THE REACTIONS OF n-OCTANE ON BIMETALLIC REFORMING CATALYSTS

THESIS

SUBMITTED FOR THE DEGREE

OF

DOCTOR OF PHILOSOPHY

OF THE

UNIVERSITY OF GLASGOW

BY

COLIN PARK, B.Sc.

DEPARTMENT OF CHEMISTRY

OCTOBER, 1994

I would like to dedicate this thesis to my mum

SUMMARY

The aim of this study was to gain a clearer understanding of the improved selectivity and activity of a bimetallic catalyst when compared with a corresponding monometallic catalyst. The role of the second metal in a bimetallic Pt-X/Al_2O_3 catalyst (where X= Re, Sn or Ge) has been studied during continuous flow experiments performed mainly at 510°C and 110 psig (9.5 atm), using n-octane as a model hydrocarbon feedstock.

Each catalyst was extensively characterised by chemisorption studies, transmission electron microscopy, EDX, physical adsorption of nitrogen and mercury porosimetry. TEM and EDX investigations showed that particle aggregation occurred on all catalysts with increasing time on stream. No alloy particles could be found on any reduced or spent Pt-Re/Al_2O_3 catalysts but alloy particles were found with both Pt-Sn/Al_2O_3 and Pt-Ge/Al_2O_3 catalysts.

In comparison with a monometallic Pt/Al_2O_3 catalyst, significant changes occurred in the aromatisation selectivities of the bimetallic catalysts. These changes have been interpreted in terms of an interaction between the small platinum particles (< 1 nm) and the second metal which is dispersed over the alumina support surface. Different methods of preparation, especially for the Pt-Sn/Al_2O_3 and Pt-Ge/Al_2O_3 catalysts, gave rise to varying degrees of interaction between the metal and the support and therefore a range of selectivities to aromatic products.

An increase in the isomerisation activity together with a decrease in the hydrocracking activity, observed with an increased time on stream, is interpreted in terms of coke deposition on, and chlorine loss from, the alumina support. The decrease in hydrogenolysis activity with time on stream, seen on all non-sulphided catalysts, has been attributed to coke deposition on the metallic sites of the catalyst.

Sulphiding either a 0.3wt%Pt/Al_2O_3-Cl or a 0.3wt%Pt-0.3wt%Re/Al_2O_3-Cl catalyst resulted in a significant increase in the aromatisation and decrease in the hydrogenolysis activity of the catalyst when compared with non-sulphided 0.3wt%Pt/Al_2O_3-Cl and 0.3wt%Pt-0.3wt%Re/Al_2O_3-Cl catalysts. The product distribution of aromatic species was altered significantly by sulphiding both the 0.3wt%Pt/Al_2O_3-Cl and the 0.3wt%Pt-0.3wt%Re/Al_2O_3-Cl catalysts, benzene and toluene being dominant over C_8 aromatic species. This is in direct contrast to the behaviour observed with a non-sulphided catalyst. With increasing sulphur content the catalyst selectivity to benzene and toluene was observed to increase as a result of an increased isomerisation and cracking activity of the sulphided catalysts. It was found that sulphur adsorbed on the catalyst surface was displaced from both sulphided 0.3wt%Pt/Al_2O_3-Cl and 0.3wt%Pt-0.3wt%Re/Al_2O_3-Cl catalysts by coke deposition with increasing time on stream.

The results obtained in this present study showed the importance of the second metal in a bimetallic catalyst. The addition of this second metal modifies both the alumina support and the small platinum particles (< 1 nm). This modification induces many changes in both the selectivity and activity of the bimetallic catalyst when compared with a monometallic catalyst.

ACKNOWLEDGEMENTS

I would like to thank my supervisor Prof. G. Webb for his help and guidance throughout this study. I would also like to thank my industrial supervisor Dr. M.A. Day (ICI Wilton) for his many helpful suggestions with this work.

I am also greatly indebted to Dr. Z. Huang for his help with this project, in particular with the electron microscopy studies and to Miss V. Yeats for processing the micrographs. Many thanks are also due to the Technical Staff at the University and to all my friends and colleagues, past and present, in the department.

I am also indebted to the many people at ICI Wilton for their help during my visits. I would especially like to thank Mr. A. Reid, Mr. R. Fletcher and Mr J. Duffie and all other members of the Micromeritics and Hydrocarbon laboratories for all their help.

I gratefully acknowledge the CASE studentship awarded by the SERC and ICI and the use of the research facilities at ICI Wilton.

Finally I would like to thank my mum, Gwen and the rest of my family for their support throughout my studies.

CONTENTS

CHAPTER THREE: PREPARATION AND CHARACTERISATION OF CATALYSTS

CHAPTER FOUR: EXPERIMENTAL

CHAPTER SIX: RESULTS

Chapter 1

Introduction

1.1. GENERAL INTRODUCTION

From its origins in the early nineteenth century, catalysis has grown into one of the most important and productive areas in industry in recent years. Today catalysts as well as being used in the petrochemical industry are widely used to produce many of the raw materials required for the plastics, paints and dye industries.

Catalytic behaviour was first noted, but not fully understood or recognised, in a wide variety of isolated experiments (1-3). These experiments included the conversion of starch to sugar by the addition of mineral acid by Kirchoff in 1812; the decomposition of hydrogen peroxide by platinum, gold and silver noted by Thenard in 1818 and the dehydrogenation of an alcohol to an ether by sulphuric acid carried out by Mitscherlich in 1834. It was not until 1835, when a common theme in this series of seemingly unrelated reactions was first postulated by Berzelius. Berzelius suggested that these reactions could take place at the surface of a solid, provided that the surface of the solid possessed what he described as a 'catalytic force'. He introduced the Greek word 'catalysis', meaning decomposition or dissolution, to describe this new phenomenon.

Since 1835, numerous scientists have suggested various definitions for 'catalysis'. But it was not until the kinetic theory of gases and basic chemical kinetics were introduced that a clearer understanding of the phenomenon 'catalysis' was gained. Ostwald, in 1911, redefined a catalyst as being any substance which could change the velocity of a chemical reaction. Ostwald postulated that a catalyst's action could

be explained if the assumption that a decrease in the activation energy, needed for a reaction to occur, was believed. To this present day, the definition of a catalyst has remained virtually the same. A catalyst is believed to be a substance which will increase the rate of a reaction by providing a different pathway with a lower activation energy and which does not alter the position of the final thermodynamic equilibrium for that particular reaction. This definition, however, only describes an ideal situation. In practice, a catalyst will undergo change during a reaction. This is especially true for heterogeneous catalysis whose surfaces are extremely sensitive to their environment. It has been well documented in the literature (2-7) that during the reaction of hydrocarbons, carbonaceous residues are deposited onto the catalyst surface. Catalysts may also undergo a variety of changes due to sintering, structural reorganisation on the surface and in many cases via secondary reactions.

Another important aspect of catalysts is their ability to direct reactions along certain pathways when a variety of options exist. This selectivity is strongly influenced by the choice of reaction conditions and the composition of the catalyst used. An example of the importance of selectivity is provided by the catalytic conversion of syngas, which can result in the formation of either hydrocarbons or alcohols, using iron or copper catalysts, respectively.

With the growing awareness of environmental problems, selectivity is again becoming increasingly more important. Industry, wishing to avoid harmful byproducts produced during certain reactions, are looking to synthesise different products from the same reactant compounds by exploring the selectivity of the

reaction with several different catalysts.

1.2 CATALYTIC REFORMING

1.2.1. Industrial Significance

Over the past 40 years catalytic reforming has rapidly grown to the point where it is now one of the most important applications of catalysis (2-4). Catalytic reforming was originally developed for the petroleum industry in the late 1940's to produce gasoline components of high anti-knock quality, in response to the developing high compression internal combustion engine. Catalytic reforming may also be used to produce aromatic compounds (in particular benzene, toluene and C_8 aromatics), which in addition to their use as fuels may also be used as a raw material for a variety of chemical processes e.g. the manufacture of plastics, paints and dyes.

The primary objective of catalytic reforming is to convert saturated hydrocarbons (low octane number) in naphtha fractions to aromatic hydrocarbons (high octane number) as selectively as possible while decreasing the overall molecular weight to a limited extent. This, therefore, results in an increase in the so called octane number of the naphtha and diminishes its knocking capacity. Naphtha fractions which are used in reforming reactions as feedstocks may vary considerably in chemical composition between different oil fields, therefore the octane ratings of straight-run gasolines would vary. This is highlighted in Table 1.2.1 where there is a considerable difference in the amounts of paraffins, naphthenes and aromatics

present in each naphtha feedstock (8). The octane number of straight-run naphthas, even with the addition of an octane enhancing component such as tetra ethyl lead, is too low to be used in commercial fuels (9).

The chemical structure of unleaded hydrocarbons in a naphtha fraction is directly related to the knocking potential and octane number (3) as illustrated in Figure 1.2.1 and summarised in Table 1.2.2.

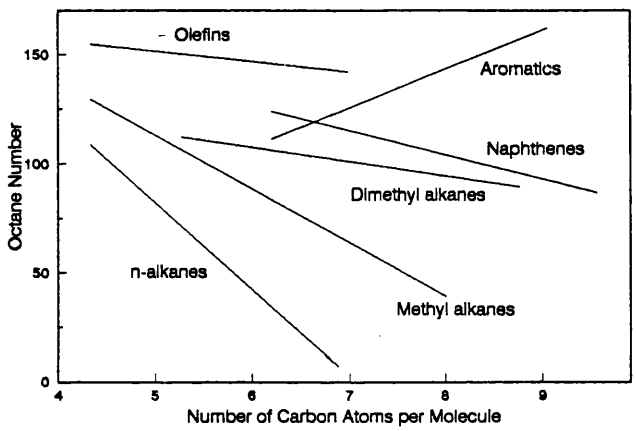

Figure 1.2.1. Variation of the Octane Number with respect to the Chemical Structure.

As shown in Figure 1.2.1 the octane number decreases with increasing carbon number or molecular weight, except for aromatic compounds where the reverse is true. The octane number of paraffins increases with the degree of substitution and unsaturation illustrating the importance of catalytic reforming. Not all compounds which have a high octane rating are suitable for use in fuels. This is clearly

Table 1.2.1. Characterisation of two typical reforming feedstocks.

	Paraffins (wt %)	Naphthenes (wt %)	Aromatics (wt %)
Arabian Light Feedstock			
C_5	-	-	-
C_6	5.49	2.30	0.41
C_7	16.83	5.80	3.18
C_8	21.38	8.27	6.80
C_9	17.26	5.95	3.08
C_{10}	2.59	0.63	-
Total	63.55	22.95	13.47
RON	50		
Nigerian Feedstock			
C_5	0.16	0.27	-
C_6	3.31	5.78	0.20
C_7	6.13	14.24	1.20
C_8	9.79	14.47	3.54
C_9	3.89	17.14	4.29
C_{10}	3.59	11.17	0.88
Total	26.81	63.07	10.10
RON	66		

Table 1.2.2. Variation of the Octane Number with Hydrocarbon Structure

	Octane Number		Octane Number
Aromatics		*Paraffins*	
Benzene	99	i-Butane	122
Toluene	124	n-Pentane	62
Ethylbenzene	124	i-Pentane	99
o-Xylene	120	n-Hexane	19
m-Xylene	145	2-Methylpentane	33
p-Xylene	146	n-Heptane	0
		2-Methylhexane	41
Naphthenes		n-Octane	-19
Cyclohexane	110	i-Octane	100

demonstrated by olefins, which have a relatively high octane rating but are the cause of engine fouling when present in fuels in high concentrations. Therefore as a result their use is strictly limited and their formation is largely desired.

It has been well documented (3, 8-10) that the octane number represents the percentage of 2,2,4 trimethyl pentane in a reference fuel blend of n-heptane and i-octane which will cause a knock at the same compression ratio as the unknown fuel mixture. Therefore, the octane rating gives an indication of a hydrocarbons ability to resist detonation under a rise in temperature due to rapid compression. The octane number scale has been defined by ascribing n-heptane a rating of 0 (as it is prone to knocking) and i-octane a rating of 100.

In general, modern car engines require fuels with an octane rating of between 91 and 98. Due to an increased awareness of the environmental pollution caused by toxic emissions from cars an increasing number of manufacturers are installing catalytic converters in their cars. This converts noxious compounds like NO_x, CO and hydrocarbons into less toxic species like CO_2, H_2O and N_2. The use of these catalytic converter required the change from leaded to lead free fuel and as a consequence the catalytic reformers must produce higher octane number fractions to compensate for the lack of lead compounds in fuel (8-10). This is generally achieved by increasing the amount of aromatics in the fuel which will in time come under scrutiny by environmental groups demanding a lower benzene content.

Industrially, catalytic reforming is generally carried out at pressures of 10 to 40 atmospheres and temperatures between 480 and 530°C. The exact reaction conditions; choice of feedstock, hydrogen to hydrocarbon ratio, WHSV, pressure, temperature and choice of catalyst depend upon the desired reaction product (4, 11, 12). The effect of changing these conditions will be discussed in greater detail later in this work.

1.2.2. Reforming Reactions

Despite the large number of catalysts available today, there are only six major reforming reactions which take place in the catalytic reforming of naphtha feedstocks (3). These reactions are shown in Figure 1.2.2 using C_6 molecules as an example.

1) Dehydrogenation of cylohexanes to aromatic species

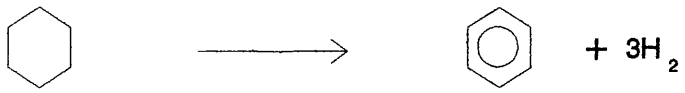

2) Dehydrogenation of alkanes to olefins

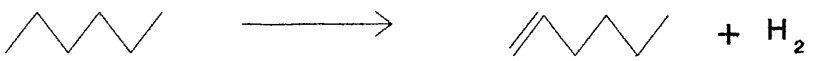

3) Isomerisation of alkanes to branched alkanes

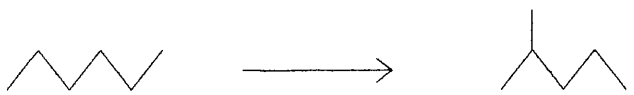

4) Dehydrocyclisation of alkanes to aromatics

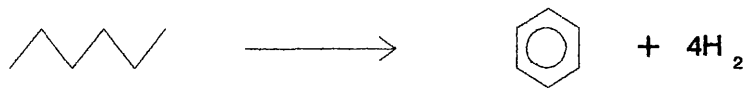

5) Hydrogenolysis & hydrocracking reactions to give low molecular weight products

6) Ring expansion

Figure 1.2.2. Major Catalytic Reforming Reactions

Of all the reactions taking place in reforming, the dehydrogenation of cyclohexane species forming aromatics occurs most readily. Isomerisation reactions and dehydrogenation of paraffins do not occur quite as rapidly and hydrocracking and dehydrocyclisation reactions occur much more slowly.

Thermodynamic data of selected reactions illustrated in Figure 1.2.2 is shown in Table 1.2.3. The thermodynamics may be considered conveniently by referring to the equilibrium constants at 500°C, K, and the heats of reaction for the conversion of C_6 species at the same temperature (13, 14).

Table 1.2.3. Thermodynamic Data on Reactions of C_6 Hydrocarbons

Reaction	K	ΔH_R (KJ mol^{-1})
Cyclohexane → Benzene + $3H_2$	6×10^5	221
Methylcyclopentane → Cyclohexane	0.086	-160
n-Hexane → Benzene + 4 H_2	0.78×10^5	266
n-Hexane → 2-Methylpentane	1.1	-5.9
n-Hexane → 3-Methylpentane	0.76	-4.6
n-Hexane → 1-Hexene + H_2	0.037	130

The dehydrogenation of cyclohexane and the dehydrocyclisation of n-hexane to give benzene are highly endothermic reactions and both evolve hydrogen. The dehydrogenation of paraffins to olefins, also an endothermic reaction, occurs to a small extent at typical reforming conditions. Although they are produced in small

quantities, olefins are believed to be important intermediates in the reforming conversions. Therefore they determine the rates of the reactions which proceed via olefin intermediates. It would therefore seem to be desirable to operate at the highest possible temperature and the lowest hydrogen pressure in order to maximise the aromatic products and olefin intermediates. In reality however, constraints are imposed on the maximum temperature and the minimum hydrogen pressure allowed. These constraints are set to maintain the catalyst activity at the highest possible level for the longest period of time.

1.3. CATALYST SUPPORTS

Initially a catalyst support was believed to be an inert substance over which an expensive metal, such as platinum, was dispersed, or a means of improving the mechanical strength of a naturally weak catalyst. However, the support has been found to contribute to the catalytic activity, depending upon the reaction and on the reaction conditions. The support may act to stabilise the catalytically active structure and has also been shown to interact with the metal dispersed upon it, as in the case of tin supported on alumina.

The supports in use today may be classified into several categories:-

a) 'Inert' supports - these have a high surface area for dispensing the active component eg. silica.

b) Catalytically 'active' supports - these include Al_2O_3, SiO_2 - Al_2O_3 and zeolites.

c) Supports which influence the active components by a strong interaction e.g. partially reducible oxides - TiO_2, V_2O_5 and Nb_2O_5.

d) Structural supports - these are becoming increasingly important for gas purification.

The selection of a support is based upon it having certain desirable properties. A fundamental requirement for any catalyst is resistance to sintering under reaction conditions. The temperature at which lattices begin to be appreciably mobile is termed the Tammann temperature; and that at which surface atoms becomes significantly mobile, the Hüttig temperature. For simple compounds without phase changes on heating and of low vapour pressure, the Tammann temperature is approximately 0.5 Tm and the Hüttig temperature is about 0.3 Tm, where Tm is the melting point in absolute units. As a result suitable supports must have reasonably high melting points as a minimum requirement. The transition metals iron, cobalt and nickel have melting points of around 1500°C and become mobile at temperatures in the region of 250 - 300°C. The platinum group metals melt at higher temperatures but are usually supported for economic reasons (15). Since platinum is very expensive, the optimal catalytic efficiency per unit mass of metal must be achieved, and therefore small particles providing a high dispersion is imperative.

1.3.1. Alumina

Stoichiometrically there is only one oxide of aluminium, that is, alumina (Al_2O_3). This simplicity, however, is compensated by the occurrence of various polymorphs,

hydrated species and so on, the formation of which depends upon the conditions of preparation. There are 27 materials that may be regarded as alumina (16). There are two forms of anhydrous alumina, namely α-Al_2O_3 and γ-Al_2O_3. Other trivalent metals (Ga and Fe) form oxides that crystallise in the same two basic structures. In α-Al_2O_3 the oxide ions form a hexagonal close packed array with the aluminium ions being distributed symmetrically among the octahedral interstices. The structure of γ-Al_2O_3 is sometimes regarded as being that of a 'defect' spinel structure, that is, having the structure of a spinel with a deficit of cations (16).

Commercially the most important support material in use today is alumina. The use of aluminas is widespread and their preparation and properties have been extensively investigated in numerous publications (17-19). Aluminas of high surface areas (100 - 600 m^2g^{-1}) are usually prepared by the thermal decomposition of crystallised aluminium hydroxides or by the precipitation of colloidal gels. The latter process is often favoured since it yields more control over the surface area and porosity of the aluminas produced. The properties of the aluminas are dependant upon the choice of gelation conditions (20).

Both γ- and η-alumina, are used extensively as supports in heterogeneous catalysis. γ-alumina is of great interest since it has a high area and is relatively stable over the temperature range of interest for most catalytic processes. η-alumina, due to its greater acidity than γ-alumina, was of particular interest as a support in catalytic reforming in the past. Interest in this support has however diminished since the discovery that the acidity of γ-alumina could be precisely controlled by the

addition of minute amounts of water and chlorine (or fluorine).

Both γ- and η-alumina possess spinel related structures, that is defect spinel structures which are slightly tetragonally distorted. The main difference structurally between γ- and η-alumina is that γ-alumina has a more ordered structure when compared to η-alumina where stacking faults are very common. This is reflected in the average Al-O bond lengths calculated from radial electron distributions, 1.818 - 1.820Å for γ-alumina and 1.825 - 1.838Å for η-alumina (21). The cation distribution is also found to be slightly different for both aluminas, γ-alumina possesses a much higher percentage of Al^{3+} ions in tetrahedral positions than η-alumina.

The surface of alumina contains hydroxyl groups in place of oxygen ions, contributing to maintaining the electrical neutrality of alumina. It has been shown by infrared adsorption that there are at least five distinct types of hydroxyl groups present surrounded by different numbers of oxides (exposed oxygen atoms) and/or anion vacancies (exposed aluminium atoms). Peri (22) also found this to be true when investigating the dehydration process of a statistical model of γ-alumina by Monte Carlo simulation. These hydroxyl groups may be regarded as being potential Brønsted acid sites (that is as a proton source) (23). During the calcination process Peri (22) attained that around 67% of the surface hydroxyl content was removed by heating γ-Al_2O_3 at approximately 500°C; this value increased to around 90% when the temperature was raised to 670°C. Coordinately unsaturated aluminium atoms on the surface may be produced as a result of the condensation of two neighbouring

surface hydroxyl groups as shown below.

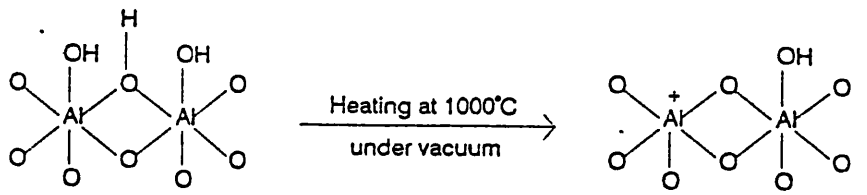

These sites may be regarded as Lewis acid sites. However, on the catalyst surface there is always sufficient adsorbed water present to result in the following reaction taking place.

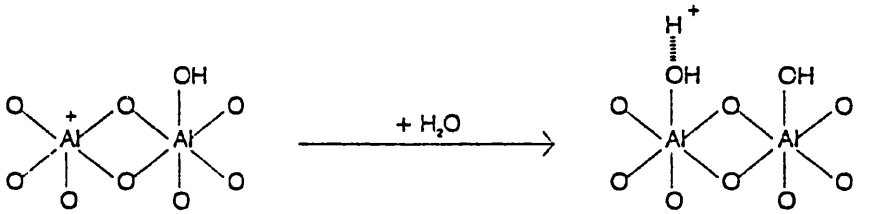

Brønsted acid sites, which initiate carbonium ion reactions, and Lewis sites, giving ion radical reactions, coexist on the catalyst surface. However, in practical usage Brønsted acid sites predominate (24).

In general aluminium hydroxides and therefore also the hydrated oxides are not strongly acidic. The measurement of the alumina surface acidity by various indicator methods (24, 25) supports the hypothesis that certain groups (OH^- groups attached to tetrahedral Al^{3+} ions) on the surface of γ-alumina and especially η-alumina are weakly acidic (15). The acidity may be markedly enhanced by deliberately incorporating halogens such as chlorine (26-28) or fluorine (29, 30) into the alumina structure. The incorporation of these will partially convert a fully hydrated alumina surface to one consisting of Cl^- and OH^- groups (for example, by treating the surface

of alumina with HCl or HF) as shown below.

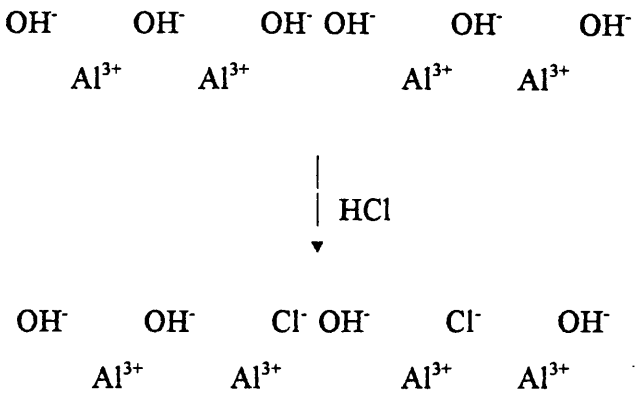

This has been found to enhance the acidity of the remaining OH^- groups substantially. Since the halide ion is very electronegative it will polarise the lattice more than the OH^- (or O^{2-}) groups it replaced. This will result in an increase in the acidity of both Brønsted and Lewis acid sites on the surface (31). It would also appear that the acidity of a group on the alumina surface can be progressively increased as more of the OH^- groups surrounding it are replaced by Cl^- (or F^-) ions (25). Halides may also be introduced inadvertently if a metal halogen compound such as $PdCl_2$, $SnCl_2$ and H_2PtCl_6 is used in the catalyst preparation.

Alumina itself is known to catalyse easy isomerisation reactions such as double-bond shifts in olefins (31, 32), though it is unable to readily catalyse skeletal isomerisation. The increase in acidity induced by the treatment of alumina with either HCl or HF is sufficient to make it a highly active catalyst for skeletal isomerisation, hydrocracking and other desirable reactions in hydrocarbon reforming. It is especially important in hydrocarbon reforming to control the strength of the surface acid sites by halogenation, and so controlling the relative rates of the several

acid-catalysed reforming reactions. Therefore the alumina support adds dual functionality to the overall catalysis (33)

Commercially aluminas are available in a wide range of surface areas (15 - 600 m^2g^{-1}) and pore sizes. The aluminas used are characterised by excellent thermal stability, though heating above 580°C will result in the closure of the micropores and therefore a reduction in the surface area (34).

In considering the individual factors which dictate the choice of catalyst support, it must be remembered that the final choice will depend on the use to which the catalyst will be put. The combination of the useful properties of aluminas make them generally the most extensively used catalyst support. However, active aluminas can dissolve or become soft and mushy under acidic conditions, conditions under which silica is stable. The relative inertness of silica may also be a very significant factor when making a choice of catalyst support. If the adsorption of products or reactants onto alumina is detrimental then the non-adsorptive character of silica may be an improvement.

1.4. REFORMING CATALYSTS

1.4.1. Early Reforming Catalysts

In the initial catalytic reforming processes, in the 1940's, alumina supported chromia or molybdena catalysts were employed. However, due to their rapid

deactivation and subsequent costly regeneration, these catalysts were extensively replaced by a bifunctional platinum catalyst in 1949. Haensel (35, 36) introduced a monometallic platinum catalyst supported on an acidic alumina which combined the dehydrogenation-hydrogenation activity of platinum with the isomerisation activity of the acidic support. The lifetime of these early catalysts was very short by todays standards. It was necessary to replace the catalysts after a period of six to twelve months on stream.

Monometallic catalysts dominated catalytic processes for many years until Chevron introduced the first bimetallic platinum-rhenium catalyst in 1967 (37). This catalyst added a further vast improvement in the stability and selectivity of reactions and lower deactivating rates resulting in prolonged lifetime on stream. The combination of metals varied considerably, tin, lead and germanium are just a few of the metals combined with platinum in the search for a better catalyst (3, 4). The reason for this improved stability and selectivity was not fully understood and has been the basis of many investigations.

1.4.2. Platinum-Rhenium Catalysts

To establish the valence state of rhenium and whether or not it was alloyed with platinum in a reduced catalyst, Johnson and LeRoy (38) and Johnson (39) used chemisorption, IR and XRD studies. A series of Pt-Re catalysts prepared by the impregnation of η- and γ-alumina with aqueous solutions of chloroplatinic acid and ammonium perrhenate were studied by these authors. The platinum and rhenium

contents ranged from 0.31 to 0.66 wt% and 0.20 to 1.18 wt% respectively. Studies on these catalysts indicated that complete reduction of Pt^{IV} to Pt^0 and partial reduction of Re^{VII} to Re^{IV} occurred during the reduction process. XRD data on the metallic residue gave no evidence for the presence of rhenium metal or a Pt-Re alloy phase.

In direct contrast results reported by Webb (40) concluded that rhenium (Re^{VII}) was completely reducible to Re^0 at temperatures of between 400 and 450°C. Several suggestions were put forward to explain the differences between these results and those of Johnson *et al.* The higher concentrations of rhenium used by Webb might have been present as larger particles and therefore they would be much easier to reduce to the metallic state. Low concentrations of rhenium on the catalyst would be much more difficult to reduce due to the larger metal support interaction. Perhaps the most significant difference between the two systems was the amount of water present on the catalyst. Johnson and LeRoy, using a static reduction technique, could not remove the water formed during the process. Webb, however, by recirculating the hydrogen was able to remove this water by means of a liquid nitrogen trap. Therefore the removal of water from the system results in the complete reduction of rhenium. Later work using chemisorption and IR (41) confirmed the results of Webb and showed that the complete reduction of Re^{VII} to Re^0 did take place.

Temperature programmed reduction (TPR) has also been extensively used to determine the oxidation state of rhenium in the bimetallic Pt-Re/Al_2O_3 catalyst

system. Results from these studies indicated that the properties of the catalyst are highly dependant upon the method of preparation. M^{c}Nicol (42) in an attempt to ascertain the reducibility of rhenium used TPR. When studying the monometallic catalysts, Pt/Al_2O_3 reduced in a single peak at 280°C and Re/Al_2O_3 at 550°C. The platinum component consumed the equivalent of four and rhenium the equivalent of seven hydrogen atoms thus indicating the complete reduction of both metal oxides to the metallic state. M^{c}Nicol concluded that as the TPR profile for a bimetallic catalyst was simply the addition of the corresponding monometallic catalysts, no interaction between the platinum and rhenium occurred.

However Bolivar *et al.* (43) when studying the reduction of $Pt\text{-}Re/Al_2O_3$ catalysts found that the presence of platinum on the catalyst strongly catalysed the reduction of rhenium. The authors postulated that hydrogen spillover was responsible for the reduction of rhenium by platinum. The difference in the results of Bolivar *et al.* and M^{c}Nicol could be explained in terms of the degree of hydration of the metal oxide. M^{c}Nicol calcined the catalysts at 525°C whereas Bolivar *et al.* dried their catalysts at 110°C. Therefore the degree of hydration has a marked effect on the ease of reduction.

Further studies carried out using TPR (44, 45) reinforced the idea of the degree of hydration strongly influencing the reduction of the metal oxides. Studies in particular by Isaacs and Petersen (46) were very significant. These authors noted that the maximum reduction temperatures of both monometallic Pt/Al_2O_3 and Re/Al_2O_3 were weakly dependent upon the calcination temperature. In general

Pt/Al_2O_3 and Re/Al_2O_3 calcined at 500 - 550°C reduce with a TPR peak at about 275 and 550°C respectively. However, after calcination at 300°C or less, the TPR peaks for Pt/Al_2O_3 and Re/Al_2O_3 fall to about 150 and 350°C respectively. This drop suggests that a higher calcination temperature enhances the interaction between the metal oxides and the Al_2O_3 support.

In marked contrast to the monometallic catalysts, the drying temperature has a significant effect on the TPR profile of a bimetallic $Pt\text{-}Re/Al_2O_3$ catalyst. Both the number and position of the peaks are highly dependent upon the drying temperature. To illustrate this point, the TPR profile of a $Pt\text{-}Re/Al_2O_3$ catalyst dried at 100 or 200°C consisted of a single peak with a maximum similar to that of a monometallic Pt/Al_2O_3 catalyst. The size of this peak corresponds to the simultaneous reduction of both platinum and rhenium. This phenomena was also noted by Bolivar *et al.* (41) and Wagstaff and Prins (47). At higher drying temperatures (< 400°C), two distinct peaks are noted. One peak is situated at a temperature characteristic of Pt/Al_2O_3 and the other at a temperature characteristic of Re/Al_2O_3. This phenomena has been reported by various authors; M°Nicol, Wagstaff and Prins (42, 47).

In order to clarify the precise effect of the drying temperature on the TPR profiles for $Pt\text{-}Re/Al_2O_3$ catalysts, three proposals were suggested.

1) The degree of hydration influences the ease of reduction of a metal oxide.

2) The degree of hydration influences the rate of hydrogen spillover.

3) The degree of hydration influences the mobility of Re_2O_x.

Isaacs and Petersen (46), as noted previously, found that the drying temperature of a monometallic catalyst had little effect upon the reduction of either Pt/Al_2O_3 or Re/Al_2O_3 catalysts and therefore the first suggestion could be discarded.

The second proposal to explain the difference in TPR profiles was based upon a hydrogen spillover mechanism (48). Atomic hydrogen produced on a reduced platinum component by dissociative adsorption of hydrogen, can migrate via the alumina support to the rhenium precursor thus promoting its reduction. Hydrogen spillover is known to be catalysed by the presence of water on the support (48, 49) and so this difference is possibly due to different degrees of alumina support hydration. However, calculations by Isaacs and Petersen, based upon the kinetic data of Kramer and Andre (50), led them to say that there was insufficient spillover to account for the observed results. However studies on the Pt-Re interaction led Mieville (51) to propose a mechanism which depended upon a small fraction of the rhenium oxide being reduced by hydrogen. It is the creation of such rhenium nuclei which subsequently catalyses the reduction of the remaining oxide.

Finally the idea of water influencing the mobility of Re_2O_x was first postulated by Bolivar *et al.* (41, 43) and has subsequently been studied by Isaacs and Petersen (46) and Wagstaff and Prins (47). It has been assumed by these authors that a hydrated Re_2O_x species is very mobile on the catalyst surface. Migration to platinum centres covered by hydrogen by this mobile species is followed by the reduction of rhenium and subsequent alloying occurs almost instantaneously. For catalysts which have been calcined at higher temperatures the surface migration by this Re_2O_x

species is hindered by dehydroxylation. It was therefore concluded that the platinum had less interaction, if any, with rhenium under these conditions and therefore results in two distinct TPR peaks. This would also imply that no Pt-Re alloy phase would be formed under such conditions.

XPS has been used to determine the valence state of rhenium in a Pt-Re/Al_2O_3 catalyst. Short *et al.* (52) examined two laboratory prepared reduced catalysts. Data from the $Re_{L_{III}}$ adsorption edge showed that rhenium was not zero valent and therefore not significantly associated with platinum. XPS data suggests that rhenium is present in the 4+ valence state. XPS methods are a good method to ascertain the valence state of rhenium due to the intense 4f peak (53). Biloen *et al.* (54) established that a Pt-Re alloy was formed. However, at the low metal loadings used in these catalysts, in addition to chlorine on the alumina support, it has been reported that an oxygen 2s satellite interferes with the rhenium 4f signal and the chlorine 2s peak with the next most intense peaks $4d_{3/2}$ and $4d_{5/2}$.

H_2/O_2 titrations have been used extensively (55) to provide vital information about Pt-Re interactions on the catalyst surface. The bimetallic Pt-Re supported catalysts showed a decrease in the hydrogen and an increase in the oxygen consumption when compared with the corresponding monometallic catalyst. A later study (41) illustrated that oxygen chemisorbed on rhenium could be readily removed even when a small amount of platinum was present. However platinum is also effective for a mechanical mixture of the two monometallic catalysts (56) therefore showing that the interaction can not be explained in terms of an alloy formation.

To investigate further the formation of a Pt-Re alloy many workers have utilised specific reforming reactions as a probe. The addition of rhenium to $Pt/\gamma\text{-}Al_2O_3$ catalysts has been shown to increase the catalytic activity and selectivity of various reforming reactions. Augustine and Sachtler (57) investigating the hydrogenolysis of cyclopentane on supported Pt-Re catalysts postulated that the formation of an alloy was responsible for the results of their studies. The high specificity of $Pt\text{-}Re/Al_2O_3$ catalysts for methane formation is assumed to be characteristic of Pt-Re alloy particles on the support. Biloen and co-workers (54) reached the same conclusions upon adding rhenium to a platinum catalyst.

Jossens and Petersen (58) compared the fouling characteristics of two model reactions catalysed by bifunctional Pt and Pt-Re catalysts. The dehydrogenation of methylcyclohexane was used as a probe for changes in the metallic function and the dehydroisomerisation reaction of methylcyclopentane to benzene was used to determine the variations in the acidic function. The addition of rhenium to a platinum reforming catalyst therefore resulted in the rates of toluene dealkylation, methylcyclopentane ring opening and long term self deactivation by methylcyclohexane all decreased dramatically. Whereas the rates for the production of toluene from methylcyclohexane and benzene from methylcyclopentane and short term self deactivation by methylcyclohexane were unaffected. The former reactions are believed to be structure sensitive while the latter are not. This idea would therefore suggest that the addition of rhenium to a $Pt/\gamma\text{-}Al_2O_3$ catalyst does directly affect the platinum component as is expected for the formation of a Pt-Re alloy.

However, other studies have led again to very different conclusions being drawn. Studies incorporating TEM, EDX and ion scattering spectroscopy (ISS) carried out by Kelley *et al.* (55) concluded that under the conditions used platinum and rhenium are not significantly alloyed. In addition these authors found that rhenium was uniformly distributed over the alumina support at low concentrations.

Short and co-workers (52) again provided further evidence of non-alloy formation by XPS. Rhenium was found to be neither present in the zero valent state nor significantly associated with the platinum component. Studies utilising infrared spectroscopy (59) conducted by Peri on adsorbed probe molecules provided evidence on the dispersion and the chemical nature of supported platinum and rhenium catalysts. Peri could find no evidence for the formation of an alloy phase or bimetallic cluster using IR. The Pt-Re/Al_2O_3 catalyst exhibited a spectra very similar to the combined spectra of both the monometallic platinum and rhenium supported catalysts. Nevertheless, Peri did not totally rule out the possibility that a small fraction of the metal may be present as an alloy or bimetallic cluster.

Experiments carried out by Bertolacini and Pellet (60) provided direct evidence ruling out the possibility of an alloy formation in a commercial catalyst. These authors found that a mechanical mixture of monometallic Pt/Al_2O_3 and Re/Al_2O_3 catalyst pellets exhibited similar behaviour to that of a Pt-Re/Al_2O_3 catalyst. In addition, analysis of the spent mechanical mixture showed that no metal transfer had taken place. Therefore on the basis of their results, Bertolacini and Pellet concluded that alloy formation, if it was present, was not responsible for the beneficial effects

seen on the addition of rhenium.

Therefore as has been shown the widespread diversity of opinion with regards to the nature of the Pt-Re interaction in supported Pt-Re/γ-Al_2O_3 catalysts emphasises the need for strict control on the preparation of the reforming catalysts. Furthermore with the many different preparation and pretreatment techniques in use the debate and controversy of alloy formation or not will continue.

1.4.3. Platinum-Tin Catalysts

Pt-Sn/Al_2O_3 catalysts were introduced not long after the Pt-Re series but did not receive widespread attention until the last fifteen years when improvements in catalytic regeneration were introduced for naphtha reforming. A lower operating pressure and the improved regeneration process has led to Pt-Sn catalysts gaining renewed commercial importance.

The addition of tin to Pt/Al_2O_3 resulted in an enhanced stability and improved selectivity towards aromatic formation. Extensive investigations have been undertaken to identify and in an attempt to understand the nature of the beneficial effects of tin by many workers (61-70). Despite these numerous studies on Pt-Sn catalysts several points of contention still exist. The main points of contention include the interaction between tin, platinum and the support; the chemical state and distribution of tin in the catalyst and the tendency for platinum and tin to form alloys.

Early work on Pt-Sn/Al_2O_3 catalysts using TPR has proved to be inconclusive (61-71). Burch and Garla.(61) have suggested that tin was not reduced to the zero valent state in the bimetallic catalysts but was present as a Sn^{II} species stabilised on the γ-alumina support. However, Burch did not rule out the possibility of an alloy formation. On the other hand, authors (62, 71, 72) contended that tin, not necessarily all the tin, was reduced to the metallic state, i.e. Sn^0. Dautzenberg *et al.* (62) in particular demonstrated that there was substantial reduction of Sn^{IV} to Sn^0 and the subsequent alloy formation. However these workers have also reported that the first 0.6 wt% Sn was not reducible due to an interaction with the alumina support. It has also been suggested by Burch and Garla, from the results of Dautzenberg *et al.*, that there is partial reduction of all the tin in the catalyst up to approximately 1.7 wt% (i.e. $Sn^{IV} \rightarrow Sn^{II}$) and the complete reduction of any additional tin (i.e. $Sn^{IV} \rightarrow Sn^0$).

This idea of having both Sn^{II} and Sn^0 species present in the catalyst has been confirmed by Lieske and Völter (69). From the results of TPR studies the majority of tin is found to reduce to Sn^{II} and a minor fraction to Sn^0. It is this small fraction of Sn^0 which forms a bimetallic alloy with platinum. In a continuation of these studies Völter *et al.* (63, 64) found that between 10 and 30% of Sn^{IV} was reduced to the zero valent state and alloyed with platinum with the majority of tin being present as a Sn^{II} species. They also reported that the extent of alloying increases with increasing tin content.

Contrasting results in the variation of the hydrogen uptake with respect to the

amount of tin added are reported in the literature. Völter *et al.* (63, 64), Palazov *et al.* (65) and Lieske and Völter (69) for example found that the addition of tin to a Pt/Al_2O_3 catalyst decreased the amount of hydrogen chemisorbed on the bimetallic $Pt\text{-}Sn/Al_2O_3$ catalyst. On the other hand, Burch (66) and Muller *et al.* (67) observed an increase in hydrogen uptake with increasing tin content. Balakrishnan and Schwank (68) found an initial increase in hydrogen uptake upon the addition of small quantities of tin ($Sn/Pt < 0.5$), but the amount of hydrogen chemisorbed tended to decrease with further additions of tin. This increased hydrogen uptake was attributed to an increase in the platinum dispersion by Burch (66), Balakrishnan and Schwank (68) as tin will not allow small platinum particles to sinter. Muller *et al.* proposed that with tin addition, hydrogen is able to migrate by a spillover mechanism onto the Sn^{II} sites.

TPR albeit a very convenient method, is an indirect method for determining the state of tin in a bimetallic Pt-Sn catalyst. More direct methods like x-ray photoelectron spectroscopy (XPS) and ESCA have been used to gain an insight into the state of tin in the bimetallic catalyst. XRD and EXAFS are two techniques which represent a diagnostic of the bulk structure..

XPS allows the determination of the chemical state of an element but cannot distinguish whether Sn^0 species is present as a Pt-Sn alloy or not. In addition, the major platinum XPS peak coincides with a large peak from the alumina support. Therefore XPS can only say if a Pt-Sn alloy is possible but cannot actually verify the presence of an alloy.

Early XPS studies revealed that tin was present only in an oxidised state, i.e. Sn^{IV} or Sn^{II} (72). Kuznetsov *et al.* (73-75) found that platinum and tin complexes impregnated on γ-alumina do not form alloys after the reduction whereas alloys were witnessed on silica supported catalysts. On γ-alumina only Sn^{IV} and Sn^{II} species could be determined after reduction in hydrogen. However, the validity of these early studies is questionable since Davis *et al.*(76) reported that the early work from their laboratories had been biased by the use of oxygen containing pump oils to maintain the high vacuum used in XPS measurements. Since then, Li *et al.* (77) have reported that a small part of the tin in a reduced Pt-Sn/Al_2O_3 catalyst is present as Sn^0. Furthermore, based on the extensive research and data by two groups of workers, Hoflund *et al.* (78-80) and Davis *et al.* (77, 81, 82), the atomic ratio of the Pt-Sn alloy phases increases with increasing tin to platinum ratios as shown in Table 1.4.1.

Table 1.4.1. Pt-Sn Alloy composition Based upon XPS data.

Pt-Sn Ratio	Support Material	
	γ-Alumina (250 m^2 g^{-1})	Silica
1:1	Pt $Sn_{0.66}$	Pt $Sn_{0.39}$
1:2.7	Pt $Sn_{1.3}$	Pt $Sn_{0.85}$
1:5	Pt $Sn_{3.4}$	Pt $Sn_{1.5}$
1:8	Pt $Sn_{3.8}$	-

XPS studies carried out by Baronetti *et al.* (70, 83) on Pt-Sn/Al_2O_3 catalysts prepared by different deposition techniques (co-impregnation and sequential impregnation) yielded some very interesting conclusions. These authors confirmed that tin was reduced to its metallic state when platinum was present in the catalyst, but not in a monometallic Sn/Al_2O_3 catalyst. Therefore this provides direct evidence that the reduction of tin is catalysed by the presence of platinum. These authors also noted that by impregnating alumina with platinum first or by coimpregnating the extent of Pt-Sn alloy increased when compared to impregnation with tin first. In both the coimpregnated and platinum impregnated first catalysts a $[PtCl_2 (SnCl_3)_2]^{2-}$ complex was formed and it was postulated that the formation of this complex enhanced the formation of alloys.

X-ray diffraction and electron microdiffraction studies (84-87) have been carried out on several Pt-Sn/γ-Al_2O_3 catalysts with varying success. Both techniques are used to characterise the bulk structure of the catalyst. Difficulties have been encountered consistently in the detection of alloy phases on a high surface area alumina support using XRD due to the highly dispersed nature of the platinum particles over the support material.

The majority of XRD studies agree that a Pt-Sn alloy is formed after reduction in hydrogen. Ushakov and Moroz (84) employing in situ XRD have reported that approximately half of the platinum on the alumina support was actually reduced at 500°C. The remainder was reported to be either ionic platinum bonded to the support or Pt^0 highly dispersed over the support. In another XRD study (85) Pt-

$Sn/\gamma\text{-}Al_2O_3$ catalysts, prepared by impregnation of alumina with a $[Pt_3Sn_8Cl_{20}]^{2-}$ complex, were investigated. This study revealed that a Pt-Sn (hcp) alloy was formed after the reduction of both a 0.6 wt%- and a 5.0 wt% Pt-Sn catalyst at 500°C for 8 hours. No other Pt-Sn alloy phase was found to be present in these catalysts.

For a series of 1.0 wt%Pt catalysts in which the tin content is varied to produce a range of Pt:Sn molar ratios from 1:1 to 1:10 the formation of an alloy phase is detected after reduction. In all these catalysts the alloyed platinum was present as a 1:1 Pt:Sn alloy, independent of the Pt:Sn molar ratio. XRD also indicated the presence of unalloyed platinum in the samples containing low tin loadings.

Davis *et al.* (85-87) used electron microdiffraction to identify the crystal structures of the alloy phases present in two $Pt\text{-}Sn/\gamma\text{-}Al_2O_3$ catalysts. One catalyst prepared by coprecipitating tin and aluminium oxide and then impregnating the resultant calcined material with chloroplatinic acid gave an Pt:Sn atomic ratio of 1:3. The second catalyst was prepared by coimpregnating $\gamma\text{-}Al_2O_3$ with an acetone solution of stannous chloride and chloroplatinic acid again to yield a Pt:Sn ratio of 1:3. A Pt-Sn alloy could not be detected for the coprecipitated catalyst but was discovered for the coimpregnated catalyst by XRD. However electron microdiffraction studies clearly identified the existence of a Pt-Sn alloy phase with a Pt:Sn ratio of 1:1 in both these catalysts. These studies also provided evidence of a second alloy phase with a Pt:Sn ratio of 1:2 in the coprecipitated catalyst.

On further examination of these catalysts by EDX spectroscopy new information

was uncovered. In the case of the coimpregnated catalyst, the dominant tin to platinum ratio was 1:1 and was therefore consistent with the XRD results. However, EDX data for the coprecipitated catalyst gave contradicting results to those of the XRD studies. EDX showed that the metal particles which were large enough for analysis consisted solely of platinum. The authors found that it was very difficult to find a metal particle with both platinum and tin present. Therefore Davis *et al.* postulated that the majority of platinum was present as metallic platinum and not as an alloy phase with tin. The few particles found with a Pt:Sn ratio of 1:2 result from platinum being present in a very tin rich or pure tin oxide region of the catalyst surface.

Transmission electron microscopy (TEM) studies on the coprecipitated and coimpregnated Pt-Sn catalysts show two distinct and contrasting structures for alumina supported catalysts of a given Pt:Sn chemical composition. For the coimpregnated catalyst both platinum and tin were found on the surface after reduction at 500°C, the migration of either metal to the bulk does not occur extensively. Following calcination, most of the tin is present as a tin aluminate species. Upon the subsequent reduction the tin is converted to Sn^{II} and Sn^{0}; the fraction of tin that is completely reduced depending ultimately on the tin loading of the catalyst. The higher the loading the higher the number of moles of Sn^{0} present. The amount of alloying in the catalyst therefore depends upon the relative amounts of tin and platinum present in the catalyst. Therefore it was concluded that for the coimpregnated catalyst the surface of the catalyst consisted of a tin aluminate species over which a mixture of platinum and Pt-Sn alloy particles were dispersed.

In direct contrast for a coprecipitated catalyst a major portion of the tin is present in the bulk of the alumina support. Therefore the surface concentration of tin was much lower than in the corresponding coimpregnated catalyst. As a result isolated tin ions are present on the support surface and on reduction some is reduced to Sn^0. Furthermore, upon reduction nearly all the platinum was present as isolated platinum atoms or as platinum metal crystallites. Therefore recent studies would appear to suggest that a lower metal loaded supported Pt-Sn catalyst will have platinum predominately present as Pt^0 with the presence of a small amount of Pt-Sn alloy.

^{119}Sn Mössbauer spectroscopy has been extensively used on a number of Pt-Sn catalysts (88-92) to provide detailed information on the bulk structure of the catalyst. Direct evidence of Pt-Sn alloy formation has been reported by many authors (88-92) using this technique. However many of these studies used high metal loadings, not characteristic of a commercial reforming catalyst. This often resulted in a very complex spectra being obtained. As a result the authors faced a degree of uncertainty in assigning Sn^0 to the exclusion of SnO phases. Mössbauer spectra clearly show changes upon the reduction of a Pt-Sn catalyst. For a reduced sample, in general, the width of the spectra peaks prevents assignment of the various states of tin.

This is highlighted in the works of Kuznetsov and co-workers (88). They reported that Pt-Sn/γ-Al_2O_3 catalysts prepared by conventional impregnation techniques are multicomponent, i.e. highly dispersed products of the interactions of Sn^{IV}, Sn^{II} and Sn^0 with both the support and platinum. Platinum according to these

authors will readily form the majority of possible alloy phases with tin.

Again Bacaud *et al.* (89) investigating the role of tin in a Pt-Sn/Al_2O_3 reforming catalyst reached similar conclusions from their work. The reduction of these Pt-Sn catalysts prepared by sequential impregnation, resulted in various quantities and compositions of Pt-Sn alloys, Sn^{IV} and Sn^{II} species. They also found that relatively high quantities of platinum did not alloy with tin and was present on the surface as metallic platinum.

Davis *et al.* (90) in a continuation of earlier work investigated alloy formation using Mössbauer spectroscopy. These authors stated that tin was observed to be in a range of oxidation states and forms as found by other authors. Tin was found to be present in forms whose isomer shifts were similar to SnO_2, SnO, $SnCl_4$, $SnCl_2$, Sn^0 and Pt-Sn alloy phases, when alumina was the support. The Pt-Sn alloy was assumed to have an atomic ratio of 1:1, as found to be the case in XRD studies on the same catalysts (86). Several conclusions were drawn as a result of these studies, lower Sn:Pt ratios ($\leq$ 5) demonstrated similar oxidised species and alloy formation. The fraction of platinum present in an alloy phase increased with an increase in the Sn:Pt atomic ratio. Complete alloy formation was only reported to have taken place at Sn:Pt ratios >5.

Extended x-ray absorption fine structure (EXAFS) and x-ray absorption near-edge structure (XANES) have been used not only to establish the presence of an alloy but also to gain information on their structure (93). Meitzner *et al.* (94-96)

using EXAFS reported that there was a significant difference in the platinum and tin components depending upon the support used. For a Pt-Sn/Al_2O_3 catalyst, it was reported that tin was not present as Sn^{IV} but largely as Sn^{II}. They also noted that there was a significant interaction between platinum and tin components as platinum is more highly dispersed on alumina when tin was present. Therefore these workers postulated that the alumina surface consisted essentially of platinum clusters dispersed upon alumina which has Sn^{II} species bound to it. For a Pt-Sn/SiO_2 catalyst, EXAFS results led to a very different conclusion being reached. The majority of tin in the silica catalyst has an oxidation state of 0 and therefore the surface of the catalyst consisted predominately of bimetallic entities or alloy particles of platinum and tin.

These conclusions were essentially reiterated by Li *et al.* (90) for a series of Pt-Sn catalysts. In general, it was found that by increasing the tin content on either alumina or silica, a corresponding decrease in the d band vacancy by tin was seen. This result is in stark contrast to the idea of a Pt-Sn alloy being formed where an increase in the d band vacancies is expected.

The ensemble effect is essentially a geometric effect in which tin atoms divide up the platinum surface into small ensembles or groups. These small ensembles are then unable to catalyse certain undesirable reactions like hydrogenolysis or the formation of carbonaceous residues (97). However (de)hydrogenation reactions can still take place at a single platinum atom.

Dautzenberg and co-workers (62) whilst investigating the reactions of n-butane over Pt-Sn/Al_2O_3 catalysts, prepared by sequential impregnation, explained the catalytic properties in terms of the formation of small ensembles of platinum. These authors found that upon alloying of platinum and tin all reactions at low temperatures (~300°C) were suppressed but a high temperatures ($\geq$ 500°C) isomerisation and methyl cyclopentane formation was suppressed whereas benzene formation remained constant. They hypothesised that the surface platinum atoms were diluted by tin and therefore the number of sites which contain three contiguous platinum atoms would significantly decrease. This hypothesis was strengthened by earlier studies by Sachtler and Van Santen (98) who reached virtually the same conclusions.

Further substantial evidence for an ensemble effect was presented by Coq and Figueras (99) whilst investigating the conversion of methyl cyclopentane on Pt-Sn/Al_2O_3 reforming catalysts. These authors believed tin diluted the large platinum ensembles into smaller groups of three or less platinum atoms as there was a decrease in hydrogenolysis and a stabilisation of the activity upon the addition of tin. Similar effects were also seen when sulphur or coke was deposited on the catalyst surface. It was this effect that led the authors to believe in the ensemble effect.

Coq and Figueras (99) noted that aromatic selectivity passes through a maximum and then decreases with increasing content. This trend was not reproducible by either coke deposition or sulphur poisoning and so the ensemble effect is no longer valid. The changes in selectivity were therefore attributed to the modification of the Pt-C bond by electron donation from the tin, i.e. an electronic effect takes place.

This idea of electron enrichment of the platinum atoms by tin weakening the Pt-C bond was first proposed by Burch and Garla (61). The weakening of this Pt-C bond is believed to be responsible for an increased resistance to coke poisoning. Tin existing as Sn^{II} species are also believed by these authors to poison the acidic cracking sites on the support and therefore explains the decrease in cracking reactions.

Several reports in the literature used CO adsorption to study the role of tin in a bimetallic Pt-Sn reforming catalyst. Palazov *et al.* (65) studied the CO adsorption on Pt-Sn catalysts at room temperature using infrared spectroscopy. They also found that by keeping the platinum content constant and increasing the tin content the peak at 2060 cm^{-1} moved to a lower frequency. This movement was attributed to an electronic effect between the platinum and tin components. The donation of electrons from tin to platinum would result in such a decrease in the CO vibration frequency. Balakrishnan and Schwank (100) applying a similar technique concluded by stating that if an electronic effect occurred between platinum and tin it was extremely small. They also postulated that Sn^{II} stabilised on alumina with platinum particles situated nearby could also produce a similar effect.

Many studies on the behaviour of Pt-Sn catalysts have been carried out using specific model reactions. Sanchez *et al.* (101), for example, examined the effect of tin addition to Pt/Al_2O_3 using ethylene hydrogenation as a probe reaction. These authors prepared two series of catalysts by sequential impregnation of alumina support by aqueous solutions of tin and platinum solutions. The platinum content

was kept constant at 0.5 wt% and the tin varied form 0 to 0.45 wt%. The presence of tin caused a decrease in ethylene hydrogenation for both series of catalysts. The hydrogen uptake decreased on catalysts which had platinum impregnated first onto the support and increased on catalysts which had been impregnated with tin first when the Sn/Pt ratio is increased. The authors attributed these findings to an electronic interaction between platinum and tin.

Studies of the reaction of neopentane over bimetallic catalysts by Balakrishnan and Schwank (100) led the authors to believe that the results of tin addition were more than a simple geometric effect. Catalysts were prepared with a constant 1.0 wt% loading of platinum and with a tin content varying from 0.1 to 5.0 wt%. It was observed that an initial loading of tin (~0.1 wt%) caused the neopentane isomerisation to increase. Further addition of tin (up to 5.0 wt%) resulted in a drastic fall in the catalyst activity. It was therefore concluded by these authors that there was an optimum level of tin content.

Davis (97) studying the effect of varying the pressure in the reaction of n-octane over various Pt-Sn catalysts found that tin led to an improvement in the stability of the catalyst by decreasing the coke deposition on the surface and by enhancing the aromatic selectivity at a given pressure. Davis in contemplation of the results postulated that electron transfer from tin to platinum is the most feasible option to produce these effects.

The main beneficial effect of a bimetallic Pt-Sn catalyst would therefore seem

to be due to an electronic interaction between the Sn^{II} species and Pt^0 particles dispersed on the catalyst surface. Pt-Sn alloy particles do not play a significant role in controlling the catalytic behaviour and as tin is always found to be present in very close proximity to platinum particles an interaction between the two is feasible. Further studies by Sexton *et al.* (72) and Adkins and Davis (81), both using XPS, led to the same conclusions. Adkins and Davis (81) went further and hypothesised that Sn^{II} was actually present as an egg-shell of tin aluminate surrounding the alumina support. This view was confirmed by Burch *et al.* (61) who discovered that tin in a Pt-Sn/Al_2O_3 catalyst was stabilised in the Sn^{II} state by an interaction with the alumina support. The tin was therefore seen to modify the electronic properties of the small platinum particles by electron donation.

1.4.4. Platinum-Germanium Catalysts

Extensive investigations have been carried out on many bimetallic systems, but the Pt-Ge system has been relatively forgotten. Although germanium is a group IVA metal like tin, the Pt-Ge system has not yet gained the same recognition as its counterpart.

Supported germanium catalysts containing 0.25 wt% Ge on γ-Al_2O_3 after being dried and calcined at 798°C were shown to reduce in a single peak at 600°C. The hydrogen consumed in the process was 40% less than that required for the complete reduction of Ge^{IV} to Ge^0 (102).

The temperature programmed reduction (TPR) profile of a calcined 0.375 wt%Pt-0.25wt%Ge/γ-Al_2O_3 catalyst showed two distinct peaks. The peak at 280°C corresponded to the reduction of the platinum component. The hydrogen consumption corresponds to a four electron reduction, i.e. $Pt^{IV} \rightarrow Pt^0$. Therefore platinum is completely reduced to the metallic state. The second peak at 600°C corresponds to the partial reduction of germanium. The hydrogen consumption, as in the monometallic germanium catalyst, was about 40% less than that required for the complete reduction of Ge^{IV}. Therefore some oxidised germanium remains in combination with the γ-Al_2O_3 support. From these results it was concluded that the interaction or alloying between platinum and germanium occurred during the reduction process of the pretreatment.

This idea of alloy formation is supported by hydrogen chemisorption measurements. The H/Pt ratio for a bimetallic Pt-Ge catalyst is equal to 1 if the reduction was carried out at 450°C. However this value progressively falls as the reduction temperature is raised into the region where the germanium component is reduced. These results imply that as germanium is reduced it is incorporated into the platinum surface, diluting it and causing chemisorption to fall as a result. Therefore part of the germanium component is completely reduced to Ge^0 with the remainder interacting with the support as a Ge^{IV} species.

Bouwman and Biloen (103) using XPS studied the bimetallic Pt-Ge/γ-Al_2O_3 system. These authors discovered that for a Pt-Ge bimetallic catalyst there was a substantial Ge 3d signal. However, with the corresponding monometallic germanium

catalyst only a very weak signal could be found. It was therefore postulated that this difference arose because of either excessive aggregation into large particles or a compound formation with γ-Al_2O_3.

XPS studies revealed that after reduction at 550°C germanium was present as $Ge^{IV}\backslash Ge^{II}$ species on the catalyst surface. Increasing the reduction temperature to 650°C resulted in an increased reduction of the germanium component and $Ge^{II}\backslash Ge^{0}$ species were found to be present. The Pt $4d_{5/2}$ photoline after pretreatment at 650°C in hydrogen lead the authors to postulate that the platinum was in an electron deficient state compared with the corresponding Pt/Al_2O_3 catalyst. This indicated that there was an alloy phase present as in the $PtGe_{0.72}$ alloy phase platinum is known to be electron deficient. The line positions of platinum in the bulk alloy and in the bimetallic catalyst are comparable. In addition the chemical shift observed between the calcined and reduced catalyst is similar to that for germanium in the bulk alloy under similar conditions. The chemical shifts observed were much larger than those for GeO_2 and germanium metal.

Bouwman and Biloen therefore concluded that platinum inhibited germanium becoming lost at high reduction temperatures and that it catalysed the reduction of germanium. The presence of germanium was noted to have several profound effects upon platinum, relatively more platinum is kept in exposed sites in a bimetallic Pt-Ge catalyst and the platinum was found to be more electron deficient than in a corresponding Pt/Al_2O_3 catalyst after reduction at 650°C. The formation of a Pt-Ge alloy phase was also considered to be highly probable.

Further studies into the behaviour of Pt-Ge catalysts was carried out by Goldwasser and co-workers (104). These authors using the hydrogenolysis of n-butane and the hydrogenation of benzene as test reactions investigated Pt-Ge\Al_2O_3-Cl catalysts. Catalysts were prepared using an impregnation technique and had a constant 1.0 wt% loading of platinum and a germanium loading of between 0 and 1.0 wt% loading. All catalysts were dried in air for 12 hours and then series A catalysts were calcined at 400°C and series B catalysts calcined at 600°C for 12 hours before the addition of platinum.

Results obtained in these studies indicated that the two series of catalysts behaved very differently. Catalysts in series A, when studied by TPR, gave results similar to those quoted previously. Again complete reduction of platinum of platinum was observed but once again only partial reduction of germanium was seen. Series A catalysts were further divided into two distinct subseries, the first from 0 to 0.3 wt%Ge (A1) and the second from 0.3 to 1.0 wt%Ge (A2). For subseries A1, germanium did not undergo any reduction and therefore remained as Ge^{IV}. For subseries A2, approximately 40 % of the amount needed for the complete reduction of Ge^{IV} to Ge^0 to take place, indicating an oxidation state of 2 for germanium after reduction. Therefore for subseries A2, the average oxidation state of germanium is independent of the %Ge on the catalyst. This result therefore makes an ensemble effect highly unlikely as the fraction of germanium reduced should depend upon the germanium content of the catalyst if a small amount of Ge^0 is formed.

Goldwasser *et al.* noted that there was a minimum amount of germanium at

which the reduction began to be observed and at which the activation energy for benzene hydrogenation increases. This increase in the activation energy, due to a drop in the specific activity, was related to an electronic interaction in the catalyst.

Experiments on the adsorption of CO, using IR, illustrated a shift to a higher frequency for the catalysts of subseries A2. These results are reinforced by early work on fluorided Pt-Ge/Al_2O_3 catalysts (105, 106) and the results were interpreted in terms of electron donation from the platinum to germanium. Therefore catalysts in the subseries A2 may be explained in terms of an electronic model, electron withdrawal from platinum by reduced germanium ions.

Results for series B catalysts suggest that after calcination at 600°C, germanium was stabilised by the alumina support. This stabilisation effect resulted in germanium not being reduced under these conditions. Again an ensemble effect can be ruled out on the basis of these results.

Work has been carried out on fluorided Pt-Ge catalysts by Romero *et al.* (105) who studied the hydrogenolysis of n-butane and the hydrogenation of benzene. They concluded that the presence of germanium in the catalyst considerably enhanced the selectivity to i-butane for the hydrogenolysis reaction, while the hydrogenation reaction went through a maximum at ~0.3 wt% Ge. Further work by these authors on Pt-Ge/Al_2O_3-F catalysts were carried out using infrared spectroscopy, electron microscopy and the measurement of model reactions. Results showed that there was a significant decrease in the CO stretching frequency when germanium was added

to the catalyst. Electron microscopy illustrated a bimodal distribution in the particle size for the bimetallic catalyst. Romero *et al.* (106) postulated that this decrease in the dispersion was due to a weaker exchange of the $PtCl_6^{2-}$ ions (metallic platinum precursors) with the presence of GeF_6^{2-} ions which compete for the same surface sites on alumina.

In a related study, Aboul-Gheit *et al.* (107) changed the halide ion to chlorine and looked at the effect of chlorine for hydroconversion processes. A 0.35wt%Pt-0.35wt%Ge/Al_2O_3 catalyst was prepared with a 3.87wt%Cl loading and one without this chlorine option was also prepared.

The combination of platinum and germanium in a catalyst resulted in a considerable suppression of the hydrogenation activity of platinum and germanium acted as a selective poison for the active hydrogenating sites of platinum in the catalysts. The addition of chlorine in the preparation of a Pt-Ge/Al_2O_3 catalyst also resulted in a similar reduction.

Catalytic behaviour of the Pt-Ge/Al_2O_3 bimetallic catalyst for n-heptane isomerisation and hydrocracking showed vast differences in activity when compared with that of benzene hydrogenation. The bimetallic catalyst displayed a lower isomerisation activity than the corresponding monometallic catalyst, especially at higher reaction temperatures, whereas its hydrocracking activity was enhanced. The addition of chlorine to a Pt-Ge/Al_2O_3 catalyst gave a considerably higher isomerisation activity compared with the chlorine free catalysts.

In a detailed study of sulphided and non-sulphided mono- and bimetallic catalysts systems by Parera *et al.* (108) several conclusions were drawn. The inclusion of germanium into a Pt/Al_2O_3 catalyst resulted in an increased yield of isomerisation products. Generally, when the n-paraffin chain length was increased aromatisation increased and hydrocracking decreased for all catalysts studied by these authors. This phenomena was explained in terms of thermodynamic and kinetic considerations by Parera *et al.* Hydrogenolysis and hydrocracking, not subjected to thermodynamic limitations, did not follow these fluctuations but remained independent of the chain length.

The main difference discovered between a sulphided Pt-Re and a Pt-Ge catalyst was in the selectivity to aromatisation and isomerisation of n-paraffins. These reactions are considered to be highly dependant upon the acidic component of the catalyst. Therefore different bimetallic catalyst systems should result in different selectivities due to the different properties of the second metal.

In general the presence of germanium as the second metal leads to a low catalyst activity and selectivity for hydrocracking reactions producing a subsequent increase in isomerisation reactions.

1.4.5. Sulphided Catalysts

Although many authors have reached conclusions on the precise role of rhenium in a bimetallic catalyst, these conclusions are not directly comparable with an

industrial catalyst. The catalyst most used commercially in recent years contains three components in the metallic function; platinum, rhenium and sulphur. Almost all Pt-Re/Al_2O_3 industrial catalysts are presulphided or continually sulphided on stream to achieve a better performance.

Sulphur when present in sufficient quantities on the catalyst surface is a well known catalyst poison. Sulphur components readily react to bond to the metallic sites of a catalyst, e.g. platinum, iridium, rhenium etc, effectively blocking these sites. Therefore if sulphur is present in sufficient quantities (~ 100 ppm) it can cause the complete deactivation of a catalyst. Therefore catalyst feedstocks must be rigidly screened and purified to ensure that sulphur poisoning does not occur.

However, under controlled circumstances, presulphiding a reforming catalyst with a small amount of sulphur can result in a drastic increase in the selectivity to aromatic products and a decrease in the hydrogenolysis activity. Catalysts are sulphided by a variety of sulphur containing compounds. The most commonly used include H_2S, thiophene and DMDS (dimethyl disulphide) with CS_2, MeSH, Et_2SH, Me_2S and EtS being used on occasion. These sulphur based compounds all have unshared electron pairs which can lead to a very strong chemisorption on the metal surface. When subjected to reduction conditions the adsorption onto the surface is usually dissociative, leaving a reduced sulphur atom bonded to the metal surface (109).

One of the most commonly used methods of presulphiding a catalyst is by

exposure to a H_2S/H_2 feed mixture. For this reason, the adsorption of H_2S on supported catalysts has been thoroughly investigated by several authors (110-113). For a γ-alumina support doped with chlorine to enhance the acidity, it has been reported (110-112, 114) that the presence of chlorine inhibits the adsorption of H_2S onto the support sites. Although H_2S adsorption is wholly reversible at 500°C on pure alumina (110), on Pt/Al_2O_3, at the same temperature, only a fraction is rapidly desorbed in a hydrogen atmosphere (110, 111).

This result has led several authors to develop the idea of having two distinct kinds of sulphur adsorbed onto the catalyst, a reversible and an irreversible sulphur. These authors concluded that the irreversible form, which does not exist on pure alumina, would be bonded to the metal component of the catalyst. The quantity of irreversible sulphur present on the catalyst surface after 30 hours desorption at 500°C in hydrogen remains independent of the sulphiding conditions (115). The Pt/Al_2O_3 catalyst used in this study was found to have a sulphur coverage of ~0.4 sulphur atoms per accessible metal atom. This idea has been extended to incorporate other metals, in particular bimetallic catalysts (116). The irreversible sulphur (S_i) adsorbed on Pt, Pt-Ir and Pt-Re alumina supported catalysts was found to have an atomic ratio of irreversible sulphur to accessible metal sites equal to 0.5. But under these identical conditions the Pt-Re catalysts were found to be more deactivated (115).

However, recently the amount of irreversibly chemisorbed sulphur, as determined using labelled $H_2{}^{35}S$ for sulphiding purposes, was found to increase in the order $Pt/Al_2O_3 < Pt\text{-}Re/Al_2O_3 < Re/Al_2O_3$ by Ponitzsch *et al.* (117).

The stability of the irreversibly adsorbed sulphur to hydrogen treatment at high temperatures suggests that a strong metal to sulphur bond has been formed. In a bimetallic catalyst, the question of which metal will the adsorbed sulphur bond to has been the subject of much deliberation. In a Pt-Re catalyst, for example, sulphur has been shown to bind preferentially to the rhenium component over the platinum. The adsorption of sulphur on metallic catalysts depends ultimately on the electronic properties of the metals involved. Table 1.4.2 illustrates the electron affinity of selected elements.

The adsorption of an electron acceptor species like sulphur will therefore be enhanced on metals with a low electron affinity, e.g. Re (118). It has also been demonstrated (119) that for a series of metallic catalysts the 'irreversible sulphur' coverage increases from Au to Re when the electronic affinities decrease in the same sequence. Therefore as rhenium has a lower electron affinity than platinum (0.15 eV compared with 2.12 eV) the formation of a Re-S bond in preference to a Pt-S bond is expected. The Pt-S bond is essentially covalent (the two electron affinities are similar) whereas a Re-S bond is polarised (large difference in the electron affinities), where the sulphur is in an negative oxidation state.

This was confirmed by the work of Kelley *et al.* (55) using ion scattering spectroscopy (ISS). These authors discovered that sulphur adsorbed on an alumina supported Pt-Re catalyst is highly associated with rhenium.

Table 1.4.2. Electron Affinity Values of selected Elements

Element	Electron Affinity (eV)	Element	Electron Affinity (eV)
Pt	2.12	Sn	1.11
S	2.08	Ru	1.05
Ir	1.60	Pd	0.56
Re	0.15	Ge	1.23

The adsorption of a sulphur species onto the metal sites of a catalyst has shown to be extremely beneficial (109, 113, 117, 119, 120). The presulphiding of a reforming catalyst has been shown to have different effects on various reactions. A marked decrease in the hydrogenolysis reaction rate due to sulphur adsorption has been reported by numerous authors (113, 115, 121, 122). This advantageous suppression of the undesirable hydrogenolysis reaction is widely used commercially in many industrial processes. The initially high hydrogenolysis activity of rhenium is strongly inhibited by sulphur and results in this sharp decline in gas production. Therefore sulphur may be regarded as being a selective poison in that when it is present in small concentrations the selectivity to desirable reactions, like aromatisation, increases and to undesirable reactions, like hydrogenolysis, is decreased.

1.5. CATALYST DEACTIVATION

1.5.1. Effect of Reaction Conditions on Coking

The rate and amount of coking is a very complicated process depending upon many individual factors. In particular the reaction conditions employed in the process highly influence coke formation.

The formation of coke is undoubtably influenced by the nature of the feedstock (60, 123-126). Since the origins of catalytic reforming it has been noted that certain feedstocks resulted in a higher level of coking. In particular Voge *et al.* (123) noted a direct relationship between the aromatic and polyaromatic content of the feed and the amount of coke deposited upon the catalyst surface. Since then a number of studies has led many authors (60, 124, 126) to believe that cyclopentane and its dehydrogenation products are particularly effective coke precursors.

Studying the reforming of various hydrocarbons at atmospheric pressure, Zhorov *et al.* (127) classed them according to their ability to cause carbon formation. Cyclohexane, used as a reference, is given a coefficient equal to one. The order found by Zhorov *et al.* was as follows:

cyclohexane (1) < benzene (3) < ethylbenzene (23) < n-hexane (35) < n-nonane (41) < methylcyclopentane (130) < indene (250) < cyclopentadiene (670)

Cooper and Trimm (126) confirmed this series at 10 atm. using hydrocarbons containing six carbon atoms. These authors found that the coking potential decreased in the following order:

methylcyclopentane > 3-methyl pentane > n-hexane > 2-methyl pentane > benzene > cyclohexane

The variation of temperature and pressure are well known to affect the degree of coking (126, 128-130). Reforming reactions are normally carried out at high temperatures (490 - 530°C) and at moderate pressures (10 - 30 atm.), conditions which favour the formation of both aromatics and coke formation. By increasing the reaction temperature (129) the formation of coke increased linearly with temperature. In the case of pressure, an increase resulted in a decline in the coke formation, however a critical level, below which coke formation is extremely rapid, has been identified (131). An increase in the pressure has been shown (7) to decrease the toxicity of the coke for the metal component. At higher pressures coke is deposited preferentially on the support than on the metal component.

The importance of the space velocity on the rate of coking was firmly established by Figoli *et al.* (130). For a fixed coking period and constant conditions, the amount of coke formed decreased with increasing space velocity. As was found in the case of pressure, a critical level for the space velocity was identified. The coking rate below this value was again found to be extremely severe.

An obvious but very important factor influencing the formation of coke is the choice of catalyst. Mono- and bimetallic catalysts are well known to produce different amounts and qualities of coke. Coke formed on monometallic catalysts is known to be more graphitic in nature than that formed on a bimetallic catalyst. Different bimetallic catalysts produce different amounts of coke (132, 133) deposited on the catalyst surface. Several studies (134, 135) have indicated that the metal loading and the subsequent size of the metal particles play a significant role in determining the degree of coking in a catalyst. Barbier *et al.* (134) noted that as the metal loading of a catalyst increased the amount of coke deposited on the catalyst also increased.

Various additives, like chlorine, sulphur etc. affect the rate of coking. The effects of these additives are discussed in further detail in Sections 1.5.3 and 1.5.6 respectively.

1.5.2. Effect of Bimetallic Catalyst on Coking

The addition of Re, Sn, Ir, Ge and S are all well known to increase the stability of the catalysts used in catalytic reforming. These additives are also known to influence the coking of the catalyst surface during a reaction. The addition of rhenium and iridium have been reported to diminish the coke deposits whereas germanium and tin have equivalent if not higher amounts of coke deposited on the catalyst surface than a monometallic Pt/Al_2O_3 catalyst (131-133).

Carter *et al.* (136) observed a decrease in the coke deposition when rhenium or iridium was added to a Pt/Al_2O_3 catalyst. These authors proposed that as rhenium and iridium are known hydrogenolysis catalysts, some of the coke precursors formed during a reaction will be removed by a hydrogenolysis reaction.

Alternatively, Parera *et al.* (130) proposed that the spillover of hydrogen onto the alumina support would lead to the removal of various coke precursors and deposits. The addition of rhenium and iridium (132, 137) has been noted to increase this rate of hydrogen migration, thus decreasing the amount of coke precursors and therefore coke deposited on the support surface.

The addition of rhenium decreases the dehydrogenation ability of platinum by increasing the surface hydrogen concentration on a platinum-rhenium catalyst (139). As has been discussed in detail in Section 1.5.5 the coking of a reforming catalyst is hypothesised to take place by a C_5 ring mechanism (138), involving the dehydrogenation and condensation of intermediate species. Suppression of the dehydrogenating ability of a catalyst would therefore result in a decrease in the formation of cyclopentadiene and other unsaturated C_5 ring compounds (139-141). This is turn would lead to a decrease in the amount of coke formed and deposited upon the catalyst surface (137, 140). This idea of rhenium suppressing the dehydrogenating capacity of platinum has been confirmed by the studies of many workers (109, 132). Parera *et al.* (108), for example, found that the amount of coke deposited upon the catalyst decreased in the sequence:

$$Pt > Pt\text{-}Ge > Pt\text{-}Re\text{-}S$$

Franck and Martino (142) found a similar phenomena in their study of platinum and platinum promoted catalysts. These authors found that the coke deposited on a catalyst declined in the following sequence:

$$Pt\text{-}Ge > Pt > Pt\text{-}Re > Pt\text{-}Ir$$

Once again the suppression of the dehydrogenating ability of platinum by the addition of a second metal was used to explain the difference in coking levels.

However, Bertolacini and Pellet (60) when studying a Pt/Al_2O_3 and $Pt\text{-}Re/Al_2O_3$ catalyst formed contrasting conclusions on the role of rhenium in a bimetallic catalyst. The platinum catalyst was found to deactivate more rapidly when a naphtha feed doped with either cyclopentane or naphthalene was used instead of a pure naphtha feed. But when these experiments were repeated using a bimetallic Pt-Re catalyst different results were obtained. Unlike monometallic platinum, platinum-rhenium catalysts were unaffected by the presence of cyclopentane in the feed. This suggested that the presence of rhenium inhibited coke formation via a cyclopentane route. However with a naphthalene doped feed the deactivation rate is rapid and rhenium does not inhibit the formation of coke. These authors postulated that rhenium therefore prevented cyclopentane dimerisation by enhancing the formation of paraffins via a ring opening mechanism therefore avoiding coke formation via cyclopentane species. Naphthalene if alternatively produced will proceed to coke despite the presence of rhenium in the catalyst.

The addition of rhenium is accompanied by an increase in the rate of hydrogenolysis (140). The addition of a small quantity of sulphur partially suppresses the hydrogenolytic capacity and increases the aromatic formation (140). Sulphur bonds preferentially to the rhenium in a bimetallic Pt-Re/Al_2O_3 catalyst and it is this Re-S species which divides up the large platinum ensembles and sterically hinders the graphitisation of the carbonaceous residues on the surface. Sulphur adsorbed on the metal sites results in carbon being quickly deposited on the support surface due to the hydrogenolysis sites being blocked by sulphur (118, 143).

Germanium and tin when added to a Pt/Al_2O_3 catalyst are thought to be inert and as a result dilute the large platinum ensembles. It is the dilution of these platinum ensembles which leads to the formation of an equivalent if not higher amount of coke on the catalyst surface. The formation of alloys and the stabilisation effects of alumina have been proposed to explain the differences in the catalyst activity and selectivity.

1.5.3. Chlorine Modification and its Effect on Coking

In reforming catalysis chlorine has been widely used to enhance the acidic sites of the alumina support (discussed in Section 1.3.1) which control the relative rates of hydrocracking and isomerisation. In addition, chlorine plays an important role in both the initial dispersion of the platinum and maintenance of its dispersion.

For monometallic Pt/Al_2O_3 catalysts it has been reported (144, 145) that there is

an optimum chlorine level of between 0.8 and 1.1 wt%. This level is in reality a compromise between the degree of isomerisation and hydrocracking. According to Parera *et al.* (131, 144, 145) the amount of coke produced on a reforming catalyst is at a minimum when the chlorine content is in the range 0.7 - 0.9 wt%. The low deactivation rate has been attributed to a maximum in the hydrogen spillover from the metal to the support surface. As a result, coke precursors, like unsaturated species, are hydrogenated to less harmful species (146).

The influence of the chlorine content on bimetallic catalysts is in many respects similar to that for a monometallic catalyst. Studies by Verderone *et al.* (144) illustrated that a bimetallic platinum-rhenium catalyst containing 0.8 - 1.0 wt% chlorine yields a good selectivity to aromatics and a low gas production, i.e. a good balance between the metal and acidic sites on the catalyst has been reached. However, increasing the chlorine content was not accompanied by an increase in coke deposition, but the corresponding drop in activity and selectivities was predicted. Bishara *et al.* (147) studying a Pt-Ir/Al_2O_3 catalyst reached very similar conclusions. These authors found that the deposition of coke was at a minimum when the catalyst contained between 0.9 and 1.1 wt% chlorine. The role of chlorine was hypothesised to increase hydrogen spillover as on a monometallic catalyst. This addition of chlorine in reasonable quantities therefore resulted in the enhancement of the reaction paths which do not lead to the formation of coke precursors.

1.5.4. Characterisation and Location of Coke Deposits

A range of techniques have been applied to the study of carbonaceous residues on the catalyst surface. Several techniques are very useful while others have a limited use.

The simplest and as a result one of the most widely used methods to characterise the coke deposits is temperature programmed oxidation (TPO) (7, 134, 148-151). TPO consists of raising the temperature in an oxygen atmosphere and analysing the combustion products from a spent catalyst to determine the H/C ratio and location of the coke on the catalyst. The thermograms generated generally show two distinct areas of coke combustion (7, 134, 151). The low temperature peak is due to coke deposited on the metal component and the peak at a higher temperature due to the coke deposited on the support.

Parera *et al.* (151) used an alumina catalyst doped with chlorine (acidic function) and a bifunctional Pt/Al_2O_3 catalyst (metal and acidic functions) to evaluate the influence of platinum on the combustion temperature of the coke deposited. The acidic catalyst, when subjected to TPO, produced a peak at 490°C and the Pt/Al_2O_3 catalyst two peaks at 280 and 490°C. Therefore the peak at 490°C was assigned to the coke deposited on the support and the peak at 280°C corresponds to the coke formed on the metallic component. Barbier *et al.* (134) found a similar result for the formation of coke on a Pt/Al_2O_3 catalyst. TPO experiments were extended to determine the location of the coking with time-on-stream by Querini *et al.* (152).

These authors found that coke was deposited mainly on the metal component initially and reached a steady level after a few days. The coke on the support (acidic component) in comparison increased throughout the time-on-stream (~210 days).

Further studies by both Parera and Barbier *et al.* (131, 137, 153) have confirmed that this is the case. The initial deposition is principally upon the metal component with further coking occurring on the alumina support (6).

TPO was also used to determine the H/C ratio of the deposited coke by measuring the oxygen consumed and the amount of CO_2 formed. Barbier (7) studying the coke formation on platinum black and on a chlorinated alumina catalyst found that coke formed on the metallic component was less dehydrogenated than that on the chlorinated alumina. Platinum black had a H/C ratio of 1.05 and chlorinated alumina a ratio of 0.5. This author also showed that as the reaction progressed the H/C ratio of the coke decreased, i.e. the hydrogen content declined. This phenomenon is widely accepted and has been termed ageing. One indirect method of characterising the coke deposits is by comparing the H/C ratios of known coke deposits with those of an unknown sample. Bolivar concluded that the coke deposited (H/C = 0.7 - 0.39) had a structure somewhere between that of polyaromatics and coals.

Raman spectroscopy being a very sensitive technique has been widely used to characterise the coke deposited on a catalyst surface (154-162). Natural, crystalline graphite displays two characteristic bands at 48 cm^{-1} and at ~ 1580 cm^{-1} (157, 161-

164). The first band is due to an interlayer and the second an intralayer vibrational mode. Pregraphitic carbon, on the other hand, shows an additional band at ~ 1360 cm^{-1}. The ratio of the intensities of the bands at 1360 and 1580 cm^{-1}, I_{1360}/I_{1580}, has been correlated to the size of the graphitic crystallites (159). When the structure of graphite becomes disordered, e.g. upon heating, the characteristic band at 1580 cm^{-1} broadens and two bands at ~ 1600 and ~ 1360 cm^{-1} appear (155, 160). The existence of the band at ~ 1360 cm^{-1} has been hypothesised to be due to:

1) Pregraphitic species or

2) The coexistence of a crystalline graphitic carbon and an amorphous carbon on the catalyst surface.

Weaker bands at 2700 and 2735 cm^{-1} have been discovered and assigned to highly organised carbon species (154).

Espinat *et al.* (158) undertook an extensive study of mono- and bimetallic catalysts to elucidate the structure of deposited carbonaceous residues. These authors found that coke contents from 0.29 - 27.3 wt% could be readily studied by Raman spectroscopy. At low carbon coverages, coke was found to be partially present as a pregraphitic structure, i.e. not just as an adsorbed polyaromatic species. The coke was found to be highly aromatic and most likely consisted of a two dimensional structure (turbostratic coke).

Espinat and co-workers found that the coke structure was most influenced by the H/Hc ratio used in the feed and the nature of the metallic phase of the catalyst. When the H/Hc ratio decreased the spectra lines broadened indicating the formation

of a less organised structure, but the I_{1600} / I_{1380} ratio increased indicating a larger crystallite size. The addition of either rhenium or iridium to a Pt/Al_2O_3 catalyst partially removes the strong dehydrogenated coke precursors as with an increase in the H/Hc ratio.

A very detailed study was carried out by Posazhenikova *et al.* (165) to characterise the coke formed during the dehydrogenation of benzene over a chromia-alumina catalyst. These authors used a variety of characterisation techniques including XRD, TEM, DTA and DTG. From the results of these studies these authors found the existence of two distinct carbonaceous phases, a crystalline graphitic structure present as large crystals (140 - 250 Å in diameter) and an amorphous phase containing small areas of crystals of 12 - 14 Å in size. DTA and DTG analysis of this coke showed the existence of two separate thermal effects at 450 - 480°C and 680°C. The first was attributed to the amorphous phase and the latter to the crystalline phase.

An x-ray diffraction pattern for a coked catalyst shows the presence of crystalline three-dimensional aggregates. However the extraction of these coke deposits, after having dissolved the alumina support with a suitable acid, e.g. HF, allows a more sensitive analysis of the extractable deposits to take place. XRD studies carried out by Barbier (7) illustrated that coke deposits were composed of pseudographitic phases with crystallographic characteristics similar to those of pure graphite. The coke deposits consisted of poorly organised arrays separated by 3.45 Å. This separation is higher than the value for pure graphite (3.35 Å) due to the presence of

C_5 rings or alkylic chains joined to the rings.

Studies by Espinat *et al.* (166) using XRD obtained an intense diffraction band (002) corresponding to the stacking of the graphitic layers. These authors measured the distance between these sheets to be 3.5 Å and calculated the regions to be close to 30 Å in size, corresponding to about ten superimposed sheets. The authors noted that it was possible to distinguish other lines on an expanded scale. The diffraction pattern obtained for the coke on the catalyst surface was found to be similar in nature to that of pure graphite.

Characterisation of coke deposits has been carried out by infrared spectroscopy by many authors (162-171). Eberly et al (167) used IR to study coking by paraffin and olefin cracking over silica-alumina catalysts. The catalyst matrix was then dissolved in KOH and the coke deposits were recovered for IR analysis. The spectra of the extracted coke deposits showed three absorption bands; the band at 3050 cm^{-1} corresponds to aromatic CH stretching, the band at 2930 - 2860 cm^{-1} to aromatic methylene and the band at 1590 - 1580 cm^{-1} to aromatic species. These authors also hypothesised that the ratio between absorbances at 3050 and 2930 - 2860 cm^{-1} was indicative of the coke aromaticity.

Subsequent studies (109, 169-171) with FTIR spectroscopy have shown the further characterisation of coke deposits. The spectra showed four absorption bands at 1420 - 1470, 2860 - 2890, 2930 - 2940, and 2960 - 2980 cm^{-1} corresponding to the CH stretching in CH_2 and CH_3 bonds. Two absorption bands at 1490 and 1590

cm^{-1} are characteristic of aromatic rings and a band at 3020 cm^{-1} is characteristic of a C-H bond in unsaturated aromatic compounds.

Auger electron spectroscopy (AES) was used by Blakely and Somorjai (172) to investigate the nature of coke formed on a stepped platinum single crystal surface. The physical structure of the coke was shown to depend upon the time-on-stream and the hydrocarbon feed. However during the dehydrogenation of cyclohexane the carbonaceous overlayer, initially ordered, becomes progressively more disordered as the reaction proceeds. Simultaneously the product distribution changes from benzene to cyclohexane being the major product, i.e. the formation of a disordered overlayer poisons the formation of benzene. The reaction is stopped at the cyclohexane intermediate in the presence of a disordered overlayer. Somorjai et al (128) in a related study used AES in conjunction with hydrogen thermal desorption (HTD) this time to define the nature of the coke deposited on a variety of single crystal platinum faces. AES determined the surface carbon to surface platinum ratio whereas HTD gave a quantitative measure of the hydrogen present. The deposited disordered carbonaceous islands produced a H/C ratio of 1.0 to 1.6 for temperatures between 300 and 450°C respectively. These values agree with previous results reported earlier (109). Further study using AES in conjunction with CO chemisorption/desorption revealed that the structure of the coke deposit varied from a two-dimensional species at low reaction temperatures to a three-dimensional species at reaction temperatures > 300°C.

1.5.5. Coke Mechanisms

Over the years, since it was discovered that coke deposition occurred during a reaction many mechanisms (169, 173-175) have been postulated to explain this laydown of coke on the catalyst surface. All these mechanisms rely upon the formation of unsaturated hydrocarbon species by an initial dehydrogenation step. These species adsorbed onto the catalyst surface are then transformed into carbonaceous residues, or coke, by a series of polymerisation and condensation reactions.

Several mechanisms have since been proposed for the formation of coke on both the acidic and metallic sites. Trimm (176), for example, proposed that the production of coke on platinum sites takes place by a series of fragmentation and successive dehydrogenation reactions. This series of reactions leads to the formation of carbon atoms which can combine to form coke deposits as detailed below.

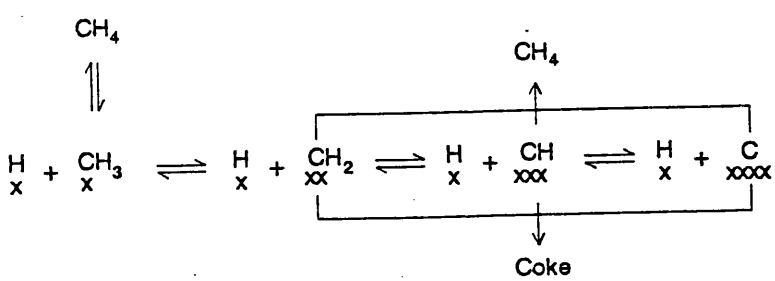

However, reaction with hydrogen can occur at any stage in this process and remove these intermediates before coking can occur.

Sárkany *et al.* (177) and Maire *et al.* (178) however proposed an alternative

mechanism for coke production on the metallic sites. These authors postulated that the formation of carbene species strongly influences the formation of coke as is shown below.

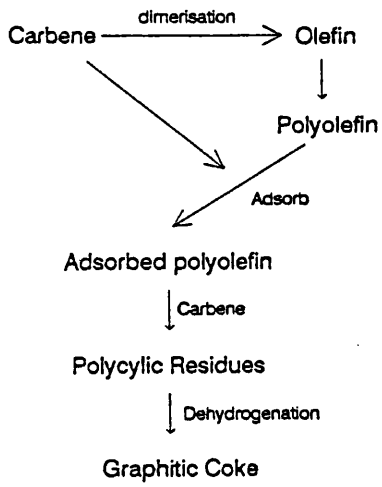

Both these mechanisms have been for coke formation on the metallic sites of a catalyst. However, on a chlorinated alumina support (acidic sites) coke can arise from the polymerisation of carbonium ions produced from olefins as detailed below.

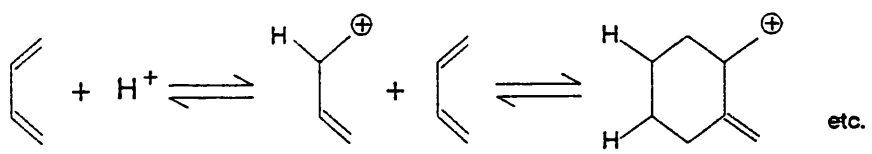

However, as has been frequently noted (109, 141, 179) coke formation increases in the presence of C_5 ring compounds, especially cyclopentadiene on Pt/Al_2O_3. Therefore it is widely accepted that unsaturated C_5 ring species are intermediates in the formation of coke. None of the previous mechanisms have taken this feature into account when trying to explain the formation of coke. Parera and co-workers (138)

noted that when they doped a naphtha feedstock with a C_5 ring species (saturated or unsaturated) an increase in the coke formation was seen. As a result of their extensive doping studies these authors proposed a coking mechanism which was centred on the C_5 ring species as shown below.

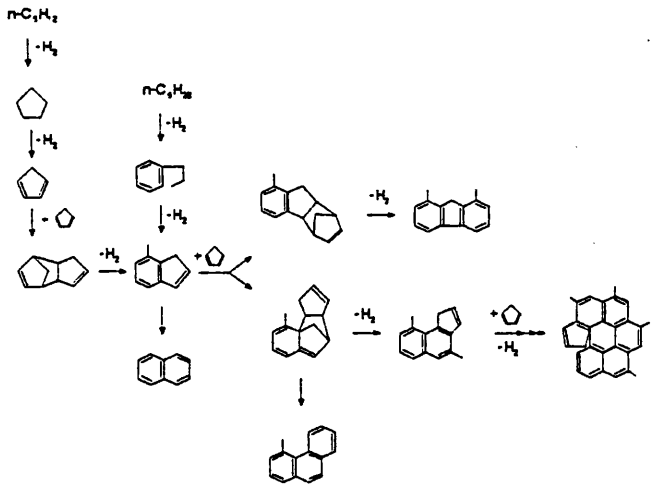

Cyclopentane is initially produced by the cyclisation of n-pentane and is then rapidly dehydrogenated to cyclopentene and cyclopentadiene due to the high dehydrogenation ability of platinum. By a diene-dienophile (Diels-Alder) condensation reaction two cyclopentadiene molecules react to form an indenic structure. This reaction is highly catalysed by the Lewis acid sites present on the catalyst support (169).

Condensation reactions end, when, due to rearrangements there are no terminal C_5 rings present in the species to react, e.g., as with naphthalene and fluorine. Condensation reactions take place either linearly or in a spiral manner as illustrated above. Species with a terminal C_5 ring species are not restricted to reacting with cyclopentadiene, olefins or conjugated olefins may also be used.

Parera and co-workers confirmed the presence of the intermediate coke species in this proposed mechanism by analysing the extracted coke deposits using GC-MS and H NMR. The authors in addition carried out experiments which confirmed their idea that a terminal C_5 ring was needed to carry on the condensation reaction. A later mechanism for the formation of polyaromatic coke species by Barbier (7) is similar to the first part of the mechanism proposed by Parera *et al.* (138).

Trimm (176) summarised the various routes to coke formation as shown below. Trimm proposed that there were three main processes to coke which are interconnected at various stages of the reaction. Gas phase reactions produce coke via a free radical mechanism and are therefore ultimately dependant upon the nature of the surface (180). Catalytic surfaces influence the nature of the coke intermediates and therefore the coke deposits themselves. Reactions to produce coke may also take place on a non-catalytic surface.

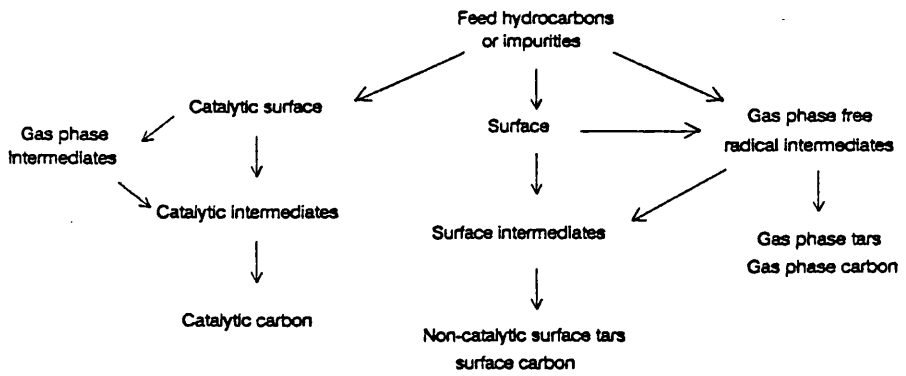

It can be seen that the mechanism of coke formation is far from straight forward. The formation of graphitic and polyaromatic coke species is complex but recent work would suggest that the most feasible route incorporates both the highly potent C_5 ring compounds and the metallic and acidic sites of a catalyst.

1.5.6. Effect of Carbonaceous Residues On Reforming Reactions

The deposition of coke upon the catalyst surface not only results in the deactivation of the catalyst but is very influential in determining the overall selectivity of the catalyst to various reactions. The selectivity of many reactions change with time-on-stream as a result of the increasing amount of coke deposited. The product selectivities generally settle down once the initial, rapid laydown of coke has finished.

Christoffel and Paál (181) noted that in the reaction of methylcyclopentane over a $Pt/\gamma\text{-}Al_2O_3\text{-}Cl$ catalyst, the formation of coke resulted in a decrease in the isomerisation and hydrogenolysis activity, but retains the (de)hydrogenation activity. These results suggest that the metal component is partially deactivated. Coke may be thought of as effectively diluting the large platinum ensembles on the catalyst surface. This results in less sites being available for more demanding reactions like hydrogenolysis but (de)hydrogenation reactions, taking place on one platinum atom, remain unaffected.

Davis *et al.* (128), using platinum single crystal surfaces for n-hexane conversion, have shown that coke formation on a catalyst is accompanied by a corresponding increase in the selectivity for aromatisation and hydrogenolysis relative to the isomerisation and C_5 cyclisation activity. It was found that on a coked catalyst the 2-methylpentane to 3-methylpentane ratio was lower than on a fresh catalyst.

Lankhorst *et al.* (135) studying the conversion of n-hexane on Pt/SiO_2 catalysts discovered that the major effect of coke deposition was to increase the selectivity to dehydrogenation relative to isomerisation products.

In direct contrast to these results, Beltramini and Trimm (182) studying n-hexane conversion over $Pt/\gamma\text{-}Al_2O_3\text{-}Cl$ catalysts, found that coke formation resulted in a significant increase in the isomerisation activity and a simultaneous decline in the dehydrocyclisation activity. A similar decrease in the dehydrocyclisation activity with increasing coke deposition was reported by Figoli *et al.* (6) when studying a $Pt/Al_2O_3\text{-}Cl$ catalyst.

The initial coke deposits may be considered to be desirable, in that they are formed on the most active catalytic sites, which if they are not deactivated, could produce an undesirable excess hydrocracking (36, 183). As a result, it is clear that some coking is desired but an excess should be avoided.

In conclusion, the metal component of the catalyst has coke deposited on the hydrogenolysis sites. This explains the initial rapid decrease in the formation of methane in most reforming catalysts. Coke deposited on the support is on the most acidic sites. Hydrocracking and isomerisation reactions decrease with time-on-stream as the quantity of coke deposited on the support increases. Therefore despite the poisoning effect, coke deposition on a catalyst surface has some beneficial effects in terms of influencing the catalytic behaviour of the catalyst.

Chapter 2

Objectives

2.1. OBJECTIVES OF THE PRESENT STUDY

The principal objective of this study was to gain a clearer understanding of the improved selectivity, activity and lifetime of a bimetallic catalyst in comparison with a monometallic catalyst.

The reactions of n-alkanes over Pt-X/Al_2O_3 catalysts (where X = Re, Sn or Ge) have been examined under typical reforming conditions (8-10 bar pressure and 470-510°C) using n-octane as a model feedstock. The objectives were to establish the influence of the second metal on the behaviour of the platinum components with respect to:

a) The deactivation phenomena.

b) The effects of surface residue formation on the catalyst selectivity for hydrogenolysis, dehydrocyclisation and cracking reactions.

The effect of presulphidation on the structure, deactivation and selectivity of the monometallic 0.3wt%Pt/Al_2O_3-Cl and bimetallic 0.3wt%Pt-0.3wt%Re/Al_2O_3-Cl catalysts were also investigated to obtain a more realistic view of catalyst behaviour under industrial conditions.

To investigate the changes in the structure of the metallic particles under the influence of the reaction conditions all catalysts used in this study were fully characterised by a variety of techniques, including CO chemisorption, dinitrogen

adsorption, mercury porosimetry, high resolution transmission electron microscopy (HRTEM) and energy dispersive x-ray (EDX) spectroscopy studies.

Chapter 3

Catalyst Preparation and Characterisation

3.1. CATALYST PREPARATION

A series of supported platinum catalysts (listed in Section 4.7) were investigated by numerous methods detailed throughout this work. Two of the catalysts studied, EUROPT-3 and -4, were commercially purchased and the remainder were prepared during the course of this study. All catalysts, with the exception of 0.3%Pt-0.3%Sn/Al_2O_3 (patent), were prepared using a commercial pelletised γ-alumina support (CK-300, Akzo Chemie Ketjen). This support was chosen as both EUROPT-3 and -4 are manufactured by Akzo using the same high purity γ-alumina support.

3.1.1. Commercial Catalysts

EUROPT-3 contains 0.3 wt% Pt and EUROPT-4 contains an additional 0.3 wt% loading of Re. Their exact physical characteristics and chemical compositions, as supplied by the manufacturer, are given in Table 3.1.1.

As illustrated in Table 3.1.1, both EUROPT-3 and -4 contain an optimum level of chlorine to enhance the acidic sites of the catalyst support. The γ-alumina support, EUROPT-3 and -4 were supplied as pellets about 4.2 mm in length and 1.7 mm in diameter. The remainder of the catalysts, listed in Section 4.7, were made in the laboratory in Glasgow by a standard wet-impregnation technique.

Table 3.1.1. Chemical and physical characteristics of EUROPT-3 and -4

	EUROPT-3	EUROPT-4
Surface Area (m^2g^{-1})	183	187
N_2 pore volume (ml g^{-1})	0.48	0.53
Pt (wt.%)	0.296	0.296
Re (wt.%)	-	0.311
Cl (wt.%)	1.00	0.95
Fe (wt.%)	0.02	0.02
S (ppm)	50	50

3.1.2. Pt-Re/Al_2O_3 Catalysts

Monometallic 0.3wt%Re/Al_2O_3, 3.0wt%Re/Al_2O_3 and bimetallic 3.0wt%Pt-3.0wt%Re/Al_2O_3 catalyst precursors were prepared by impregnation of γ-alumina with the appropriate concentrations of NH_4ReO_4 aqueous solution and H_2PtCl_6 aqueous solution to give the appropriate metal loadings. After impregnation the pellets were dried in flowing air at 110°C for four hours. The bimetallic catalyst precursor was obtained by impregnating γ-alumina with the appropriate concentrations of NH_4ReO_4 aqueous solution and then drying at 110°C in flowing air. This was then impregnated with the required concentration of H_2PtCl_6 aqueous solution and finally dried in air for a further four hours.

3.1.3. Pt-Sn/Al_2O_3 Catalysts

Supported bimetallic Pt-Sn catalysts were prepared with platinum and tin loadings varying from 0.3 wt% to 3.0 wt% with a constant molar ratio of Pt:Sn of 1:1. Again as described earlier commercial pelletised γ-alumina (CK-300) was used as a support, except in the case of the 0.3%Pt-0.3%Sn/Al_2O_3 (patent) catalyst.

For catalysts (a) and (b), refer to Table 3.1.2, γ-alumina pellets were impregnated with the required concentration of H_2PtCl_6 in dilute HCl and then dried in air at 110°C for four hours. This was then impregnated with an aqueous solution of $SnCl_2.2H_2O$ and dried once more in flowing air at 110°C for four hours. One very interesting and important feature of the second impregnation step was that the pellets changed from being colourless to a deep red colour. This change in colour has been previously reported by Bond and Hellier (184) and Davies *et al.* (185) and was attributed to the formation of the Pt-Sn complex $[Pt(SnCl_3)_2Cl_2]^{2-}$ ion.

Catalysts (c) and (d) were prepared in a similar manner to catalysts (a) and (b) except that the first impregnation step was carried out using $SnCl_2.2H_2O$ in dilute HCl followed by H_2PtCl_6 in the second step. There was no colour change in the pellets for the catalysts prepared by this method.

Catalyst (e) was prepared following a patented method (186). Briefly, this method involved the preparation of an alumina gel containing the appropriate quantities of aluminium powder, $SnCl_2.2H_2O$ and dilute HCl. This tin containing

alumina-gel was then condensed and aged in oil. After this it was impregnated with an aqueous solution of H_2PtCl_6 and finally dried and calcined in flowing air at 530°C for two hours. This catalyst was prepared in the form of granules of varying size. Therefore to produce a catalyst with a uniform size it was ground and sieved to a size of 425-850μm.

Catalyst (f) was prepared in exactly the same way as catalysts (c) and (d) except that a methanol solution was used in the place of the aqueous solution.

Catalyst (g) was prepared by coimpregnating γ-alumina with the appropriate quanties of $SnCl_2.2H_2O$ and H_2PtCl_6 in dilute HCl. During this process no colour change was observed on the support pellets.

Catalysts (h) and (i) was prepared by impregnating γ-alumina support with the appropriate quanties of $SnCl_2.2H_2O$ aqueous solution and then drying in flowing air at 110°C.

All the catalysts mentioned above (a → i) underwent a standard activation procedure before use in the microreactor, described in Section 4.8.

Table 3.1.2. Summary of the Platinum-Tin Catalysts Prepared

Catalyst	
(a)	0.3wt%Pt-0.3wt%Sn/γ-Al_2O_3 (Pt impreg. first)
(b)	3.0wt%Pt-3.0wt%Sn/γ-Al_2O_3 (Pt impreg. first)
(c)	0.3wt%Pt-0.3wt%Sn/γ-Al_2O_3 (Sn impreg. first)
(d)	1.0wt%Pt-1.0wt%Sn/γ-Al_2O_3 (Sn impreg. first)
(e)	0.3wt%Pt-0.3wt%Sn/γ-Al_2O_3 (Patent)
(f)	0.3wt%Pt-0.3wt%Sn/γ-Al_2O_3 (Methanol)
(g)	0.3wt%Pt-0.3wt%Sn/γ-Al_2O_3 (Coimpregnated)
(h)	0.3wt%Sn/γ-Al_2O_3
(i)	3.0wt%Sn/γ-Al_2O_3

3.1.4. Pt-Ge/Al_2O_3 Catalysts

Supported platinum-germanium catalysts were prepared with platinum and germanium loadings varying from 0.3 to 1.0 wt% with a constant Pt:Ge molar ratio of 1:1. All catalysts were prepared using the commercial pelletised γ-alumina (CK-300) as a support.

Catalysts (1) and (4) were prepared by impregnating γ-alumina with the required concentration of a germanium solution (Germanium ICP/DCP standard solution, Aldrich Chemical Company) in dilute HCl before being dried in air for four hours

at 110°C. This was then impregnated with H_2PtCl_6 in dilute HCl before being dried once again in air. The resultant catalyst precursors were a pale pink colour.

Catalyst (2) was prepared by impregnating an existing monometallic 0.3wt%Pt/Al_2O_3 catalyst (EUROPT-3) with a germanium solution in dilute HCl. This catalyst was then dried in air as before with the catalyst pellets remaining colourless.

Catalyst (3) was prepared by co-impregnating γ-alumina with the appropriate quantities of germanium and H_2PtCl_6 in dilute HCl. This catalyst was then dried in air at 110°C and the pellets were pale pink in colour as in the Ge impregnated first catalysts.

Catalyst (5) was prepared by impregnating the γ-alumina support with the appropriate quantities of a germanium solution before being dried in air at 110°C.

All catalysts underwent the standard activation procedure, detailed in Section 4.8, before use in n-octane reforming reactions.

Table 3.1.3. Summary of the Platinum-Germanium Catalysts Prepared

Catalyst	
1	0.3wt%Pt-0.3wt%Ge/γ-Al_2O_3 (Ge impreg. first)
2	0.3wt%Pt-0.3wt%Ge/γ-Al_2O_3 (Pt impreg. first)
3	0.3wt%Pt-0.3wt%Ge/γ-Al_2O_3 (Coimpregnated)
4	1.0wt%Pt-1.0wt%Ge/γ-Al_2O_3 (Ge impreg. first)
5	0.3wt%Ge/γ-Al_2O_3

3.2. CHARACTERISATION BY CHEMISORPTION STUDIES

3.2.1. Pulse Flow Carbon Monoxide Chemisorption Studies on Pt-Re/Al_2O_3

Carbon monoxide (CO) chemisorption was used to further characterise the catalysts used in this study. A chemisorption system similar to the one described by Jackson *et al.* (187) in an earlier publication. The calcined precursor was reduced by hydrogen *in situ* in this system. Approximately 0.5 g of a 0.3 wt% loading catalyst and 0.1 - 0.2 g of a higher loading catalyst was used in these experiments. The sample was ramped from ambient temperature to 400°C (or higher, see Table 3.2.1) in flowing hydrogen and held at this temperature for 2 hours (as in the standard pretreatment). Following reduction the catalyst was cooled to room temperature in a flow of helium. After flushing with helium, a known volume (4.70 cm^3, 16 mmHg) of CO (adsorbate gas) was injected into the carrier gas stream and therefore to the catalyst. The amount of CO gas passing over the catalyst was

accurately measured using a TCD in conjunction with a chart recorder. This was repeated until the adsorption peak stabilised indicating that adsorption had ended. The amount of CO adsorbed onto the catalyst was calculated from the difference in the peak areas obtained.

Assuming CO forms a linearly bound species (41, 187) with platinum, the total number of exposed platinum atoms and therefore the metal dispersion may be ascertained. Carbon monoxide is known to adsorb onto the platinum surface in two possible ways, a bridged and a linear species. In practice however, the latter is known to predominate (187). The maximum number of CO molecules that can adsorb per surface platinum atom has been extensively studied by several groups with some diversity in the results. The maximum number of CO molecules that care adsorbed per surface platinum atom has been reported to be 0.87±0.07 (188, 189), 0.77 (190), 0.76 (191) and 0.75 (192, 193). In these studies it was assumed that the platinum is well dispersed and therefore have taken the maximum value of CO/Pt surface molecules to be 0.76. The experimentally observed CO/Pt ratio of 0.5462 for EUROPT-4 will therefore give a platinum dispersion of 71.87%. One CO molecule adsorbed per Pt molecule can only be achieved experimentally with a very pure platinum foil in an ultrahigh vacuum at 270°C. The experimental CO/Pt ratio and the corrected platinum dispersion and results from the CO experiments are detailed in Table 3.2.1.

It has been well documented in the literature (41, 136, 194) that when rhenium is completely reduced to its metallic form CO can adsorb linearly to it. However in

Table 3.2.1. CO chemisorption results for Pt-Re/γ-Al_2O_3 Catalysts

	Reduction Temperature (°C)	CO Adsorbed (moles g^{-1} catalyst)	No. of CO molecules adsorbed (g^{-1} catalyst)	No. of Pt metal surface atoms (g^{-1} catalyst)	No. of bulk metal atoms (g^{-1} catalyst)	CO_{ads}/Pt_{exp}	CO_{ads}/Pt *(a)*
EUROPT-3	400	9.8×10^{-6}	5.90×10^{18}	5.90×10^{18}	9.26×10^{18}	0.6373	83.85
EUROPT-4	400	8.4×10^{-6}	5.06×10^{18}	5.06×10^{18}	9.26×10^{18}	0.5462	71.87
3.0wt%Pt-3.0wt %Re/Al_2O_3	400	2.2×10^{-5}	1.32×10^{19}	1.32×10^{19}	9.26×10^{19}	0.1431	18.82
3.0wt%Pt/Al_2O_3	400	2.15×10^{-5}	1.29×10^{19}	1.29×10^{19}	9.26×10^{19}	0.1398	18.40
3.0wt%Pt/Al_2O_3	680	4.2×10^{-5}	2.53×10^{19}	2.53×10^{19}	9.26×10^{19}	0.2731	35.94
0.3wt%Re/Al_2O_3	400	-	-	-	-	-	-
3.0wt%Re/Al_2O_3	400	-	-	-	-	-	-

(a) - assuming a surface stoichiometry of CO:Pt = 0.76:1

these experiments, no CO was found to adsorb onto the Re after reduction at 400°C and 680°C for the 3.0wt%Pt-3.0wt%Re/Al_2O_3 catalyst. This would suggest that the Re present in this catalyst is not in its metallic form. EDX spectroscopy was used to determine the state of Re in the bimetallic Pt-Re catalysts. A quantitative analysis of the results show that Re is actually present as a layer of ReO_2 in these catalysts and will therefore not adsorb any CO. As a direct result of these findings any CO adsorbed on the bimetallic Pt-Re catalysts must be adsorbed by the Pt.

Additional information may be drawn from CO chemisorption results as detailed in Table 3.2.2. The metal surface area (g^{-1} catalyst) is obtained by using the following expression:

$$S_c = n_{CO} N_A \sigma \qquad (3.1)$$

where

S_C = metal surface area (m^2g^{-1} catalyst).

n_{CO} = moles of CO adsorbed at STP (g^{-1} catalyst).

N_A = Avagadros number.

σ = Pt cross sectional area, $\sigma = 8.9Å^2$ for Pt (204, 205).

The metal surface area, S_M, per gram of platinum may be readily calculated by:

$$S_M = \frac{N_A \sigma R_{CO/Pt}}{M.W.} \qquad (3.2)$$

where

$R_{CO/Pt}$ = ratio of CO molecules adsorbed per Pt atom.

$M.W.$ = molecular weight of platinum.

Table 3.2.2. CO Chemisorption Results for Pt-Re/γ-Al_2O_3 Catalysts

	No. of Surface Atoms (g^{-1} catalyst)	Pt Surface Area (m^2g^{-1} catalyst)	Metal Surface Area (m^2g^{-1} catalyst)	Crystallite Face Diagonal (nm)	Reduction Temperature (°C)
EUROPT-3	5.90×10^{18}	0.5252	175.0806	1.8785	400
EUROPT-4	5.06×10^{18}	0.4502	150.0683	2.1916	400
3.0wt%Pt-3.0wt%Re/Al_2O_3	1.32×10^{19}	1.1791	39.3043	8.3677	400
3.0wt%Pt/Al_2O_3	1.29×10^{19}	1.1523	38.4105	8.5624	680
3.0wt%Pt/Al_2O_3	2.53×10^{19}	2.2510	75.0347	4.3831	400

Platinum crystallites may be regarded as being cubes which have one face in contact with the support and the other five faces are exposed to the adsorbing gas. However, electron microscopy studies have suggested that platinum crystallites are roughly spherical in shape, but the volume/surface ratio is constant for both spheres and for cubes (188). Therefore the metal area of a catalyst containing 1 gram of platinum is given by the following expression:

$$S_M = \frac{5000}{l\,\rho} \qquad (3.3)$$

where

l = the length of a cube length (in nm).

ρ = density of platinum (ρ = 21.5 g cm^3).

Therefore the length of a cube edge, l, of a platinum crystallite can be calculated using the value of S_M obtained in equation 2. The mean diameter (face diagonal) of the crystallite may be readily calculated using Pythagora's theorem as detailed below. The mean diameter, l_{diag}, is therefore calculated by

$$l_{diag} = 2\,(\,l_{edge}\,)^2 \qquad (3.4)$$

as the length of any cube edge is the same.

3.2.2. Chemisorption Studies On Pt-Sn/Al_2O_3 Catalysts

Metallic platinum adsorbs both CO and O_2 whereas metallic tin will only adsorb oxygen. Therefore oxygen chemisorption was used in conjunction with CO chemisorption to fully characterise the Pt-Sn/Al_2O_3 series of catalysts.

An O/Pt stoichiometry of unity has been reported (192, 193), but later studies reported a stoichiometry of 0.5 (187, 195). Under the experimental conditions used in these studies the ratio of chemisorbed oxygen to total platinum was found to be O/Pt = 1.0. However, the value obtained for oxygen chemisorption on EUROPT-3 is larger than expected when compared to the result obtained from CO chemisorption. The value for oxygen chemisorption suggests that all the platinum are surface atoms. One explanation for this observed difference is that platinum has retained some hydrogen which reacts with the oxygen to form water resulting in additional oxygen being consumed.

Both the 0.3wt% and the 3.0wt%Sn/Al_2O_3 catalysts did not adsorb oxygen at room temperature in close agreement with results reported by Lieske and Völter (69). This indicated that the tin was in an ionic state in the Sn/Al_2O_3 catalysts after reduction at 400°C. In contrast unsupported tin oxide is reduced to metallic tin at the same temperature (63). Therefore it is feasible that the tin oxide in these catalysts is stabilised by an interaction with the alumina support, possibly by the formation of a surface Sn^{II} alumina complex.

In a bimetallic Pt-Sn catalyst, if any metallic tin was formed the amount of oxygen adsorbed would increase when compared with the monometallic catalyst. This was found to be the case, as detailed in Table 3.2.3, for several bimetallic catalysts. The excess adsorption of oxygen allowed the amount of metallic tin in the catalysts to be estimated by making two important asumptions:

1) The ratios of adsorbed CO and O_2 to platinum were unchanged by tin

2) Tin adsorbs oxygen as SnO

The results indicated that approximately 15 to 30% of the tin was reduced to the metallic state after reduction at 400°C, the remainder being retained as an oxide. However, enrichment of the surface of a Pt-Sn alloy by tin has been reported (196,197) and may occur in these catalysts. This would lead to the amount of metallic tin in the catalyst being overestimated. However it would appear that only a minor part of tin was alloyed with platinum after reduction. The fraction of tin reduced to the metallic state increased when the dispersion of platinum increased in the catalysts.

3.2.3. Chemisorption Studies On Pt-Ge/Al_2O_3 Catalysts

The chemisorption results of these catalysts are outlined in Table 3.2.4. As with the Pt-Sn/Al_2O_3 catalysts, Section 3.2.2, a CO/Pt stoichiometry of 0.76 and an O/Pt stoichiometry of 1 are used (187, 192, 193, 198) and an O/Ge stoichiometry of 1 was used. Metallic germanium is known to adsorb oxygen (199) but in these studies a reduced 0.3wt%Ge/Al_2O_3 catalyst did not adsorb any oxygen at room temperature.

Table 3.2.3. CO and O_2 Chemisorption Results for EUROPT-3 and Pt-Sn/Al_2O_3 Catalysts

	Amount Adsorbed (moles g^{-1} catalyst) (x 10^{18})		No. of molecules adsorbed (g^{-1} catalyst) (x 10^{-6})		No. of Pt metal surface atoms (g^{-1} catalyst) (x 10^{18})		No. of bulk metal atoms (g^{-1} catalyst) (x 10^{18})		Dispersion (a) (%)	
	CO	O_2	CO	O_2	CO	O_2	CO	O_2	CO	O_2
EUROPT-3	5.90	4.63	9.80	7.69	5.90	9.26	9.26	9.26	83.85	100.00
0.3%Pt-0.3%Sn (Sn impreg. 1st)	4.07	5.69	6.76	9.45	4.07	11.38	9.26	9.26	57.83	122.88
0.3%Pt-0.3%Sn (Pt impreg. 1st)	3.80	4.49	6.31	7.46	3.80	8.98	9.26	9.26	53.99	96.97
0.3%Pt-0.3%Sn (Coimpreg.)	4.07	4.82	6.76	8.00	4.07	9.64	9.26	9.26	57.83	104.09
0.3%Pt-0.3%Sn (Patent)	4.35	5.69	7.22	9.45	4.35	11.38	9.26	9.26	61.81	122.88
0.3%Pt-0.3%Sn (Methanol)	3.33	4.12	5.53	6.84	3.33	8.24	9.26	9.26	47.31	88.98
1.0%Pt-1.0%Sn (Sn impreg. 1st)	13.27	17.43	22.04	28.94	13.27	34.86	30.87	30.87	56.56	112.93
3.0%Pt-3.0%Sn (Pt impreg. 1st)	9.30	18.10	15.44	30.06	9.30	36.20	92.61	92.61	13.21	39.09

(a) - Calculated assuming a surface stoichiometry of CO:Pt = 0.76:1, O:Pt = 1:1, O:Sn = 1:1

This suggests that germanium in the reduced 0.3wt%Ge/Al_2O_3 catalyst is in an ionic state in agreement with previous studies (104, 133).

If any metallic germanium was found on the bimetallic Pt-Ge catalysts during the activation pretreatment, more oxygen would be adsorbed than in the monometallic catalyst. This was found to be true for the reduced 0.3wt%Pt-0.3wt%Ge/Al_2O_3 (coimpregnated) and 1.0wt%Pt-1.0wt%Ge/Al_2O_3 catalysts as detailed in Table 3.2.4. The excess adsorption of oxygen was used to estimate the amount of metallic germanium in the bimetallic catalysts by making two general assumptions:

1) The ratios of adsorbed CO and O_2 to platinum were not changed by germanium
2) Germanium adsorbs oxygen as GeO

The results indicated that only approximately 5% of the germanium present in the catalyst was reduced to the metallic state in the two reduced catalysts.

3.3. PHYSICAL ADSORPTION OF GASES BY SOLIDS

The adsorption of a gas by a solid can, in principle, be used to determine the surface area and the pore structure of a variety of solid materials, such as industrial adsorbents, catalysts, ceramics and pigments. The measurement of adsorption at the gas/solid interface also forms an essential part of many fundamental investigations into the nature and behaviour of solid surfaces.

Table 3.2.4. CO and O_2 Chemisorption Results for EUROPT-3 and Pt-Ge/Al_2O_3 Catalysts

	Amount Adsorbed (moles g^{-1} catalyst) (x 10^{18})		No. of molecules adsorbed (g^{-1} catalyst) (x 10^{-6})		No. of Pt metal surface atoms (g^{-1} catalyst) (x 10^{18})		No. of bulk metal atoms (g^{-1} catalyst) (x 10^{18})		Dispersion (a) (%)	
	CO	O_2	CO	O_2	CO	O_2	CO	O_2	CO	O_2
EUROPT-3	5.90	4.63	9.80	7.69	5.90	9.26	9.26	9.26	83.85	100.00
0.3%Pt-0.3%Ge (Ge impreg. 1st)	4.15	2.64	6.89	4.38	4.15	5.28	9.26	9.26	58.97	57.02
0.3%Pt-0.3%Ge (Pt impreg. 1st)	3.31	1.95	5.50	3.24	3.31	3.90	9.26	9.26	47.03	42.12
0.3%Pt-0.3%Ge (Coimpreg.)	2.95	2.36	4.90	3.92	2.95	4.72	9.26	9.26	41.92	50.97
1.0%Pt-1.0%Ge (Ge impreg. 1st)	8.45	7.10	14.03	11.79	8.45	14.20	30.87	30.87	36.02	46.00
0.3%Ge/Al_2O_3	0	0	0	0						

(a) - Calculated assuming a surface stoichiometry of CO:Pt = 0.76:1, O:Pt = 1:1, O:Ge = 1:1

3.3.1. Surface Area Measurement by N_2 Adsorption

To accurately measure the total surface area of a solid a physical adsorption technique is required, but even with this the adsorption isotherm varies considerably with the nature of the solid (adsorbent). The majority of these isotherms, however, may be grouped into five classifications as illustrated in Figure 3.3.1a, as originally proposed by Brunauer, Deming, Deming and Teller (BDDT) (200). The classification of the different hysteresis loops is illustrated in Figure 3.3.1b.

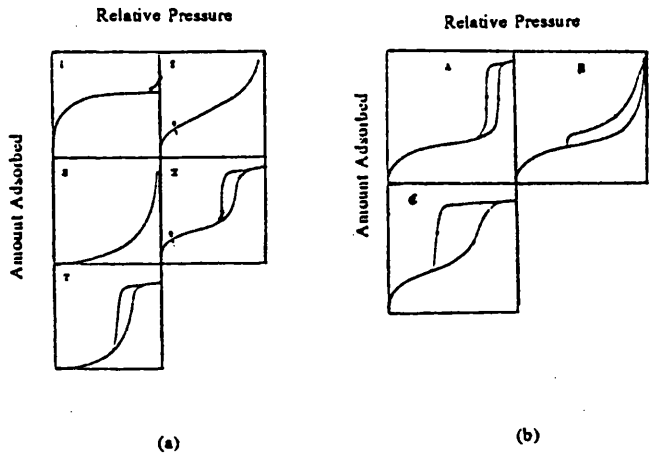

Figure 3.3.1. Clasification of the different adsorption isotherms and hysteresis loops.

In all cases as the partial pressure is increased the amount of vapour adsorbed increases becoming at some point equivalent to a monolayer. The monolayer coverage is then increased to a multilayer, which eventually merges into a condensed phase as P/P° approaches unity. At point B, shown in isotherms type II and IV, monolayer coverage is complete and therefore multilayer adsorption begins.

3.3.2. BET Theory

The Brunauer-Emmett-Teller (BET) gas adsorption theory (201) has become the most widely used standard procedure for the determination of the surface area of solids since its introduction in 1938.

The BET theory is largely based upon the kinetic model of the adsorption process developed by Langmuir. Langmuir postulated that the surface of a solid could be thought of as an array of adsorption sites. Therefore by introducing several fundamental assumptions Brunauer, Emmett and Teller were able to simplify and adapt the Langmuir mechanism to extend to multilayer adsorption on solid surfaces.

The BET theory is based on several assumptions:-

a) Adsorption in the first layer is assumed to take place on a surface of uniform site energy.

b) For the first layer, the rate of evaporation is equal to the rate of condensation and the heat of adsorption is independent of coverage.

c) For the second and subsequent layers, the rate of adsorption is proportional to the fraction of the lowest layer still vacant. The rate of desorption is proportional to the amount present in that layer.

d) The heat of adsorption for all types except the first layer is assumed to be equal to the heat of condensation of the adsorbed gas.

e) When $P = P^{\circ}$, there is an infinite number of layers.

Therefore summation of the amount adsorbed in all layers yields the following expression:

$$\frac{V}{V_m} = \frac{C\left(\frac{P}{P^o}\right)}{\left(1 - \frac{P}{P^o}\right)\left(1 + (C - 1)\frac{P}{P^o}\right)} \qquad (3.5)$$

where

V = volume of gas adsorbed at pressure P.

V_m = volume of gas adsorbed in a monolayer.

P^o = saturation vapour pressure.

C = constant, related exponentially to the heats of adsorption and condensation of the gas.

where

$$C = e^{\frac{(q_1 - q_c)}{RT}} \qquad (3.6)$$

where

q_1 = heat of adsorption on the first layer.

q_c = heat of condensation of the adsorbed gas on all other layers.

R = Gas constant.

The value of C ultimately decides the shape of the isotherm. As C increases, the curve in the region of point B becomes sharper. One advantage of having a

larger value of C is that the surface area may be determined more accurately. Equation 3.5 may be rearranged and expressed in the more familiar form:

$$\frac{P}{V\,(P - P^{o})} = \frac{1}{V_m\,C} + \frac{(C - 1)}{V_m\,C}\,\frac{P}{P^{o}} \qquad (3.7)$$

A plot of P/ V(P° - P) against P/P° cedes a straight line of gradient (C - 1)/V_mC and intercept 1/V_mC. Solution of these two simultaneous equations gives the values of C and V_m. The BET equation will only apply however if P/P° lies between the values of 0.05 and 0.30, if P/P° is outside these values the linearity of the plot will not hold. BET plots derived from the corresponding isotherms for catalysts are shown in Figure 3.3.2.

The specific surface area of the catalyst may then be calculated from V_m as the average area occupied by an adsorbed molecule is known:

$$A_{sp} = \frac{n_{ads}\,A_m}{wt} \qquad (3.8)$$

where

n_{ads} = number of molecules of adsorbate in the monolayer.

A_m = cross sectional area of the adsorbate molecule.

wt = weight of the sample.

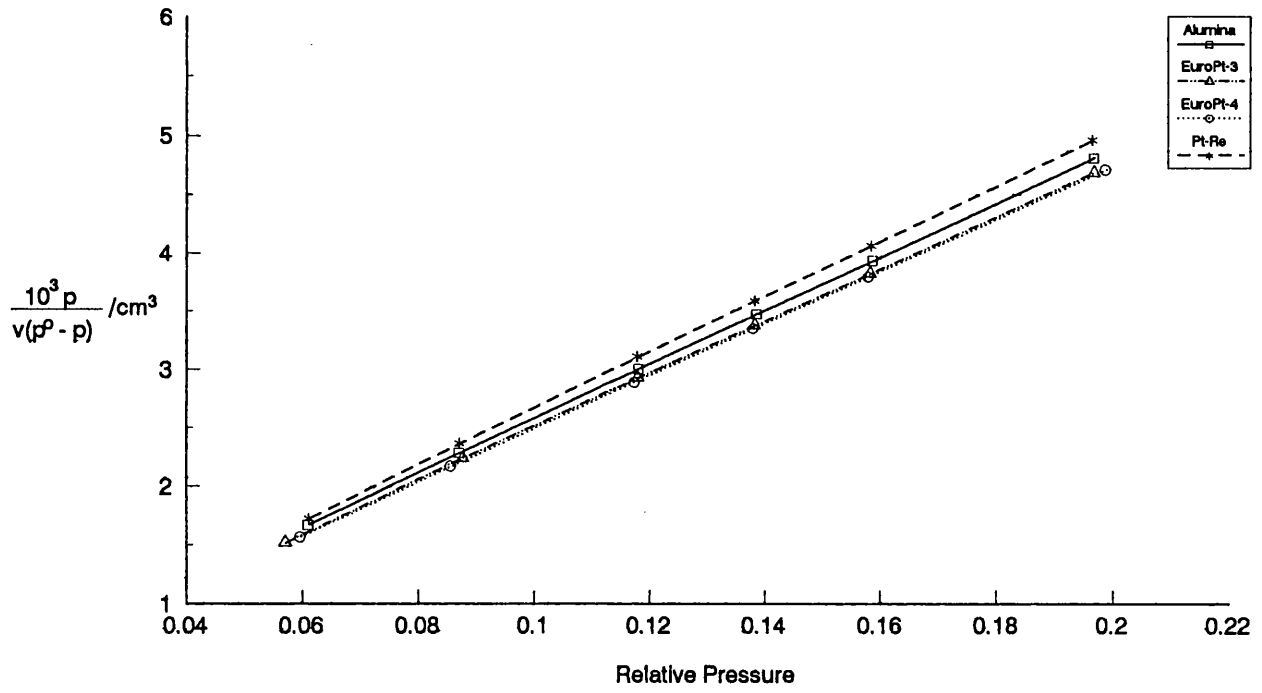

Figure 3.3.2. BET plot of catalysts calculated from N_2 adsorption studies

The cross sectional area of the adsorbed nitrogen molecule is calculated to be 0.162 nm^2 from measurements on adsorbents whose area can be directly obtained. It is assumed that for a given adsorbate and temperature that A_m remains constant and independent of the nature of the adsorbent. If the constant C is significantly large, e.g. greater than 50, the isotherm should have a well-defined point B and the intercept is relatively small compared to the slope.

3.3.3. Determination of the Pore Structure

The possibility of determining the pore size distribution of a porous solid from the hysteresis loop of a type IV isotherm has long been recognised.

The initial section of a type IV isotherm adsorption is restricted to a thin layer on the walls of the pores, until at the inception of the hysteresis loop capillary condensation begins at the smallest pores. As the pressure is progressively increased, larger pores are filled until at the saturation pressure the entire system is full of condensate. In most cases the desorption branch of an isotherm is used to relate the amount of adsorbate lost in a desorption step to the average size of the pore emptied in that step. A pore will lose its condensed liquid adsorbate, otherwise known as the core or capillary of the pore, at a particular relative pressure related to the core radius by the Kelvin equation. The mesopore size can therefore be calculated by utilising the Kelvin equation as shown:

$$\frac{1}{r_1} + \frac{1}{r_2} = -\frac{R\,T}{\gamma V_L} \ln \frac{P}{P^o} \qquad (3.9)$$

where

P/P^o = relative pressure at which condensation takes place

r_k = radius of curvature for a meniscus associated with a cylindrical pore.

V_L = molar volume of condensed liquid.

γ = surface tension.

If $r_1 = r_2 = r_k$, replacing $1/r_1 + 1/r_2$ by $1/r_k$ gives

$$\frac{2}{r_k} = -\frac{R\,T}{\gamma V_L} \ln \frac{P}{P^o} \qquad (3.10)$$

Then multiplying both sides of the equation by $-\gamma V_L/RT$ and rearranging gives the following expression:

$$\ln \frac{P}{P^o} = -\frac{2\gamma V_L}{r_k\,R\,T} \qquad (3.11)$$

Once the core of the pore has evaporated in the desorption step, a layer of adsorbate remains on the pore walls. The thickness of this layer is therefore calculated for a particular relative pressure by the Halsey equation:

$$t_i = m\left[\frac{n}{\ln(\frac{P}{P^o})}\right]^x \qquad (3.12)$$

where

t_i = adsorbed layer thickness.

m = monolayer thickness.

n = Halsey equation numerator.

x = Halsey exponent.

The thickness, t_i, of the adsorbed layer decreases with each progressive pressure drop. Therefore the measured volume of gas desorbed in one step is composed of the volume of the cores evaporated in that step and the volume desorbed from the walls of pores whose cores have already been evaporated in previous steps. It is the composite nature of the amount given up at each stage, which complicates the pore size distribution calculation. These ideas have been incorporated into a method proposed by Barret, Joyner and Halendo (BJH method) (202).

A method to calculate the pore volume and pore area distributions based upon the BJH expression, is used in the Digisorb instrument. In these calculations several assumptions were made: a) the surface of the solid is clean and uniform; b) the pores are straight, cylindrical and non intersecting; c) the volume of gas adsorbed external to the pores is negligible. The pore area distributions determined for catalysts are illustrated in Figures 3.3.3 to 3.3.14. The results from the nitrogen adsorption studies are summarised in Table 3.3.1. The adsorption/desorption isotherms determined for the four catalyst samples all displayed characteristic features of a type IV isotherm, with hysteresis loop type H1.

Table 3.3.1. Summary of the N_2 adsorption data

Sample	BET Surface Area ($m^2 g^{-1}$)	Cumulative Pore Volume (cc/g)	Mean Pore Diameter (Å)	Median Pore Diameter (Å)
γ-Al_2O_3 *	188.1546	0.5161	138.7394	88.74
EUROPT-3	190.2074	0.4784	138.7308	87.8
EUROPT-4	190.8198	0.4835	139.2577	88.7
3.0%Pt-0.3%Re/Al_2O_3 *	177.5434	0.4343	138.7792	88.7

* Values represent the mean of five separate experiments.

3.4. MERCURY POROSIMETRY

Compared with nitrogen capillary condensation, mercury porosimetry offers several advantages, including high speed analysis, a large measuring range and simple theoretical analysis of the results.

However, the method is destructive in the sense that in most cases not all the mercury can be recovered from the pore network of the sample. Therefore no repeat analysis of the sample is possible. Comparisons between the methods used in the measurement of pore distributions and investigations of capillary phenomena have been widely reported in the literature (2, 203, 208, 209).

Mercury porosimetry essentially consists of measuring the extent of mercury penetration into an evacuated solid as a function of the applied pressure. The

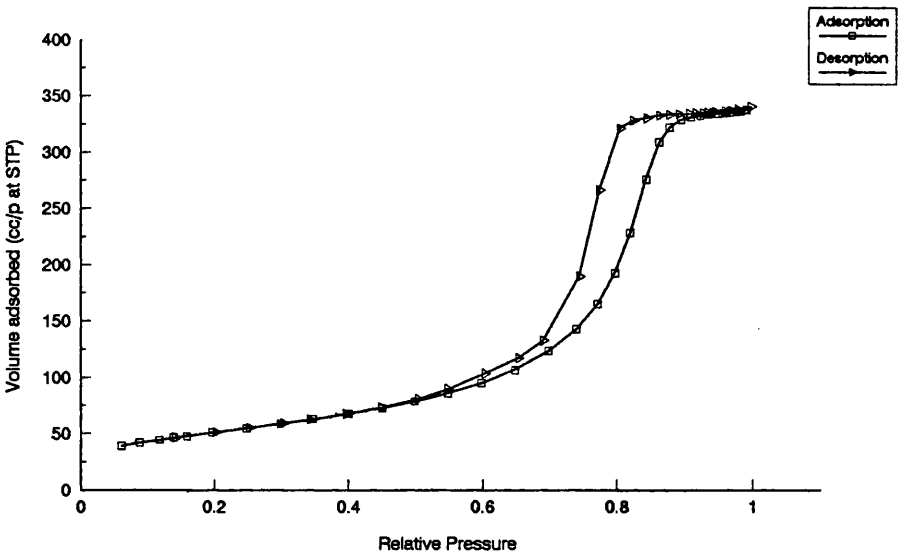

Figure 3.3.3. Typical isotherm for nitrogen physisorption on gamma-alumina

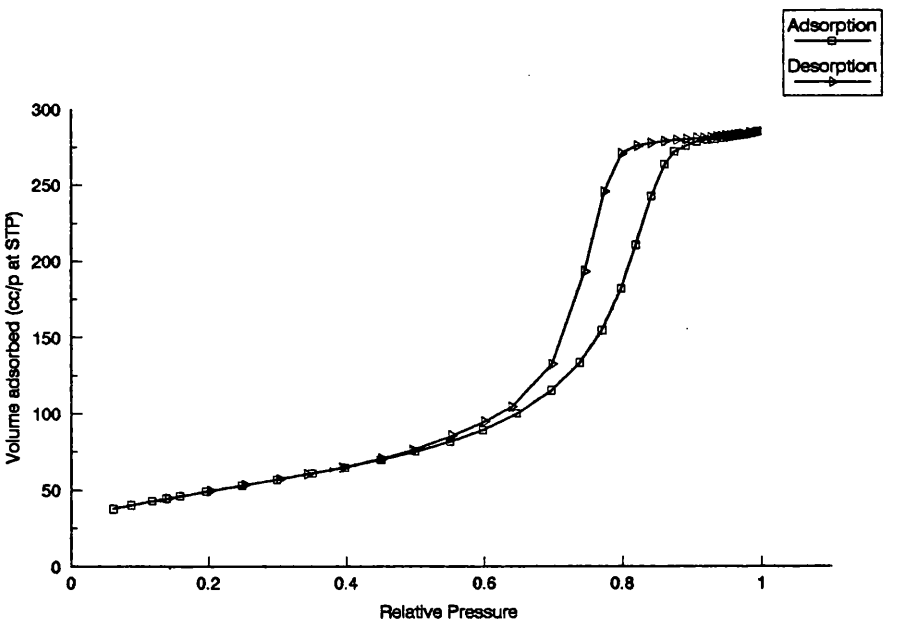

Figure 3.3.4. Typical isotherm for nitrogen physisorption on 3.0%Pt-3.0%Re/Alumina

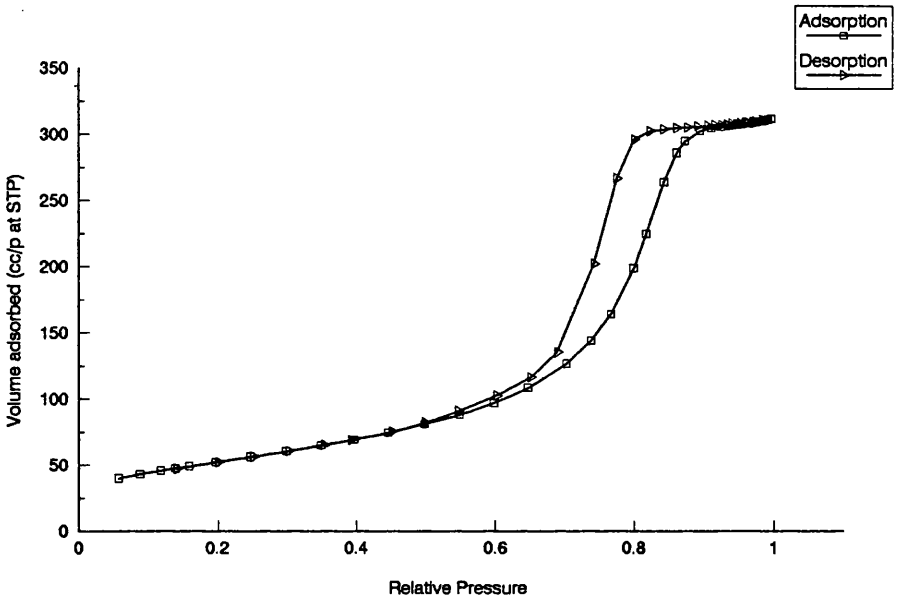

Figure 3.3.5. Typical isotherm for nitrogen physisorption on EUROPT-3

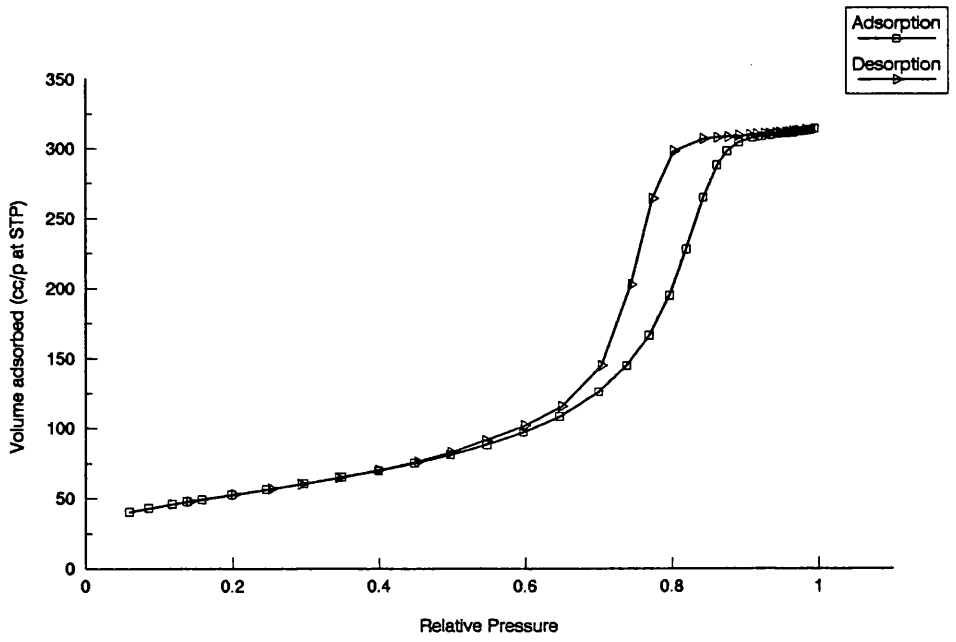

Figure 3.3.6. Typical isotherm for nitrogen physisorption on EUROPT-4

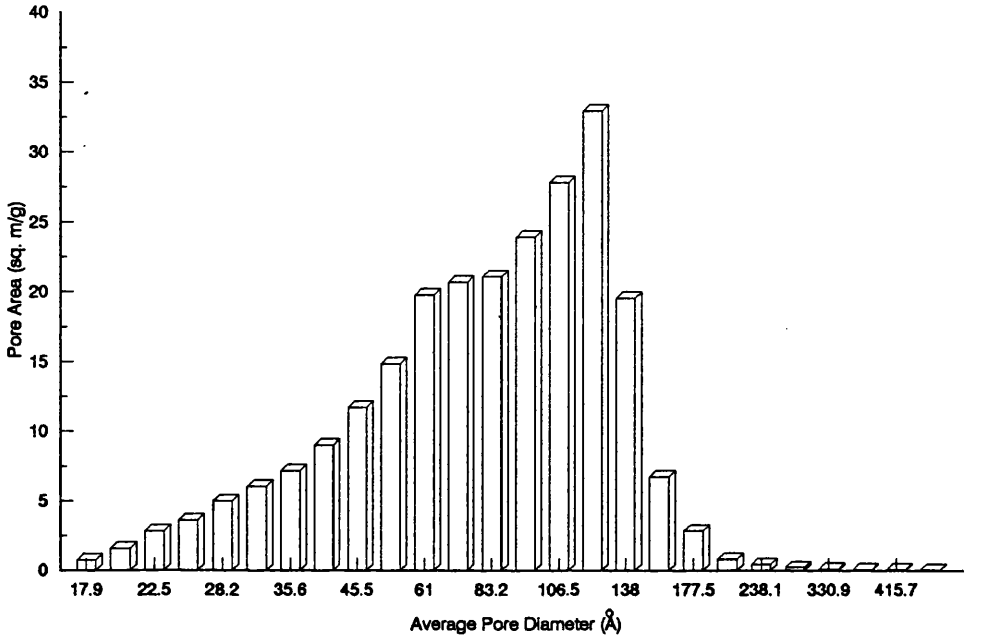

Figure 3.3.7. Pore Area distribution for gamma-alumina

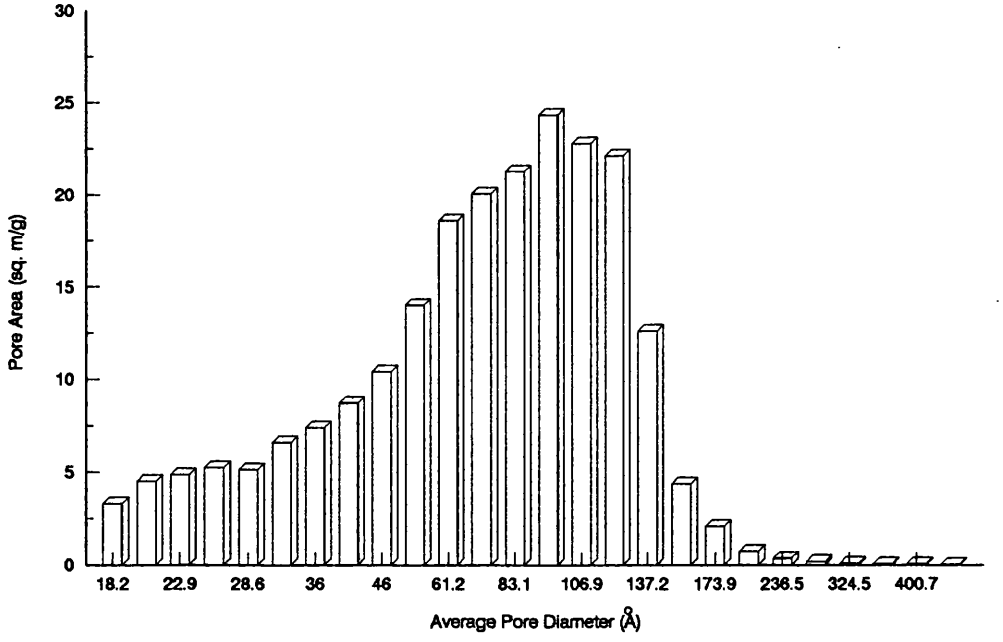

Figure 3.3.8. Pore Area distribution for 3.0%Pt-3.0%Re/Alumina

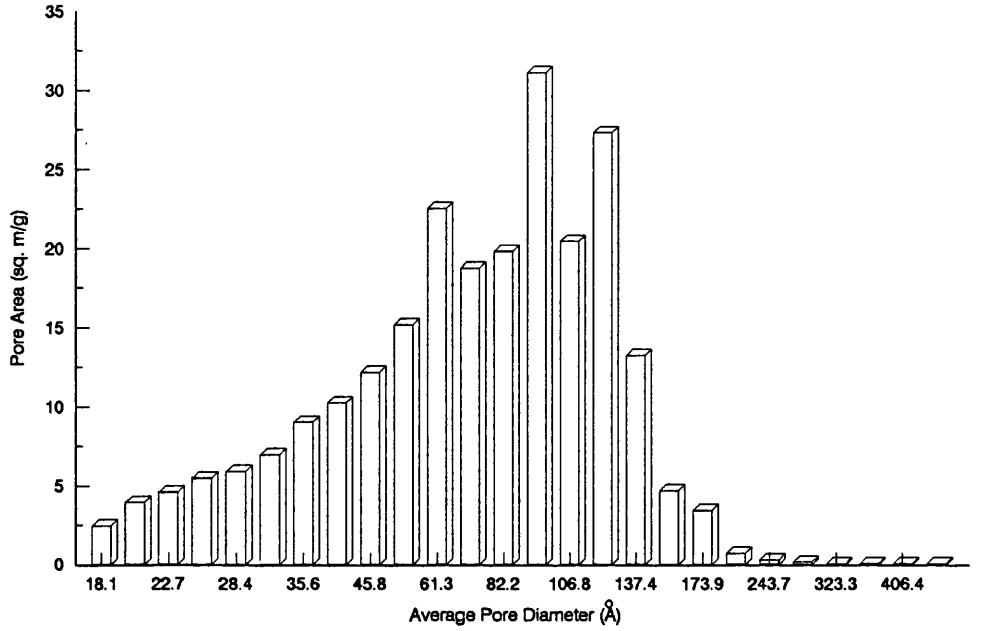

Figure 3.3.9. Pore Area distribution for EUROPT-3

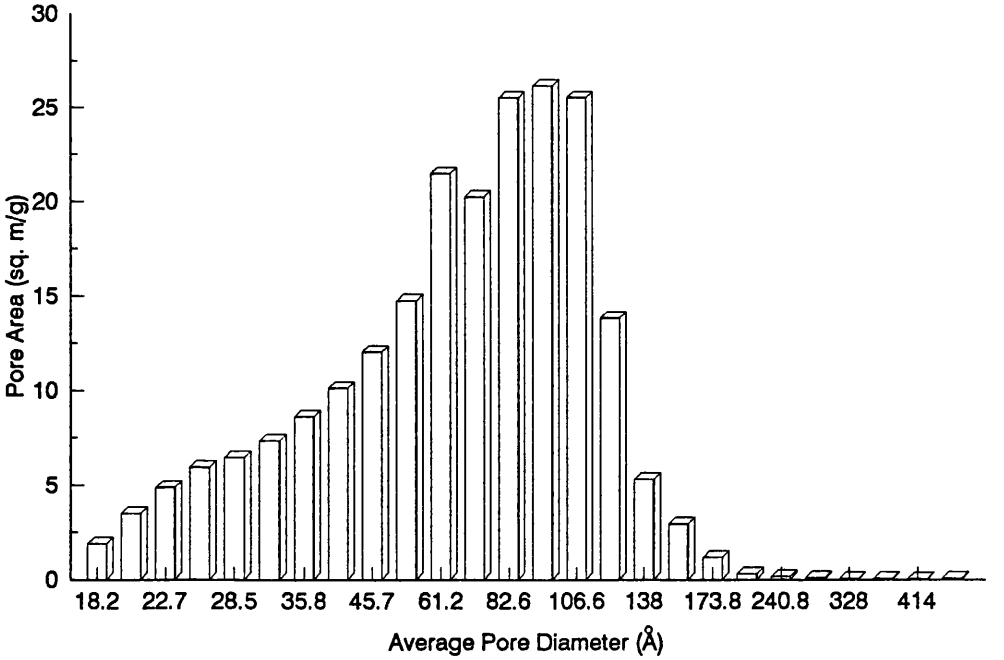

Figure 3.3.10. Pore Area distribution for EUROPT-4

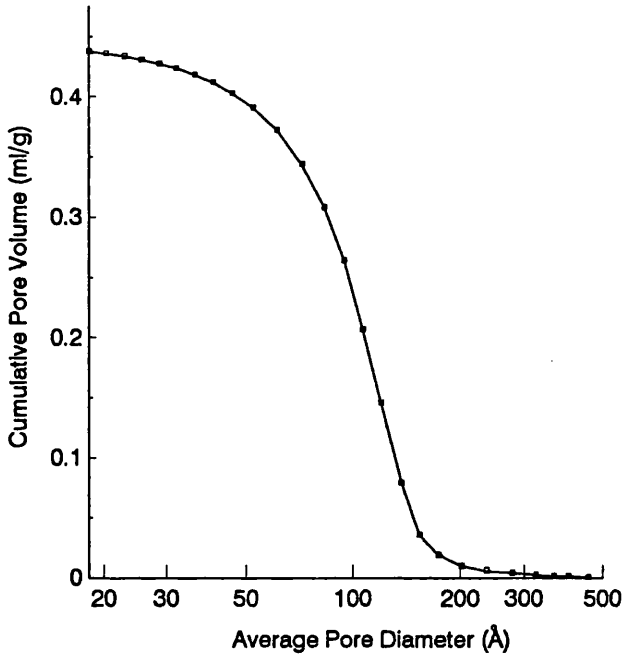

Figure 3.3.11. Pore distribution of 3.0%Pt-3.0%Re/Alumina

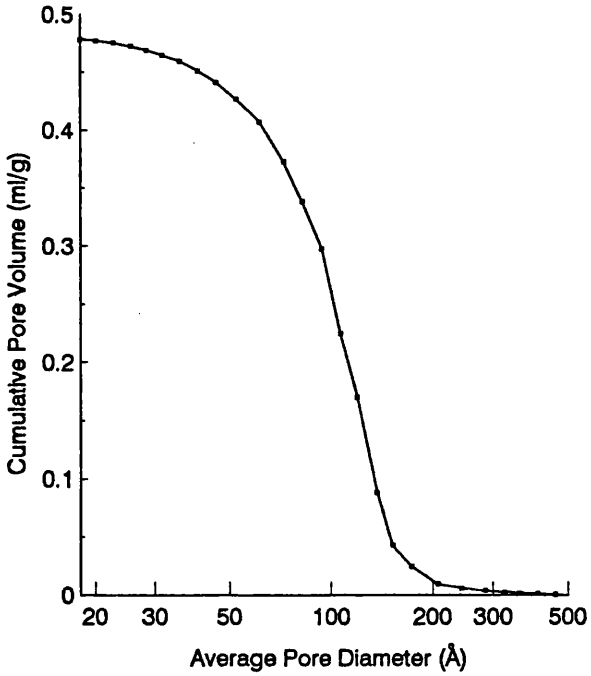

Figure 3.3.12. Pore distribution of EUROPT-3

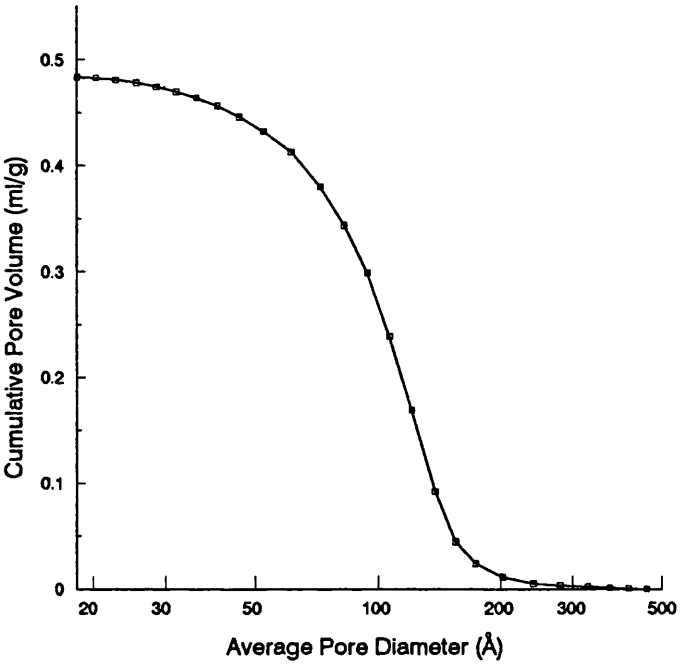

Figure 3.3.13. Pore distribution of EUROPT-4

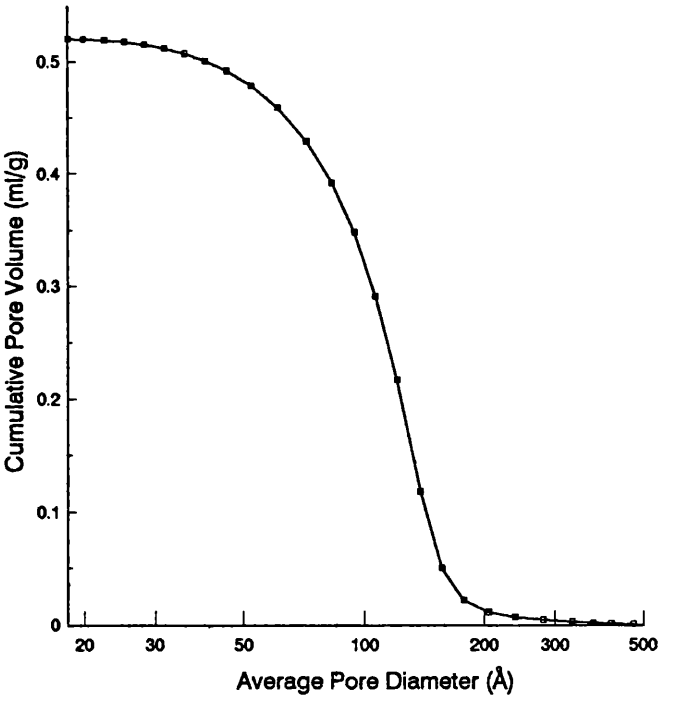

Figure 3.3.14. Pore distribution of gamma alumina

saturation intrusion volume of mercury is taken to be a measure of the total pore volume of the solid.

The experimental range of this technique ultimately depends upon the porosimeter available but generally will extend from ~10 nm (at a preesure of ~5000 atm) to ~ 7.5 μm (at atmospheric pressure). The upper limit may be extended to 10 μm by reducing the preesure applied to below atmospheric (203). Therefore the range of this technique overlaps with that of gas adsorption as the lower limit of mercury porosimetry is ~ 15 Å and the upper limit of gas adsorption is in the region of 100-200 Å. However, due to the dubiety of the results at the extreme limits of these two techniques there is in many cases a lack of compatability between the results obtained.

The contact angle, θ, of mercury while advancing over or receding from the solid surface is always greater than 90°. The contact angle is usually in the range 130°-150° (203, 206, 207). The most commonly used value being $\theta = 140°$, but this depends upon the purity and structure of the solid surface. As the contact angle of mercury is greater than 90° the mercury meniscus will be convex in shape.

3.4.1. Hysteresis

One feature common to both nitrogen capillary condensation and mercury porosimetry techniques is hysteresis. That is the curves of penetration and withdrawal of mercury, in this case, do not coincide. This is a very common feature of these

techniques. Several explanations have been postulated to explain this phenomena. One of the simplist and most widely held explanations of reproducible hysteresis in mercury porosimetry is based upon an 'ink bottle' model (210, 211). The pressure needed to force mercury into a pore with a narrow (cylindrical) neck of radius r_n, will be:

$$P_n = - \frac{2\gamma \ Cos \ \theta}{r_n} \qquad (3.13)$$

But mercury is then trapped in the pore, radius r_w, until the pressure has dropped to P_w, allowing the mercury to exit. This is expressed in equation:

$$P_w = - \frac{2\gamma \ Cos\theta}{r_w} \qquad (3.14)$$

Since by definition of the shape of an 'ink bottle' r_n will be less than r_w. Therefore the pressure P_n for intrusion will always be greater than that required for extrusion P_w, and as a result hysteresis is observed.

The 'ink bottle' explanation is regarded as being simplistic in that the majority of real solids the pores are interconnected. A more realistic model of a porous solid would therefore be a three-dimensional array of pores interconnected by narrow channels as shown in Figure 3.4.1.

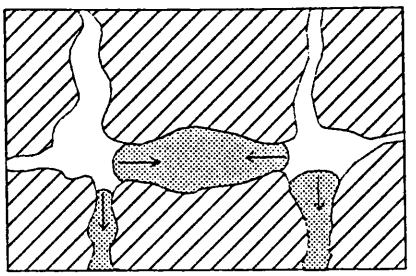

Figure 3.4.1. Representation of the Pore Network in a Porous Solid

Therefore penetration into a series of pores by mercury through one of these narrow channels will only take place at a higher intrusion pressure. The withdrawal of mercury will mainly be through a different set of pores, thus leaving behind small pockets of mercury entrapped in the channels. This entrapment of mercury is shown as the hysteresis loop does not close.

3.4.2. Pore Structure Determination

The calculation of pore radii from mercury porosimetry experiments is based upon the Washburn equation:

$$r_p = \frac{2\gamma \, Cos\theta}{\Delta P} \qquad (3.15)$$

where

r_p = radius of the pore, assumed to be cylindrical.

ΔP = applied pressure required to force mercury into the pores.

γ = surface tension of penetrating liquid (Hg has a value of 480 dynes cm^{-1}).

θ = contact angle of the penetrating and receding liquid (θ = 140° for Hg).

3.4.3. Surface Area Measurements by Mercury Porosimetry

The surface area of the porous solid may be determined from mercury porosimetry. The work, dw, needed to force a volume, dν, of mercury into the pores of a solid with respect to the work required to form an area, dA, of mercury solid interface may be calculated using the following equation:

$$dw = \gamma \, Cos \, \theta \, dA = -\rho dv \qquad (3.16)$$

Like the corresponding equation for nitrogen capillary condensation, equation is based upon the assumption that the pores are cylindrical. Integrating equation over the range of the mercury penetration curve gives an expression for the surface area, A, of all the pore walls penetrated by mercury:

$$A = -\frac{1}{\gamma \, Cos\theta} \int_{V_{min}}^{V_{max}} \rho dv \qquad (3.17)$$

3.5. CHARACTERISATION BY ELECTRON MICROSCOPY

3.5.1. HRTEM

High resolution transmission electron microscopy studies were carried out using an ABT-EM002B high resolution microscope into which an energy dispersive x-ray (EDX) LINK 200-QX system was installed with a windowless detector. Catalysts having undergone the standard pretreatment procedure (detailed previously in Section 4.8) and after use in the microreactor were investigated. The TEM samples were prepared by placing a drop of ethanol solution containing the ground catalyst powder in suspension on a carbon film coated copper grid. The alcohol evaporated leaving the particles finely distributed upon the grid. TEM specimens were prepared in a dry box under a nitrogen atmosphere to avoid contamination by air. The oxygen concentration in the dry-box was around 10 ppm.

When the carbonaceous residues present on spent catalyst samples were investigated a carbon free silica grid was used. This was to avoid complications arising from mistaking carbon on the specimen grid for carbon on the catalysts.

3.5.2. EDX

As described in the previous Section an EDX system with an improved LaB_6 filament was used to measure the spectra of reduced and spent catalyst samples. As the high resolution electron microscope is fitted with an EDX system, EDX spectra were collected on the catalyst samples once the TEM work was finished. This is

advantageous as the sample under investigation was not exposed to contamination by the air as measurements take place in the same chamber.

An electron beam of ~10 nm in diameter, which covered a particle, was used to generate an EDX spectrum. The collection time was usually 100 seconds. During the collection, the beam was sometimes spread (i.e. underfocussed and overfocussed) for a period of time to obtain an image of the particle. The beam was then relocated on the particle to compensate for any spectrum shift. In this way, a good platinum signal could be obtained for a 20Å platinum particle on a thin alumina support.

Quantitative EDX analysis was also carried out on the samples to ascertain the stoichiometry of the area studied. Along with micro-beam diffraction a very detailed picture of the area can be gained.

3.5.3. Micro-beam Diffraction

Micro-beam diffraction (MBD) patterns were obtained by illuminating an area of the spectrum using an electron beam ranging from 6 to 10 nm in diameter. The recorded diffraction patterns obtained are illustrated with the corresponding micrograph. The lattice spacings, d, of the sample may be easily determined by measurement of the distance between the unscatttered beam and the diffracted beam. From these spacings the diffraction pattern may be indexed to a known phase. This technique is especially useful in determining the various different alloy phases present in both the reduced and spent catalyst particles.

Chapter 4

Experimental

4.1. INTRODUCTION

In order to determine the activity, selectivity and stability of a range of mono- and bimetallic catalysts, a high pressure microreactor was designed and built in the initial stages of this project. This system was capable of operating at temperatures in excess of 600°C and pressures up to 200 psig. The microreactor was designed in such a way that allowed continuous flow experiments to be carried out. The system consisted of three main sections:-

1) The feed system.

2) The reactor system.

3) The analytical system.

4.2. THE FEED SYSTEM

The feed system was designed to allow a constant, regulated flow of n-octane and hydrogen to be delivered to the reactor. A schematic diagram of this section is shown in Figure 4.2.1.

4.2.1. n-Octane Feed System

The flow of liquid n-octane was delivered and regulated by means of a Labatron (LDP-20) precision metering pump. The Labatron pump was capable of working at backpressures of up to 50 atmospheres. The liquid n-octane was driven to the

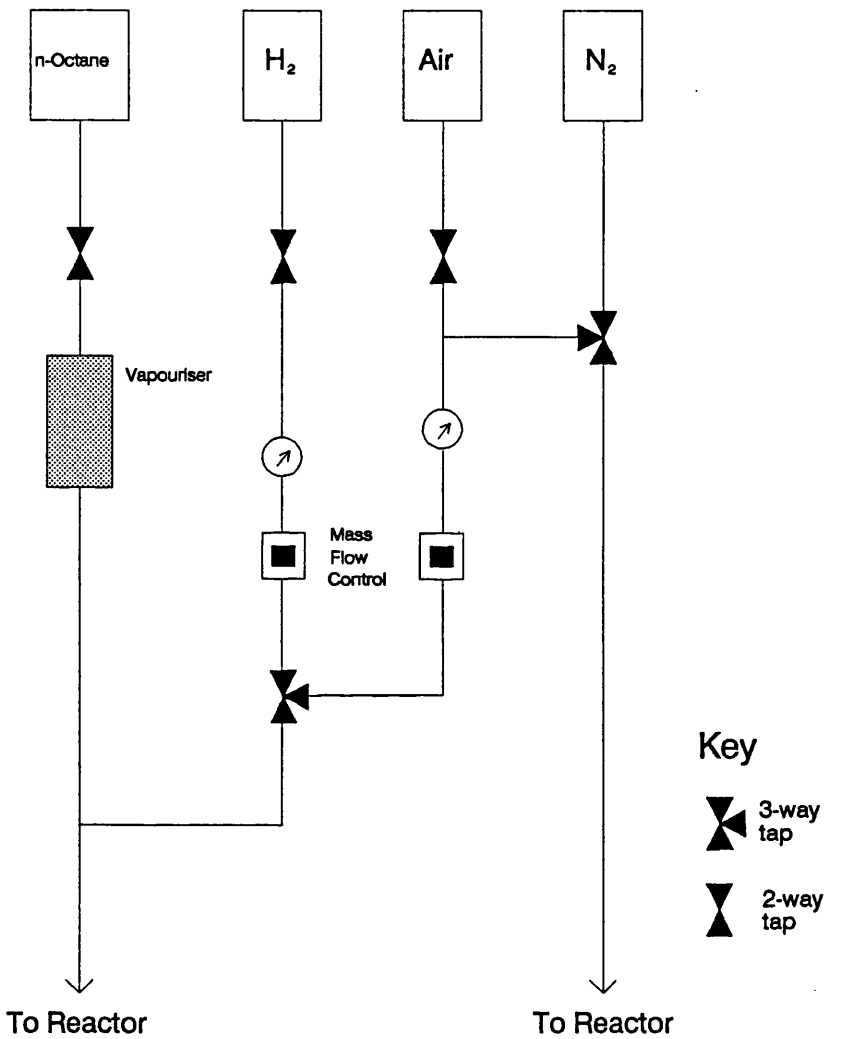

Figure 4.2.1. Schematic Diagram of the Reactor Feed System

vaporisation unit which was designed to discharge the liquid n-octane from the narrow bore tubing as a fine spray, see Figure 4.2.2, by the pump. The vaporisation unit was enclosed in a heated insulated box maintained at approximately 230°C. This is well in excess of the boiling point of n-octane (125 - 127°C), ensuring that the n-octane is instantly vaporised before it entered the reactor system of the microreactor. All tubing carrying gaseous n-octane from this unit was also maintained at a high temperature within the insulated box to ensure that no n-octane condensed out in the metal tubing, thus disrupting the flow to the reactor. The n-octane flow rate was accurately measured by the calibrated potentiometer on the Labatron pump.

4.2.2. Dihydrogen Feed System

The dihydrogen flow to the reactor was regulated by the use of a mass flow control unit (see Appendix 1). The mass flow unit was calibrated against a graduated bubble flowmeter. A plot of dihydrogen flow rate versus the potentiometer response is shown in Figure 4.2.3. The desired constant flow of dihydrogen was readily attained using this system. The feed system could therefore deliver a constant, known ratio of hydrogen to hydrocarbon to the reactor section of the microreactor.

4.2.3. Air, Dinitrogen and Helium Gas Feed

In addition to dihydrogen, the feed system was capable of delivering other gases.

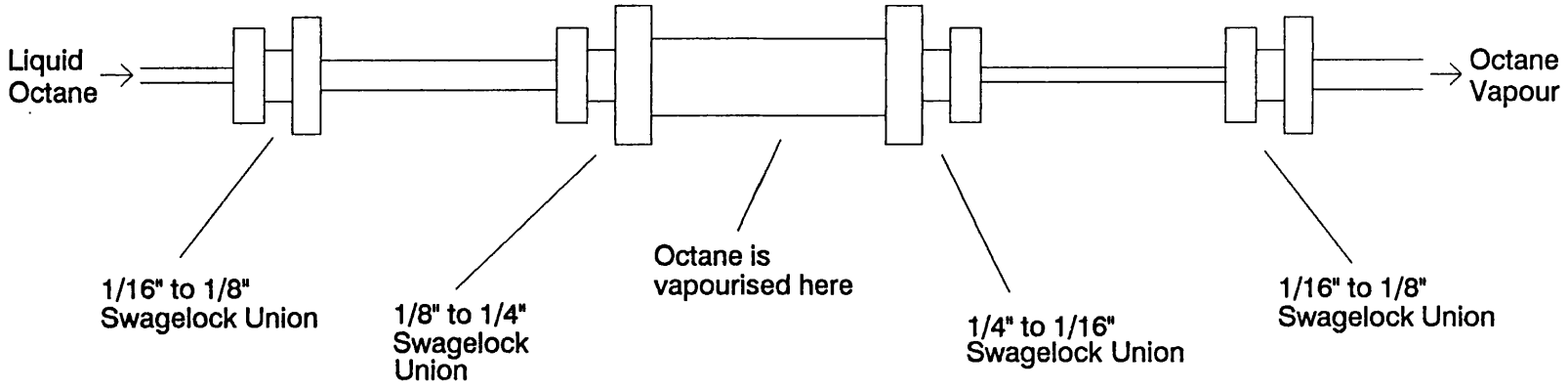

Figure 4.2.2. Octane Vapourisation Unit

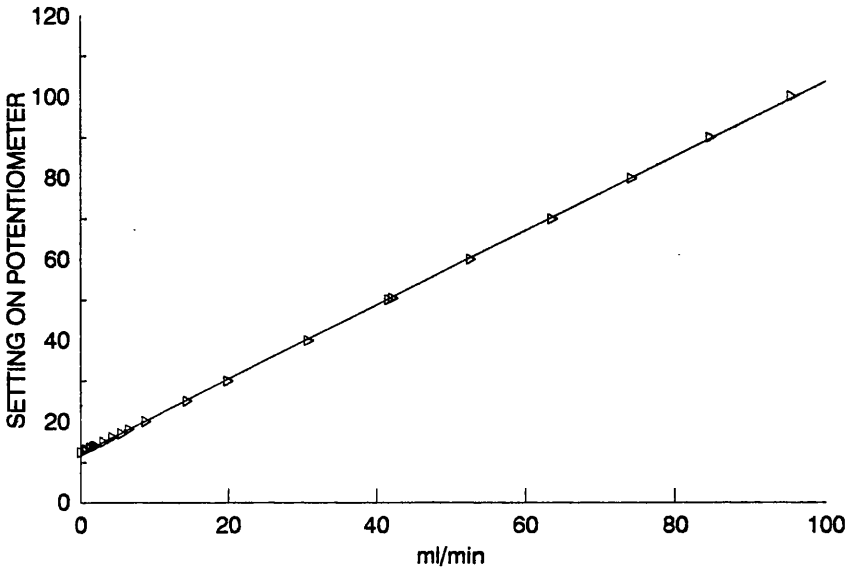

Figure 4.2.3. Calibration of the Hydrogen Mass Flow Control Unit

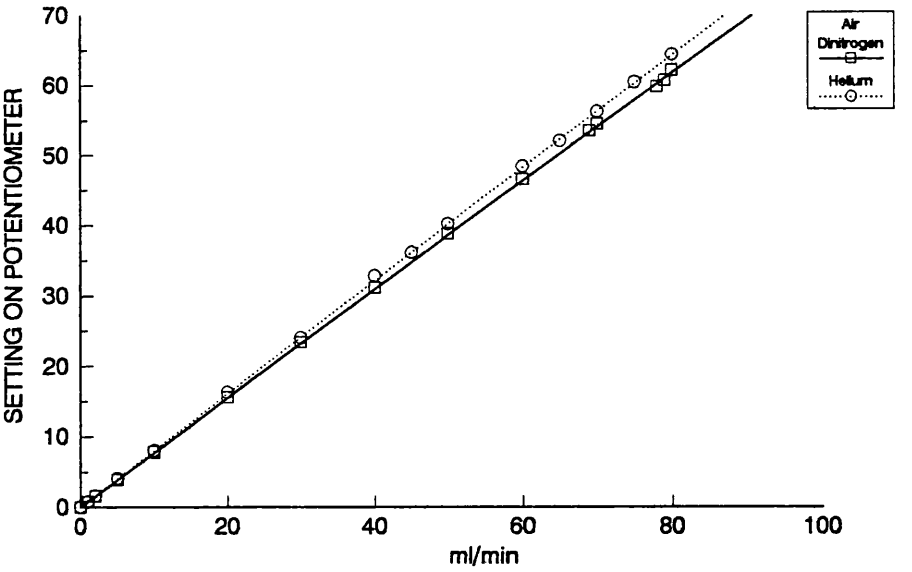

Figure 4.2.4. Calibration of the Mass Flow Control Unit for Air, Dinitrogen and Helium

This facility was used during the standard pretreatment of the catalyst samples, prior to the reforming run, as outlined in Section 4.8. Dinitrogen was also used to flush out the microreactor system after each reforming run.

As with dihydrogen the desired gas flow was accurately controlled by means of mass flow control units see Appendix 1). The mass flow control units were calibrated against a graduated bubble flowmeter. Figure 4.2.4 shows plots of the air, dinitrogen and helium flow versus the potentiometer response.

4.3. THE REACTOR SYSTEM

A diagram of the reactor system is shown in Figure 4.3.1.

4.3.1. The Reactor Block

The reactor was constructed from a rectangular brass block as shown in Figure 4.3.2. Brass was chosen as it gave a more isothermal region than stainless steel. The reactor was enclosed within an insulated box along with the vaporisation unit. When the reactor was at reaction temperature, the temperature within the box remained constant at approximately 230°C, thus ensuring that the vaporisation unit and all metal tubing needed no additional heating to avoid condensation of hydrocarbon products.

The reactor and bypass tubes consisted of 20 cm lengths of 1/8" stainless steel

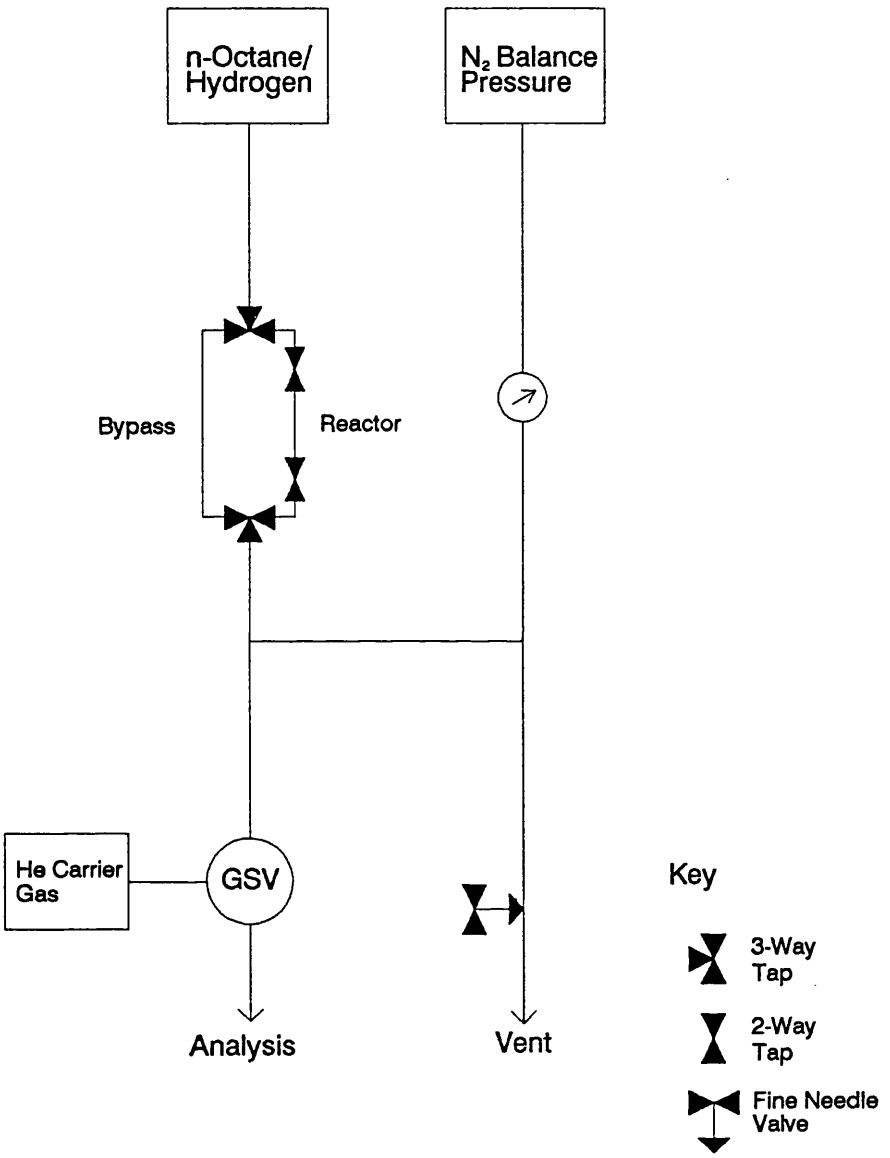

Figure 4.3.1. Schematic Diagram of the Reactor System

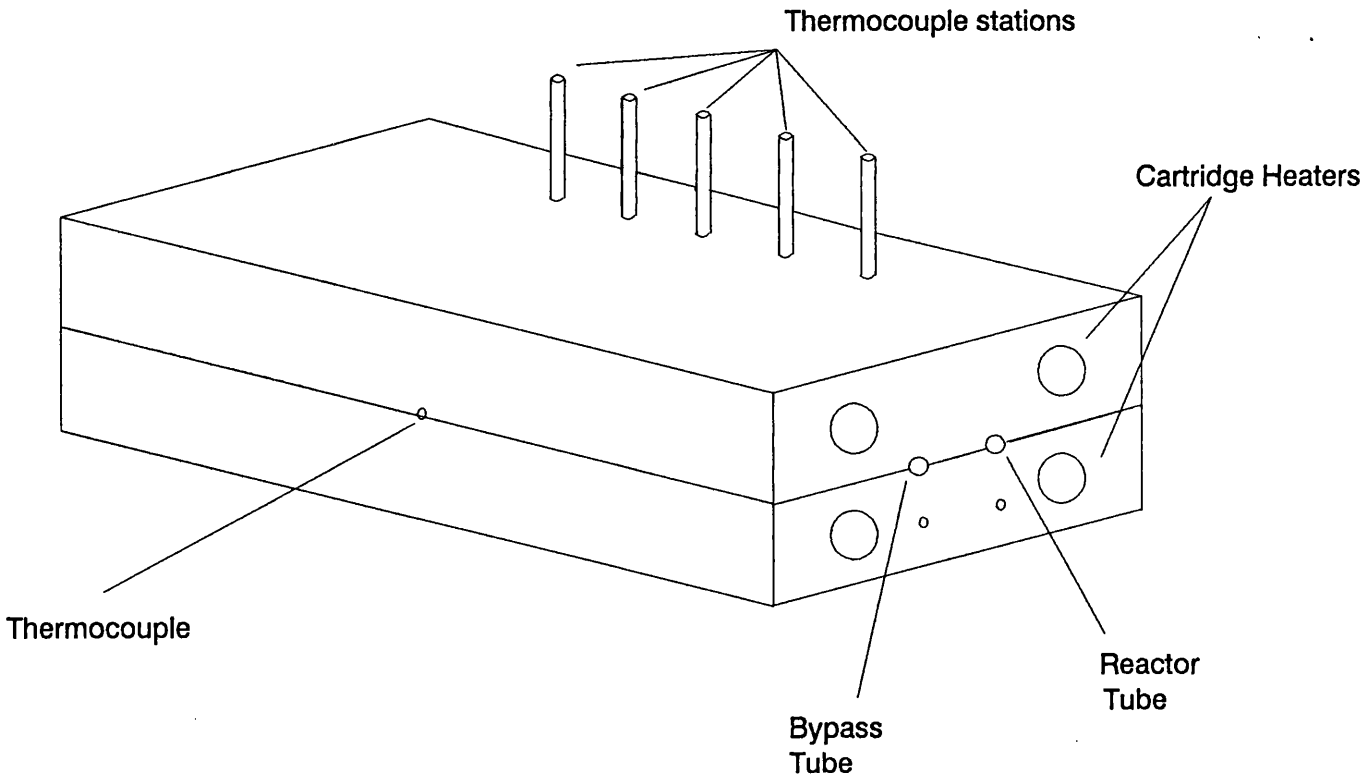

Figure 4.3.2. Diagram of the Reactor Block

tubing. The catalyst samples were held in place in the reactor tube by glass wool plugs. The temperature of the reactor block was accurately controlled by means of an F.G.H. temperature programmer in conjunction with a 10A solid state relay and four 240 W cartridge heaters positioned as shown in Figure 4.3.2. The temperature during a reforming run was monitored continuously by several Cr/Al thermocouples positioned in the reactor block.

Switching between the reactor and bypass tubes was carried out using high temperature 3-way valves. High temperature valves were used due to the elevated temperatures inside the insulated box.

The bypass tube was situated parallel to the reactor tube and was identical in all respects except that it contained no catalyst sample. During reforming runs the bypass enabled the desired flow of hydrogen and n-octane to be established before it was introduced to the catalyst. The bypass tube also enabled blank experiments to be carried out *in situ*. These blank experiments were used to determine if there was any residual activity in the reactor tube.

4.3.2. Tubular Reactors, Heat and Mass Transfer Considerations

A tubular plug flow reactor was used in this study. The reactor was operated under continuous flow conditions such that the reactant concentration varied with the axial position in the catalyst bed.

One of the major drawbacks associated with using tubular reactors is in the elimination of diffusion constraints through the catalyst bed. It is of the utmost importance that the observed product distributions are not in any way influenced by either axial or radial mass and heat mass transfer limitations. In reactor tubes of very small diameter it has been well established that gas phase reactant molecules will display only laminar flow. Mixing of the gas phase proceeds through the radial diffusion of the gas molecules from the centre of the catalyst sample to the reactor wall and vice versa.

The rate of this radial diffusion may be expressed by the following equation:-

$$t = \frac{(dT)^2}{8dR} \qquad (4.1)$$

where

t = time taken for a gas phase molecule to travel from the centre of the reactor tube to the wall

dT = reactor tube diameter

dR = radial diffusivity

Therefore, as the diameter of the reactor tube decreases the rate of radial mixing increases. Within reactor tubes of small diameter heat transfer will occur by convection in which the gas phase molecules themselves transport the heat and, therefore, as a result heat transfer will occur as rapidly as mass transfer. Hence, even in the presence of various exothermic and endothermic reactions, the temperature gradient across the diameter of a catalyst reactor tube is negligible.

4.3.3. Reactor Pressure Control

The microreactor was designed to operate at pressure in excess of atmosphere. High pressures within the system were achieved by using a fine metering needle valve situated downstream of the reactor block.

After the catalyst had been reduced, the reaction pressure was initially set using dinitrogen, drawn from the gas feed system described in Section 4.2. Once the desired pressure had been set, gaseous n-octane and dihydrogen were allowed to flow through the reactor. The gas stream coming from the reactor was split into two by a T junction. The dinitrogen supply was fed into the system after the T junction and before the fine metering needle valve.

The total pressure within the system was then made up by dinitrogen, dihydrogen and n-octane. An important feature of the system was that if the flow through the fine metering needle valve was greater than the combined n-octane and dihydrogen flow, the reactor pressure remained unchanged. When the feed gases were initially introduced there was a corresponding drop in the contribution of dinitrogen to the absolute pressure of the system. The actual pressure in the microreactor was monitored throughout a reforming run by a Budenburg pressure gauge (as shown in Figure 4.3.1).

4.3.4. Gas Sampling

The gas stream from the reactor was sampled at regular intervals by an eight port high temperature gas sampling valve (GSV). This GSV was situated inside an oven, held at a constant temperature of 140°C, thus ensuring no hydrocarbon condensed out in the tubing. The two sample loops in use were also maintained at this temperature. The effluent gas was vented to the atmosphere. A schematic diagram of the gas sampling valve is shown in Figure 4.3.3.

4.4. THE ANALYTICAL SYSTEM

A schematic diagram of the analytical system is shown in Figure 4.4.1.

Reformate products of n-octane ranged widely from light aliphatic gases through naphthenes and medium aliphatics (both normal and branched isomers) to aromatic species such as xylenes. A quantitative separation of these products was required and the analytical system used was based upon an established method for the resolution of mixtures of paraffins, naphthenes and aromatics. The acronym PNA is used to refer to this system.

The PNA system involved the separation of aromatic hydrocarbons from the paraffins and naphthenes. Non-aromatic hydrocarbons were resolved by a combination of 5A and 13X activated molecular sieves. The 5A molecular sieve adsorbs all molecules with a critical diameter of up to 5Å. In the sodium

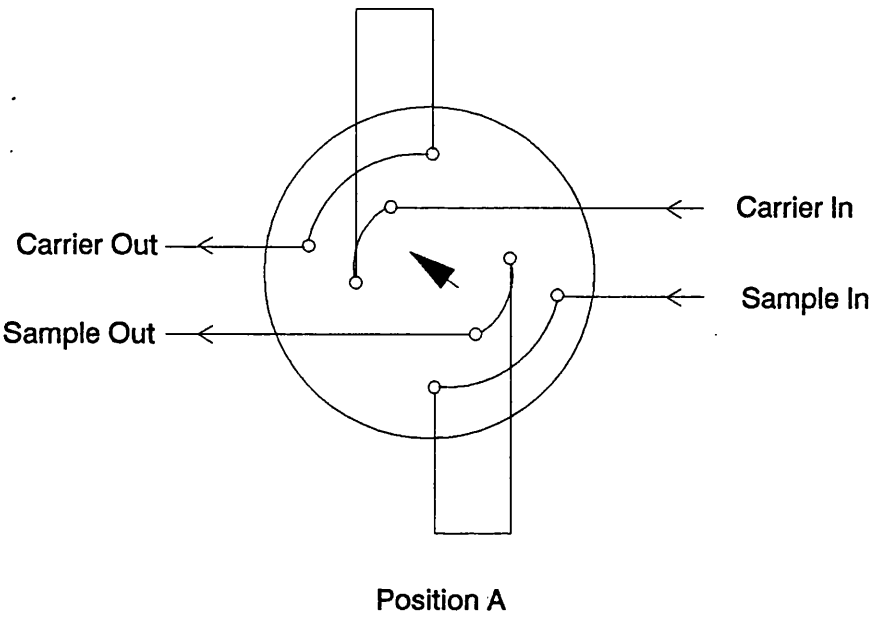

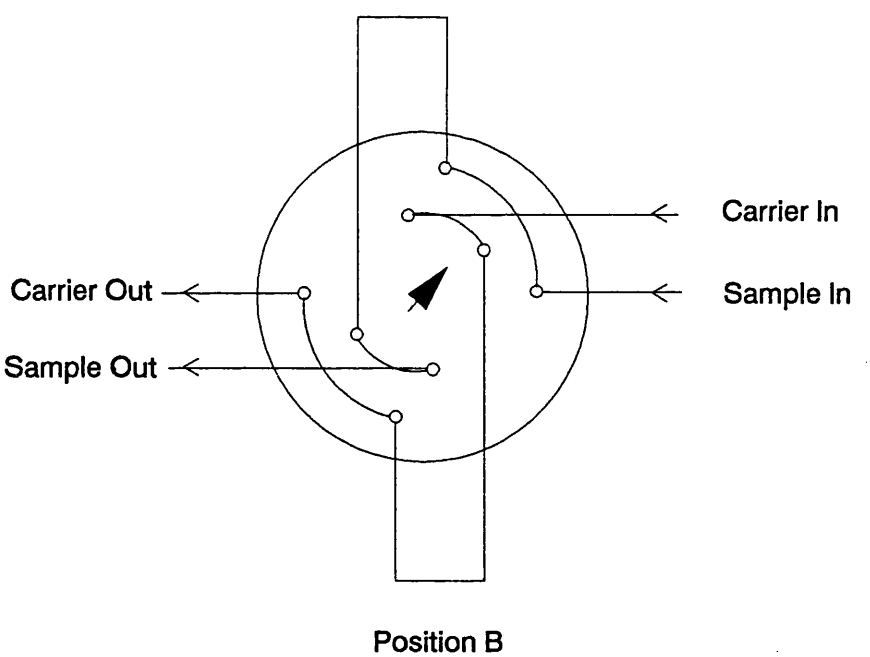

Figure 4.3.3. Schematic diagram of the gas sampling valve.

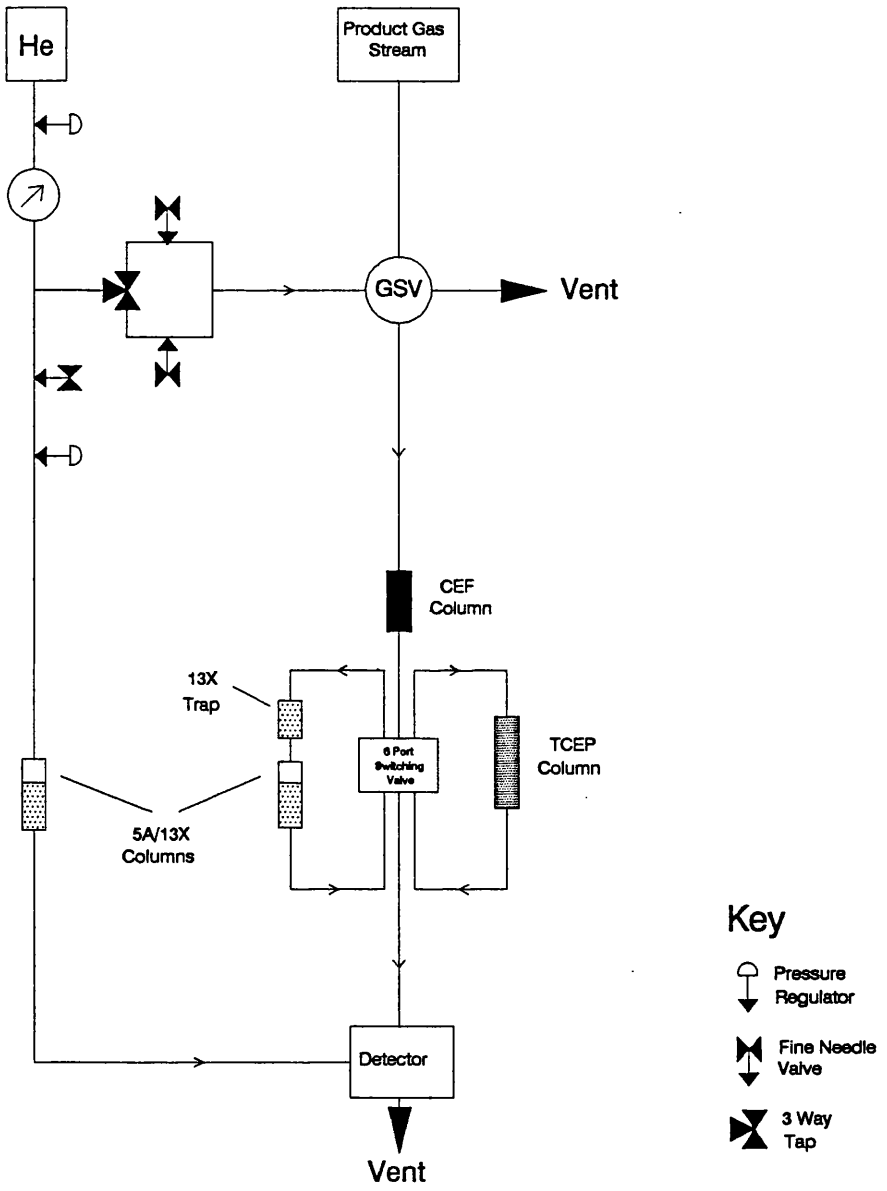

Figure 4.4.1. Schematic Diagram of the Analytical System

aluminosilicate framework, some of the sodium has been replaced by calcium. This sieve separates straight chain hydrocarbons (C_3 - C_{22}) from branched chain and cyclic hydrocarbons. The 13X molecular sieve, in comparison, has a more open aluminosilicate framework with a pore diameter of 10Å and can be used to separate cyclic and non-cyclic paraffins by carbon number. The adsorbed molecules were subsequently displaced from the molecular sieve pores by raising the temperature (as described in Section 4.4.1).

The reforming sample was injected into the analytical section of the microreactor by means of the sample valve, described previously in Section 4.3.4.

4.4.1. PNA System Operation

Helium carrier gas was initially directed through the 13X trap and 5A/13X column. The 13X trap, held at room temperature was enclosed by a tubular glass furnace and the 5A/13X column held at 150°C in the chromatographic oven. At this stage the TCEP column used for aromatic separation was isolated using a 6-port switching valve.

The sample was injected and allowed to elute via the CEF column until all the non-aromatics had reached the 13X trap. As this was at room temperature all paraffins with the exception of methane were trapped. Methane was therefore the first product to be detected. At this stage benzene, the first aromatic product, was reaching the end of the CEF column. The 6-port switching valve was switched to

direct all aromatic products towards the TCEP column, before benzene could proceed towards the 13X trap. The CEF column, the TCEP column and the 6 port switching valve were held at a constant 90°C in an oven. All the aromatics were detected within 30 minutes, during which time the non-aromatics were held in the 13X trap.

After the detection and measurement of the aromatics was complete the 6 port valve was switched to allow the carrier gas to flow through the 5A/13X column. Both the 13X trap and the 5A/13X column were held at their initial temperatures for a further 10 minutes allowing ethane to elute. Then the 13X trap was heated rapidly to 450°C (about 2 minutes) whilst the 5A/13X column was maintained at 100°C. After 15 minutes, when all non-aromatics had been displaced on to the 5A/13X column, the 13X trap was cooled to room temperature.

The 5A/13X column was then ramped at 3° min^{-1} and held at 398°C until all paraffins were displaced from the 5A/13X column. The temperature was raised at the rate of 3° min^{-1} to allow the adsorbed hydrocarbons to be removed sequentially in order of increasing carbon number.

Due to the different temperature regimes and column packings, fine metering needle valves were used to set the flow rate at 30 ml min^{-1} through both the TCEP and 5A/13X columns. A 3-way tap enabled the carrier gas to be directed through either needle valve as required.

The carrier gas flow rate through the 5A/13X column decreased with increasing

temperature. This manifested in a rising baseline in the non-aromatic chromatogram. To attenuate this, the reference gas flow was directed through a second identical 5A/13X column.

In order to avoid condensation of gaseous hydrocarbons, all metal tubing in the reactor and analytical sections of the microreactor was maintained at elevated temperatures. This was achieved by building the system inside several ovens. These were easily and accurately maintained at elevated temperatures to avoid cold spots within the line. The length of tubing, connecting the 13X trap to the analytical system, which was situated outwith the ovens, was maintained at approximately 160°C by means of Electrothermal heating tape, lagged with high temperature insulating tape, again to avoid cold spots and any condensation in the line.

After a reforming run had been completed, the used catalyst samples were transferred to a high resolution electron microscope without exposure to the atmosphere. This enabled any change in the structure of the catalyst i.e. the particle size, and any change as a result of reaction usage to be determined.

4.5. SULPHIDATION OF CATALYSTS

To investigate the activity and selectivity of the catalysts mentioned previously under realistic industrial conditions, EUROPT-3 and EUROPT-4 were sulphided with variable amounts of H_2S. As sulphur may be regarded as a poison and is very destructive, it was decided to sulphide the catalysts in a specially constructed system.

The sulphidation system is shown schematically in Figure 4.5.1 and consists of four basic sections:-

1) The feed system
2) The gas sampling valve
3) The reactor system
4) Lead acetate trap

4.5.1. The Feed System

This section was designed to allow a known amount of H_2S to be delivered to the reactor system. The use of fine metering needle valves allowed the flow of both dinitrogen and H_2S to be set accurately at the desired rate. The flow rate of each gas was measured against a graduated bubble flowmeter at the start of each sulphiding experiment.

4.5.2. The Gas Sampling Valves

A schematic diagram of the gas sampling valves (GSV) is shown in Figure 4.5.2. Two four-port sample valves were used in this system to achieve the desired result. The use of the GSV allowed a known amount of H_2S to be injected on to the catalyst surface when desired. This was a very important feature of the system as sulphur (in any form, H_2S, DMDS, thiophene, etc.) acts as a poison for reforming catalysts if present in sufficient quantities. It was therefore very important to be able

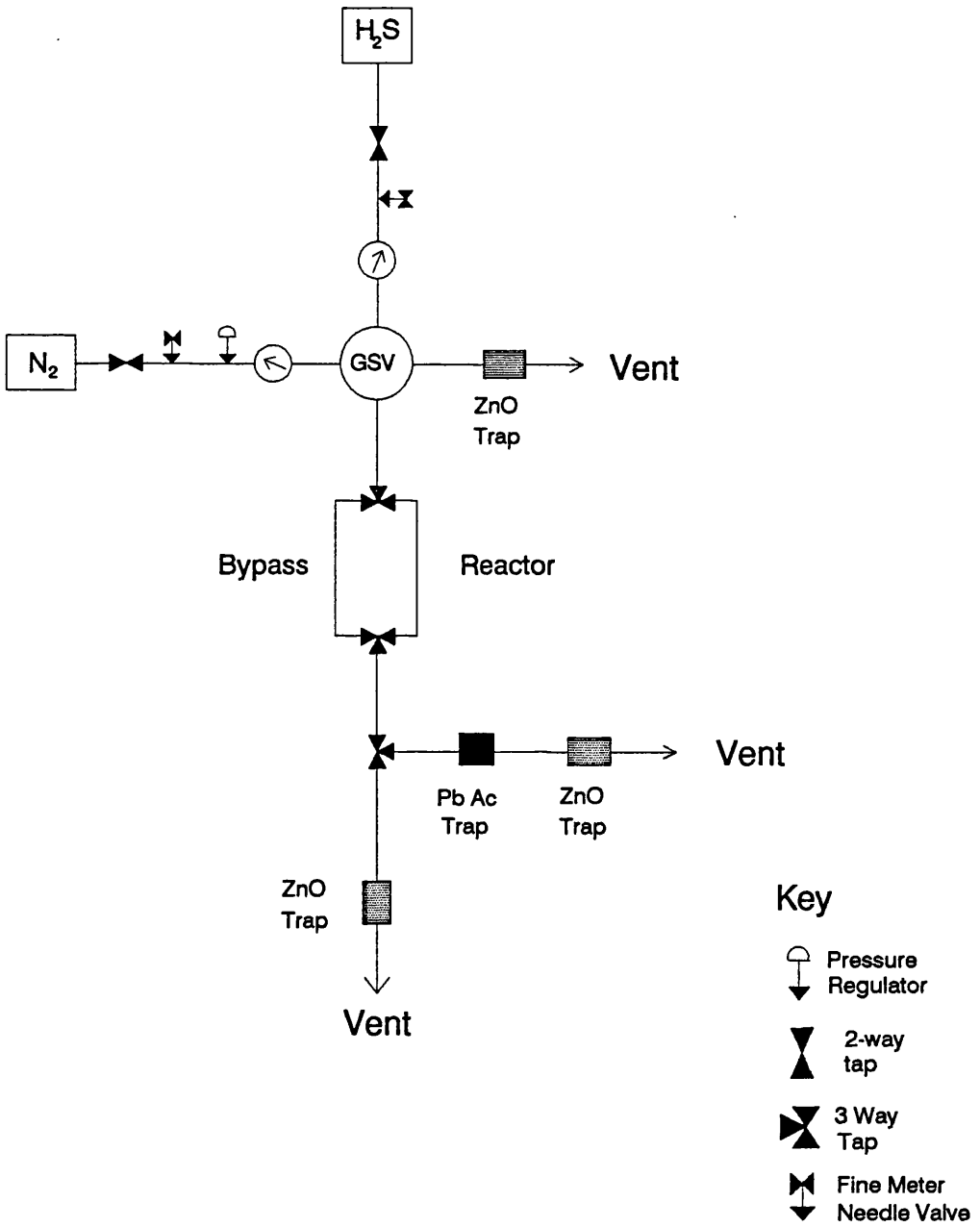

Figure 4.5.1. Schematic Diagram of the Sulphiding Apparatus

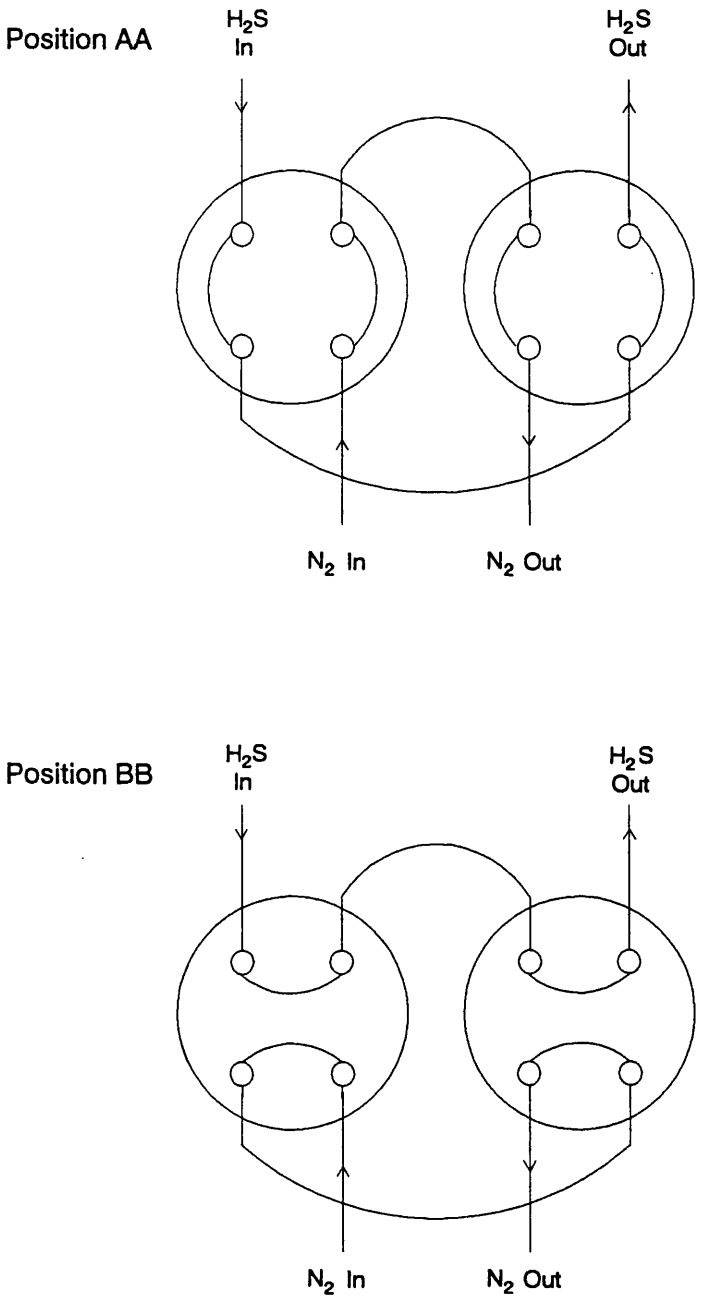

Figure 4.5.2. Schematic Diagram of the Gas Sample Valve used in the Sulphiding System

to control the exact amount of H_2S being added to the catalyst sample, hence the use of the sample valves in this system.

Dinitrogen was used as a carrier gas to transport the injected H_2S sample on to the catalyst sample situated in the reactor tube.

4.5.3. The Reactor System

The reactor vessel consisted of a 20 cm length of 1/8 " o.d. stainless steel tubing (identical to that used in the reforming experiments). The reactor and bypass were identical in every respect except that the reactor tube contained the catalyst sample to be sulphided. The catalyst sample was held in place by glass wool plugs.

The reactor and bypass tubes were enclosed within a furnace to allow the sulphidation to be carried out at elevated temperatures (up to 500°C) if desired, the temperature of the furnace being monitored by a Cr/Al thermocouple positioned in the furnace. The furnace was in turn was positioned within an insulated box to maintain a steady temperature.

During the sulphidation experiments the bypass enabled the desired flow rates of H_2S and dinitrogen to be established before being introduced to the catalyst sample.

4.5.4. Lead Acetate Trap

The gas stream exiting from the reactor could be directed towards the lead acetate trap by means of a 3-way tap. The trap was used to indicate the breakthrough point of H_2S, that is when the catalyst uptake of H_2S had reached a maximum. When H_2S was detected, the clear lead acetate instantly turned a dense black colour thus indicating the presence of H_2S.

The effluent gas stream from each section was vented to the atmosphere through zinc oxide (ZnO) traps. These traps were used to adsorb any H_2S remaining in the gas stream, thus eliminating the possibility of any H_2S being vented into the atmosphere. As a further precaution against any H_2S pollution, the entire sulphiding system was built within a fumehood.

After the catalyst had been sulphided, the sample was weighed to determine the extent of the sulphur uptake. The samples were then transferred to the microreactor for further study in n-octane reforming runs. Part of the sulphided catalyst sample was retained for further examination by EDX and HRTEM.

4.6. POISONING OF A REFORMING CATALYST

In addition to investigating the effect of partially sulphiding reduced EUROPT catalysts, they were poisoned using H_2S. This enabled the full extent of sulphiding a EUROPT catalyst to be studied under typical reforming conditions.

The catalyst to be poisoned was activated as detailed in Section 4.8. The reduced catalyst was then transferred to a glass reactor vessel without exposure to air. The catalyst was arranged into three separate beds within this vessel by means of glass wool plugs as illustrated in Figure 4.6.1. This arrangement ensured that there was an even adsorption of H_2S throughout the catalyst pellets in the three beds. Table 4.6.1 lists the % uptake of H_2S by each catalyst.

Table 4.6.1. % Uptake of H_2S by EUROPT-3 and EUROPT-4.

	EUROPT-3 % Uptake of H_2S	EUROPT-4 % Uptake of H_2S
Bed 3	0.925	0.926
Bed 2	0.770	0.805
Bed 1	0.794	0.963
Overall Uptake Of H_2S	0.830	0.897

The reactor vessel was placed in a furnace at 20°C to enable all poisoning experiments to be carried out at the same temperature. The reduced catalyst was then introduced to a 2%H_2S/N_2 gas mixture and the gas eluting from the reactor vessel was sampled by means of a gas sampling valve. The sampled mixture was analysed using a Poropak QS chromatographic column, held at 40°C in an oven, in conjunction with a thermal conductivity detector. This enabled the exact amount of H_2S exiting the reactor vessel to be determined during the reaction until a constant level was reached. Results of the poisoning experiments are shown in Table 4.6.2.

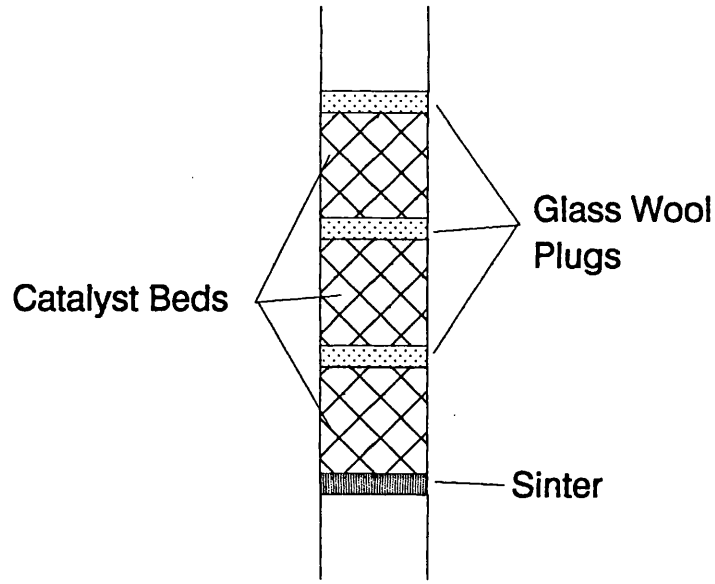

Figure 4.6.1. Arrangement of Catalyst Sample in the Reactor Vessel during the poisoning experiments

For both EUROPT catalysts no further adsorption of H_2S was observed after two hours. The breakthrough point of H_2S was almost immediate for both EUROPT catalysts indicating the very small amount of H_2S needed to sulphide either catalyst.

Table 4.6.2. H_2S detected for EUROPT catalysts with time-on-stream.

EUROPT-3		EUROPT-4	
Time (minutes)	Area of H_2S Detected	Time (minutes)	Area of H_2S Detected
0	107935	0	98192
26	111295	24	108114
41	113454	49	113084
71	114223	67	113820
83	116077	91	114764
110	116393	107	114757

The poisoned catalyst was transferred from the glass reactor vessel into an 1/8" o.d. stainless steel reactor tube (described in Section 4.3.1) without exposure to the air. The poisoned catalyst was then rereduced in hydrogen at 400°C, as described in Section 4.8, for two hours in the microreactor system. After this period of time the reactor was ramped to the reaction temperature and the reaction conditions were set as for a typical reforming run.

4.7. CATALYSTS

A variety of mono- and bimetallic catalysts were examined in the microreactor. These were as follows:-

EUROPT-3 - 0.3%Pt/Al_2O_3-Cl

EUROPT-4 - 0.3%Pt-0.3%Re/Al_2O_3-Cl

0.3%Pt-0.3%Sn/Al_2O_3 - Pt impregnated first.

- Sn impregnated first.

- Pt & Sn coimpregnated.

- by methanol.

- Patent.

0.3%Pt-0.9%Sn/Al_2O_3 - Pt impregnated first

1.0%Pt-1.0%Sn/Al_2O_3 - Sn impregnated first

3.0%Pt-3.0%Sn/Al_2O_3 - Pt impregnated first.

3.0%Pt-3.0%Re/Al_2O_3 - Re impregnated first.

0.3% Re/Al_2O_3

0.3% Sn/Al_2O_3

3.0% Sn/Al_2O_3

0.3%Pt-0.3%Ge/Al_2O_3 - Ge impregnated first.

- Pt & Ge coimpregnated.

- Pt impregnated first (EUROPT-3 impregnated with Ge)

1.0%Pt-1.0%Ge/Al_2O_3 - Ge impregnated first

0.3% Ge/Al_2O_3

4.8. ACTIVATION OF CATALYSTS

All catalysts used in these studies were activated *in situ* by a standard procedure. This consisted of 3 steps:-

1) Calcination

Heating to 400°C at 5° min^{-1} in flowing air (60 ml min^{-1}). Held at 400°C for 4 hours and then cooled to room temperature.

2) Flushing

Switch to He flow (60 ml min^{-1}). Held for one hour at room temperature.

3) Reduction

Switch to dihydrogen flow (60 ml min^{-1}) and heated to 400°C at 5° min^{-1}. Held at 400°C for 2 hours.

4.9. SUMMARY OF THE PNA COLUMNS_

1. CEF . This allows the elution of aliphatics < C_{10}, before benzene. Held at 90°C. This is a stainless steel column, (i.d. = 1.8 mm, length = 2.0 m), containing cyano ethyl formamide, 22.5% w/w on acid washed Chromosorb P (60 - 80 mesh).

2. TCEP This separates aromatic products. Held at 90°C. Triscyano ethoxy propane, 5% w/w on acid washed Chromosorb P (60 - 80 mesh) in a stainless steel column, i.d. = 2.4 mm, length = 2.0 m

3. 13X Trap This traps and holds the non aromatics while the aromatics are detected. 13X molecular sieve (60 - 80 mesh) in a stainless steel column, i.d. = 1.8 mm, length = 15 cm.

Temperature is raised from ambient to 450°C.

4. 5A/13X This separates the paraffins by carbon number and by bulk hydrocarbon type. This column contains two sections. A 5A molecular sieve section (60 - 80 mesh), length = 30 cm and a 13X molecular sieve section (60 - 80 mesh), length = 90 cm. Both sections are contained within one length of stainless steel column, i.d. = 1.8 mm.

The temperature is raised from 100°C to 398°C at 3° min^{-1}.

Columns 3 and 4 were initially activated by heating to 100°C and holding at this temperature for 30 minutes. The temperature was then ramped to 450°C (5A trap) and to 398°C (5A/13X column) at 3° min^{-1} and held at these temperatures for a further 4 hours.

4.10. HYDROCARBON DETECTION AND CALIBRATION

A thermal conductivity detector and a Schimadzu Chromatopac integrator were used in the detection, measurement and display of the chromatographic data.

The retention times and response factors of all potential reaction products were determined by injecting a known volume of each potential product into the PNA system. By varying the volume a corresponding range of peak areas was obtained for each potential product. The calibration procedure was repeated until at least four reproducible results for each volume were obtained. Therefore all retention times and response factors represent average values. The retention times were measured from the point of injection into the system.

Appendix 2 shows plots of the average area of the chromatographic peak versus the number of moles for each potential product.

Table 4.10.1 shows the retention times and response factors of all relevant compounds.

Table 4.10.1. Retention times and Response Factors of all Relevant Products

Expected Product	Retention Time (min)	Conversion Factor (Area Units x 10^{-13} mol^{-1})
Benzene	4.31	0.866
Toluene	6.02	0.942
Ethylbenzene	8.67	1.029
m/p - Xylene	9.41	1.031
o - Xylene	12.49	1.112
Methane	2.18	173.853
Ethane	8.54	166.390
Propane	28.61	143.644
i - Butane	56.04	126.304
n - Butane	56.97	121.746
Cyclopentane	72.25	0.932
i - Pentane	76.57	0.930
n - Pentane	79.82	0.738
Cyclohexane	89.43	0.930
i - Hexane	93.62	0.930
n - Hexane	98.56	0.952
Cycloheptane	107.62	0.937
i - Heptane	111.87	0.938
n - Heptane	114.74	0.919
Cyclooctane	120.86	0.884
i - Octane	122.35	0.927
n - Octane	126.38	0.930

4.11. MATERIALS USED

4.11.1. n-Octane

The n-octane liquid feedstock used throughout this study was supplied by the Aldrich Chemical Company Ltd. The purity of this feedstock was measured by gas chromatography and the purity was always found to be > 99%. Therefore the n-octane was used as supplied without any further purification.

4.11.2. Gaseous Feedstocks

The cylinder gaseous feedstocks, Hydrogen, Nitrogen, Helium and Air (supplied by B.O.C. Ltd.), were all used without further purification.

Chapter 5

Treatment of Results

5.1. n-OCTANE REFORMING REACTION CONDITIONS

The reaction of n-octane and hydrogen on the catalysts mentioned in the previous section were investigated. Reforming reactions were performed at a pressure of 110 psig, spacial velocity (WHSV) 2 h^{-1}, molar ratio of hydrogen:hydrocarbon = 6 and an initial temperature of 510°C.

5.2.1. Calculation of the Yield, Conversion and Selectivity

The yield, conversion and selectivity values quoted in this report are defined in the following way:

Yield:-

the amount of a given reaction product, i, related to the amount of starting material, expressed by the equation:

$$(\%)Yield = \frac{n_i (M_i)}{N (X)} \times \frac{100}{1} \qquad (5.1)$$

where

n_i = the number of carbon atoms in product species i.

M_i = the number of moles of product species i.

N = the number of carbon atoms in the reactant molecule.

X = the number of moles of hydrocarbon reactant.

The gaseous products were sampled at regular intervals by a gas sampling valve; the sample loops each having a volume of 2 or 5 ml. The number of moles of hydrocarbon reactant, X, is defined as the amount of n-octane that would have been present in the sample loop had no reaction taken place. Knowing the molar ratio of hydrogen to hydrocarbon and the values of pressure, temperature and volume the value of X was readily calculated.

Conversion:-

the amount of starting material, i, transformed into products, expressed by the equation:

$$(\%)\ Conversion = \frac{\sum_{i=1}^{i=j} n_i\ (M_i)}{n_i\ (M_i)} \quad x \quad \frac{100}{1} \qquad (5.2)$$

Selectivity:-

the amount of a given reaction product, i, related to the amount of starting material converted, expressed by the equation:

$$(\%)\ Selectivity = \frac{n_i\ (M_i)}{\sum_{i=1}^{i=j} n_i\ (M_i)} \quad x \quad \frac{100}{1} \qquad (5.3)$$

5.2.2. Calculation of the Selectivities to Major Reactions

The major reactions which take place in catalytic reforming may be summarised by taking into account the selectivity towards related groups of hydrocarbon products. Four major reactions, aromatisation, hydrogenolysis, isomerisation and hydrocracking may be represented by the following summations:-

a) Aromatisation - defined as the sum of the selectivities for all aromatic species

b) Hydrogenolysis - defined as the selectivity of methane

c) Isomerisation - defined as the sum of the selectivities of i-heptane and i-octane

d) Hydrocracking - defined as the sum of the selectivities of i-butane, i-pentane and i-hexane

In this way any changes in the selectivities to the major reforming reactions may be followed throughout a reforming run.

5.2.3. Calculation of the Carbon Mass Balance

The carbon mass balance sums the number of moles of carbon atoms eluted from the reactor with respect to the number of moles introduced to the reactor. Therefore the carbon mass balance was calculated in the following way:

$$\textit{The number of carbon moles introduced} = N(X) \qquad (5.4)$$

$$\textit{The number of moles of carbon eluted} = \sum_{i=1}^{i=j} n_i\,(M_i) + N(Y) \qquad (5.5)$$

where Y = the number of moles of unreacted hydrocarbon feed eluted from the reactor.

5.2.4. Calculation of the Propane to Methane Ratio

To assess the relative activities of the acidic and metallic sites throughout a reforming reaction, the ratio of propane to methane product yields were studied with respect to the reaction time. The formation of propane, via hydrocracking reactions, takes place on the acidic sites of the catalyst. In comparison, methane production by hydrogenolysis is widely accepted to take place on the metallic sites of the catalyst. Therefore the propane to methane ratio can be used to ascertain the appropriate relationship between the acidic and metallic sites of the catalyst.

5.3. BLANK RUN

A 'blank run' was carried out in the microreactor to establish the catalytic properties of the stainless steel tubing used in the construction of the system. The blank runs were examined under identical conditions to those used in a normal reforming reaction, i.e. WHSV = 2 h^{-1}, H_2: n-octane = 6:1, T = 510 °C and P = 110 psig (8.5 atm). The only difference being the absence of a catalyst sample in the reactor tube for a blank run.

The blank run provided a valuable insight into the inherent properties of an empty reactor tube as illustrated presented in Table 5.3.1. These results represent

the mean of four different blank runs.

Table 5.3.1. Product distribution and mean % Yield obtained from blank runs.

Product	Mean % Yield
Benzene	1.472×10^{-3}
Toluene	2.933×10^{-4}
Methane	5.183
Ethane	1.454
i - Octane	2.593×10^{-4}
n - Octane	88.983
Δ Octane	4.419

The results in Table 5.3.1 show that the stainless steel tubing does in fact influence the product distribution, especially to methane and ethane. It is also noticeable that there is approximately 4.5% of a difference in the n-octane entering and exiting the reactor. This difference is attributed to the formation of carbonaceous residues on the walls of the metal tubing in the system.

All the results quoted in this work have been amended to take into account the contribution of the stainless steel tubing. Therefore this meant that the values quoted were a true representation of the catalytic activity of the catalysts involved in these reactions.

Chapter 6

Results

Table 6.1. % Coke Deposited on the Catalyst after use in n-Octane Reforming Reactions

Catalyst	Time on Stream (hrs)	% Coke (wt)	Catalyst	Time on Stream (hrs)	% Coke (wt)
EUROPT-3.1	55	13.88	0.3%Sn/Al_2O_3	31	12.38
EUROPT-3.2	70	6.73	3.0%Sn/Al_2O_3	32	18.21
EUROPT-4.1	51	15.39	EUROPT-3 (Poisoned)	104	1.68
EUROPT-4.2	40	9.09	EUROPT-4 (Poisoned)	106	2.32
EUROPT-4.3	42	11.36	EUROPT-3 (4 pulses H_2S)	96	2.99
3.0%Pt-3.0%Re/Al_2O_3	26	16.08	EUROPT-3 (3 pulses H_2S)	95	5.34
0.3%Pt-0.9%Sn/Al_2O_3 (Pt impregnated first)	31	11.04	EUROPT-3 (2 pulses H_2S)	96	6.74
0.3%Pt-0.3%Sn/Al_2O_3 (Pt impregnated first)	45	23.84	EUROPT-4 (4 pulses H_2S)	75	3.75
0.3%Pt-0.3%Sn/Al_2O_3 (Sn impregnated first)	51	12.96	EUROPT-4 (2 pulses H_2S)	96	6.90
0.3%Pt-0.3%Sn/Al_2O_3 (Coimpregnated)	43	6.50	0.3%Pt-0.3%Ge/Al_2O_3 (Ge impregnated first)	74	8.49
0.3%Pt-0.3%Sn/Al_2O_3 (Patent)	45	14.99	0.3%Pt-0.3%Ge/Al_2O_3 (Pt impregnated first)	76	9.95
0.3%Pt-0.3%Sn/Al_2O_3 (Methanol)	46.5	17.42	0.3%Pt-0.3%Ge/Al_2O_3 (Coimpregnated)	95	4.93
1.0%Pt-1.0%Sn/Al_2O_3	45.5	8.12	1.0%Pt-1.0%Ge/Al_2O_3	75	8.60
3.0%Pt-3.0%Sn/Al_2O_3	20.5	6.50	0.3%Ge/Al_2O_3	95	5.01

6.1. EUROPT-3.1 (510°C, 110 psig)

The hydrogen and n-octane feed mixture was passed over ~0.4 g of EUROPT-3, 0.3wt%Pt/Al_2O_3-Cl, catalyst for 51 hours. Throughout this period the reaction conditions were held constant at 510°C, 110 psig (8.5 atm), WHSV = 2 h^{-1} and a hydrogen to n-octane molar ratio of 6:1. By sampling the gas stream exiting the reactor at regular intervals, the yield, selectivity and conversion were calculated (see Section 5.2) giving a detailed analysis of the product distribution with time. The results of this study are presented in Tables 6.1.1 to 6.1.3 and Figures 6.1.1 to 6.1.9.

As seen in Figure 6.1.1 the conversion of n-octane to C_1 - C_4 species decreased with reaction time. For these products there was an initial rapid fall in the conversion with the yield stabilising after approximately 50 hours. Methane was produced in the largest quantities followed by propane and then ethane. Iso- and n-butane products were inseparable in this run and therefore the combined yield is quoted.

Conversion to cycloparaffins, Figure 6.1.2, was low throughout the run. The yield of cyclopentane was constant while the yields of both cyclohexane and cycloheptane decreased with time reaching a constant yield after 50 hours on stream. In contrast, the yield of cyclooctane increased rapidly and reached a steady state after about 25 hours on stream. Iso-paraffin formation was much higher than that of the corresponding cycloparaffins. The yield of i-paraffins, Figure 6.1.3, decreases with increasing carbon number initially but after 20 hours on stream the yield of i-heptane

Table 6.1.1. %Yield of individual products and % Conversion versus time-on-stream for EUROPT-3.1.

Products	The % Yield of Selected Products										
Time (hrs)	2.5	5.5	8.5	20	23	26	29	32	44.5	47.5	51
Benzene	0.2888	0.2636	0.2485	0.2303	0.2170	0.2086	0.2048	0.2032	0.1873	0.1854	0.1817
Toluene	3.3540	3.5878	3.2388	2.8320	2.6442	2.4329	2.2003	2.1548	1.8643	1.8077	1.7647
Ethylbenzene m/p-Xylene	8.6673	8.1013	7.6445	7.4174	7.0564	6.7479	6.4416	6.3306	5.8585	5.7625	5.7535
o-Xylene	4.7174	5.1175	4.6765	4.3473	4.2335	4.1210	3.9029	3.8644	3.7960	3.7312	3.7032
Methane	8.5825	6.4151	5.4170	4.8592	4.7057	4.6366	4.5923	4.5618	4.4804	4.4781	4.4802
Ethane	4.4676	3.8658	3.6651	3.4611	3.3190	3.1964	3.1168	3.0131	2.8536	2.7860	2.6950
Propane	6.9187	5.8713	5.5187	4.7293	4.2454	3.9445	3.8303	3.8204	3.2654	3.1486	3.0603
i-Butane n-Butane	10.5688	8.5689	7.6507	7.0546	6.7650	6.4298	6.3490	6.1983	5.4837	5.3223	5.1031
Cyclopentane	0.0008	0.0010	0.0013	0.0009	0.0009	0.0008	0.0007	0.0006	0.0003	0.0003	0.0003
i-Pentane	0.5249	0.3217	0.3028	0.2851	0.2755	0.2755	0.2754	0.2474	0.2514	0.2442	0.2396
n-Pentane	0	0	0	0	2.2×10^{-5}	3.2×10^{-5}	4.5×10^{-5}	5.3×10^{-5}	9.9×10^{-5}	0.0001	0.0001
Cyclohexane	0.0122	0.0108	0.0093	0.0071	0.0067	0.0058	0.0054	0.0049	0.0022	0.0022	0.0022
i-Hexane	0.2979	0.2770	0.2665	0.2631	0.2581	0.2521	0.2460	0.2394	0.2083	0.1842	0.1622
n-Hexane	0.0144	0.0148	0.0146	0.0117	0.0095	0.0103	0.0099	0.0096	0.0054	0.0051	0.0049
Cycloheptane	0.0165	0.0156	0.0137	0.0104	0.0090	0.0082	0.0073	0.0069	0.0053	0.0049	0.0051
i-Heptane	0.0393	0.0345	0.0322	0.0311	0.0306	0.0301	0.0299	0.0299	0.0288	0.0274	0.0264
n-Heptane	-	0.0140	0.0133	0.0101	0.0094	0.0088	0.0081	0.0075	0.0045	0.0042	0.0039
Cyclooctane	0.0008	0.0022	0.0048	0.0090	0.0149	0.0180	0.0205	0.0206	0.0210	0.0210	0.0210
i-Octane	0.0110	0.0197	0.0227	0.0317	0.0336	0.0361	0.0381	0.0384	0.0448	0.0448	0.0458
Conversion of n-Octane	48.4144	42.5024	38.7411	35.5915	33.8346	32.3654	31.2793	30.7519	28.3612	27.7601	27.2534

In the following Tables the precision of the major reaction products should be taken to three significant figures, where more significant figures are shown.

Table 6.1.2. %Selectivity of individual products versus time-on-stream for EUROPT-3.1.

Products	The % Selectivity of Selected Products										
Time (hrs)	2.5	5.5	8.5	20	23	26	29	32	44.5	47.5	51
Benzene	0.5964	0.6201	0.6412	0.6472	0.6413	0.6446	0.6546	0.6608	0.6603	0.6678	0.6669
Toluene	6.9277	8.4415	8.3601	7.9571	7.8150	7.5231	7.0344	7.0070	6.5733	6.5120	6.4753
Ethylbenzene m/p-Xylene	17.902	19.061	19.732	20.840	20.856	20.849	20.594	20.586	20.657	20.758	21.111
o-Xylene	9.7437	10.570	12.071	12.215	12.512	12.733	12.478	12.566	13.385	13.441	13.588
Methane	17.727	15.093	13.983	13.653	13.908	14.326	14.682	14.834	15.797	16.131	16.440
Ethane	9.2279	9.0954	9.4605	9.7246	9.8096	9.8761	9.9646	9.7981	10.062	10.036	9.8888
Propane	14.290	13.814	14.245	13.288	12.548	12.188	12.245	12.423	11.513	11.342	11.229
i-Butane n-Butane	21.830	20.161	19.748	19.821	19.994	19.866	20.298	20.156	19.335	19.172	18.725
Cyclopentane	0.0017	0.0023	0.0032	0.0025	0.0028	0.0024	0.0021	0.0021	0.0012	0.0012	0.0012
i-Pentane	1.0842	0.7569	0.7817	0.8011	0.8143	0.8511	0.8804	0.8044	0.8865	0.8797	0.8791
n-Pentane	0	0	0	0	6.6×10^{-5}	0.0001	0.0001	0.0002	0.0003	0.0004	0.0004
Cyclohexane	0.0251	0.0254	0.0241	0.0199	0.0198	0.0179	0.0174	0.0159	0.0076	0.0077	0.0079
i-Hexane	0.6154	0.6517	0.6879	0.7392	0.7629	0.7791	0.7865	0.7784	0.7346	0.6636	0.5950
n-Hexane	0.0297	0.0348	0.0377	0.0328	0.0282	0.0318	0.0316	0.0313	0.0192	0.0185	0.0178
Cycloheptane	0.0340	0.0366	0.0355	0.0292	0.0267	0.0253	0.0233	0.0226	0.0188	0.0177	0.0185
i-Heptane	0.0812	0.0811	0.0832	0.0873	0.0905	0.0929	0.0957	0.0972	0.1014	0.0985	0.0970
n-Heptane	-	0.0330	0.0342	0.0284	0.0279	0.0272	0.0258	0.0243	0.0158	0.0150	0.0143
Cyclooctane	0.0018	0.0052	0.0123	0.0253	0.0441	0.0558	0.0654	0.0669	0.0740	0.0755	0.0771
i-Octane	0.0228	0.0463	0.0587	0.0890	0.0993	0.1114	0.1219	0.1249	0.1432	0.1613	0.1682

Table 6.1.3. Carbon Mass Balance of the EUROPT-3.1. catalyst

Time (hrs)	No. of moles of Carbon In	No. of moles of Carbon Out	Δ Carbon
2.5	7.1545×10^{-4}	5.9376×10^{-4}	1.2169×10^{-4}
5.5	7.1545×10^{-4}	5.9494×10^{-4}	1.2051×10^{-4}
8.5	7.1545×10^{-4}	6.0235×10^{-4}	1.1310×10^{-4}
20	7.1545×10^{-4}	6.2427×10^{-4}	9.1183×10^{-5}
23	7.1545×10^{-4}	6.2737×10^{-4}	8.8078×10^{-5}
26	7.1545×10^{-4}	6.3027×10^{-4}	8.5187×10^{-5}
29	7.1545×10^{-4}	6.3325×10^{-4}	8.2203×10^{-5}
32	7.1545×10^{-4}	6.3642×10^{-4}	7.9033×10^{-5}
44.5	7.1545×10^{-4}	6.4043×10^{-4}	7.5017×10^{-5}
47.5	7.1545×10^{-4}	6.4112×10^{-4}	7.4334×10^{-5}
51	7.1545×10^{-4}	6.4235×10^{-4}	7.3106×10^{-5}

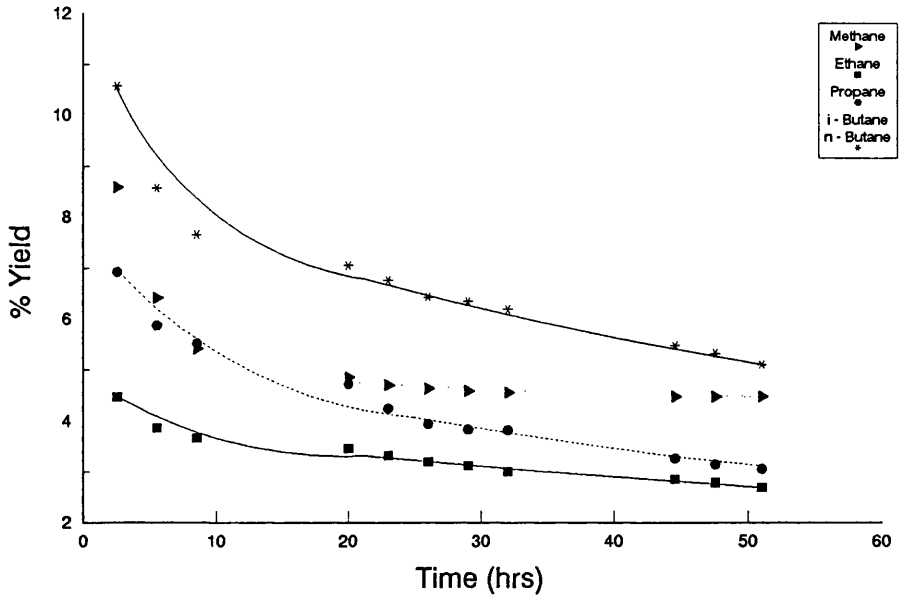

Figure 6.1.1. % Yield to Individual Hydrocarbon Products on EUROPT-3.1.

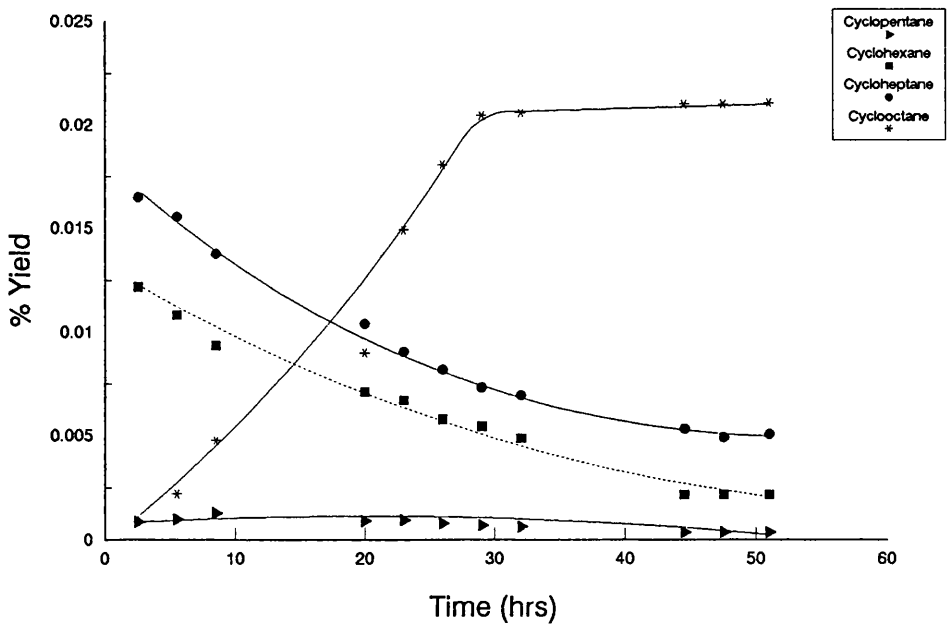

Figure 6.1.2. % Yield to Cycloparaffin Products on EUROPT-3.1.

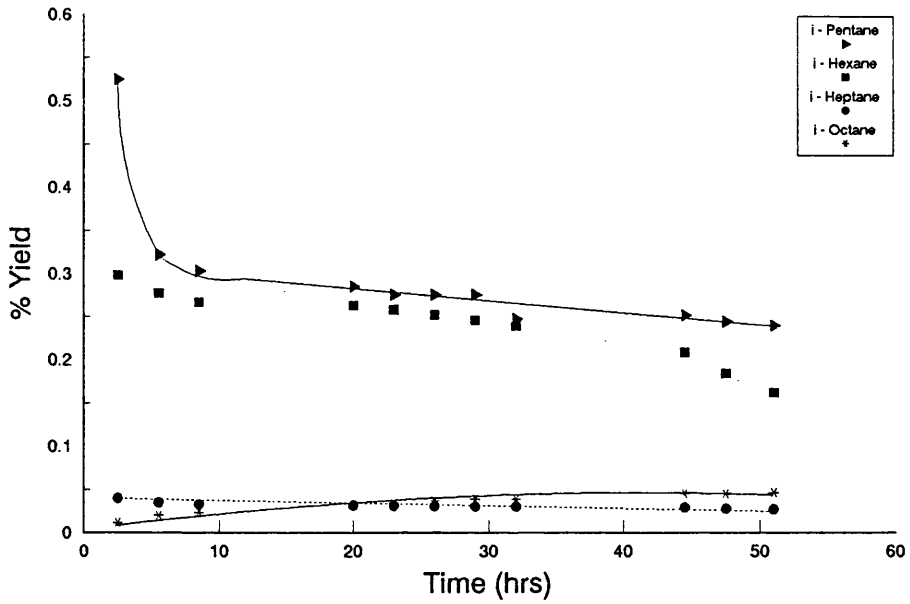

Figure 6.1.3. % Yield of i-Paraffins on EUROPT-3.1.

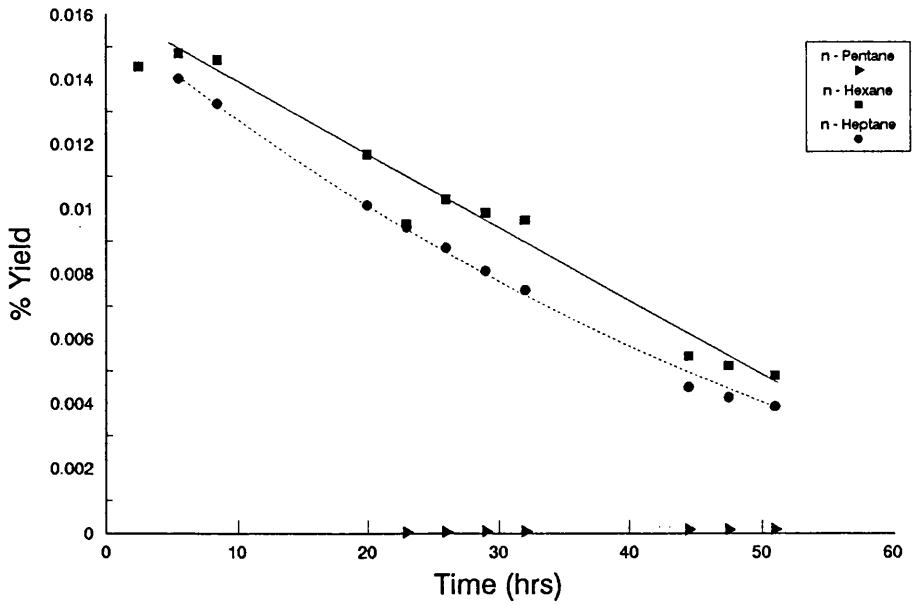

Figure 6.1.4. % Yield of n-Paraffins on EUROPT-3.1.

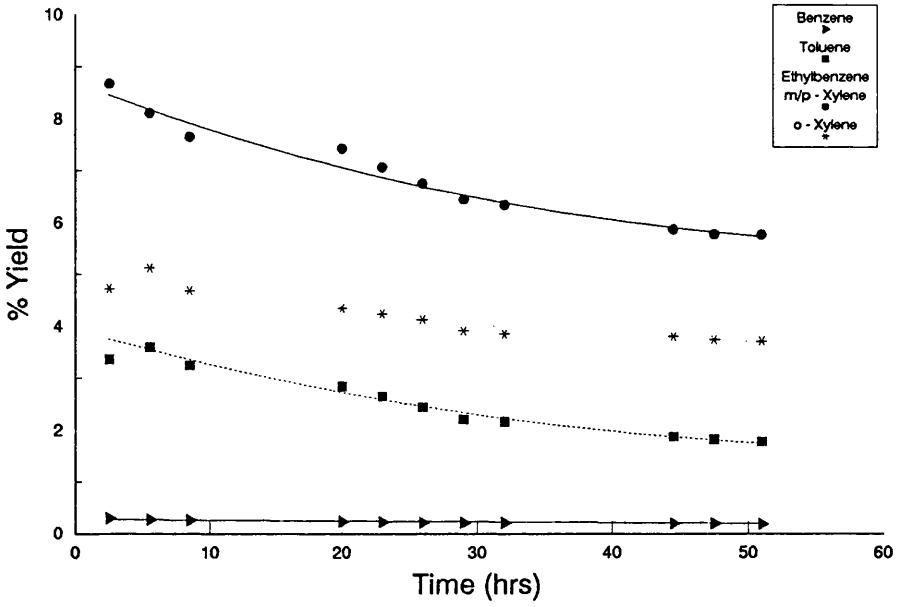

Figure 6.1.5. % Yield to Aromatic Products on EUROPT-3.1.

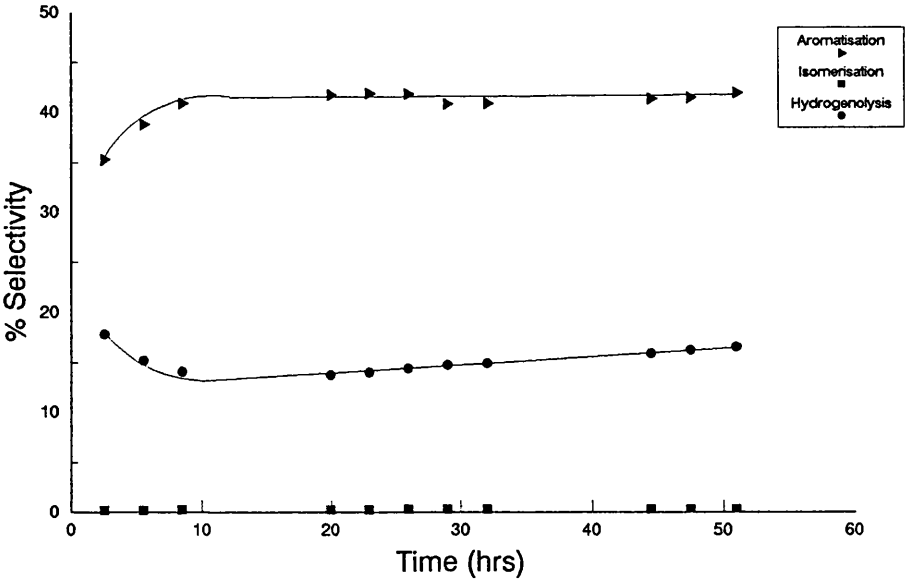

Figure 6.1.6. % Selectivity to Major Reactions on EUROPT-3.1.

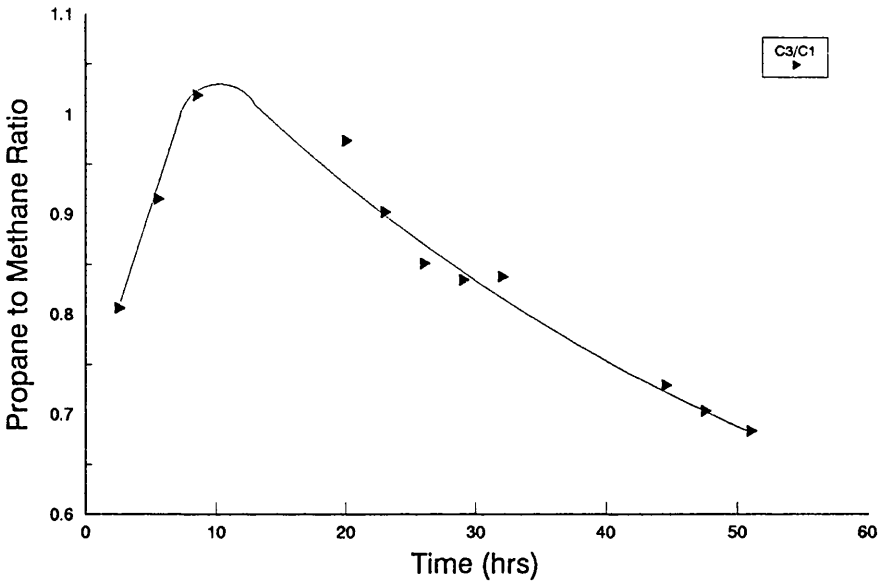

Figure 6.1.7. Propane to Methane Ratio on EUROPT-3.1.

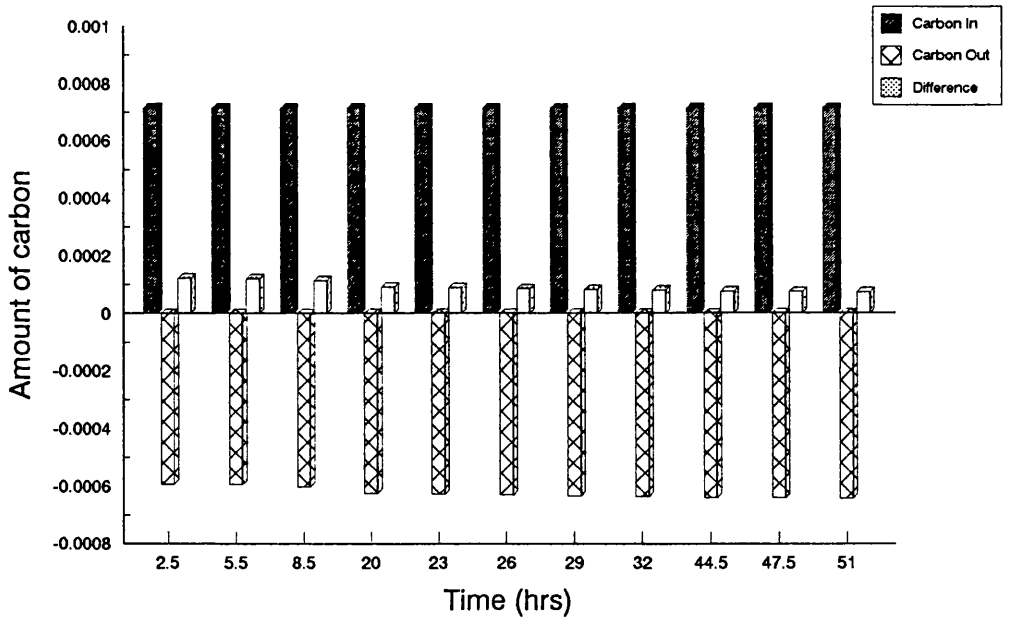

Figure 6.1.8. The Carbon Mass Balance on EUROPT-3.1.

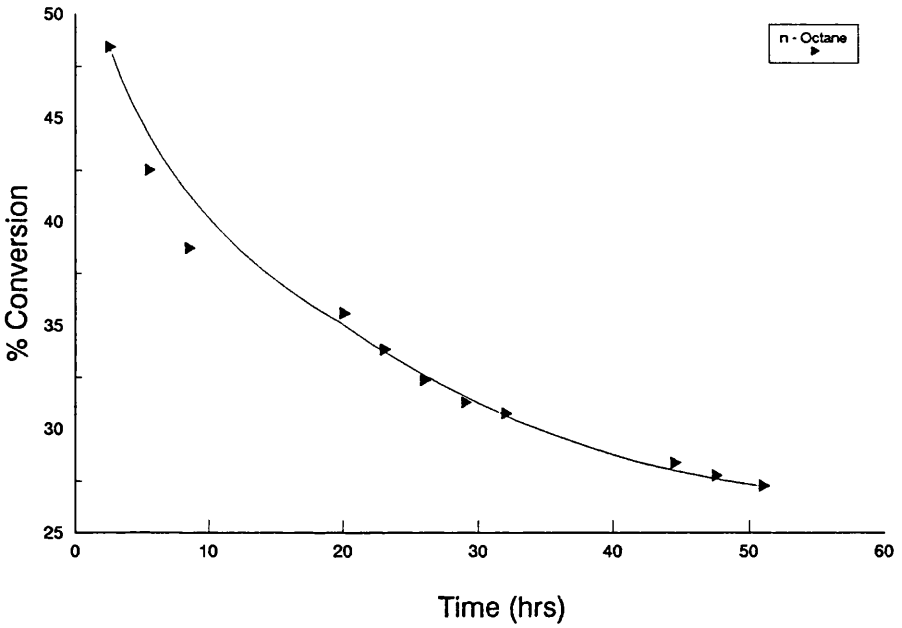

Figure 6.1.9. % Conversion of n-Octane on EUROPT-3.1.

decreased below that of i-octane. The i-pentane yield declined rapidly initially and then gradually until the reaction was stopped whereas the yield of i-hexane declined steadily throughout this study.

The yield of n-paraffins was similar to that of cycloparaffins, extremely small, as shown in Figure 6.1.4. No n-pentane could be detected until after 20 hours on stream. The yield of n-hexane and n-heptane in comparison decreased steadily with time and did not show any sign of reaching a constant level.

The full range of expected aromatic products; benzene, toluene, ethylbenzene, m/p-xylene and o-xylene, was found and the yield plotted against reaction time in Figure 6.1.5. C_9 aromatic species could be detected in several samples but the yields were very small and inconsistent and consequently they are not reported in these studies. The yield of all aromatic products follows a similar trend, decreasing with time on stream. The principal aromatic product throughout this run was found to be ethylbenzene/m/p-xylene followed by o-xylene, toluene and finally benzene. A steady level of conversion was reached before the reaction was stopped in all cases.

The selectivity to individual hydrocarbon products is detailed in Table 6.1.2. The selectivities of the major reactions are summarised in Figure 6.1.6. Hydrocracking selectivity was not calculated for EUROPT-3.1 due to the combination of the i- and n-butane yields. A rapid decline in the hydrogenolysis activity was observed in the first 10 hours, but the level then rose steadily to ~15%. Aromatisation activity differed by undergoing an initial increase to ~42% and then

maintaining this level throughout the run. The isomerisation activity was seen to increase with reaction time. Hydrocracking activity, although not calculated, exceeded that of isomerisation throughout the run. Therefore, summation of the major reactions results in the following sequence:

Aromatisation > Hydrogenolysis > Hydrocracking > Isomerisation

The ratio of propane to methane is illustrated in Figure 6.1.7 as a function of the reaction time. The C_3/C_1 ratio increases steadily and reaches a maximum value of 1.1 after ~12 hours on stream. This initial rise demonstrates that the metal component is being deactivated preferentially in the first 12 hours of the reaction. The ratio steadily decreases after this indicating that the acidic sites are being deactivated slowly after the initial period of rapid coke laydown.

The carbon mass balance (CMB), Figure 6.1.8 and Table 6.1.3, shows that in the initial 20 hours of the experiment a large difference in the carbon going into and coming out of the reactor has been found. This difference in carbon has been attributed to coke deposition upon the catalyst surface and slowly decreases with time. This corresponds to fewer sites being available for coking as the coke laydown on the surface increases.

The total conversion of n-octane on EUROPT-3.1, shown in Figure 6.1.9, decreases rapidly from 48 to 27%. A constant conversion was not reached after 50 hours on stream but the deactivation rate had decreased drastically. The % coke deposited upon the surface of the spent catalyst is detailed in Table 6.1.

6.2. EUROPT-3.2 (490°C, 110 psig)

The reaction conditions were as described in the previous Section except that the reaction was carried out at 490°C. The results of this run are expressed in Tables 6.2.1 to 6.2.3 and Figures 6.2.1 to 6.2.7.

The yield of C_1 - C_4 species, as shown in Figure 6.2.1, decreases steadily throughout the 70 hours on stream. Methane is by far the dominant species followed closely by propane and finally ethane with a steady yield being gained after ~40 hours on stream. Iso- and n-butane were separable in this run with the yield of n-butane being approximately 3 times that of i-butane. Both yields reach a constant level before the reaction was stopped.

Figure 6.2.2 illustrates the yield of cycloparaffins from n-octane. The yield of these species is very small and decrease to a steady state with time. Cyclopentane dominates throughout the run followed initially by cyclopentane and then cyclohexane. However after 20 hours on stream the yield of cyclopentane falls below that of cyclohexane. The conversion to i-paraffins is shown in Figure 6.2.3. The combined yields of both i- and n-pentane and cyclo- and i-octane are quoted in Figure 6.2.3. The combined yield of i- and n-pentane decreases steadily while the remainder are approximately constant throughout the run. The yield of n-hexane and n-heptane both decrease with reaction time as shown in Figure 6.2.4, reaching a steady level before the reaction is stopped.

Table 6.2.1. %Yield of individual products and % Conversion versus time-on-stream for EUROPT-3.2.

Products	The % Yield of Selected Products											
Time (hrs)	1.5	4	19	22.05	25	28	42	45	48	51	66.35	69.5
Benzene	0.1604	0.1406	0.0692	0.0644	0.0565	0.0503	0.0326	0.0309	0.0285	0.0264	0.0222	0.0227
Toluene	4.5048	4.1080	1.9975	1.8109	1.5137	1.3597	0.9763	0.8689	0.8329	0.8277	0.7742	0.7801
Ethylbenzene	0.3016	0.2061	0.1282	0.0947	0.0797	0.0750	0.0555	0.0517	0.0494	0.0424	0.0408	0.0391
m/p - Xylene	3.6813	3.0809	1.9923	1.6494	1.5291	1.2447	0.9352	0.8252	0.7872	0.7065	0.6152	0.6298
o - Xylene	1.4113	1.2551	0.4706	0.4370	0.3776	0.3483	0.2713	0.2774	0.2623	0.2501	0.1691	0.1733
Methane	11.624	10.455	7.6505	7.3306	6.8980	6.2741	5.5832	5.4898	5.4166	5.4482	5.5428	5.5274
Ethane	4.9460	4.5118	4.2052	4.0331	3.8180	3.7627	3.7257	3.7060	3.7104	3.7085	3.6492	3.5873
Propane	8.3311	8.1317	6.9742	6.5651	6.2290	5.8258	5.1602	5.0320	4.9139	4.8747	4.8104	4.7973
i-Butane	2.9195	2.7618	2.3835	2.1615	2.0295	1.9720	1.7235	1.6909	1.5760	1.4973	1.2371	1.2175
n-Butane	8.4061	7.9993	6.1324	6.8932	6.5387	6.3892	5.7352	5.6795	5.3770	5.1459	4.7323	4.6257
Cyclopentane	0.0031	0.0021	0.0009	0.0009	0.0008	0.0007	0.0006	0.0005	0.0005	0.0005	0.0004	0.0003
i-Pentane n-Pentane	0.0887	0.0851	0.0781	0.0700	0.0623	0.0549	0.0504	0.0460	0.0410	0.0377	0.0324	0.0295
Cyclohexane	0.0016	0.0012	0.0011	0.0010	0.0009	0.0008	0.0527	0.0008	0.0008	0.0460	0.0007	0.0429
i-Hexane	0.0297	0.0287	0.0246	0.0224	0.0207	0.0189		0.0169	0.0167		0.0146	
n-Hexane	0.0521	0.0467	0.0430	0.0385	0.0358	0.0337		0.0324	0.0325		0.0295	
Cycloheptane	0.0049	0.0046	0.0031	0.0029	0.0027	0.0026	0.0024	0.0021	0.0019	0.0018	0.0134	0.0015
i-Heptane	0.0187	0.0178	0.0152	0.0151	0.0149	0.0149	0.0146	0.0145	0.0143	0.0139		0.0132
n-Heptane	0.0385	0.0364	0.0346	0.0329	0.0322	0.0300	0.0288	0.0292	0.0283	0.0273	0.0258	0.0259
Cyclooctane i-Octane	0.0303	0.0297	0.0255	0.0250	0.0246	0.0246	0.0243	0.0231	0.0228	0.0223	0.0218	0.0218
Conversion of n-Octane	46.5539	42.9023	32.2297	31.2486	29.2647	27.4829	24.3724	23.8178	23.1128	22.6772	21.7318	21.3314

Table 6.2.2. %Selectivity of individual products versus time-on-stream for EUROPT-3.2.

Products	The % Selectivity of Selected Products											
Time (hrs)	1.5	4	19	22.05	25	28	42	45	48	51	66.35	69.5
Benzene	0.3445	0.3278	0.2148	0.2060	0.1932	0.1829	0.1339	0.1298	0.1233	0.1165	0.1020	0.1063
Toluene	9.6766	9.5752	6.1976	5.7950	5.1723	4.9474	4.0056	3.6480	3.6036	3.6500	3.5624	3.6571
Ethylbenzene	0.6479	0.4804	0.3977	0.3031	0.2725	0.2730	0.2276	0.2170	0.2136	0.1872	0.1876	0.1835
m/p - Xylene	7.9076	7.1811	6.1816	5.2784	5.2250	4.5289	3.8370	3.4646	3.4059	3.1154	2.8308	2.9524
o - Xylene	3.0316	2.9255	1.4601	1.3985	1.2901	1.2674	1.1130	1.1645	1.1347	1.1030	0.7782	0.8126
Methane	24.969	24.368	23.738	23.459	23.571	22.829	22.908	23.049	23.435	24.025	25.506	25.912
Ethane	10.624	10.516	13.048	12.906	13.047	13.691	15.286	15.560	16.053	16.353	16.792	16.817
Propane	17.896	18.954	21.639	21.009	21.285	21.198	21.172	21.127	21.260	21.496	22.135	22.490
i-Butane	6.2713	6.4374	7.3952	6.9170	6.9349	7.1755	7.0716	7.0992	6.8188	6.6026	5.6927	5.7076
n-Butane	18.057	18.645	19.027	22.059	22.343	23.248	23.532	23.846	23.264	22.692	21.776	21.685
Cyclopentane	0.0067	0.0049	0.0029	0.0029	0.0027	0.0025	0.0025	0.0022	0.0020	0.0020	0.0017	0.0015
i-Pentane n-Pentane	0.1905	0.1984	0.2422	0.2242	0.2130	0.2000	0.2083	0.1933	0.1772	0.1663	0.1492	0.1384
Cyclohexane	0.0034	0.0029	0.0033	0.0031	0.0031	0.0028	0.2163	0.0034	0.0034	0.2027	0.0031	0.2012
i-Hexane	0.0638	0.0669	0.0765	0.0718	0.0709	0.0688		0.0711	0.0722		0.0671	
n-Hexane	0.1120	0.1089	0.1333	0.1233	0.1222	0.1226		0.1360	0.1406		0.1357	
Cycloheptane	0.0104	0.0107	0.0096	0.0091	0.0092	0.0095	0.0097	0.0090	0.0084	0.0081	0.0618	0.0069
i-Heptane	0.0402	0.0416	0.0470	0.0482	0.0510	0.0541	0.0601	0.0610	0.0621	0.0615		0.0619
n-Heptane	0.0828	0.0849	0.1075	0.1054	0.1100	0.1090	0.1181	0.1226	0.1223	0.1202	0.1189	0.1216
Cyclooctane i-Octane	0.0651	0.0691	0.0791	0.0801	0.0840	0.0894	0.0997	0.0968	0.0984	0.0983	0.1005	0.1020

Table 6.2.3. Carbon Mass Balance of the EUROPT-3.2. catalyst

Time (hrs)	No. of moles of Carbon In	No. of moles of Carbon Out	Δ Carbon
1.5	1.6924×10^{-4}	1.4864×10^{-4}	2.0603×10^{-5}
4	1.6924×10^{-4}	1.5139×10^{-4}	1.7853×10^{-5}
19	1.6924×10^{-4}	1.5321×10^{-4}	1.6035×10^{-5}
22.05	1.6924×10^{-4}	1.5410×10^{-4}	1.5140×10^{-5}
25	1.6924×10^{-4}	1.5559×10^{-4}	1.3651×10^{-5}
28	1.6924×10^{-4}	1.5985×10^{-4}	9.3932×10^{-6}
42	1.6924×10^{-4}	1.5995×10^{-4}	9.2918×10^{-6}
45	1.6924×10^{-4}	1.5999×10^{-4}	9.2539×10^{-6}
48	1.6924×10^{-4}	1.6040×10^{-4}	8.8432×10^{-6}
51	1.6924×10^{-4}	1.6085×10^{-4}	8.3897×10^{-6}
66.35	1.6924×10^{-4}	1.6215×10^{-4}	7.0927×10^{-6}
69.5	1.6924×10^{-4}	1.6216×10^{-4}	7.0790×10^{-6}

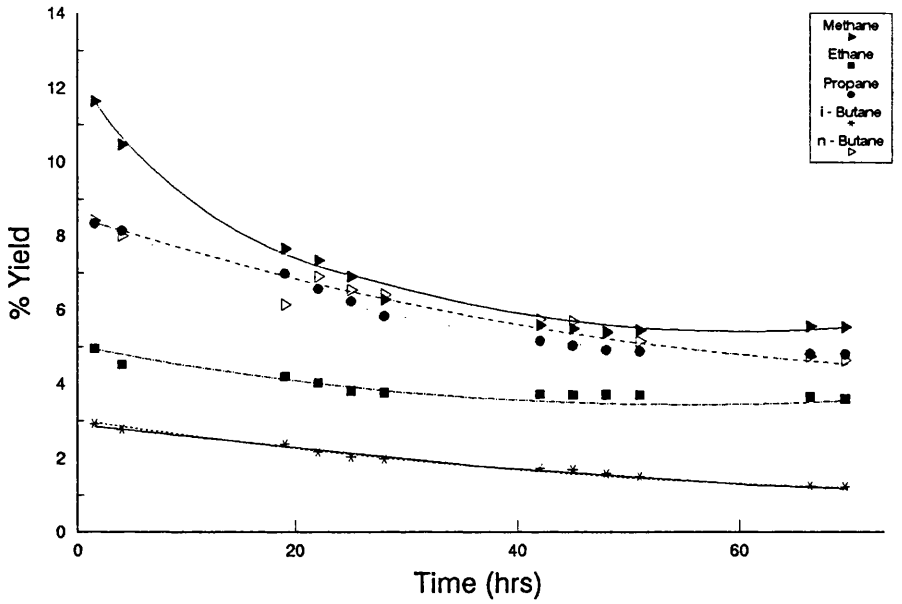

Figure 6.2.1. % Yield to Individual Hydrocarbon Products on EUROPT-3.2.

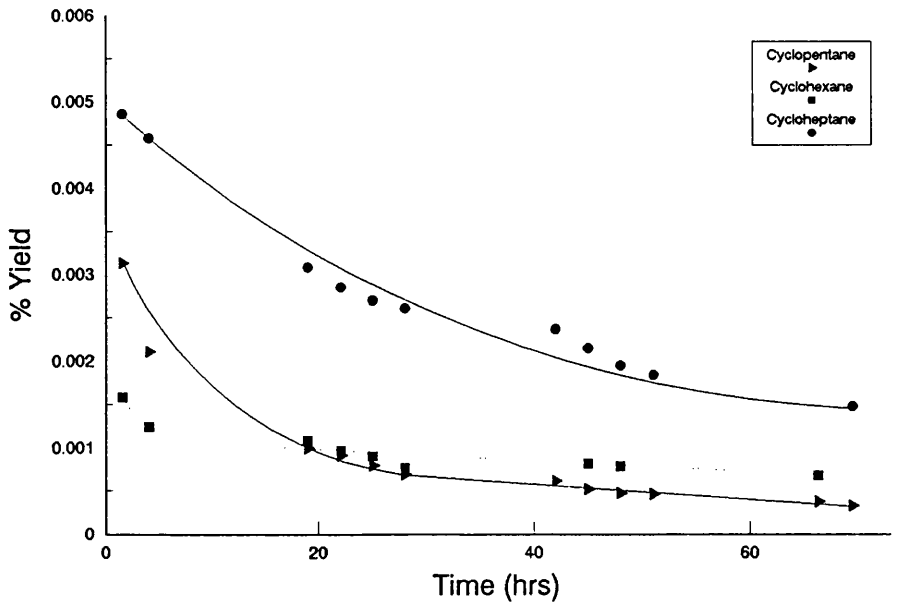

Figure 6.2.2. % Yield to Cycloparaffin Products on EUROPT-3.2.

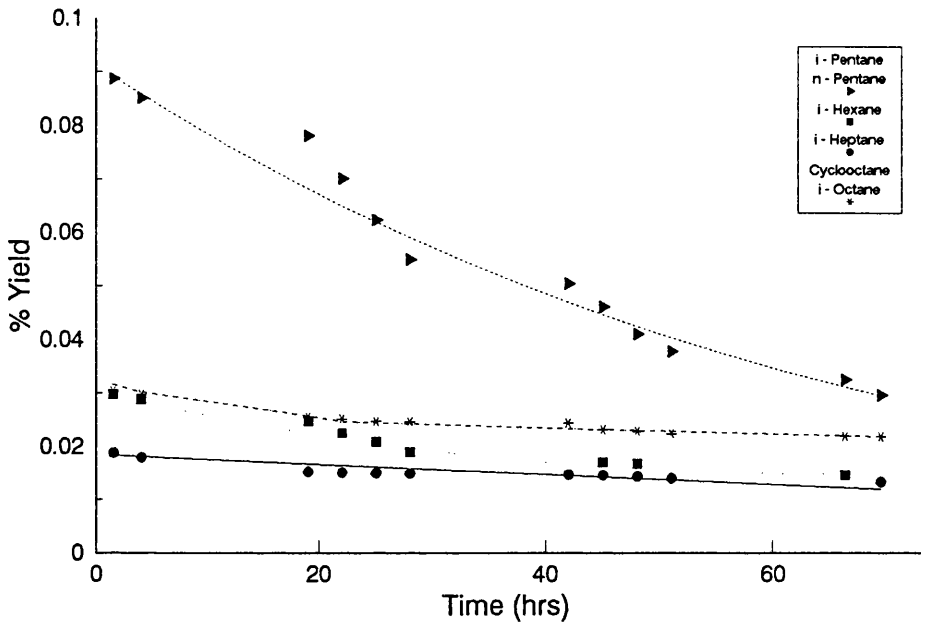

Figure 6.2.3. % Yield to Paraffin Products on EUROPT-3.2.

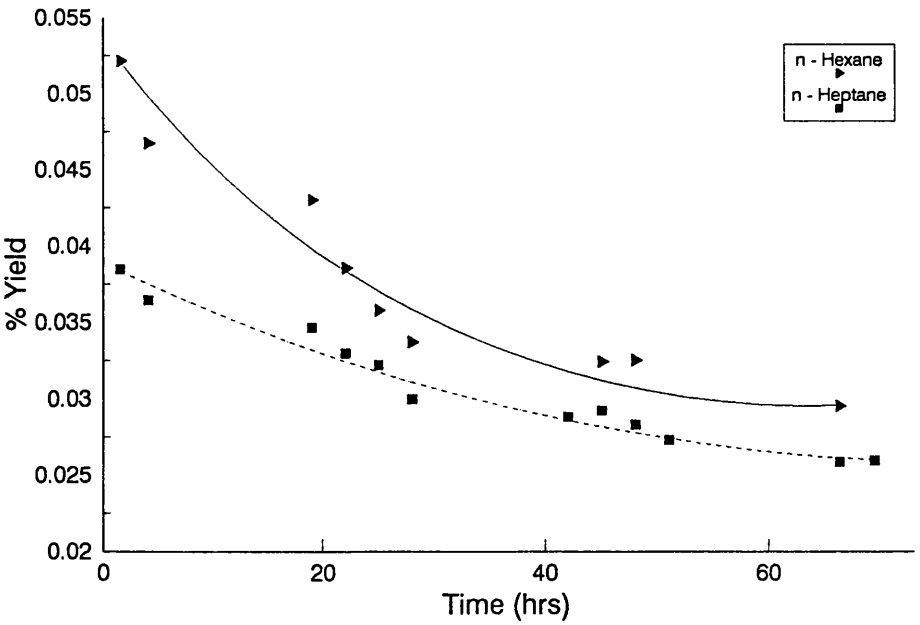

Figure 6.2.4. % Yield to n-Paraffins on EUROPT-3.2.

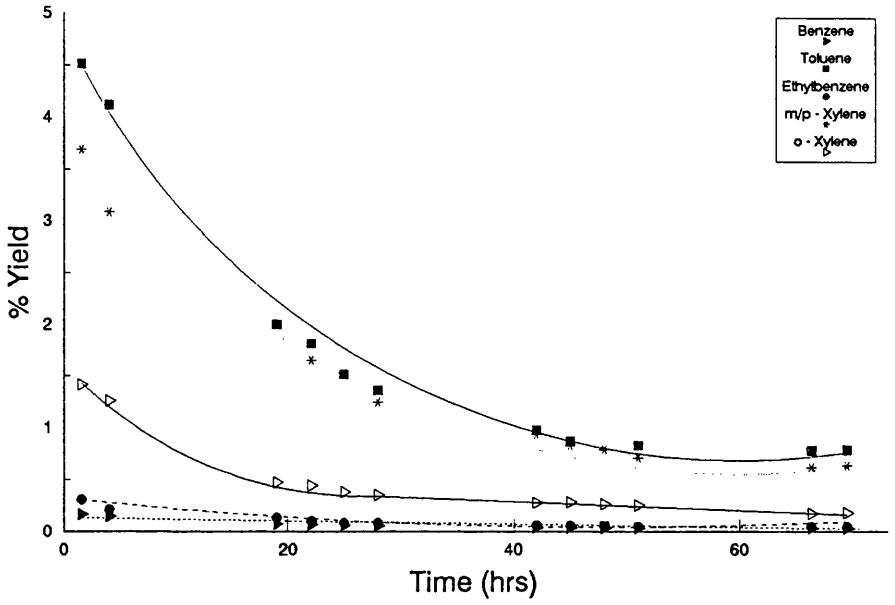

Figure 6.2.5. % Yield to Aromatic Products on EUROPT-3.2.

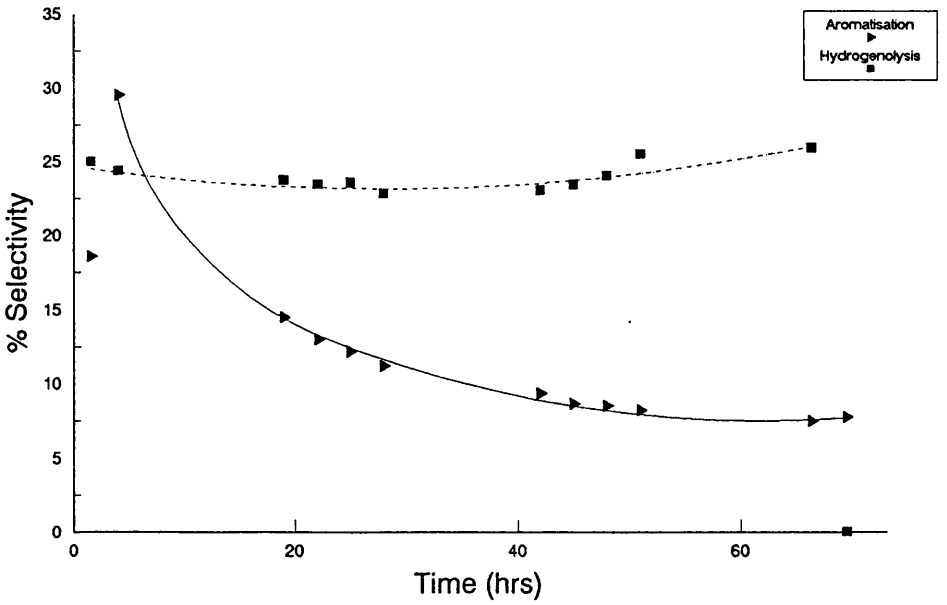

Figure 6.2.6. % Selectivity to the Major Reactions on EUROPT-3.2.

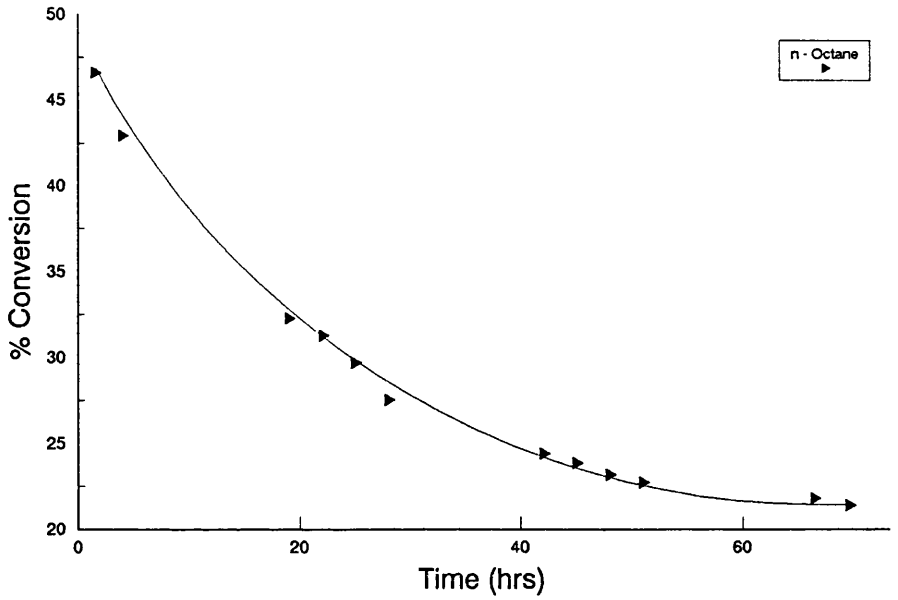

Figure 6.2.7. % Conversion of n-Octane on EUROPT-3.2.

The yield of aromatics followed a different trend than that observed at 510°C. Toluene is the dominant product in this run followed by m/p-xylene, o-xylene, ethylbenzene and then benzene. All these species undergo a rapid decline before stabilising to a constant ratio. This is especially noticeable in the case of both toluene and m/p-xylene.

All product yields were considerably lower, with the exception of methane, when compared to the run at the higher temperature. The yield of methane increased slightly from the value obtained at 510°C.

The selectivity of individual products is shown in Table 6.2.2 and the selectivity to the major reactions is shown in Figure 6.2.6. The aromatisation activity decreases sharply in the first 20 hours of the reaction before reaching a constant level after ~68 hours. The hydrogenolysis activity on the other hand is seen to increase steadily becoming the dominant reaction after ~7 hours on stream. Hydrocracking and isomerisation reactions, though not included in Figure 6.2.6, have lower activities. The order of the selectivities to the major reactions at 490°C is as follows:

Hydrogenolysis > Aromatisation > Hydrocracking > Isomerisation

The aromatisation activity is approximately ¼ that at 510°C after 50 hours on stream. The hydrogenolysis activity was higher in this run than at the higher temperature.

The ratio of propane to methane, as seen before, increases steadily to a value of ~0.925 after 25 hours before falling steadily to the end of the reaction. The carbon

mass balance, Table 6.2.3, shows that the carbon deposition decreases with increasing reaction time. The results of both the CMB and the C_3/C_1 ratio suggests that after an initial large deposition of carbon on the metallic sites the coke is deposited slowly onto the acidic sites on the support.

The total conversion of n-octane is expressed in Figure 6.2.7. As with the reaction at 510°C, the conversion falls constantly before reaching a steady level. However at this lower temperature the conversion of n-octane is ~5% lower than that at 510°C.

The % coke deposited upon the catalyst surface, detailed in Table 6.1, is less than that deposited on the EUROPT-3 catalyst at the higher temperature. Therefore decreasing the temperature results in a corresponding decrease in both the carbon deposition and the aromatic production. The hydrogenolysis activity, in contrast, was found to increase when the temperature is decreased. The overall conversion of n-octane and the corresponding yields of individual products is lower explaining why reforming reactions are carried out at such high temperatures.

6.3. EUROPT-4.1 (510°C, 110 psig)

The catalyst tested, under reaction conditions stated previously in Section 6.1, for 51 hours was a bimetallic 0.3wt%Pt-0.3wt%Re/Al_2O_3-Cl (EUROPT-4) catalyst. The results of this run are shown in Tables 6.3.1 to 6.3.3 and in Figures 6.3.1 to 6.3.7.

Table 6.3.1. %Yield of individual products and % Conversion versus time-on-stream for EUROPT-4.1.

Products	The % Yield of Selected Products										
Time (hrs)	2.5	5.5	8.5	20.25	23.25	26.25	29.25	32.25	44	47	50.5
Benzene	0.5789	0.6520	0.7102	0.7737	0.8256	0.7977	0.8454	0.8608	0.8755	0.8678	0.8802
Toluene	4.3724	3.7680	3.4850	3.1059	3.0073	2.9333	2.8461	2.5828	2.4616	2.4412	2.3949
Ethylbenzene	10.092	10.925	11.151	11.909	12.266	12.468	12.271	12.183	12.181	12.030	12.180
m/p-Xylene											
o-Xylene	5.6403	5.9310	6.9814	7.5911	7.8829	8.2181	8.2391	8.3019	8.3454	8.4052	8.3870
Methane	10.349	7.4813	5.6977	5.2031	4.8944	4.6549	4.3912	4.1680	3.8981	3.8213	3.7894
Ethane	5.0854	4.3040	3.7928	3.4374	2.8973	2.6392	2.5107	2.5855	2.4268	2.3231	2.3212
Propane	7.1020	6.3296	6.1018	5.4030	5.2072	5.1910	5.0332	4.9853	4.7055	4.6317	4.5915
i-Butane	4.0021	2.9966	2.0129	1.6967	1.4012	1.1708	1.2098	1.3992	1.3034	1.2999	1.3017
n-Butane	9.4899	7.2918	6.6461	5.8762	5.1050	4.4612	3.7002	4.0600	3.9997	3.9841	3.9880
Cyclopentane	0.0006	0.0011	0.0017	0.0033	0.0045	0.0052	0.0058	0.0054	0.0055	0.0055	0.0056
i-Pentane	0.0866	0.1066	0.1169	0.1420	0.1490	0.1576	0.1663	0.1676	0.2116	0.2144	0.2177
n-Pentane	0.0008	0.0012	0.0015	0.0032	0.0039	0.0041	0.0043	0.0043	0.0043	0.0043	0.0043
Cyclohexane	0.0002	0.0004	0.0007	0.0018	0.0032	0.0047	0.0059	0.0065	0.0084	0.0085	0.0086
i-Hexane	0.0188	0.0305	0.0402	0.0551	0.0608	0.0642	0.0693	0.0746	0.0841	0.0852	0.0852
n-Hexane	0.0019	0.0033	0.0034	0.0070	0.0079	0.0087	0.0100	0.0109	0.0143	0.0145	0.0146
Cycloheptane	0.0011	0.0013	0.0015	0.0017	0.0018	0.0019	0.0020	0.0021	0.0028	0.0029	0.0029
i-Heptane	0.1487	0.1607	0.1653	0.2142	0.2211	0.2305	0.2421	0.2483	0.2502	0.2523	0.2561
n-Heptane	0.0052	0.0067	0.0083	0.0101	0.0105	0.0112	0.0121	0.0135	0.0159	0.0178	0.0182
Cyclooctane	0.0113	0.0114	0.0119	0.0150	0.0164	0.0172	0.0181	0.0199	0.0224	0.0247	0.0255
i-Octane	0.0318	0.0369	0.0436	0.0632	0.0936	0.1065	0.1166	0.1285	0.1341	0.1366	0.1367
% Conversion of n-Octane	57.0192	50.0395	46.9741	45.5128	44.1547	43.1458	41.6990	41.8084	40.9510	40.5708	40.6094

Table 6.3.2. %Selectivity of individual products versus time-on-stream for EUROPT-4.1.

Products	The % Selectivity of Selected Products										
Time (hrs)	2.5	5.5	8.5	20.25	23.25	26.25	29.25	32.25	44	47	50.5
Benzene	1.0153	1.3030	1.5118	1.6999	1.8699	1.8487	2.0275	2.0589	2.1378	2.1389	2.1674
Toluene	7.6682	7.5301	7.4189	6.8242	6.8108	6.7985	6.8253	6.1777	6.0110	6.0172	5.8975
Ethylbenzene m/p-Xylene	17.699	21.833	23.739	26.167	27.780	28.897	29.427	29.141	29.746	29.651	29.994
o-Xylene	9.8920	11.8527	14.8623	16.679	17.853	19.047	19.759	19.857	20.379	20.717	20.653
Methane	18.150	14.951	12.130	11.432	11.085	10.789	10.531	9.9693	9.5190	9.4189	9.3313
Ethane	8.9187	8.6012	8.0743	7.5525	6.5617	6.1169	6.0211	6.1841	5.9262	5.7260	5.7159
Propane	12.455	12.649	12.990	11.871	11.793	12.031	12.070	11.924	11.491	11.416	11.306
i-Butane	7.0189	5.9885	4.2851	3.7279	3.1735	2.7136	2.9013	3.3467	3.1829	3.2040	3.2053
n-Butane	16.643	14.572	14.149	12.911	11.562	10.340	8.8735	9.7109	9.7670	9.8200	9.8204
Cyclopentane	0.0010	0.0021	0.0035	0.0073	0.0102	0.0121	0.0140	0.0130	0.0133	0.0135	0.0138
i-Pentane	0.1519	0.2131	0.2489	0.3119	0.3374	0.3653	0.3988	0.4008	0.5167	0.5283	0.5361
n-Pentane	0.0014	0.0024	0.0032	0.0069	0.0088	0.0094	0.0102	0.0104	0.0106	0.0107	0.0107
Cyclohexane	0.0004	0.0009	0.0014	0.0040	0.0073	0.0108	0.0142	0.0156	0.0206	0.0210	0.0213
i-Hexane	0.0329	0.0610	0.0856	0.1210	0.1376	0.1488	0.1661	0.1785	0.2053	0.2101	0.2097
n-Hexane	0.0034	0.0065	0.0073	0.0154	0.0178	0.0202	0.0240	0.0261	0.0350	0.0357	0.0358
Cycloheptane	0.0019	0.0025	0.0032	0.0037	0.0040	0.0043	0.0048	0.0051	0.0068	0.0071	0.0070
i-Heptane	0.2608	0.3212	0.3519	0.4706	0.5007	0.5343	0.5805	0.5938	0.6111	0.6219	0.6306
n-Heptane	0.0091	0.0134	0.0177	0.0221	0.0239	0.0260	0.0290	0.0323	0.0389	0.0438	0.0449
Cyclooctane	0.0198	0.0229	0.0253	0.0329	0.0372	0.0400	0.0434	0.0476	0.0548	0.0609	0.0629
i-Octane	0.0558	0.0737	0.0928	0.1389	0.2119	0.2469	0.2796	0.3074	0.3274	0.3367	0.3366

Table 6.3.3. Carbon Mass Balance of the EUROPT-4.1. catalyst

Time (hrs)	No. of moles of Carbon In	No. of moles of Carbon Out	Δ Carbon
2.5	9.6151×10^{-4}	9.2113×10^{-4}	4.0373×10^{-5}
5.5	9.6151×10^{-4}	9.3166×10^{-4}	2.9847×10^{-5}
8.5	9.6151×10^{-4}	9.3955×10^{-4}	2.1956×10^{-5}
20.25	9.6151×10^{-4}	9.4402×10^{-4}	1.7482×10^{-5}
23.25	9.6151×10^{-4}	9.4809×10^{-4}	1.3415×10^{-5}
26.25	9.6151×10^{-4}	9.5399×10^{-4}	7.5154×10^{-6}
29.25	9.6151×10^{-4}	9.5575×10^{-4}	5.7597×10^{-6}
32.25	9.6151×10^{-4}	9.5604×10^{-4}	5.4643×10^{-6}
44	9.6151×10^{-4}	9.5981×10^{-4}	1.6919×10^{-6}
47	9.6151×10^{-4}	9.6088×10^{-4}	6.2382×10^{-7}
50.5	9.6151×10^{-4}	9.6104×10^{-4}	4.6801×10^{-7}

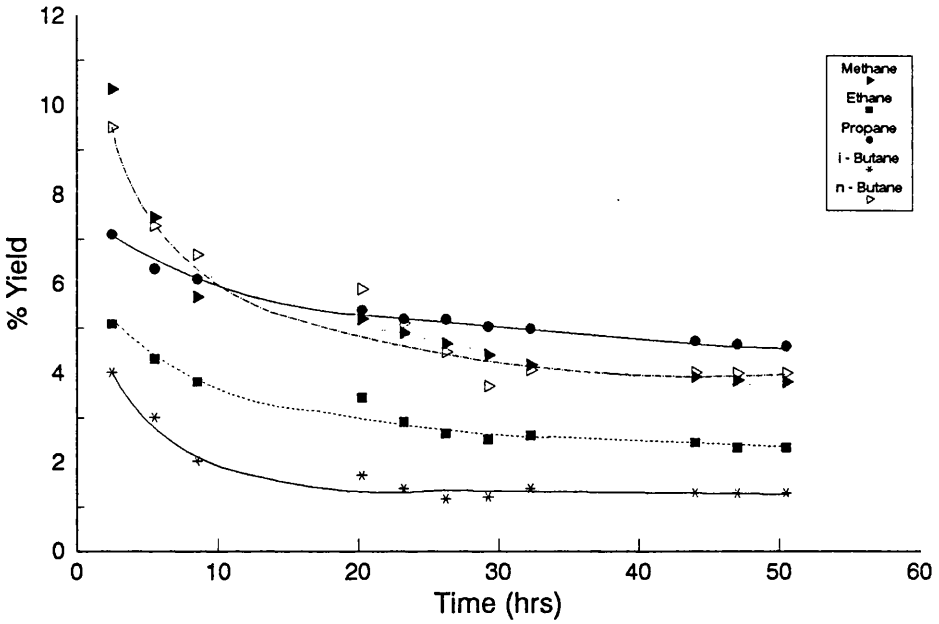

Figure 6.3.1. % Yield to Individual Hydrocarbon Products on EUROPT-4.1.

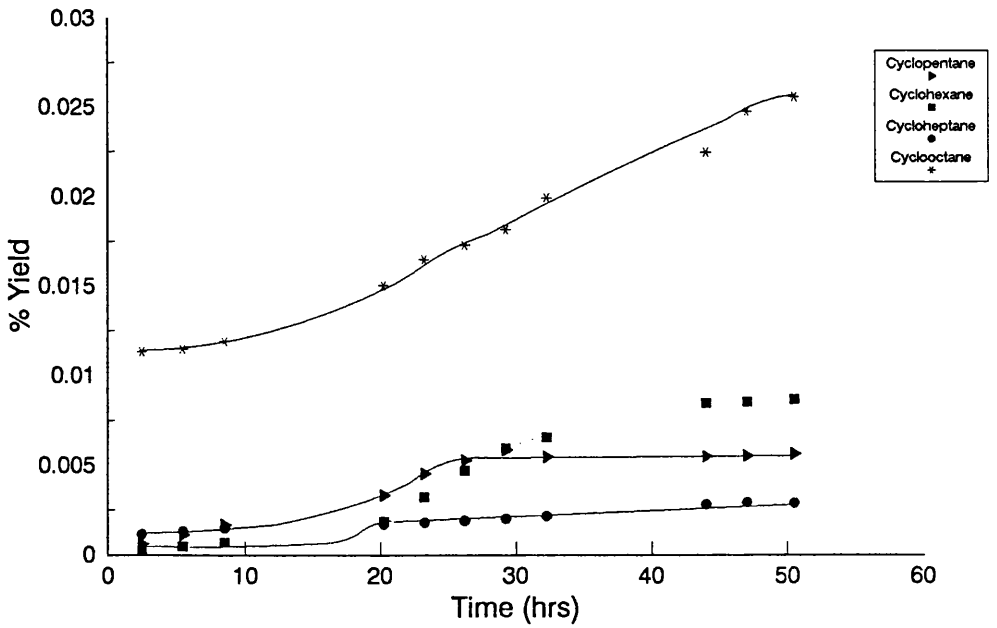

Figure 6.3.2. % Yield to Cycloparaffin Products on EUROPT-4.1.

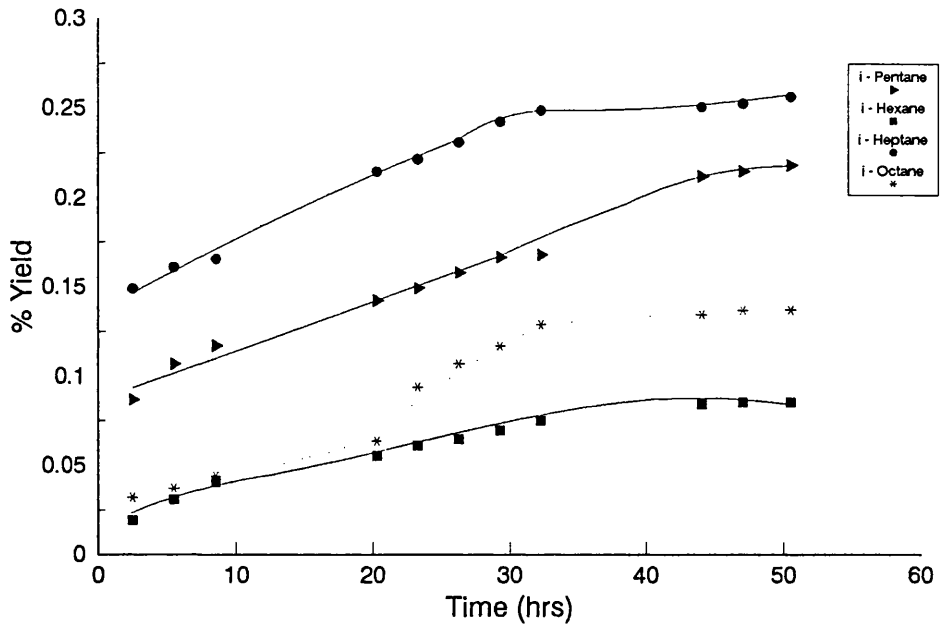

Figure 6.3.3. % Yield of i-Paraffin Products on EUROPT-4.1.

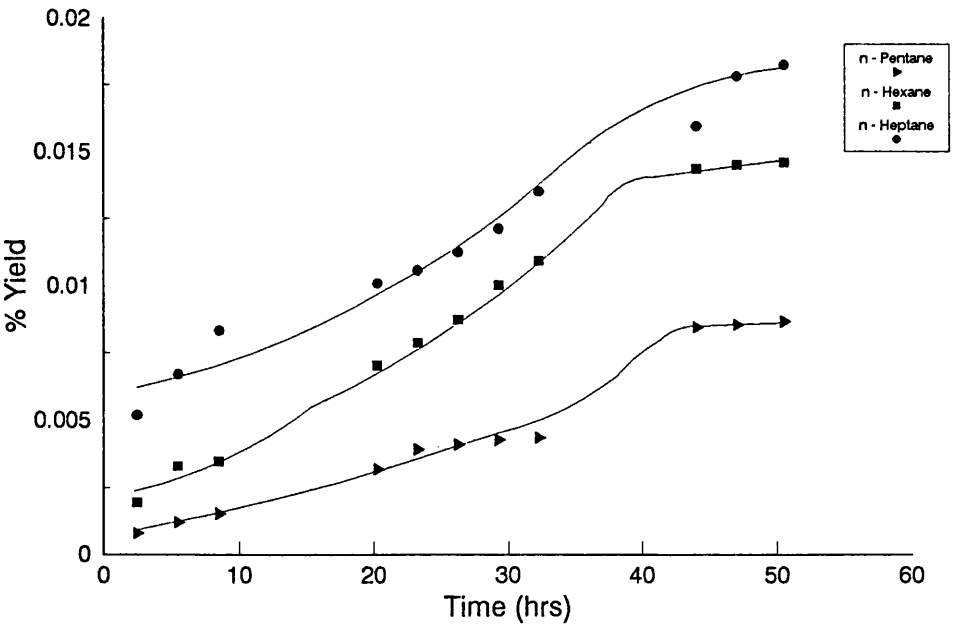

Figure 6.3.4. % Yield of n-Paraffin Products on EUROPT-4.1.

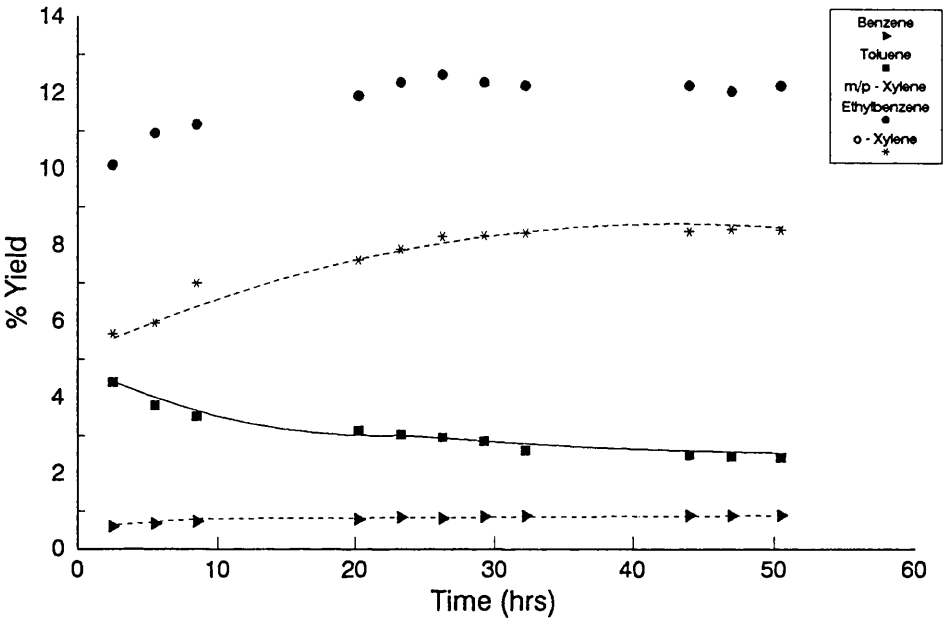

Figure 6.3.5. % Yield of Aromatic Products on EUROPT-4.1.

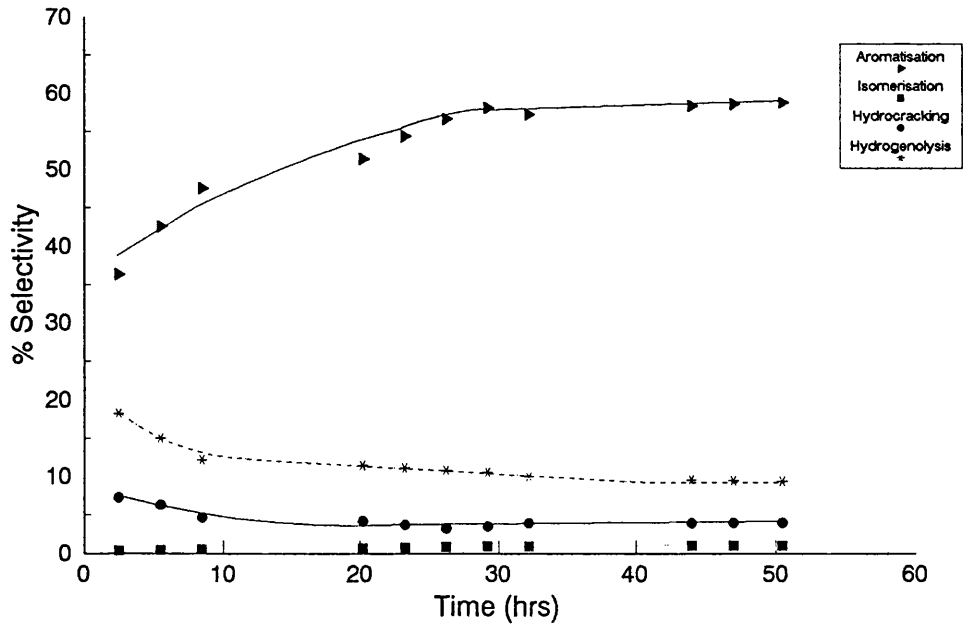

Figure 6.3.6. % Selectivity to the Major Reactions on EUROPT-4.1.

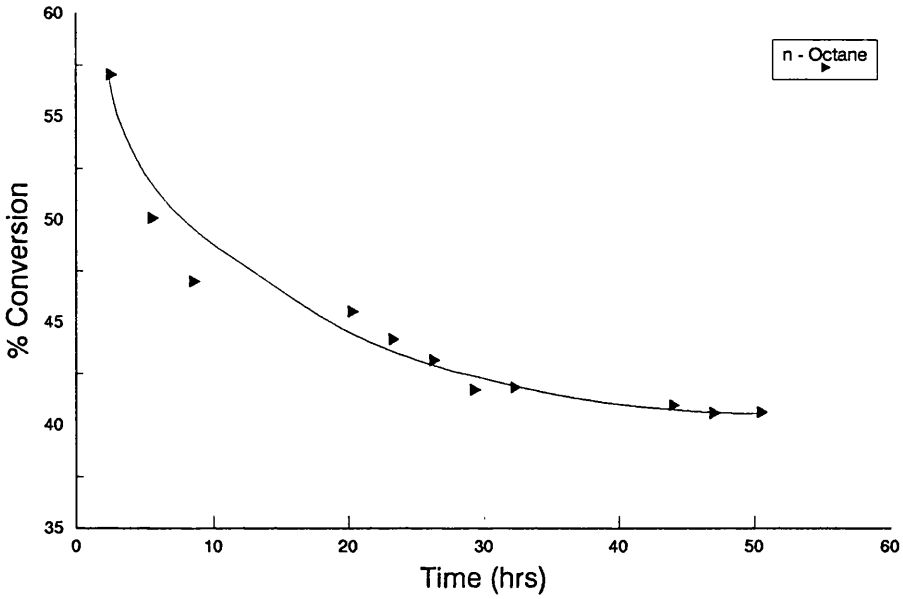

Figure 6.3.7. % Conversion of n-Octane on EUROPT-4.1.

Figure 6.3.1 displays the yield of C_1 - C_4 products with respect to the reaction time. The yields of these species decrease rapidly before reaching a steady conversion. Initially methane is dominant but after ~10 hours on stream propane becomes the dominant product. The yield of methane declines sharply whereas that of propane decreases slowly with time on stream. Ethane is always produced in lower quantities than either methane or propane. The yields of i- and n-butane both decrease sharply in the first 15 hours of the reaction before reaching a constant level. The yield of n-butane is approximately 3 - 4 times higher than that of i-butane throughout the run.

The yield of both cycloparaffins and n-paraffins is very small when compared to other product yields. The yield of cycloparaffins is seen in Figure 6.3.2 to increase with time and with carbon number initially. After ~26 hours, however, the yield of cyclohexane becomes greater than that of cyclooctane. Figure 6.3.3 illustrates that the yield of i-paraffins increases with time reaching a constant level after ~35 hours. The conversion to i-heptane is greatest followed by i-pentane, i-octane and finally i-hexane. The yield of n-paraffins, Figure 6.3.4. increases with reaction time and again with carbon number.

The conversion of n-octane to aromatics produced the full complement of expected products. The yields of ethylbenzene/m/p-xylene, benzene and o-xylene all increase with time as shown in Figure 6.3.5. The yield of toluene in comparison decreases slightly over the 50 hours on stream. The combined yields of ethylbenzene and m/p-xylene (~13%) are the most abundant, closely followed by o-

xylene (~8%). The yield of toluene despite decreasing is followed by benzene which is produced in very small quantities. The overall aromatic trend is the same as that produced with the monometallic EUROPT-3.1 catalyst. But in contrast to the results with EUROPT-3.1 the yields of all aromatic species, except toluene, increased with time on EUROPT-4.1.

The selectivities calculated for the individual products are shown in Table 6.3.2. Selectivity to the major reactions, shown in Figure 6.3.6, illustrates the following order:

Aromatisation > *Hydrogenolysis* > Hydrocracking > Isomerisation

Aromatisation and isomerisation activities both increase whereas those of hydrogenolysis and hydrocracking decrease with time. Aromatisation activity increases from 36% to a constant 58% after 30 hours on stream. In comparison on EUROPT-3, under the same conditions, the activity rose from 35 to 42% over the same period of time. In addition the hydrogenolysis activity on EUROPT-4.1 (~9%) is approximately half that on EUROPT-3.1 (16%) after 50 hours on stream. The production of n-paraffin species is also higher than that observed on EUROPT-3.1 under the same conditions.

The propane to methane ratio for EUROPT-4.1 increased steadily for the first 20 hours indicating that the metal sites are being deactivated quicker than the acidic sites on the catalyst. The ratio then levelled out at ~1.2 until the reaction was stopped. The carbon mass balance, Table 6.3.3, indicated that once again the carbon deposition decreased with time on stream. These results again suggest that the coke

is deposited on the metal sites initially before being deposited on the support.

Total conversion of n-octane, illustrated in Figure 6.3.7, decreases steadily for ~40 hours on stream before reaching a constant level of ~41%. This is higher than the corresponding conversion on EUROPT-3.1 where a final conversion of ~27% was reached. The deactivation of EUROPT-4.1 was not as severe as that undergone by EUROPT-3.1. The % coke deposited on the catalyst surface is shown in Table 6.1. The difference in the % coke deposited on both EUROPT-3.1 and -4.1 is within experimental error, ~1.5%. Therefore the addition of a 0.3wt% loading of rhenium has added stability and altered the selectivity to products. The level of coke has not decreased but its detrimental effect has.

6.4. EUROPT-4.2 (490°C, 110 psig)

The temperature was lowered to 490°C in this run while the other reaction conditions were kept constant. The results obtained are shown in Figures 6.4.1 to 6.4.6 and in Tables 6.4.1 to 6.4.3.

Figure 6.4.1 displays the decreasing product yields of C_1 - C_4 species with reaction time. Methane is preferentially formed followed by propane and then ethane. Unlike the reaction at 510°C the yield of propane does not rise above that of methane at this lower temperature. The yields of both methane and propane are slightly higher than in the reaction at 510°C. The yield of n-butane is once again approximately 4 times greater than that of i-butane.

Table 6.4.1. %Yield of individual products and % Conversion versus time on stream for EUROPT-4.2.

Products	The % Yield of Selected Products							
Time (hrs)	1.5	4.333	15.017	18.25	21.25	24.25	27.25	39.3
Benzene	0.2105	0.1974	0.1706	0.1690	0.1469	0.1505	0.1363	0.1361
Toluene	3.4112	3.3242	3.3160	3.0306	3.0217	2.9016	2.4547	2.1492
Ethylbenzene	2.9820	2.9420	2.1660	2.1068	2.1129	2.1253	2.0836	1.8427
m/p-Xylene								
o-Xylene	1.7008	1.6500	1.3118	1.2874	1.2489	1.1956	1.1656	1.1724
Methane	9.3816	8.9186	8.0383	7.6665	7.5712	7.4074	7.2593	7.3481
Ethane	4.9714	4.7513	3.9899	4.0586	3.7862	3.6693	3.1449	2.5503
Propane	8.0155	7.6367	6.2663	6.0408	5.7862	5.4722	5.2743	4.2516
i-Butane	2.0078	1.7421	1.0768	1.0384	0.9693	0.9500	0.8496	0.6989
n-Butane	7.1534	6.0499	4.0762	3.8588	3.3130	2.9801	2.8417	2.8851
Cyclopentane	0.1685	0.1783	0.0005	0.0005	0.0005	0.0003	0.0982	0.0004
i-Pentane			0.1642	0.1636	0.0345	0.0989		0.0653
n-Pentane					0.0864			
Cyclohexane	0.1376	0.1227	0.1249	0.1193	0.1020	0.0986	0.0851	0.0728
i-Hexane								
n-Hexane								
Cycloheptane	0.0185	0.0183	0.0178	0.0209	0.0237	0.0212	0.0201	0.0170
i-Heptane	0.0555	0.0472	0.0572	0.0614	0.0587	0.0534	0.0510	0.0432
n-Heptane	0.0554	0.0467	0.0510	0.0557	0.0550	0.0519	0.0535	0.0462
Cyclooctane	0.0376	0.0353	0.0436	0.0420	0.0421	0.0414	0.0404	0.0378
i-Octane	0.1450	0.1217	0.1027	0.0988	0.0964	0.0979	0.0957	0.0881
% Conversion of n-Octane	40.4524	37.7825	30.9739	29.8189	28.9834	27.3690	25.6541	23.4053

Table 6.4.2. %Selectivity of individual products versus time on stream for EUROPT-4.2.

Products	The % Selectivity of Selected Products							
Time (hrs)	1.5	4.333	15.017	18.25	21.25	24.25	27.25	39.3
Benzene	0.5204	0.5224	0.5509	0.5667	0.5069	0.5500	0.5314	0.5814
Toluene	8.4326	8.7982	10.7059	10.1632	10.4256	10.6019	9.5685	9.1826
Ethylbenzene	7.3717	7.7867	6.9930	7.0654	7.2901	7.7653	8.1218	7.8730
m/p-Xylene								
o-Xylene	4.2045	4.3672	4.2353	4.3174	4.3091	4.3684	4.5434	5.0093
Methane	23.1916	23.6052	25.9518	25.7104	26.1225	27.0650	28.2968	31.3953
Ethane	12.2896	12.5755	12.8816	13.6107	13.0635	13.4066	12.2588	10.8963
Propane	19.8147	20.2122	20.2308	20.2582	19.9640	19.9941	20.5595	18.1651
i-Butane	4.9633	4.6110	3.4763	3.4823	3.3443	3.4712	3.3119	2.9862
n-Butane	17.6835	16.0124	13.1601	12.9409	11.4306	10.8885	11.0769	12.3268
Cyclopentane	0.4164	0.4718	0.0015	0.0016	0.0016	0.0012	0.3828	0.0015
i-Pentane			0.5303	0.5485	0.1192	0.3613		0.2790
n-Pentane					0.2980			
Cyclohexane	0.3402	0.3248	0.4032	0.4000	0.3518	0.3602	0.3318	0.3112
i-Hexane								
n-Hexane								
Cycloheptane	0.0458	0.0484	0.0573	0.0700	0.0818	0.0776	0.0785	0.0724
i-Heptane	0.1373	0.1249	0.1847	0.2059	0.2024	0.1952	0.1989	0.1846
n-Heptane	0.1370	0.1236	0.1648	0.1869	0.1897	0.1895	0.2086	0.1974
Cyclooctane	0.0929	0.0934	0.1407	0.1407	0.1451	0.1513	0.1573	0.1616
i-Octane	0.3585	0.3222	0.3317	0.3312	0.3325	0.3575	0.3730	0.3765

Table 6.4.3. Carbon Mass Balance of the EUROPT-4.2. catalyst

Time (hrs)	No. of moles of Carbon In	No. of moles of Carbon Out	Δ Carbon
1.5	3.3852×10^{-4}	3.2844×10^{-4}	1.0079×10^{-5}
4.333	3.3852×10^{-4}	3.3099×10^{-4}	7.5305×10^{-6}
15.017	3.3852×10^{-4}	3.3157×10^{-4}	6.9475×10^{-6}
18.25	3.3852×10^{-4}	3.3186×10^{-4}	6.6610×10^{-6}
21 25	3.3852×10^{-4}	3.3252×10^{-4}	6.0018×10^{-6}
24.25	3.3852×10^{-4}	3.3275×10^{-4}	5.7711×10^{-6}
27.5	3.3852×10^{-4}	3.3298×10^{-4}	5.5408×10^{-6}
39.3	3.3852×10^{-4}	3.3470×10^{-4}	4.4167×10^{-6}

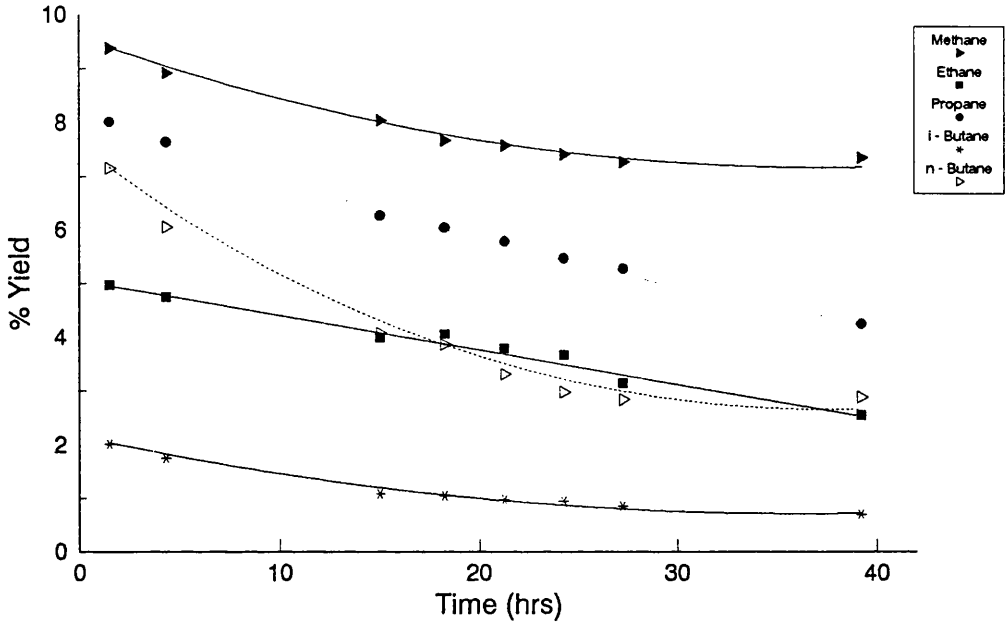

Figure 6.4.1. % Yield to Individual Hydrocarbon Products on EUROPT-4.2.

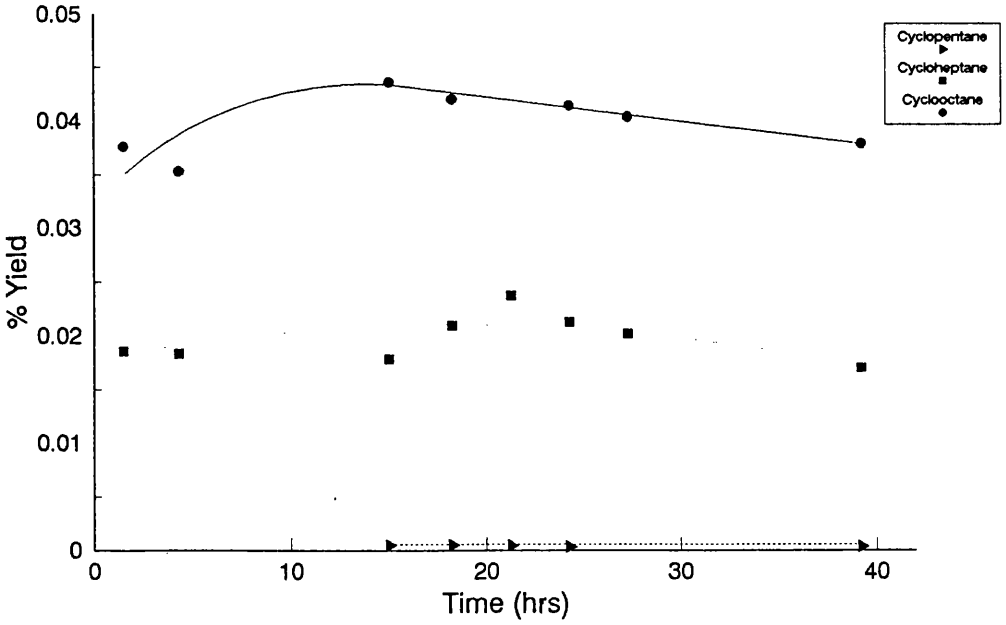

Figure 6.4.2. % Yield of Cycloparaffin Products on EUROPT-4.2.

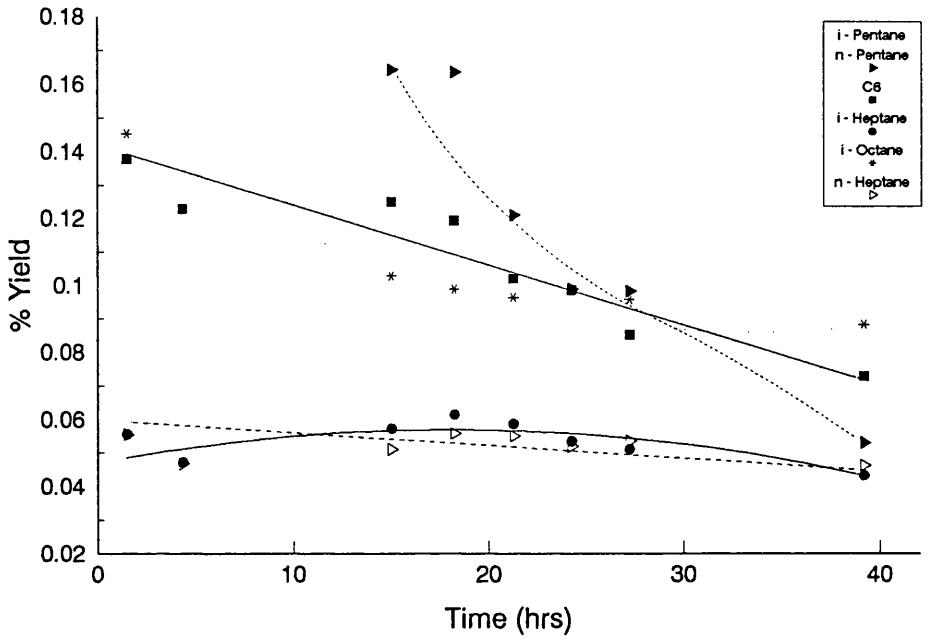

Figure 6.4.3. % Yield of i- and n-Paraffin Products on EUROPT-4.2.

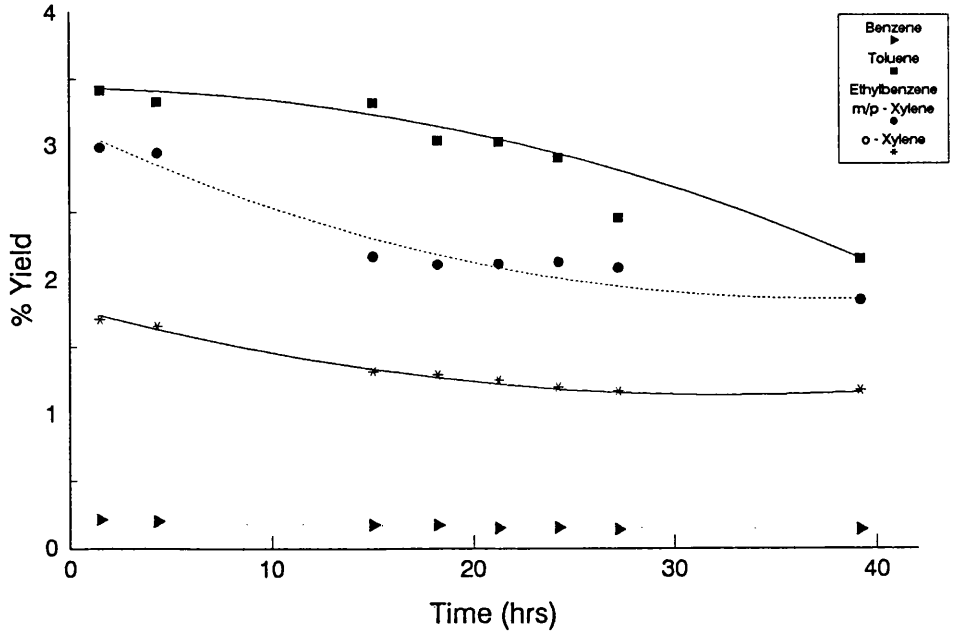

Figure 6.4.4. % Yield of Aromatic Products on EUROPT-4.2.

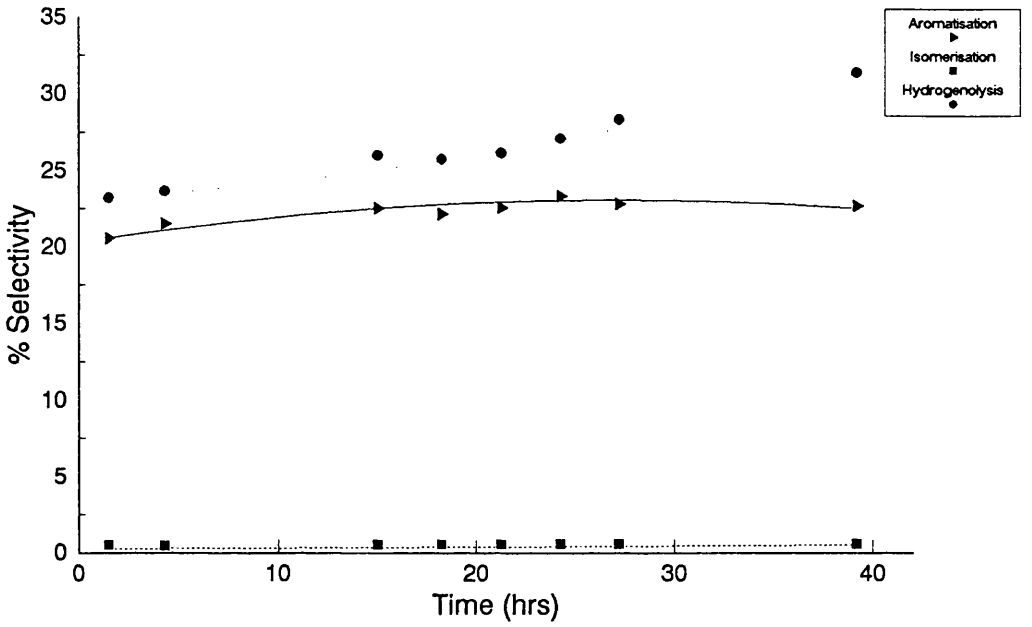

Figure 6.4.5. % Selectivity to the Major Reaction Products on EUROPT-4.2.

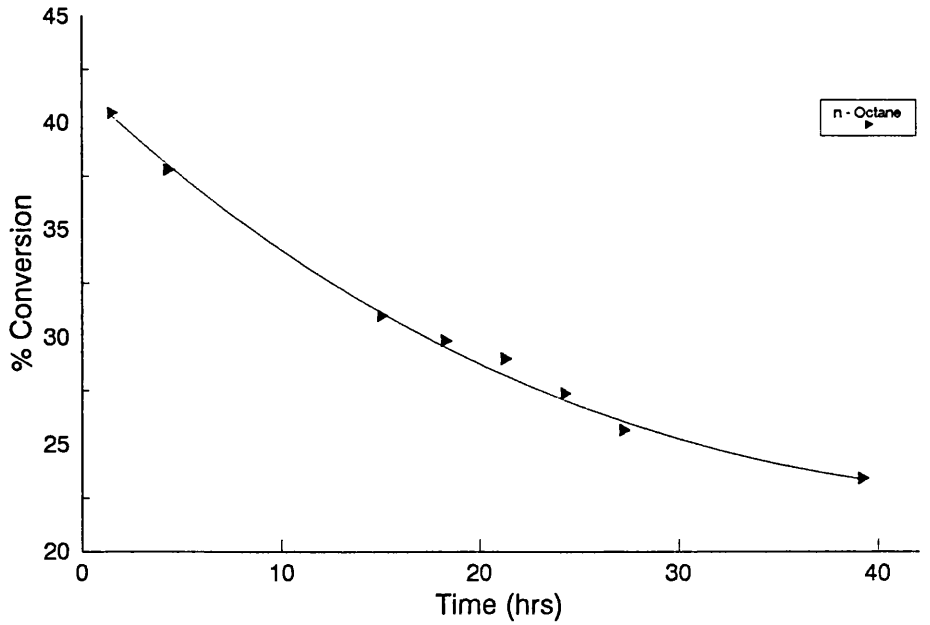

Figure 6.4.6. % Conversion of n-Octane on EUROPT-4.2.

The yield of paraffins was again low leading to several species being indistinguishable from one another as in the case of the C_6 products. The conversion to both cyclooctane and cycloheptane, Figure 6.4.2, is seen to increase before decreasing steadily until the reaction was stopped. Cyclopentane was not detected initially but increased steadily after the first 15 hours on stream. The conversion to cycloparaffins was found to increase with carbon number. Figure 6.4.3 shows the conversion to both i- and n-paraffins. The yield of i-octane decreases with time, whereas the yield if i-heptane goes through a maximum before decreasing. The yield of n-heptane, in contrast, is shown to decrease steadily with time.

The yield of aromatic products follows a similar pattern to that observed on EUROPT-3.1. Toluene once again has become the major product followed by ethylbenzene/m/p-xylene, o-xylene and finally benzene. The yield of all aromatic species decreases with reaction time. The overall yield of aromatics has fallen by lowering the temperature 20°, this is especially noticeable for the xylene species. At 510°C, the combined yield of ethylbenzene/m/p-xylene is constant at 12% and o-xylene at 8% whereas at 490°C the yields have dropped to ~2% and 1.4% respectively. The yields of both benzene and toluene decreased slightly in comparison when the temperature was lowered.

The selectivities of the individual hydrocarbon products are shown in Table 6.4.2. The order of the selectivities to the major reactions has altered from that at the higher temperature. As with EUROPT-3, hydrogenolysis has become the most favoured reaction at 490°C. The order of selectivities is therefore as follows:

Hydrogenolysis > Aromatisation > Hydrocracking > Isomerisation

Hydrogenolysis activity increases steadily with time whereas aromatisation activity, after an initial rise, reaches a steady value of ~21%. This is almost a third of the value found for the reaction at 510°C. The hydrogenolysis activity over the same period of time, in total contrast, almost trebles for the reaction at 490°C compared to that at 510°C.

Interestingly the propane to methane ratio rises slightly in the first 5 hours before decreasing rapidly. This would suggest that the coke is deposited preferentially upon the support after 5 hours. The support is much more deactivated in this run than the metal component. The carbon mass balance for the reaction, Table 6.4.3, shows that the carbon difference decreases with increasing reaction time.

The total conversion of n-octane, shown in Figure 6.4.6, decreases steadily from the start to a value of ~23% at the end of the run. This is a large decrease (18%) in the conversion when compared with EUROPT-4.1, but the deactivation rate was slower. The % coke deposited upon the catalyst surface was 9.1% by weight. This is ~6% smaller than the amount deposited at 510°C. The coking rate and level has decreased slightly but the selectivity to aromatics has fallen dramatically and as a result the hydrogenolysis activity has gained in importance.

6.5. EUROPT-4.3 (510°C, 130 psig)

The conversion of n-octane over EUROPT-4.3 was carried out at 130 psig (10 atm) with the temperature being maintained at 510°C throughout the run. The hydrogen to hydrocarbon ratio and the WHSV were held at 6 and 2 respectively. The results of this study are detailed in Figures 6.5.1 to 6.5.7 and in Tables 6.5.1 to 6.5.3.

The product yields of all C_1 - C_4 species are illustrated in Figure 6.5.1 and are shown to decrease with reaction time. Methane is produced in the highest quantity, followed by propane and then ethane. The yield of methane does not fall drastically in the initial hours of the reaction as in the reaction at 110 psig. By the end of the run, the methane yield is ~2% higher than that at 110 psig, the yield of both propane and ethane falling in comparison.

Figures 6.5.2 to 6.5.4 show the conversion to cycloparaffins, i-paraffins and n-paraffins respectively. The yield of cycloparaffins is once again very small and with an increase in the carbon number a corresponding increase in the yield was noted. The yield of cycloheptane decreased whereas the yield of other cycloparaffins increased with time. The yield of i-paraffin products is shown in Figure 6.5.3 to decrease with time. The yield of i- and n-pentane are combined in this run as their chromatographic peaks could not always be resolved. The product yield of i-paraffins is shown to decrease with carbon number. Figure 6.5.4 illustrates the decreasing yield of both n-hexane and n-heptane with time and carbon number.

Table 6.5.1. %Yield of individual products and % Conversion versus time on stream for EUROPT-4.3.

Products	The % Yield of Selected Products							
Time (hrs)	1.25	4	18.75	21.75	24.75	27.75	30.75	41.5
Benzene	0.8163	0.7371	0.6753	0.6685	0.5942	0.5875	0.5534	0.4778
Toluene	3.1211	2.9574	2.7325	2.7231	2.6541	2.6609	2.6154	2.4639
Ethylbenzene m/p-Xylene	2.7688	2.6893	2.6017	2.5541	2.5381	2.4660	2.3756	2.1926
o-Xylene	2.8145	2.8915	3.0531	3.0488	3.0875	3.0901	3.1781	3.2393
Methane	6.8877	6.2972	5.9152	5.7960	5.6900	5.5934	5.5066	5.1891
Ethane	3.2212	2.9189	2.3468	2.2081	2.1453	2.1201	2.0529	1.7883
Propane	6.2212	5.9191	5.1483	5.1328	5.0807	4.9945	5.0883	4.8037
i-Butane	1.8406	1.5492	1.3155	1.2373	1.1092	1.0978	1.0632	0.9989
n-Butane	6.0332	4.6391	4.0267	3.8915	3.5407	3.2998	3.2191	3.1076
Cyclopentane	0.0003	0.0003	0.0004	0.0004	0.0004	0.0004	0.0443	0.0004
i-Pentane	0.0547	0.0510	0.0483	0.0448	0.0459	0.0449		0.0423
n-Pentane								
Cyclohexane	0.0004	0.0004	0.0004	0.0004	0.0003	0.0003	0.0004	0.0005
i-Hexane	0.0138	0.0130	0.0122	0.0117	0.0116	0.0113	0.0111	0.0105
n-Hexane	0.0458	0.0450	0.0429	0.0423	0.0415	0.0409	0.0357	0.0335
Cycloheptane	0.0009	0.0008	0.0008	0.0008	0.0008	0.0007	0.0006	0.0006
i-Heptane	0.0219	0.0214	0.0197	0.0185	0.0171	0.0167	0.0162	0.0158
n-Heptane	0.0610	0.0555	0.0505	0.0499	0.0493	0.0486	0.0438	0.0420
Cyclooctane	0.0016	0.0021	0.0022	0.0022	0.0021	0.0022	0.0024	0.0026
i-Octane	0.0430	0.0419	0.0392	0.0386	0.0382	0.0380	0.0370	0.0349
% Conversion of n-Octane	33.9679	30.8300	28.0314	27.4698	26.6468	26.1140	25.8441	24.4442

Table 6.5.2. %Selectivity of individual products versus time on stream for EUROPT-4.3.

Products	The % Selectivity of Selected Products							
Time (hrs)	1.25	4	18.75	21.75	24.75	27.75	30.75	41.5
Benzene	2.4032	2.3908	2.4091	2.4337	2.2299	2.2497	2.1415	1.9547
Toluene	9.1883	8.7065	9.7480	9.9131	9.9602	10.1895	10.1198	10.0798
Ethylbenzene	8.1511	8.7228	9.2813	9.2978	9.5248	9.4433	9.1919	8.9698
m/p-Xylene								
o-Xylene	8.2858	9.3787	10.8917	11.0986	11.5869	11.8331	12.2971	13.2517
Methane	20.2771	20.4256	21.1020	21.0995	21.3532	21.4192	21.3070	21.2285
Ethane	9.4831	9.4677	8.3720	8.0383	8.0510	8.1185	7.9433	7.3157
Propane	18.3149	19.1990	18.3663	18.6854	19.0668	19.1256	19.6886	19.6517
i-Butane	5.4187	5.0249	4.6928	4.5043	4.1625	4.2038	4.1137	4.0863
n-Butane	17.7615	15.0473	14.3648	14.1665	13.2874	12.6360	12.4560	12.7129
Cyclopentane	0.0008	0.0010	0.0013	0.0015	0.0015	0.0017	0.1715	0.0014
i-Pentane	0.1609	0.1655	0.1723	0.1630	0.1721	0.1721		0.1729
n-Pentane								
Cyclohexane	0.0013	0.0012	0.0013	0.0014	0.0012	0.0012	0.0014	0.0022
i-Hexane	0.0405	0.0421	0.0434	0.0426	0.0435	0.0431	0.0431	0.0431
n-Hexane	0.1349	0.1458	0.1531	0.1539	0.1554	0.1567	0.1382	0.1371
Cycloheptane	0.0026	0.0026	0.0027	0.0028	0.0028	0.0027	0.0024	0.0025
i-Heptane	0.0644	0.0696	0.0660	0.0673	0.0644	0.0639	0.0627	0.0646
n-Heptane	0.1795	0.1799	0.1779	0.1815	0.1849	0.1860	0.1694	0.1718
Cyclooctane	0.0046	0.0068	0.0077	0.0080	0.0081	0.0083	0.0093	0.0106
i-Octane	0.1266	0.1359	0.1399	0.1407	0.1432	0.1457	0.1431	0.1429

Table 6.5.3. Carbon Mass Balance of the EUROPT-4.3. catalyst

Time (hrs)	No. of moles of Carbon In	No. of moles of Carbon Out	Δ Carbon
1.25	3.5368×10^{-4}	3.4479×10^{-4}	8.8863×10^{-6}
4	3.5368×10^{-4}	3.4589×10^{-4}	7.7888×10^{-6}
18.75	3.5368×10^{-4}	3.4978×10^{-4}	3.9013×10^{-6}
21.25	3.5368×10^{-4}	3.5038×10^{-4}	3.2957×10^{-6}
24.75	3.5368×10^{-4}	3.5099×10^{-4}	2.6903×10^{-6}
27.75	3.5368×10^{-4}	3.5124×10^{-4}	2.4403×10^{-6}
30.75	3.5368×10^{-4}	3.5153×10^{-4}	2.1442×10^{-6}
41.5	3.5368×10^{-4}	3.5298×10^{-4}	6.9281×10^{-7}

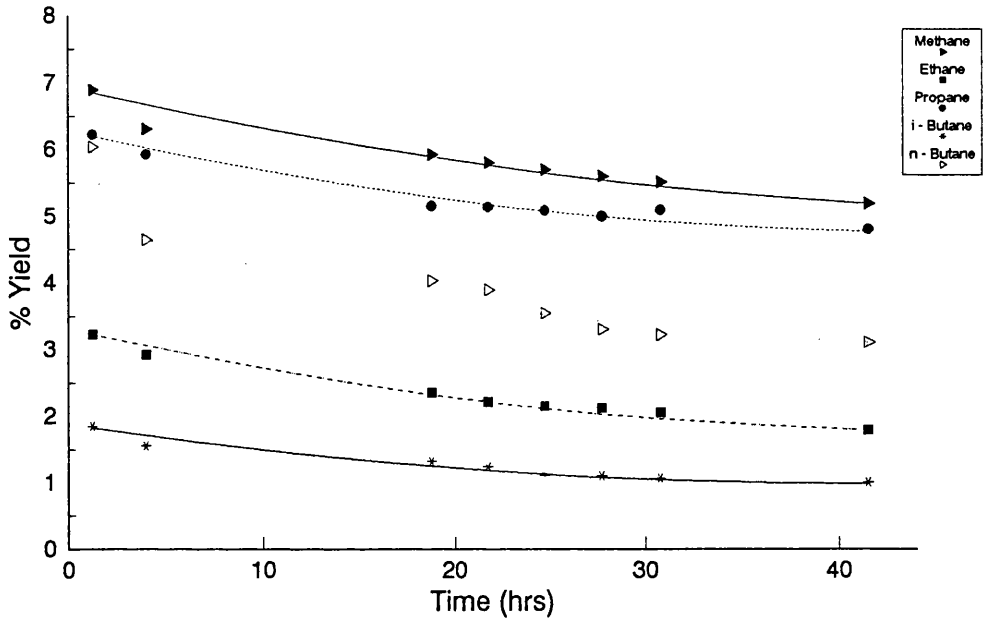

Figure 6.5.1. % Yield to Individual Hydrocarbon Products on EUROPT-4.3.

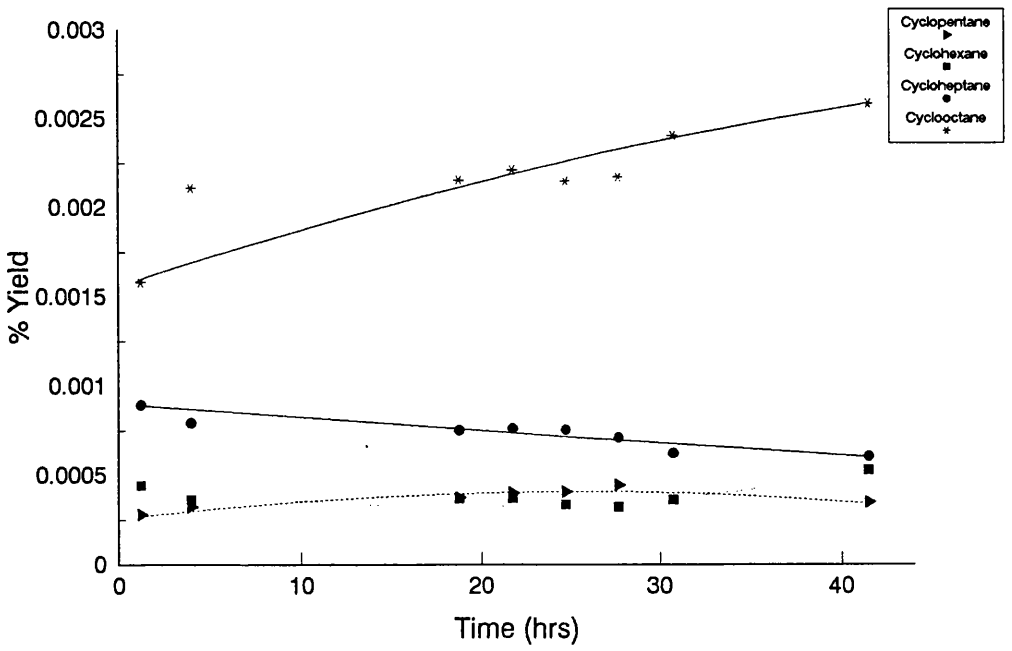

Figure 6.5.2. % Yield of Cycloparaffin Products on EUROPT-4.3.

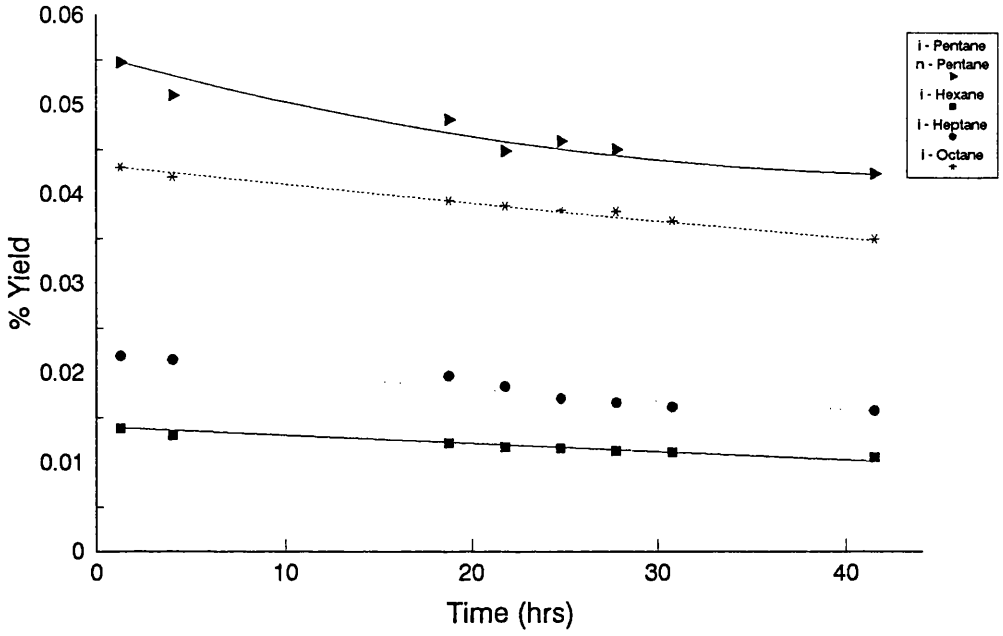

Figure 6.5.3. % Yield of i-Paraffin Products on EUROPT-4.3.

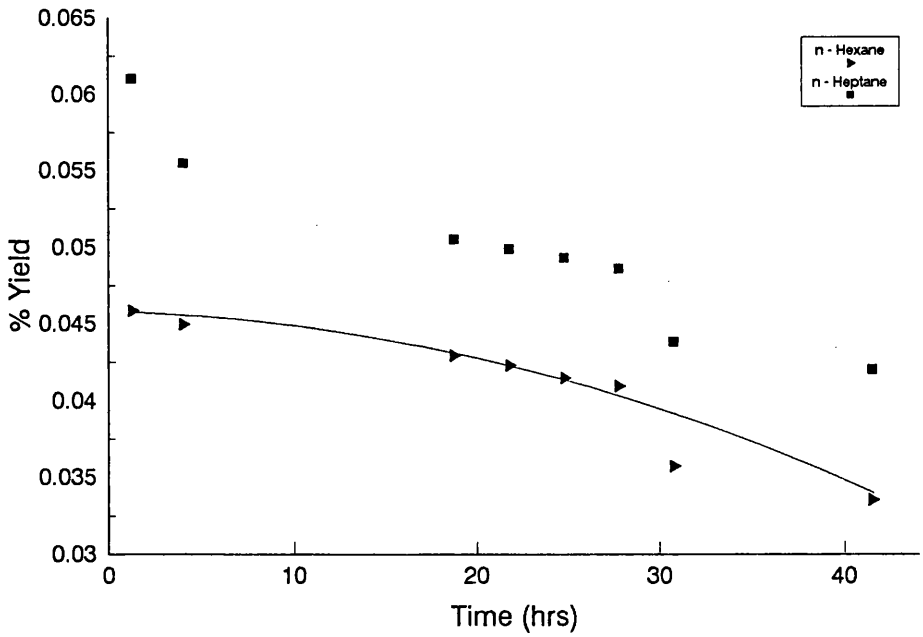

Figure 6.5.4. % Yield of n-Paraffin Products on EUROPT-4.3.

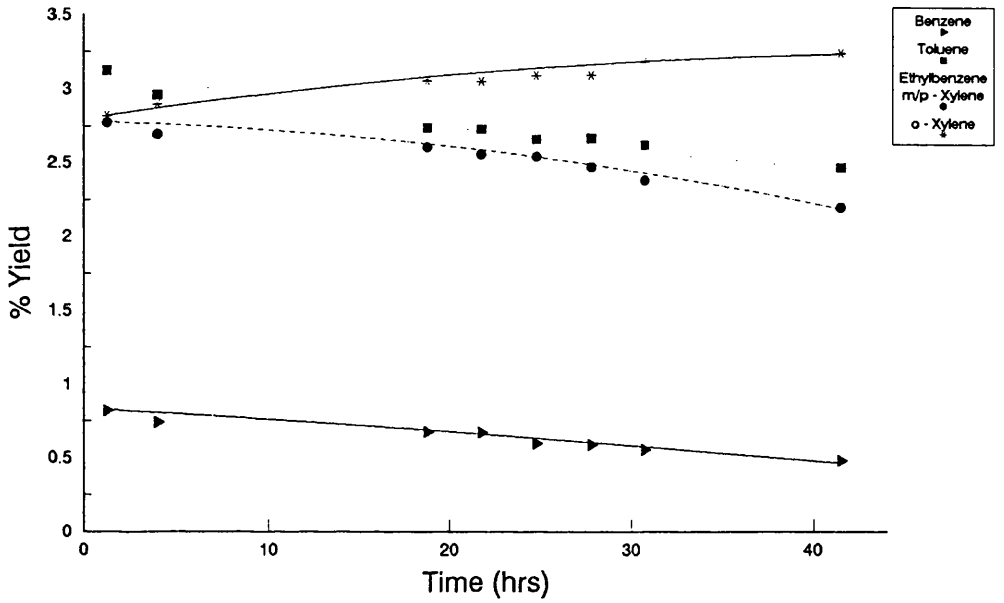

Figure 6.5.5. % Yield of Aromatic Products on EUROPT-4.3.

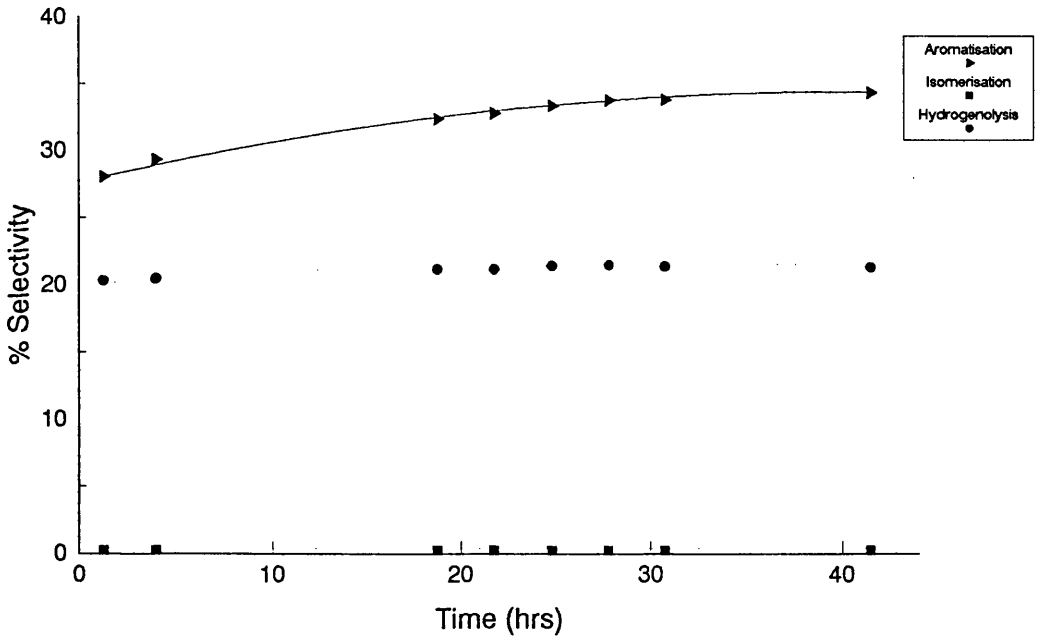

Figure 6.5.6. % Selectivity to Major Reactions on EUROPT-4.3.

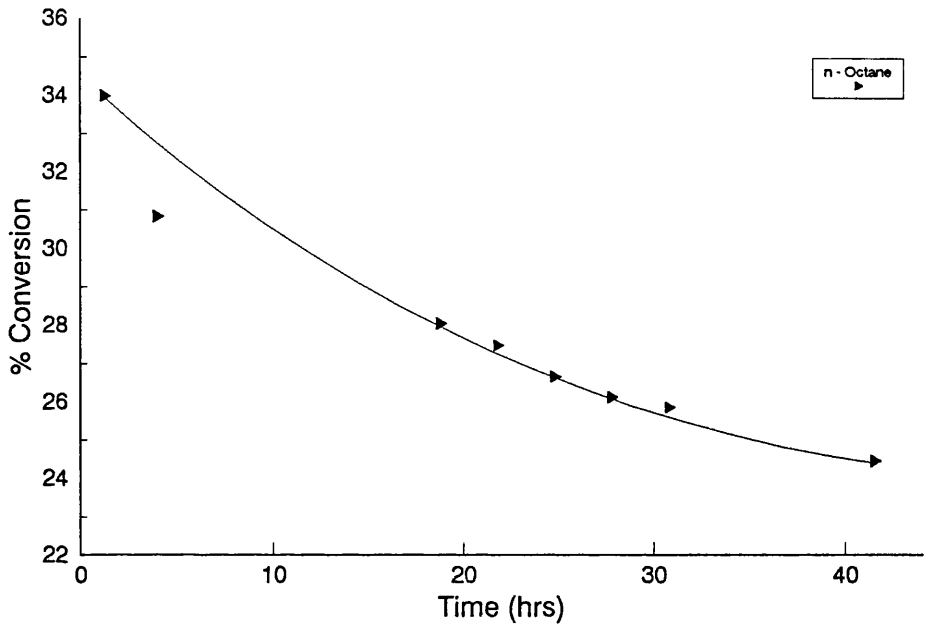

Figure 6.5.7. % Conversion of n-Octane on EUROPT-4.3.

The % yield of aromatic products is much lower than that observed with the lower pressure. The product yield for toluene and xylene species has dropped to ~3% and benzene to ~0.5%, drastically lower than seen at 110 psig. The yield of o-xylene increases while that of benzene, toluene and ethylbenzene/m/p-xylene decreases with time. After ~10 hours on stream o-xylene becomes the dominant reaction product followed by toluene, ethylbenzene/m/p-xylene and finally benzene. Toluene formation once again becomes more important as the xylene yields fall dramatically.

The selectivities to the individual hydrocarbon products are detailed in Table 6.5.2. The selectivities to the major reactions are shown in Figure 6.5.6. As shown the aromatisation activity is highest and levels out at ~33%. This value is ~½ that of the activity at 110 psig. The major reaction selectivities decrease in the order:

Aromatisation > Hydrogenolysis > Hydrocracking > Isomerisation

The hydrogenolysis activity is constant at ~20% which is almost double that with EUROPT-4.1.

The propane to methane ratio and the carbon mass balance are similar to those in previous Sections indicating the metallic sites are initially deactivated by coke deposition before the alumina support is coked.

The total conversion of n-octane is shown in Figure 6.5.7 and can be seen to decrease steadily with time. The deactivation rate is extremely slow almost ½ that of the other reactions with EUROPT-4. The conversion reaches a steady value of

~25% after 42 hours on stream.

The % coke deposited on EUROPT-4.3, detailed in Table 6.1, is less than that deposited on EUROPT-4.1. Therefore increasing the pressure results not only in a lower coke deposition but also in a lower yield of aromatics. This explains why reforming reactions are carried out preferentially at lower pressures even though the deactivation rate is higher.

6.6. 3.0wt%Pt-3.0wt%Re/Al_2O_3 (510°C, 110 psig)

The reforming of n-octane was carried out under conditions described in Section 6.1. The conversion of n-octane over this catalyst was extremely low. The product distribution was very limited with small quantities of aromatics being produced. The dominant product was by far methane, with this species having a selectivity of ~99% throughout the reaction. The yield of methane and consequently the conversion falls dramatically from ~12.6 to 3% after 25 hours on stream, after which the conversion was so low that the reaction was stopped.

6.7. 0.3wt%Re/Al_2O_3 and 3.0wt%Re/Al_2O_3 (510°C, 110 psig)

Both catalysts were tested under conditions stated in Section 6.1. The conversion of n-octane over both these monometallic catalysts was very low, ~5% for the 0.3wt%Re/Al_2O_3 and ~4.3% for the 3.0wt%Re/Al_2O_3 catalyst. At these low conversions the main product with both catalysts was methane. The product yields

of aromatics and non-aromatic species was very low. Due to the very low conversions and poor selectivity of both these catalysts the reforming reaction were stopped after ~24 hours.

6.8. 0.3wt%Pt-0.3wt%Sn/Al_2O_3 - Coimpregnated (510°C, 110 psig)

The 0.3wt%Pt-0.3wt%Sn/Al_2O_3 coimpregnated catalyst was tested, under identical conditions described in Section 6.1, in the microreactor. The results are presented in Figures 6.8.1 to 6.8.7 and Tables 6.8.1 to 6.8.3.

Figure 6.8.1 illustrates the decreasing yield of C_1 - C_4 products with the reaction time. The yield of both methane and n-butane decrease rapidly in the first 10 hours of this study. Methane is predominately produced, followed by propane and ethane. The yield of n-butane at a constant level of 3.8% is more than double that of i-butane.

The conversion to cycloparaffins is detailed in Figure 6.8.2. The yield of both cyclohexane and cyclopentane increase rapidly with time whereas the yield of cycloheptane increases to a maximum after 35 hours before decreasing rapidly. Figure 6.8.3 illustrates the yield of i-paraffin products. In this study the combined yields of cyclooctane and i-octane are quoted. As illustrated the yield of i-paraffin species increases with time and with decreasing carbon number, disregarding the combined octane yield. The conversion to n-paraffins is shown in Figure 6.8.4 to decrease in the order from n-hexane, n-heptane to n-pentane. The yield of both

Table 6.8.1. %Yield of individual products and % Conversion versus time on stream for 0.3wt%Pt-0.3wt%Sn/Al_2O_3 (Coimpregnated)

Products	The % Yield of Selected Products								
Time (hrs)	2	12.5	15.5	18.5	21.5	24.5	36.5	39.5	42.67
Benzene	1.8286	1.6777	1.6572	1.6371	1.6230	1.6039	1.5866	1.5761	1.5608
Toluene	5.0906	4.5160	4.2975	4.0839	3.9540	3.8320	3.7327	3.5420	3.6148
Ethylbenzene m/p-Xylene	11.0894	10.4569	9.6634	9.2264	9.0095	8.9060	9.0317	8.9833	8.9017
o-Xylene	6.2738	5.8589	5.6627	5.5524	5.4272	5.4379	5.3399	5.2364	5.2146
Methane	12.1983	8.4335	7.9408	7.6120	7.2724	7.0996	6.6349	5.6207	5.4250
Ethane	3.1771	2.6349	1.9021	1.7959	1.4777	1.2445	1.0886	0.9898	0.9821
Propane	6.0422	5.4731	5.0556	4.7550	4.4672	4.2420	3.8855	3.8975	3.8201
i-Butane	4.0989	3.3132	2.3395	2.2839	2.2130	2.1664	1.7163	1.6815	1.5965
n-Butane	11.1147	5.6904	4.6193	4.6630	4.4376	4.1063	3.9406	3.9097	3.7968
Cyclopentane	0.0008	0.0013	0.0026	0.0031	0.0040	0.0047	0.0097	0.0111	0.0128
i-Pentane	0.1028	0.1063	0.1049	0.1098	0.1202	0.1260	0.1445	0.1563	0.1722
n-Pentane	0.0001		-	0.0002	0.0002	0.0003	0.0005	0.0006	0.0007
Cyclohexane	0.0006	0.0007	0.0011	0.0018	0.0027	0.0048	0.0130	0.0160	0.0197
i-Hexane	0.0409	0.0472	0.0505	0.0558	0.0588	0.0610	0.0773	0.0834	0.0891
n-Hexane	0.0203	0.0258	0.0272	0.0303	0.0344	0.0395	0.0535	0.0579	0.0612
Cycloheptane	0.0046	0.0049	0.0062	0.0060	0.0076	0.0095	0.0155	0.0141	0.0100
i-Heptane	0.0155	0.0158	0.0218	0.0269	0.0305	0.0364	0.0482	0.0567	0.0578
n-Heptane	-	0.0080	0.0084	0.0094	0.0132	0.0160	0.0238	0.0280	0.0314
Cyclooctane i-Octane	0.0844	0.1277	0.1499	0.1740	0.1843	0.1916	0.2973	0.3645	0.4381
% Conversion of n-Octane	61.1837	48.3922	43.5105	42.0269	40.3375	39.1285	37.6401	36.2254	35.8054

Table 6.8.2. %Selectivity of individual products versus time on stream for 0.3wt%Pt-0.3wt%Sn/Al_2O_3 (Coimpregnated)

Products	The % Selectivity of Selected Products								
Time (hrs)	2	12.5	15.5	18.5	21.5	24.5	36.5	39.5	42.67
Benzene	2.9887	3.4670	3.8087	3.8953	4.0236	4.0991	4.2152	4.3508	4.3590
Toluene	8.3202	9.3320	9.8768	9.7174	9.8022	9.7935	9.9167	9.7777	10.0958
Ethylbenzene m/p-Xylene	18.1248	21.6087	22.2093	21.9536	22.3352	22.7608	23.9949	24.7984	24.8614
o-Xylene	10.2541	12.1070	13.0145	13.2116	13.4544	13.8974	14.1867	14.4550	14.5638
Methane	19.9372	17.4273	18.2503	18.1122	18.0290	18.1444	17.6273	15.5158	15.1515
Ethane	5.1927	5.4449	4.3716	4.2733	3.6634	3.1806	2.8920	2.7323	2.7429
Propane	9.8756	11.3099	11.6194	11.3142	11.0745	10.8412	10.3226	10.7590	10.6691
i-Butane	6.69943.	6.8465	5.3768	5.4343	5.4863	5.5367	4.5597	4.6418	4.4589
n-Butane	18.1661	11.7589	10.6165	11.0953	11.0011	10.4944	10.4690	10.7928	10.6041
Cyclopentane	0.0012	0.0028	0.0059	0.0073	0.0099	0.0120	0.0258	0.0305	0.03565
i-Pentane	0.1681	0.2196	0.2411	0.2612	0.2979	0.3221	0.3839	0.4316	0.4810
n-Pentane	0.0002		-	0.0004	0.0005	0.0007	0.0013	0.0016	0.0018
Cyclohexane	0.0010	0.0014	0.0026	0.0042	0.0067	0.0124	0.0346	0.0441	0.0550
i-Hexane	0.0668	0.0975	0.1161	0.1327	0.1457	0.1559	0.2054	0.2301	0.2488
n-Hexane	0.0332	0.0533	0.0624	0.0720	0.0852	0.1011	0.1422	0.1598	0.1708
Cycloheptane	0.0075	0.0102	0.0143	0.0143	0.0189	0.0242	0.0413	0.0390	0.0280
i-Heptane	0.0254	0.0326	0.0501	0.0641	0.0757	0.0931	0.1281	0.1564	0.1615
n-Heptane	-	0.0165	0.0192	0.0224	0.0326	0.0409	0.0632	0.0773	0.0877
Cyclooctane	0.1379	0.2638	0.3444	0.4141	0.4570	0.4896	0.7898	1.0061	1.2235
i-Octane									

Table 6.8.3. Carbon Mass Balance for 0.3wt%Pt-0.3wt%Sn/Al_2O_3 (Coimpregnated) (510°C, 110 psig)

Time (hrs)	No. of moles of Carbon In	No. of moles of Carbon Out	Δ Carbon
2	3.7170×10^{-4}	3.4082×10^{-4}	3.0877×10^{-5}
12.5	3.7170×10^{-4}	3.4609×10^{-4}	2.5609×10^{-5}
15.5	3.7170×10^{-4}	3.5115×10^{-4}	2.0550×10^{-5}
18.5	3.7170×10^{-4}	3.5328×10^{-4}	1.8419×10^{-5}
21.5	3.7170×10^{-4}	3.5602×10^{-4}	1.5684×10^{-5}
24.5	3.7170×10^{-4}	3.5947×10^{-4}	1.2232×10^{-5}
36.5	3.7170×10^{-4}	3.6496×10^{-4}	6.7425×10^{-6}
39.5	3.7170×10^{-4}	3.6726×10^{-4}	4.4352×10^{-6}
42.67	3.7170×10^{-4}	3.6738×10^{-4}	4.3166×10^{-6}

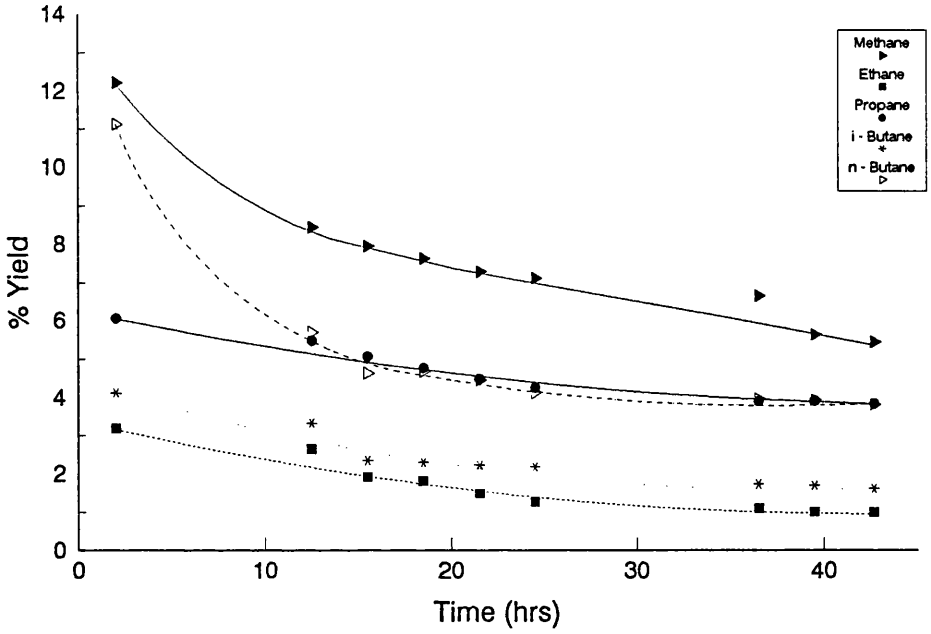

Figure 6.8.1. % Yield to Individual Hydrocarbon Products on 0.3%Pt-0.3%Sn /Alumina (Coimpregnated)

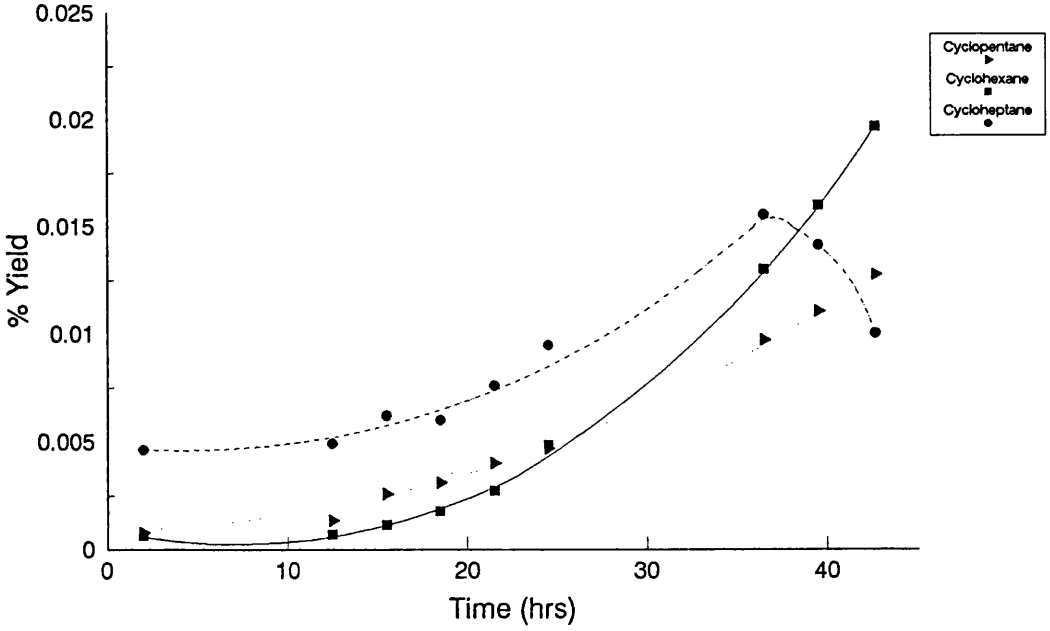

Figure 6.8.2. % Yield of Cycloparaffin Products on 0.3%Pt-0.3%Sn /Alumina (Coimpregnated)

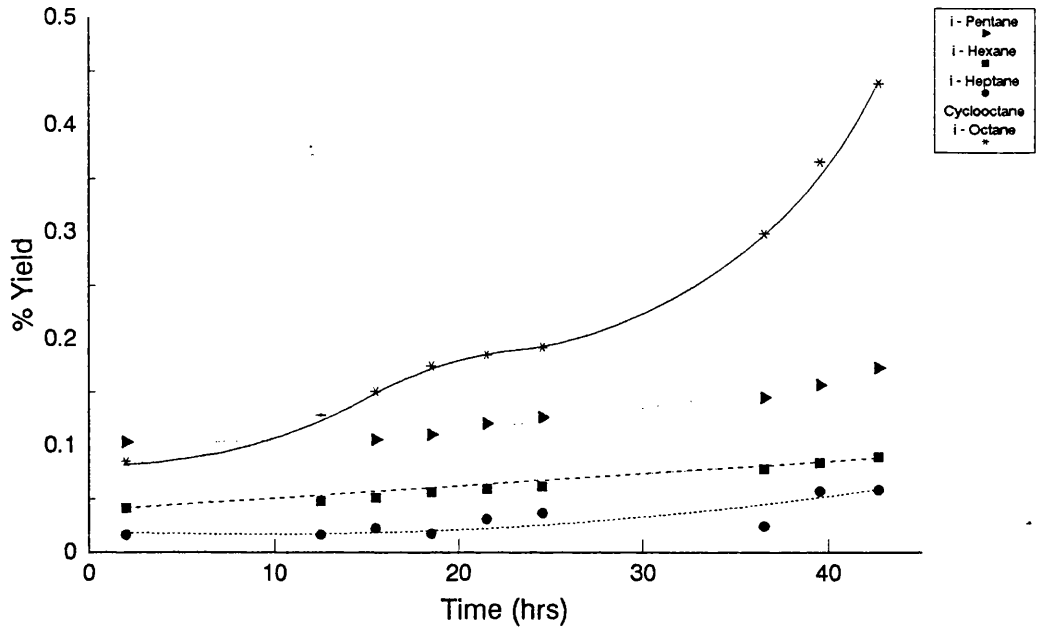

Figure 6.8.3. % Yield of i-Paraffin Products on 0.3%Pt-0.3%Sn /Alumina (Coimpregnated)

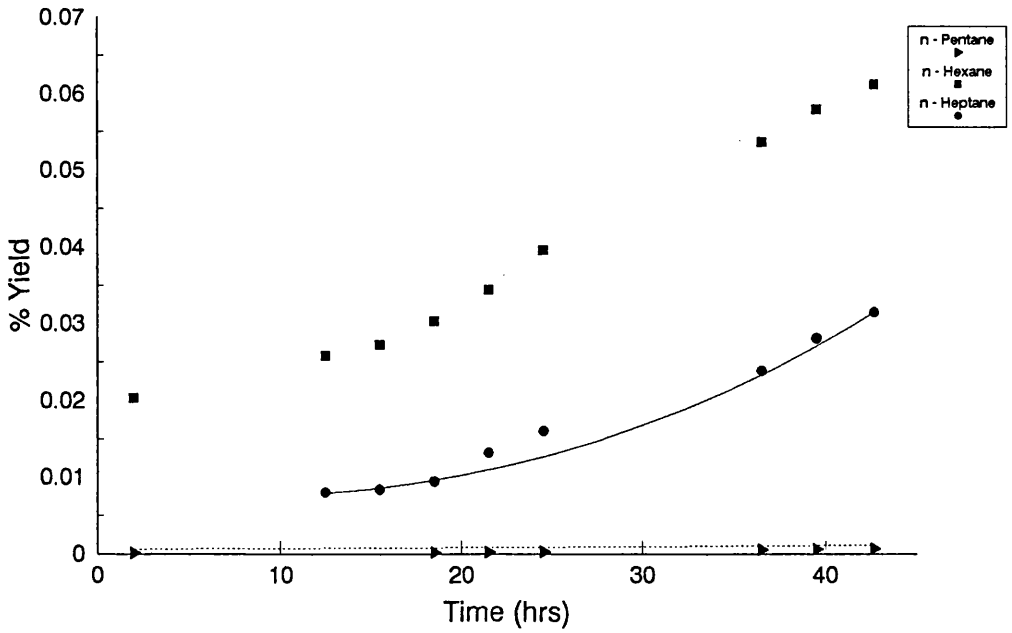

Figure 6.8.4. % Yield of n-Paraffin Products on 0.3%Pt-0.3%Sn /Alumina (Coimpregnated)

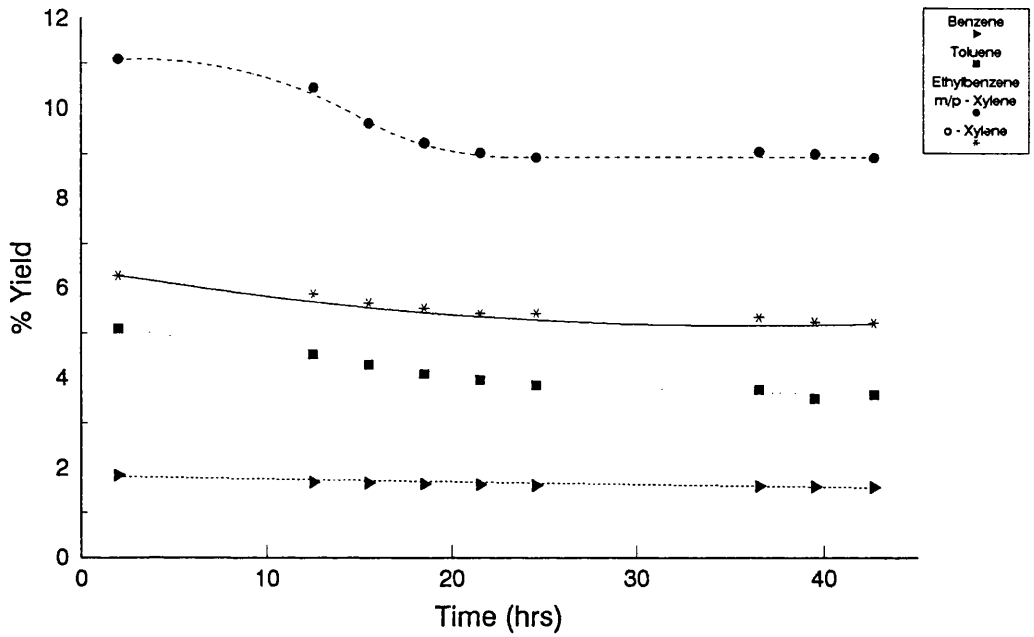

Figure 6.8.5. % Yield of Aromatic Products on 0.3%Pt-0.3%Sn /Alumina (Coimpregnated)

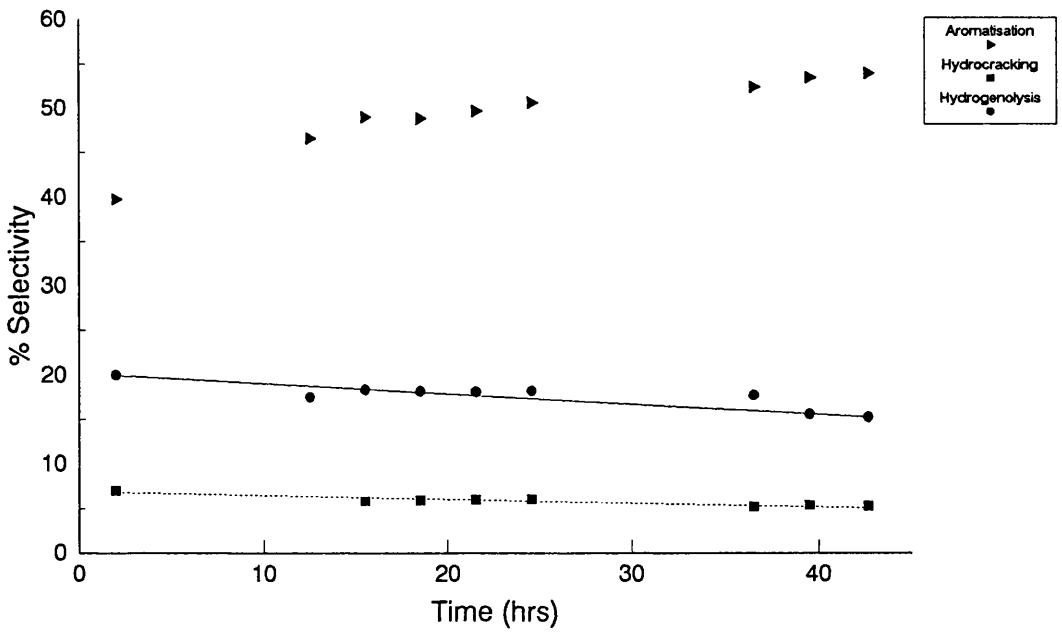

Figure 6.8.6. % Selectivity to the Major Reactions on 0.3%Pt-0.3%Sn /Alumina (Coimpregnated)

cycloparaffins and n-paraffins is in general much smaller than the corresponding yield of i-paraffin products.

Conversion to aromatic species is shown in Figure 6.8.5 to decrease with time on stream. The yields of o-xylene, toluene, and benzene decrease gradually while that of ethylbenzene/m/p-xylene decreases steadily before reaching a constant level after 20 hours. Aromatics are produced in the following decreasing order from ethylbenzene/m/p-xylene, o-xylene, toluene to benzene.

Table 6.8.2 details the selectivities to individual reaction products. The summation of the major reactions is illustrated in Figure 6.8.6. Aromatisation is shown to increase steadily with time to reach a constant selectivity of 54% after 43 hours. Hydrogenolysis activity decreases steadily throughout this time from 20 to 15%. The resulting order of selectivity to the major reactions is:

Aromatisation > *Hydrogenolysis* > *Hydrocracking* > *Isomerisation*

The propane to methane ratio for this reaction increases initially before reaching a steady value. However after 37 hours on stream the ratio rises sharply from this level to reach a constant ratio of 0.7. This would suggest that initially carbon was deposited on the metallic sites before being deposited on the alumina support. After 37 hours the metallic sites were once again deactivated quicker than the acidic sites. Table 6.8.3 shows the carbon mass balance for this run. There was an initial large uptake of carbon by the catalyst but this progressively decreased with reaction time.

The total conversion of n-octane decreases rapidly before reaching a constant level at 36%. The conversion rate is higher than that with EUROPT-3.1 (27%) but lower than with EUROPT-4.1 (41%) under identical conditions. Methane production was however greater than on both EUROPT catalysts.

The % coke deposited upon this catalyst after 43 hours on stream was 6.50% by weight, almost half the value deposited upon both EUROPT catalysts under identical conditions.

6.9. 0.3wt%Pt-0.3wt%Sn/Al_2O_3 - Sn impregregnated first (510°C, 110 psig)

The catalyst tested was prepared by sequential impregnation with tin being impregnated onto the alumina support first. The reaction conditions were identical to those described in Section 6.1. The results with respect to the reaction time are presented in Figures 6.9.1 to 6.9.7 and in Tables 6.9.1 to 6.9.3.

Figure 6.9.1 shows that the product yield of C_1 - C_4 species decreases with time. Unfortunately i- and n-butane could not be separated and are therefore quoted as a combined value. Methane production was again much larger than in either EUROPT catalysts. The product yield decreased in the order from methane, propane to ethane throughout the 51 hours on stream.

The yield of cycloparaffins, Figure 6.9.2, increases with time with the yield of cyclohexane and cycloheptane increasing rapidly from the start. The yield of

Table 6.9.1. %Yield of individual products and % Conversion versus time on stream for 0.3wt%Pt-0.3wt%Sn/Al_2O_3 (Sn impregnated first).

Products	The % Yield of Selected Products										
Time (hrs)	2.5	5.5	8.6	11.57	22.77	25.92	29.12	32.33	35.65	46.83	50.33
Benzene	0.6191	0.6599	0.7024	0.7675	0.9053	0.9892	1.0414	1.1254	1.1024	1.1438	1.1628
Toluene	8.8346	7.6890	3.9215	9.3790	10.3923	10.5204	10.4766	10.8419	10.9070	10.8144	10.6548
Ethylbenzene m/p-Xylene	4.4533	4.6207	5.1024	5.5925	5.9486	6.2140	6.5775	6.6432	6.8924	6.9138	6.9390
o-Xylene	0.6810	0.7022	0.7224	0.7785	1.2722	1.5233	1.7437	1.8228	1.8912	2.0443	2.0992
Methane	13.1941	9.0524	8.9365	8.1705	7.9854	8.0212	7.8248	7.5189	7.6326	7.5075	7.4328
Ethane	2.1126	1.8501	1.4406	1.1357	0.9722	0.8735	0.8422	0.8571	0.8247	0.7959	0.7907
Propane	7.0655	6.1948	5.1741	4.6122	3.8650	3.7490	3.4249	3.2119	3.0633	2.9929	2.9200
i-Butane	14.2404	13.6081	12.9516	9.2676	7.6362	7.4530	6.8139	6.7506	6.2586	6.0170	6.0776
n-Butane											
Cyclopentane	0.0012	0.0013	0.0014	0.0015	0.0017	0.0018	0.0020	0.0021	0.0022	0.0895	0.0903
i-Pentane	0.0485	0.0536	0.0576	0.0590	0.0727	0.0793	0.0811	0.0821	0.0839		
n-Pentane	-	0.0002	0.0004	0.0007	0.0012	0.0015	0.0018	0.0021	0.0021	0.0021	0.0021
Cyclohexane	0.0025	0.0050	0.0068	0.0078	0.0106	0.0123	0.0134	0.0138	0.0141	0.1120	0.1142
i-Hexane	0.1351	0.1260	0.1218	0.1178	0.1074	0.1024	0.0950	0.0929	0.0892		
n-Hexane	0.0016	0.0027	0.0049	000077	0.0104	0.0111	0.0119	0.0124	0.0129	0.0162	0.0169
Cycloheptane	0.0021	0.0030	0.0043	0.0053	0.0073	0.0081	0.0095	0.0090	0.0098	0.0109	0.0107
i-Heptane	0.0181	0.0192	0.0208	0.0246	0.0287	0.0332	0.0344	0.0350	0.0357	0.0377	0.0390
n-Heptane		0.0041	0.0053	0.0060	0.0077	0.0080	0.0084	0.0090	0.0093	0.0106	0.0103
Cyclooctane	0.1150	0.1439	0.1667	0.2022	0.2589	0.2853	0.3134	0.3297	0.3492	0.4622	0.4074
i-Octane											
% Conversion of n-Octane	51.5247	44.7363	44.3417	40.1362	39.4839	39.8867	39.3160	39.3599	39.1806	38.9708	38.7677

Table 6.9.2. % Selectivity versus time on stream for 0.3wt%Pt-0.3wt%Sn/Al_2O_3 (Sn impregnated first).

Products	The % Selectivity of Selected Products										
Time (hrs)	2.5	5.5	8.6	11.57	22.77	25.92	29.12	32.33	35.65	46.83	50.33
Benzene	1.2016	1.4751	1.5841	1.9123	2.2927	2.4801	2.6487	2.8594	2.8137	2.9351	2.9994
Toluene	17.1463	17.1875	20.12001	23.3679	26.3203	26.3757	26.6471	27.5455	27.8378	27.7499	27.4838
Ethylbenzene m/p-Xylene	8.6431	10.3287	11.5071	13.9338	15.0658	15.5790	16.7299	16.3782	17.5914	17.7410	17.8988
o-Xylene	1.3217	1.5695	1.6293	1.9398	3.2221	3.8191	4.4352	4.6311	4.8270	5.2456	5.4148
Methane	25.6073	20.2351	20.1537	20.3568	20.2245	20.1100	19.9024	19.1030	19.4805	19.2646	19.1727
Ethane	4.1001	4.13568	3.2488	2.8296	2.4623	2.1898	2.1421	2.1775	2.1049	2.0422	2.0395
Propane	13.7127	13.8474	11.6687	11.4915	9.7889	9.3991	8.7113	8.1604	7.8184	7.6797	7.5321
i-Butane	27.6380	30.4185	29.2087	23.0904	19.3400	18.6855	17.3311	17.1509	15.9736	15.4397	15.6770
n-Butane											
Cyclopentane	0.0024	0.0029	0.0031	0.0037	0.0043	0.0046	0.0050	0.0052	0.0056	0.2297	0.2329
i-Pentane	0.0941	0.1198	0.1300	0.1470	0.1842	0.1989	0.2063	0.2085	0.2141		
n-Pentane	-	0.0006	0.0010	0.0016	0.0029	0.0037	0.0046	0.0053	0.0054	0.0054	0.0053
Cyclohexane	0.0049	0.0111	0.0152	0.0195	0.0269	0.0307	0.0341	0.0352	0.0359	0.2874	0.2945
i-Hexane	0.2623	0.2816	0.2746	0.2935	0.2721	0.2566	0.2417	0.2361	0.2277		
n-Hexane	0.0030	0.0061	0.0111	0.0192	0.0264	0.0278	0.0304	0.0315	0.0330	0.0416	0.0437
Cycloheptane	0.0041	0.0067	0.0098	0.0133	0.0185	0.0203	0.0242	0.0230	0.0250	0.0280	0.0275
i-Heptane	0.0351	0.0429	0.0468	0.0614	0.0728	0.0833	0.0876	0.0890	0.0910	0.0967	0.1006
n-Heptane		0.0093	0.0121	0.0151	0.0196	0.0201	0.0214	0.0227	0.0238	0.0272	0.0266
Cyclooctane	0.2232	0.3217	0.3760	0.5037	0.6558	0.7154	0.7971	0.8376	0.8911	1.1860	1.0509
i-Octane											

Table 6.9.3. Carbon Mass Balance for 0.3wt%Pt-0.3wt%Sn/Al_2O_3 (Sn impregnated first) (510°C, 110 psig)

Time (hrs)	No. of moles of Carbon In	No. of moles of Carbon Out	Δ Carbon
2.5	5.9897×10^{-4}	5.1040×10^{-4}	8.8564×10^{-5}
5.5	5.9897×10^{-4}	5.4391×10^{-4}	5.5059×10^{-5}
8.6	5.9897×10^{-4}	5.5675×10^{-4}	4.2218×10^{-5}
11.57	5.9897×10^{-4}	5.5908×10^{-4}	3.9943×10^{-5}
22.77	5.9897×10^{-4}	5.6365×10^{-4}	3.5317×10^{-5}
25.92	5.9897×10^{-4}	5.6439×10^{-4}	3.4576×10^{-5}
29.12	5.9897×10^{-4}	5.6879×10^{-4}	3.0181×10^{-5}
32.33	5.9897×10^{-4}	5.7142×10^{-4}	2.7542×10^{-5}
35.65	5.9897×10^{-4}	5.7213×10^{-4}	2.6835×10^{-5}
46.83	5.9897×10^{-4}	5.7383×10^{-4}	2.5133×10^{-5}
50.33	5.9897×10^{-4}	5.7284×10^{-4}	2.6128×10^{-5}

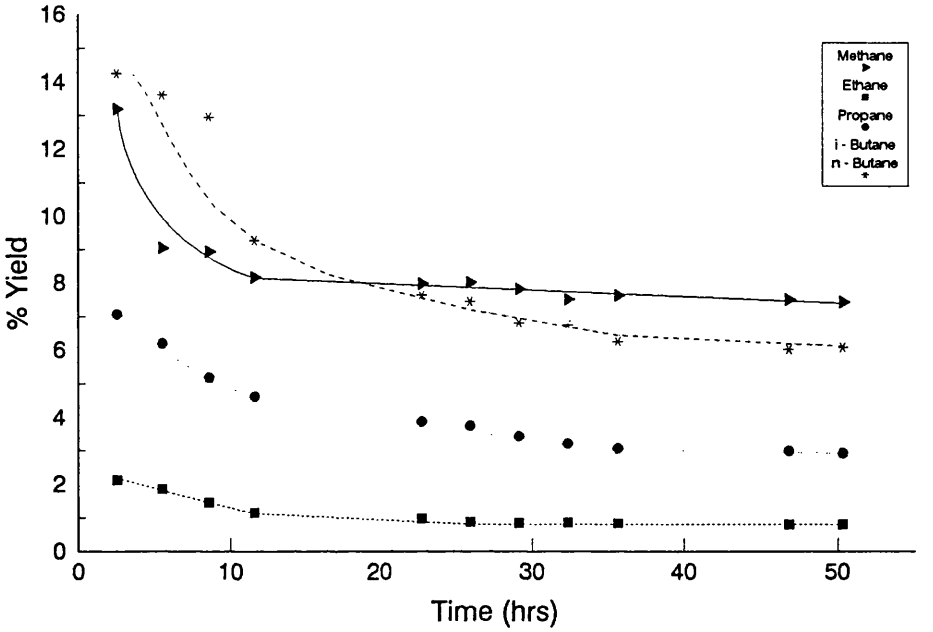

Figure 6.9.1. % Yield to Individual Hydrocarbon Products on 0.3%Pt-0.3%Sn /Alumina (Sn impregnated first)

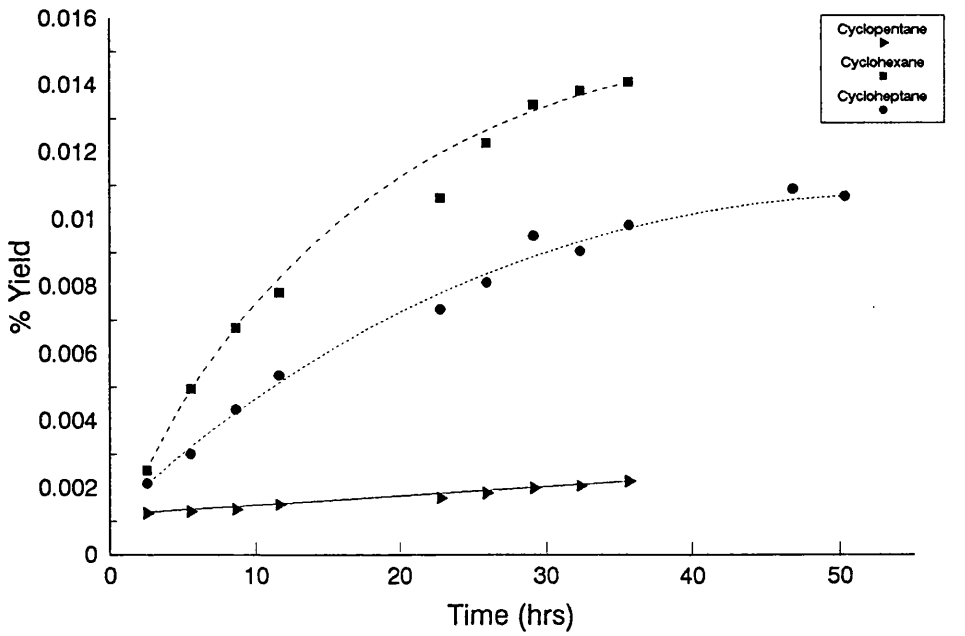

Figure 6.9.2. % Yield to Cycloparaffin Products on 0.3%Pt-0.3%Sn /Alumina (Sn impregnated first)

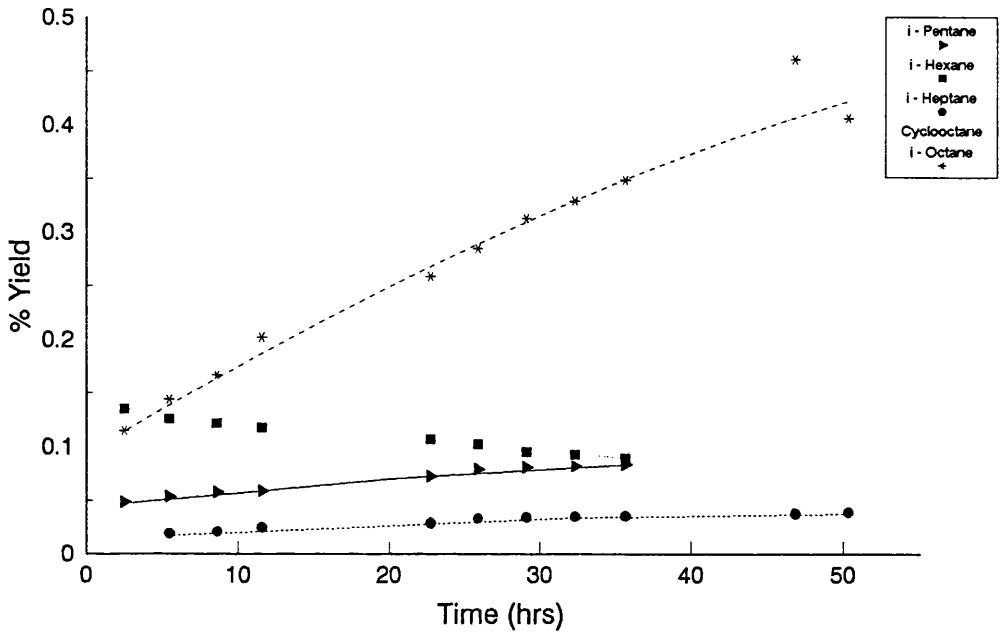

Figure 6.9.3. % Yield to i-Paraffin Products on 0.3%Pt-0.3%Sn /Alumina (Sn impregnated first)

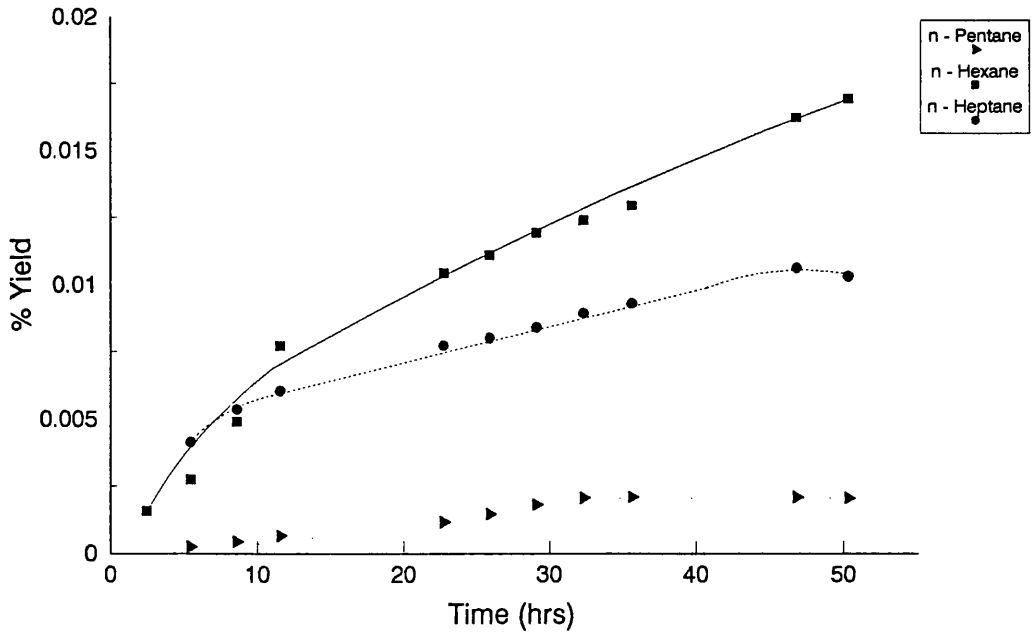

Figure 6.9.4. % Yield to n-Paraffin Products on 0.3%Pt-0.3%Sn /Alumina (Sn impregnated first)

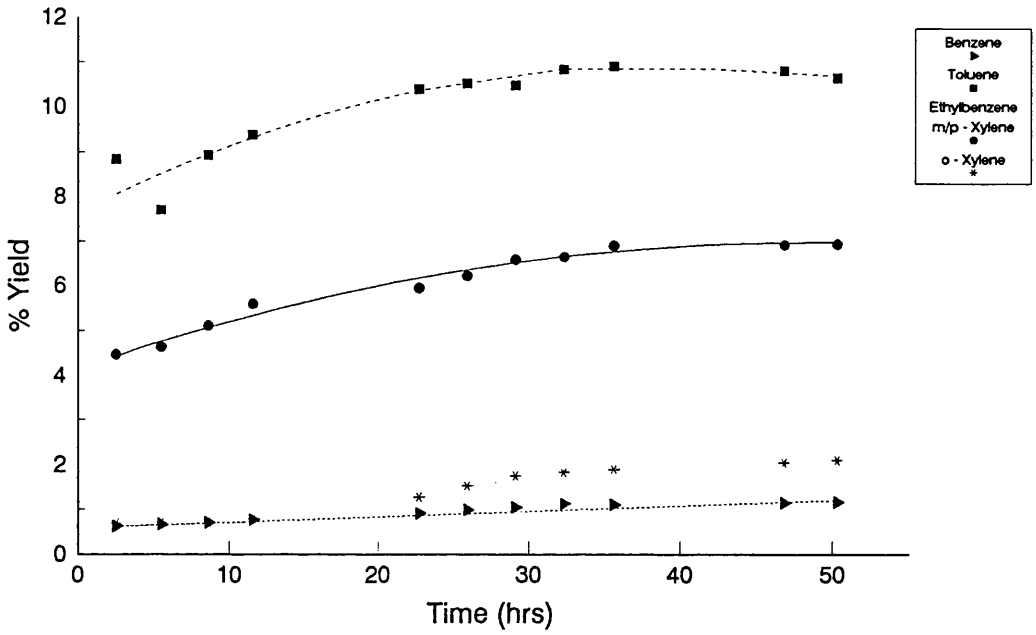

Figure 6.9.5. % Yield to Aromatic Products on 0.3%Pt-0.3%Sn /Alumina (Sn impregnated first)

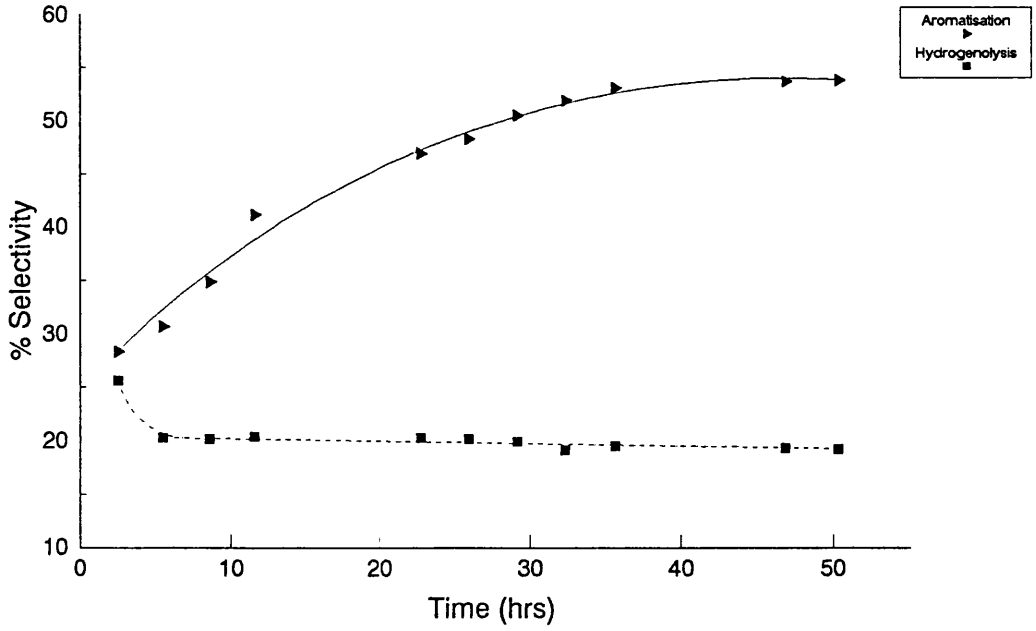

Figure 6.9.6. % Selectivity to the Major Reactions on 0.3%Pt-0.3%Sn /Alumina (Sn impregnated first)

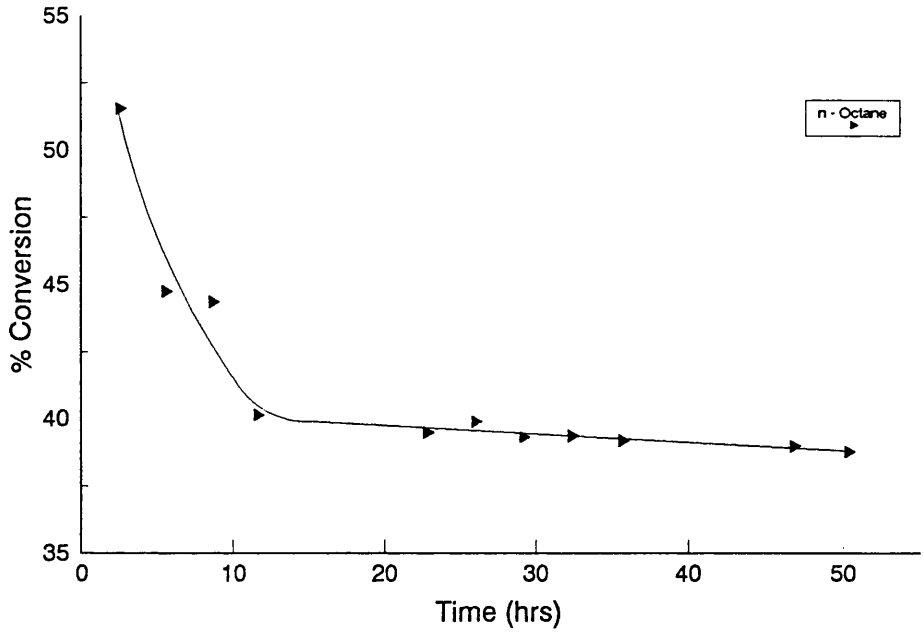

Figure 6.9.7. % Conversion of n-Octane on 0.3%Pt-0.3%Sn /Alumina (Sn impregnated first)

cyclopentane rises steadily during this time. Figure 6.9.3 illustrates the variation of i-paraffins with reaction time. The yields of both i-hexane and i-pentane are only quoted to 36 hours as they are indistinguishable from the corresponding cycloparaffins after this time. The yield of i-hexane decreases whereas the yields of i-pentane, i-hexane and cyclooctane/i-octane increase with time. The product yields of n-paraffins falls in the order from n-hexane, n-heptane to n-pentane. In this reaction the formation of i-paraffins is preferred to that of either cyclo- or i-paraffins.

The conversion of n-octane to aromatic species is detailed in Figure 6.9.5. All aromatic species are shown to increase with time before reaching a constant level. Toluene is the dominant species with a constant level of ~10% after 51 hours. This is followed by the combined yield of ethylbenzene/m/p-xylene, o-xylene and finally benzene. In comparison with the coimpregnated 0.3wt%Pt-0.3wt%Sn/Al_2O_3 catalyst the xylene yields are very small in this catalyst.

The selectivities to individual reaction products are shown in Table 6.9.2. The selectivities to the major reactions are shown in Figure 6.9.11. Aromatisation activity increases rapidly from 28% to a constant level of 54% at the end of the run. Hydrogenolysis activity on the other hand decreases initially until it reaches a steady level of 19%. The order of the selectivities to the major reactions is as follows:

Aromatisation > Hydrogenolysis > Hydrocracking > Isomerisation

The propane to methane ratio shows that the initial coke deposition is upon the metallic sites as the ratio rises for the first 6 hours. After this time the ratio falls

steadily indicating that the support is being deactivated preferentially in this period. The carbon mass balance, Table 6.9.3, reinforces this idea showing a progressively decreasing carbon uptake with time on stream.

The total conversion of n-octane rapidly decreases in the first 12 hours before levelling out at ~39%. Once again this value is between that of monometallic EUROPT-3.1 and bimetallic EUROPT-4.1. The % coke deposited upon the catalyst surface is 12.96%, almost double that for the Pt-Sn coimpregnated catalyst and very similar to the amount deposited on both EUROPT catalysts.

6.10. 0.3wt%Pt-0.9wt%Sn/Al_2O_3 - Pt impregnated first (510°C, 110 psig)

This catalyst was tested under identical conditions stated previously in Section 6.1. The conversion of n-octane over this catalyst is shown in Figure 6.10.1.

As can be seen from Figure 6.10.1 the total conversion of n-octane was constant until 30 hours on stream when it rapidly declined to a value of ~2%. The catalyst died in the microreactor and a very low conversion of n-octane was achieved. The % coke deposited upon the catalyst surface in this time was found to be 11.04% (Table 6.1).

Electron microscopy studies on the spent catalyst revealed that only a Pt-Sn alloy phase, Sn^{II} and no platinum particles could be found. This would indicate that after the 30 hour period all the available platinum had been alloyed with the excess of tin

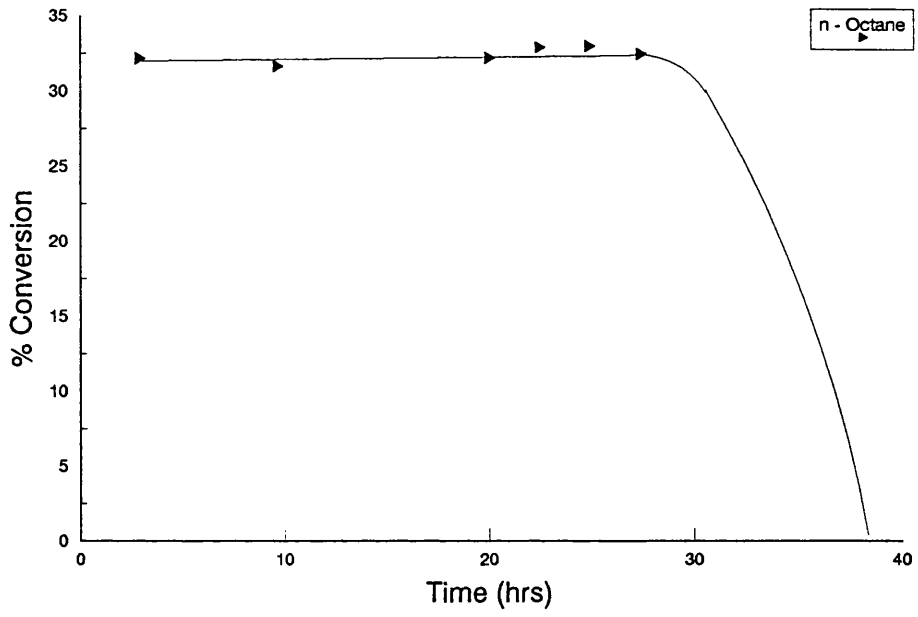

Figure 6.10.1. % Conversion of n-Octane on 0.3%Pt-0.9%Sn /Alumina (Pt impregnated first)

on the catalyst surface. This therefore explains both the reforming and electron microscopy results.

6.11. 0.3wt%Pt-0.3wt%Sn/Al_2O_3 - Pt impregnated first (510°C, 110 psig)

Reaction conditions were as stated in Section 6.1. The results of these experiments are illustrated in Tables 6.11.1 to 6.11.7 and Figures 6.11.1 to 6.11.3.

Figure 6.11.1 details the decreasing yield of C_1 - C_4 species with reaction time. Methane is produced in the largest quantities followed by propane and then ethane. The yield of n-butane is approximately 2 - 3 times that of i-butane in the run. The yield of paraffins is shown in Figures 6.11.2 to 6.11.4. Figure 6.11.2 illustrates the increasing cycloparaffin yield with reaction time. The product yield decreases in the order from cyclooctane, cycloheptane, cyclopentane to cyclohexane. The yield of cyclooctane rises steadily throughout the run where the yield of the other cycloparaffins is constant. The yields of i-paraffin products are shown in Figure 6.11.3. The yield of i-heptane decreases whereas the yield of the other i-paraffins increases with time. The yield of i-octane is the greatest followed initially by i-heptane and i-pentane, but after ~28 hours the yield of i-pentane increases above that of i-heptane. These are followed by i-hexane which is formed in very small quantities. The yield of n-paraffins, shown in Figure 6.11.4, increases with carbon number.

Table 6.11.1. %Yield of individual products and % Conversion versus time on stream for 0.3wt%Pt-0.3wt%Sn/Al_2O_3 (Pt impregnated first).

Products	The % Yield of Selected Products								
Time (hrs)	1.5	4.5	17.9	21	24	27	30.1	41.75	44.75
Benzene	3.3590	3.0348	2.8701	2.7333	2.6830	2.7063	2.6605	1.9737	1.9160
Toluene	5.0347	4.6563	4.0431	3.9152	3.7606	3.5976	3.3288	2.1477	2.2320
Ethylbenzene	3.1919	4.8459	5.5230	5.5591	5.8226	6.3683	6.2184	6.6437	6.5663
m/p-Xylene	1.3108	1.2395	1.1892	1.2453	1.0183	0.9129	0.8875	0.6921	0.6404
o-Xylene	3.5930	3.1886	2.6151	2.4570	2.3840	2.2688	2.0805	1.6649	1.5679
Methane	11.2186	8.7265	7.6895	7.4993	7.2682	7.1277	7.0659	6.5472	6.4787
Ethane	2.0223	18.7856	1.8984	1.9082	1.8882	1.9029	1.8020	1.7730	1.7722
Propane	7.0906	6.3220	5.7233	5.5831	5.3047	5.1096	4.9004	4.5949	4.4959
i-Butane	2.9159	2.7613	2.4960	2.3569	2.2531	2.1416	2.0656	1.8204	1.8197
n-Butane	5.49190	5.1253	5.2658	5.2042	5.0892	4.8127	4.8296	4.7528	4.7616
Cyclopentane	0.0003	0.0004	0.0004	0.0004	0.0004	0.0004	0.0004	0.0004	0.0004
i-Pentane	0.0084	0.0088	0.0105	0.0109	0.0110	0.0112	0.0116	0.0117	0.0117
n-Pentane	0.0095	0.0098	0.0111	0.0120	0.0118	0.0120	0.0125	0.0127	0.0128
Cyclohexane	0.0002	0.0003	0.0003	0.0003	0.0003	0.0003	0.0003	0.0003	0.0003
i-Hexane	0.0044	0.0045	0.0050	0.0063	0.0065	0.0071	0.0076	0.0079	0.0082
n-Hexane	0.0135	0.0140	0.0157	0.0173	0.0183	0.0189	0.0192	0.0201	0.0207
Cycloheptane	0.0006	0.0006	0.0007	0.0008	0.0007	0.0008	0.0008	0.0008	0.0009
i-Heptane	0.0118	0.0116	0.0115	0.0112	0.0113	0.0111	0.0109	0.0105	0.0103
n-Heptane	0.0243	0.0248	0.0254	0.0255	0.0255	0.0255	0.0259	0.0264	0.0284
Cyclooctane	0.0011	0.0010	0.0364	0.0012	0.0016	0.0017	0.0018	0.0022	0.0025
i-Octane	0.0348	0.0352		0.0367	0.0358	0.0369	0.0376	0.0386	0.0392
% Conversion of n-Octane	45.3374	41.8897	39.4305	38.5841	37.5954	37.0741	35.9678	32.7419	32.3860

Table 6.11.2. % Selectivity to individual products versus time on stream for 0.3wt%Pt-0.3wt%Sn/Al_2O_3 (Pt impregnated first).

Products	The % Selectivity of Selected Products								
Time (hrs)	1.5	4.5	17.9	21	24	27	30.1	41.75	44.75
Benzene	7.4089	7.2446	7.2788	7.0841	7.1365	7.2996	7.3969	6.0280	5.9160
Toluene	11.1049	11.1157	10.2537	10.1472	10.0029	9.7038	9.2551	6.5594	6.8920
Ethylbenzene	7.0403	11.5682	14.0069	14.4077	15.4876	17.1773	17.2887	20.2912	20.2751
m/p-Xylene	2.8911	2.9589	3.0160	3.2285	2.7086	2.4624	2.4676	2.1139	1.9774
o-Xylene	7.9250	7.6119	6.6322	6.3678	6.3412	6.1195	5.7843	5.0848	4.8414
Methane	24.7447	20.8320	19.5015	19.4361	19.3328	19.2255	19.6451	19.9964	20.0046
Ethane	4.4605	4.4845	4.8145	4.9455	5.0224	5.1327	5.0101	5.4149	5.4722
Propane	15.6395	15.0920	14.5148	14.4700	14.1100	13.7821	13.6245	14.0338	13.8821
i-Butane	6.4315	6.5919	6.3301	6.1086	5.9930	5.7764	5.7429	5.5598	5.6187
n-Butane	12.1134	12.2351	13.3545	13.4878	13.5367	12.9812	13.4276	14.5160	14.7025
Cyclopentane	0.0007	0.0009	0.0011	0.0011	0.0011	0.0011	0.0011	0.0013	0.0013
i-Pentane	0.0185	0.0210	0.0267	0.0283	0.0293	0.0302	0.0321	0.0357	0.0361
n-Pentane	0.0210	0.0234	0.0282	0.0310	0.0315	0.0323	0.0349	0.0388	0.0395
Cyclohexane	0.0005	0.0006	0.0008	0.0008	0.0008	0.0008	0.0008	0.0009	0.0009
i-Hexane	0.0096	0.0108	0.0127	0.0163	0.0174	0.0193	0.0212	0.0241	0.0252
n-Hexane	0.0299	0.0334	0.0397	0.0448	0.0488	0.0510	0.0532	0.0613	0.0639
Cycloheptane	0.0014	0.0015	0.0019	0.0020	0.0020	0.0021	0.0021	0.0024	0.0028
i-Heptane	0.0261	0.0277	0.0291	0.0289	0.0301	0.0300	0.0302	0.0320	0.0317
n-Heptane	0.0536	0.0593	0.0644	0.0662	0.0679	0.0689	0.0721	0.0805	0.0878
Cyclooctane	0.0023	0.0025	0.0923	0.0032	0.0041	0.0046	0.0051	0.0067	0.0076
i-Octane	0.0767	0.0839		0.0951	0.0953	0.0994	0.1046	0.1180	0.1212

Table 6.11.3. Carbon Mass Balance for 0.3wt%Pt-0.3wt%Sn/Al_2O_3 (Pt impregnated first) (510°C, 110 psig)

Time (hrs)	No. of moles of Carbon In	No. of moles of Carbon Out	Δ Carbon
1.5	4.3572×10^{-4}	4.1103×10^{-4}	2.4686×10^{-5}
4.5	4.3572×10^{-4}	4.1601×10^{-4}	1.9710×10^{-5}
17.9	4.3572×10^{-4}	4.2389×10^{-4}	1.1822×10^{-5}
21	4.3572×10^{-4}	4.2573×10^{-4}	9.9846×10^{-6}
24	4.3572×10^{-4}	4.2661×10^{-4}	9.1077×10^{-6}
27	4.3572×10^{-4}	4.2781×10^{-4}	7.9087×10^{-6}
30.1	4.3572×10^{-4}	4.2827×10^{-4}	7.4477×10^{-6}
41.75	4.3572×10^{-4}	4.3087×10^{-4}	4.8436×10^{-6}
44.75	4.3572×10^{-4}	4.3104×10^{-4}	4.6796×10^{-6}

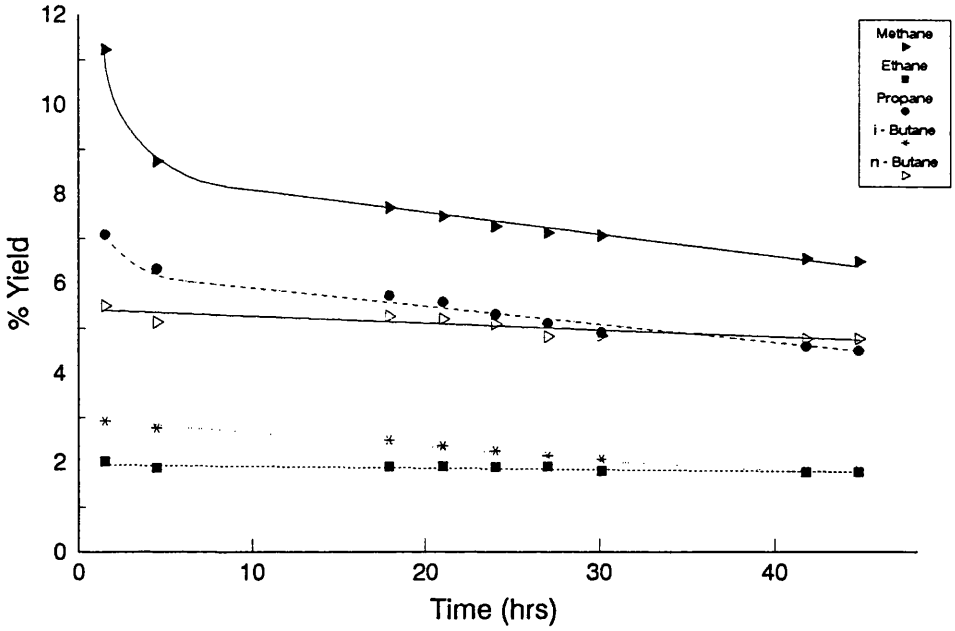

Figure 6.11.1. % Yield to Individual Hydrocarbon Products on 0.3%Pt-0.3%Sn /Alumina (Pt impregnated first)

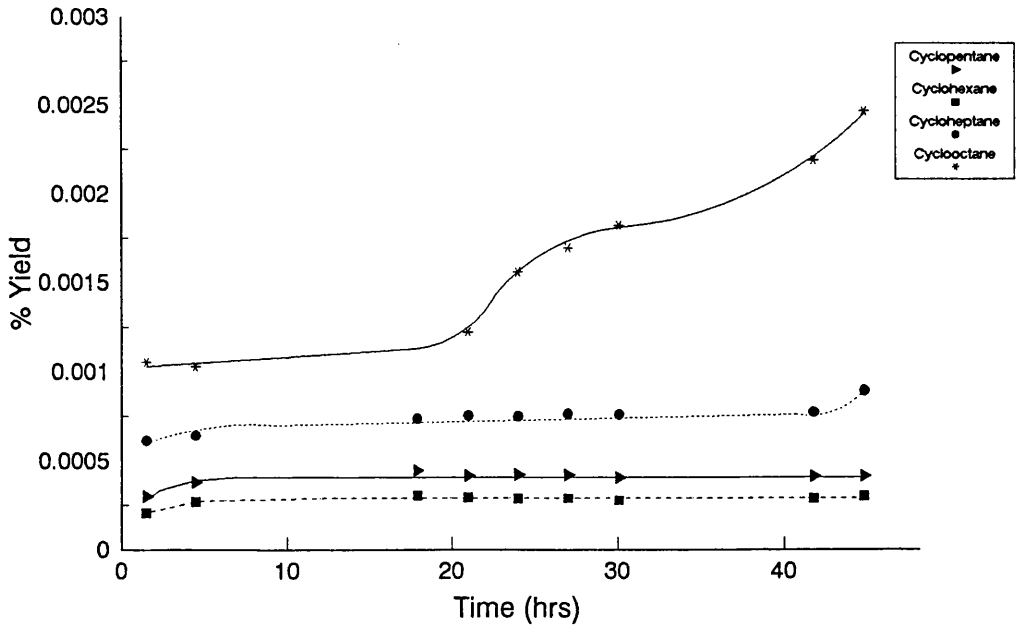

Figure 6.11.2. % Yield of Cycloparaffin Products on 0.3%Pt-0.3%Sn /Alumina (Pt impregnated first)

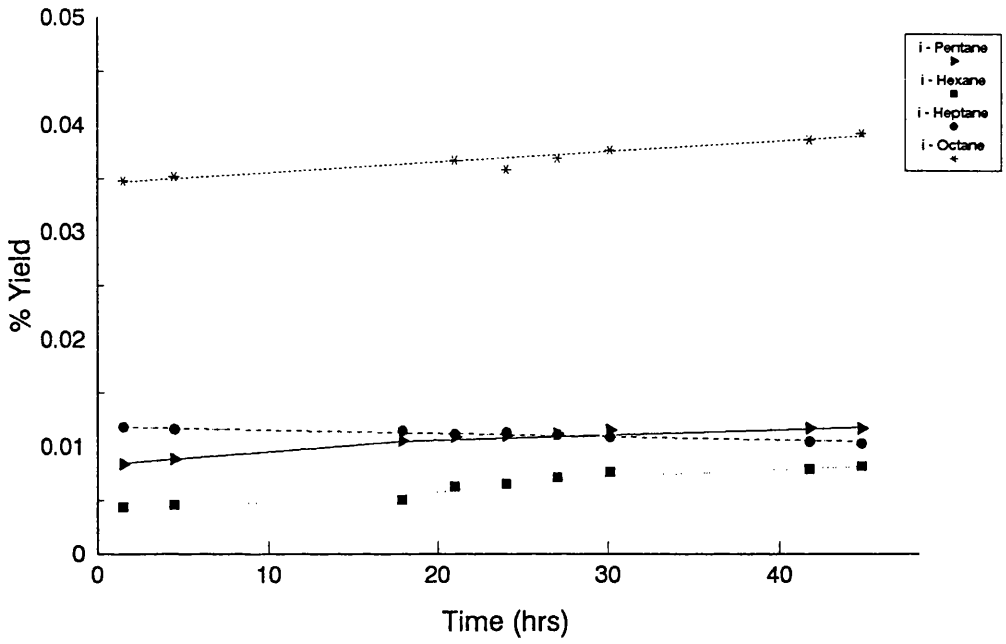

Figure 6.11.3. % Yield of i-Paraffin Products on 0.3%Pt-0.3%Sn /Alumina (Pt impregnated first)

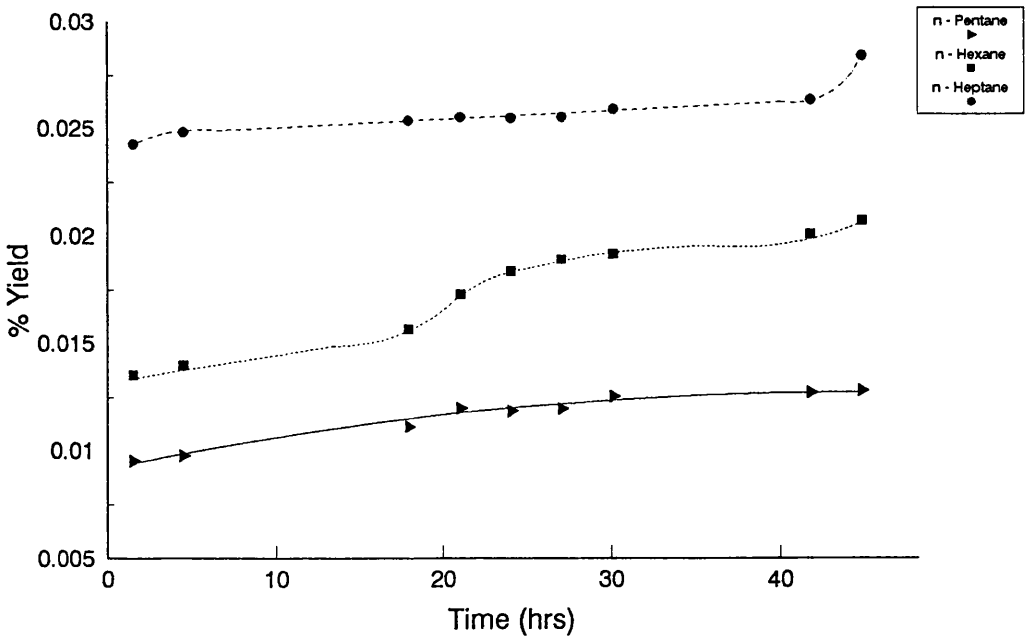

Figure 6.11.4. % Yield of n-Paraffin Products on 0.3%Pt-0.3%Sn /Alumina (Pt impregnated first)

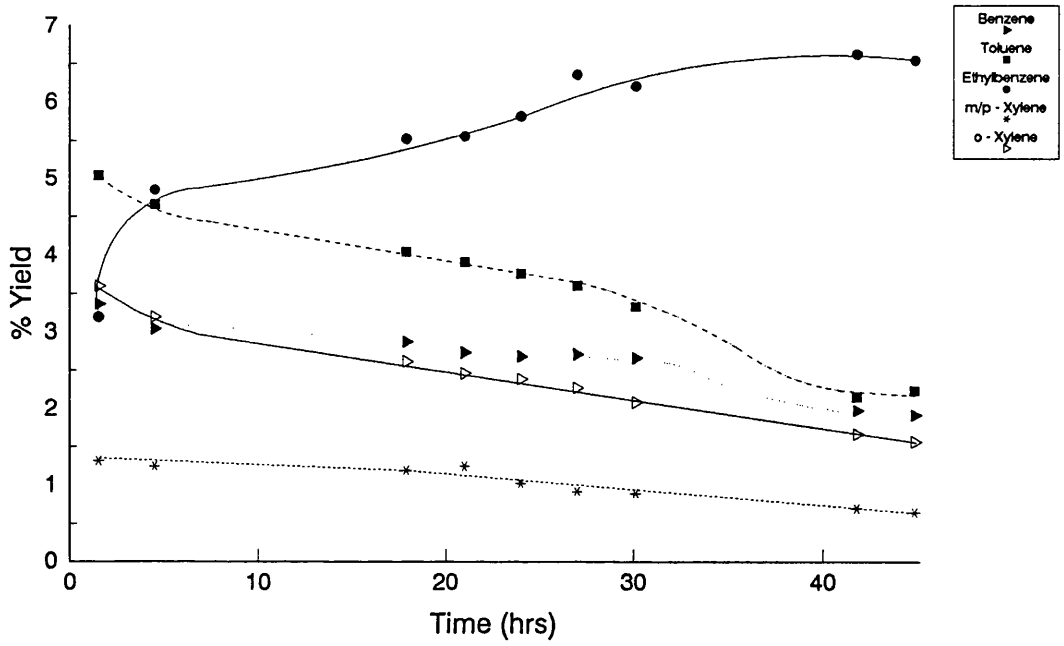

Figure 6.11.5. % Yield of Aromatic Products on 0.3%Pt-0.3%Sn /Alumina (Pt impregnated first)

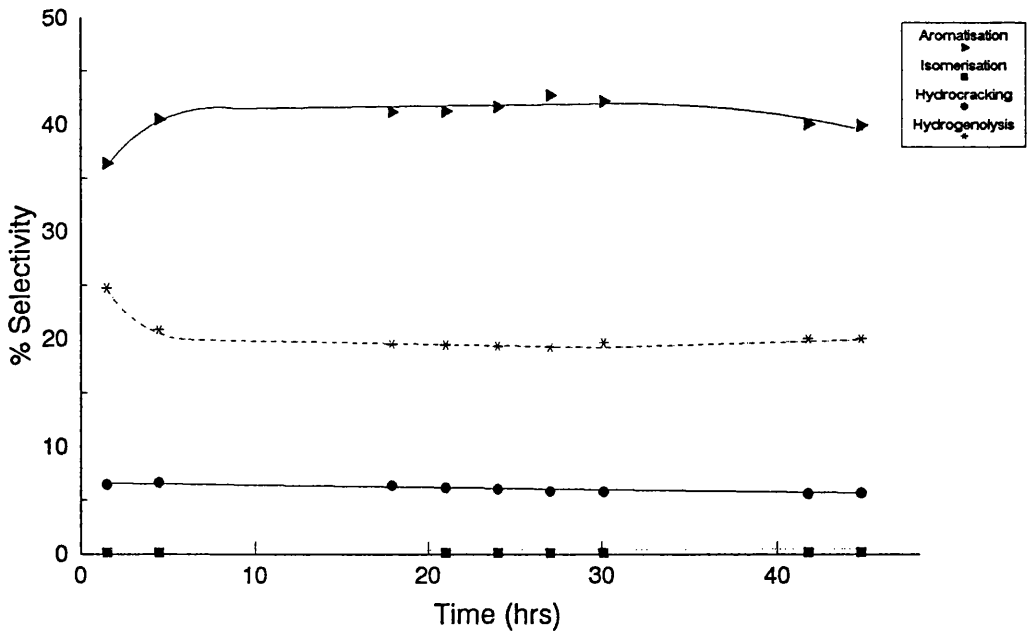

Figure 6.11.6. % Selectivity to the Major Reactions on 0.3%Pt-0.3%Sn /Alumina (Pt impregnated first)

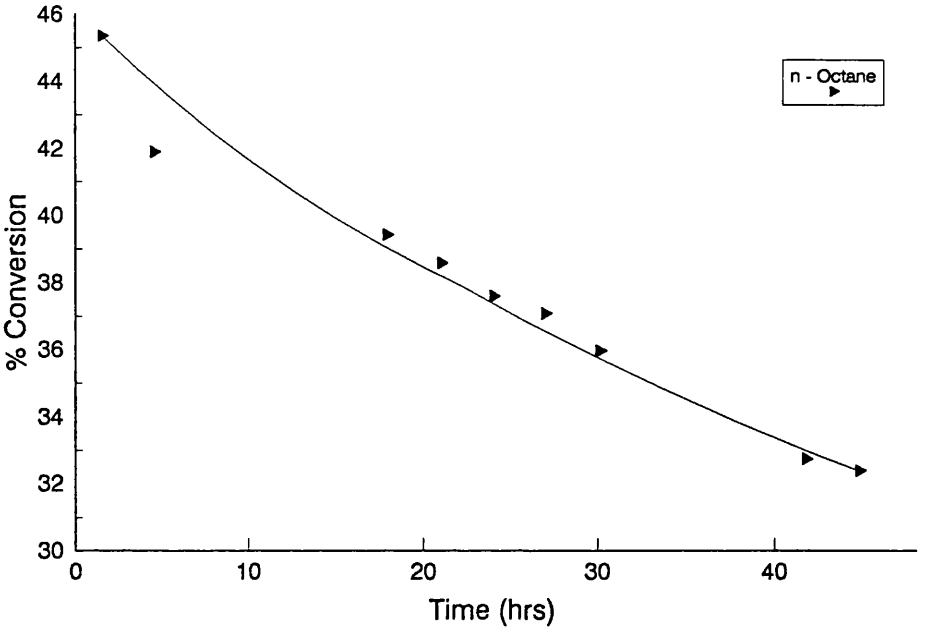

Figure 6.11.7. % Conversion of n-Octane on 0.3%Pt-0.3%Sn /Alumina (Pt impregnated first)

The product yields of aromatic species are shown in Figure 6.11.5 with respect to the reaction time. The yield of ethylbenzene increases before reaching a constant value while the yield of all other aromatics decrease with time. The order of aromatic formation was initially toluene, o-xylene, ethylbenzene and then m/p-xylene. However after ~5 hours on stream this order changed to ethylbenzene being the dominant product followed by toluene, benzene, o-xylene and m/p-xylene.

The selectivities to individual hydrocarbon species are shown in Table 6.11.2. The selectivities of the major reactions are shown in Figure 6.11.6. The order of the selectivities is as follows:

Aromatisation > Hydrogenolysis > Hydrocracking > Isomerisation

The aromatisation activity increases initially before reaching a constant value of ~42% before falling to ~40% after 45 hours on stream. The hydrogenolysis activity, after an initial decrease, remains constant at 20% throughout the run. The selectivity to aromatisation reactions is less than either the corresponding 0.3wt%Pt-0.3wt%Sn/Al_2O_3 coimpregnated or tin impregnated first catalysts. The aromatisation activity is very similar to that of the monometallic EUROPT-3.1 catalyst under the same conditions. The selectivity to hydrogenolysis was similar to that of the tin impregnated first catalyst but higher than either EUROPT catalyst.

The propane to methane ratio increases steadily before reaching a constant level indicating that the metallic sites were initially more deactivated than the acidic sites. The carbon mass balance again illustrates the decreasing carbon deposition with time on the catalyst surface.

The total conversion of n-octane, illustrated in Figure 6.11.7, decreases with time before reaching a constant conversion of ~32%. This level of conversion is higher than with EUROPT-3.1 but lower than with EUROPT-4.1, the 0.3wt%Pt-0.3wt%Sn/Al_2O_3 tin impregnated first and the coimpregnated catalysts.

The % coke deposited upon the catalyst surface was 23.84% by weight. This is almost double the amount deposited on either of the EUROPT catalysts and much greater than on any other catalyst tested.

6.12. 0.3wt%Pt-0.3wt%Sn/Al_2O_3 - Patent (510°C, 110 psig)

The reaction conditions were as described in Section 6.1 with the results of this study being expressed in Tables 6.12.1 to 6.12.3 and Figures 6.12.1 to 6.12.6.

The yield of C_1 - C_4 species is shown in Figure 6.12.1 to decrease with time on stream. Both the yields of methane and propane decrease rapidly in the initial 20 hours of the reaction before reaching constant levels of 2.4 and 1.7% respectively. Ethane, in comparison, is produced in much smaller quantities. The yield of n-butane, approximately 4 times that of i-butane, levels off at ~3.4%.

The yields of paraffin products as a function of time are illustrated in Figures 6.12.2 and 6.12.3. Several individual hydrocarbon species could not be separated and therefore combined values are quoted. The yield of cycloparaffins is extremely small and initially increase with increasing carbon number. The final product yields

Table 6.12.1. %Yield of individual products and % Conversion versus time on stream for 0.3wt%Pt-0.3wt%Sn/Al_2O_3 (Patent).

Products	The % Yield of Selected Products									
Time (hrs)	1.5	4.4	17.55	20.55	23.5	26.5	29.5	41.5	44.5	48
Benzene	7.8439	6.3628	4.9131	4.7364	4.5840	4.3645	4.1653	3.1232	3.0838	3.0445
Toluene	4.7969	4.1581	3.4380	3.4007	3.3693	3.2745	3.2039	2.4425	2.4005	2.4362
Ethylbenzene	0.2281	0.2146	0.1983	0.2012	0.1990	0.1925	0.1935	0.1874	0.1893	0.1883
m/p-Xylene	0.0587	0.0527	0.0427	0.0411	0.0400	0.0372	0.0356	0.0303	0.0303	0.0291
o-Xylene	0.7170	0.6724	0.5946	0.5505	0.5832	0.5380	0.5293	0.4776	0.4842	0.4731
Methane	6.1892	4.3748	3.4239	3.1367	3.0325	2.9341	2.8048	2.3802	2.3670	2.3859
Ethane	1.8487	1.4922	1.2457	1.0867	0.8795	0.7653	0.7560	0.7483	0.6937	0.6748
Propane	4.1776	3.6985	2.2316	2.0317	1.9115	1.8944	1.9005	1.7360	1.6423	1.7041
i-Butane	1.6533	1.4555	1.1660	1.1274	1.1331	1.1053	1.1225	0.9042	0.7695	0.7369
n-Butane	5.4638	5.0978	4.3540	4.1849	4.1394	4.1143	4.0355	3.5494	3.4157	3.3690
Cyclopentane	0.0001	0.0001	0.0002	0.0002	0.0002	0.0003	0.0004	0.0004	0.0005	0.0005
i-Pentane n-Pentane	0.0487	0.0389	0.0259	0.0250	0.0238	0.0226	0.0200	0.0159	0.0146	0.0135
Cyclohexane	0.0002	0.0002	0.0002	0.0003	0.0003	0.0003	0.0004	0.0004	0.0004	0.0004
i-Hexane n-Hexane	0.0194	0.0202	0.0259	0.0267	0.0261	0.0279	0.0305	0.0327	0.0328	0.0323
Cycloheptane	0.0003	0.0003	0.0003	0.0004	0.0003	0.0004	0.0004	0.0005	0.0073	0.0005
i-Heptane	0.0092	0.0088	0.0077	0.0078	0.0077	0.0071	0.0071	0.0068		0.0067
n-Heptane	0.0104	0.0106	0.0111	0.0111	0.0113	0.0124	0.0125	0.0153	0.0147	0.0149
Cyclooctane	-	-	-	-	-	-	-	-	-	-
i-Octane	0.0117	0.0126	0.0159	0.0162	0.0164	0.0169	0.0171	0.0175	0.0169	0.0175
% Conversion of n-Octane	33.0772	27.6711	21.6953	20.9551	19.9578	19.3080	18.8353	15.6686	15.1634	15.1282

Table 6.12.2 % Selectivity of individual products versus time on stream for 0.3wt%Pt-0.3wt%Sn/Al_2O_3 (Patent).

Products	The % Selectivity of Selected Products									
Time (hrs)	1.5	4.4	17.55	20.55	23.5	26.5	29.5	41.5	44.5	48
Benzene	23.7140	22.9943	22.6461	23.0089	22.9685	22.6046	22.1143	19.9326	20.3369	20.1244
Toluene	14.5023	15.0270	15.8467	16.5201	16.8820	16.9592	17.0103	15.58888	15.8307	16.1038
Ethylbenzene	0.6895	0.7754	0.9140	0.9776	0.9972	0.9972	1.0272	1.1962	1.2482	1.2445
m/p-Xylene	0.1775	0.1903	0.1970	0.1998	0.2005	0.1924	0.1891	0.1935	0.1997	0.1927
o-Xylene	2.16772	2.4300	2.7408	2.6744	2.9222	2.7864	2.8100	3.0483	3.1930	3.1273
Methane	18.7115	15.8100	15.7819	15.2377	15.1947	15.1965	14.8913	15.1906	15.6101	15.7712
Ethane	5.5889	5.3927	5.7420	5.2793	4.4070	5.1792	4.0136	4.7758	4.5749	4.4605
Propane	12.6298	13.3659	10.2860	9.8701	9.5776	9.8113	10.0902	11.0782	10.8310	11.2647
i-Butane	4.9983	5.2601	5.3744	5.4768	5.6776	5.7245	5.9594	5.7709	5.0747	4.8708
n-Butane	16.5184	18.4228	20.0689	20.3299	20.7410	21.3087	21.4255	22.6528	22.5259	22.2699
Cyclopentane	0.0003	0.0004	0.0009	0.0012	0.0012	0.0014	0.0020	0.0028	0.0030	0.0031
i-Pentane n-Pentane	0.1474	0.1407	0.1194	0.1212	0.1194	0.1170	0.1063	0.1016	0.0963	0.0890
Cyclohexane	0.0005	0.0007	0.0011	0.0013	0.0016	0.0018	0.0020	0.0027	0.0028	0.0029
i-Hexane n-Hexane	0.0585	0.0730	0.1192	0.1297	0.1308	0.1445	0.1621	0.2085	0.2162	0.2137
Cycloheptane	0.0009	0.0011	0.0016	0.0017	0.0017	0.0018	0.0020	0.0031	0.0480	0.0032
i-Heptane	0.0278	0.0317	0.0356	0.0378	0.0484	0.0368	0.0376	0.0433		0.0441
n-Heptane	0.0313	0.0382	0.0511	0.0538	0.0564	0.0644	0.0664	0.0976	0.0969	0.0986
Cyclooctane	-	-	-	-	-	-	-	-	-	-
i-Octane	0.0354	0.0457	0.0734	0.0786	0.0824	0.0877	0.0907	0.1116	0.1115	0.1156

Table 6.12.3. Carbon Mass Balance for 0.3wt%Pt-0.3wt%Sn/Al_2O_3 (Patent) (510°C, 110 psig)

Time (hrs)	No. of moles of Carbon In	No. of moles of Carbon Out	Δ Carbon
1.5	4.0993×10^{-4}	3.9124×10^{-4}	1.8690×10^{-5}
4.4	4.0993×10^{-4}	3.9475×10^{-4}	1.5183×10^{-5}
17.55	4.0993×10^{-4}	3.9860×10^{-4}	1.1335×10^{-5}
20.55	4.0993×10^{-4}	3.9921×10^{-4}	1.0727×10^{-5}
23.5	4.0993×10^{-4}	3.9899×10^{-4}	1.0946×10^{-5}
26.5	4.0993×10^{-4}	3.9936×10^{-4}	1.0577×10^{-5}
29.5	4.0993×10^{-4}	3.9964×10^{-4}	1.0290×10^{-5}
41.5	4.0993×10^{-4}	4.0133×10^{-4}	8.6067×10^{-6}
44.5	4.0993×10^{-4}	4.0234×10^{-4}	7.5889×10^{-6}
48	4.0993×10^{-4}	4.0186×10^{-4}	8.0704×10^{-6}

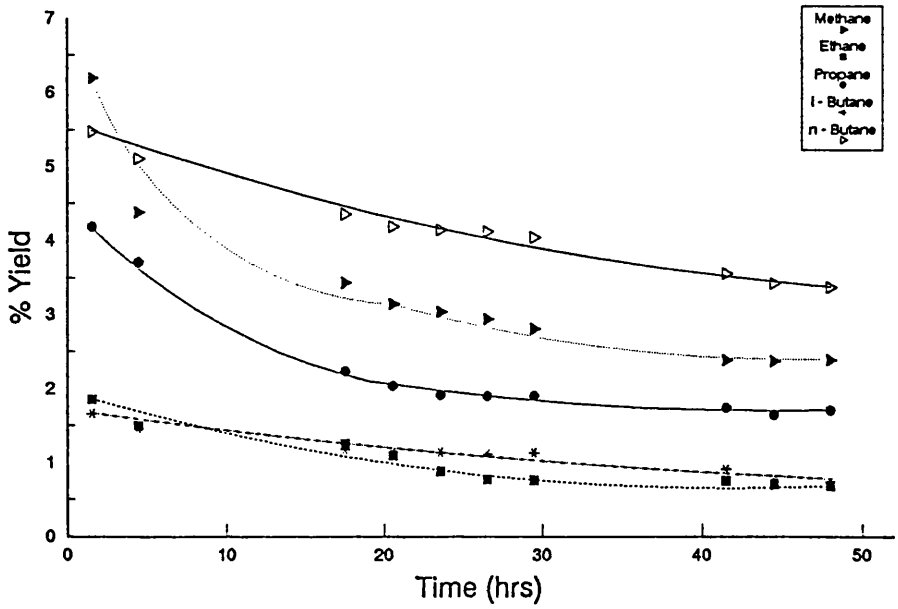

Figure 6.12.1. % Yield to Individual Hydrocarbon Products on 0.3%Pt-0.3%Sn/Alumina (Patent)

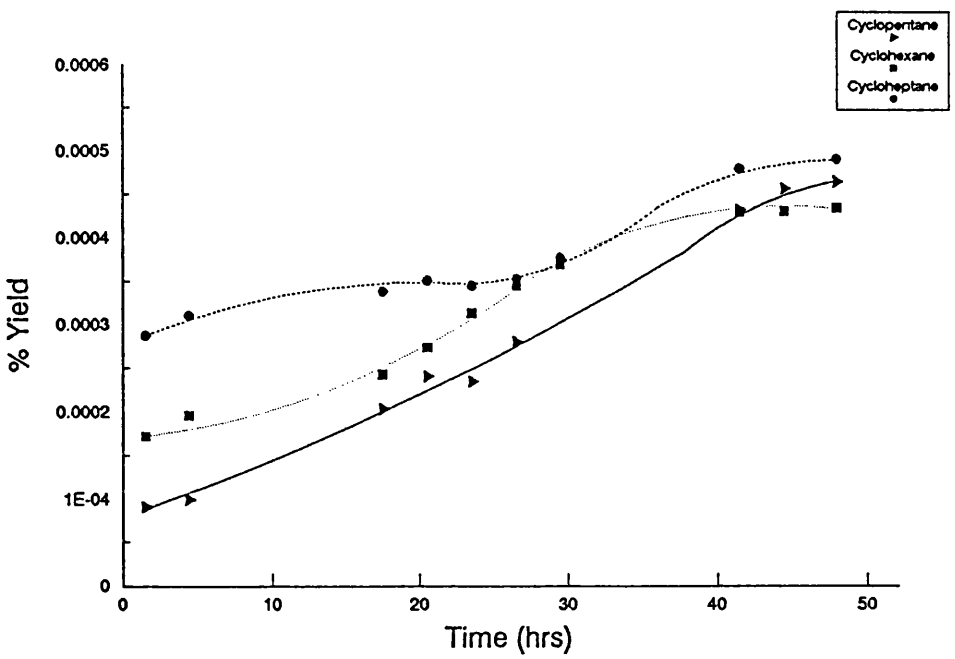

Figure 6.12.2. % Yield to Cycloparaffin Products on 0.3%Pt-0.3%Sn/Alumina (Patent)

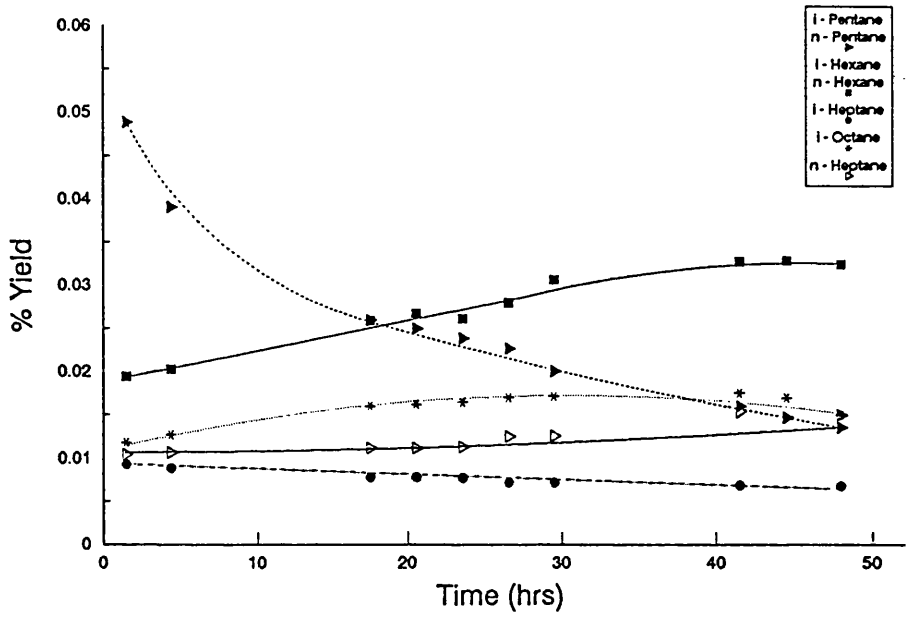

Figure 6.12.3. % Yield to i- and n-Paraffins on 0.3%Pt-0.3%Sn /Alumina (Patent)

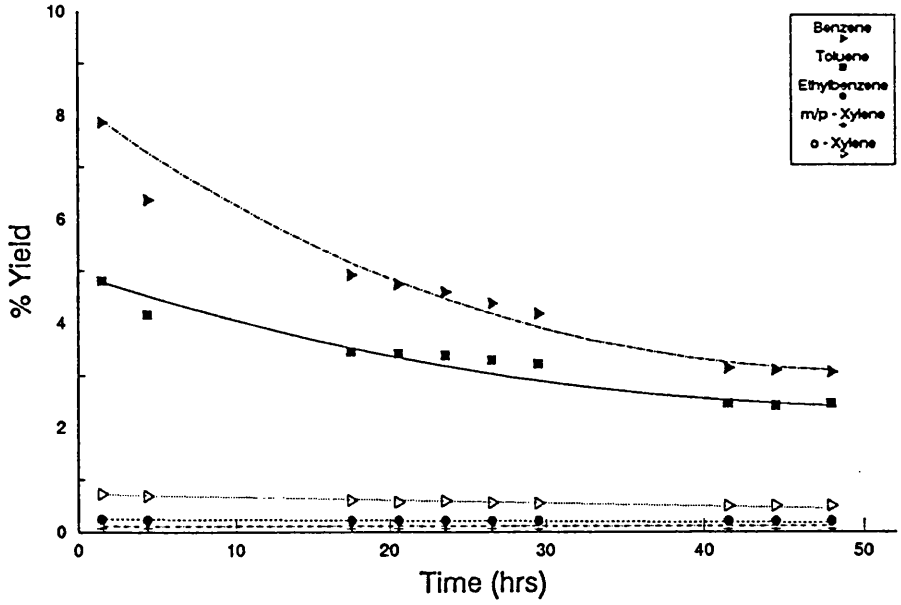

Figure 6.12.4. % Yield to Aromatic Products on 0.3%Pt-0.3%Sn /Alumina (Patent)

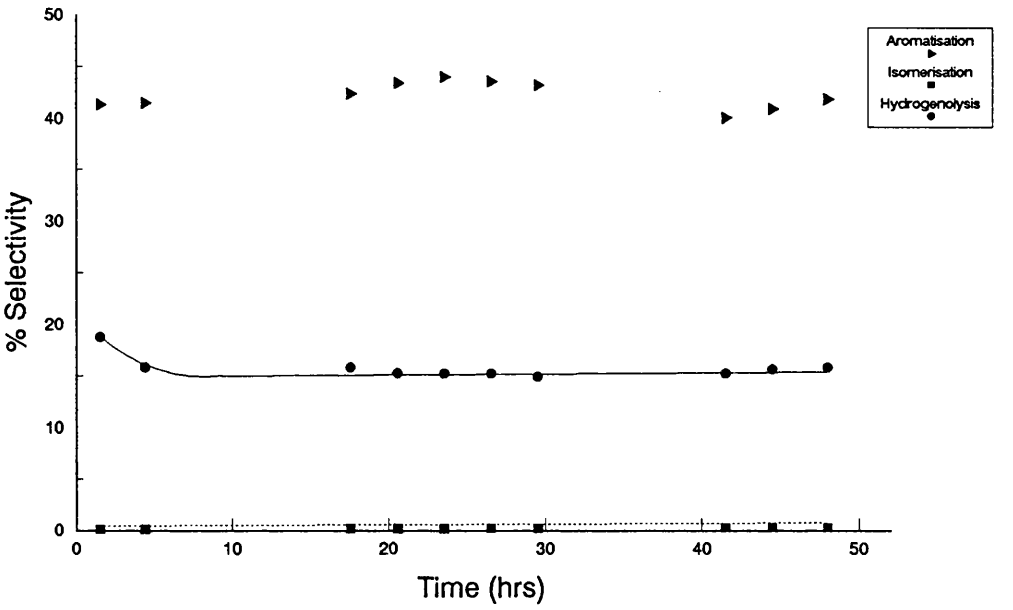

Figure 6.12.5. % Selectivity to Major Reactions on 0.3%Pt-0.3%Sn /Alumina (Patent)

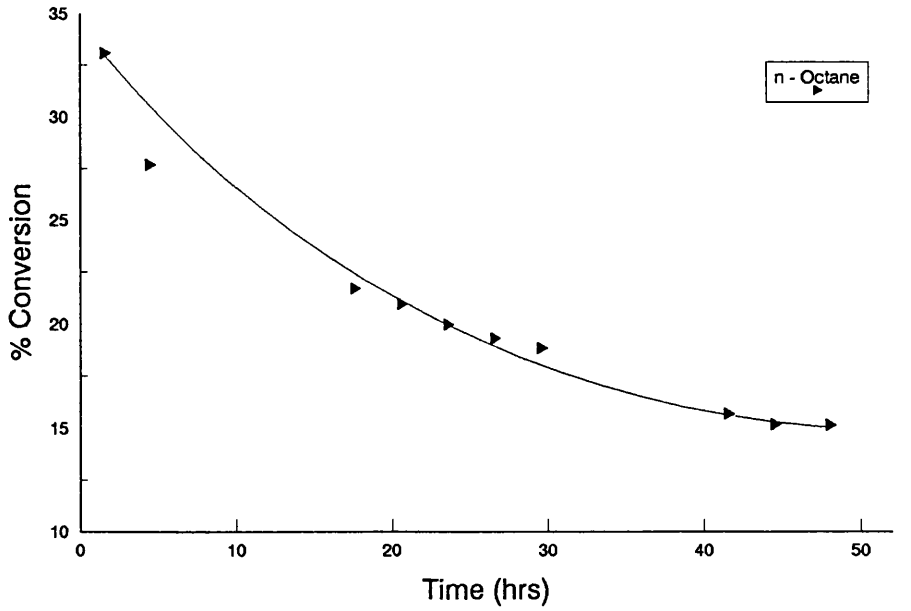

Figure 6.12.6. % Conversion of n-Octane on 0.3%Pt-0.3%Sn /Alumina (Patent)

illustrate that cycloheptane is still produced in the largest quantities followed by cyclopentane and finally by cyclohexane. Figure 6.12.3 shows the combined and individual yields of paraffinic species. The combined yields of i- and n-pentane decreases whereas that of i- and n-hexane increases with time. The product yield of i-octane increases with time and that of i-heptane decreases.

The formation of aromatics on this catalyst, Figure 6.12.4, follows the order from benzene, toluene, o-xylene, ethylbenzene to m/p-xylene. The yield of C_8 aromatics on this catalyst is many times lower than that on the EUROPT catalysts or on the platinum-tin catalysts prepared using pelletised γ-Al_2O_3 (CK-300). The yield of C_8 aromatics never exceeds 1% whereas the constant yield of benzene and toluene is 3 and 2.5% respectively. The yield of all the individual aromatic species decreases with time.

Table 6.12.2 shows the selectivity of hydrocarbon products with time and the selectivities to the major reactions are detailed in Figure 6.12.5. The major reactions again follow the decreasing order:

Aromatisation > Hydrogenolysis > Hydrocracking > Isomerisation

Aromatisation activity increases gradually to a maximum after 25 hours before decreasing slowly to approximately the original value. Hydrogenolysis activity in comparison decreases initially before attaining a constant level of ~15%. The overall aromatisation activity of this catalyst is similar to that of the catalyst in Section 6.11. However one advantage was that the hydrogenolysis activity had dropped by ~5%.

The propane to methane ratio increases rapidly to a maximum after 5 hours before decreasing steadily. After 25 hours the ratio again increases slightly before reaching a steady level. This would suggest that an initial rapid deposition of coke on the metallic sites is followed by coke deposition upon the support. The carbon mass balance is again typical of these reactions, the amount of carbon deposition decreasing with time on stream.

The total conversion of n-octane is illustrated in Figure 6.12.6. The conversion undergoes a steady decline in the first 40 hours of the reaction before reaching a constant conversion of ~15%. This value is much lower than that of either the EUROPT catalysts or of one of the Pt-Sn/Al_2O_3 catalysts. Although the conversion of this catalyst is low the selectivity to aromatics has not fallen considerably.

The % coke deposited on this catalyst was 14.99% by weight as detailed in Table 6.1. The % coke deposited upon this catalyst is comparable to the amount on EUROPT-4.1.

6.13. 0.3wt%Pt-0.3wt%Sn/Al_2O_3 - Methanol (510°C, 110 psig)

The reaction conditions were as described in Section 6.1 with the results of this study being expressed in Tables 6.13.1 to 6.13.3 and Figures 6.13.1 to 6.13.7.

The product yields of C_1 - C_4 species are shown to decrease with time in Figure 6.13.1. Yet again methane is found to be the dominant species (~5%) closely

Table 6.13.1. %Yield of individual products and % Conversion versus time on stream for 0.3wt%Pt-0.3wt%Sn/Al_2O_3 (Methanol).

Products	The % Yield of Selected Products							
Time (hrs)	2	5	18.95	22	25	28	43.2	46.25
Benzene	2.5920	1.9322	1.4107	1.4482	1.4650	1.4576	1.4144	1.4044
Toluene	2.6296	3.2588	3.5534	3.5135	3.4700	3.4265	3.3196	3.3812
Ethylbenzene	3.1641	3.9156	5.4967	5.6130	5.7408	5.8343	5.6680	5.7695
m/p-Xylene								
o-Xylene	1.7228	2.5679	2.4191	2.5860	2.8673	2.9279	3.2573	3.2288
Methane	8.6005	6.6072	6.0952	5.8952	5.5088	5.2666	5.2109	5.1483
Ethane	2.1316	1.8774	1.4427	1.2389	1.1040	0.9891	0.7381	0.6955
Propane	7.1898	6.0844	5.3613	5.1365	4.9750	4.8172	4.8044	4.7954
i-Butane	3.2838	2.0107	1.2173	0.9406	0.8136	0.9164	0.7841	0.7526
n-Butane	7.6508	6.6741	5.9704	5.5780	5.0520	5.2980	5.3084	5.0856
Cyclopentane	0.0004	0.0003	0.0003	0.0003	0.0003	0.0002	0.0002	0.0002
i-Pentane	0.0344	0.0318	0.0286	0.0261	0.0234	0.0196	0.0184	0.0178
n-Pentane	0.0071	0.0068	0.0076	0.0077	0.0080	0.0085	0.0089	0.0090
Cyclohexane	0.0007	0.0007	0.0008	0.0009	0.0009	0.0012	0.0011	0.0012
i-Hexane	0.0165	0.0593	0.0621	0.0631	0.0171	0.0181	0.0183	0.0185
n-Hexane	0.0382				0.0445	0.0486	0.0482	0.0493
Cycloheptane	0.0015	0.0011	0.0010	0.0009	0.0009	0.0009	0.0009	0.0009
i-Heptane	0.0194	0.0153	0.0146	0.0145	0.0145	0.0138	0.0136	0.0131
n-Heptane	0.0252	0.0282	0.0310	0.0329	0.0346	0.0366	0.0370	0.0380
Cyclooctane	0.0372	0.0077	0.0085	0.0091	0.0098	0.0099	0.0100	0.0102
i-Octane		0.0303	0.0321	0.0312	0.0315	-	0.0336	0.0327
% Conversion of n-Octane	39.1454	35.1099	33.4324	32.1364	31.1476	31.0910	30.6955	30.4523

Table 6.13.2. % Selectivity of individual products and versus time on stream for 0.3wt%Pt-0.3wt%Sn/Al_2O_3 (Methanol).

Products	The % Selectivity of Selected Products							
Time (hrs)	2	5	18.95	22	25	28	43.2	46.25
Benzene	6.6214	5.5033	4.2196	4.5065	4.7035	4.6880	4.6078	4.6118
Toluene	6.7176	9.2818	10.6286	10.9330	11.1405	11.0210	10.8145	11.1032
Ethylbenzene	8.0829	11.1523	16.4414	17.4660	18.4311	18.7651	18.4654	18.9461
m/p-Xylene								
o-Xylene	4.4010	7.3140	7.2359	8.0469	9.2056	9.4171	10.6116	10.5832
Methane	21.9707	18.8187	18.2314	18.3443	17.6861	16.9393	16.9762	16.9060
Ethane	5.4453	5.3471	4.3153	3.8552	3.5445	3.1813	2.4045	2.2838
Propane	18.3669	17.3296	16.0361	15.9836	15.9724	15.4938	15.6518	15.7474
i-Butane	8.3888	5.7269	3.6410	2.9271	2.6120	2.9476	2.5544	2.4715
n-Butane	19.5447	19.0091	17.8583	17.3571	16.2195	17.0405	17.2938	16.7004
Cyclopentane	0.0010	0.0010	0.0009	0.0009	0.0008	0.0008	0.0008	0.0008
i-Pentane	0.0878	0.0905	0.0855	0.0811	0.0753	0.0631	0.0600	0.0586
n-Pentane	0.0181	0.0194	0.0228	0.0239	0.0257	0.0273	0.0290	0.0296
Cyclohexane	0.0017	0.0021	0.0025	0.0027	0.0029	0.0038	0.0037	0.0038
i-Hexane	0.0420	0.1689	0.1856	0.1962	0.0549	0.0581	0.0595	0.0608
n-Hexane	0.0976				0.1429	0.1563	0.1572	0.1619
Cycloheptane	0.0037	0.0031	0.0030	0.0029	0.0030	0.0029	0.0029	0.0029
i-Heptane	0.0485	0.0437	0.0436	0.0451	0.0466	0.0444	0.0444	0.0429
n-Heptane	0.0643	0.0804	0.0927	0.1024	0.1109	0.1179	0.1207	0.1249
Cyclooctane	0.0951	0.0219	0.0256	0.0283	0.0314	0.0318	0.0325	0.0334
i-Octane		0.0862	0.0960	0.0971	0.1012	-	0.1093	0.1074

Table 6.13.3. Carbon Mass Balance for 0.3wt%Pt-0.3wt%Sn/Al_2O_3 (Methanol) (510°C, 110 psig)

Time (hrs)	No. of moles of Carbon In	No. of moles of Carbon Out	Δ Carbon
2	4.2743×10^{-4}	3.9618×10^{-4}	3.1254×10^{-5}
5	4.2743×10^{-4}	4.0572×10^{-4}	2.1715×10^{-5}
18.95	4.2743×10^{-4}	4.1130×10^{-4}	1.6128×10^{-5}
22	4.2743×10^{-4}	4.1386×10^{-4}	1.3572×10^{-5}
25	4.2743×10^{-4}	4.1489×10^{-4}	1.2544×10^{-5}
28	4.2743×10^{-4}	4.1640×10^{-4}	1.1031×10^{-5}
43.2	4.2743×10^{-4}	4.2161×10^{-4}	5.8171×10^{-6}
46.25	4.2743×10^{-4}	4.2189×10^{-4}	5.5445×10^{-6}

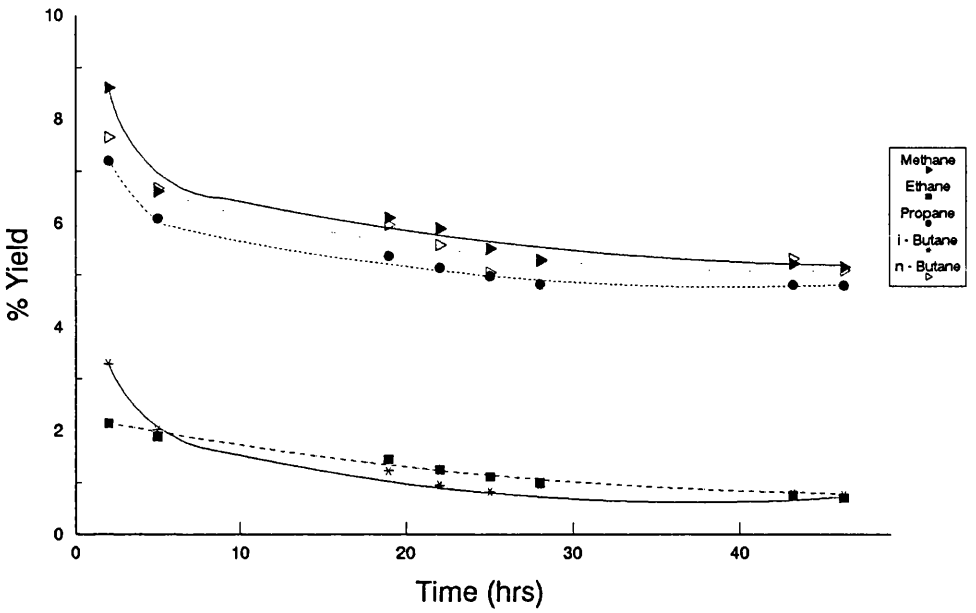

Figure 6.13.1. % Yield to Individual Hydrocarbon Products on 0.3%Pt-0.3%Sn/Alumina (Methanol)

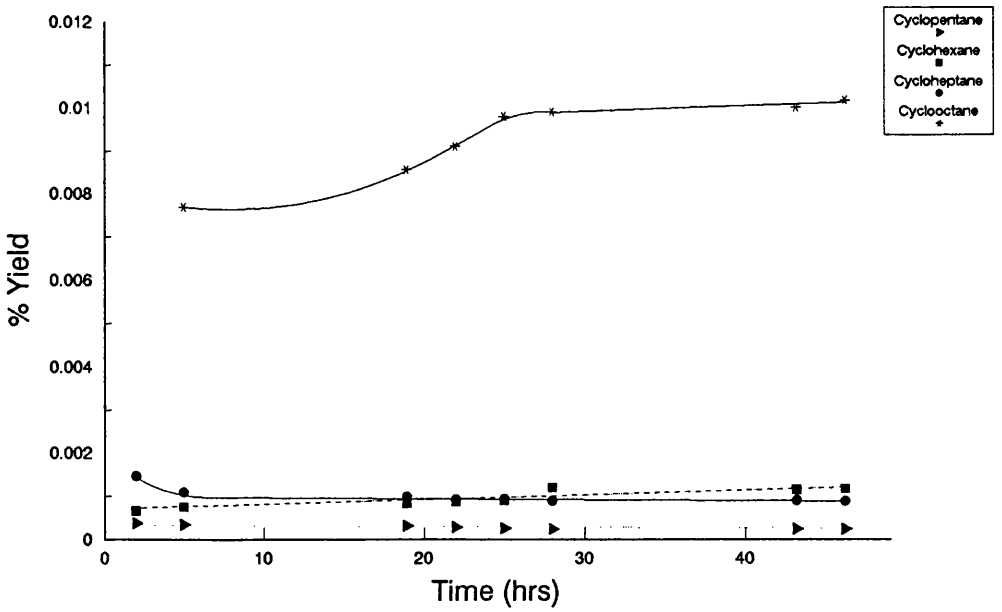

Figure 6.13.2. % Yield to Cycloparaffin Products on 0.3%Pt-0.3%Sn/Alumina (Methanol)

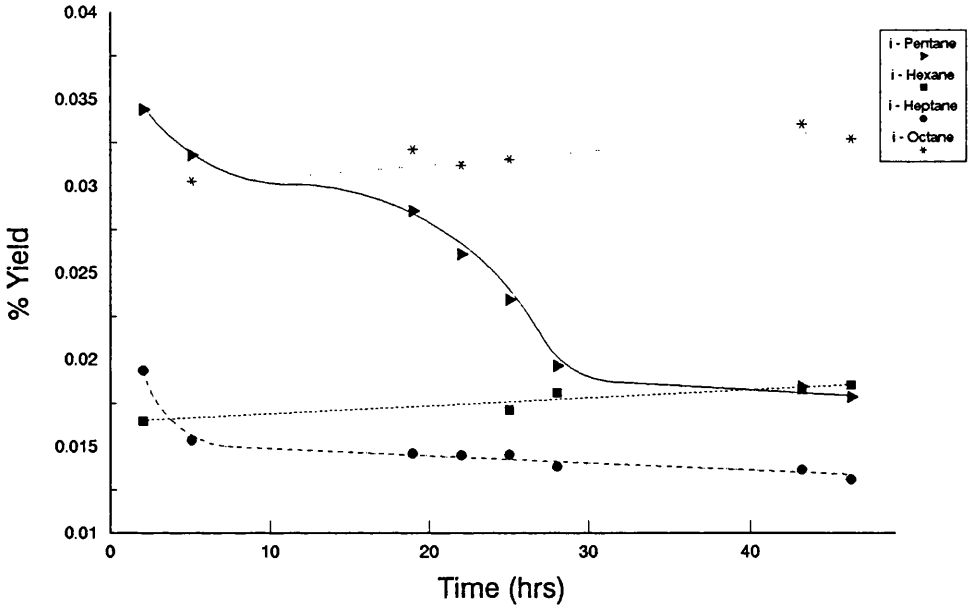

Figure 6.13.3. % Yield of i-Paraffins on 0.3%Pt-0.3%Sn /Alumina (Methanol)

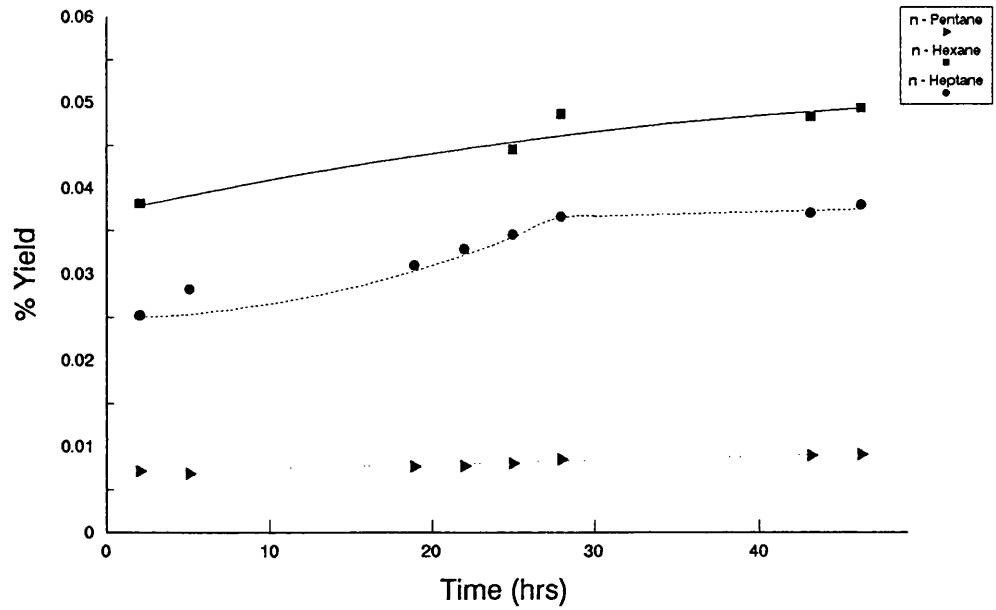

Figure 6.13.4. % Yield of n-Paraffins on 0.3%Pt-0.3%Sn /Alumina (Methanol)

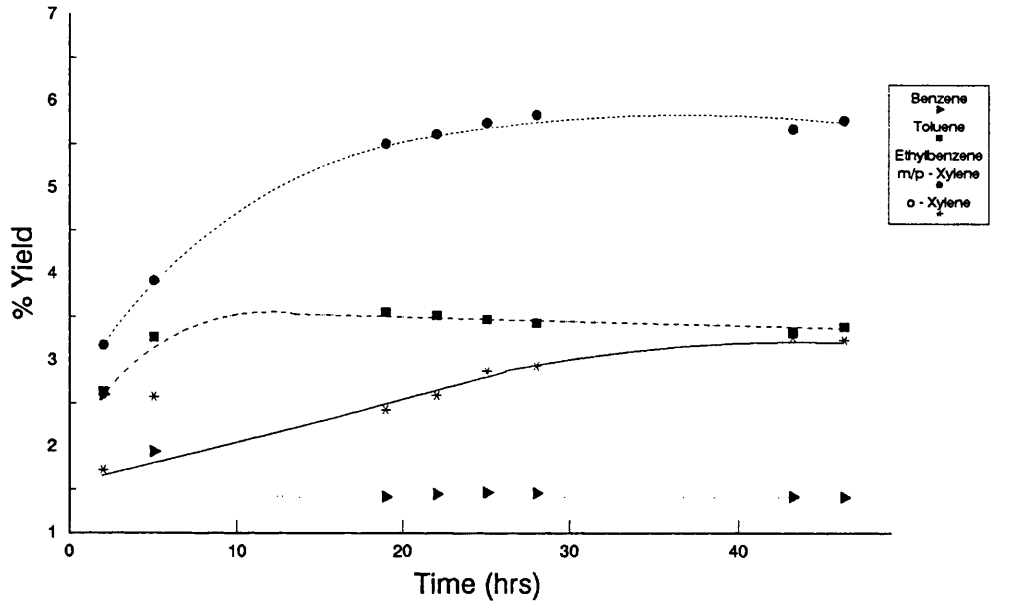

Figure 6.13.5. % Yield of Aromatic Products on 0.3%Pt-0.3%Sn /Alumina (Methanol)

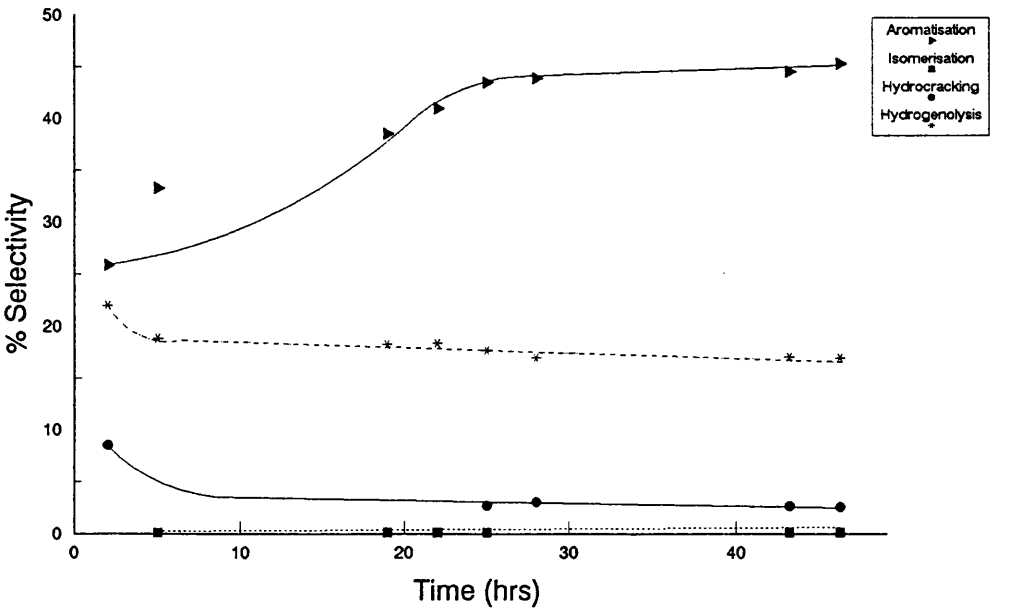

Figure 6.13.6. % Selectivity to the Major Reactions on 0.3%Pt-0.3%Sn /Alumina (Methanol)

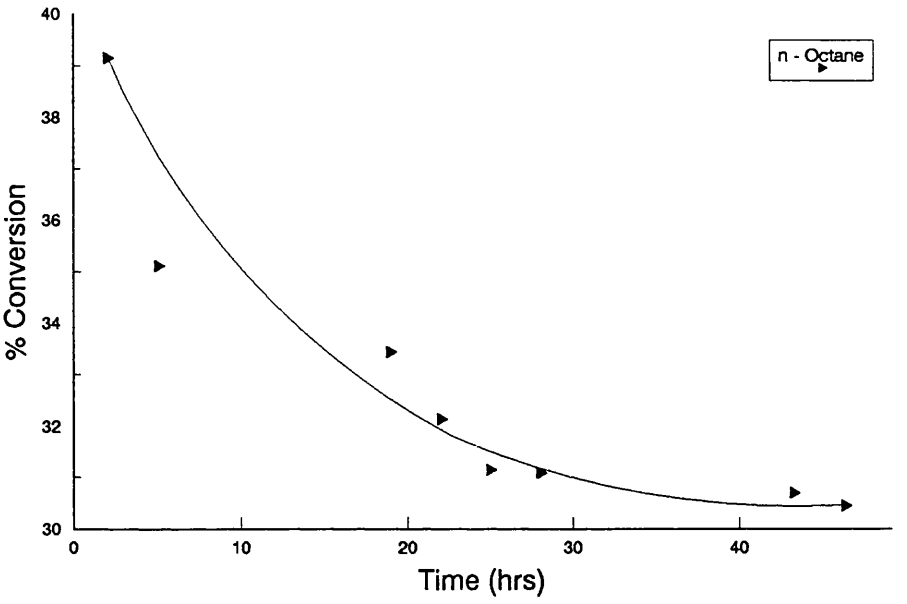

Figure 6.13.7. % Conversion of n-Octane on 0.3%Pt-0.3%Sn /Alumina (Methanol)

followed by propane and then ethane. All undergo an initial rapid decline in activity before reaching a steady yield. The yield of n-butane is again many times (~6) higher than that of i-butane over this catalyst.

The yield to paraffin species is illustrated in Figures 6.13.2 to 6.13.4. The yield of cycloparaffins is very small, initially increasing with carbon number. However after 23 hours the yield of cyclohexane increases above that of cyclopentane. The yield of both cyclohexane and cyclooctane increased while the yield of cyclopentane and cycloheptane decreased with time. Figure 6.13.3 shows that the yields of both i-pentane and i-heptane decrease while the yields of i-hexane and i-octane increase with time. The yields of n-paraffin products, Figure 6.13.4, increase with time and decrease in the order from n-hexane, n-heptane to n-pentane.

The product yields of all aromatics are detailed in Figure 6.13.5. The yield of benzene decreases while the yields of all other aromatic species increase with time before reaching a steady state. The yield of aromatics decrease in the following order from ethylbenzene/m/p-xylene, toluene, o-xylene to benzene. As with the EUROPT catalysts C_8 aromatic species are dominant.

Table 6.13.2 illustrates the selectivities of the individual hydrocarbon products with time. The selectivity of the major reactions is detailed in Figure 6.13.6. The activity of aromatisation increases steadily for the first 25 hours of the reaction before reaching a constant level of 45%. This level is higher than with a monometallic platinum catalyst but much smaller than with a bimetallic Pt-Re/Al_2O_3

catalyst. This catalyst was slightly more selective towards aromatic species than the corresponding catalyst with platinum impregnated first, but less selective than the catalyst which had been coimpregnated or had tin impregnated in an aqueous solution first. The selectivity to the major reactions decreases in the following order:

Aromatisation > *Hydrogenolysis* > *Hydrocracking* > *Isomerisation*

Hydrogenolysis activity was constant at 17% after 20 hours on stream in keeping with the results from other Pt-Sn/Al_2O_3 catalysts.

The propane to methane ratio increases sharply in the first few hours of the reaction before decreasing steadily. However the ratio increases after ~20 hours until a constant ratio is achieved after 40 hours on stream. This suggests that after the initial carbon deposition on the metal sites the support was deactivated. But after 20 hours on stream more coke was deposited upon the metal sites before being deposited once again on the support. The carbon mass balance demonstrates that the amount of coke deposited upon the catalyst surface in this run decreases with time on stream.

The total conversion of n-octane, detailed in Figure 6.13.7, decreases steadily for the first 40 hours of the reaction before a constant level of ~30% is achieved. The % coke deposited upon the catalyst is 17.42% by weight. This is greater than on either EUROPT catalyst and on most Pt-Sn/Al_2O_3 catalysts.

6.14. 1.0wt%Pt-1.0wt%Sn/Al_2O_3 - Sn impregnated first (510°C, 110 psig)

The catalyst was tested in the microreactor system under conditions stated previously in Section 6.1. The results of this experiment are detailed in Figures 6.14.1 to 6.14.7 and Tables 6.14.1 to 6.14.3.

Figure 6.14.1 shows the yield of C_1 - C_4 species decreasing with time on stream. The i- and n-butane yield increases with time before reaching a constant yield of 12%. Methane is produced in greater quantities than either propane or ethane. Both the yields of propane and methane decrease before reaching a constant level while the yield of ethane decreases constantly with time.

The product yields of paraffinic species are outlined in Figures 6.14.2 to 6.14.4. The product yields of both cycloparaffins and n-paraffins are small when compared with those of i-paraffin species. The yield of all cycloparaffin species increases with time on stream and with carbon number. Figure 6.14.3 illustrates the behaviour of i-pentane, i-hexane, i-heptane and the combination of cyclo- and i-octane with time. The yield of all these species increases with increasing time on stream. The combination of cyclo- and i-octane species has the highest product yield. The yield of i-paraffin products decreases with increasing carbon number. In comparison the product yield of n-paraffins, Figure 6.14.4, increases with increasing carbon number and with time over this catalyst.

The product yields of aromatic species formed in this experiment increases with

Table 6.14.1. %Yield of individual products and % Conversion versus time on stream for 1.0wt%Pt-1.0wt%Sn/Al_2O_3 (Sn impregnated first).

Products	The % Yield of Selected Products								
Time (hrs)	2	5	17.83	21	24	27	30	42.05	45
Benzene	0.5112	0.7661	1.0823	1.0023	1.0870	1.1019	1.0533	1.0842	1.0796
Toluene	1.3405	2.1382	3.4823	4.0752	4.6875	4.8868	5.0538	5.3010	5.4040
Ethylbenzene	4.5630	5.0640	6.5456	6.3865	6.6395	7.0830	7.4817	8.3803	8.3975
m/p-Xylene									
o-Xylene	3.0447	2.7247	3.1820	3.6861	4.3298	5.0268	5.6784	5.3442	5.5833
Methane	13.1013	10.9195	8.7435	8.3226	7.9714	7.7652	7.6321	7.3670	7.2199
Ethane	2.5527	2.2774	1.8670	1.7617	1.6137	1.5722	1.4835	1.0304	0.9969
Propane	8.7545	8.4291	6.8783	6.2932	5.4998	4.9825	4.6002	4.4652	4.3175
i-Butane	5.3224	6.5115	7.8944	8.5094	9.0652	9.8927	10.3412	12.0627	12.1086
n-Butane									
Cyclopentane	0.0002	0.0002	0.0005	0.0004	0.0005	0.0005	0.0005	0.0006	0.0006
i-Pentane	0.0146	0.0234	0.0447	0.0455	0.0472	0.0486	0.0498	0.0582	0.0604
n-Pentane	0.0001	0.0001	-	0.0002	0.0001	0.0002	0.0001	0.0002	0.0002
Cyclohexane	0.0001	0.0001	0.0006	0.0007	0.0006	0.0007	0.0007	0.0007	0.0007
i-Hexane	0.0100	0.0160	0.0322	0.0396	0.0432	0.0426	0.0429	0.0492	0.0510
n-Hexane	0.0001	0.0004	0.0008	0.0010	0.0010	0.0010	0.0010	0.0010	0.0011
Cycloheptane	0.0003	0.0003	0.0007	0.0007	0.0008	0.0008	0.0008	0.0008	0.0008
i-Heptane	0.0048	0.0052	0.0245	0.0248	0.0246	0.0251	0.0253	0.0302	0.0313
n-Heptane	0.0002	0.0006	0.0015	0.0017	0.0020	0.0020	0.0019	0.0019	0.0020
Cyclooctane	0.0211	0.0275	0.0577	0.0584	0.0594	0.0606	0.0614	0.0660	0.0704
i-Octane									
% Conversion of n-Octane	39.2417	38.9042	39.8388	40.2099	41.0734	42.4931	43.8946	45.2437	45.3257

Table 6.14.2. % Selectivity of individual products versus time on stream for 1.0wt%Pt-1.0wt%Sn/Al_2O_3 (Sn impregnated first).

Products	The % Selectivity of Selected Products								
Time (hrs)	2	5	17.83	21	24	27	30	42.05	45
Benzene	1.3026	1.9691	2.7167	2.4928	2.6464	2.5931	2.3997	2.3964	2.3819
Toluene	3.4160	5.4960	8.7410	10.1349	11.4125	11.5003	11.5136	11.7166	11.9226
Ethylbenzene	11.6279	13.0165	16.4303	15.8829	16.1649	16.6685	17.0448	18.5227	18.5270
m/p-Xylene									
o-Xylene	7.7587	7.0037	7.9872	9.1671	10.5416	11.8298	12.9363	11.8121	12.3182
Methane	33.3862	28.0676	21.9472	20.6978	19.4076	18.2740	17.3872	16.2829	15.9290
Ethane	6.5051	5.8538	4.6864	4.3812	3.9289	3.6999	3.3797	2.2774	2.1994
Propane	22.3092	21.6664	17.2653	15.6509	13.3903	11.7254	10.4801	9.8691	9.5255
i-Butane	13.5632	16.7373	19.8158	21.1625	22.0708	23.2807	23.5593	26.6615	26.7147
n-Butane									
Cyclopentane	0.0004	0.0006	0.0012	0.0011	0.0012	0.0011	0.0012	0.0013	0.0013
i-Pentane	0.0371	0.0601	0.1123	0.1132	0.1148	0.1145	0.1136	0.1285	0.1331
n-Pentane	0.0002	0.0002	-	0.0004	0.0004	0.0004	0.0003	0.0004	0.0004
Cyclohexane	0.0003	0.0004	0.0016	0.0017	0.0016	0.0016	0.0015	0.0015	0.0015
i-Hexane	0.0256	0.0412	0.0808	0.0984	0.1052	0.1001	0.0977	0.1088	0.1125
n-Hexane	0.0002	0.0009	0.0021	0.0024	0.0025	0.0024	0.0022	0.0020	0.0024
Cycloheptane	0.0007	0.0009	0.0019	0.0018	0.0019	0.0018	0.0017	0.0017	0.0017
i-Heptane	0.0122	0.0133	0.0616	0.0616	0.0599	0.0590	0.0577	0.0668	0.0691
n-Heptane	0.0005	0.0015	0.0037	0.0043	0.0049	0.0048	0.0044	0.0043	0.0044
Cyclooctane	0.0538	0.0706	0.1449	0.1453	0.1447	0.1425	0.1398	0.1458	0.1552
i-Octane									

Table 6.14.3. Carbon Mass Balance for 1.0wt%Pt-1.0wt%Sn/Al_2O_3 (Sn impregnated first) (510°C, 110 psig)

Time (hrs)	No. of moles of Carbon In	No. of moles of Carbon Out	Δ Carbon
2	4.6045×10^{-4}	4.4392×10^{-4}	1.6528×10^{-5}
5	4.6045×10^{-4}	4.4513×10^{-4}	1.5326×10^{-5}
17.83	4.6045×10^{-4}	4.5017×10^{-4}	1.0282×10^{-5}
21	4.6045×10^{-4}	4.5169×10^{-4}	8.7660×10^{-6}
24	4.6045×10^{-4}	4.5237×10^{-4}	8.0861×10^{-6}
27	4.6045×10^{-4}	4.5351×10^{-4}	6.9433×10^{-6}
30	4.6045×10^{-4}	4.5470×10^{-4}	5.7537×10^{-6}
42.05	4.6045×10^{-4}	4.5586×10^{-4}	4.5898×10^{-6}
45	4.6045×10^{-4}	4.5591×10^{-4}	4.5371×10^{-6}

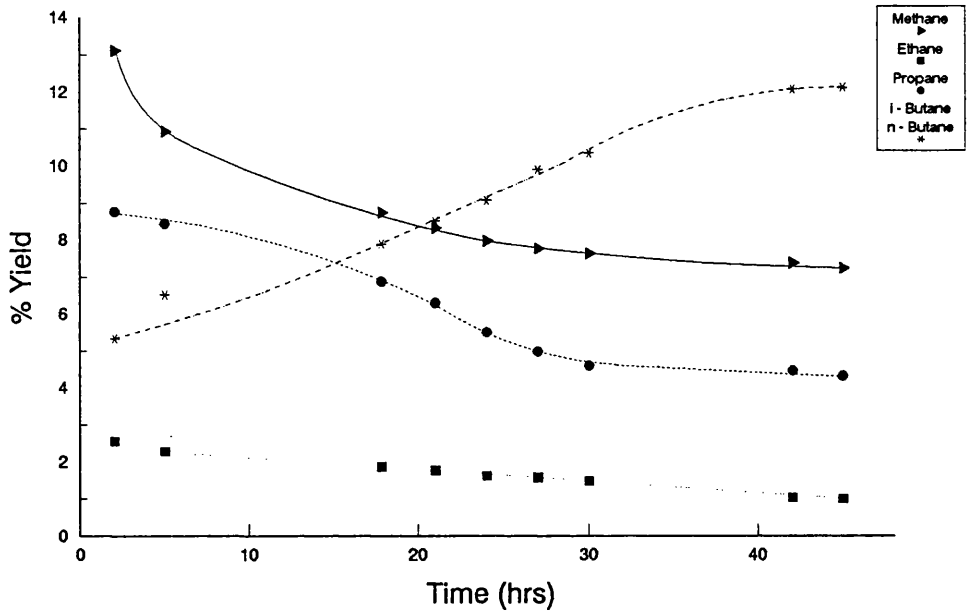

Figure 6.14.1. % Yield of Individual Hydrocarbon Products on 1.0%Pt-1.0%Sn/Alumina

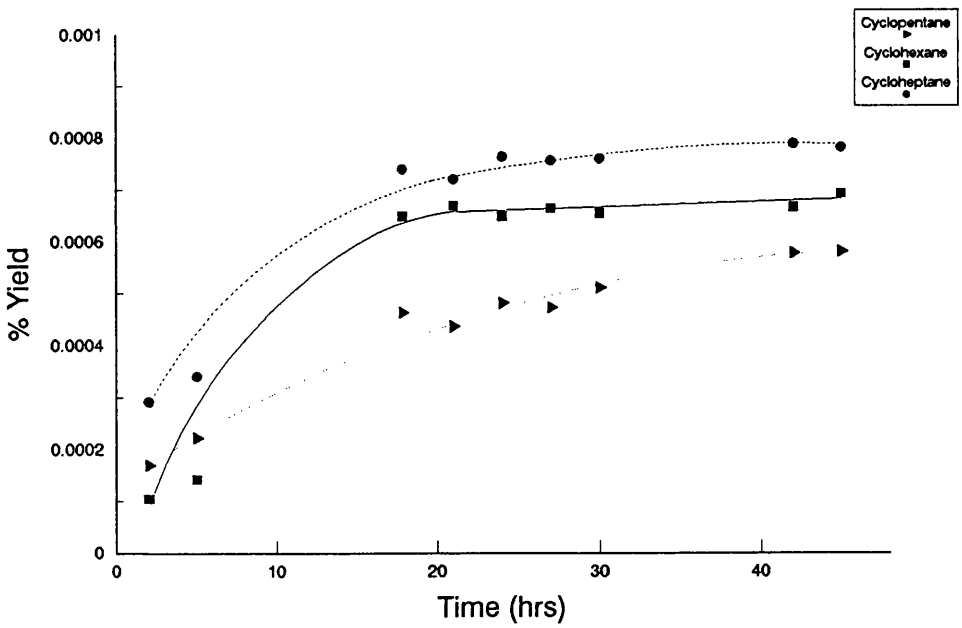

Figure 6.14.2. % Yield of Cycloparaffin Products on 1.0%Pt-1.0%Sn/Alumina

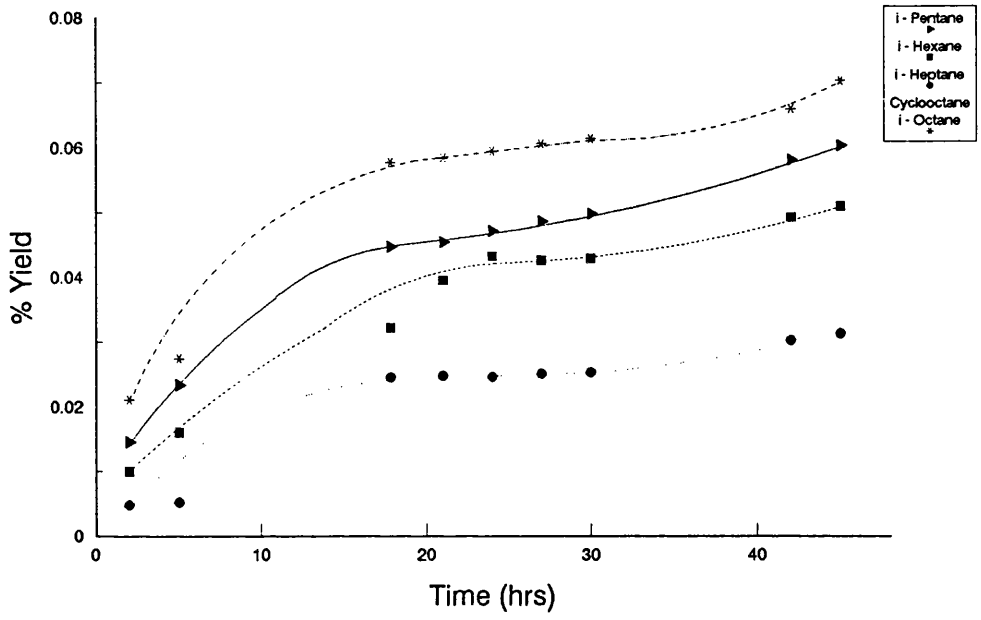

Figure 6.14.3. % Yield of i-Paraffins on 1.0%Pt-1.0%Sn/Alumina

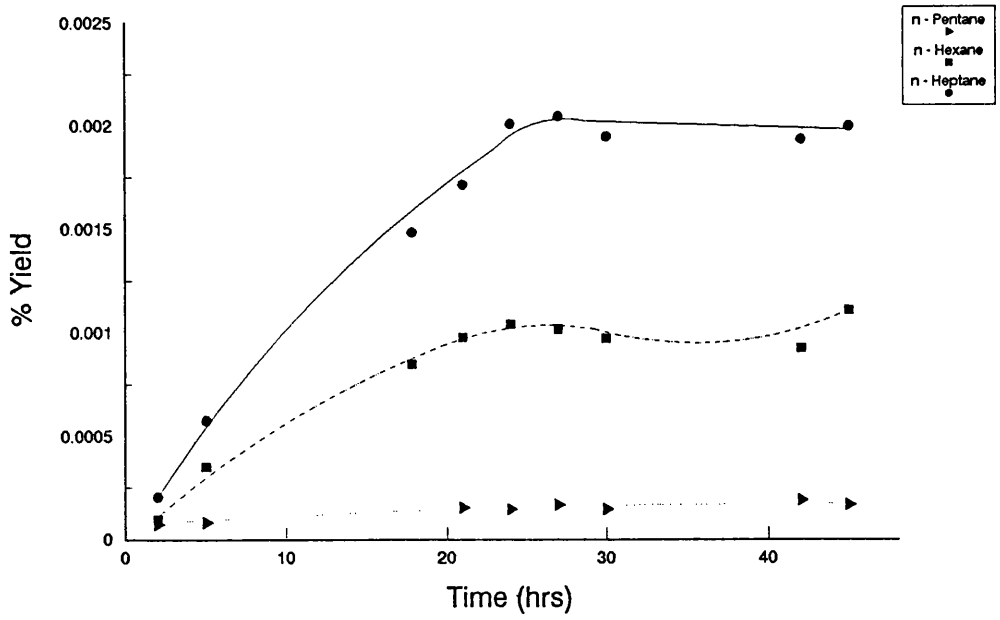

Figure 6.14.4. % Yield of n-Paraffins on 1.0%Pt-1.0%Sn/Alumina

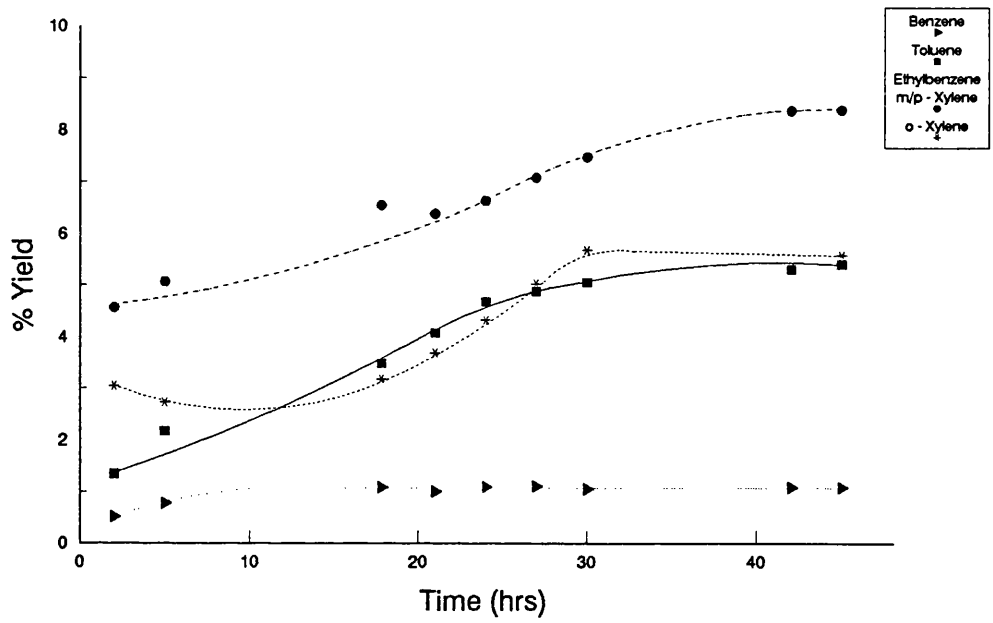

Figure 6.14.5. % Yield of Aromatic Products on 1.0%Pt-1.0%Sn/Alumina

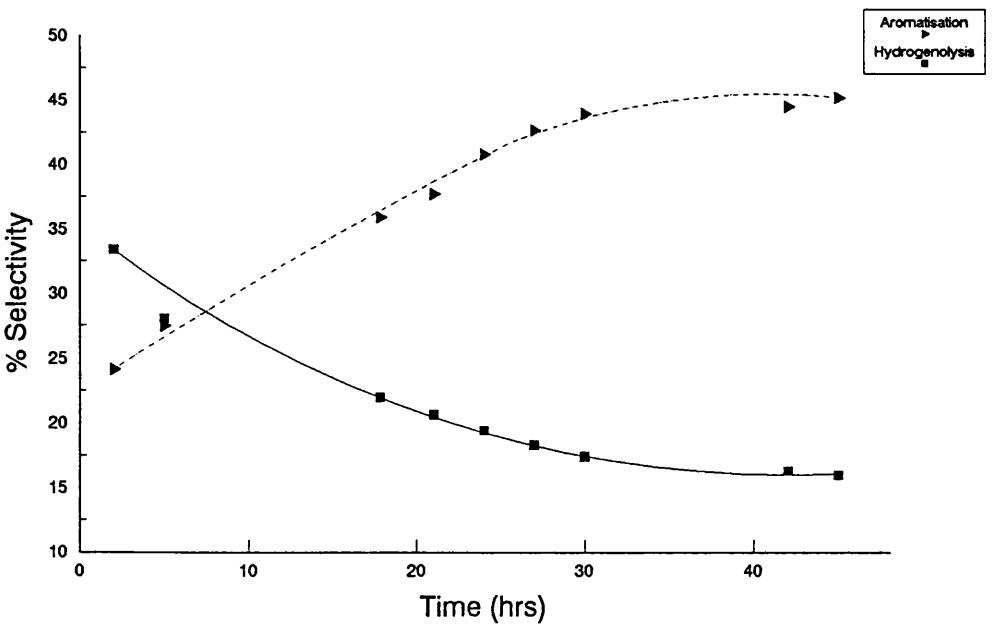

Figure 6.14.6. % Selectivity to the Major Reactions on 1.0%Pt-1.0%Sn/Alumina

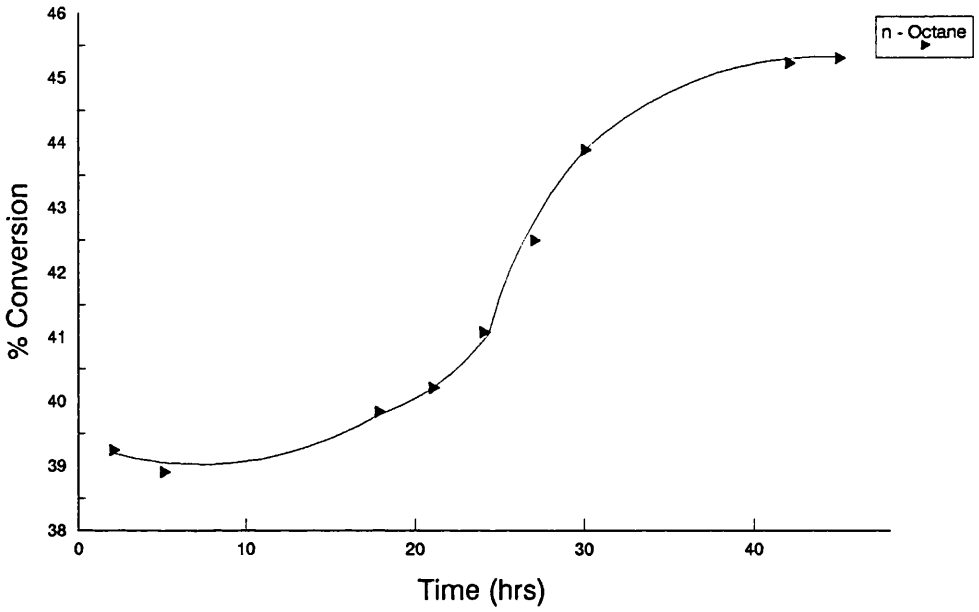

Figure 6.14.7. % Conversion of n-Octane on 1.0%Pt-1.0%Sn/Alumina

aromatic species decreases from ethylbenzene/m/p-xylene, o-xylene, toluene to benzene.

Table 6.14.2 shows the individual selectivity to hydrocarbon species with respect to time. The selectivity of this catalyst to the major reforming reactions is shown in Figure 6.14.6. Initially hydrogenolysis is dominant but the activity falls rapidly with time to reach a constant level of ~16% after 40 hours. Aromatisation activity in comparison increases steadily until reaching a constant level of 45%. Therefore the order of selectivities for the major reactions is as follows:

Aromatisation > Hydrogenolysis > Hydrocracking > Isomerisation

As in previous Sections a typical propane to methane ratio and carbon mass balance were obtained for this catalyst. The propane to methane ratio increases initially to a maximum after ~10 hours and then decreases steadily until it reaches a steady level. The carbon mass balance, Table 6.14.3, shows that the carbon deposition decreases with reaction time as less sites are available for coking. Therefore an initial rapid deposition of coke occurs on the metallic sites in preference to the support, but after ~10 hours the support is preferentially deactivated.

Figure 6.14.7 shows the total conversion of n-octane as a function of time. Unlike other Pt-Sn/Al_2O_3 catalysts the conversion of n-octane increases readily on this catalyst until a constant conversion of ~45% is reached. The % coke deposited on the catalyst was found to be 8.12% by weight. In comparison with the 0.3wt%

bimetallic catalysts the amount of coke is generally lower on this catalyst.

6.15. 3.0wt%Pt-3.0wt%Sn/Al_2O_3 - Pt impregnated first (510°C, 110 psig)

The conversion of n-octane over this catalyst was very low with the product distribution being limited. The major reforming product in this reaction was methane, which had a selectivity > 95% throughout the run. The yield and hence the selectivity of aromatic products was very small in comparison with methane. The total conversion of n-octane decreases steadily from ~8.4 to ~2.7% after 26 hours on stream. The reaction was stopped at this time due to the very low conversion.

6.16. 0.3wt%Sn/Al_2O_3 (510°C, 110 psig)

This monometallic catalyst was tested under conditions stated previously in Section 6.1. The results of this experiment is outlined in Figures 6.16.1 to 6.16.6 and Tables 6.16.1 to 6.16.3.

Figure 6.16.1 shows the decreasing yield of C_1 - C_4 species with reaction time. Methane has the highest product yield initially but after 23 hours the yield of methane and propane are similar. The yield of both ethane and i-butane is very low and never exceeds 1%. The yield of n-butane is ~4 - 5 times that of i-butane throughout the run.

Table 6.16.1. %Yield of individual products and % Conversion versus time on stream for 0.3wt%Sn/Al_2O_3

Products	The % Yield of Selected Products						
Time (hrs)	1.5	4.5	18.17	21.25	24.25	27.25	30.25
Benzene	0.1262	0.1153	0.1122	0.1032	0.0906	0.0927	0.0891
Toluene	0.2118	0.1953	0.1703	0.1649	0.1513	0.1424	0.1388
Ethylbenzene	0.2780	0.2682	0.2307	0.2141	0.2012	0.1921	0.2031
m/p-Xylene							
o-Xylene	0.2375	0.2157	0.1870	0.1740	0.1600	0.1499	0.1395
Methane	6.2956	5.3062	4.2952	3.7445	3.6492	3.5669	3.5207
Ethane	0.7574	0.7218	0.6697	0.6573	0.6456	0.6378	0.6313
Propane	5.1765	4.8826	3.8532	3.7489	3.6944	3.5833	3.5161
i-Butane	0.4642	0.4272	0.3683	0.3590	0.3540	0.3492	0.3454
n-Butane	3.2641	2.9793	2.4294	2.2687	1.9807	1.6575	1.4490
Cyclopentane	0.0008	0.0008	0.0007	0.0007	0.0006	0.0006	0.0006
i-Pentane	0.0456	0.0414	0.0364	0.0344	0.0382	0.0321	0.0319
n-Pentane							
Cyclohexane	0.0310	0.0291	0.0262	0.0260	0.0249	0.0239	0.0239
i-Hexane							
n-Hexane							
Cycloheptane	0.0005	0.0004	0.0004	0.0003	0.0003	0.0003	0.0003
i-Heptane	0.0133	0.0139	0.0149	0.0157	0.0160	0.0159	0.0159
n-Heptane							
Cyclooctane	0.0049	0.0046	0.0040	0.0039	0.0038	0.0037	0.0037
i-Octane	0.0477	0.0550	0.0603	0.0647	0.0694	0.0718	0.0749
% Conversion of n-Octane	16.9541	15.2568	12.4587	11.5804	11.0753	10.5201	10.1839

Table 6.16.2. %Selectivity of individual products versus time on stream for 0.3wt%Sn/Al_2O_3

Products	The % Selectivity of Selected Products						
Time (hrs)	1.5	4.5	18.17	21.25	24.25	27.25	30.25
Benzene	0.7445	0.7559	0.9005	0.8912	0.8181	0.8812	0.8749
Toluene	1.2492	1.2804	1.3673	1.4242	1.3658	1.3537	1.3627
Ethylbenzene	1.6400	1.7579	1.8514	1.8489	1.8163	1.8256	1.9942
m/p-Xylene							
o-Xylene	1.4011	1.4139	1.5007	1.5029	1.4448	1.4248	1.3695
Methane	37.1272	34.7790	34.4755	32.3347	32.9492	33.9052	34.5710
Ethane	4.4672	4.7309	5.3751	5.6757	5.8289	6.0629	6.1987
Propane	30.5325	32.0027	30.9275	32.3731	33.3573	34.0616	34.5257
i-Butane	2.7380	2.8003	2.9560	3.1005	3.1967	3.3192	3.3913
n-Butane	19.2525	19.5281	19.4993	19.5910	17.8839	15.7559	14.2279
Cyclopentane	0.0048	0.0052	0.0057	0.0059	0.0058	0.0057	0.0055
i-Pentane	0.2692	0.2713	0.2920	0.2866	0.2899	0.3052	0.3129
n-Pentane							
Cyclohexane	0.1827	0.1905	0.2103	0.2243	0.2244	0.2273	0.2351
i-Hexane							
n-Hexane							
Cycloheptane	0.0027	0.0026	0.0028	0.0029	0.0030	0.0030	0.0029
i-Heptane	0.0784	0.0908	0.1197	0.1356	0.1449	0.1509	0.1565
n-Heptane							
Cyclooctane	0.0288	0.0301	0.0320	0.0335	0.0343	0.0350	0.0359
i-Octane	0.2813	0.3604	0.4842	0.5587	0.6269	0.6829	0.7355

Table 6.16.3. Carbon Mass Balance for 0.3wt%Sn/Al_2O_3 (510°C, 110 psig)

Time (hrs)	No. of moles of Carbon In	No. of moles of Carbon Out	Δ Carbon
1.5	4.2734×10^{-4}	4.1158×10^{-4}	1.5757×10^{-5}
4.5	4.2734×10^{-4}	4.1717×10^{-4}	1.0162×10^{-5}
18.17	4.2734×10^{-4}	4.2135×10^{-4}	5.9863×10^{-6}
21.25	4.2734×10^{-4}	4.2314×10^{-4}	4.1995×10^{-6}
24.25	4.2734×10^{-4}	4.2439×10^{-4}	2.9509×10^{-6}
27.25	4.2734×10^{-4}	4.2552×10^{-4}	1.8127×10^{-6}
30.25	4.2734×10^{-4}	4.2583×10^{-4}	1.5047×10^{-6}

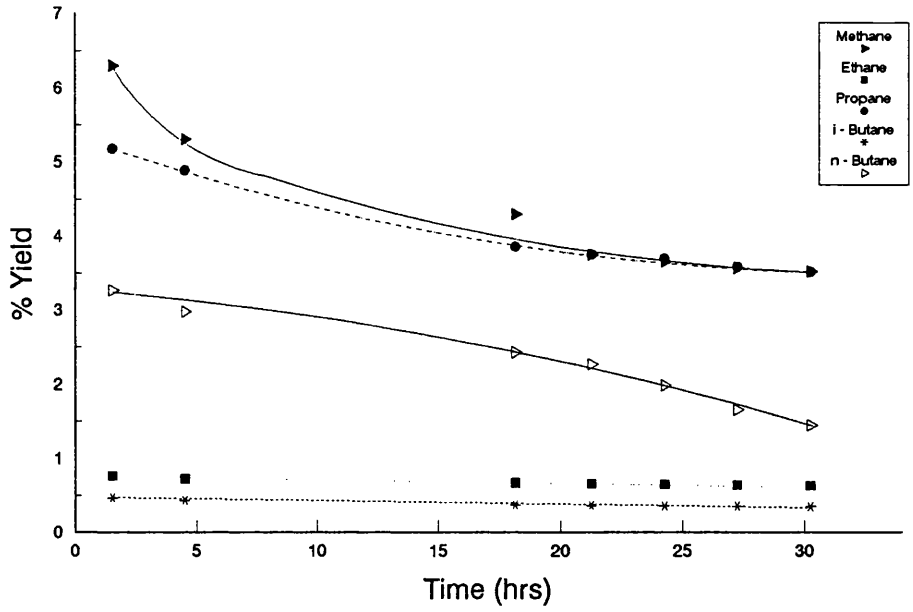

Figure 6.16.1. % Yield of Individual Hydrocarbon Products on 0.3%Sn/Alumina

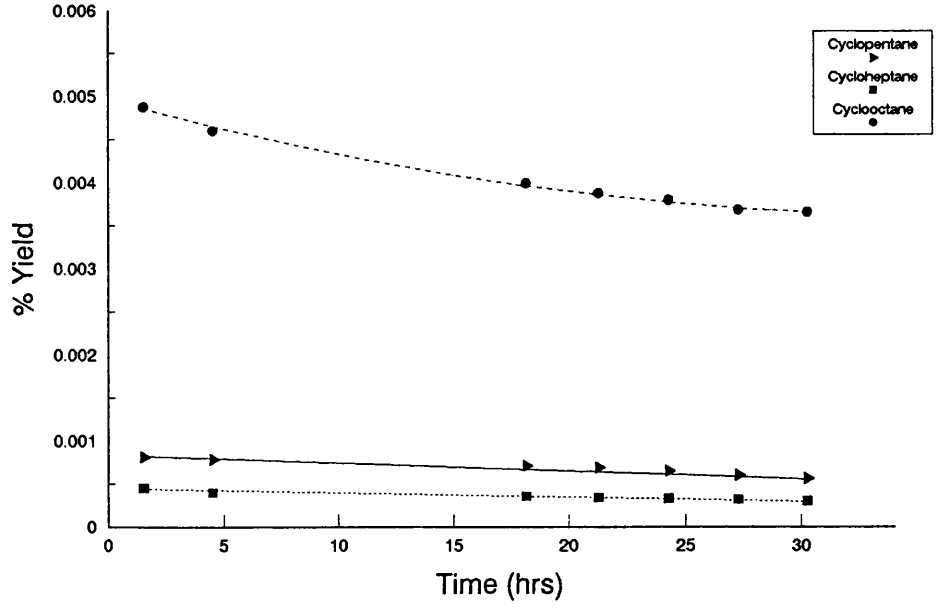

Figure 6.16.2. % Yield of Cycloparaffin Products on 0.3%Sn/Alumina

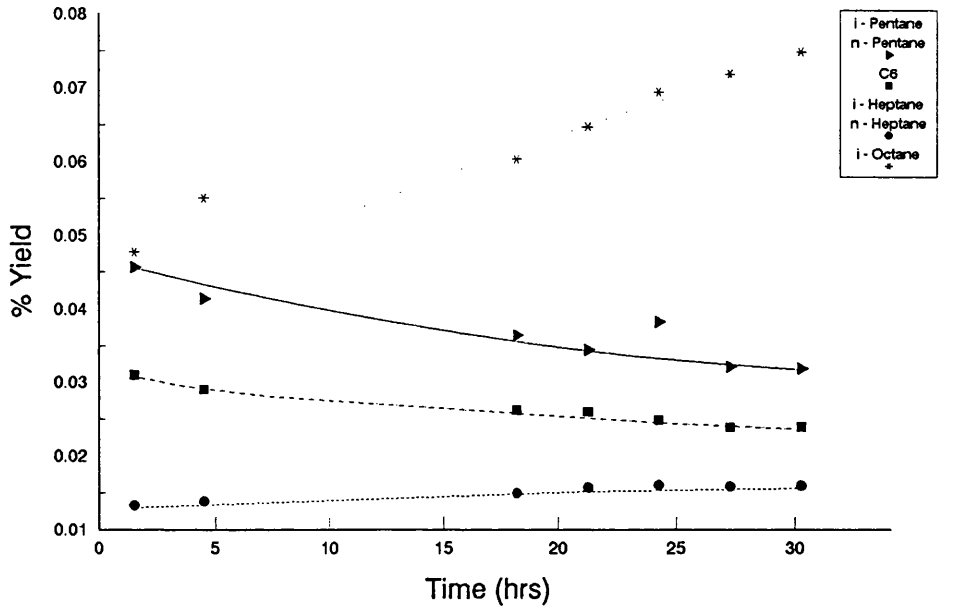

Figure 6.16.3. % Yield of i- and n-Paraffins on 0.3%Sn/Alumina

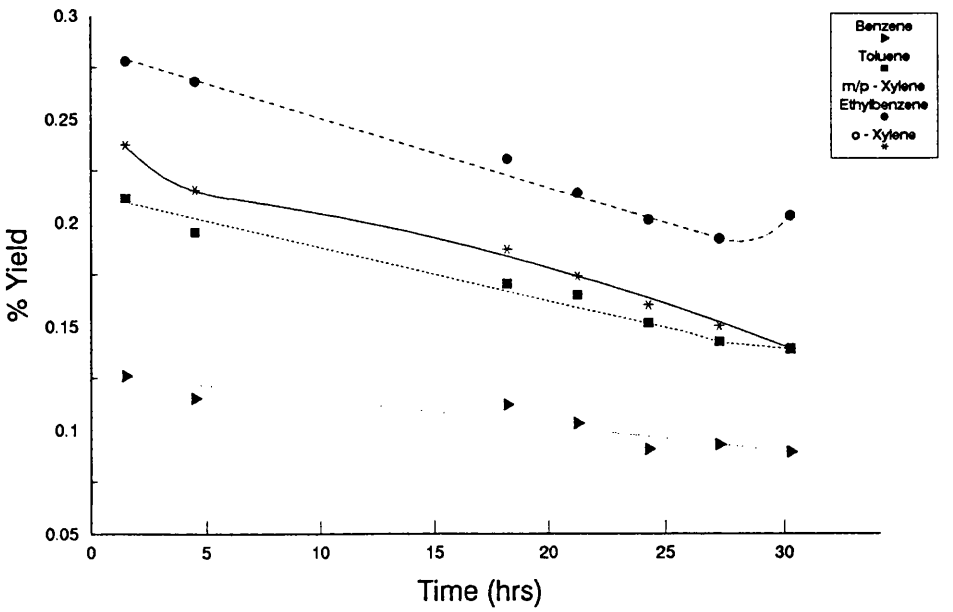

Figure 6.16.4. % Yield aromatic products on 0.3%Sn/Alumina

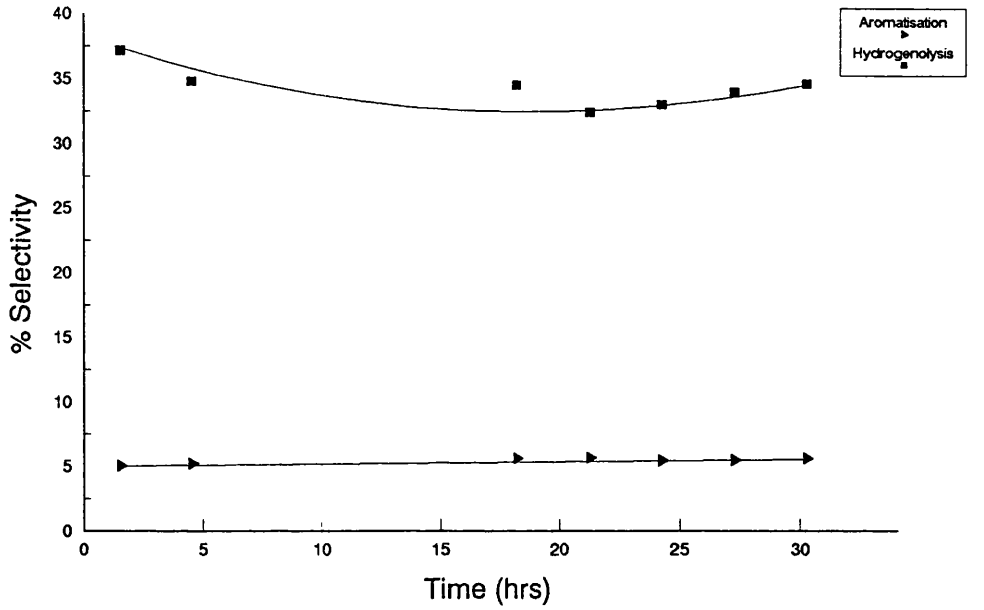

Figure 6.16.5. % Selectivity to the Major Reactions on 0.3%Sn/Alumina

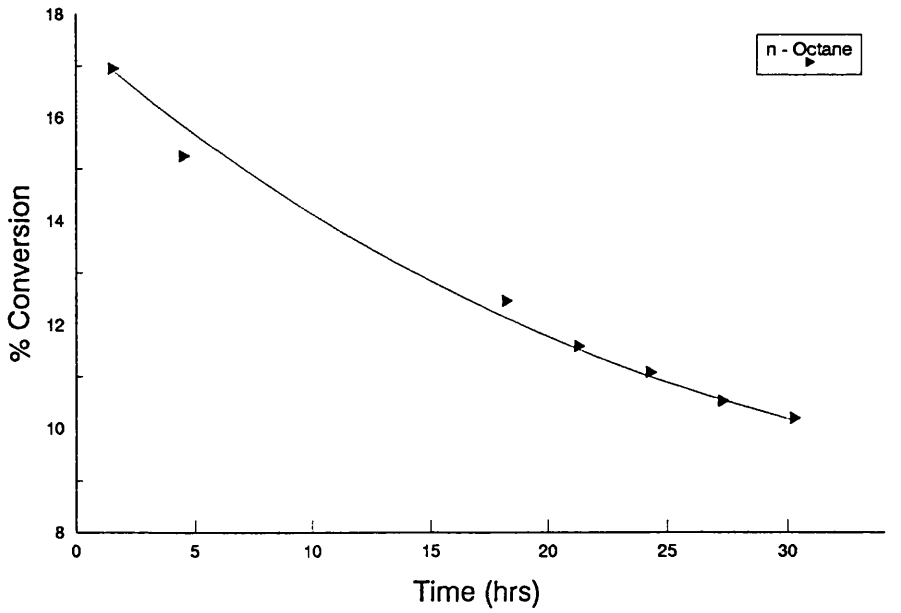

Figure 6.16.6. % Conversion of n-Octane on 0.3%Sn/Alumina

Figures 6.16.2 and 6.16.3 illustrate the yield of paraffin products with time. As with the bimetallic catalysts the yield of cycloparaffins is very small. The yield of cycloparaffins decreases with time in the order from cyclooctane, cyclopentane and finally cycloheptane. The combined yields of several i- and n-paraffin species are quoted as the individual yields are indistinguishable. The yield of i-octane increases with reaction time in Figure 6.16.3 whereas the yield of the combined species decreases with time and with increasing carbon number.

Figure 6.16.4 illustrates the decreasing yield of aromatics with time. The aromatic yields are much lower than on the corresponding bimetallic catalyst. The yield of ethylbenzene/m/p-xylene is steady at ~0.2% in this catalyst. The yield of aromatic products decreases in the order from ethylbenzene/m/p-xylene, o-xylene, toluene to benzene.

The selectivity to individual hydrocarbon species is shown in Table 6.16.2 and the selectivity to the major reactions is shown in Figure 6.16.5. Due to the inability to separate certain species, only the activity of the hydrogenolysis and aromatisation reactions could be calculated. Hydrogenolysis activity is very high on this catalyst at ~34%, whereas the aromatisation activity is very low at ~6%. The absence of a 0.3wt% loading of platinum has a pronounced effect on the selectivity and conversion of n-octane.

The propane to methane ratio increases steadily to a maximum before decreasing slowly and the carbon mass balance shows a decrease in the carbon deposition with

time. Therefore there is an initial rapid coke deposition on the metallic sites and then coke is deposited mainly on the support.

The total conversion of n-octane decreases steadily from 17 to 10% after 30 hours on stream. This value is again much lower than that on the corresponding bimetallic 0.3wt%Pt-0.3wt%Sn/Al_2O_3 catalyst. The % coke deposited upon the catalyst surface is 12.38% by weight (Table 6.1). This value is similar to that of many of the bimetallic Pt-Sn/Al_2O_3 catalysts.

6.17. 3.0wt%Sn/Al_2O_3 (510°C, 110 psig)

The catalyst was tested in the microreactor system under conditions stated previously in Section 6.1. The results of this experiment are detailed in Figures 6.17.1 to 6.17.7 and Tables 6.17.1 to 6.17.3.

The product yield of C_1 - C_4 species decreases with time on stream as shown in Figure 6.17.1. In comparison with the 0.3wt%Sn/Al_2O_3 the yields of methane and propane have decreased significantly by ~3%. Methane is yet again the dominant product followed by propane and then ethane. The yield of n-butane in this study is approximately twice that of i-butane.

Figures 6.17.2 to 6.17.4 illustrate the yields of paraffin products with time. Once again the yield of cycloparaffins is very small in comparison with other paraffinic species. The yield of cyclooctane is seen to increase whereas the yield of other

Table 6.17.1. %Yield of individual products and % Conversion versus time on stream for 3.0wt%Sn/Al_2O_3

Products	The % Yield of Selected Products						
Time (hrs)	2.5	8.33	18.6	21.75	25.2	28.27	31.33
Benzene	0.3079	0.2736	0.2638	0.2538	0.2469	0.2296	0.2175
Toluene	0.4755	0.4233	0.3974	0.3844	0.3777	0.3634	0.3561
Ethylbenzene	0.3591	0.3373	0.2878	0.2795	0.2673	0.2614	0.2617
m/p-Xylene	0.1895	0.1612	0.1326	0.1346	0.1170	-	0.0962
o-Xylene	0.2178	0.1710	0.1455	0.1405	0.1052	0.0987	0.0889
Methane	3.2243	2.7988	2.6674	2.3355	2.3572	2.2822	2.2101
Ethane	0.5084	0.4266	0.3897	0.2805	0.2534	0.2166	0.2155
Propane	2.4352	1.8243	1.5087	1.3076	1.2906	1.3002	1.2923
i-Butane	1.3961	1.2588	1.2171	1.1879	1.1462	1.1207	1.1328
n-Butane	3.1854	2.8058	2.3599	2.0092	1.9388	1.8927	1.8601
Cyclopentane	0	0	0	0	0	0	0
i-Pentane	0.0018	0.0016	0.0015	0.0015	0.0015	0.0013	0.0014
n-Pentane	0.0030	0.0030	0.0029	0.0039	0.0041	0.0040	0.0041
Cyclohexane	0.0001	0	0	0	0	0	0
i-Hexane	0.0020	0.0019	0.0018	0.0018	0.0100	0.0016	0.0016
n-Hexane	0.0079	0.0072	0.0066	0.0071		0.0070	0.0066
Cycloheptane	0.0016	0.0007	0.0005	0.0005	0.0005	0.0005	0.0004
i-Heptane	0.0018	0.0016	0.0016	0.0020	0.0019	0.0019	0.0019
n-Heptane	0.0056	0.0055	0.0053	0.0066	0.0067	0.0066	0.0068
Cyclooctane	0.0005	0.0004	0.0004	0.0005	0.0006	0.0006	0.0006
i-Octane	0.0051	0.0050	0.0049	0.0035	0.0036	0.0035	0.0034
% Conversion of n-Octane	12.3288	10.5078	9.3959	8.3411	8.1291	7.7925	7.7582

Table 6.17.2. % Selectivity of individual products versus time on stream for 3.0wt%Sn/Al_2O_3

Products	The % Selectivity of Selected Products						
Time (hrs)	2.5	8.33	18.6	21.75	25.2	28.27	31.33
Benzene	2.4971	2.6042	2.8072	3.0424	3.0368	2.9467	2.8037
Toluene	3.8567	4.0289	4.2296	4.6089	4.6467	4.6633	4.5900
Ethylbenzene	2.9123	3.2096	3.0632	3.3506	3.2877	3.3547	3.3730
m/p-Xylene	1.5374	1.5345	1.4117	1.6139	1.4387	-	1.2394
o-Xylene	1.7668	1.6275	1.5487	1.2613	1.2942	1.2666	1.1465
Methane	26.1523	26.6356	28.3891	27.9999	28.9971	29.2866	28.4868
Ethane	4.1239	4.0596	4.1480	3.3634	3.1175	2.780	2.7781
Propane	19.7524	17.3610	16.0576	15.6772	15.8764	16.6847	16.6572
i-Butane	11.3242	11.9793	12.9540	14.2419	14.0998	14.3819	14.6020
n-Butane	25.8372	26.7022	25.1167	24.0884	23.8506	24.2890	23.9760
Cyclopentane	0.0003	0.0002	0.0002	0.0002	0.0002	0.0002	0.0002
i-Pentane	0.0144	0.0155	0.0163	0.0184	0.0181	0.0167	0.0182
n-Pentane	0.0246	0.0281	0.0314	0.0467	0.0504	0.0509	0.0535
Cyclohexane	0.0010	0.0008	0.0006	0.0007	0.0007	-	0.0007
i-Hexane	0.0165	0.0181	0.0196	0.0213	0.1234	0.0207	0.0212
n-Hexane	0.0644	0.0688	0.0707	0.0848		0.0896	0.0850
Cycloheptane	0.0132	0.0069	0.0057	0.0058	0.0057	0.0061	0.0057
i-Heptane	0.0144	0.0156	0.0171	0.0238	0.0229	0.0241	0.0242
n-Heptane	0.0455	0.0520	0.0564	0.0793	0.0820	0.0852	0.0874
Cyclooctane	0.0040	0.0040	0.0042	0.0063	0.0068	0.0077	0.0077
i-Octane	0.0415	0.0475	0.0521	0.0416	0.0443	0.0455	0.0436

Table 6.17.3. Carbon Mass Balance for 3.0wt%Sn/Al_2O_3 (510°C, 110 psig)

Time (hrs)	No. of moles of Carbon In	No. of moles of Carbon Out	Δ Carbon
2.5	4.3725×10^{-4}	4.2056×10^{-4}	1.6686×10^{-5}
8.33	4.3725×10^{-4}	4.2906×10^{-4}	8.1908×10^{-6}
18.6	4.3725×10^{-4}	4.3286×10^{-4}	4.3914×10^{-6}
21.75	4.3725×10^{-4}	4.3405×10^{-4}	3.1945×10^{-6}
25.2	4.3725×10^{-4}	4.3472×10^{-4}	2.5292×10^{-6}
28.27	4.3725×10^{-4}	4.3561×10^{-4}	1.6335×10^{-6}
31.33	4.3725×10^{-4}	4.3652×10^{-4}	7.2556×10^{-7}

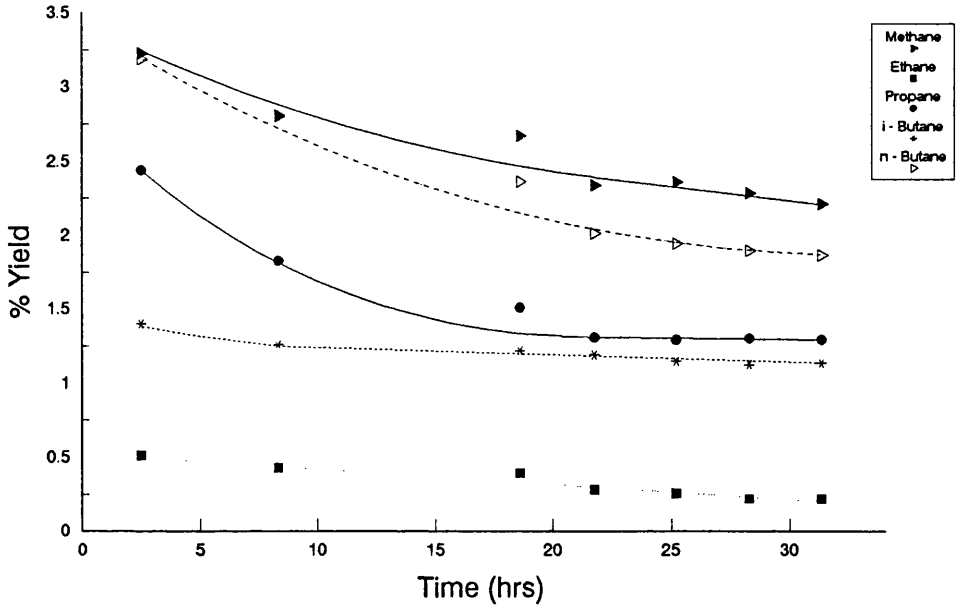

Figure 6.17.1. % Yield of Individual Hydrocarbon Products on 3.0%Sn/Alumina

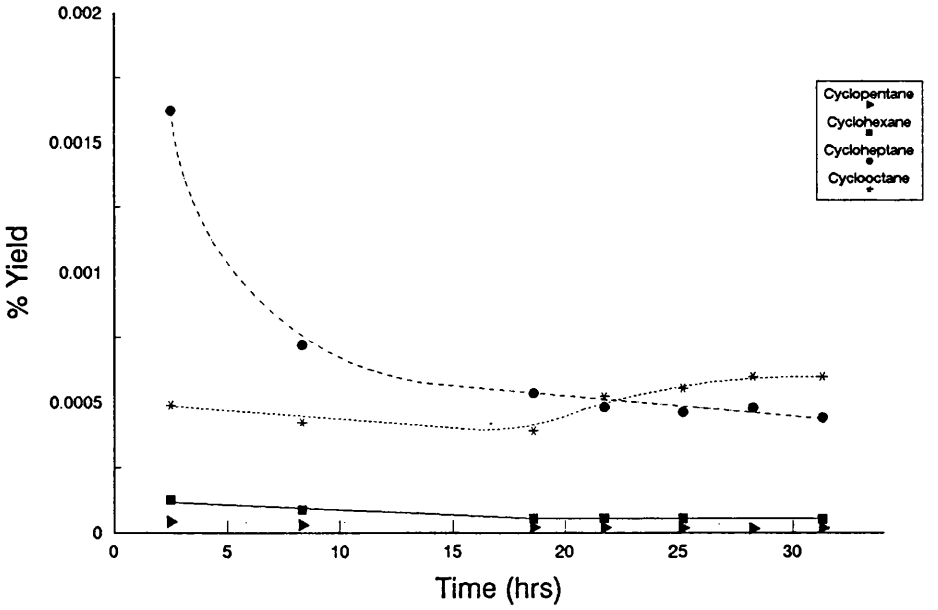

Figure 6.17.2. % Yield of Cycloparaffin Products on 3.0%Sn/Alumina

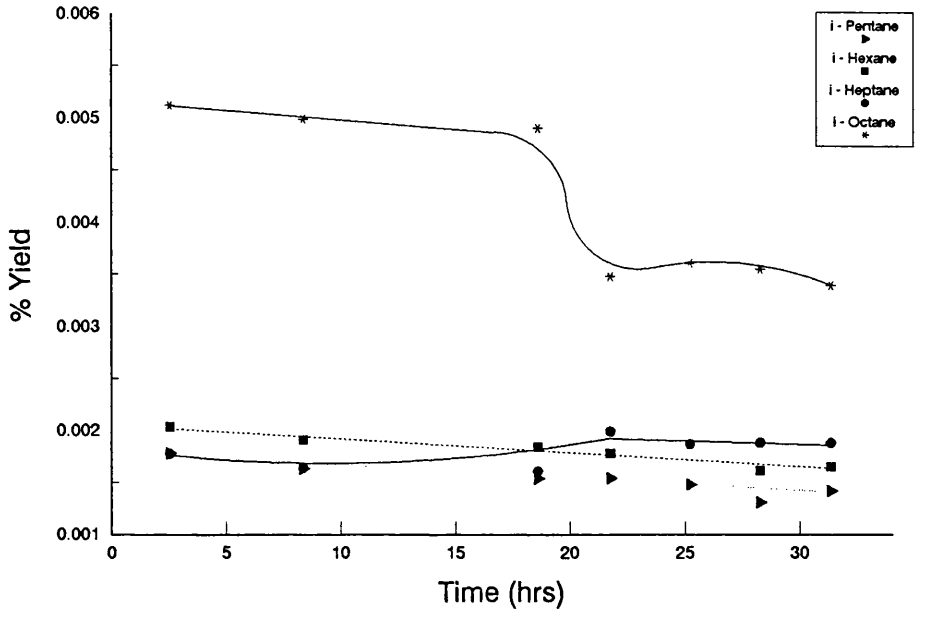

Figure 6.17.3. % Yield of i-Paraffins on 3.0%Sn/Alumina

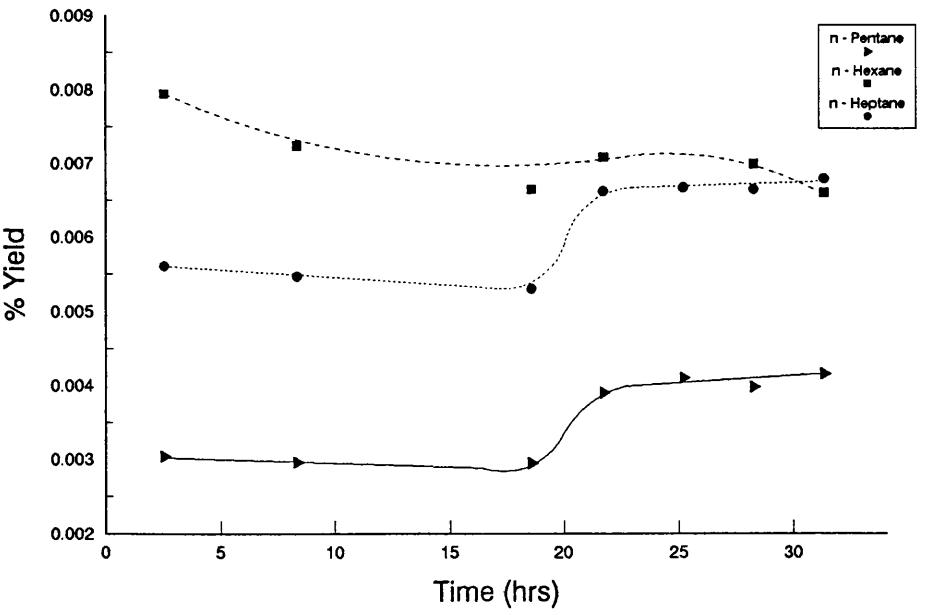

Figure 6.17.4. % Yield of n-Paraffins on 3.0%Sn/Alumina

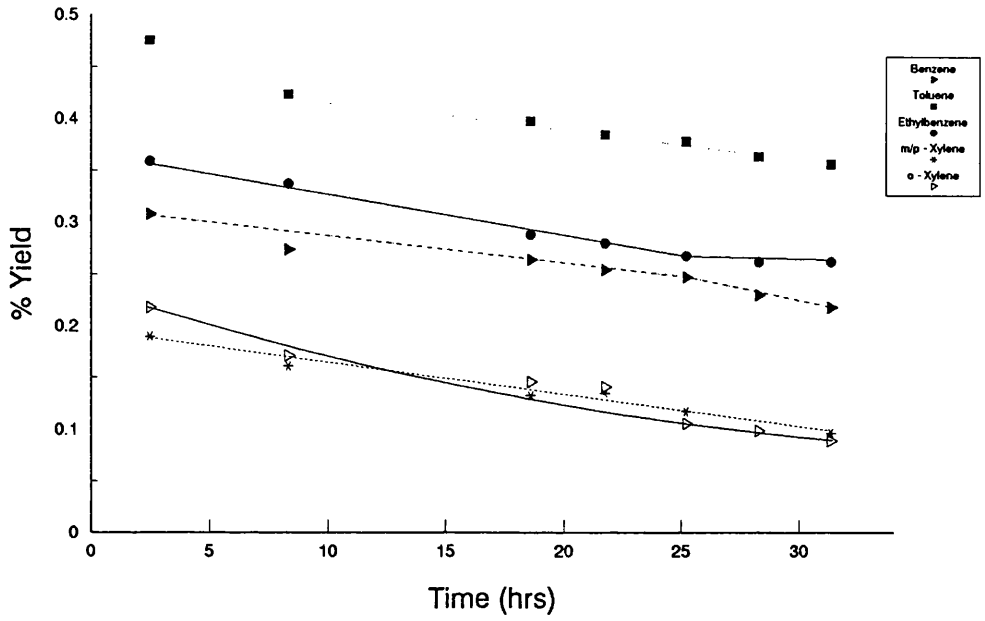

Figure 6.17.5. % Yield aromatic products on 3.0%Sn/Alumina

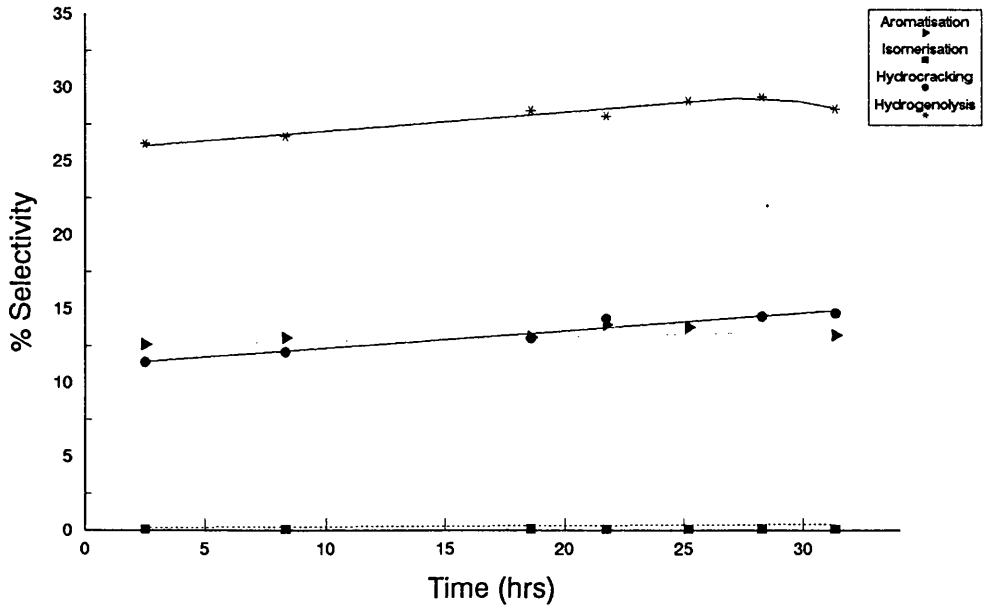

Figure 6.17.6. % Selectivity to the Major Reactions on 3.0%Sn/Alumina

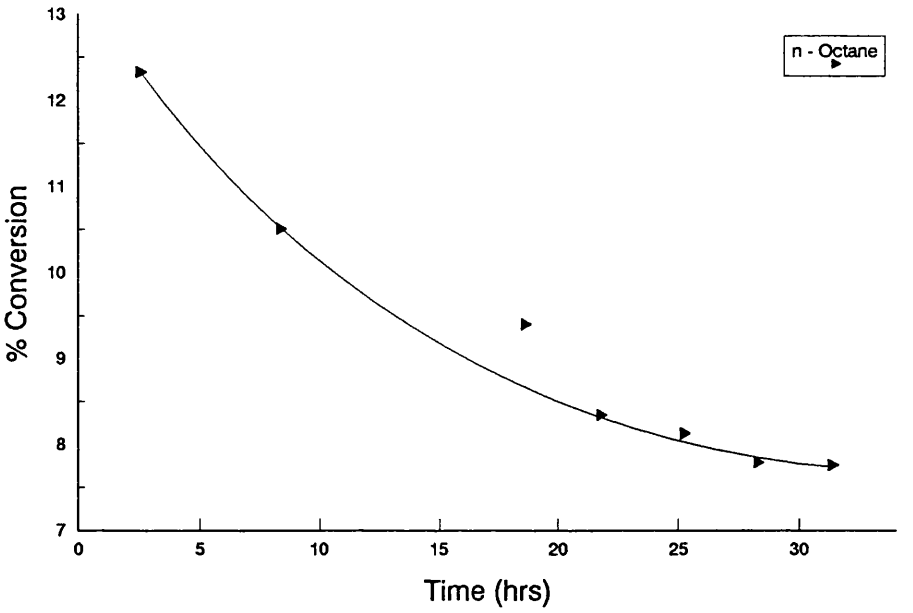

Figure 6.17.7. % Conversion of n-Octane on 3.0%Sn/Alumina

cycloparaffin species decrease with time. Cycloheptane in particular decreases dramatically during the first 15 hours of the reaction. At the end of the run the product yield of cycloparaffins increases with carbon number. Figure 6.17.3 shows the yields of i-paraffin products with time. The yield of i-heptane increases before reaching a steady level whereas the other i-paraffins decrease with time. Figure 6.17.4 shows that the yields of both n-pentane and n-heptane increase rapidly after 17 hours before reaching a steady yield. The yield of n-hexane in contrast decreases with time.

Figure 6.17.5 illustrates the decreasing yield of aromatic products with time. Toluene in this case is the dominant species followed by ethylbenzene, benzene and then the xylene isomers. Once again the yield of aromatics is extremely low as noted in the previous Section. However with this catalyst the yields of the C_8 aromatic species have dropped significantly when compared with the 0.3wt%Sn/Al_2O_3 catalyst.

The selectivities of individual hydrocarbon species are shown in Table 6.17.2 and the selectivity to the major reactions is detailed in Figure 6.17.6. As with the 0.3wt%Sn/Al_2O_3 catalyst hydrogenolysis was found to be the dominant reaction. Initially this was followed by aromatisation but after 16 hours on stream the activity of hydrocracking increased above that of aromatisation. Isomerisation activity is always very small. The activity of all major reactions increases with reaction time as shown in Figure 6.17.6.

The initial propane to methane ratio, in this case, decreases sharply before rising slightly after 25 hours on stream. This indicates that the support was initially deactivated preferentially. The carbon mass balance typically shows the carbon deposition to decrease with reaction time.

The conversion of n-octane, shown in Figure 6.17.7, decreases steadily from ~12.5% to ~8% after 32 hours where it reaches a constant level. This level of conversion is similar to that with the 0.3wt%Sn/Al_2O_3 catalyst although the higher metal loaded catalyst is not deactivated as quickly. In comparison with a platinum monometallic catalyst the conversion is very low. The % coke deposited on the catalyst surface was 18.21% by weight. The addition of large amounts of tin to a support material has shown to be detrimental to both the selectivity and conversion.

6.18 Poisoned EUROPT Catalysts

The poisoned EUROPT-3 and -4 catalysts were tested under identical conditions stated previously in Section 6.1. The catalysts were poisoned for 2 hours in a stream of 2% H_2S/N_2 gaseous mixture. The two catalysts behaved similarly and therefore only the results of the poisoned EUROPT-3 catalyst are illustrated in Figures 6.18.1 to 6.18.5 and in Tables 6.18.1 and 6.18.2.

The yield of most products was very low and many species could not be detected. Figure 6.18.1 illustrates the increasing yield of methane and propane with time on stream. No propane could be detected until after 75 hours on stream. The

Table 6.18.1. %Yield of individual products and % Conversion versus time-on-stream for the poisoned EUROPT-3 catalyst.

Products	The % Yield of Selected Products																
Time (hrs)	1.5	4.5	18.05	21.15	24.15	27.15	44	47.5	51	54.5	70.5	74	77.5	81	96	99	103
Benzene	-	-	-	-	-	-	-	-	-	-	6×10^{-6}	6×10^{-6}	6×10^{-6}	7×10^{-6}	1×10^{-5}	1×10^{-5}	1×10^{-5}
Toluene	-	-								-	-	-	-	-	4×10^{-6}	5×10^{-6}	5×10^{-6}
Ethylbenzene	-	-	-	-	-	-	-	-	-	-	-	-	-	7×10^{-6}	8×10^{-6}	9×10^{-6}	9×10^{-6}
m/p - Xylene																	
o - Xylene	-	-	-	-	-	-	-	-	-	-	-	-	4×10^{-6}	-	7×10^{-6}	8×10^{-6}	8×10^{-6}
Methane	0.0640	0.0623	0.0665	0.0675	0.0732	0.0785	0.0761	0.0889	0.0957	0.0982	0.0999	0.1151	0.1161	0.1206	0.1211	0.1151	0.1146
Propane													0.0034	-	0.0046	0.0051	0.0062
Conversion of n-Octane	0.0640	0.0623	0.0665	0.0675	0.0732	0.0785	0.0761	0.0889	0.0957	0.0982	0.0999	0.1151	0.1120	0.1206	0.1258	0.1203	0.1209

Table 6.18.2. Carbon Mass Balance for the poisoned EUROPT-3 catalyst (510°C, 110 psig)

Time (hrs)	No. of moles of Carbon In	No. of moles of Carbon Out	Δ Carbon
1.5	1.2820×10^{-4}	1.2730×10^{-4}	8.9905×10^{-7}
4.5	1.2820×10^{-4}	1.2701×10^{-4}	1.1860×10^{-6}
18.05	1.2820×10^{-4}	1.2517×10^{-4}	3.0323×10^{-6}
21.15	1.2820×10^{-4}	1.2472×10^{-4}	3.4838×10^{-6}
24.15	1.2820×10^{-4}	1.2444×10^{-4}	3.7650×10^{-6}
27.15	1.2820×10^{-4}	1.2426×10^{-4}	3.9430×10^{-6}
44	1.2820×10^{-4}	1.2410×10^{-4}	4.1005×10^{-6}
47.5	1.2820×10^{-4}	1.2403×10^{-4}	4.1695×10^{-6}
51	1.2820×10^{-4}	1.2381×10^{-4}	4.3892×10^{-6}
54.5	1.2820×10^{-4}	1.2362×10^{-4}	4.5854×10^{-6}
70.5	1.2820×10^{-4}	1.2280×10^{-4}	5.4004×10^{-6}
74	1.2820×10^{-4}	1.2258×10^{-4}	5.6180×10^{-6}
77.5	1.2820×10^{-4}	1.2258×10^{-4}	5.6174×10^{-6}
81	1.2820×10^{-4}	1.2246×10^{-4}	5.7406×10^{-6}
96	1.2820×10^{-4}	1.2065×10^{-4}	7.5492×10^{-6}
99	1.2820×10^{-4}	1.2063×10^{-4}	7.5712×10^{-6}
103	1.2820×10^{-4}	1.2047×10^{-4}	7.7348×10^{-6}

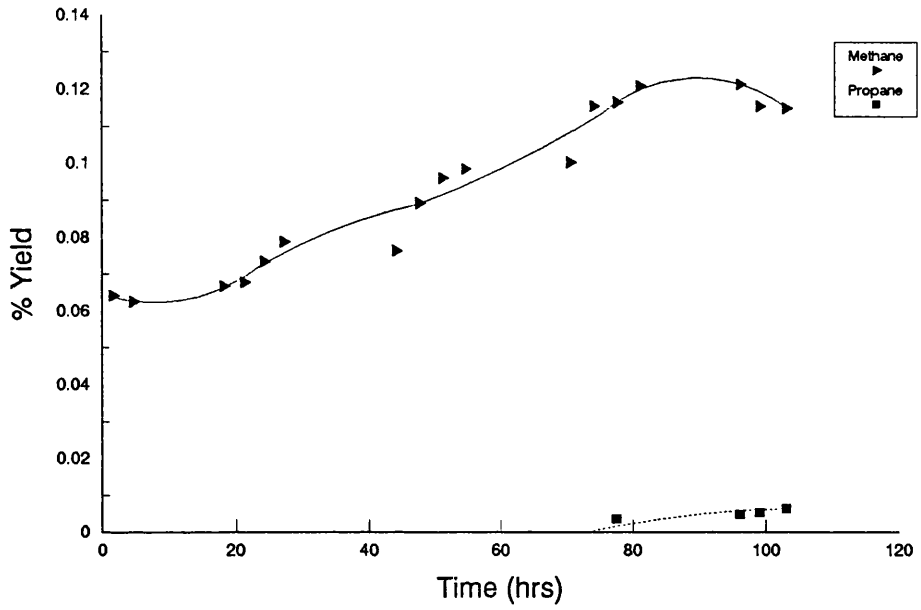

Figure 6.18.1. % Yield of Individual Hydrocarbon Products on a poisoned EUROPT-3 catalyst

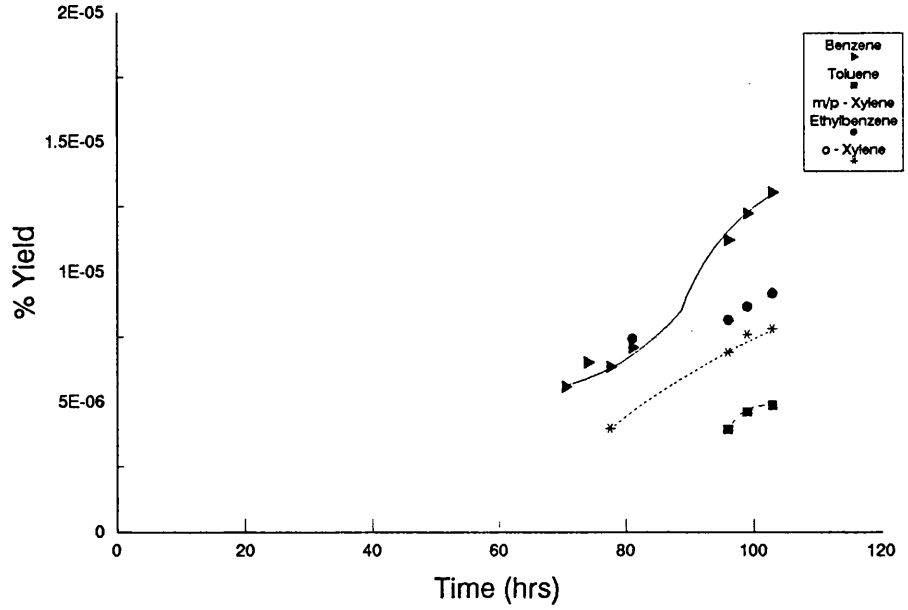

Figure 6.18.2. % Yield of Aromatic Products on a poisoned EUROPT-3 catalyst

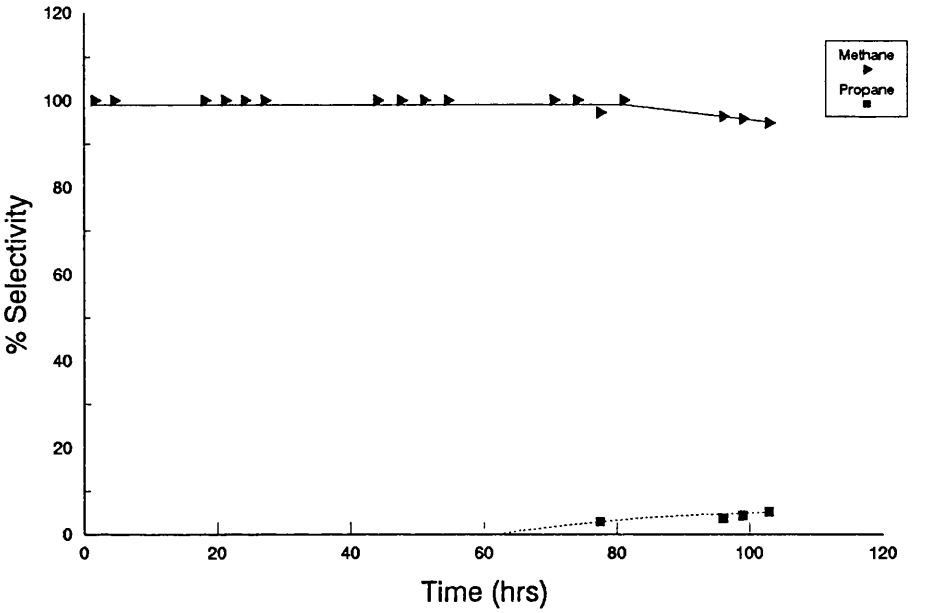

Figure 6.18.3. % Selectivity of Individual Hydrocarbon Products on a poisoned EUROPT-3 catalyst

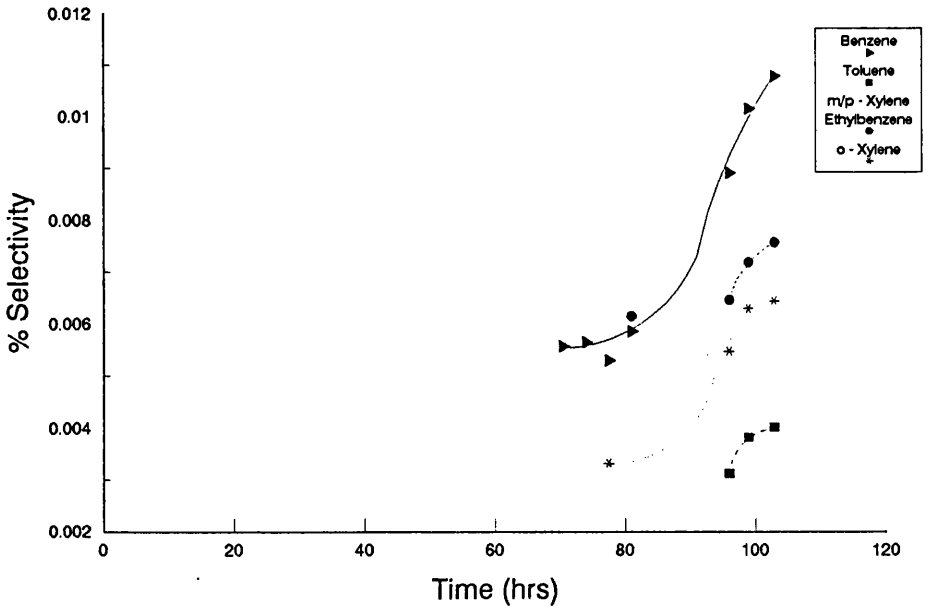

Figure 6.18.4. % Selectivity of Aromatic Products on a poisoned EUROPT-3 catalyst

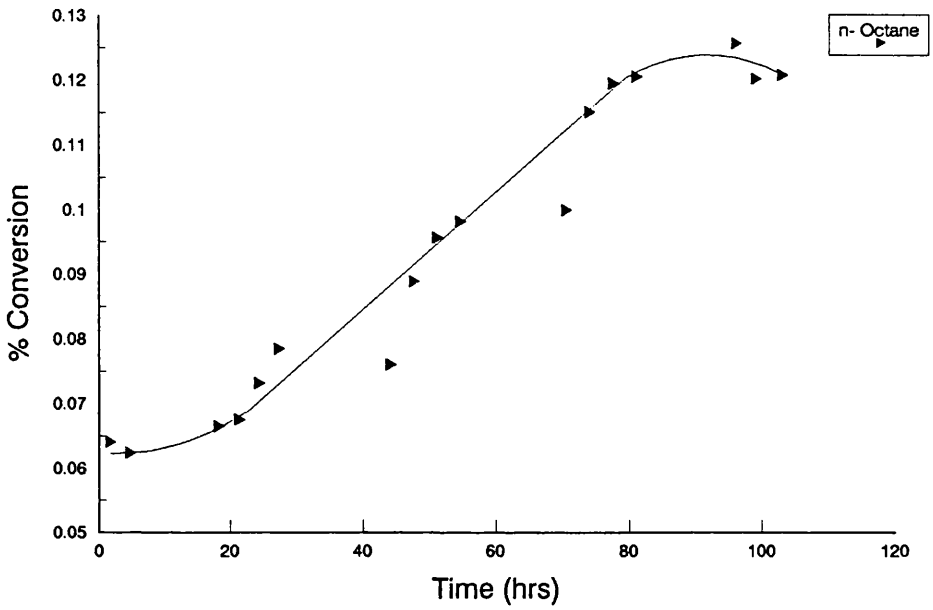

Figure 6.18.5. % Conversion of n-Octane on a poisoned EUROPT-3 catalyst

yield of both methane and propane has been drastically lowered (by ~100 times) by the addition of a large quantity of sulphur to the catalyst.

Figure 6.18.2 shows the yield of aromatic species with time. The yield of aromatic species is very low in comparison with an unsulphided EUROPT-3.1 catalyst and no aromatic products were detected until after 15 hours on stream. The aromatic yields after this time increased gradually with benzene being produced in the highest quantities followed by ethylbenzene/m/p-xylene, o-xylene and then toluene. Toluene was only detectable after 96 hours on stream.

Figures 6.18.3 and 6.18.4 illustrate the selectivities to the observed hydrocarbon products with time. The selectivity to the major reactions was not calculated due to the lack of products formed during the reaction. However, hydrogenolysis dominated the reactions (> 90%) followed by aromatisation (<1%).

The propane to methane ratio increased slightly in the last 25 hours of the reaction. The carbon mass balance, Table 6.18.2, showed that the carbon deposition increased gradually with reaction time. The results suggest that in the last 25 hours of the reaction more coke is deposited onto the metallic sites than on the acidic sites of the catalyst.

The total conversion of n-octane, illustrated in Figure 6.18.5, increases from 0.06 to 0.12% in the 103 hours on stream. The deposition of a large amount of sulphur onto the catalyst surface has been shown to be highly detrimental to both the catalyst

selectivity and conversion. The % coke deposited upon the poisoned EUROPT-3 and -4 catalysts was 1.68 and 2.32% respectively. This value is many factors smaller than the coke deposited on non-sulphided catalysts. The adsorption of sulphur on to a catalyst therefore deters the formation of coke.

6.19. EUROPT-3-S (4 pulses of H_2S, 510°C, 110 psig)

The partially sulphided EUROPT-3 catalyst was tested under conditions described in Section 6.1. This catalyst had been sulphided with 4 pulses of H_2S at 400°C before being reduced again. The results of this run are reported in Figures 6.19.1 to 6.19.6 and in Tables 6.19.1 to 6.19.3.

The product yield of C_1 - C_4 species, with the exception of methane, increase with reaction time. Methane in contrast decreases steadily until it reaches a constant yield of ~1%. The order of the product yields is as follows from propane, methane to ethane. The yield of n-butane in this run was ~2 times that of i-butane. The yield of all C_1 - C_4 species, especially that of methane, was lower than that on an unsulphided catalyst.

The yield of paraffinic species is outlined in Figures 6.19.2 and 6.19.3 against time. Yet again the yield of cycloparaffins is very small in comparison to both i- and n-paraffin products. The yield of cyclooctane decreases while that of cyclopentane, cyclohexane and cycloheptane increases with time. Initially cyclooctane is the dominant product but after ~12 hours on stream the yield fell

Table 6.19.1a. % Yield of individual products and % Conversion versus time on stream for EUROPT-3 (4 pulses of H_2S)

Products	% Yield of Selected Products								
Time (hrs)	1.5	4.5	7.67	20.8	23.75	26.75	29.75	44.7	47.75
Benzene	12.5780	11.7710	11.8311	11.6932	11.6560	9.7559	9.8551	9.3348	10.0715
Toluene	11.0683	10.5366	9.4347	7.9100	6.4975	5.8754	4.9675	4.3556	4.8716
Ethylbenzene	4.0980	3.7700	4.0513	3.6977	3.5343	3.4886	3.5577	3.5788	3.4276
m/p-Xylene									
o-Xylene	-	-	0.0010	-	-	0.0008	0.0008	0.0013	0.0014
Methane	2.2242	2.2479	2.2195	2.1571	2.1181	2.0545	2.0989	1.7367	1.6921
Ethane	-	-	0.0481	-	-	-	0.0539	-	0.0629
Propane	1.9191	2.5368	2.7305	3.4283	3.6430	3.2170	3.6002	3.2679	3.5665
i-Butane	1.0742	1.1569	1.3086	1.5493	2.0991	2.3522	2.3861	2.3172	2.5305
n-Butane	2.7507	2.4736	2.4249	3.4625	3.3631	3.1440	3.2432	3.3394	3.5207
Cyclopentane	0.0302	0.0002	0.0003	0.0002	0.0003	0.0003	0.0003	0.0003	0.0003
i-Pentane		0.0311	0.0325	0.0452	0.0444	0.0440	0.0434	0.0491	0.0493
n-Pentane									
Cyclohexane	0.0011	0.0012	0.0011	0.0013	0.0013	0.0013	0.0014	0.0012	0.0015
i-Hexane	0.0322	0.0290	0.0293	0.0252	0.0268	0.0305	0.0320	0.0297	0.0280
n-Hexane									
Cycloheptane	0.0003	0.0051	0.0005	0.0006	0.0006	0.0007	0.0006	0.0007	0.0008
i-Heptane	0.0039		0.0047	0.0037	0.0039	0.0038	0.0038	0.0040	0.0038
n-Heptane	0.0168	0.0133	0.0114	0.0087	0.0085	0.0080	0.0083	0.0084	0.0081
Cyclooctane	0.0019	0.0015	0.0015	0.0011	0.0011	0.0010	0.0011	0.0010	0.0010
i-Octane	0.0202	0.0225	0.0185	0.0207	0.0230	0.0260	0.0266	0.0270	0.0266
% Conversion of n-Octane	35.8191	34.5969	34.1493	34.0047	33.0210	30.0039	29.8775	28.0532	29.8642

Table 6.19.1b. % Yield of individual products and % Conversion versus time on stream for EUROPT-3 (4 pulses of H_2S)

Products	% Yield of Selected Products							
Time (hrs)	50.75	53.8	68.75	71.75	74.75	81.4	92.8	95.75
Benzene	9.8138	9.4921	9.7132	10.7052	10.6179	10.0273	9.7256	10.1787
Toluene	4.4142	4.2620	4.0808	4.6173	4.7972	4.7629	4.7882	4.8102
Ethylbenzene	3.5174	3.9167	4.5450	4.8831	5.1994	5.6653	5.9251	6.0725
m/p-Xylene								
o-Xylene	0.0014	0.0014	0.0013	0.0014	0.0018	0.0015	0.0017	0.0017
Methane	1.6204	1.6494	1.3184	1.0318	0.9025	0.8454	0.8097	0.7882
Ethane	0.0602	0.0588	0.0692	0.0722	0.0747	0.0806	0.0939	0.0961
Propane	3.6387	3.4088	3.5039	3.6687	3.7504	3.6511	3.4431	3.5591
i-Butane	2.2995	2.1723	2.0608	2.1998	2.0068	2.2026	2.2341	2.3745
n-Butane	3.1135	2.9759	2.9052	3.1258	3.6550	3.6621	3.6204	3.6441
Cyclopentane	0.0003	0.0003	0.0037	0.0003	0.0003	0.0004	0.0004	0.0004
i-Pentane	0.0468	0.0439	0.0525	0.0503	0.0500	0.0589	0.0548	0.0460
n-Pentane								
Cyclohexane	0.0012	0.0010	0.0010	0.0011	0.0012	0.0012	0.0012	0.0013
i-Hexane	0.0301	0.0289	0.0317	0.0317	0.0313	0.0449	0.0522	0.0458
n-Hexane								
Cycloheptane	0.0007	0.0007	0.0007	0.0007	0.0008	0.0008	0.0009	0.0008
i-Heptane	0.0040	0.0039	0.0036	0.0035	0.0034	0.0033	0.0034	0.0034
n-Heptane	0.0085	0.0078	0.0085	0.0077	0.0074	0.0081	0.0079	0.0078
Cyclooctane	0.0010	0.0009	0.0009	0.0009	0.0009	0.0009	0.0009	0.0009
i-Octane	0.0285	0.0305	0.0297	0.0325	0.0352	0.0373	0.0380	0.0387
% Conversion of n-Octane	28.6002	28.0493	28.3268	30.4341	31.1362	31.0527	30.8013	31.6702

Table 6.19.2a. % Selectivity of individual products versus time on stream for EUROPT-3 (4 pulses of H_2S)

Products	% Selectivity of Selected Products								
Time (hrs)	1.5	4.5	7.67	20.8	23.75	26.75	29.75	44.7	47.75
Benzene	35.1152	34.0233	34.6452	34.3869	35.2986	35.5154	32.9852	33.2753	33.7244
Toluene	30.9007	30.4554	27.6279	23.2614	19.6768	19.5822	16.6262	15.5261	16.3125
Ethylbenzene	11.4408	10.8969	11.8634	10.8741	10.7033	11.6271	11.9077	12.2184	11.4774
m/p-Xylene									
o-Xylene	-	-	0.0030	-	-	0.0028	0.0026	0.0051	0.0048
Methane	6.2095	6.4975	6.4995	6.3436	6.4144	6.8473	27.0249	6.1907	5.6659
Ethane	-	-	0.1407	-	-	-	0.1803	-	0.2107
Propane	5.3577	7.3325	7.9957	10.0817	11.0325	10.7221	12.0498	11.6488	11.9422
i-Butane	2.9990	3.3441	3.8321	4.5561	6.3569	7.8395	7.9862	8.2600	7.6999
n-Butane	7.6794	7.1497	7.1009	10.1823	10.1846	10.4786	10.8550	11.9038	10.4255
Cyclopentane	0.0844	0.0006	0.0008	0.0007	0.0009	0.0010	0.0010	0.0010	0.0011
i-Pentane		0.0899	0.0950	0.1328	0.1345	0.1466	0.1453	0.1756	0.1650
n-Pentane									
Cyclohexane	0.0030	0.0034	0.0033	0.0039	0.0039	0.0045	0.0047	0.0043	0.0050
i-Hexane	0.0898	0.0839	0.0857	0.0741	0.0813	0.1068	0.1072	0.1060	0.0936
n-Hexane									
Cycloheptane	0.0010	0.0146	0.0013	0.0019	0.0019	0.0020	0.0020	0.0027	0.0027
i-Heptane	0.0110		0.0137	0.0108	0.0117	0.0126	0.0126	0.0144	0.0126
n-Heptane	0.0470	0.0385	0.0333	0.0256	0.0256	0.0276	0.0277	0.0300	0.0273
Cyclooctane	0.0053	0.0045	0.0044	0.0034	0.0034	0.0036	0.0036	0.0037	0.0035
i-Octane	0.0563	0.0652	0.0541	0.0608	0.0698	0.0887	0.0890	0.0963	0.0890

Table 6.19.2b. % Selectivity of individual products versus time on stream for EUROPT-3 (4 pulses of H_2S)

Products	% Selectivity of Selected Products							
Time (hrs)	50.75	53.8	68.75	71.75	74.75	81.4	92.8	95.75
Benzene	34.3138	33.8409	34.2898	35.1751	34.1015	32.2911	32.0962	32.1396
Toluene	15.4341	15.1947	14.4062	15.1716	15.4071	15.3382	15.8018	15.1884
Ethylbenzene	12.2987	13.9636	16.0450	16.0448	16.6989	18.2441	19.5539	19.1741
m/p-Xylene								
o-Xylene	0.0050	0.0049	0.0047	0.0046	0.0058	0.0047	0.0058	0.0053
Methane	5.6658	5.8805	4.6543	3.3902	2.8985	2.7225	2.6720	2.4887
Ethane	0.2103	0.2095	0.2442	0.2371	0.2399	0.2597	0.3097	0.3035
Propane	12.7227	12.1529	12.3695	12.0546	12.0450	11.7577	11.3630	11.2381
i-Butane	8.0402	7.7446	7.2751	7.2281	6.4453	7.0867	7.3729	7.4976
n-Butane	10.8863	10.6094	10.2562	10.2706	11.7389	11.7932	11.9481	11.5064
Cyclopentane	0.0011	0.0010	0.0013	0.0011	0.0010	0.0013	0.0014	0.0013
i-Pentane	0.1635	0.1566	0.1853	0.1651	0.1607	0.1898	0.1807	0.1453
n-Pentane								
Cyclohexane	0.0041	0.0037	0.0037	0.0036	0.0038	0.0038	0.0040	0.0041
i-Hexane	0.1053	0.1029	0.1118	0.1043	0.1004	0.1446	0.1721	0.1447
n-Hexane								
Cycloheptane	0.0025	0.0024	0.0025	0.0024	0.0025	0.0027	0.0028	0.0027
i-Heptane	0.0136	0.0139	0.0126	0.0115	0.0110	0.0107	0.0112	0.0106
n-Heptane	0.0274	0.0280	0.0300	0.0254	0.0238	0.0261	0.0260	0.0246
Cyclooctane	0.0034	0.0033	0.0032	0.0030	0.0028	0.0028	0.0030	0.0029
i-Octane	0.0997	0.1086	0.1048	0.1068	0.1131	0.1202	0.1255	0.1220

Table 6.19.3. Carbon Mass Balance for EUROPT-3 (4 Pulses of H_2S) (510°C, 110 psig)

Time (hrs)	No. of moles of Carbon In	No. of moles of Carbon Out	Δ Carbon
1.5	4.3572×10^{-4}	3.8587×10^{-4}	4.9846×10^{-5}
4.5	4.3572×10^{-4}	3.9450×10^{-4}	4.1219×10^{-5}
7.67	4.3572×10^{-4}	4.0801×10^{-4}	2.7701×10^{-5}
20.8	4.3572×10^{-4}	4.1559×10^{-4}	2.0129×10^{-5}
23.75	4.3572×10^{-4}	4.1631×10^{-4}	1.9408×10^{-5}
26.75	4.3572×10^{-4}	4.1343×10^{-4}	2.2281×10^{-5}
29.75	4.3572×10^{-4}	4.1379×10^{-4}	2.1921×10^{-5}
44.7	4.3572×10^{-4}	4.1359×10^{-4}	2.2127×10^{-5}
47.75	4.3572×10^{-4}	4.1380×10^{-4}	2.1912×10^{-5}
50.75	4.3572×10^{-4}	4.1373×10^{-4}	2.1985×10^{-5}
53.8	4.3572×10^{-4}	4.1713×10^{-4}	1.8581×10^{-5}
68.75	4.3572×10^{-4}	4.1898×10^{-4}	1.6735×10^{-5}
71.75	4.3572×10^{-4}	4.2274×10^{-4}	1.2971×10^{-5}
74.75	4.3572×10^{-4}	4.2280×10^{-4}	1.2916×10^{-5}
81.4	4.3572×10^{-4}	4.2115×10^{-4}	1.4569×10^{-5}
92.8	4.3572×10^{-4}	4.2926×10^{-4}	6.4549×10^{-6}
95.75	4.3572×10^{-4}	4.3023×10^{-4}	5.4895×10^{-6}

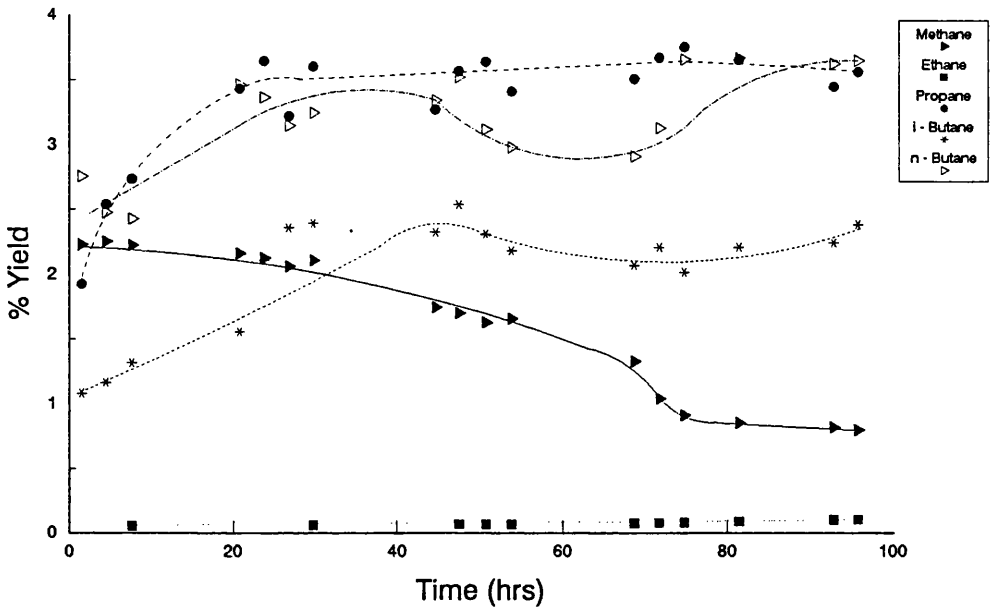

Figure 6.19.1. % Yield of Individual Hydrocarbon Products on a EUROPT-3 catalyst (4 pulses of H_2S)

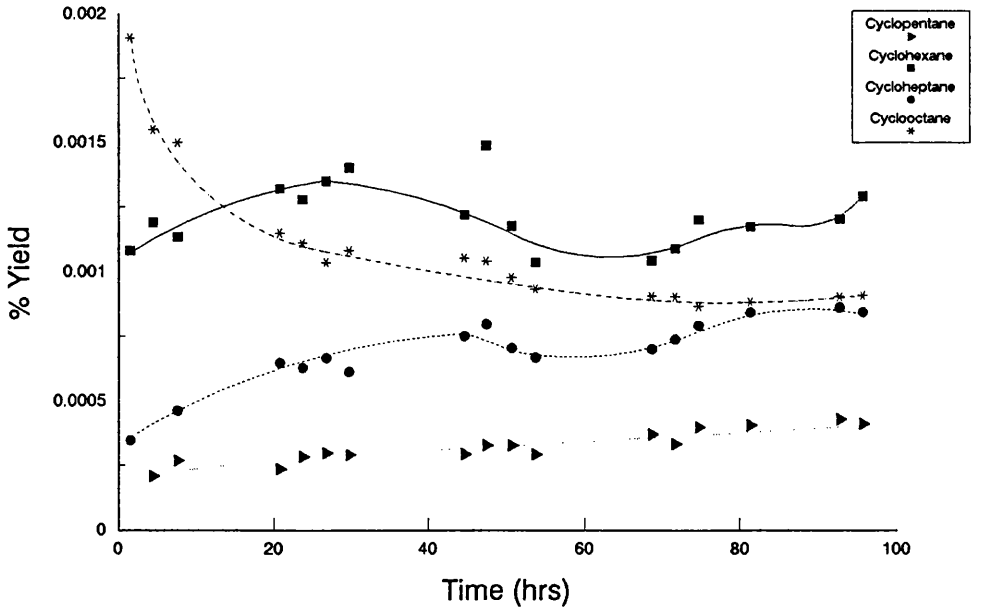

Figure 6.19.2. % Yield of Cycloparaffin Products on a EUROPT-3 catalyst (4 Pulses H_2S)

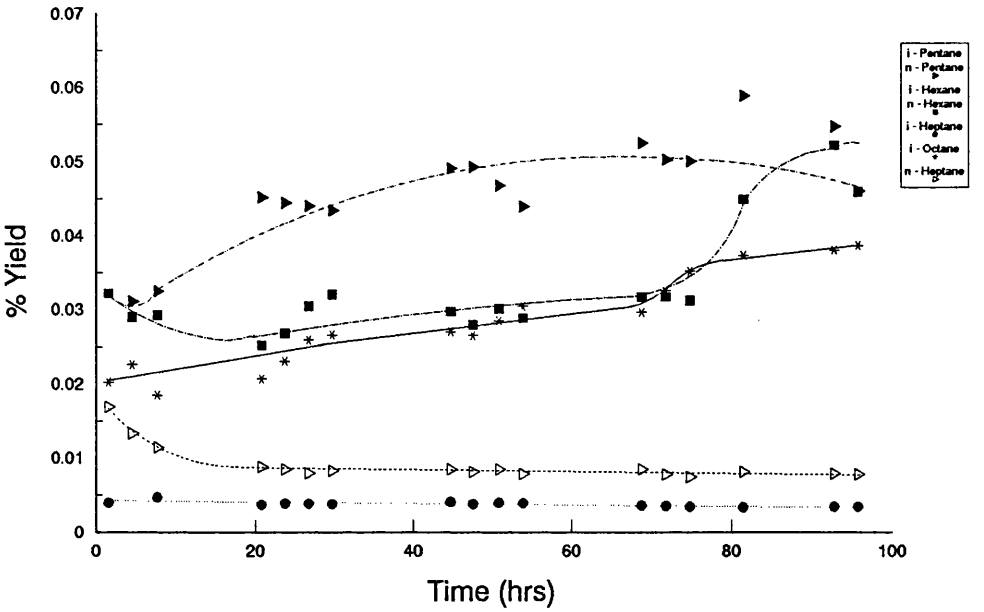

Figure 6.19.3. % Yield of i- and n-Paraffin Products on a EUROPT-3 catalyst (4 pulses of H_2S)

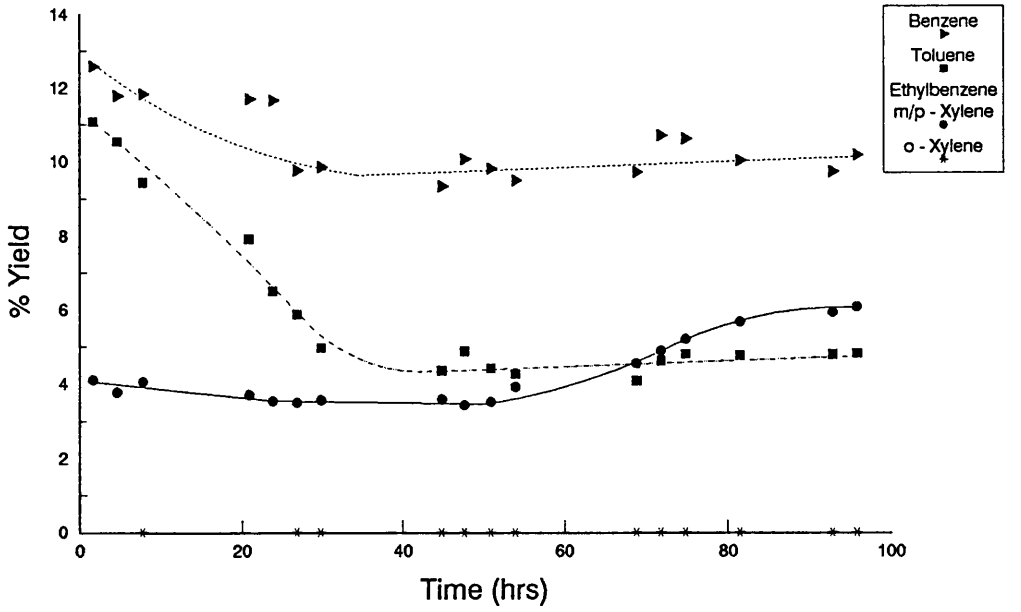

Figure 6.19.4. % Yield of Aromatic Products on a EUROPT-3 catalyst (4 Pulses H_2S)

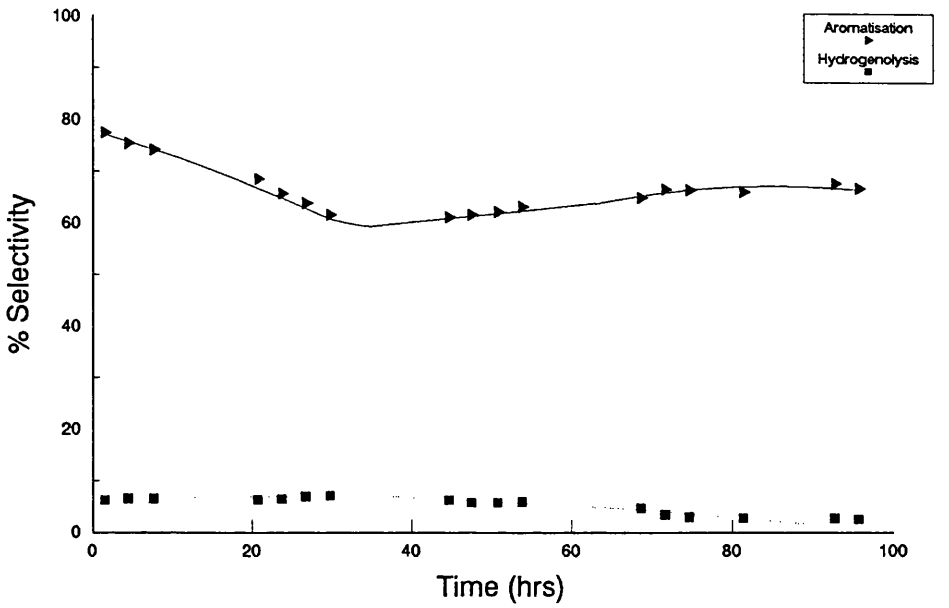

Figure 6.19.5. % Selectivity to the Major Reactions on a EUROPT-3 catalyst (4 pulses of H_2S)

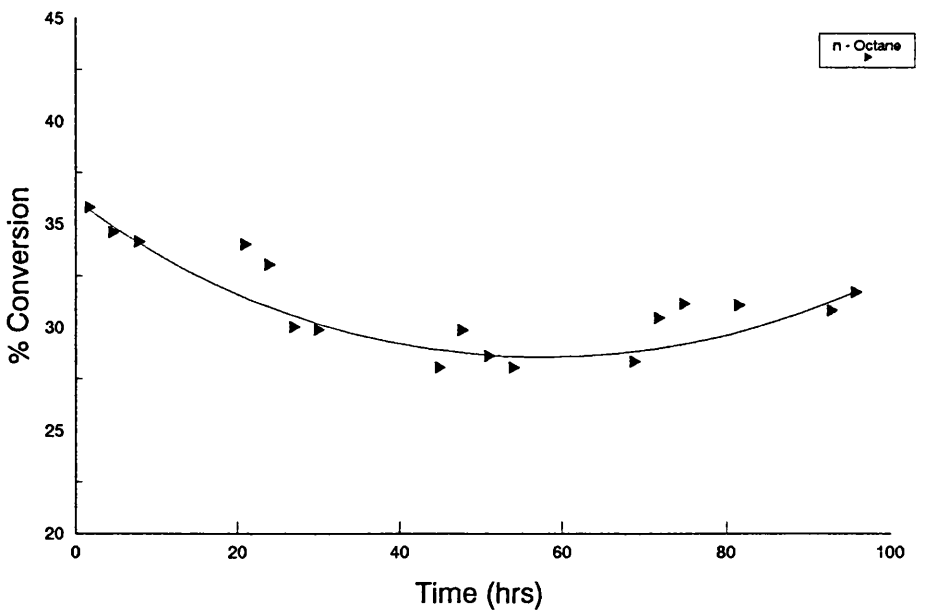

Figure 6.19.6. % Conversion of n-Octane on a EUROPT-3 catalyst (4 Pulses H_2S)

below that of cyclohexane. These products were followed by cycloheptane and finally cyclopentane. Once again certain species were indistinguishable and therefore are reported as combined values. The combined yield of i- and n-pentane and i- and n-hexane increase with time on stream. The yield of i-octane also increases steadily while the yield of both i- and n-heptane decreases with time.

The range of aromatic products obtained is illustrated in Figure 6.19.4. One notable difference between a sulphided and an unsulphided EUROPT-3.1 catalyst is in the product distribution of aromatics. The yield of C_8 aromatics is significantly lower and the yield of benzene and toluene higher with a sulphided catalyst. Benzene, in this run, reaches a constant value of ~10% whereas with an unsulphided EUROPT-3.1 catalyst, Section 6.1, this value is significantly lower at ~0.2%. The yield of both benzene and toluene decrease while the yield of the xylene isomers and ethylbenzene increase with time on stream.

Table 6.19.2 details the selectivities of individual hydrocarbon products with time. Figure 6.19.5 illustrates the selectivity to the major reactions. The order of decreasing selectivity is as follows:

Aromatisation > Hydrogenolysis > Hydrocracking > Isomerisation

The aromatisation activity reaches a constant level at 66% after falling from ~78%. Hydrogenolysis activity is in contrast very low, falling to a value of ~2.5% in comparison with ~15% on an unsulphided EUROPT-3.1 catalyst.

The propane to methane ratio increases initially to a constant ratio before increasing to a value of 4.4 after 40 hours. The carbon mass balance, Table 6.19.3, shows that the carbon deposition on this catalyst decreases with time. Initially the coke deposition deactivates the metallic sites preferentially, but after 40 hours the acidic sites on the support are deactivated quicker.

The total conversion of n-octane, Figure 6.19.6, decreases from ~35% through a minimum at ~50 hours to ~31% after 103 hours. The conversion of this catalyst has improved along with the selectivity in comparison with an unsulphided catalyst. The % coke deposited upon this catalyst was 2.99% by weight, higher than that on the poisoned catalyst but much lower than with an unsulphided catalyst.

6.20. EUROPT-3-S (3 pulses of H_2S, 510°C, 110 psig)

The partially sulphided catalyst was tested under conditions described in Section 6.1. This catalyst had been sulphided with 3 pulses of H_2S at 400°C before being reduced in hydrogen once again. The results of this run are reported in Figures 6.20.1 to 6.20.6 and in Tables 6.20.1 to 6.20.3.

The product yield of C_1 - C_4 species is shown in Figure 6.20.1. The yield of both propane and methane decrease while that of i- and n-butane rise initially before decreasing gradually with time. The yield of methane and propane reach constant levels of ~2.2 and 4.2% respectively. The yield of n-butane is only ~1.4 times greater than i-butane with a steady value of ~4.5%.

Table 6.20.1. % Yield of individual products and % Conversion versus time on stream for EUROPT-3 (3 pulses of H_2S)

Products	% Yield of Selected Products													
Time (hrs)	3	18.1	21.05	24	27	42.1	45	48	51	67.25	70.25	73.25	91.75	94.75
Benzene	7.0213	6.2404	6.3135	6.5570	6.6290	6.8497	6.7103	6.0195	6.0112	6.0776	6.0759	6.0576	6.1060	6.0954
Toluene	5.4393	5.2011	5.2247	5.2876	5.3006	5.2918	5.2056	5.0593	5.0515	4.9750	4.9341	4.8987	4.6215	4.6034
Ethylbenzene	3.5966	4.3810	4.5188	4.6129	4.9444	4.8460	4.6733	4.3437	4.2196	4.1203	3.9833	4.1662	4.1856	3.9843
m/p-Xylene														
o-Xylene	2.3992	1.8778	1.8013	1.7252	1.6592	1.6524	1.4811	1.3998	1.3028	1.0942	1.1009	1.0838	1.1519	1.0595
Methane	3.0090	2.8833	2.7046	2.5829	2.5215	2.0295	2.4262	2.4749	2.3534	2.1449	2.1054	2.2201	2.1113	2.2013
Ethane	-	-	-	-	-	0.0604	0.0604	0.0762	-	-	-	0.1004	-	-
Propane	5.7731	5.4906	5.4752	5.4784	5.4919	5.3490	5.0744	4.8653	4.6417	4.5766	4.5120	4.4468	4.2717	4.2842
i-Butane	2.7272	2.8218	3.1889	3.4738	3.5284	3.9824	3.9109	3.6062	3.4451	3.3287	3.3180	3.2803	3.2550	3.2174
n-Butane	4.2352	4.5645	4.6477	4.8488	4.8800	4.9631	4.8323	4.6737	4.6325	4.5806	4.5948	4.5014	4.4849	4.4331
Cyclopentane	0.0009	0.0006	0.0006	0.0005	0.0005	0.0005	0.0005	0.0005	0.0005	0.0004	0.0005	0.0004	0.0004	0.0005
i-Pentane	0.0387	0.0383	0.0378	0.0384	0.0393	0.0382	0.0383	0.0388	0.0391	0.0404	0.0423	0.0433	0.0432	0.0443
n-Pentane	0.0167	0.0172	0.0171	0.0208	0.0222	0.0230	0.0226	0.0232	0.0251	0.0271	0.0263	0.0271	0.0264	0.0265
Cyclohexane	0.0009	0.0008	0.0007	0.0007	0.0007	0.0007	0.0007	0.0007	0.0007	0.0007	0.0007	0.0007	0.0007	0.0007
i-Hexane	0.0305	0.0354	0.0371	0.0390	0.0441	0.0469	0.0464	0.0468	0.0478	0.0476	0.0469	0.0467	0.0502	0.0508
n-Hexane														
Cycloheptane	0.0006	0.0006	0.0006	0.0005	0.0005	-	0.0005	0.0005	0.0004	0.0004	0.0004	0.0004	-	0.0004
i-Heptane	0.0037	0.0037	0.0038	0.0039	0.0042	0.0052	0.0053	0.0058	0.0061	0.0069	0.0072	0.0074	0.0071	0.0072
n-Heptane														
Cyclooctane	0.0004	-	-	0.0005	0.0005	0.0005	0.0006	0.0006	0.0006	0.0006	0.0006	0.0006	0.0007	0.0007
i-Octane	0.0689	0.0559	0.0524	0.0497	0.0484	0.0393	0.0345	0.0336	0.0333	0.0342	0.0321	0.0316	0.0302	0.0301
% Conversion of n-Octane	34.3622	33.6130	34.0246	34.7207	35.1153	35.6787	34.5239	32.6692	31.8111	31.0562	30.7814	30.9136	30.3470	30.0397

Table 6.20.2. % Selectivity of individual products versus time on stream for EUROPT-3 (3 pulses of H_2S)

Products	% Selectivity of Selected Products													
Time (hrs)	3	18.1	21.05	24	27	42.1	45	48	51	67.25	70.25	73.25	91.75	94.75
Benzene	20.4331	18.5654	18.5557	18.8849	18.8779	19.1982	19.4367	18.4257	18.8965	19.5697	19.7389	19.5951	20.1206	20.2910
Toluene	15.8293	15.4735	15.3556	15.2289	15.0948	14.8319	15.0783	15.4866	15.8795	16.0195	16.0294	15.8464	15.2289	15.3243
Ethylbenzene	10.4667	13.0338	13.2809	13.2858	14.0804	13.5824	13.5364	13.2961	13.2645	13.2673	12.9406	13.4768	13.7925	13.2635
m/p-Xylene														
o-Xylene	6.9822	5.5864	5.2940	4.9689	4.7249	4.6312	4.2900	4.2848	4.0954	3.5234	3.5766	3.5059	3.7958	3.5270
Methane	8.7567	8.5779	7.9489	7.4390	7.1805	7.0897	7.0277	7.5757	7.3979	6.9066	6.8399	7.1818	6.9572	7.3281
Ethane	-	-	-	-	-	0.1693	0.1749	0.2332	-	-	-	0.3247	-	-
Propane	16.8007	16.3347	16.0918	15.7785	15.6396	14.9922	14.6981	14.8926	14.5915	14.7365	14.6581	14.3845	14.0763	14.2619
i-Butane	7.9367	8.3949	9.3723	10.0051	10.0482	11.1619	11.3281	11.0386	10.8298	10.7181	10.7792	10.6113	10.7261	10.7104
n-Butane	12.3251	13.5796	13.6700	13.9653	13.8972	13.9105	13.9969	14.3061	14.5626	14.7493	14.9272	14.5613	14.7788	14.7574
Cyclopentane	0.0026	0.0019	0.0018	0.0016	0.0014	0.0014	0.0015	0.0015	0.0014	0.0014	0.0015	0.0014	0.0014	0.0016
i-Pentane	0.1126	0.1140	0.1110	0.1107	0.1119	0.1072	0.1111	0.1187	0.1229	0.1301	0.1374	0.1401	0.1422	0.1474
n-Pentane	0.0485	0.0513	0.0503	0.0599	0.0632	0.0645	0.0654	0.0769	0.0789	0.0871	0.0856	0.0877	0.0872	0.0883
Cyclohexane	0.0025	0.0023	0.0020	0.0020	0.0020	0.00196	0.0021	0.0021	0.0021	0.0022	0.0021	0.0022	0.0023	0.0023
i-Hexane	0.0888	0.1053	0.1090	0.1124	0.1257	0.1315	0.1345	0.1434	0.1501	0.1532	0.1524	0.1510	0.1654	0.1692
n-Hexane														
Cycloheptane	0.0017	0.0018	0.0016	0.0014	0.0015	-	0.0014	0.0014	0.0013	0.0013	0.0013	0.0013	-	0.0013
i-Heptane	0.0108	0.0111	0.0112	0.0111	0.0118	0.0147	0.0153	0.0178	0.0190	0.0222	0.0233	0.0240	0.0235	0.0239
n-Heptane														
Cyclooctane	0.0013	-	-	0.0014	0.0013	0.0015	0.0016	0.0018	0.0019	0.0019	0.0020	0.0021	0.0022	0.0024
i-Octane	0.2006	0.1662	0.1539	0.1431	0.1377	0.1100	0.1000	0.1029	0.1046	0.1101	0.1042	0.1024	0.0995	0.1000

Table 6.20.3. Carbon Mass Balance for EUROPT-3 (3 Pulses of H_2S) (510°C, 110 psig)

Time (hrs)	No. of moles of Carbon In	No. of moles of Carbon Out	Δ Carbon
3	2.4051×10^{-4}	2.2712×10^{-4}	1.3385×10^{-5}
18.1	2.4051×10^{-4}	2.2862×10^{-4}	1.1886×10^{-5}
21.05	2.4051×10^{-4}	2.3024×10^{-4}	1.0263×10^{-5}
24	2.4051×10^{-4}	2.3211×10^{-4}	8.4011×10^{-6}
27	2.4051×10^{-4}	2.3413×10^{-4}	6.3806×10^{-6}
42.1	2.4051×10^{-4}	2.3423×10^{-4}	6.2746×10^{-6}
45	2.4051×10^{-4}	2.3529×10^{-4}	5.2147×10^{-6}
48	2.4051×10^{-4}	2.3604×10^{-4}	4.4648×10^{-6}
51	2.4051×10^{-4}	2.3654×10^{-4}	3.9637×10^{-6}
67.25	2.4051×10^{-4}	2.3900×10^{-4}	1.5097×10^{-6}
70.25	2.4051×10^{-4}	2.3920×10^{-4}	1.3077×10^{-6}
73.25	2.4051×10^{-4}	2.3941×10^{-4}	1.1005×10^{-6}
91.75	2.4051×10^{-4}	2.4044×10^{-4}	6.8677×10^{-8}
94.75	2.4051×10^{-4}	2.4046×10^{-4}	5.0354×10^{-8}

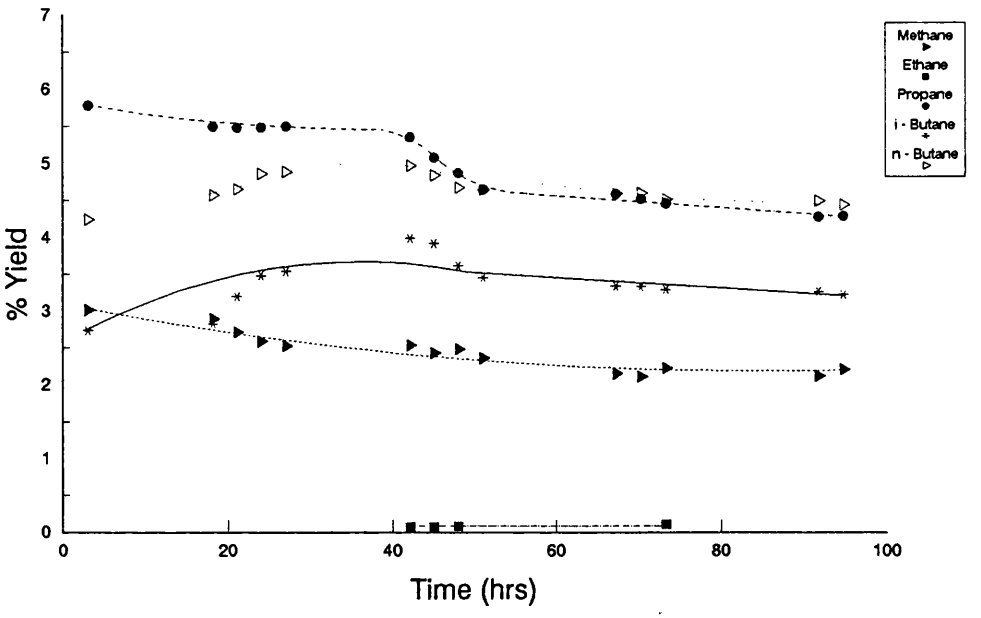

Figure 6.20.1. % Yield of Individual Hydrocarbon Products on a EUROPT-3 catalyst (3 pulses of H_2S)

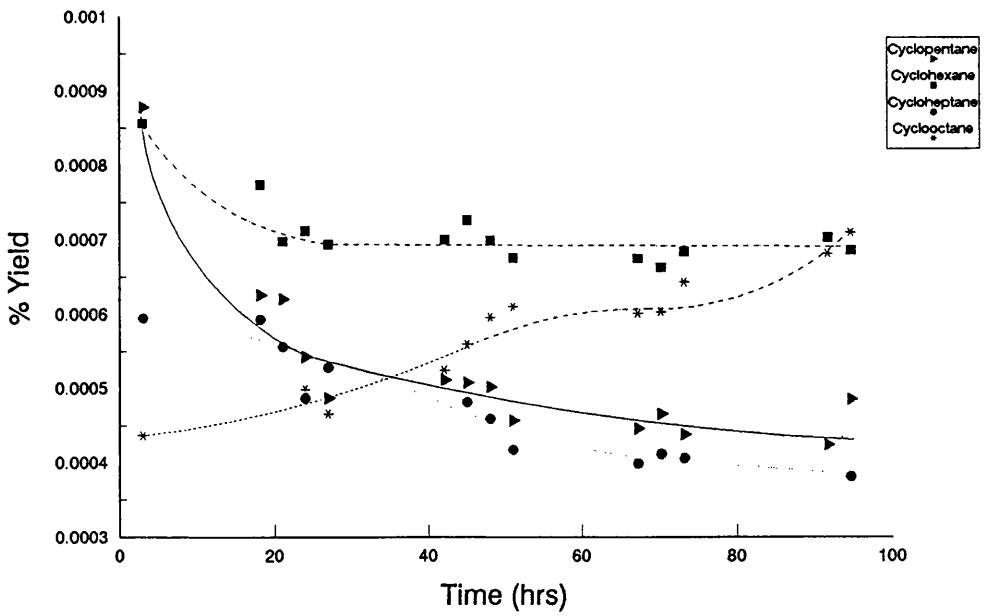

Figure 6.20.2. % Yield of Cycloparaffin Products on a EUROPT-3 catalyst (3 Pulses H_2S)

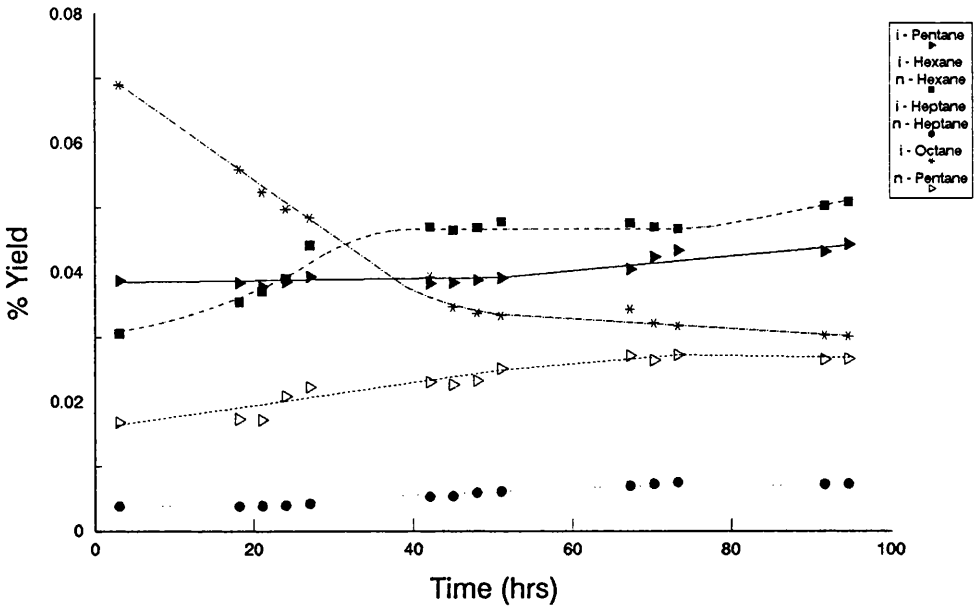

Figure 6.20.3. % Yield of i- and n-Paraffin Products on a EUROPT-3 catalyst (3 pulses of H_2S)

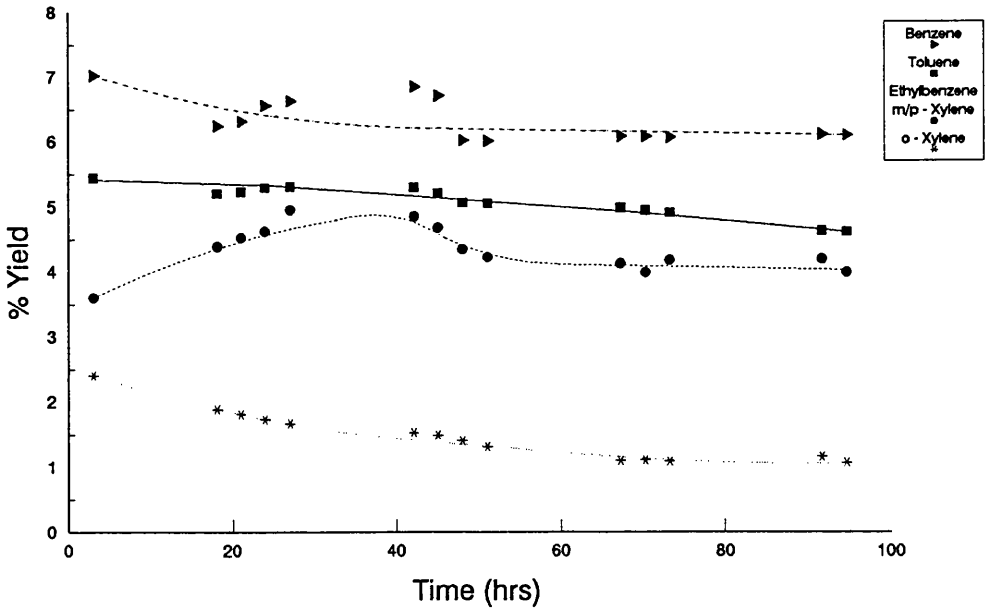

Figure 6.20.4. % Yield of Aromatic Products on a EUROPT-3 catalyst (3 Pulses H_2S)

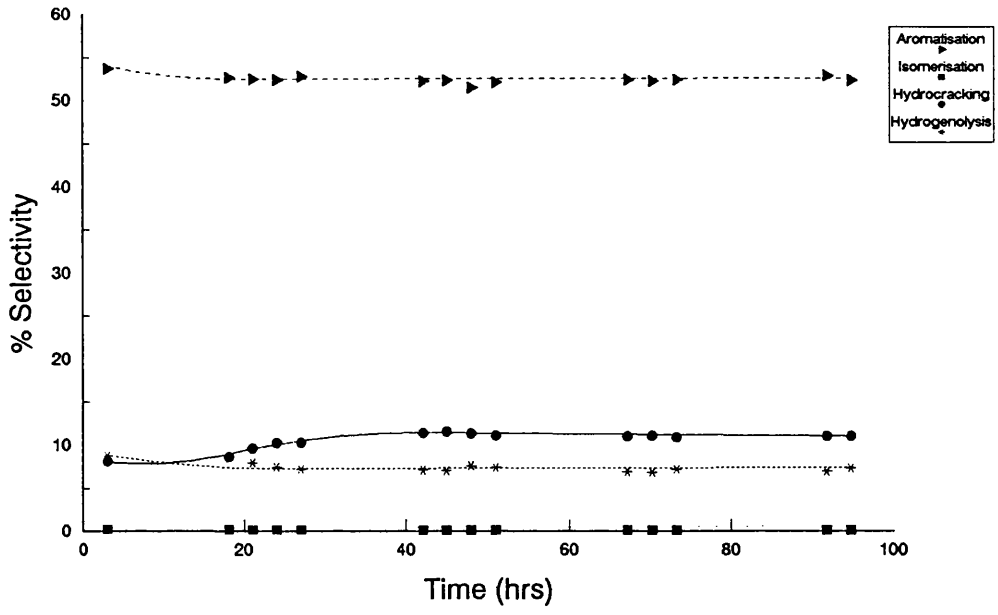

Figure 6.20.5. % Selectivity to the Major Reactions on a EUROPT-3 catalyst (3 pulses of H_2S)

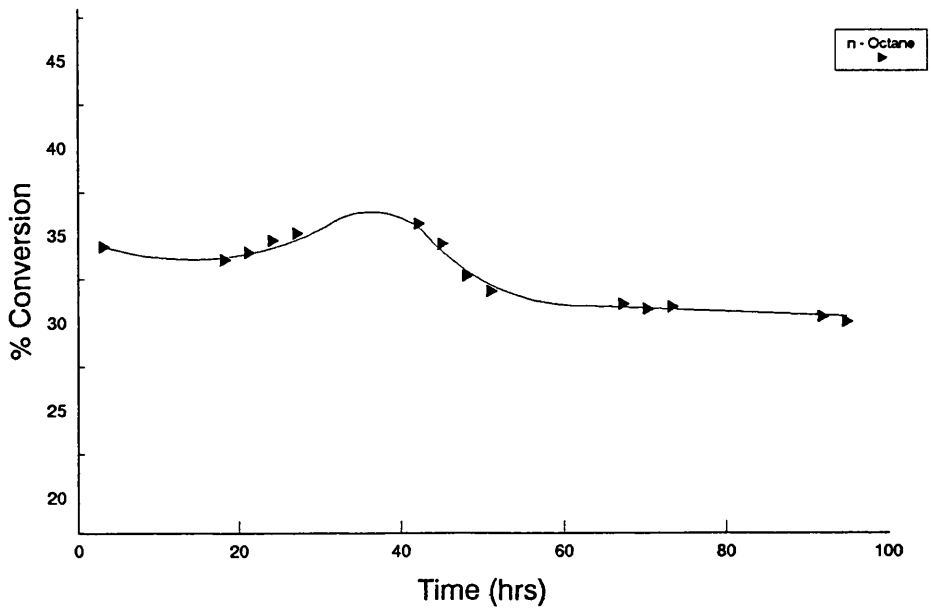

Figure 6.20.6. % Conversion of n-Octane on a EUROPT-3 catalyst (3 Pulses H_2S)

Figure 6.20.2 and 6.20.3 show the variation in the product yields for paraffin products with respect to time. The yield of cyclooctane increases whereas the yield of other cycloparafiin products decrease with time. Both cyclopentane and cyclohexane undergo rapid initial falls in the yields before reaching a constant level. The combined values of i- and n-hexane and i- and n-heptane are used as they are inseparable during analysis. The yield of i-octane decreases as shown in Figure 6.20.3 while the combined yields and those of i- and n-pentane increase with time. Once again the cycloparaffin yield was many times smaller than that of i- or n-paraffins.

Figure 6.20.4 details the increasing yield of aromatic species with decreasing carbon number and with time. As noted in the previous Section, the yield of benzene is the highest followed by toluene, ethylbenzene/m/p-xylene and finally o-xylene. In comparison with the partially sulphided catalyst in Section 6.19, the benzene and toluene yields have fallen while the yields of xylenes and ethylbenzene have increased significantly. The yield of C_8 aromatics is still significantly lower than those observed on an unsulphided EUROPT-3.1 catalyst.

The selectivities of individual hydrocarbon species are shown in Table 6.20.2. The selectivity to the major reactions is detailed in Figure 6.20.5. Aromatisation activity is dominant with a constant selectivity at 52%, while the hydrogenolysis activity falls to ~7% after 95 hours on stream. The selectivities of the major reactions decrease in the order:

Aromatisation > Hydrocracking > Hydrogenolysis > Isomerisation

The activity of aromatisation, isomerisation and hydrogenolysis reactions decrease while the hydrocracking activity increases with reaction time.

The propane to methane ratio increases slowly to a maximum at ~26 hours and then decreases gradually. The carbon mass balance illustrates that the carbon deposition on the catalyst decreases with time. Therefore coke is initially deposited upon the metallic sites before being deposited upon the support after ~26 hours.

The total conversion of n-octane increases to ~36% before falling to a constant level of 30%. This is greater than with an unsulphided EUROPT-3.1 catalyst but less than the catalyst in the previous Section. The % coke is 5.34% by weight which is higher than on the previous two sulphided catalysts but much less than with the unsulphided catalyst.

6.21. EUROPT-3-S (2 pulses of H_2S, 510°C, 110 psig)

The partially sulphided monometallic catalyst was tested under conditions described in Section 6.1. This catalyst had been sulphided with 2 pulses of H_2S at 400°C before being reduced in hydrogen. Results from this reforming run are reported in Figures 6.21.1 to 6.21.6 and in Tables 6.21.1 to 6.21.3.

The decreasing product yields of all C_1 - C_4 species are detailed in Figure 6.21.1. The yield of ethane is undetectable until after 44 hours on stream. The yields of methane and propane are lower than in an unsulphided catalyst and reach steady

Table 6.21.1. % Yield of individual products and % Conversion versus time on stream for EUROPT-3 (2 pulses of H_2S)

Products	% Yield of Selected Products													
Time (hrs)	1.5	4.25	19.25	22.25	25.25	28.25	44	47	50.25	68	71	74	92	95
Benzene	5.0084	5.1200	5.4522	5.1722	5.0500	4.8757	3.6802	3.4608	3.3959	3.2445	3.1284	3.1041	2.9904	2.8975
Toluene	3.8438	3.8070	3.6725	3.5207	3.3155	3.1719	2.7578	2.5741	2.3786	2.2802	2.2750	2.2579	2.0736	2.0104
Ethylbenzene	0.8850	1.0663	1.1976	1.2606	1.2587	1.3020	1.3324	1.3172	1.3267	1.5140	1.5089	1.5316	1.6538	1.6623
m/p-Xylene														
o-Xylene	0.7145	1.0667	1.1170	1.3337	1.3659	1.3894	1.5055	1.5084	1.5092	1.5087	1.5077	1.5090	1.5206	1.5205
Methane	2.7361	2.4933	2.4178	2.4018	2.3011	2.3894	2.1116	1.9184	1.7391	1.6720	1.6155	1.3809	1.4411	1.4562
Ethane	0.0470	0.0610	-	-	-	0.0645	0.0749	-	-	-	-	-	-	-
Propane	2.5864	2.4916	2.2684	2.2079	2.1705	2.1397	2.0888	2.0588	2.0190	1.8860	1.9118	1.8901	1.9192	1.8627
i-Butane	1.9920	1.9611	1.9021	1.8217	1.8122	1.8065	1.6949	1.6436	1.5822	1.5155	1.4224	1.4576	1.3490	1.3283
n-Butane	3.5614	3.3762	3.2785	3.1642	3.0650	2.9726	2.9856	2.8407	2.8795	2.7968	2.6847	2.6571	2.3914	2.3504
Cyclopentane	0.0007	0.0006	0.0005	0.0005	0.0005	0.0005	0.0004	0.0004	0.0004	0.0003	0.0003	0.0003	0.0003	0.0003
i-Pentane	0.0239	0.0253	0.0229	0.0219	0.0213	0.0206	0.0203	0.0199	0.0198	0.0195	0.0188	0.0183	0.0174	0.0170
n-Pentane	0.0196	0.0195	0.0179	0.0176	0.0171	0.0168	0.0158	0.0153	0.0150	0.0140	0.0137	0.0133	0.0132	0.0131
Cyclohexane	0.0007	0.0006	0.0006	0.0005	0.0005	0.0005	0.0006	0.0006	0.0006	0.0006	0.0006	0.0006	0.0005	0.0005
i-Hexane	0.0411	0.0405	0.0390	0.0386	0.0379	0.0369	0.0350	0.0348	0.0334	0.0327	0.0320	0.0312	0.0301	0.0293
n-Hexane														
Cycloheptane	0.0009	0.0008	0.0007	0.0007	0.0007	0.0006	0.0006	0.0006	0.0006	0.0006	0.0005	0.0005	0.0004	0.0004
i-Heptane	0.0220	0.0214	0.0193	0.0187	0.0178	0.0172	0.0170	0.0165	0.0161	0.0153	0.0150	0.3014	0.0144	0.0143
n-Heptane														
Cyclooctane	0.0008	0.0008	0.0007	0.0007	0.0006	0.0006	0.0006	0.0006	0.0005	0.0005	0.0005	0.0005	0.0005	0.0005
i-Octane	0.0311	0.0301	0.0278	0.0261	0.0251	0.0242	0.0209	0.0203	0.0188	0.0171	0.0167	0.0170	0.0173	0.0170
% Conversion of n-Octane	21.5155	21.5829	21.4356	21.0081	20.4602	20.2298	18.3430	17.4312	16.9356	16.5183	16.1524	15.8847	15.4330	15.1807

Table 6.21.2. % Selectivity of individual products versus time on stream for EUROPT-3 (2 pulses of H_2S)

Products	% Selectivity of Selected Products													
Time (hrs)	1.5	4.25	19.25	22.25	25.25	28.25	44	47	50.25	68	71	74	92	95
Benzene	23.2781	23.7227	25.4355	24.6200	24.6818	24.1018	20.0630	19.8543	20.0522	19.6417	19.3683	19.5416	19.3764	19.0870
Toluene	17.8651	17.6389	17.1326	16.7589	16.2048	15.6792	15.0349	14.7671	14.0453	13.8043	14.0845	14.2141	13.4359	13.2429
Ethylbenzene	4.1134	4.9406	5.5868	6.0007	6.1518	6.4362	7.2637	7.5567	7.8340	9.1656	9.3416	9.6420	10.7158	10.9502
m/p-Xylene														
o-Xylene	3.3209	4.94213	5.2110	6.3484	6.6759	3.8680	8.2075	8.6537	8.9115	9.1338	9.3341	9.4994	9.8529	10.0161
Methane	12.7170	11.5523	11.2792	11.4326	11.2467	11.8115	11.5115	11.0058	10.2689	10.1220	10.0019	8.6934	9.3375	9.5925
Ethane	0.2187	0.2826	-	-	-	0.3188	0.4086	-	-	-	-	-	-	-
Propane	12.0209	11.5442	10.5824	10.5097	10.6085	10.5771	11.3873	11.8110	11.9217	11.4177	11.8358	11.8986	12.4360	12.2700
i-Butane	9.2585	9.0863	8.8737	8.6712	8.8574	8.9301	9.2399	9.4292	9.3427	9.1744	8.8060	9.1758	8.7408	8.7498
n-Butane	16.5527	15.6428	15.2948	15.0618	14.9801	14.6942	16.2767	16.2967	17.0026	16.9312	16.6208	16.7274	15.4952	15.4830
Cyclopentane	0.0032	0.0028	0.0023	0.0024	0.0023	0.0023	0.0022	0.0023	0.0021	0.0020	0.0019	0.0018	0.0018	0.0017
i-Pentane	0.1112	0.1173	0.1071	0.1045	0.1041	0.1021	0.1109	0.1142	0.1170	0.1180	0.1165	0.1157	0.1125	0.1121
n-Pentane	0.0911	0.0906	0.0835	0.0838	0.0837	0.0829	0.0861	0.0880	0.0888	0.0350	0.0850	0.0838	0.0853	0.0862
Cyclohexane	0.0032	0.0030	0.0028	0.0026	0.0024	0.0023	0.0034	0.0035	0.0035	0.0037	0.0036	0.0035	0.0034	0.0032
i-Hexane	0.1912	0.1879	0.1819	0.1838	0.1851	0.1826	0.1910	0.1998	0.1973	0.1980	0.1984	0.1966	0.1951	0.1931
n-Hexane														
Cycloheptane	0.0041	0.0037	0.0033	0.0033	0.0032	0.0032	0.0033	0.0034	0.0033	0.0031	0.0029	0.0029	0.0028	0.0029
i-Heptane,	0.1021	0.0989	0.0902	0.0889	0.0868	0.0850	0.0928	0.0948	0.0952	0.0929	0.0927	0.0930	0.0933	0.0943
n-Heptane														
Cyclooctane	0.0039	0.0038	0.0034	0.0033	0.0030	0.0032	0.0033	0.0032	0.0031	0.0029	0.0030	0.0030	0.0031	0.0030
i-Octane	0.1447	0.1396	0.1296	0.1241	0.1225	0.1195	0.1138	0.1162	0.1108	0.1037	0.1031	0.1071	0.1121	0.1120

Table 6.21.3. Carbon Mass Balance for EUROPT-3 (2 Pulses of H_2S) (510°C, 110 psig)

Time (hrs)	No. of moles of Carbon In	No. of moles of Carbon Out	Δ Carbon
1.5	2.5265×10^{-4}	2.3104×10^{-4}	2.1610×10^{-5}
4.25	2.5265×10^{-4}	2.3267×10^{-4}	1.9981×10^{-5}
19.25	2.5265×10^{-4}	2.3684×10^{-4}	1.5807×10^{-5}
22.25	2.5265×10^{-4}	2.3760×10^{-4}	1.5047×10^{-5}
25.25	2.5265×10^{-4}	2.4012×10^{-4}	1.2533×10^{-5}
28.25	2.5265×10^{-4}	2.4111×10^{-4}	1.1536×10^{-5}
44	2.5265×10^{-4}	2.4234×10^{-4}	1.0307×10^{-5}
47	2.5265×10^{-4}	2.4513×10^{-4}	7.5196×10^{-6}
50.25	2.5265×10^{-4}	2.4602×10^{-4}	6.6273×10^{-6}
68	2.5265×10^{-4}	2.4811×10^{-4}	4.5371×10^{-6}
71	2.5265×10^{-4}	2.4914×10^{-4}	3.5121×10^{-6}
74	2.5265×10^{-4}	2.5016×10^{-4}	2.4843×10^{-6}
92	2.5265×10^{-4}	2.5112×10^{-4}	1.5293×10^{-6}
95	2.5265×10^{-4}	2.5142×10^{-4}	1.2254×10^{-6}

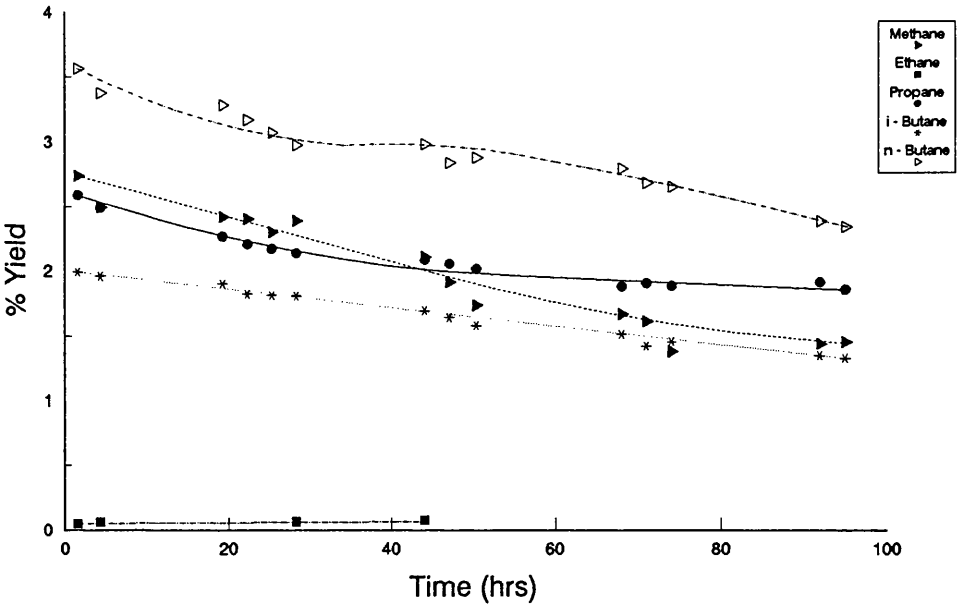

Figure 6.21.1. % Yield of Individual Hydrocarbon Products on a EUROPT-3 catalyst (2 pulses of H_2S)

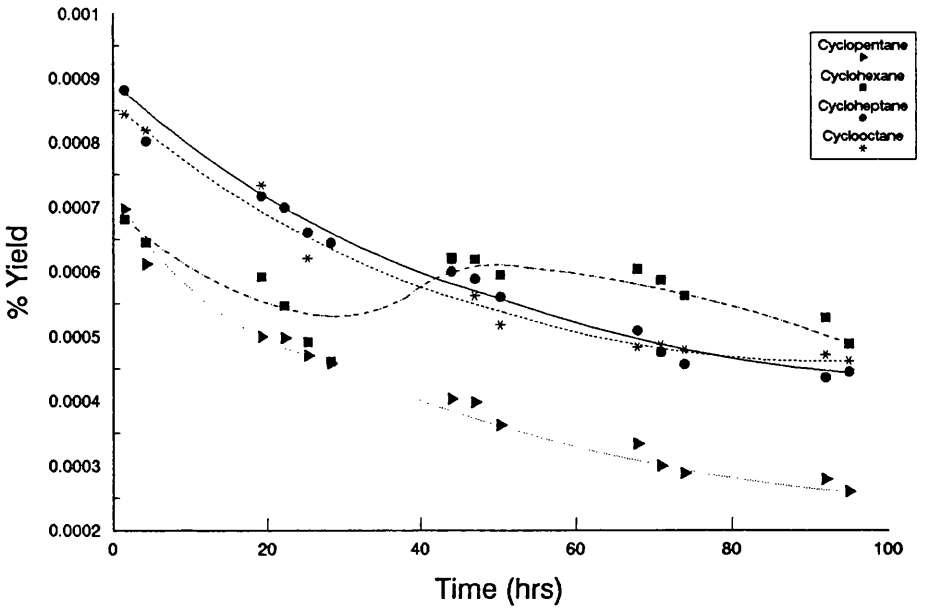

Figure 6.21.2. % Yield of Cycloparaffin Products on a EUROPT-3 catalyst (2 Pulses H_2S)

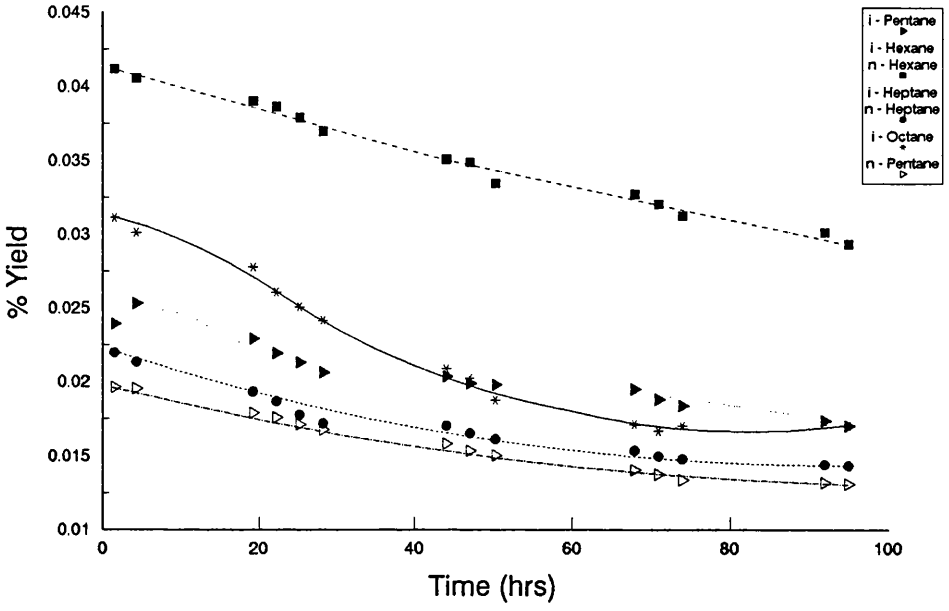

Figure 6.21.3. % Yield of i- and n-Paraffin Products on a EUROPT-3 catalyst (2 pulses of H_2S)

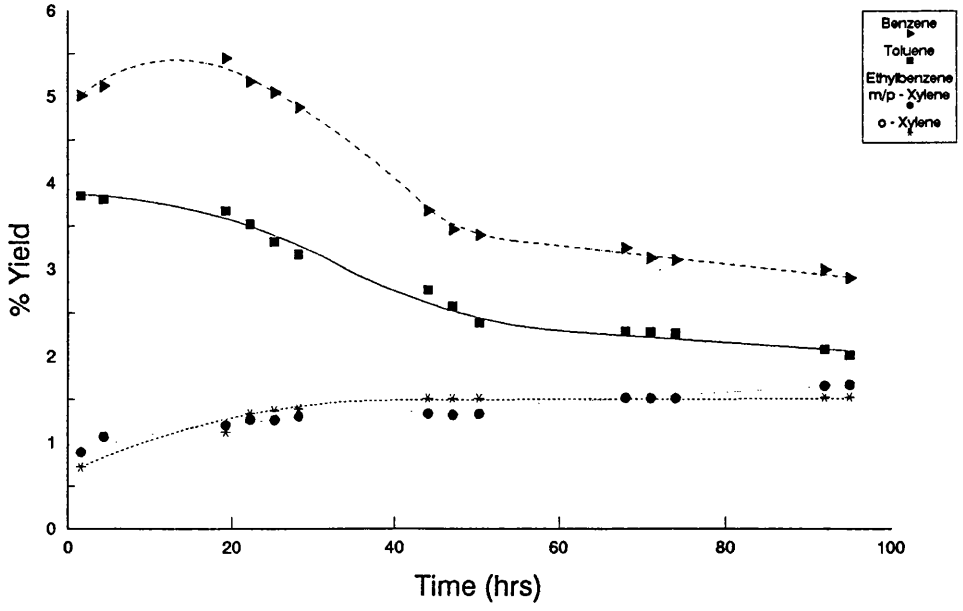

Figure 6.21.4. % Yield of Aromatic Products on a EUROPT-3 catalyst (2 Pulses H_2S)

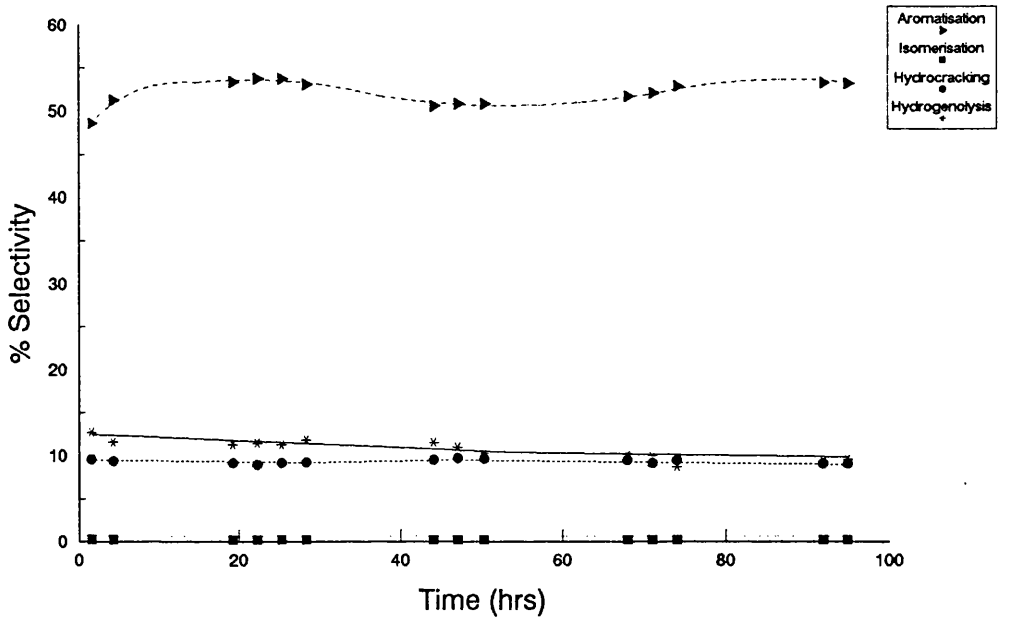

Figure 6.21.5. % Selectivity to the Major Reactions on a EUROPT-3 catalyst (2 pulses of H_2S)

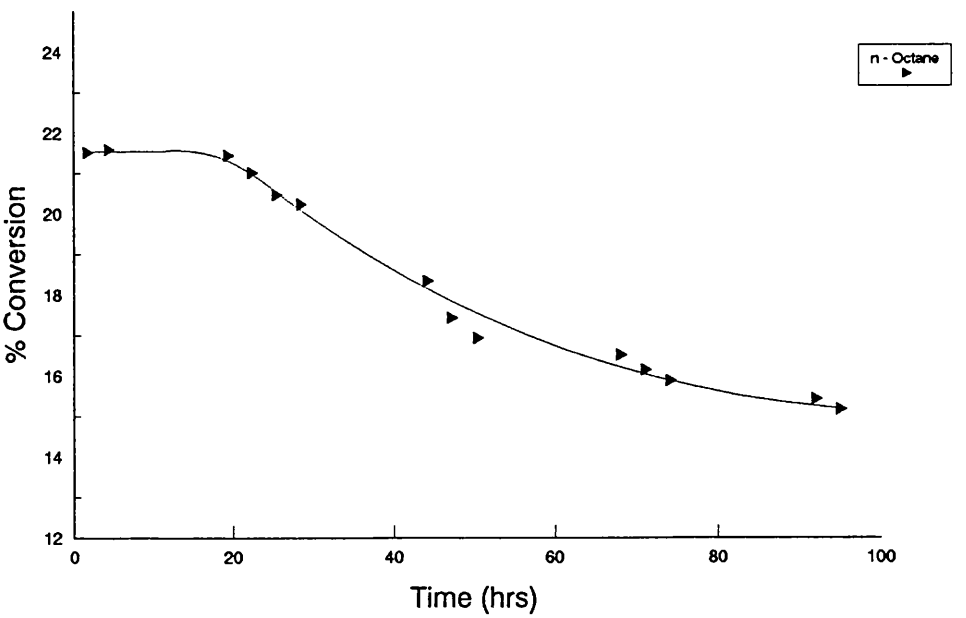

Figure 6.21.6. % Conversion of n-Octane on a EUROPT-3 catalyst (2 Pulses H_2S)

levels of ~1.5 and 1.9% respectively. The yield of n-butane is ~1.5 times that of i-butane throughout the run.

The yields of paraffinic species are illustrated in Figures 6.21.2 and 6.21.3. Figure 6.21.2 shows the yield of cycloparaffins decreasing with reaction time. The yields of cyclopentane, cycloheptane and cyclooctane decrease steadily whereas that of cyclohexane initially decreases before going through a maximum after ~50 hours and then decreasing slowly. Yet again combined values of i- and n-paraffins are quoted in Figure 6.21.3. The combined product yields of all i- and n-paraffins decrease with increasing carbon number and with time.

Figure 6.21.4 shows the variation in the yields of aromatic products with time. The yield of both benzene and toluene decrease before reaching constant values of ~2.9 and 2% respectively. The yield of the C_8 aromatics in comparison to benzene and toluene increase with time. The yield of benzene and toluene are lower than on the previous sulphided catalysts but the yield of C_8 aromatics has increased.

Table 6.21.2 illustrate the selectivity to the individual hydrocarbon species with time. The selectivity to the major reactions is shown in Figure 6.21.5. Aromatisation activity is the highest with a constant selectivity of ~53%. The selectivity decreases in the order from:

Aromatisation > Hydrogenolysis > Hydrocracking > Isomerisation

Only the selectivity to aromatisation increases, the other activities decrease with time. Hydrogenolysis activity reaches a steady value of ~9.5%, higher than in the

previous two sulphided catalysts (Sections 6.19 and 6.20).

The propane to methane ratio decreases for the first 40 hours before rising to a constant level after ~75 hours. This suggests that coke was initially deposited upon the acidic sites and then after 40 hours it was deposited on the metallic sites. After 75 hours the coke once again deactivated the acidic sites quicker than the metallic sites. The carbon mass balance obtained from this run again showed that carbon deposition on the catalyst surface decreased with reaction time.

The total conversion of n-octane with respect to the reaction time is detailed in Figure 6.21.6. The conversion is stable at ~21.5% for the first 20 hours before decreasing steadily to ~15% after ~95 hours. In comparison the conversion at the end of the run is ~ half that of the previous partially sulphided catalyst.

6.22. EUROPT-4-S (4 pulses of H_2S, 510°C, 110 psig)

This partially sulphided catalyst was tested under conditions described in Section 6.1. This catalyst had been sulphided with 4 pulses of H_2S at 400°C before being further reduced in hydrogen. The results of this experiment are reported in Figures 6.22.1 to 6.22.6 and in Tables 6.22.1 to 6.22.3.

The product yields of C_1 - C_4 species are shown in Figure 6.22.1 to increase with time. The yield of methane is very small, ~0.5% after 75 hours when compared with that of an unsulphided EUROPT-4.1 catalyst (~3.8%). The yield of propane is

Table 6.22.1. % Yield of individual products and % Conversion versus time on stream for EUROPT-4 (4 pulses of H_2S)

Products	% Yield of Selected Products													
Time (hrs)	1.5	4.5	7.5	20.75	23.75	26.75	29.75	45.33	48	51.25	57.4	68.35	71.25	74.25
Benzene	6.7288	6.5200	6.9654	7.3605	7.5105	7.7390	8.0023	10.4720	9.7075	8.6816	8.5775	8.7193	9.1408	9.6612
Toluene	3.6417	5.3455	6.6508	8.0708	8.2296	8.4722	8.4168	9.4963	10.7637	10.1628	9.4789	9.2036	8.8566	8.9648
Ethylbenzene	1.7173	1.6589	2.1284	3.7932	4.9519	5.7446	6.5270	7.1996	6.8555	6.7700	7.0510	7.0182	7.1235	7.1565
m/p-Xylene														
o-Xylene	0.5310	0.9521	1.2668	1.9034	2.0984	2.5662	2.4253	3.2135	3.4250	3.4518	3.8660	3.7895	3.8705	3.7888
Methane	0.0948	0.1095	0.1616	0.2002	0.2291	0.2351	0.2494	0.2966	0.3226	0.3634	0.4108	0.4256	0.3855	0.4624
Ethane	-	0.0289	-	0.0321	0.0347	0.0368	-	0.0390	0.0472	0.0545	0.0604	0.0568	0.0606	0.0599
Propane	1.6903	2.2517	2.5712	2.6898	2.8011	2.8161	2.9217	3.0390	3.0246	3.1697	3.3619	3.3929	3.2786	3.3377
i-Butane	1.1769	1.5267	1.6447	1.7088	1.8415	1.8620	1.8232	1.8768	1.7847	1.7381	1.6988	1.6577	1.8249	1.7917
n-Butane	1.6067	2.1228	2.1139	2.4655	2.5989	2.7118	2.7519	2.7275	2.6092	2.5456	2.6992	2.5446	2.6360	2.6653
Cyclopentane	0.0001	0.0002	0.0002	0.0003	0.0003	0.0003	0.0003	0.0004	0.0003	0.0004	0.0004	0.0004	0.0004	0.0004
i-Pentane	0.0280	0.0299	0.0303	0.0319	0.0327	0.0342	0.0351	0.0358	0.0344	0.0346	0.0359	0.0362	0.0373	0.0382
n-Pentane														
Cyclohexane	0.0003	0.0003	0.0003	0.0004	0.0004	0.0005	0.0006	0.0004	0.0004	0.0004	0.0004	0.0005	0.0005	0.0005
i-Hexane	0.0220	0.0257	0.0267	0.0301	0.0308	0.0334	0.0354	0.0393	0.0404	0.0397	0.0384	0.0378	0.0403	0.0429
n-Hexane														
Cycloheptane	0.0003	0.0003	0.0004	0.0005	0.0005	0.0005	0.0006	0.0005	0.0006	0.0006	0.0005	0.0006	0.0006	0.0006
i-Heptane	0.0220	0.0241	0.0255	0.0289	0.0282	0.0317	0.0330	0.0352	0.0387	0.0458	0.0476	0.0457	0.0460	0.0458
n-Heptane														
Cyclooctane	0.0388	0.0389	0.0362	0.0452	0.0469	0.0477	0.0489	0.0492	0.0569	0.0605	0.0632	0.0611	0.0623	0.0603
i-Octane														
% Conversion of n-Octane	17.2989	22.8871	23.6223	28.3616	30.4354	32.3271	33.2716	38.5212	38.7116	37.1193	37.3910	36.9905	37.3646	38.0772

Table 6.22.2. % Selectivity of individual products versus time on stream for EUROPT-4 (4 pulses of H_2S)

Products	% Selectivity of Selected Products													
Time (hrs)	1.5	4.5	7.5	20.75	23.75	26.75	29.75	45.33	48	51.25	57.4	68.35	71.25	74.25
Benzene	38.8974	28.4875	29.4865	25.9523	24.6768	23.9242	24.0516	27.1851	25.0764	23.3884	22.9401	23.5718	24.4639	25.3728
Toluene	21.0519	23.3559	28.1546	28.4568	27.0395	26.2077	25.2973	24.6521	27.8049	27.3788	25.3506	24.8811	23.7032	23.5437
Ethylbenzene	9.9274	7.2481	9.0103	13.3744	16.2703	16.8466	19.6174	18.6900	17.7092	18.2385	18.8574	18.9730	19.0649	18.7947
m/p-Xylene														
o-Xylene	3.0697	4.1598	5.3628	6.7113	6.8947	7.9383	7.2895	8.3421	8.8476	9.2993	10.3393	10.2446	10.3588	9.9503
Methane	0.5480	0.4783	0.6843	0.7059	0.7528	0.7273	0.7497	0.7699	0.8333	0.9789	1.0987	1.1507	1.0317	1.2144
Ethane	-	0.1263	-	0.1133	0.1139	0.1137	-	0.1012	0.1219	0.1468	0.1616	0.1536	0.1622	0.1574
Propane	9.7710	9.8383	10.8845	9.4841	9.2033	8.7112	8.7815	7.8893	7.8130	8.5393	8.9913	9.1723	8.7747	8.7655
i-Butane	6.8031	6.6708	6.9623	6.0250	6.0505	5.7598	5.4798	4.8722	4.6103	4.6824	4.5433	4.4813	4.8840	4.7055
n-Butane	9.2876	9.2752	8.9489	8.6931	8.5389	8.3886	8.2710	7.0806	6.7400	6.8579	7.2189	6.8790	7.0549	6.9998
Cyclopentane	0.0006	0.0008	0.0009	0.0009	0.0009	0.0008	0.0008	0.0009	0.0008	0.0010	0.0010	0.0010	0.0010	0.0011
i-Pentane	0.1620	0.1305	0.1282	0.1125	0.1075	0.1058	0.1054	0.0928	0.0890	0.0933	0.0929	0.0978	0.0998	0.1002
n-Pentane														
Cyclohexane	0.0015	0.0012	0.0012	0.0014	0.0014	0.0016	0.0017	0.0010	0.0011	0.0010	0.0011	0.0012	0.0013	0.0014
i-Hexane	0.1269	0.0129	0.1129	0.1062	0.1011	0.1033	0.1065	0.1020	0.1042	0.1068	0.1028	0.1023	0.1080	0.1127
n-Hexane														
Cycloheptane	0.0018	0.0020	0.0016	0.0016	0.0016	0.0017	0.0017	0.0014	0.0014	0.0015	0.0014	0.0015	0.0016	0.0016
i-Heptane	0.1273	0.1052	0.1078	0.1017	0.0926	0.0979	0.0991	0.0915	0.0998	0.1233	0.1273	0.1236	0.1232	0.1204
n-Heptane														
Cyclooctane	0.2244	0.1700	0.1533	0.1595	0.1542	0.1476	0.1470	0.1277	0.1470	0.1631	0.1691	0.1651	0.1668	0.1585
i-Octane														

Table 6.22.3. Carbon Mass Balance for EUROPT-4 (4 Pulses of H_2S) (510°C, 110 psig)

Time (hrs)	No. of moles of Carbon In	No. of moles of Carbon Out	Δ Carbon
1.5	4.4559×10^{-4}	4.1517×10^{-4}	3.0418×10^{-5}
4.5	4.4559×10^{-4}	4.1639×10^{-4}	2.9198×10^{-5}
7.5	4.4559×10^{-4}	4.1704×10^{-4}	2.8548×10^{-5}
20.75	4.4559×10^{-4}	4.2389×10^{-4}	2.1698×10^{-5}
23.75	4.4559×10^{-4}	4.2418×10^{-4}	2.1408×10^{-5}
26.75	4.4559×10^{-4}	4.2501×10^{-4}	2.0578×10^{-5}
29.75	4.4559×10^{-4}	4.2531×10^{-4}	2.0278×10^{-5}
45.33	4.4559×10^{-4}	4.2708×10^{-4}	1.8508×10^{-5}
48	4.4559×10^{-4}	4.2784×10^{-4}	1.7748×10^{-5}
51.25	4.4559×10^{-4}	4.2899×10^{-4}	1.6598×10^{-5}
57.4	4.4559×10^{-4}	4.3004×10^{-4}	1.5548×10^{-5}
68.35	4.4559×10^{-4}	4.3268×10^{-4}	1.2908×10^{-5}
71.25	4.4559×10^{-4}	4.3306×10^{-4}	1.2528×10^{-5}
74.25	4.4559×10^{-4}	4.3325×10^{-4}	1.2338×10^{-5}

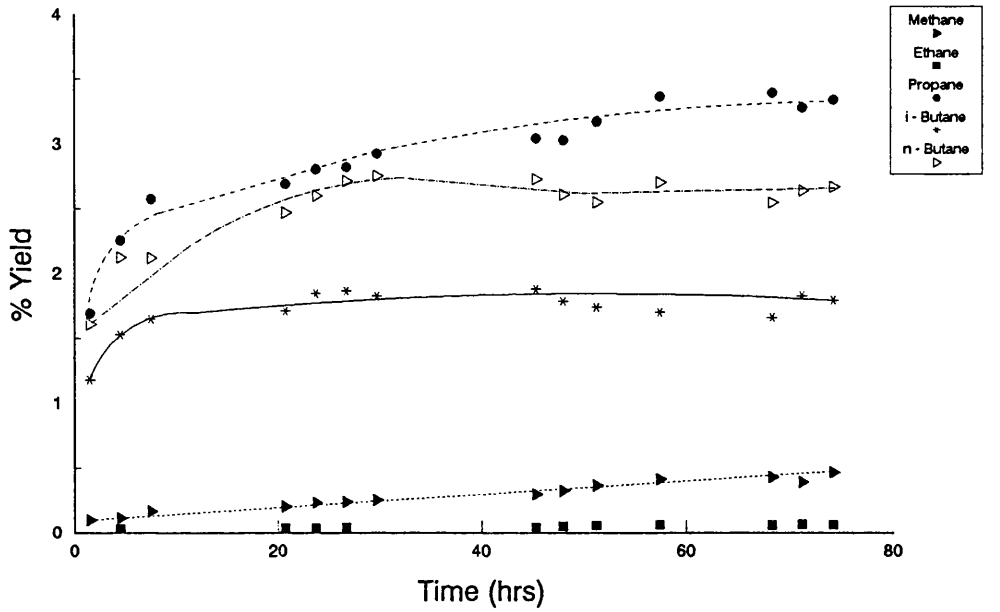

Figure 6.22.1. % Yield of Individual Hydrocarbon Products on a EUROPT-4 catalyst (4 pulses of H_2S)

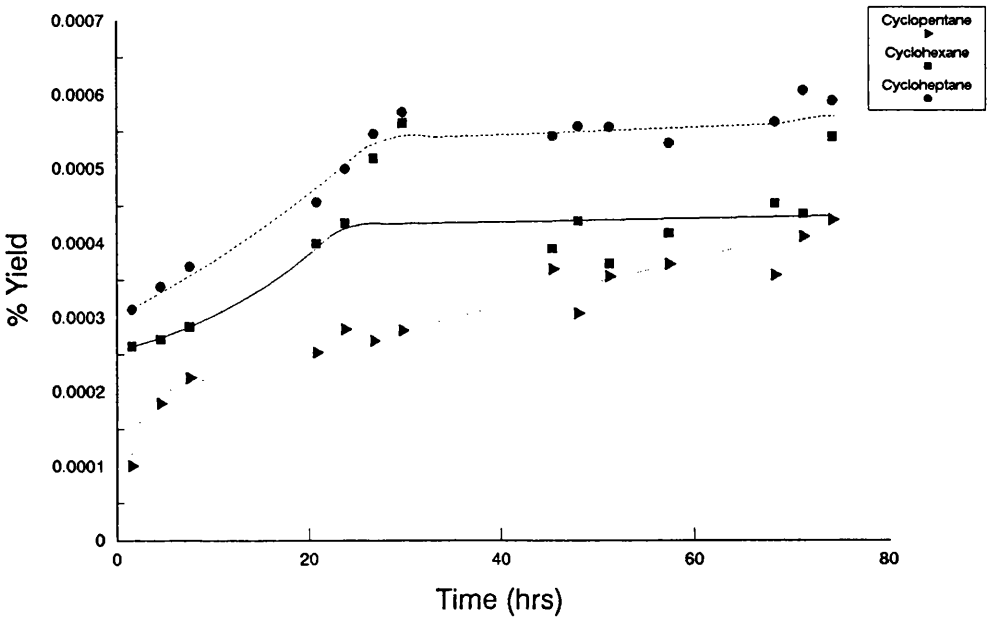

Figure 6.22.2. % Yield of Cycloparaffin Products on a EUROPT-4 catalyst (4 Pulses H_2S)

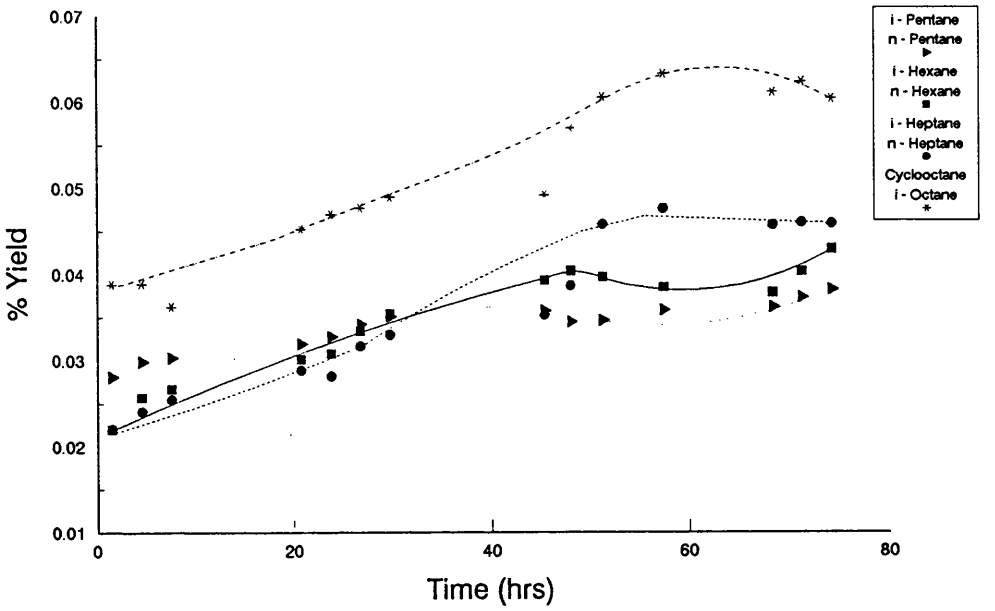

Figure 6.22.3. % Yield of i- and n-Paraffin Products on a EUROPT-4 catalyst (4 pulses of H_2S)

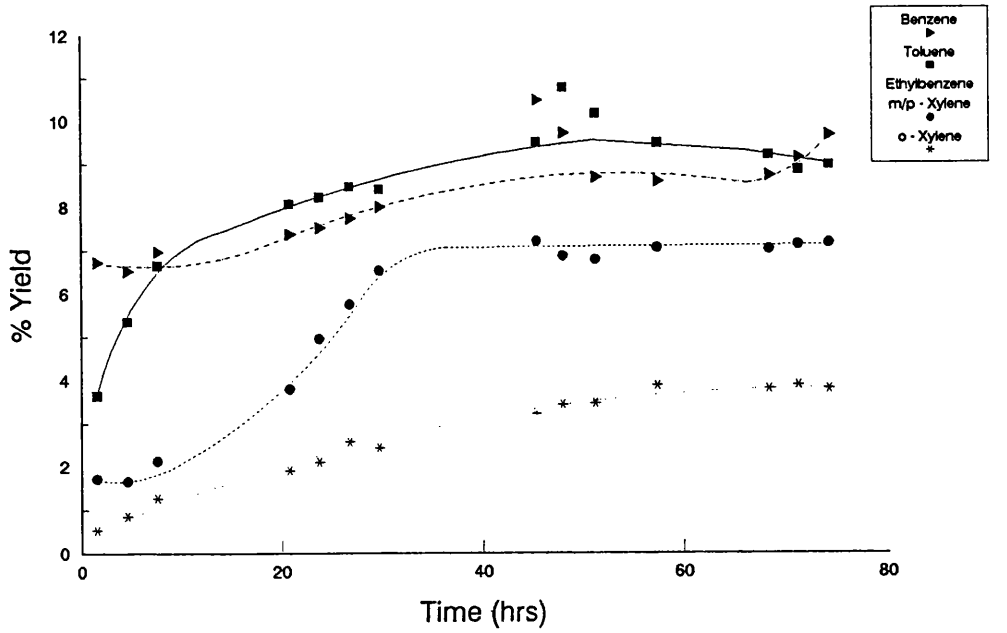

Figure 6.22.4. % Yield of Aromatic Products on a EUROPT-4 catalyst (4 Pulses H_2S)

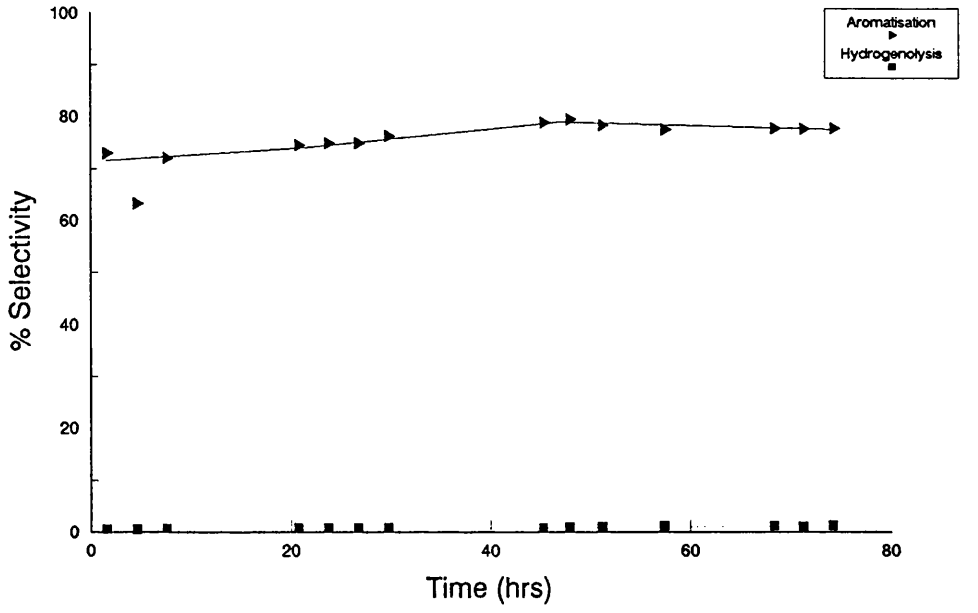

Figure 6.22.5. % Selectivity of the Major Reactions on a EUROPT-4 catalyst (4 pulses of H_2S)

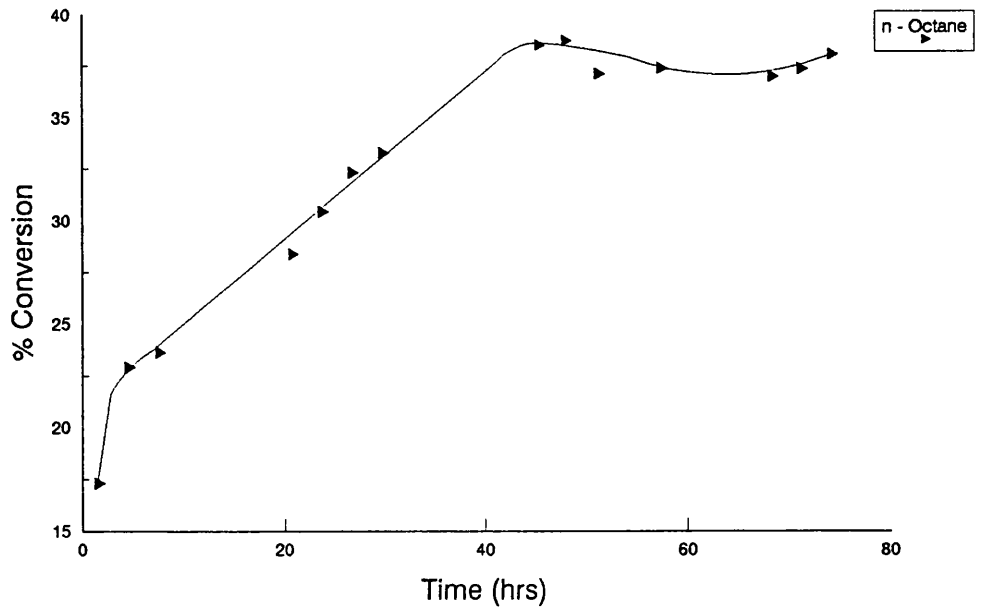

Figure 6.22.6. % Conversion of n-Octane on a EUROPT-4 catalyst (4 Pulses H_2S)

constant at ~3.3%, many times higher than either methane or ethane. The yields of i- and n-butane are similar at the start of the reaction but n-butane reaches a constant yield of 2.8%, 1.5 times that of i-butane after 76 hours on stream.

The yield of paraffinic species is shown in Figures 6.22.2 and 6.22.3. The yield of cycloparaffins increases with time before reaching a constant level and with increasing carbon number. The combined yields of i- and n-pentane, hexane and heptane along with the yield of cyclo- and i-octane are presented in Figure 6.22.3. Initially the i- and n-paraffin yield decreases with increasing carbon number, but after ~33 hours on stream this order changed and the yield now increased with increasing carbon number.

The yield of aromatic species increases with time as illustrated in Figure 6.22.4. The yield of aromatic products increases in the order from o-xylene, ethylbenzene/m/p-xylene, toluene to benzene. The yield of both toluene and benzene are higher and that of o-xylene and ethylbenzene/m/p-xylene is lower than that with an unsulphided EUROPT-4.1 catalyst (Section 6.3). In comparison with the EUROPT-3 catalyst, with the same amount of H_2S initially adsorbed, the yield of benzene is lower, o-xylene and toluene higher and the yield of ethylbenzene/m/p-xylene is approximately the same.

The selectivity to the individual hydrocarbon species is shown in Table 6.22.2. Figure 6.22.5 shows the selectivity to the four major reactions with time. Aromatisation is the dominant reaction with a constant selectivity of ~78%.

Hydrogenolysis activity in comparison is very low at ~1.2%. The order of selectivities to the major reactions is as follows:

Aromatisation > Hydrocracking > Hydrogenolysis > Isomerisation

In comparison with an unsulphided bimetallic EUROPT-4.1 catalyst the aromatisation activity has increased while the hydrogenolysis activity decreased significantly.

The propane to methane ratio increases initially to a maximum after 5 hours and then decreases steadily throughout the reaction. The carbon mass balance again shows that carbon deposition decreases with time. These results suggest that after an initial rapid coking of the metallic sites the support is deactivated slowly.

The total conversion of n-octane increases to a constant level of ~38% as shown in Figure 6.22.6. The conversion increases rapidly over the first 10 hours and then steadily before reaching a constant conversion. The conversion of n-octane is approximately the same as with an unsulphided EUROPT-4.1 catalyst but much higher than with the corresponding sulphided EUROPT-3 catalyst (Section 6.19). The % coke deposited on the catalyst was 3.75% by weight, higher than on the corresponding EUROPT-3 catalyst but lower than that on an unsulphided EUROPT-4.1 catalyst.

6.23. EUROPT-4-S (2 pulses of H_2S, 510°C, 110 psig)

This partially sulphided catalyst was tested under conditions described in Section 6.1. This catalyst had been sulphided with 2 pulses of H_2S at 400°C before being reduced again. The results are reported in Figures 6.23.1 to 6.23.6 and in Tables 6.23.1 to 6.23.3.

The product yields of C_1 - C_4 species are shown in Figure 6.23.1 to increase with time. The yield of methane is still very low compared to that with an unsulphided catalyst and has a constant yield of ~3.4%. The yield of propane as with the previous partially sulphided EUROPT-4 catalyst (Section 6.22) is ~3 times that of methane. In comparison with an unsulphided EUROPT-4.1 catalyst the yields of i- and n-butane are much higher and increase with reaction time. The yield of n-butane is ~1.5 times that of i-butane.

Figures 6.23.2 to 6.23.4 show the yield of paraffin products with time. The yield of all cycloparaffins increases with time in the decreasing order from cyclooctane, cyclohexane, cyclopentane to cycloheptane in Figure 6.23.2. As with the cycloparaffin products, the yield of i-paraffins increases with time in the order from i-hexane, i-heptane, i-octane and i-pentane. The yield of both n-hexane and n-heptane increases steadily with the reaction time in Figure 6.23.4. The yield of n-pentane, in contrast, decreases to a constant value with time. One noticeable feature was that the yield of cycloparaffins was much smaller than that of either i- or n-paraffins.

Table 6.23.1. % Yield of individual products and % Conversion versus time on stream for EUROPT-4 (2 pulses of H_2S)

Products	% Yield of Selected Products														
Time (hrs)	1.5	4.5	19.33	22	25	28	43.2	46.25	49.25	52.25	67.15	70.63	73.5	91.45	95.65
Benzene	2.9433	2.9096	2.7743	2.6347	2.5776	2.4598	2.3623	2.2692	2.2364	2.1651	2.1005	1.9857	1.9321	1.8948	1.9125
Toluene	4.2984	4.2348	4.2159	4.1618	4.1140	3.7356	3.5210	3.3438	3.2509	3.2297	2.9268	2.8824	2.4298	2.3630	2.4516
Ethylbenzene	0.5240	0.6318	1.1006	1.3931	1.7764	2.0076	2.1660	2.2693	2.3703	2.5062	3.1473	3.2340	3.4307	3.6286	3.6459
m/p-Xylene															
o-Xylene	0.0320	0.0421	0.8867	1.0589	1.2236	1.3282	1.6516	1.7115	1.9264	2.0529	2.4806	2.6244	2.6847	2.7451	2.8621
Methane	0.6269	0.7526	0.8901	1.5618	1.6028	1.6268	1.7301	2.0661	2.2260	2.5218	2.7315	2.9390	3.1816	3.3573	3.4046
Ethane	-	0.8357	-	1.2790	1.5833	1.6253	1.6246	1.7031	1.7788	1.9842	1.9042	2.0410	2.1696	2.4118	2.9053
Propane	3.0561	3.3759	5.2351	5.6436	5.9613	6.2715	7.8878	8.4293	8.4668	9.2095	9.3623	9.4059	9.7253	10.5967	10.6048
i-Butane	1.6635	2.3899	6.1276	6.2930	5.7893	5.9285	7.6394	7.9682	8.3160	8.6521	9.6290	10.0905	10.8088	10.6031	11.0423
n-Butane	3.2829	4.5175	9.2392	10.2381	11.8845	11.3255	13.6836	14.7824	15.6249	15.1514	15.5737	15.9077	15.6650	15.7663	15.8264
Cyclopentane	-	0.0010	0.0010	0.0010	0.0011	0.0012	0.0012	0.0012	0.0012	0.0013	0.0014	0.0015	0.0014	0.0015	0.0015
i-Pentane	0.0147	0.0155	0.0167	0.0187	0.0229	0.0240	0.0245	0.0260	0.0298	0.0320	0.0343	0.0381	0.0405	0.0444	0.0421
n-Pentane	0.0492	0.0522	0.0511	0.0525	0.0488	0.0513	0.0515	0.0473	0.0449	0.0423	0.0376	0.0367	0.0369	0.0324	0.0327
Cyclohexane	-	-	-	0.0012	-	-	-	-	-	-	-	-	-	0.0018	0.0018
i-Hexane	0.0022	0.0024	0.0027	0.0032	0.0039	0.0041	0.0040	0.0048	0.0051	0.0055	0.0057	0.0061	-	0.0081	0.0083
n-Hexane	0.0124	0.0154	0.0169	0.0177	0.0213	0.0239	0.0274	0.0292	0.0311	0.0332	0.0353	0.0357	0.0388	0.0474	0.0477
Cycloheptane	0.0004	0.0004	0.0004	0.0004	0.0004	0.0005	0.0005	0.0006	0.0006	0.0006	0.0006	0.0006	0.0006	0.0007	0.0007
i-Heptane	0.0056	0.0062	0.0064	0.0068	0.0074	0.0078	0.0088	0.0096	0.0102	0.0108	0.0112	0.0118	0.0120	0.0134	0.0130
n-Heptane	0.0217	0.0307	0.0414	0.0523	0.0536	0.0550	0.0552	0.0556	0.0574	0.0589	0.0559	0.0595	0.0652	0.0724	0.0741
Cyclooctane	0.0014	0.0015	0.0015	0.0016	0.0016	0.0016	0.0166	0.0017	0.0017	0.0017	0.0018	0.0018	0.0018	0.0018	0.0018
i-Octane	0.0174	0.0182	0.0203	0.0217	0.0228	0.0233	0.0248	0.0250	0.0253	0.0259	0.0267	0.0287	0.0309	0.0330	0.0343
% Conversion of n-Octane	16.5703	19.8332	30.6279	34.4410	36.6965	36.5015	42.4651	44.7440	46.4036	47.6843	50.0663	51.3310	52.2566	53.6176	54.9135

Table 6.23.2. % Selectivity of individual products versus time on stream for EUROPT-4 (2 pulses of H_2S)

Products	% Selectivity of Selected Products														
Time (hrs)	1.5	4.5	19.33	22	25	28	43.2	46.25	49.25	52.25	67.15	70.63	73.5	91.45	95.65
Benzene	17.7628	14.6702	9.0580	7.6498	7.0241	6.7388	5.5628	5.0715	4.8194	4.5405	4.1955	3.8683	3.6973	3.5338	3.4828
Toluene	25.9406	21.3518	13.7650	12.0837	11.2110	10.2341	8.2916	7.4732	7.0057	6.7718	5.8458	5.6153	4.6497	4.4072	4.4645
Ethylbenzene	3.2710	3.1858	3.5933	4.0450	4.8407	5.5000	5.1007	5.0717	5.1079	5.2558	6.2862	6.3003	6.5650	6.7676	6.6394
m/p-Xylene															
o-Xylene	0.1928	0.2121	2.8951	3.0746	3.3343	3.6388	3.8894	3.8250	4.1514	4.3051	4.9547	5.1128	5.1394	5.1198	5.2120
Methane	3.7831	3.7947	2.9062	4.5346	4.3676	4.4568	4.0741	4.6176	4.7970	5.2885	5.4557	5.7257	6.0883	6.2616	6.2000
Ethane	-	4.2134	-	3.7137	4.3145	4.4526	3.8257	3.8062	3.8333	4.1610	3.8034	3.9762	4.1519	4.4980	5.2907
Propane	18.4433	17.0215	17.0924	16.3863	16.2449	17.1814	18.5748	18.8390	18.2460	19.3135	18.6998	18.3240	18.6107	19.7523	19.3118
i-Butane	10.0392	12.0502	20.0065	18.2717	15.7760	16.2419	17.9875	17.8085	17.9210	18.1446	19.2324	19.6577	20.6842	19.7754	20.1086
n-Butane	19.8120	22.7775	30.1658	29.7264	32.3859	31.0275	32.2232	33.0378	33.6718	31.7744	31.1061	30.9903	29.9771	29.4051	28.8206
Cyclopentane	-	0.0050	0.0034	0.0028	0.0029	0.0032	0.0027	0.0027	0.0026	0.0026	0.0029	0.0028	0.0028	0.0028	0.0280
i-Pentane	0.0888	0.0779	0.0545	0.0543	0.0623	0.0657	0.0577	0.0581	0.0643	0.0670	0.0686	0.0743	0.0774	0.0828	0.0766
n-Pentane	002971	0.2633	0.1669	0.1524	0.1331	0.1407	0.1213	0.1057	0.0967	0.0887	0.0751	0.0715	0.0706	0.0605	0.0595
Cyclohexane	-	-	-	0.0035	-	-	-	-	-	-	-	-	-	0.0330	0.0326
i-Hexane	0.0135	0.0119	0.0088	0.0092	0.0106	0.0113	0.0094	0.0107	0.0109	0.0116	0.0113	0.0118	-	0.0151	0.0151
n-Hexane	0.0751	0.0778	0.0552	0.0514	0.0581	0.0656	0.0645	0.0653	0.0670	0.0696	0.0704	0.0695	0.0743	0.0885	0.0868
Cycloheptane	0.0024	0.0021	0.0014	0.0013	0.0012	0.0013	0.0013	0.0013	0.0012	0.0012	0.0012	0.0012	0.0012	0.0013	0.0013
i-Heptane	0.0339	0.0311	0.0209	0.0198	0.0202	0.0214	0.0207	0.0214	0.0219	0.0226	0.0224	0.0229	0.0230	0.0250	0.0237
n-Heptane	0.1307	0.1548	0.1352	0.1519	0.1461	0.1567	0.1300	0.1243	0.1237	0.1235	0.1117	0.1160	0.1248	0.1350	0.1349
Cyclooctane	0.0086	0.0073	0.0049	0.0045	0.0044	0.0045	0.0039	0.0038	0.0037	0.0036	0.0035	0.0034	0.0034	0.0033	0.0032
i-Octane	0.1049	0.0916	0.0664	0.0631	0.0622	0.0637	0.0585	0.0559	0.0545	0.0544	0.0533	0.0559	0.0591	0.0615	0.0625

Table 6.23.3. Carbon Mass Balance for EUROPT-4 (2 Pulses of H_2S) (510°C, 110 psig)

Time (hrs)	No. of moles of Carbon In	No. of moles of Carbon Out	Δ Carbon
1.5	4.2714×10^{-4}	4.0384×10^{-4}	2.3298×10^{-5}
4.5	4.2714×10^{-4}	4.0611×10^{-4}	2.1028×10^{-5}
19.33	4.2714×10^{-4}	4.1192×10^{-4}	1.5218×10^{-5}
22	4.2714×10^{-4}	4.1208×10^{-4}	1.5058×10^{-5}
25	4.2714×10^{-4}	4.1231×10^{-4}	1.4828×10^{-5}
28	4.2714×10^{-4}	4.1245×10^{-4}	1.4688×10^{-5}
43.2	4.2714×10^{-4}	4.1642×10^{-4}	1.0718×10^{-5}
46.25	4.2714×10^{-4}	4.1699×10^{-4}	1.0148×10^{-5}
49.25	4.2714×10^{-4}	4.2035×10^{-4}	6.7878×10^{-6}
52.25	4.2714×10^{-4}	4.2109×10^{-4}	6.0478×10^{-6}
67.15	4.2714×10^{-4}	4.2219×10^{-4}	4.9478×10^{-6}
70.63	4.2714×10^{-4}	4.2236×10^{-4}	4.7778×10^{-6}
73.5	4.2714×10^{-4}	4.2265×10^{-4}	4.4878×10^{-6}
91.45	4.2714×10^{-4}	4.2311×10^{-4}	4.0278×10^{-6}
95.65	4.2714×10^{-4}	4.2329×10^{-4}	3.8478×10^{-6}

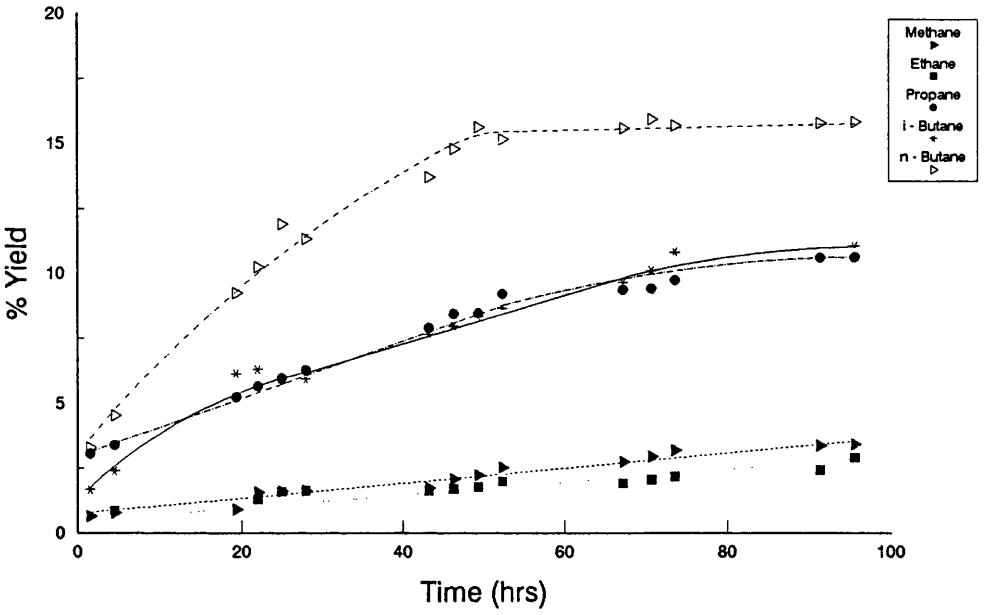

Figure 6.23.1. % Yield of Individual Hydrocarbon Products on a EUROPT-4 catalyst (2 pulses of H_2S)

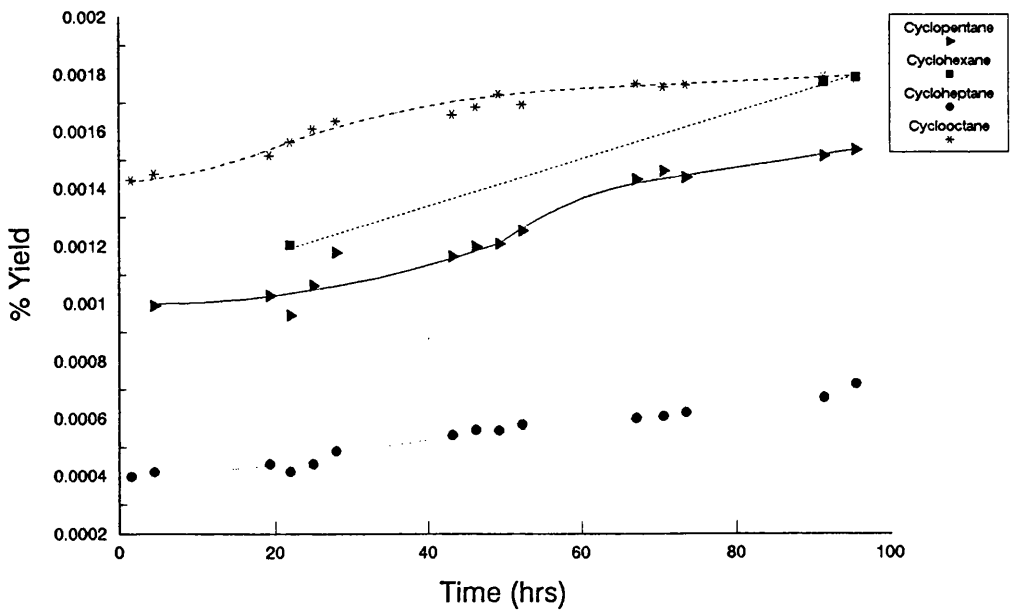

Figure 6.23.2. % Yield of Cycloparaffin Products on a EUROPT-4 catalyst (2 Pulses H_2S)

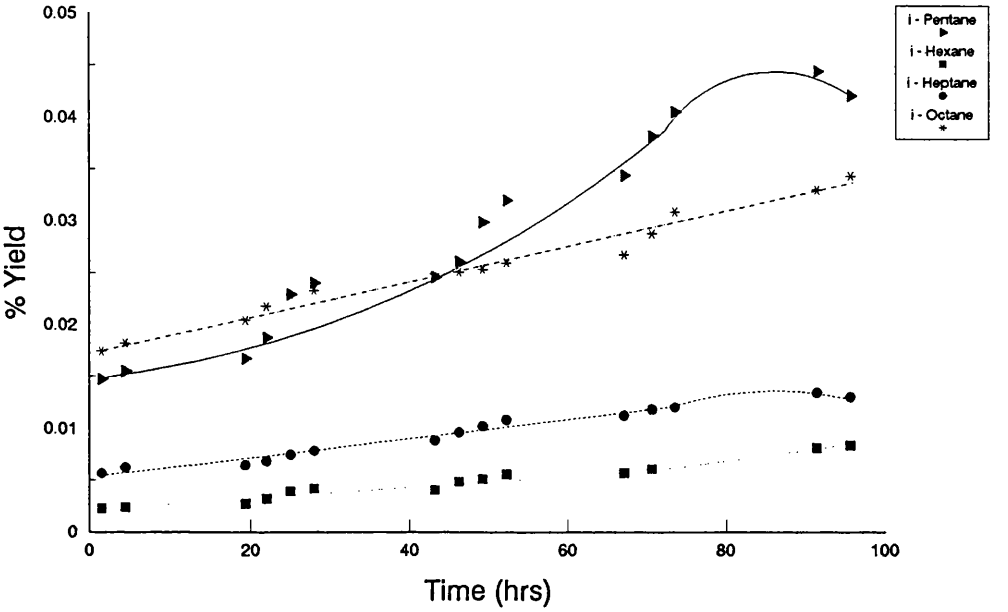

Figure 6.23.3. % Yield of i- and n-Paraffin Products on a EUROPT-4 catalyst (2 pulses of H_2S)

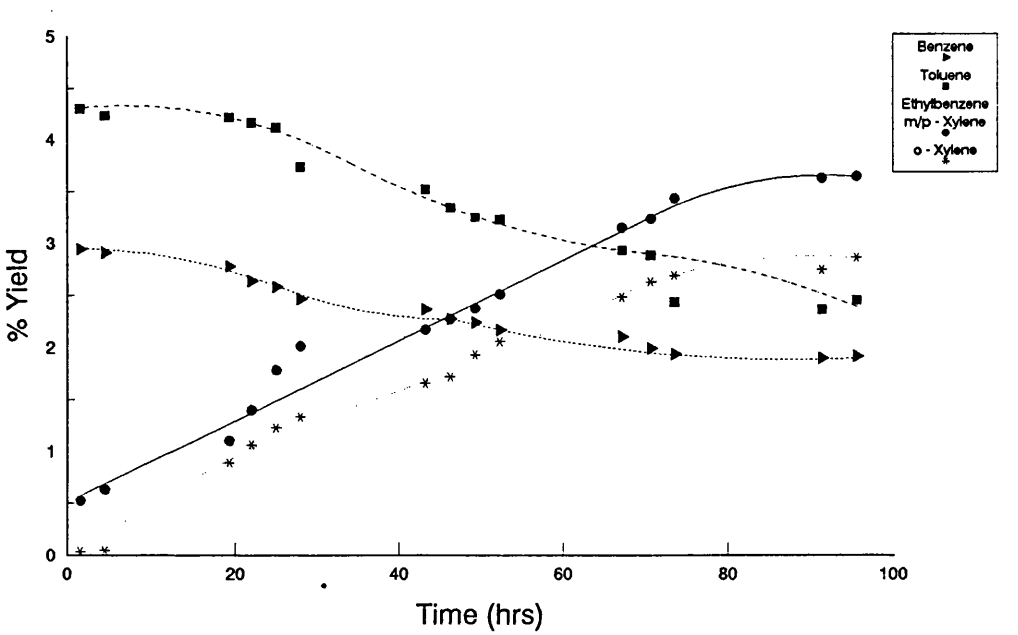

Figure 6.23.4. % Yield of Aromatic Products on a EUROPT-4 catalyst (2 Pulses H_2S)

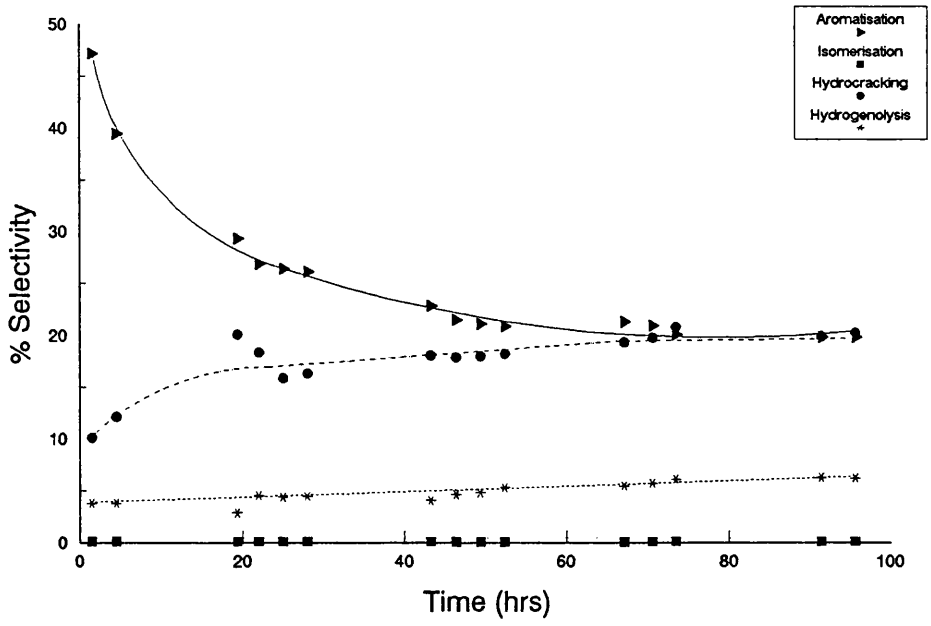

Figure 6.23.5. % Selectivity of the Major Reactions on a EUROPT-4 catalyst (2 pulses of H_2S)

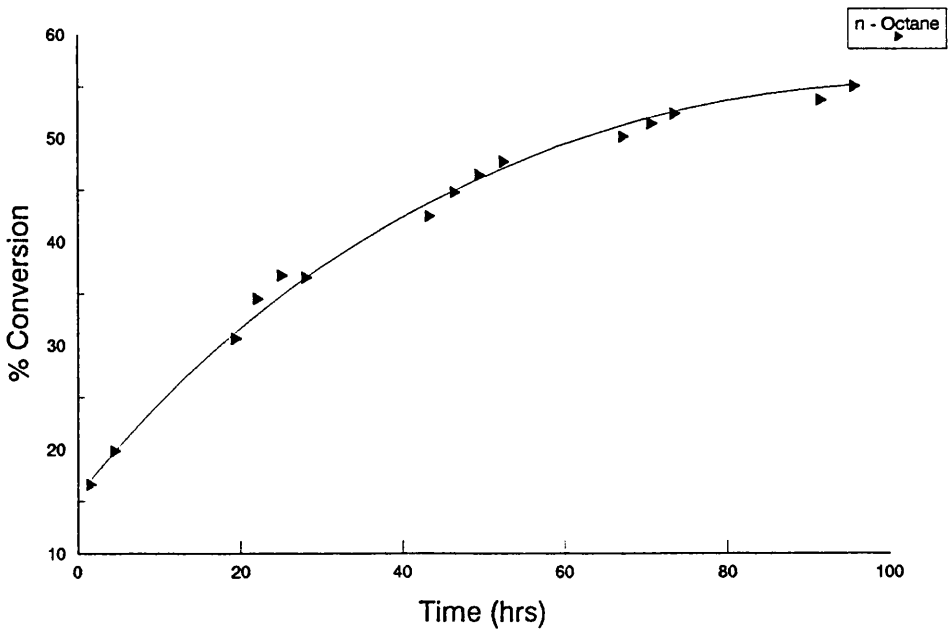

Figure 6.23.6. % Conversion of n-Octane on a EUROPT-4 catalyst (2 Pulses H_2S)

The full range of aromatics was found and the product yields are summarised in Figure 6.23.5. The yield of both benzene and toluene decreases while the yield of ethylbenzene and the xylenes increase steadily throughout the reaction. After ~96 hours the product yield decreased in the order ethylbenzene/m/p-xylene, o-xylene, toluene and then benzene as with an unsulphided EUROPT-4.1 catalyst. However the yield of C_8 aromatic species was much lower than with the EUROPT-4.1 catalyst. In comparison with the sulphided EUROPT-4 catalyst (Section 6.22) the yield of all aromatics, especially those of benzene and toluene, has decreased significantly.

The selectivity of the individual products is summarised in Table 6.23.2. The selectivity to the major reactions is shown in Figure 6.23.5. The selectivity to aromatisation and isomerisation decreases while that of hydrogenolysis and hydrocracking increases with time. The selectivity to aromatisation falls from 47 to ~20% after 96 hours on stream. Aromatisation activity is almost a third of that with EUROPT-4.1 (58%) and a quarter of that with the other partially sulphided EUROPT-4 catalyst. The order of the major reactions is as follows:

Aromatisation > Hydrocracking > Hydrogenolysis > Isomerisation

The hydrocracking activity has increased considerably in this run in comparison with the unsulphided and other partially sulphided EUROPT-4 catalyst. Hydrogenolysis activity has also gained importance with a value of ~6.2% at the end of the run.

The propane to methane ratio decreases for the first 22 hours before increasing to a maximum after 40 hours and then decreasing gradually until the reaction ends. The carbon mass balance is typical of a reforming reaction and demonstrates that the carbon deposition decreases with reaction time. These results suggest that coke is deposited on to the support preferentially in the first 20 hours before being deposited upon the metallic sites. After this had occurred the support was once again coked.

The overall conversion of n-octane increases with time, as seen in Figure 6.23.6, before reaching a constant level at 55%. This value is higher than both the partially sulphided EUROPT-4 (Section 6.22) and EUROPT-4.1 catalysts (Section 6.3). Although the conversion is higher, the selectivity of the other two catalysts to the aromatisation reaction is significantly higher. The % coke deposited upon the catalyst surface after the reaction had ended is 6.90% by weight, detailed in Table 6.1. This value is ~½ that of the unsulphided EUROPT-4.1 catalyst and approximately equal to the corresponding EUROPT-3 catalyst.

6.24. 0.3wt%Pt-0.3wt%Ge/Al_2O_3 - Ge impregnated first (510°C, 110 psig)

The catalyst was tested under conditions described in Section 6.1. Results from this reforming run are reported in Figures 6.24.1 to 6.24.6 and in Tables 6.24.1 to 6.24.3.

The product yields of all C_1 - C_4 species are detailed in Figure 6.24.1. Throughout this run no ethane could be detected from the sampled products. The

Table 6.24.1. % Yield of individual products and % Conversion versus time on stream for 0.3wt%Pt-0.3wt%Ge/Al_2O_3 (Ge impregnated first).

Products	% Yield of Selected Products											
Time (hrs)	2	5	8	22.15	25.15	28.15	31.15	46.5	49.5	52.8	70.55	73.5
Benzene	3.1090	3.5358	4.2702	4.4864	4.6429	4.6713	4.5983	4.7476	4.7854	4.7911	4.8771	5.1298
Toluene	1.4911	1.6546	2.0347	2.2772	2.3546	2.3832	2.3808	2.4768	2.3975	2.4641	2.8748	2.8348
Ethylbenzene	0.1074	0.1358	0.1654	0.1757	0.1915	0.1922	0.1882	0.2210	0.1922	0.1980	0.2688	0.3148
m/p-Xylene												
o-Xylene	0.0569	0.0607	0.0666	0.1012	0.0881	0.0967	0.0923	0.1194	0.0971	0.1177	0.1535	0.1444
Methane	3.1752	2.9125	2.5727	2.4558	2.3228	2.1365	2.0185	1.7603	1.5919	1.4246	1.4040	1.3338
Ethane	-	-	-	-	-	-	-	0.0399	-	-	-	-
Propane	5.9924	6.3680	6.8986	6.3216	6.3649	6.5698	6.3780	0.3844	6.2681	6.4691	6.4375	6.4927
i-Butane	5.0888	5.5266	6.0926	5.5157	5.8685	5.8587	5.8695	5.6788	5.7026	5.5516	6.1501	5.8491
n-Butane	6.2769	6.7581	7.4855	7.2669	7.1378	7.0746	7.0074	6.9109	6.9290	6.6956	7.3755	6.8274
Cyclopentane	0.0002	0.0002	0.0003	0.0003	0.0002	0.0002	0.0002	0.0002	0.0003	0.0002	0.0002	0.0002
i-Pentane	0.0561	0.0543	0.0605	0.0597	0.0610	0.0616	0.0623	0.0632	0.0618	0.0613	0.0650	0.0634
n-Pentane	0.0264	0.0271	0.0861	0.0303	0.0258	0.0255	0.0276	0.0333	0.0331	0.0339	0.0371	0.0359
Cyclohexane	0.0002	0.0003	0.0002	0.0002	0.0004	0.0004	0.0015	0.0017	0.0017	0.0017	0.0021	0.0019
i-Hexane	0.0371	0.0346	0.0501	0.0486	0.0480	0.0491	0.0567	0.0597	0.0525	0.0613	0.0674	0.0656
n-Hexane												
Cycloheptane	0.0006	0.0007	0.0004	0.0004	0.0011	0.0011	0.0012	0.0012	0.0012	0.0012	0.0012	0.0012
i-Heptane	0.0030	0.0035	0.0050	0.0056	0.0067	0.0077	0.0078	0.0095	0.0090	0.0097	0.0114	0.0119
n-Heptane												
Cyclooctane	0.0039	0.0039	0.0044	0.0065	0.0079	0.0079	0.0089	0.0086	0.0114	0.0111	0.0144	0.0152
i-Octane	0.0159	0.0157	0.0174	0.0207	0.0241	0.0251	0.0287	0.0381	0.0404	0.0367	0.0441	0.0494
% Conversion of n-Octane	26.4075	27.0923	29.7602	28.7728	29.1465	29.1607	28.6779	28.5549	28.1780	27.9290	29.7842	29.1717

Table 6.24.2. % Selectivity of individual products and % Conversion versus time on stream for 0.3wt%Pt-0.3wt%Ge/Al_2O_3 (Ge impregnated first).

Products	% Selectivity of Selected Products											
Time (hrs)	2	5	8	22.15	25.15	28.15	31.15	46.5	49.5	52.8	70.55	73.5
Benzene	11.7733	13.0511	14.3486	15.5925	15.9296	16.0192	16.0342	16.6264	16.9825	17.1544	16.3749	17.5849
Toluene	5.6465	6.1074	6.8370	7.9145	8.0788	8.1725	8.1275	8.6740	8.5684	8.8228	9.6522	9.7175
Ethylbenzene	0.4066	0.5011	0.5557	0.6105	0.6569	0.6592	0.6561	0.7740	0.6821	0.7089	0.9025	1.0793
m/p-Xylene												
o-Xylene	0.2155	0.2239	0.2237	0.3516	0.3023	0.3317	0.3218	0.4181	0.3446	0.4122	0.5153	0.4951
Methane	12.0239	10.7501	8.6447	8.5352	7.9694	7.3266	7.0385	6.1646	5.6600	5.1006	4.7138	4.5723
Ethane	-	-	-	-	-	-	-	0.1397	-	-	-	-
Propane	22.6923	23.5047	23.1804	21.9706	21.8378	22.5295	22.2403	22.3585	22.2446	23.1626	21.6137	22.2569
i-Butane	19.2702	20.3990	20.4723	19.1697	20.1347	20.0909	20.4668	19.8875	20.2377	19.8776	20.6490	20.0206
n-Butane	23.7695	24.9448	25.1527	25.2562	24.4895	24.2609	24.4348	24.2021	24.5900	23.9737	24.7632	23.4040
Cyclopentane	0.0008	0.0007	0.0009	0.0009	0.0008	0.0007	0.0009	0.0007	0.0009	0.0008	0.0008	0.0008
i-Pentane	0.2123	0.2003	0.2032	0.2074	0.2092	0.2111	0.2174	0.2214	0.2193	0.2196	0.2181	0.2172
n-Pentane	0.0998	0.1000	0.1212	0.1055	0.0885	0.0874	0.0963	0.1168	0.1176	0.1215	0.1246	0.1232
Cyclohexane	0.0009	0.0009	0.0007	0.0009	0.0012	0.0013	0.0053	0.0060	0.0059	0.0062	0.0069	0.0064
i-Hexane	0.1404	0.1278	0.1685	0.1689	0.1648	0.1682	0.1978	0.2090	0.1865	0.2196	0.2262	0.2249
n-Hexane												
Cycloheptane	0.0022	0.0025	0.0014	0.0016	0.0039	0.0038	0.0041	0.0041	0.0044	0.0043	0.0040	0.0042
i-Heptane	0.0113	0.0131	0.0170	0.0194	0.0229	0.0242	0.0272	0.0333	0.0319	0.0349	0.0384	0.0410
n-Heptane												
Cyclooctane	0.0146	0.0144	0.0146	0.0226	0.0277	0.0269	0.0309	0.0302	0.0404	0.0397	0.0484	0.0523
i-Octane	0.0603	0.0581	0.0575	0.0721	0.0826	0.0858	0.1002	0.1335	0.1432	0.1314	0.1479	0.1694

Table 6.24.3. Carbon Mass Balance for 0.3wt%Pt-0.3wt%Ge/Al_2O_3 (Ge impregnated first) (510°C, 110 psig)

Time (hrs)	No. of moles of Carbon In	No. of moles of Carbon Out	Δ Carbon
2	2.0165×10^{-4}	1.4615×10^{-4}	5.5503×10^{-5}
5	2.0165×10^{-4}	1.4940×10^{-4}	5.2253×10^{-5}
8	2.0165×10^{-4}	1.6292×10^{-4}	3.8733×10^{-5}
22.15	2.0165×10^{-4}	1.5812×10^{-4}	4.3533×10^{-5}
25.15	2.0165×10^{-4}	1.6105×10^{-4}	4.0603×10^{-5}
28.15	2.0165×10^{-4}	1.6014×10^{-4}	4.1513×10^{-5}
31.15	2.0165×10^{-4}	1.5785×10^{-4}	4.3803×10^{-5}
46.5	2.0165×10^{-4}	1.5749×10^{-4}	4.4163×10^{-5}
49.5	2.0165×10^{-4}	1.5572×10^{-4}	4.5933×10^{-5}
52.8	2.0165×10^{-4}	1.5457×10^{-4}	4.7083×10^{-5}
70.55	2.0165×10^{-4}	1.6424×10^{-4}	3.7413×10^{-5}
73.5	2.0165×10^{-4}	1.6159×10^{-4}	4.0063×10^{-5}

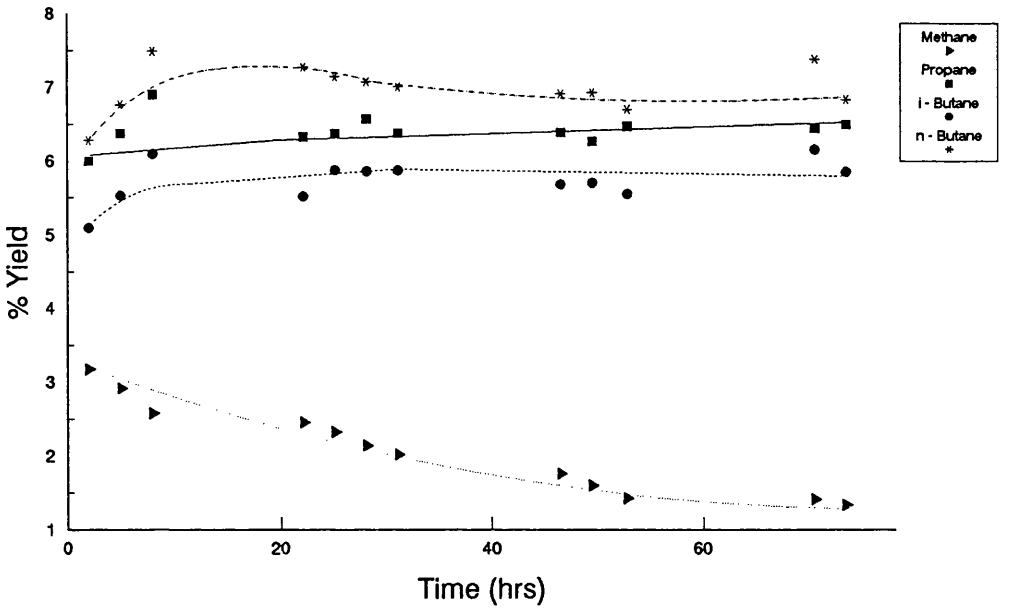

Figure 6.24.1. % Yield of Individual Hydrocarbon Products on 0.3wt%Pt-0.3wt%Ge/Alumina (Ge impregnated first)

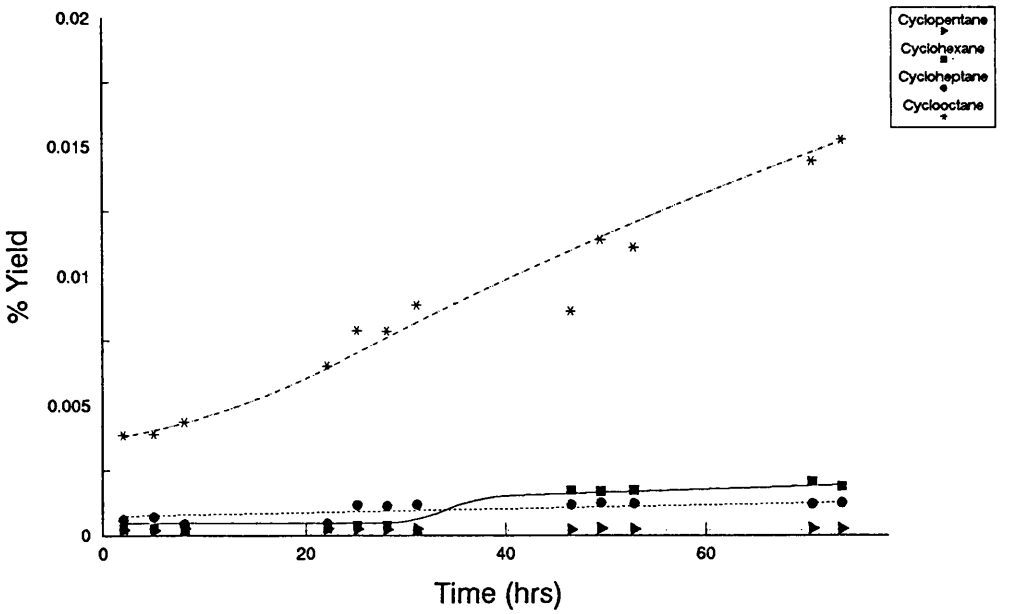

Figure 6.24.2. % Yield of Cycloparaffin Products on 0.3wt%Pt-0.3wt%Ge/ Alumina (Ge impregnated first)

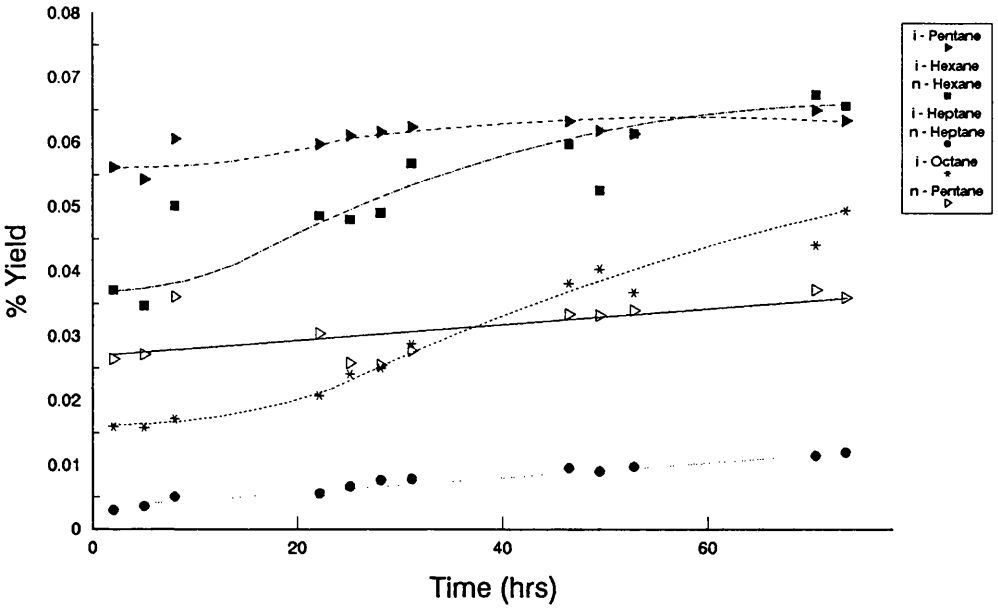

Figure 6.24.3. % Yield of i- and n-Paraffin Products on 0.3wt%Pt-0.3wt%Ge/Alumina (Ge impregnated first)

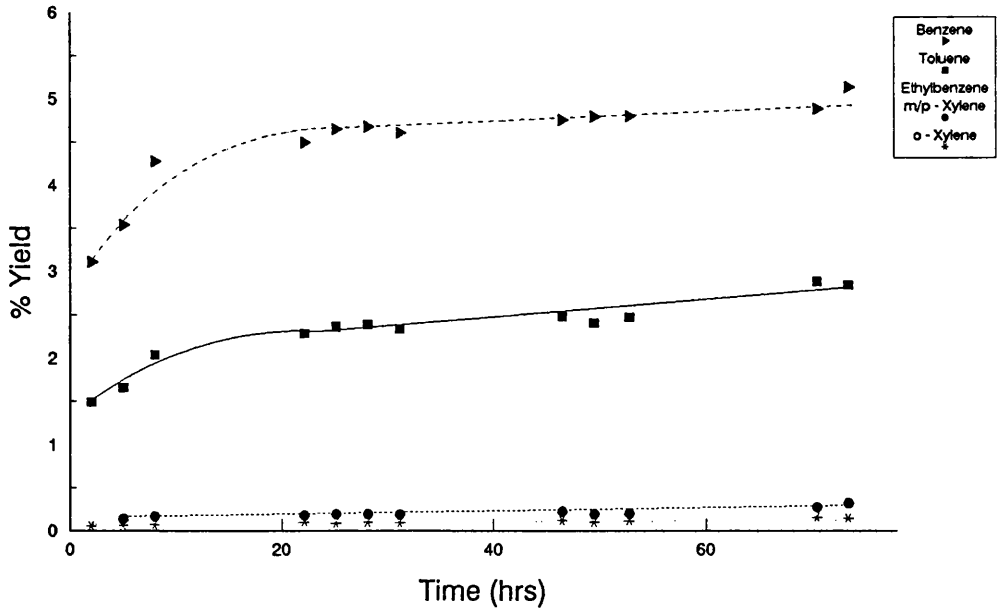

Figure 6.24.4. % Yield of Aromatic Products on 0.3wt%Pt-0.3wt%Ge/ Alumina (Ge impregnated first)

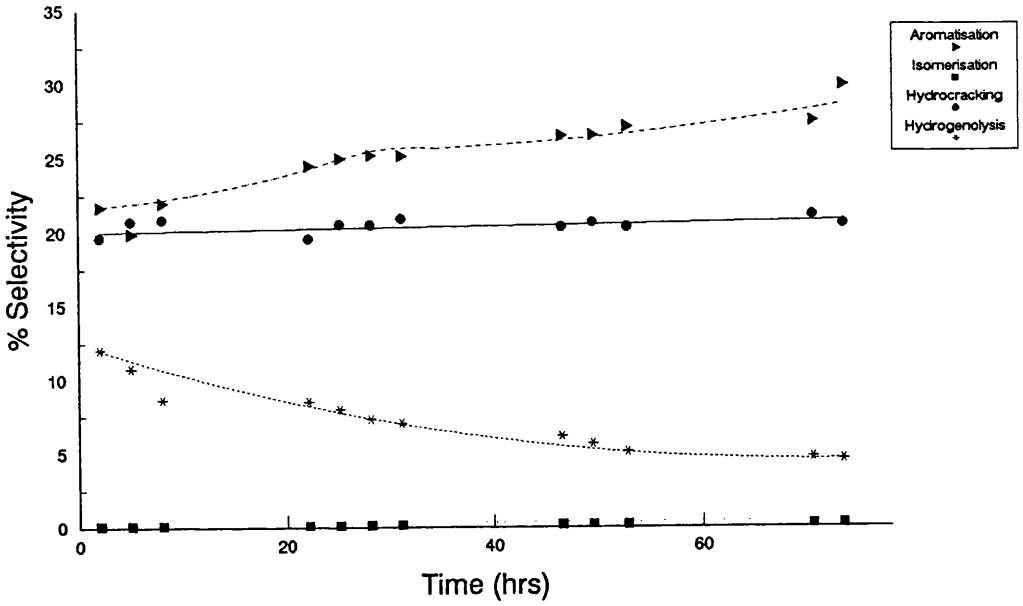

Figure 6.24.5. % Selectivity of the Major Reactions on 0.3wt%Pt-0.3wt%Ge/Alumina (Ge impregnated first)

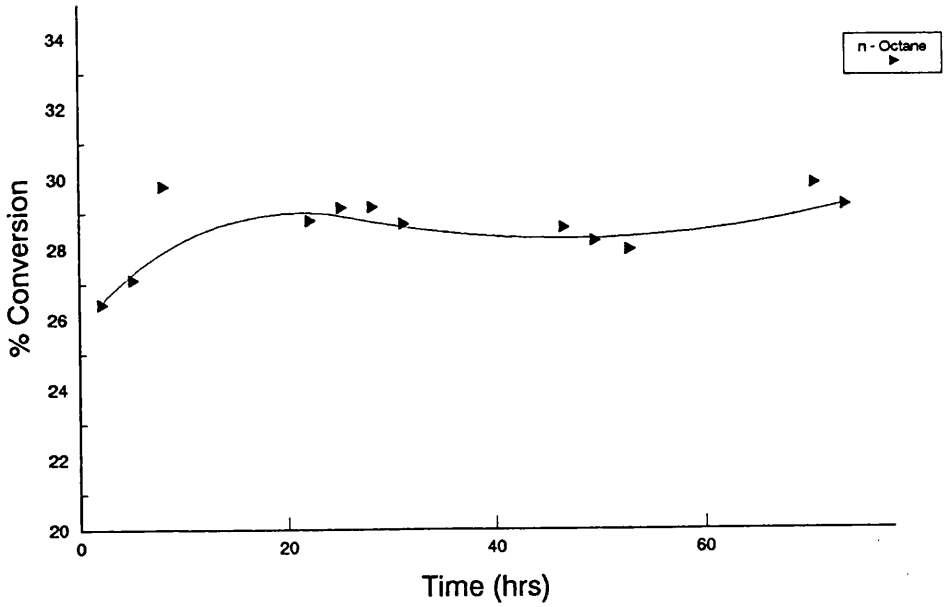

Figure 6.24.6. % Conversion of n-Octane on 0.3wt%Pt-0.3wt%Ge/ Alumina (Ge impregnated first)

yield of methane produced by this catalyst is very low in comparison with a corresponding Pt-Sn/Al_2O_3 or a Pt-Re/Al_2O_3 catalyst. The methane yield falls to a constant level of 1.3% whereas that of propane levels off at 6.5%. The yield of n-butane is ~1.2 times greater than that of i-butane at a steady yield.

Figures 6.24.2 and 6.24.3 show the yield of paraffin products against reaction time. The yield of all cycloparaffins increases with time initially and with carbon number. However, after ~38 hours on stream the yield of cyclohexane increases above that of cycloheptane before reaching a steady yield. The yield of cyclooctane increases steadily throughout the run. Once again combined values of i- and n-paraffins are used in Figure 6.24.3 as certain reaction products could not be separated. The combined yields of i- and n-paraffins increases with time and with decreasing carbon number for C_5 to C_7 species. The yield of i-octane is shown to increase with time in Figure 6.24.3.

The yield of aromatic species is shown to increase with reaction time in Figure 6.24.4. The product yield decreases in the following order from benzene, toluene, ethylbenzene/m/p-xylene and o-xylene. The yields of both benzene and toluene are much higher than those of ethylbenzene/m/p-xylene and o-xylene. This is in contrast to both the Pt-Re/Al_2O_3 and Pt-Sn/Al_2O_3 catalyst systems but is similar to a sulphided EUROPT-3 or -4 catalyst. The combined yield of all C_8 aromatics is ~0.45% after 74 hours on stream.

The selectivity to the individual hydrocarbon products is shown in Table 6.24.2.

The selectivity to the major reactions is detailed in Figure 6.24.5. The order of decreasing selectivity is as follows:

Aromatisation > Hydrocracking > Hydrogenolysis > Isomerisation

The selectivity of both aromatisation and isomerisation reactions increases to a steady level of 29 and 0.2% respectively, while the hydrogenolysis activity decreases with time to 4.6%. The hydrocracking activity stays approximately constant throughout the reaction. In comparison with the Pt-Re/Al_2O_3 or Pt-Sn/Al_2O_3 systems the aromatisation and hydrogenolysis activities have decreased while that of hydrocracking has increased.

The propane to methane ratio increases steadily before reaching a constant ratio after ~70 hours on stream. The ratio is very high (~4.5) due to the very low methane yield in comparison with that of propane. The carbon mass balance shows that carbon deposition on this catalyst decreases very slowly with the reaction time.

The conversion of n-octane increases from 26 to 29% with reaction time as shown in Figure 6.24.12. The value is in general lower than either the bimetallic Pt-Re/Al_2O_3 or the Pt-Sn/Al_2O_3 catalysts but higher than the monometallic EUROPT-3.1 catalyst. However this catalyst displays a poor selectivity to aromatics. The % coke, detailed in Table 6.1, is 8.49% by weight, lower than on the EUROPT catalysts and many of the Pt-Sn/Al_2O_3 catalysts.

6.25. 0.3wt%Pt-0.3wt%Ge/Al_2O_3 - Pt impregnated first (510°C, 110 psig)

This catalyst was tested under conditions described in Section 6.1 was prepared by impregnating monometallic EUROPT-3 catalyst with germanium. Results from this reforming run are reported in Figures 6.25.1 to 6.25.6 and in Tables 6.25.1 to 6.25.3.

The yields of C_1 - C_4 species are presented in Figure 6.25.1. The yield of all species, with the exception of propane, decrease with reaction time. As with the previous Pt-Ge/Al_2O_3 catalyst (Section 6.24) the yield of methane is very small, levelling off at ~1.3%. The yield of propane increases with time to ~5.45%, many times greater than the yield of methane. The yield of n-butane decreases quicker than that of i-butane and therefore is only slightly higher when the reaction is stopped.

Figures 6.25.2 to 6.25.4 illustrate the yields of cyclo-, i- and n-paraffins with respect to the reaction time. The yields of cycloparaffins increase with reaction time as outlined in Figure 6.25.2. The yields of cyclooctane, cycloheptane and cyclohexane increase steadily while the yield of cyclopentane decreases initially before increasing throughout the run. The yield of i-paraffins is detailed in Figure 6.25.3. The yields of i-octane, i-heptane and the combined yield of i- and n-hexane increase through a maximum before decreasing slightly towards the end of the reaction. The yield of i-pentane decreases with reaction time. The product yield decreases from i-pentane, i-octane to i-heptane. The yield of both n-pentane and n-

Table 6.25.1. % Yield of individual products and % Conversion versus time on stream for 0.3wt%Pt-0.3wt%Ge/Al_2O_3 (Pt impregnated first).

Products	% Yield of Selected Products											
Time (hrs)	1.5	18.75	21.75	24.65	27.65	42.75	45.65	48.75	51.65	69	72	75.25
Benzene	3.6388	4.9148	5.1864	4.5505	5.1612	5.3401	5.4180	5.3604	5.0173	4.8089	4.6759	4.6238
Toluene	1.5587	2.1042	2.1187	2.0587	1.7262	3.9550	4.0693	4.0772	3.9532	3.8786	3.8723	3.7855
Ethylbenzene	0.3704	0.6277	0.6367	0.7858	0.8964	2.4077	2.4162	2.4551	2.3792	2.8954	2.6500	2.7985
m/p-Xylene												
o-Xylene	0.0746	0.1130	0.1228	0.1484	0.1503	0.2407	0.2785	0.3984	0.4826	0.8006	0.9577	1.0408
Methane	1.8859	1.7648	1.5639	1.5499	1.4481	1.4756	1.3946	1.3804	1.3519	1.3586	1.2767	1.2508
Ethane	-	0.0333	-	0.0414	-	-	0.0084	-	-	-	-	0.0313
Propane	3.3015	5.6321	6.4307	7.3562	6.7666	5.9411	5.7547	5.7468	5.8922	5.6449	5.2735	5.4442
i-Butane	8.3911	7.3610	7.4235	7.3975	7.2089	6.3453	6.4813	7.1710	6.7636	5.7156	5.7429	5.4546
n-Butane	12.6327	10.1447	11.4983	10.5462	10.5518	9.9322	9.6978	9.8296	7.6017	7.0073	7.0557	6.6817
Cyclopentane	-	0.0004	0.0002	0.0001	0.0001	0.0001	0.0002	0.0002	0.0002	0.0002	0.0002	0.0002
i-Pentane	0.0765	0.0678	0.0624	0.0624	0.0659	0.0644	0.0628	0.0623	0.0436	0.0574	0.0564	0.0540
n-Pentane	0.0505	0.0475	0.0474	0.0446	0.0443	0.0426	0.0403	0.0422	0.0425	0.0416	0.0412	0.0395
Cyclohexane	-	-	0.0001	0.0001	0.0001	-	0.0403	0.0001	0.0001	-	-	0.0002
i-Hexane	0.0246	0.0447	0.0569	0.0543	0.0621	0.0739	0.0775	0.0732	0.0624	0.0803	0.0799	0.0748
n-Hexane												
Cycloheptane	0.0006	0.0005	0.0002	0.0002	0.0002	-	-	-	0.0015	-	-	-
i-Heptane	0.0049	0.0061	0.0065	0.0067	0.0075	0.0080	0.0098	0.0083	0.0078	0.0067	0.0067	0.0642
n-Heptane	-	0.0158	0.0185	0.0186	0.0190	0.0226	0.0204	0.0196	0.0198	0.0161	0.0159	0.0139
Cyclooctane	-	0.0038	-	0.0037	0.0045	-	0.0042	0.0050	0.0047	0.0056	0.0054	0.0056
i-Octane	0.0183	0.0166	0.0161	0.0152	0.0154	0.0296	0.0297	0.0299	0.0294	0.0298	0.0278	0.0269
% Conversion of n-Octane	32.0492	32.8984	35.1893	34.6406	34.1285	36.0453	35.7638	36.6600	33.6537	32.3469	31.7382	31.3319

Table 6.25.2. % Selectivity of individual products versus time on stream for 0.3wt%Pt-0.3wt%Ge/Al_2O_3 (Pt impregnated first).

Products	% Selectivity of Selected Products											
Time (hrs)	1.5	18.75	21.75	24.65	27.65	42.75	45.65	48.75	51.65	69	72	75.25
Benzene	11.3537	14.9393	14.7384	13.1363	15.1228	14.0362	15.1494	14.6220	14.9086	14.8665	14.7327	14.7575
Toluene	4.8635	6.3962	6.0209	5.9429	5.0579	10.3956	11.3782	11.1217	11.7467	11.9907	12.2008	12.0819
Ethylbenzene	1.1558	1.9079	1.8093	2.2685	2.6264	6.3286	6.7559	6.6970	7.0696	9.9526	8.3496	8.9317
m/p-Xylene												
o-Xylene	0.2328	0.3435	0.3490	0.4284	0.4403	6.3278	0.7786	1.0867	1.4341	2.4749	3.0176	3.3219
Methane	5.8843	5.3643	4.4443	4.4744	4.2432	3.8785	3.8996	3.7655	4.0170	4.2000	4.0226	3.9922
Ethane	-	0.1013	-	0.1196	-	-	0.0234	-	-	-	-	0.0999
Propane	10.3012	10.1198	18.2747	21.2357	19.8267	15.6160	16.0908	15.6602	17.5083	17.4511	16.6157	17.3758
i-Butane	26.1820	22.3748	21.0959	21.3550	21.1227	16.6784	18.1226	19.5608	20.0976	17.6696	18.0946	17.4090
n-Butane	39.4790	30.8365	32.6755	30.4445	30.9178	26.1062	27.1163	26.8130	22.5881	21.6631	22.2309	21.3256
Cyclopentane	-	0.0011	0.0007	0.0004	0.0004	0.0003	0.0006	0.0005	0.0006	0.0007	0.0005	0.0008
i-Pentane	0.2387	0.2061	0.1774	0.1801	0.1932	0.1693	0.1757	0.1700	0.1295	0.1773	0.1778	0.1724
n-Pentane	0.1577	0.1429	0.1347	0.1287	0.1299	0.1121	0.1127	0.1152	0.1262	0.1288	0.1298	0.1262
Cyclohexane	-	0.0001	0.0002	0.0002	0.0002	-	0.0003	0.0004	0.0004	-	-	0.0007
i-Hexane	0.0769	0.1360	0.1616	0.1567	0.1820	0.1942	0.2167	0.1997	0.1856	0.2483	0.2517	0.2387
n-Hexane												
Cycloheptane	0.0019	0.0016	0.0005	0.0006	0.0007	-	-	-	0.0044	-	-	-
i-Heptane	0.0154	0.0185	0.0185	0.0195	0.0218	0.0211	0.0273	0.0227	0.0232	0.0206	0.0210	0.0201
n-Heptane	-	0.0481	0.0524	0.0538	0.0558	0.0594	0.0571	0.0536	0.0588	0.0497	0.0501	0.0434
Cyclooctane	-	0.0114	-	0.0107	0.0131	-	0.0118	0.0137	0.0138	0.0155	0.0169	0.0177
i-Octane	0.0570	0.0505	0.0459	0.0440	0.0450	0.0763	0.0829	0.0816	0.0875	0.0920	0.0877	0.0843

Table 6.25.3. Carbon Mass Balance for 0.3wt%Pt-0.3wt%Ge/Al_2O_3 (Pt impregnated first) (510°C, 110 psig)

Time (hrs)	No. of moles of Carbon In	No. of moles of Carbon Out	Δ Carbon
1.5	4.3563×10^{-4}	3.7599×10^{-4}	5.9632×10^{-5}
18.75	4.3563×10^{-4}	3.7664×10^{-4}	5.8982×10^{-5}
21.75	4.3563×10^{-4}	3.8019×10^{-4}	5.5432×10^{-5}
24.65	4.3563×10^{-4}	3.8795×10^{-4}	4.7678×10^{-5}
27.65	4.3563×10^{-4}	3.8533×10^{-4}	5.0291×10^{-5}
42.75	4.3563×10^{-4}	4.2491×10^{-4}	1.0715×10^{-5}
45.65	4.3563×10^{-4}	4.3400×10^{-4}	1.6243×10^{-6}
48.75	4.3563×10^{-4}	4.2986×10^{-4}	5.7688×10^{-6}
51.65	4.3563×10^{-4}	4.2853×10^{-4}	7.1005×10^{-6}
69	4.3563×10^{-4}	4.3270×10^{-4}	2.9286×10^{-6}
72	4.3563×10^{-4}	4.3563×10^{-4}	2.0961×10^{-9}
75.25	4.3563×10^{-4}	4.3543×10^{-4}	2.0065×10^{-7}

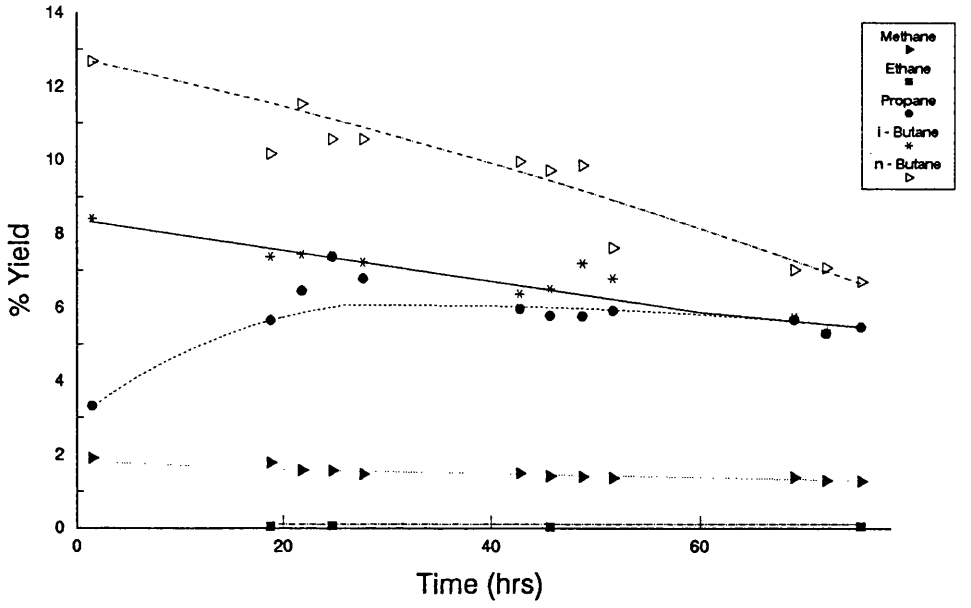

Figure 6.25.1. % Yield of Individual Hydrocarbon Products on 0.3wt%Pt-0.3wt%Ge/Alumina (Pt impregnated first)

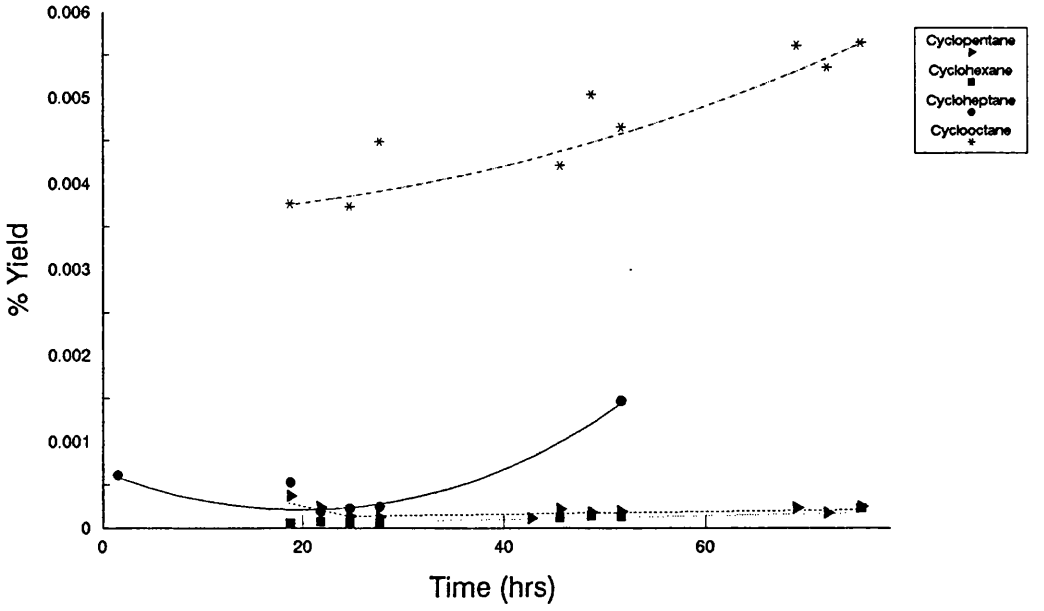

Figure 6.25.2. % Yield of Cycloparaffin Products on 0.3wt%Pt-0.3wt%Ge/ Alumina (Pt impregnated first)

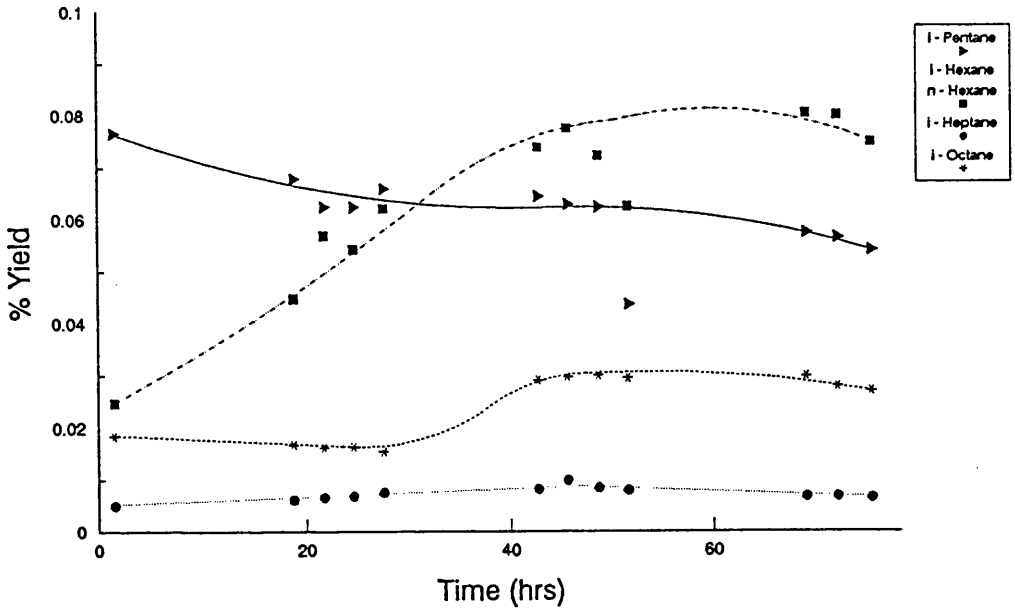

Figure 6.25.3. % Yield of i-Paraffin Products on 0.3wt%Pt-0.3wt%Ge/ Alumina (Pt impregnated first)

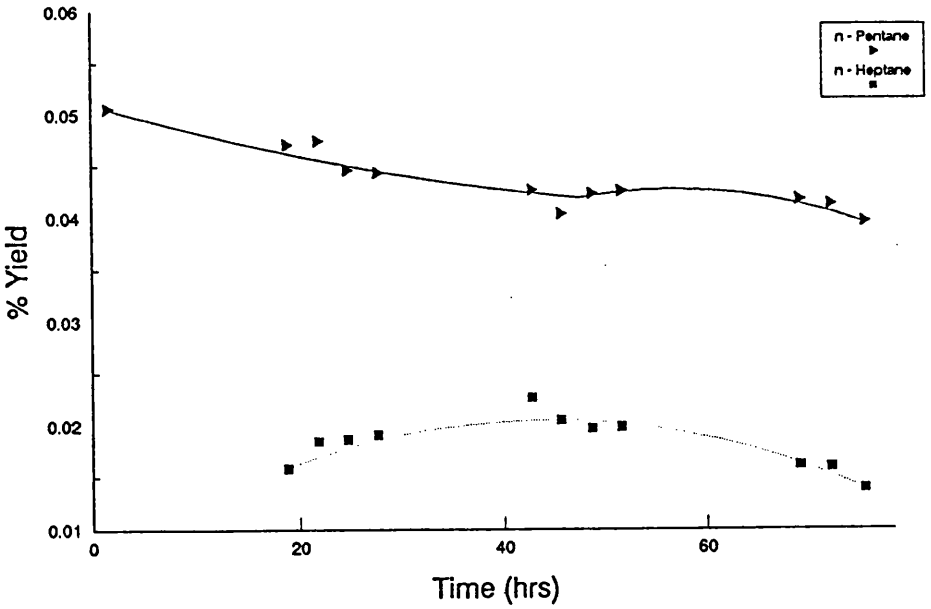

Figure 6.25.4. % Yield of n-Paraffin Products on 0.3wt%Pt-0.3wt%Ge/ Alumina (Pt impregnated first)

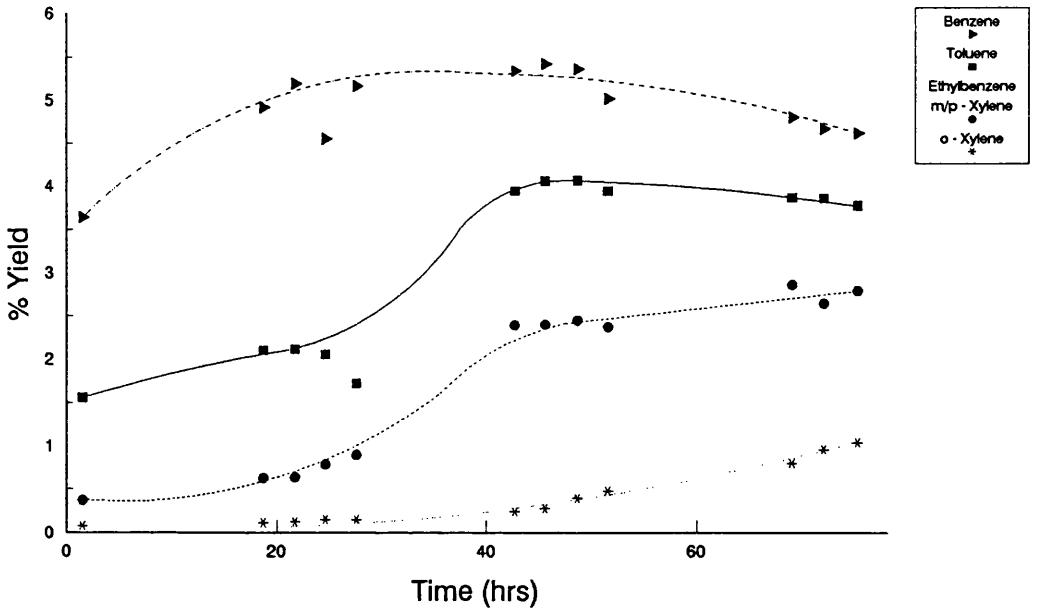

Figure 6.25.5. % Yield of Aromatic Products on 0.3wt%Pt-0.3wt%Ge/ Alumina (Pt impregnated first)

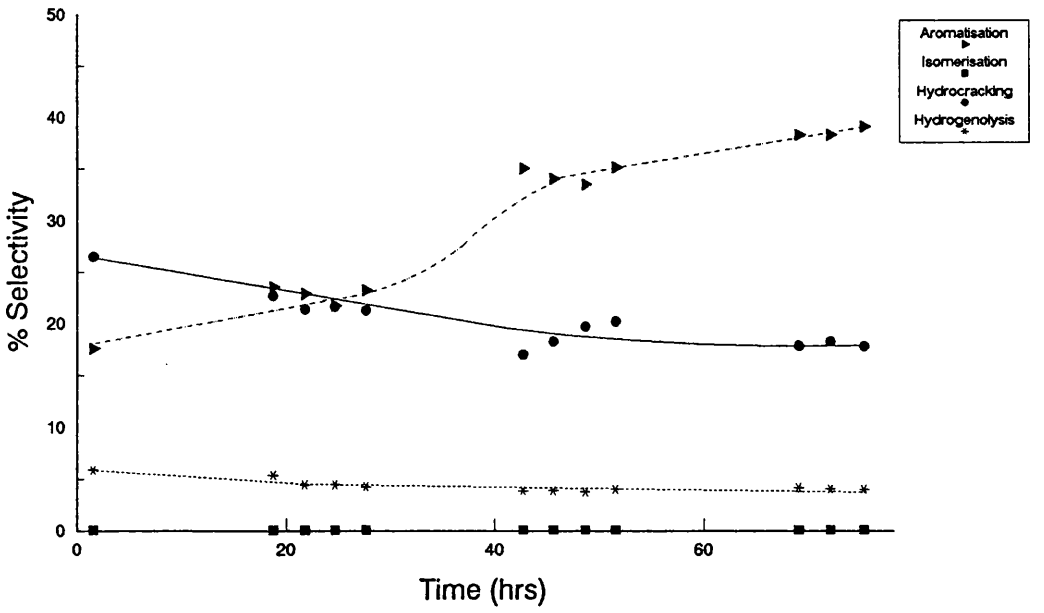

Figure 6.25.6. % Selectivity to the Major Reactions on 0.3wt%Pt-0.3wt%Ge/ Alumina (Pt impregnated first)

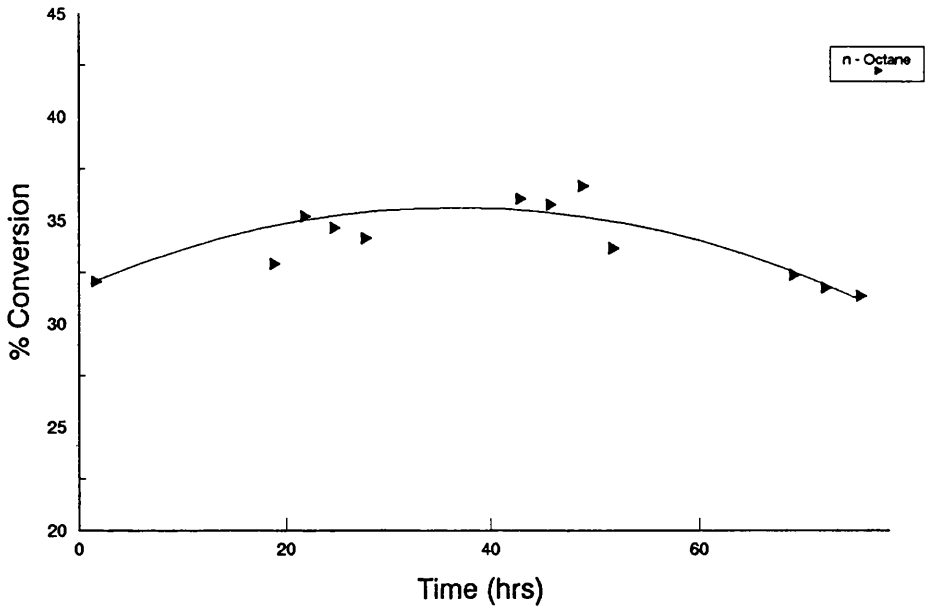

Figure 6.25.7. % Conversion of n-Octane on 0.3wt%Pt-0.3wt%Ge/ Alumina (Pt impregnated first)

heptane decrease with time and the yield of n-pentane is higher than that of n-heptane.

The yields of all aromatic species produced in this reforming run are presented in Figure 6.25.5. As with the previous Pt-Ge/Al_2O_3 catalyst, the yields of both benzene and toluene are greater than those of the C_8 aromatic species. The yields of both benzene and toluene increase through a maximum before decreasing. The yields of C_8 aromatic species increase with the reaction time. In comparison with the corresponding Pt-Ge/Al_2O_3 catalyst which had germanium impregnated first, the benzene yield is lower and the yields of toluene and C_8 aromatic species have increased. The yield of C_8 aromatic species is still very low when compared with a Pt-Re/Al_2O_3 or Pt-Sn/Al_2O_3 catalyst.

The selectivity to individual hydrocarbon products is shown in Table 6.25.2. The summation of the selectivities to the major reactions is shown in Figure 6.25.5. The aromatisation and isomerisation activity increase to 39 and 0.1% respectively whereas the hydrocracking and hydrogenolysis activity decreases to 18 and 4% respectively with time. Initially hydrocracking is the prominent reaction on this catalyst but after ~20 hours the aromatisation activity increases above that of hydrocracking. These reactions are followed by hydrogenolysis and finally isomerisation.

The propane to methane ratio initially increases before decreasing with time indicating an initial carbon deposition on the metallic sites and then on the alumina

support. The ratio is again high (~4) due to the low yields of methane. The carbon mass balance shows a rapid decrease in the carbon deposition after ~28 hours on stream.

The total n-octane conversion increases before decreasing steadily as shown in Figure 6.25.6. After 75 hours on stream 31.3% of n-octane was converted into hydrocarbon products. This value is higher than the corresponding germanium impregnated first catalyst. However the conversion is still not as high as either Pt-Re/Al_2O_3 or Pt-Sn/Al_2O_3 bimetallic catalysts. The selectivity to the major reactions however had improved in comparison with the germanium impregnated first catalyst. The % coke deposited upon the surface of this catalyst is 9.95% by weight. This is higher than the other Pt-Ge/Al_2O_3 catalysts studied but lower than on either EUROPT catalysts.

6.26. 0.3wt%Pt-0.3wt%Ge/Al_2O_3 - Coimpregnated (510°C, 110 psig)

This bimetallic catalyst was tested under conditions described in Section 6.1. Results from this reforming run are reported in Figures 6.26.1 to 6.26.6 and in Tables 6.26.1 to 6.26.3.

The yields of C_1 - C_4 species are presented in Figure 6.26.1. In this experiment no trace of ethane was found throughout the 95 hours on stream. The yield of propane increased while the yield of methane was very low, in keeping with the other Pt-Ge/Al_2O_3 catalysts examined. One interesting feature of this reforming run

Table 6.26.1. % Yield of individual products and % Conversion versus time on stream for 0.3wt%Pt-0.3wt%Ge/Al_2O_3 (Coimpregnated).

Products	% Yield of Selected Products															
Time (hrs)	1.5	4	19.25	22.25	25.25	28.25	43.15	46.2	49.25	52.25	66.9	69.9	73.05	76	91.85	95
Benzene	2.5755	2.6405	2.9415	3.1503	3.2448	3.5296	4.0126	4.1232	4.1960	4.2714	4.9716	5.0827	5.6533	5.6528	5.7752	5.9546
Toluene	1.9524	2.1214	2.3273	2.4120	2.4549	2.5620	2.6035	2.7828	3.0938	3.2528	3.8364	4.1991	4.5294	4.5616	5.0688	5.4027
Ethylbenzene	1.0073	1.0693	1.3834	1.4524	1.4868	1.5010	1.7517	2.0543	2.2352	2.4103	2.7128	2.8603	3.0919	3.4240	3.4328	3.4155
m/p-Xylene																
o-Xylene	0.4676	0.5112	0.9094	1.0609	1.1230	1.3038	1.5418	1.6455	1.8992	2.0351	2.3401	2.2828	2.2958	2.2760	2.2220	2.2397
Methane	3.0990	2.9361	2.6424	2.5472	2.4886	2.4256	2.0754	2.0098	1.9665	1.8843	1.7357	1.6969	1.7060	1.7804	1.7950	1.7716
Ethane	-	-	-	-	-	-	-	-	-	-	-	-	-	-	-	-
Propane	3.3828	3.8727	4.1405	4.7910	5.2867	5.8546	5.8618	6.7874	7.0620	7.1852	6.6503	6.5850	6.3808	6.2322	6.3384	6.5606
i-Butane	8.7221	8.2253	8.2122	7.8296	6.9445	5.9800	4.7349	5.3931	4.8598	4.6773	4.6121	4.2181	4.1357	3.9694	3.8589	3.8948
n-Butane	11.7971	10.0934	8.9444	7.9883	8.0625	6.9278	6.4348	6.2568	5.8788	5.5285	5.5248	5.0846	4.5804	4.5247	4.7321	4.7251
Cyclopentane	0.0004	0.0004	0.0003	0.0003	0.0003	0.0002	0.0002	0.0002	0.0002	0.0002	0.0002	0.0002	0.0002	0.0002	0.0002	0.0002
i-Pentane	0.0361	0.0370	0.0428	0.0455	0.0449	0.0468	0.0586	0.0608	0.0641	0.0647	0.0681	0.0679	0.0707	0.0711	0.0784	0.0770
n-Pentane	0.0292	0.0301	0.0308	0.0322	0.0335	0.0348	0.0439	0.0463	0.0483	0.0493	0.0509	0.0506	0.0508	0.0506	0.0508	0.0507
Cyclohexane	0.0004	0.0004	0.0004	0.0004	0.0004	0.0004	0.0003	0.0003	0.0003	0.0003	0.0003	0.0003	0.0002	0.0003	0.0003	0.0003
i-Hexane	-	0.0574	0.0604	0.0580	0.0561	0.0544	0.0442	0.0427	0.0424	0.0422	0.0407	0.0399	0.0404	0.0404	0.0332	0.0332
n-Hexane	0.0294	0.0332	0.0355	0.0368	0.0370	0.0372	0.0376	0.0380	0.0391	0.0386	0.0391	0.0413	0.0402	0.0399	0.0432	0.0428
Cycloheptane	-	-	-	-	-	-	-	-	-	-	-	-	-	-	-	-
i-Heptane	0.0155	0.0150	0.0128	0.0122	0.0115	0.0110	0.0112	0.0111	0.0106	0.0165	0.0104	0.0103	-	0.0103	0.0100	0.0098
n-Heptane	0.0463	0.0472	0.0432	0.0425	0.0419	0.0416	0.0418	0.0409	0.0412	0.0410	0.0415	0.0412	0.0449	0.0438	0.0418	0.0421
Cyclooctane	0.0052	0.0049	0.0046	0.0046	0.0046	0.0046	0.0042	0.0042	-	0.0038	-	0.0035	0.0035	0.0034	0.0034	0.0034
i-Octane	0.0347	0.0369	0.0399	0.0438	0.0452	0.0490	0.0493	0.0518	0.0560	0.0613	0.0624	0.0648	0.0675	0.0670	0.0671	0.0677
% Conversion of n-Octane	33.2010	31.7325	31.7718	31.5087	31.3671	30.3643	29.3079	31.3492	31.4935	31.5568	32.6975	32.3293	32.6918	32.7481	33.5519	34.2919

Table 6.26.2. % Selectivity of individual products versus time on stream for 0.3wt%Pt-0.3wt%Ge/Al_2O_3 (Coimpregnated).

Products	% Selectivity of Selected Products															
Time (hrs)	1.5	4	19.25	22.25	25.25	28.25	43.15	46.2	49.25	52.25	66.9	69.9	73.05	76	91.85	95
Benzene	7.7572	8.3210	9.2581	9.9982	10.3445	11.6242	13.6910	13.1524	13.3233	13.5357	15.2049	15.7218	17.2929	17.2614	17.2129	17.3644
Toluene	5.8805	6.6853	7.3251	7.6552	7.8262	8.4377	8.8834	8.8767	9.8237	10.3077	11.7330	12.9885	13.8549	13.9293	15.1075	15.7550
Ethylbenzene	3.0339	3.3696	4.3541	4.6094	4.7401	4.9432	5.9770	6.5529	7.0973	7.6380	8.2966	8.8474	9.4576	10.4556	10.2314	9.9602
m/p-Xylene																
o-Xylene	1.4083	1.4083	1.6111	2.8622	3.5802	4.2937	5.2608	5.2490	6.0305	6.4490	7.1567	7.0611	7.0227	6.9501	6.6225	6.5314
Methane	9.334	9.2527	8.3169	8.0842	7.9337	7.9883	7.0813	6.4111	6.2443	5.9713	5.3082	5.2487	5.2183	5.4366	5.3500	5.1661
Ethane	-	-	-	-	-	-	-	-	-	-	-	-	-	-	-	-
Propane	10.1888	12.2041	13.0320	15.2055	16.8544	19.2812	20.0008	21.6508	22.4237	22.7693	20.3389	20.3684	19.5181	19.0309	18.8915	19.1315
i-Butane	26.2705	25.9209	25.8476	24.8492	22.1394	19.6940	16.1556	17.2032	15.4312	14.8220	14.1054	13.0472	12.6507	12.1209	11.5014	11.3577
n-Butane	35.5323	31.8078	28.1519	25.3541	25.7038	22.8157	21.9558	19.9585	18.6668	17.5191	16.8969	15.7274	14.0107	13.8167	14.1038	13.7792
Cyclopentane	0.0013	0.0012	0.0010	0.0010	0.0010	0.0008	0.0009	0.0007	0.0007	0.0007	0.0006	0.0006	0.0006	0.0006	0.0006	0.0005
i-Pentane	0.1087	0.1167	0.1348	0.1444	0.1432	0.1541	0.1998	0.1941	0.2035	0.2050	0.2083	0.2100	0.2162	0.2177	0.2338	0.2246
n-Pentane	0.0879	0.0948	0.0970	0.1022	0.1067	0.1147	0.1499	0.1478	0.1533	0.1561	0.1558	0.1565	0.1554	0.1545	0.1513	0.1480
Cyclohexane	0.0012	0.0013	0.0013	0.0013	0.0012	0.0013	0.0011	0.0009	0.0008	0.0009	0.0009	0.0008	0.0008	0.0009	0.0008	0.0008
i-Hexane	-	0.1810	0.1902	0.1842	0.1787	0.1793	0.1509	0.1362	0.1345	0.1337	0.1245	0.1234	0.1236	0.1235	0.0990	0.0969
n-Hexane	0.0885	0.1045	0.1118	0.1169	0.1178	0.1224	0.1282	0.1213	0.1242	0.1223	0.1196	0.1276	0.1231	0.1217	0.1289	0.1248
Cycloheptane	-	-	-	-	-	-	-	-	-	-	-	-	-	-	-	-
i-Heptane	0.0468	0.0473	0.0402	0.0388	0.0365	0.0361	0.0380	0.0354	0.0336	0.0333	0.0319	0.0318	-	0.0314	0.0299	0.0287
n-Heptane	0.1395	0.1488	0.1358	0.1350	0.1337	0.1369	0.1427	0.1305	0.1308	0.1299	0.1269	0.1274	0.1373	0.1387	0.1247	0.1229
Cyclooctane	0.0158	0.0154	0.144	0.0146	0.0146	0.0151	0.0145	0.0133	-	0.0120	-	0.0109	0.0106	0.0105	0.0101	0.0100
i-Octane	0.1045	0.1164	0.1257	0.1389	0.1441	0.1612	0.1683	0.1652	0.1778	0.1941	0.1909	0.2005	0.2065	0.2047	0.2001	0.1974

Table 6.26.3. Carbon Mass Balance for 0.3wt%Pt-0.3wt%Ge/Al_2O_3 (Coimpregnated) (510°C, 110 psig)

Time (hrs)	No. of moles of Carbon In	No. of moles of Carbon Out	Δ Carbon
1.5	2.0288×10^{-4}	1.6467×10^{-4}	3.8214×10^{-5}
4	2.0288×10^{-4}	1.7184×10^{-4}	3.1044×10^{-5}
19.25	2.0288×10^{-4}	1.7438×10^{-4}	2.8504×10^{-5}
22.25	2.0288×10^{-4}	1.7543×10^{-4}	2.7454×10^{-5}
25.25	2.0288×10^{-4}	1.7568×10^{-4}	2.7204×10^{-5}
28.25	2.0288×10^{-4}	1.7567×10^{-4}	2.7214×10^{-5}
43.15	2.0288×10^{-4}	1.7754×10^{-4}	2.5344×10^{-5}
46.2	2.0288×10^{-4}	1.7839×10^{-4}	2.4494×10^{-5}
49.25	2.0288×10^{-4}	1.7901×10^{-4}	2.3874×10^{-5}
52.25	2.0288×10^{-4}	1.7985×10^{-4}	2.3034×10^{-5}
66.9	2.0288×10^{-4}	1.8114×10^{-4}	2.1744×10^{-5}
69.9	2.0288×10^{-4}	1.8283×10^{-4}	2.0054×10^{-5}
73.05	2.0288×10^{-4}	1.8326×10^{-4}	1.9624×10^{-5}
76	2.0288×10^{-4}	1.8411×10^{-4}	1.8774×10^{-5}
91.85	2.0288×10^{-4}	1.8973×10^{-4}	1.3154×10^{-5}
95	2.0288×10^{-4}	1.9114×10^{-4}	1.1744×10^{-5}

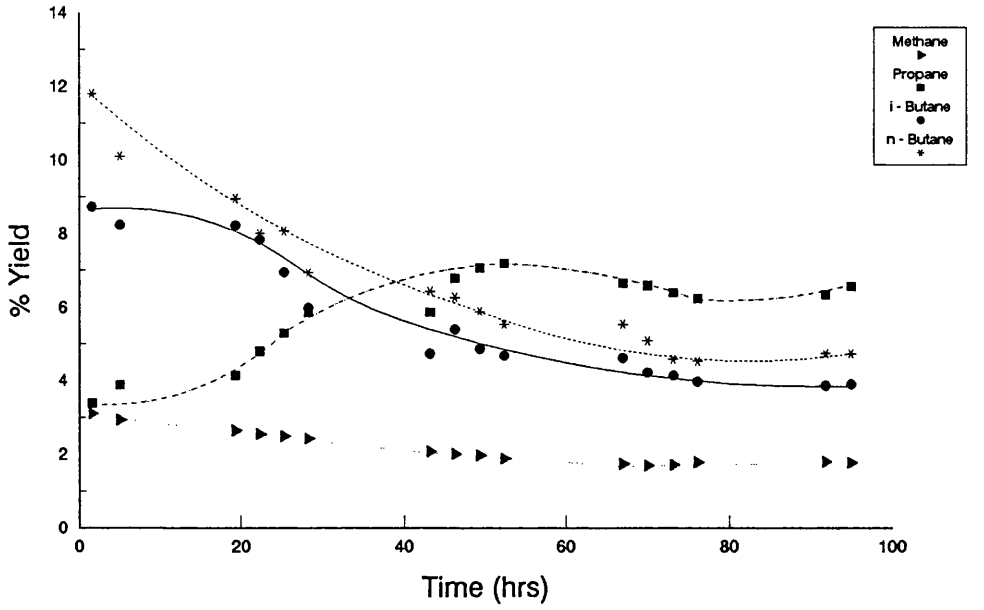

Figure 6.26.1. % Yield of Individual Hydrocarbon Products on 0.3wt%Pt-0.3wt%Ge/Alumina (Coimpregnated)

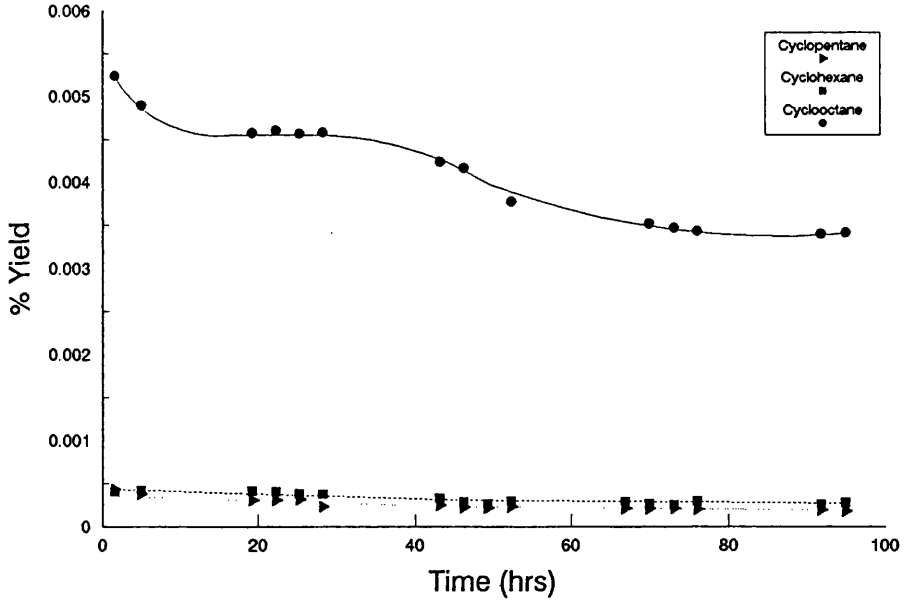

Figure 6.26.2. % Yield of Cycloparaffin Products on 0.3wt%Pt-0.3wt%Ge/ Alumina (Coimpregnated)

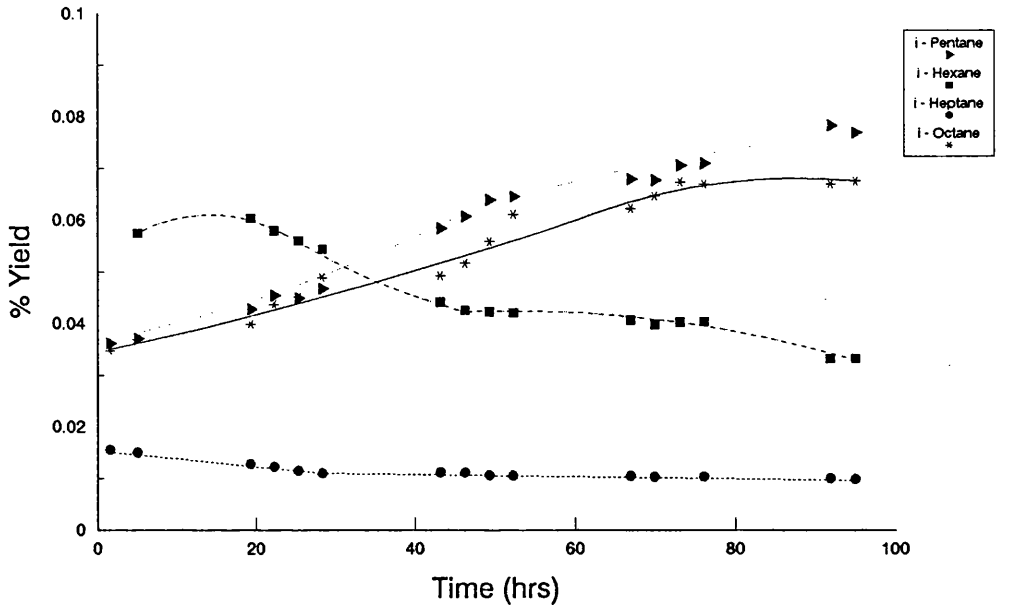

Figure 6.26.3. % Yield of i-Paraffin Products on 0.3wt%Pt-0.3wt%Ge/ Alumina (Coimpregnated)

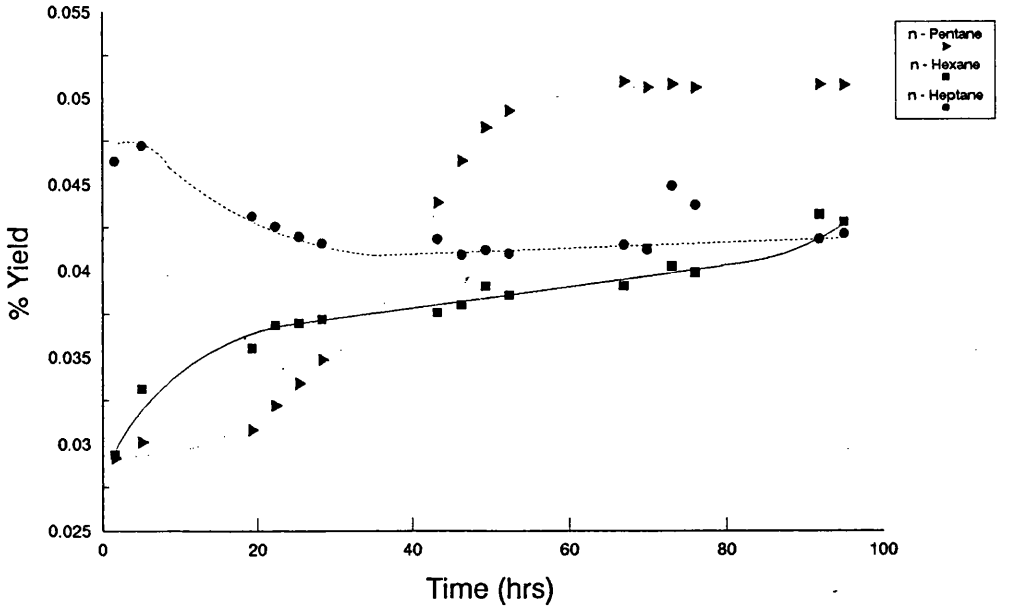

Figure 6.26.4. % Yield of n-Paraffin Products on 0.3wt%Pt-0.3wt%Ge/ Alumina (Coimpregnated)

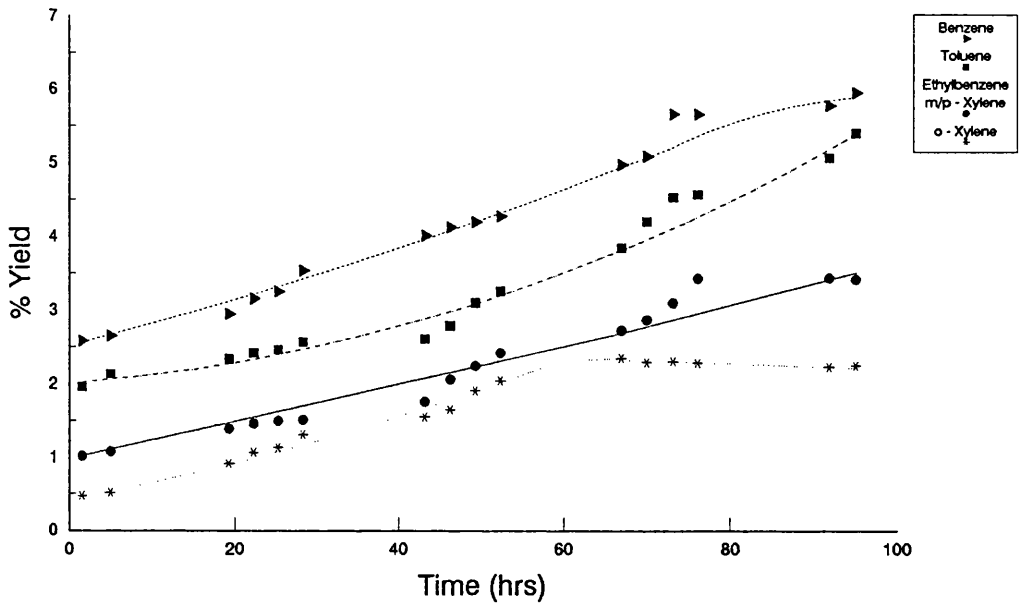

Figure 6.26.5. % Yield of Aromatic Products on 0.3wt%Pt-0.3wt%Ge/ Alumina (Coimpregnated)

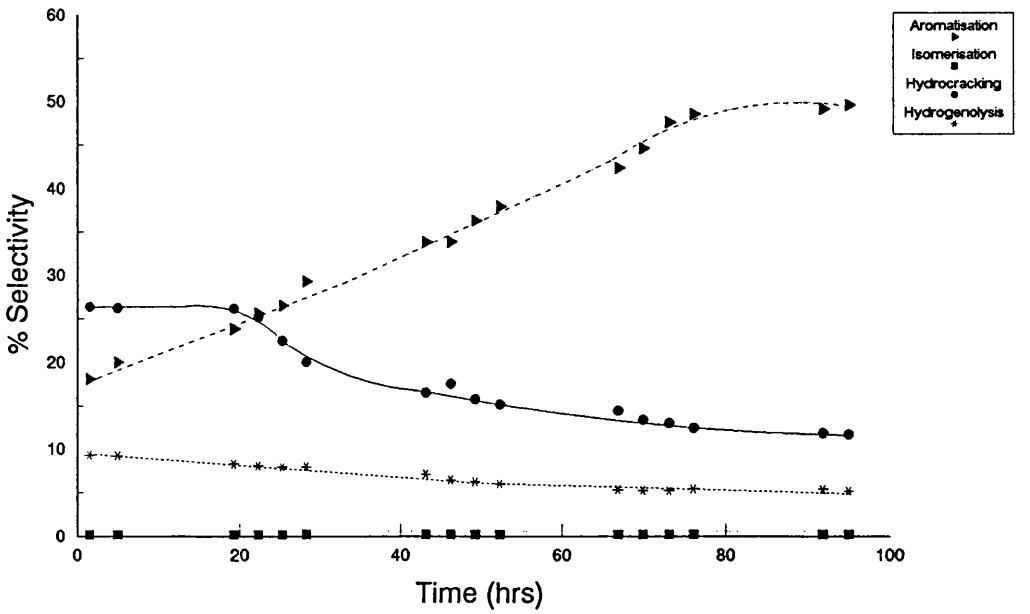

Figure 6.26.6. % Selectivity to the Major Reactions on 0.3wt%Pt-0.3wt%Ge/ Alumina (Coimpregnated)

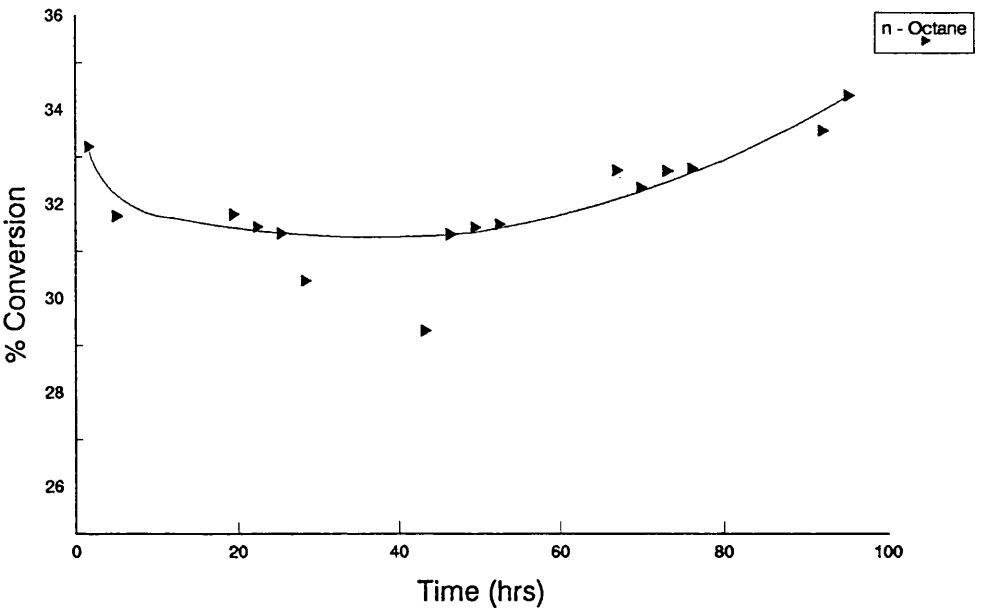

Figure 6.26.7. % Conversion of n-Octane on 0.3wt%Pt-0.3wt%Ge/ Alumina (Coimpregnated)

was that the yield of i-butane was greater than that of n-butane throughout the run by ~1%.

Figures 6.26.2 to 6.26.4 illustrate the variation of cyclo-, i- and n-paraffins with time. The yield of cycloparaffins, Figure 6.26.2, decreases with reaction time and with decreasing carbon number. Figure 6.26.3 details the yields of i-paraffins with time. The yield of i-pentane and i-octane increases while that of i-hexane and i-heptane decrease before reaching a constant value. The yield of both n-pentane and n-hexane increase with time while the yield of n-heptane decreases in the first 30 hours before increasing steadily. The yield of n-paraffins decreases with increasing carbon number at the end of the reforming run.

The yield of aromatic species increases with time as shown in Figure 6.26.5. The yield of C_8 aromatic species again is lower than either benzene or toluene. The aromatic yield decreases in the order from benzene, toluene, ethylbenzene/m/p-xylene to o-xylene. The yield of C_8 aromatic species on this catalyst has improved in comparison with the catalysts in Sections 6.24 and 6.25. The yield of benzene and toluene has increased when compared with the germanium impregnated first catalyst but is similar to the platinum impregnated first catalyst.

The selectivity to the individual hydrocarbon products is summarised in Table 6.26.2. The selectivity to the major reactions is presented in Figure 6.26.5. The selectivity of isomerisation and aromatisation reactions increase to 0.2 and 50% respectively while the activity of hydrocracking and hydrogenolysis reactions fall to

12 and 5% respectively. The aromatisation activity is significantly higher with this coimpregnated catalyst than with either catalyst prepared by sequential impregnation. The hydrogenolysis activity in comparison is approximately the same.

The propane to methane ratio initially increases before declining gradually suggesting carbon deposition takes place on the metallic sites initially. The carbon mass balance shows that the carbon deposition increases in the first 40 hours before decreasing with time as expected.

The total conversion of n-octane increases with time to ~ 34% after 95 hours on stream. This conversion is once again higher than that with a monometallic EUROPT-3.1 catalyst but is less than that with the bimetallic EUROPT-4.1 catalyst under the same conditions. The % coke, shown in Table 6.1, is 4.93% by weight. This value is very low when compared with that of the other Pt-Ge/Al_2O_3 catalysts. Indeed this catalyst produces the least amount of coke seen on any non sulphided catalyst.

6.27. 1.0wt%Pt-1.0wt%Ge/Al_2O_3 - Ge impregnated first (510°C, 110 psig)

The catalyst was tested again under conditions described in Section 6.1. Results from this reforming run are reported in Figures 6.27.1 to 6.27.6 and in Tables 6.27.1 to 6.27.3.

Table 6.27.1. % Yield of individual products and % Conversion versus time on stream for 1.0wt%Pt-1.0wt%Ge/Al_2O_3 (Ge impregnated first).

Products	% Yield of Selected Products												
Time (hrs)	1.5	4.5	19.75	22.68	25.75	28.67	44.2	47	49.9	52.75	68.33	71.33	74.45
Benzene	3.8971	3.2037	3.1444	2.7639	6.8371	2.7132	2.6651	2.6715	2.4248	2.2121	2.1734	2.1666	1.9315
Toluene	3.3781	3.1129	2.7737	2.5402		2.0107	1.6345	1.4405	1.3052	1.1890	1.2345	1.2765	1.2342
Ethylbenzene	0.1541	0.1386	0.0685	0.0551		0.0512	0.0398	0.0354	0.0297	0.0266	0.0163	0.0158	0.0163
m/p-Xylene													
o-Xylene	-	0.0233	0.0174	0.0167		0.0146	0.0104	0.0096	0.0094	0.0085	0.0075	0.0072	0.0071
Methane	1.6922	1.5257	1.2700	1.2530	1.3253	1.0775	0.7296	0.7366	0.8023	0.7348	0.7087	0.6772	0.7192
Ethane	-	-	-	-	0.0008	-	-	0.0005	0.0005	-	-	-	-
Propane	-	3.8952	3.0707	2.4658	2.5175	2.8444	2.8340	2.8243	2.5507	2.6320	2.5656	2.4003	2.4402
i-Butane	5.0416	5.2061	3.9312	3.8958	4.1759	4.0217	3.7522	3.8146	3.6167	3.2284	3.2283	3.3210	3.3627
n-Butane	11.1648	10.2543	6.7951	6.0610	6.4351	6.0975	6.4090	5.9743	5.7686	5.7819	5.5593	5.4253	5.3326
Cyclopentane	0.0004	0.0003	0.0003	0.0003	0.0003	0.0003	0.0003	0.0003	0.0003	0.0003	0.0002	0.0002	0.0002
i-Pentane	0.0569	0.0536	0.0458	0.0453	0.0441	0.0466	0.0438	0.0455	0.0431	0.0394	0.0384	0.0385	0.0399
n-Pentane	0.0405	0.0417	0.0357	0.0349	0.0364	0.0361	0.0353	0.0351	0.0335	0.0322	0.0303	0.0307	0.0287
Cyclohexane	0.0004	0.0005	0.0039	0.0003	0.0003	0.0003	0.0002	0.0002	0.0002	0.0002	0.0002	0.0002	0.0002
i-Hexane	0.0270	0.0267	0.0238	0.0228	0.0235	0.0219	0.0224	0.0220	0.0204	0.0188	0.0177	0.0170	0.0171
n-Hexane													
Cycloheptane	0.0007	0.0004	-	0.0004	0.0004	0.0004	-	0.0003	0.0002	0.0003	0.0002	-	0.0002
i-Heptane	0.0165	0.0163	0.0156	0.0146	0.0148	0.0146	0.0138	0.0145	0.0144	0.0140	0.0128	0.0134	0.0127
n-Heptane													
Cyclooctane	0.0003	0.0004	0.0004	0.0005	0.0005	0.0006	0.0007	0.0008	0.0006	0.0006	0.0006	0.0006	0.0006
i-Octane	0.0515	0.0500	0.0388	0.0386	0.0388	0.0376	0.0329	0.0321	0.0306	0.0274	0.0179	0.0174	0.0173
% Conversion of n-Octane	25.5221	27.5497	21.2318	19.2992	21.4509	18.9891	18.2240	17.6580	16.6513	15.9466	15.6119	15.4078	15.1608

Table 6.27.2. % Selectivity of individual products versus time on stream for 1.0wt%Pt-1.0wt%Ge/Al_2O_3 (Ge impregnated first).

Products	% Selectivity of Selected Products												
Time (hrs)	1.5	4.5	19.75	22.68	25.75	28.67	44.2	47	49.9	52.75	68.33	71.33	74.45
Benzene	15.2694	11.6287	14.8100	14.3215		14.2883	14.6240	15.1291	14.5623	13.8722	13.9215	14.0617	12.7403
Toluene	13.2360	11.2994	13.0639	13.1622	31.8732	10.5886	8.9691	8.1577	7.8387	7.4560	7.9071	8.2846	8.1409
Ethylbenzene	0.6036	0.5032	0.3227	0.2854		0.2696	0.2183	0.2003	0.1785	0.1666	0.1044	0.1022	0.1078
m/p-Xylene													
o-Xylene	-	0.0847	0.0820	0.0866		0.0768	0.0569	0.0543	0.0566	0.0534	0.0483	0.0470	0.0470
Methane	6.6303	5.5380	5.9817	6.4925	6.1783	5.6744	4.0037	4.1717	4.8184	4.6082	4.5392	4.3955	4.7437
Ethane	-	-	-	-	0.0039	-	-	0.0026	0.0027	-	-	-	-
Propane	-	14.1387	14.4629	12.7769	11.7363	14.9792	15.5510	15.9947	15.3183	16.5054	16.4338	15.5786	16.0954
i-Butane	19.7537	18.8971	18.5156	20.6529	19.4672	21.1792	20.5895	21.6025	21.7204	20.2452	20.6783	21.5540	22.1804
n-Butane	43.7457	37.2211	32.0046	31.4055	29.9993	32.1107	35.1679	33.8336	34.6437	36.2577	35.6095	35.2110	35.1734
Cyclopentane	0.0015	0.0010	0.0013	0.0015	0.0013	0.0014	0.0018	0.0015	0.0016	0.0016	0.0014	0.0014	0.0013
i-Pentane	0.2229	0.1946	0.2158	0.2345	0.2057	0.2454	0.2406	0.2575	0.2588	0.2473	0.2462	0.2500	0.2629
n-Pentane	0.1588	0.1515	0.1680	0.1806	0.1696	0.1962	0.1936	0.1985	0.2010	0.2017	0.1940	0.1992	0.1894
Cyclohexane	0.0017	0.0017	0.0018	0.0016	0.0016	0.0014	0.0012	0.0011	0.0012	0.0014	0.0012	0.0012	0.0011
i-Hexane	0.1060	0.0970	0.1119	0.1180	0.1094	0.1154	0.1228	0.1247	0.1228	0.1182	0.1131	0.1103	0.1130
n-Hexane													
Cycloheptane	0.0026	0.0016	-	0.0022	0.0018	0.0019	-	0.0017	0.0014	0.0017	0.0015	-	0.0014
i-Heptane	0.0647	0.0593	0.0734	0.0757	0.0691	0.0767	0.0756	0.0820	0.0864	0.0881	0.0822	0.0866	0.0841
n-Heptane													
Cyclooctane	0.0013	0.0013	0.0019	0.0025	0.0023	0.0030	0.0037	0.0040	0.0038	0.0040	0.0039	0.0036	0.0037
i-Octane	0.2019	0.1815	0.1826	0.1999	0.1811	0.1979	0.1804	0.1820	0.1835	0.1715	0.1144	0.1130	0.1142

Table 6.27.3. Carbon Mass Balance for 1.0wt%Pt-1.0wt%Ge/Al_2O_3 (Ge impregnated first) (510°C, 110 psig)

Time (hrs)	No. of moles of Carbon In	No. of moles of Carbon Out	Δ Carbon
1.5	3.1255×10^{-4}	2.9509×10^{-4}	1.7460×10^{-5}
4.5	3.1255×10^{-4}	2.9764×10^{-4}	1.4915×10^{-5}
19.75	3.1255×10^{-4}	2.9817×10^{-4}	1.4382×10^{-5}
22.67	3.1255×10^{-4}	3.0104×10^{-4}	1.1509×10^{-5}
25.75	3.1255×10^{-4}	2.9885×10^{-4}	1.3699×10^{-5}
28.67	3.1255×10^{-4}	3.0074×10^{-4}	1.1814×10^{-5}
44.2	3.1255×10^{-4}	3.0146×10^{-4}	1.1095×10^{-5}
47	3.1255×10^{-4}	3.0149×10^{-4}	1.1057×10^{-5}
49.9	3.1255×10^{-4}	3.0255×10^{-4}	9.9967×10^{-6}
52.75	3.1255×10^{-4}	3.0263×10^{-4}	9.9227×10^{-6}
68.33	3.1255×10^{-4}	3.0356×10^{-4}	8.9887×10^{-6}
71.33	3.1255×10^{-4}	3.0413×10^{-4}	8.4181×10^{-6}
74.45	3.1255×10^{-4}	3.1039×10^{-4}	2.1557×10^{-6}

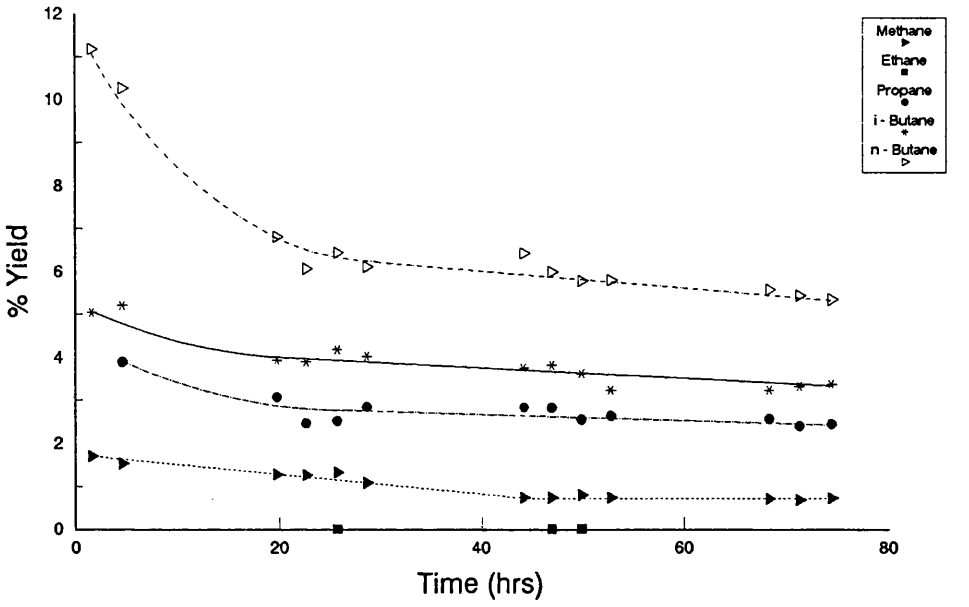

Figure 6.27.1. % Yield of Individual Hydrocarbon Products on a 1.0wt%Pt-1.0wt%Ge/Alumina (Ge impregnated first)

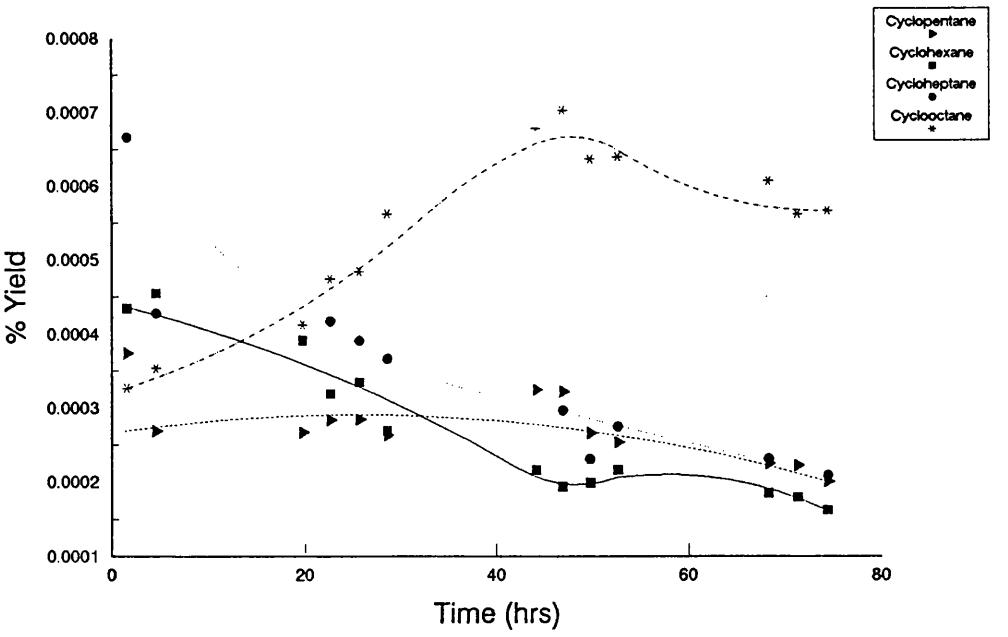

Figure 6.27.2. % Yield of Cycloparaffin Products on a 1.0wt%Pt-1.0wt%Ge/ Alumina (Ge impregnated first)

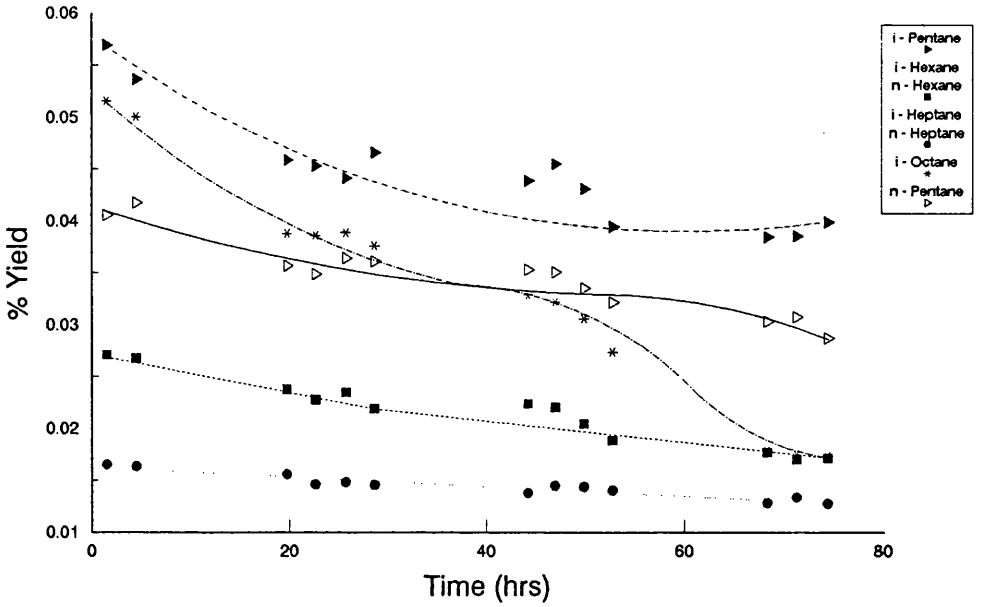

Figure 6.27.3. % Yield of i- and n-Paraffin Products on a 1.0wt%Pt-1.0wt%Ge/Alumina (Ge impregnated first)

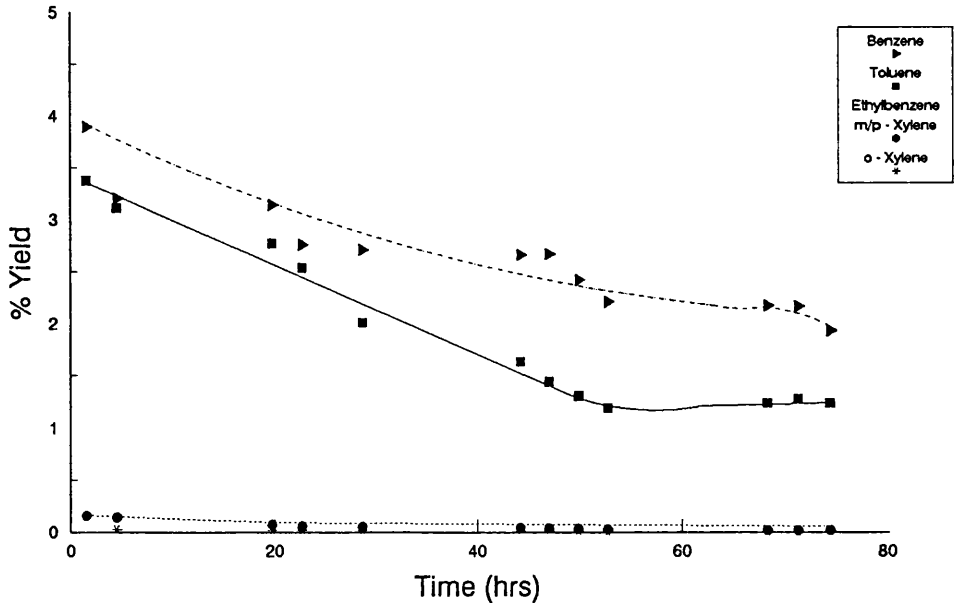

Figure 6.27.4. % Yield of Aromatic Products on a 1.0wt%Pt-1.0wt%Ge/ Alumina (Ge impregnated first)

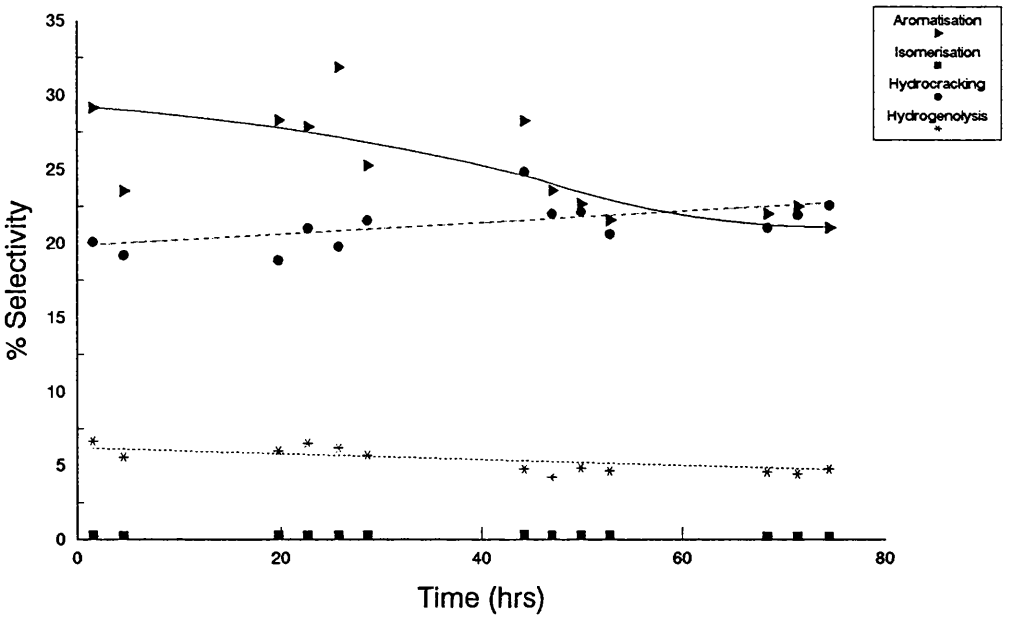

Figure 6.27.5. % Selectivity to the Major Reactions on a 1.0wt%Pt-1.0wt%Ge/Alumina (Ge impregnated first)

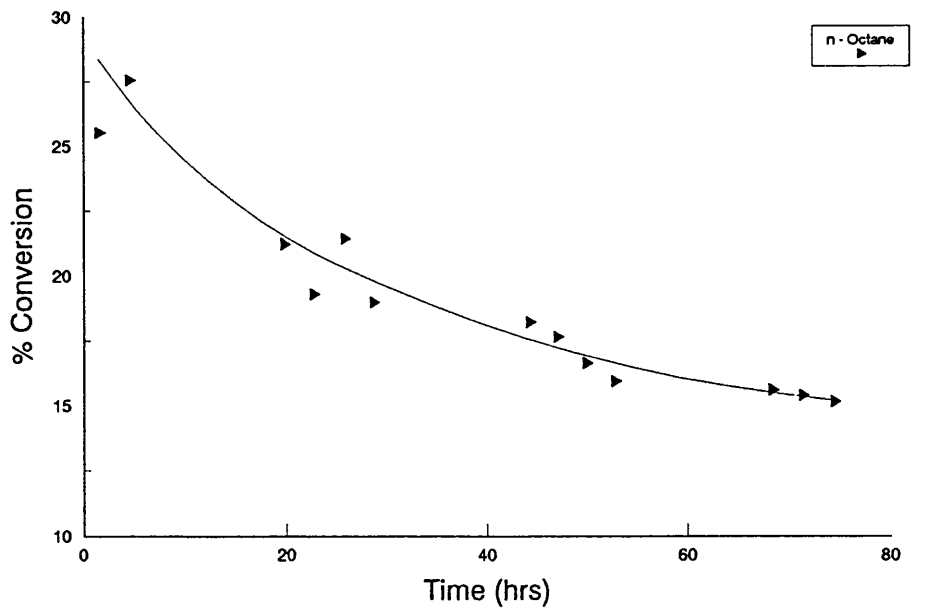

Figure 6.27.6. % Conversion of n-Octane on a 1.0wt%Pt-1.0wt%Ge/ Alumina (Ge impregnated first)

The yield of C_1 - C_4 species decreases with time in Figure 6.27.1. In this reforming run ethane was found in very low concentrations throughout the run. The yield of methane is again very small and levels out at 0.7%, lower than on the 0.3wt%Pt-0.3wt%Ge/Al_2O_3 catalysts. The yield of propane has also fallen when compared to these catalysts. The yield of n-butane levels out at ~5.4%, which is approximately 1.6 times that of i-butane.

The yield of cycloparaffins is shown in Figure 6.27.2. The yield of cyclooctane increases with time through a maximum after ~50 hours before decreasing slowly. The yields of cyclopentane, cyclohexane and cycloheptane all decrease with time. The yields of the combined i- and n-paraffins are quoted in Figure 6.27.3 as the species could not be separated in the experiment. The yields of all combined species and i-octane decrease with time and the combined species decrease with increasing carbon number.

Figure 6.27.4 illustrates the decreasing yield of all aromatic products with the reaction time. The yield of aromatic species on this catalyst is significantly smaller than on a 0.3wt%Pt-0.3wt%Ge/Al_2O_3 catalyst. The yield of benzene and toluene are significantly lower at 1.9 and 1.3% respectively when the reaction was stopped.

Table 6.27.2 illustrates the selectivity of this catalyst to the individual hydrocarbon species. The selectivity to the major reactions is shown in Figure 6.27.5. The aromatisation, hydrogenolysis and isomerisation reactions all decrease while the activity of hydrocracking reaction increases with time. Aromatisation

activity falls from 29 to 21% over the 75 hours on stream. This was the lowest value seen for aromatisation reactions on any Pt-Ge/Al_2O_3 catalyst. Hydrocracking reactions become dominant after 60 hours on stream when they increase to a higher level, 23%, than aromatisation reactions. Hydrogenolysis activity is again between 4 and 5%, which is typical of all the Pt-Ge/Al_2O_3 catalysts tested.

The propane to methane ratio increases initially with time before decreasing slowly suggesting that coke is deposited upon the metallic sites preferentially. Coke is then deposited upon the support after ~60 hours in this reaction. The carbon mass balance illustrates that carbon deposition decreases with time as less sites become available for coking.

The total n-octane conversion decreases with time over this catalyst as seen in Figure 6.27.6. The conversion falls from a value of 25 - 15% in 75 hours. This catalyst has shown to have a lower conversion than a corresponding 0.3wt%Pt-0.3wt%Ge/Al_2O_3 catalyst. The % coke deposited upon this catalyst is 8.60% by weight.

6.28. 0.3wt%Ge/Al_2O_3 (510°C, 110 psig)

This monometallic catalyst was tested again under conditions described in Section 6.1. Results from this reforming run are reported in Figures 6.28.1 to 6.28.7 and in Tables 6.28.1 to 6.28.3.

Table 6.28.1. % Yield of individual products and % Conversion versus time on stream for 0.3wt%Ge/Al_2O_3

Products	% Yield of Selected Products													
Time (hrs)	1	3.75	19.5	22.4	25.3	28.2	43.6	46.5	49.5	67.25	70.25	73.25	91.65	94.5
Benzene	0.5359	0.4848	0.4159	0.4223	0.4246	0.4164	0.3914	0.3619	0.3405	0.2998	0.2779	0.2528	0.2381	0.2320
Toluene	0.0635	0.0594	0.0626	0.0595	0.0584	0.0416	0.0418	0.0306	0.0319	0.0261	0.0186	0.0193	-	0.0099
Ethylbenzene	-	0.1485	-	0.0267	0.0195	0.0172	0.0074	0.0061	0.0043	-	0.0034	-	-	0.0037
m/p-Xylene														
o-Xylene	-	-	0.0151	-	0.0082	-	-	-	-	-	-	-	-	-
Methane	1.6298	1.7104	1.5984	1.7082	2.1389	1.9564	1.8591	1.7907	1.5096	1.6588	1.7219	1.6697	1.6663	1.5091
Ethane	-	-	0.0009	-	-	-	-	-	-	-	-	-	-	-
Propane	-	-	1.8878	1.7655	-	-	1.5872	1.3656	-	-	-	-	1.2854	-
i-Butane	2.1082	1.9491	1.5031	1.5414	1.5483	1.3884	1.6867	1.1000	1.0289	1.1397	1.1802	1.1394	1.1186	1.0012
n-Butane	3.2130	3.0335	2.4848	2.4532	2.4262	2.5733	2.0178	2.1516	1.9776	1.9175	1.9870	2.1089	2.0846	1.9249
Cyclopentane	0.0004	0.0002	0.0004	0.0003	0.0004	0.0002	0.0387	0.0430	0.0001	0.0002	0.0388	-	0.0001	-
i-Pentane	0.0461	0.0390	0.0347	0.0406	0.0419	0.0388			0.0388	0.0382		0.0349	0.0290	0.0290
n-Pentane		0.0086	0.0083											
Cyclohexane	-	-	-	-	0.0001	0.0002	0.0004	0.0007	0.0008	-	0.0006	-	-	-
i-Hexane	0.0164	0.0153	0.0153	0.0149	0.0130	0.0124	0.0113	0.0091	0.0088	0.0091	0.0082	0.0081	0.0081	0.0079
n-Hexane	0.0103	0.0124	0.0146	0.0161	0.0186	0.0186	0.0221	0.0199	0.0191	0.0201	0.0201	0.0169	0.0196	0.0195
Cycloheptane	0.0004	-	-	-	-	-	0.0007	-	-	-	-	-	0.0009	-
i-Heptane	0.0146	0.0146	-	0.0149	0.0139	0.0139	0.0121	-	-	0.0097	0.0097	-	0.0102	0.0099
n-Heptane	0.0183	0.0181	0.0207	0.0155	0.0147	0.0164	0.0166	0.0183	0.0208	0.0185	0.0215	0.0226	0.0226	0.0221
Cyclooctane	0.0217	0.0213	0.0216	0.0212	0.0215	0.0212	0.0211	0.0215	0.0221	0.0219	0.0226	0.0228	0.0217	0.0206
i-Octane														
% Conversion of n-Octane	7.6786	7.5153	8.0842	8.1003	6.7483	6.5152	7.1147	6.9185	5.0034	5.1597	5.3104	5.2954	6.5053	4.7897

Table 6.28.2. % Selectivity of individual products versus time on stream for 0.3wt%Ge/Al_2O_3

Products	% Selectivity of Selected Products													
Time (hrs)	1	3.75	19.5	22.4	25.3	28.2	43.6	46.5	49.5	67.25	70.25	73.25	91.65	94.5
Benzene	6.97969	6.4514	5.1449	5.2128	6.2925	6.3917	5.5018	5.2308	6.8048	5.8110	5.2337	4.7749	3.6595	4.8443
Toluene	0.8274	0.7905	0.7742	0.7344	0.8653	0.6390	0.5878	0.4423	0.6374	0.5060	0.3495	0.3639	-	0.2057
Ethylbenzene	-	1.9756	-	0.3295	0.2882	0.2642	0.1035	0.0886	0.0858	-	0.0641	-	-	0.0763
m/p-Xylene														
o-Xylene	-	-	0.1872	-	0.1210	-	-	-	-	-	-	-	-	-
Methane	21.2247	22.7589	19.7723	21.0884	31.6958	30.0283	26.1305	25.8833	30.1720	32.1498	32.4245	31.5307	25.6143	31.5068
Ethane	-	-	0.0109	-	-	-	-	-	-	-	-	-	-	-
Propane	-	-	23.3514	21.7953	-	-	22.3094	19.7382	-	-	-	-	19.7600	-
i-Butane	27.4561	25.9356	18.5934	19.0288	22.9443	21.3102	15.2747	15.8996	20.5641	22.0880	22.2237	21.5161	17.1946	20.9034
n-Butane	41.8430	40.3644	30.7363	30.2847	35.9530	39.4962	28.3617	31.0909	39.5258	37.1633	37.4161	39.8257	32.0454	40.1885
Cyclopentane	0.0048	0.0031	0.0047	0.0393	0.0062	0.0036	0.5445	0.6210	0.0016	0.0031	0.7310	-	0.0018	-
i-Pentane	0.6000	0.5192	0.4295	0.5015	0.6213	0.5960			0.7757	0.7400		0.6589	0.4464	0.6052
n-Pentane		0.1150	0.1032											
Cyclohexane	-	-	-	-	0.0219	0.0036	0.0052	0.0103	0.0161	-	0.0119	-	-	-
i-Hexane	0.2141	0.2037	0.1888	0.1845	0.1934	0.1908	0.1589	0.1320	0.1775	0.1772	0.1539	0.1533	0.1249	0.1645
n-Hexane	0.1341	0.1645	0.1801	0.1988	0.2750	0.2847	0.3104	0.2879	0.3809	0.3900	0.3786	0.3198	0.3006	0.4075
Cycloheptane	0.0046	-	-	-	-	-	0.0103	-	-	-	-	-	0.0143	-
i-Heptane	0.1900	0.1944	-	0.1839	0.2055	0.2133	0.1705	-	-	0.1872	0.1833	-	0.1574	0.2072
n-Heptane	0.2387	0.2404	0.2555	0.1913	0.2174	0.2523	0.2337	0.2640	0.4161	0.3593	0.4045	0.4270	0.3472	0.4606
Cyclooctane	0.2830	0.2832	0.2674	0.2621	0.3189	0.3261	0.2971	0.3110	0.4421	0.4250	0.4253	0.4297	0.3338	0.4300
i-Octane														

Table 6.28.3. Carbon Mass Balance for 0.3wt%Ge/Al_2O_3 (510°C, 110 psig)

Time (hrs)	No. of moles of Carbon In	No. of moles of Carbon Out	Δ Carbon
1	2.4859×10^{-4}	2.1888×10^{-4}	2.9719×10^{-5}
3.75	2.4859×10^{-4}	2.1898×10^{-4}	2.9619×10^{-5}
19.5	2.4859×10^{-4}	2.2090×10^{-4}	2.7693×10^{-5}
22.4	2.4859×10^{-4}	2.2190×10^{-4}	2.6691×10^{-5}
25.3	2.4859×10^{-4}	2.2046×10^{-4}	2.8139×10^{-5}
28.2	2.4859×10^{-4}	2.2110×10^{-4}	2.7499×10^{-5}
43.6	2.4859×10^{-4}	2.2847×10^{-4}	2.0125×10^{-5}
46.5	2.4859×10^{-4}	2.3115×10^{-4}	1.7448×10^{-5}
49.5	2.4859×10^{-4}	2.3173×10^{-4}	1.6860×10^{-5}
67.25	2.4859×10^{-4}	2.3921×10^{-4}	9.3894×10^{-6}
70.25	2.4859×10^{-4}	2.4045×10^{-4}	8.1424×10^{-6}
73.25	2.4859×10^{-4}	2.4205×10^{-4}	6.5495×10^{-6}
91.65	2.4859×10^{-4}	2.4781×10^{-4}	7.8482×10^{-7}
94.5	2.4859×10^{-4}	2.4808×10^{-4}	5.1735×10^{-7}

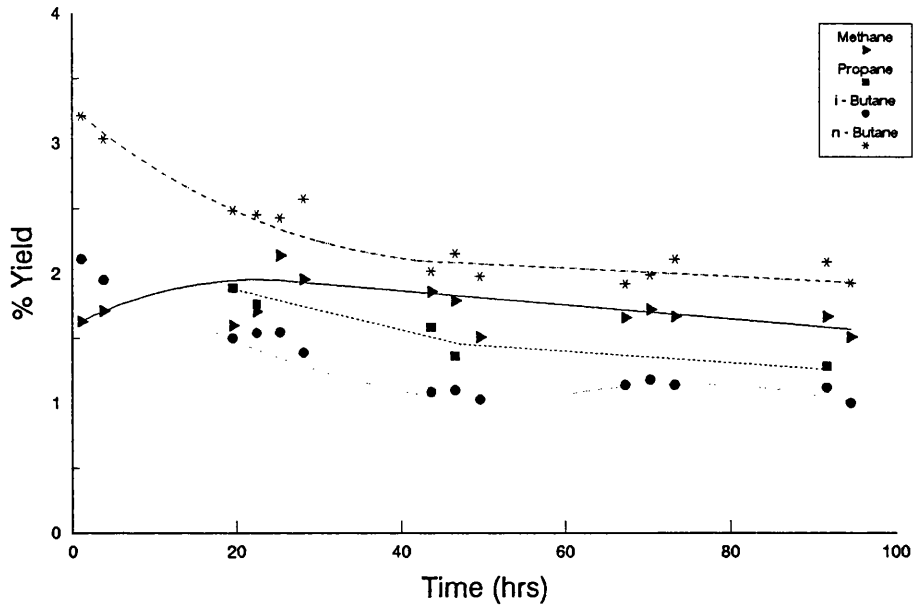

Figure 6.28.1. % Yield of Individual Hydrocarbon Products on 0.3wt%Ge/Alumina

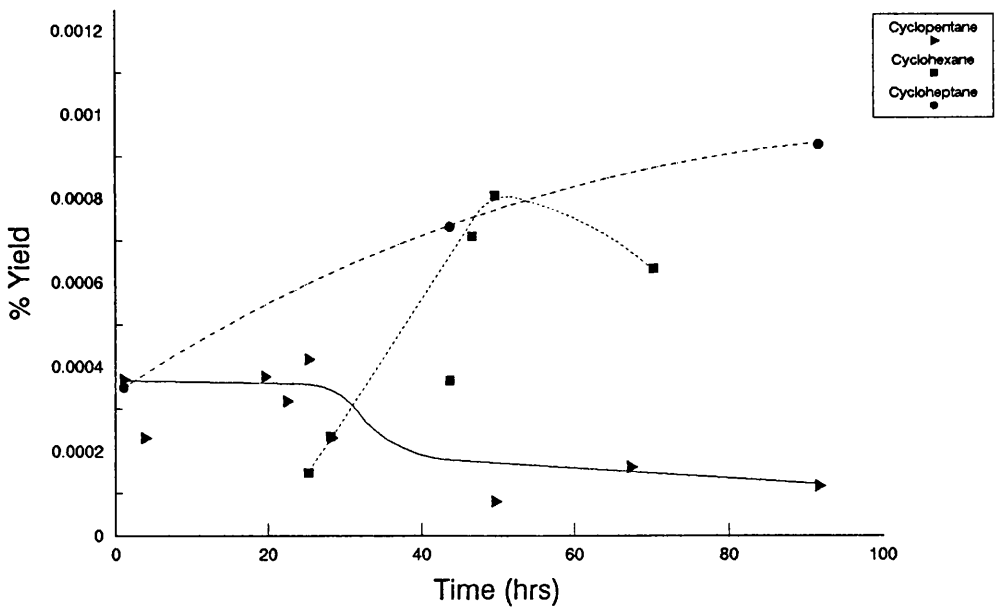

Figure 6.28.2. % Yield of Cycloparaffin Products on 0.3wt%Ge/ Alumina

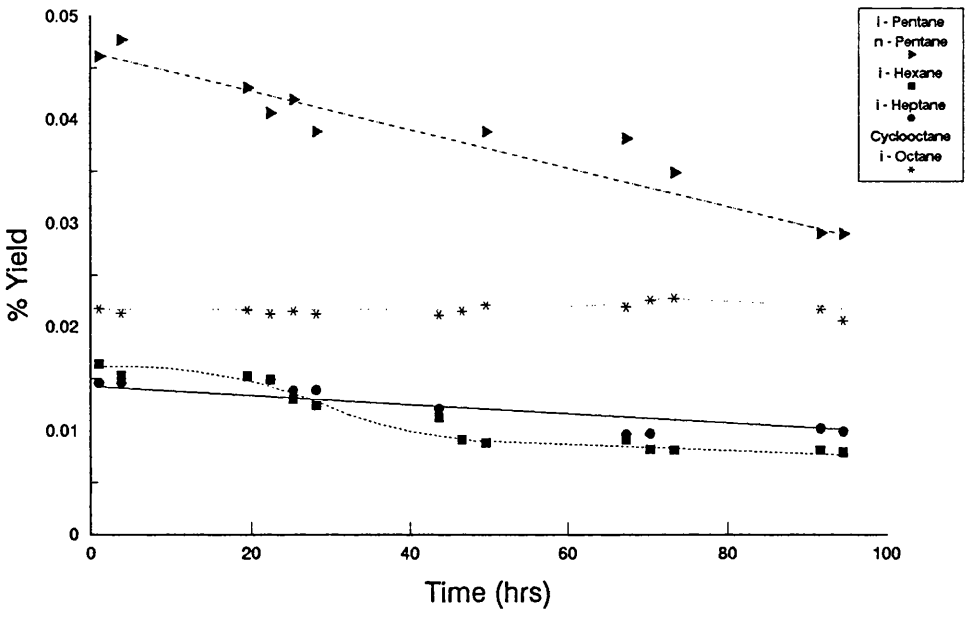

Figure 6.28.3. % Yield of Paraffin Products on 0.3wt%Ge/Alumina

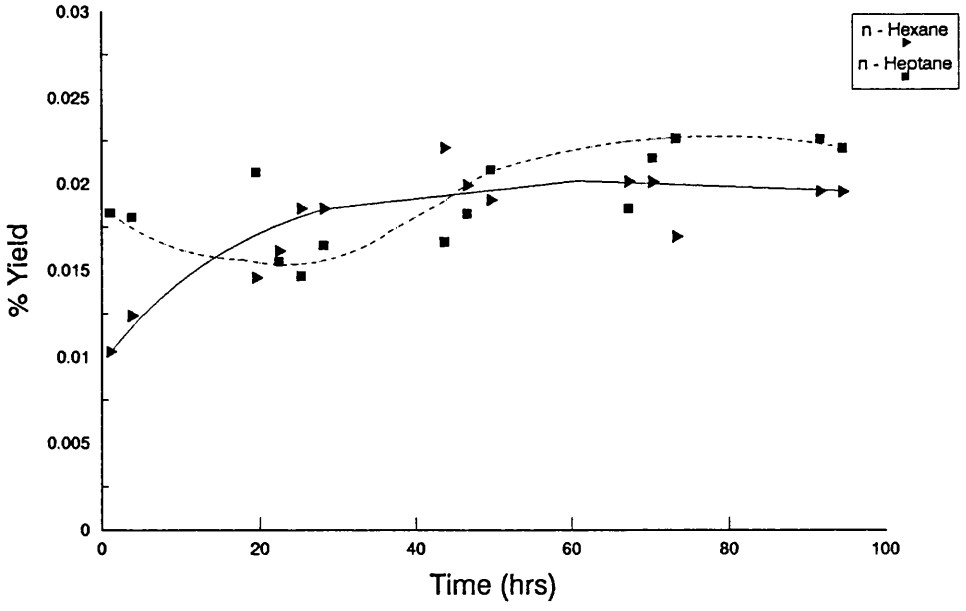

Figure 6.28.4. % Yield of n-Paraffin Products on 0.3wt%Ge/Alumina

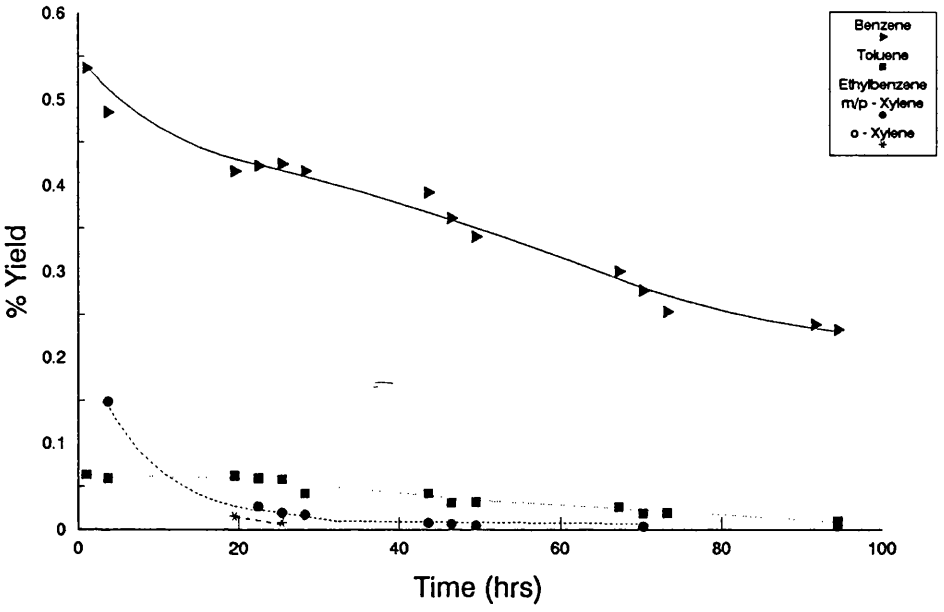

Figure 6.28.5. % Yield of Aromatic Products on 0.3wt%Ge/Alumina

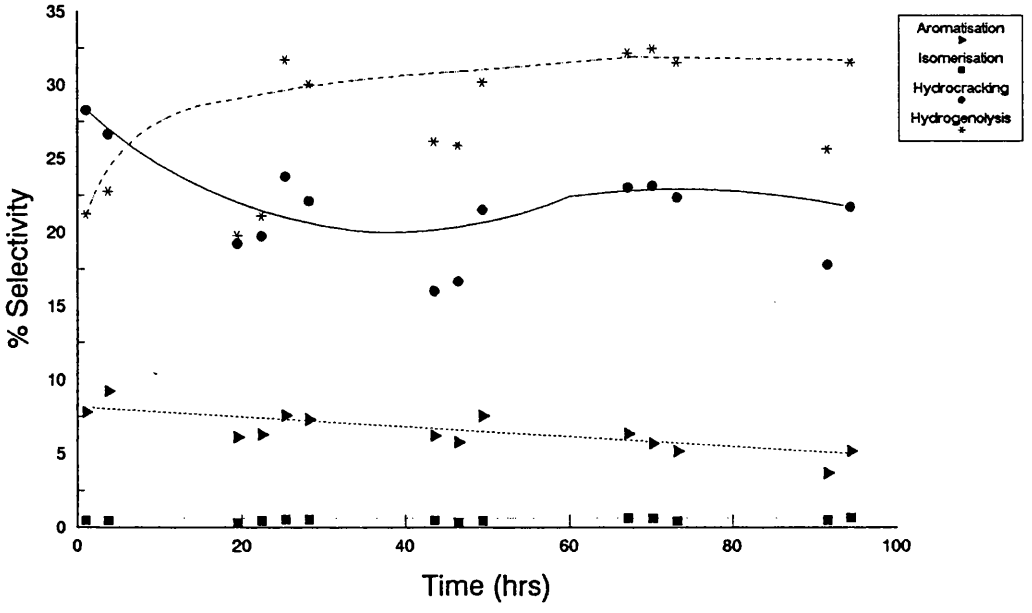

Figure 6.28.6. % Selectivity to the Major Reactions on 0.3wt%Ge/Alumina

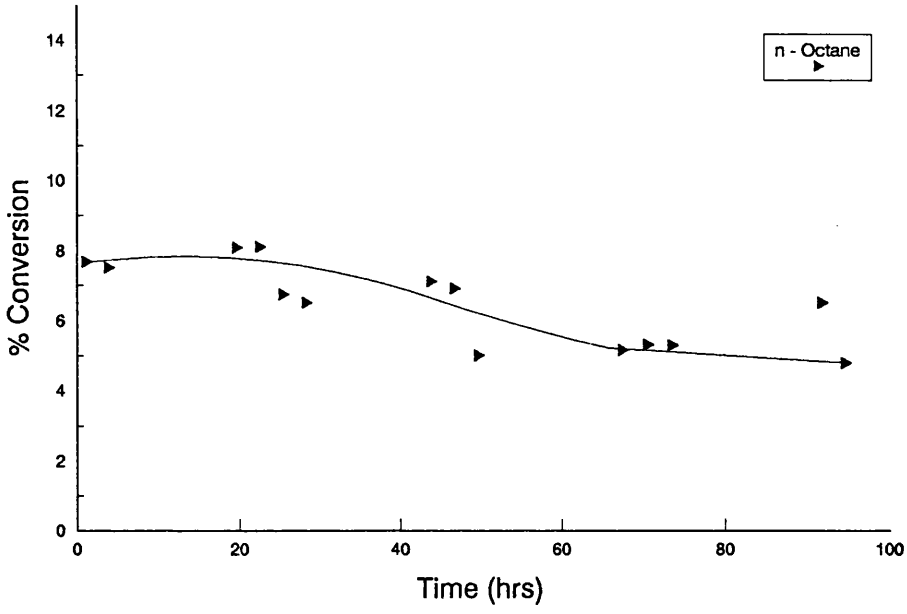

Figure 6.28.7. % Conversion of n-Octane on 0.3wt%Ge/Alumina

The product yields of C_1 - C_4 species are presented in Figure 6.28.1. In this experiment no trace of ethane was found throughout the 95 hours on stream. The yield of methane was very low, always less than 2% and that of propane levels out at 1.3%. The yield of n-butane is approximately twice that of i-butane throughout the run.

Figures 6.28.2 to 6.28.4 illustrate the yields of cycloparaffins, i-paraffins and n-paraffins with time on stream. The yield of cycloparaffins is very small compared to that of i- and n-paraffins. The yield of i-paraffins decreases with time as shown in Figure 6.28.3. The yield of n-paraffins increases with time and with carbon number as detailed in Figure 6.28.4.

The yield of aromatic products is extremely low as illustrated in Figure 6.28.5. The yield of all aromatic products decreases with time. The yield of C_8 aromatic species are particularly small, with o-xylene being undetectable after 25 hours on stream.

The selectivities of the individual hydrocarbon species are presented in Table 6.28.2. The selectivity to the four major reactions is shown in Figure 6.28.6. Hydrogenolysis activity increases initially to ~32% while the hydrocracking activity decreases to 22%. Aromatisation activity falls from 7 to 5% throughout the run while isomerisation activity increases to ~0.7%.

The propane to methane ratio decreases with time indicating that the support is deactivated more than the metal component. The carbon mass balance is typical in that the carbon deposition decreases with time.

The total n-octane conversion decreases to a constant level of ~5% with time. This value is similar to that deposited upon the corresponding monometallic Re or Sn catalyst. The % coke is 5.01%, similar to the amount found to be present upon the coimpregnated Pt-Ge/Al_2O_3 catalyst.

6.29. NITROGEN ADSORPTION

To determine the validity of the results obtained from nitrogen adsorption studies a 'null hypothesis' was devised to evaluate whether the addition of a metal loading to an alumina support could be distinguished from the support itself. The null hypothesis states that there is no difference between the sample and the population mean, i.e., the sample is drawn from the population and any observed difference is due to a sampling error. Therefore a series of repeat experiments was carried out, under identical conditions, on both γ-alumina and 3.0wt%Pt-3.0wt%Re/Al_2O_3 catalyst to test this null hypothesis. The results of these repeat experiments are shown in Table 6.29.1, the values depicting the mean of five independent experiments.

Therefore in these experiments, as $n < 50$, a correction is used to take into account the possible error in estimating the standard deviation, σ, from the normal population distribution by using σ_{n-1} (s). The appropriate distribution when using σ_{n-1}

is better known as the students t-distribution. This is similar to that of the normal distribution as it is symmetrical about zero and approximately bell shaped. However the exact contour of the distribution is determined by the degrees of freedom.

Table 6.29.1. Selected Values Calculated from Nitrogen Adsorption Results

	BET Surface Area (m^2g^{-1})	Cumulative Pore Volume (ccg^{-1})	Mean Pore Diameter (Å)	Median Pore Diameter (Å)
γ-alumina	188.1546	0.5161	138.7394	88.74
σ_{n-1}	3.7784	0.0067	0.8204	1.6402
3.0wt%Pt-3.0wt%Re/Al_2O_3	177.5434	0.4343	138.7792	88.7
σ_{n-1}	2.8755	0.0058	0.6124	1.3078

Therefore in this case on the basis of two samples, the significance of the results may be calculated using the following equations:

$$t = \frac{\bar{x}_1 - \bar{x}_2}{S_p \sqrt{\frac{1}{n_1} + \frac{1}{n_2}}} \qquad (6.1)$$

where

$$S_p^2 = \frac{(n_1 - 1)\, S_1^2 + (n_2 - 1)\, S_2^2}{n_1 + n_2 - 2} \qquad (6.2)$$

where

x_i = the mean value of sample i

n_i = the size of sample i

S_i = the corrected standard deviation, σ_{n-1} , of the sample i

$n_1 + n_2 - 2$ = degrees of freedom

The significance of the results between γ-alumina and 3.0wt%Pt-3.0wt%Re/Al_2O_3 is shown in Table 6.29.2. The critical region is when t > 2.896, i.e., when the difference is due to the presence of metal particles deposited upon the γ-alumina support and not due to a sampling error.

Table 6.29.2. Significance of the Results Between γ-alumina and 3.0wt%Pt-3.0wt%Re/Al_2O_3

	BET Surface Area	Cumulative Pore Volume	Median Pore Diameter	Mean Pore Diameter
S_p^2	11.2723	0.0039	0.5240	17.6029
t	4.9972	20.6724	0.0874	0.0150

Therefore there is a significant difference between the surface area and the cumulative pore volume of γ-alumina and 3.0wt%Pt-3.0wt%Re/Al_2O_3 but not between the pore diameters. As there is no significant difference in the pore diameter it may be assumed that the metal particles in the 3.0wt%Pt-3.0wt%Re/Al_2O_3 catalyst do not block the entrances to the pores but rather fill up the pores instead. This is shown in the values for both the surface area and the cumulative pore

volumes as they decrease significantly from those of the γ-alumina support.

In comparison, the results from EUROPT-3, EUROPT-4 and γ-alumina studies show no significant difference and the null hypothesis therefore holds in these cases.

6.30. MERCURY POROSIMETRY

All the catalysts used in these studies, with the exception of the Pt-Sn (Patent) catalyst, were supported on the same high purity γ-alumina. It was therefore decided to investigate the pore structure of this support and a 3.0wt%Pt-3.0wt%Re/Al_2O_3 catalyst. The 3.0wt%Pt-3.0wt%Re/Al_2O_3 catalyst was investigated to determine the effect of adding a metal loading, to an alumina support, on the pore structure.

The catalyst samples, ~0.5g, were loaded into the porosimeter and evacuated. A pressure was then applied to the penetrometer columns and progressively increased from ~0.48 to ~60 000 psia. As the pressure increased, the cumulative intrusion volume was measured at various points. The cumulative and incremental volume changes for both γ-alumina and 3.0wt%Pt-3.0wt%Re/Al_2O_3 against the applied pressure are illustrated in Figures 6.30.1 to 6.30.4.

From Table 6.30.1 it can be seen that the addition of a 3.0wt% loading of both platinum and rhenium to a γ-alumina support has a dramatic effect upon both the intrusion volume and the total pore area. Both these values decrease significantly

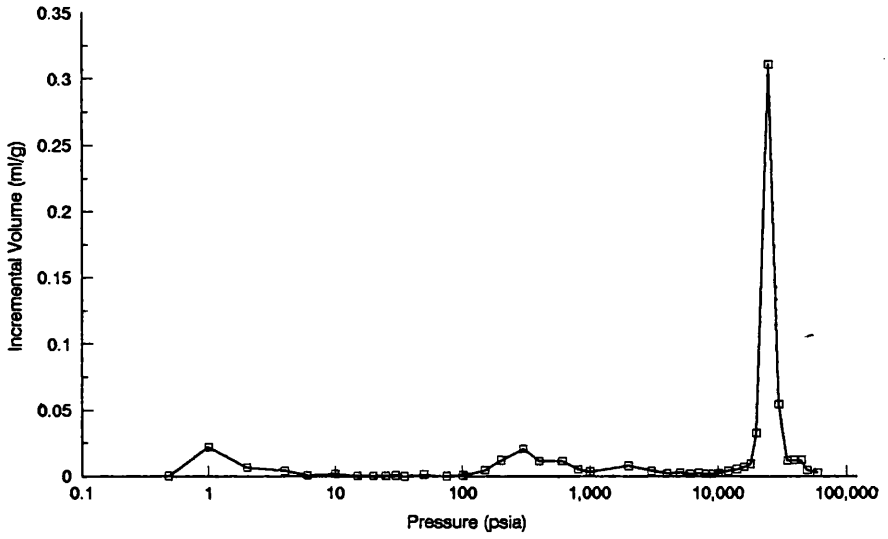

Figure 6.30.1. Incremental mercury intrusion volume versus applied pressure for gamma alumina

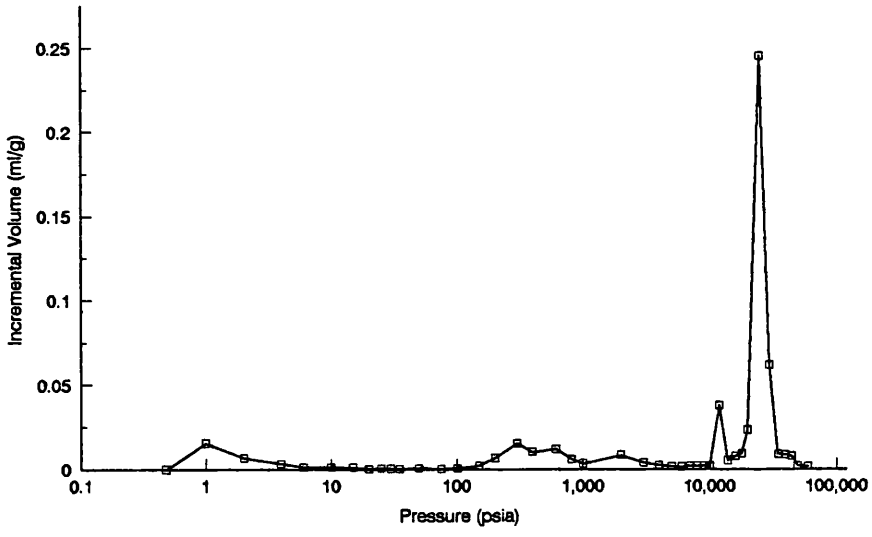

Figure 6.30.2. Incremental mercury intrusion volume versus applied pressure for 3.0%Pt-3.0%Re/Alumina

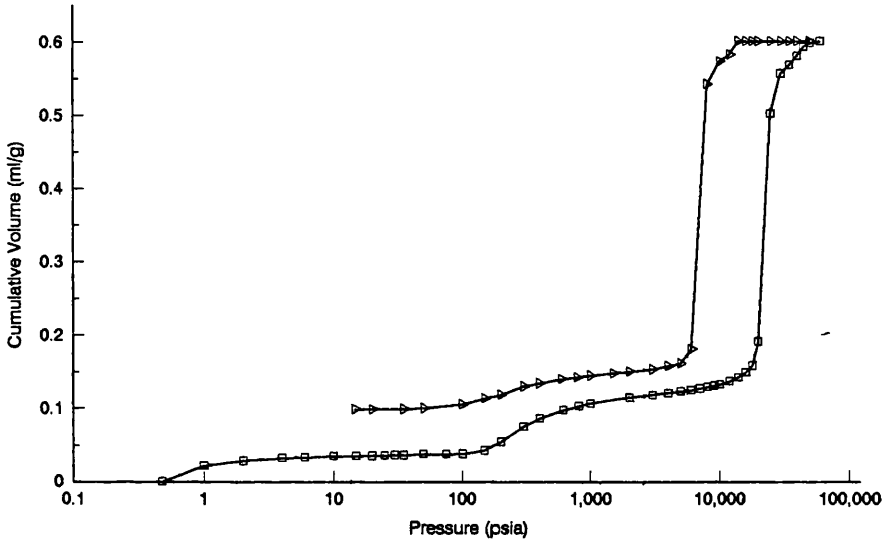

Figure 6.30.3. Cumulative mercury intrusion volume versus applied pressure for gamma alumina

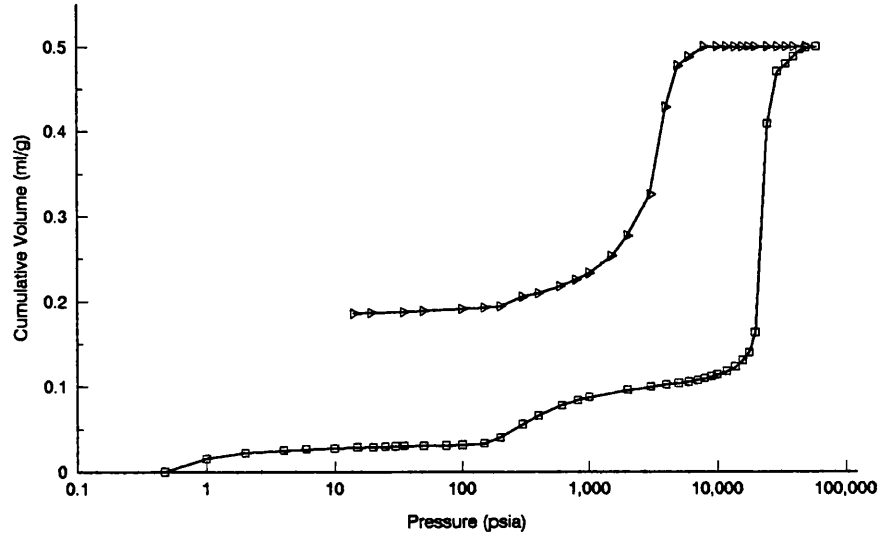

Figure 6.30.4. Cumulative mercury intrusion volume versus applied pressure for 3.0%Pt-3.0%Re/Alumina

due to the presence of metal particles deposited in the pore network of the support.

Table 6.30.1. Summary of the results obtained from Mercury Porosimetry Experiments

	Intrusion Volume	Total Pore Area	Median Pore Diameter (Area)	Median Pore Diameter (Volume)
γ-alumina	0.5919	206.4955	9.35×10^{-3}	9.7×10^{-3}
σ_{n-1}	0.0141	2.9607	7.07×10^{-5}	0
3.0wt%Pt-3.0wt%Re/Al_2O_3	0.4971	171.2315	9.30×10^{-3}	9.7×10^{-3}
σ_{n-1}	3.96×10^{-3}	0.4999	0	0

γ-alumina and 3.0wt%Pt-3.0wt%Re/Al_2O_3 catalysts exhibit very different behaviour as shown in Figures 6.30.3 and 6.30.4. The hysteresis loop of the 3.0wt%Pt-3.0wt%Re/Al_2O_3 catalyst is much broader than that of γ-alumina. The broadening of the hysteresis loop signifies that mercury is having difficulty exiting the material. This suggests that a small amount of mercury is entrapped within the pore network of the alumina support by metal particles. The final volume of mercury which is permanently left behind in the pore network is significantly higher in the bimetallic catalyst than in γ-alumina due to the presence of platinum particles.

Figures 6.30.5 and 6.30.6 illustrate the cumulative pore volume versus the

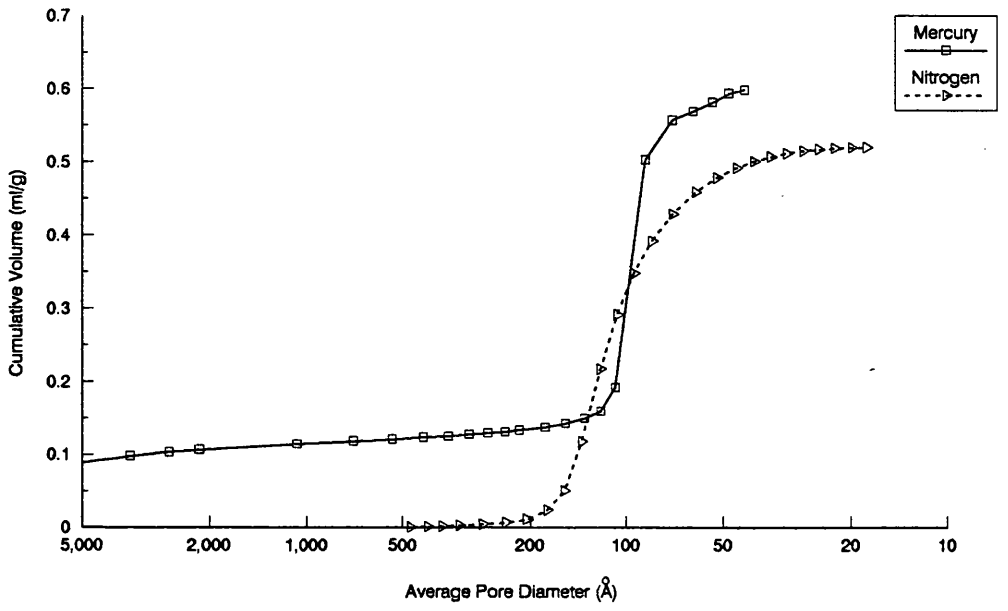

Figure 6.30.5. Comparison of mercury porosimetry and nitrogen adsorption techniques for gamma alumina

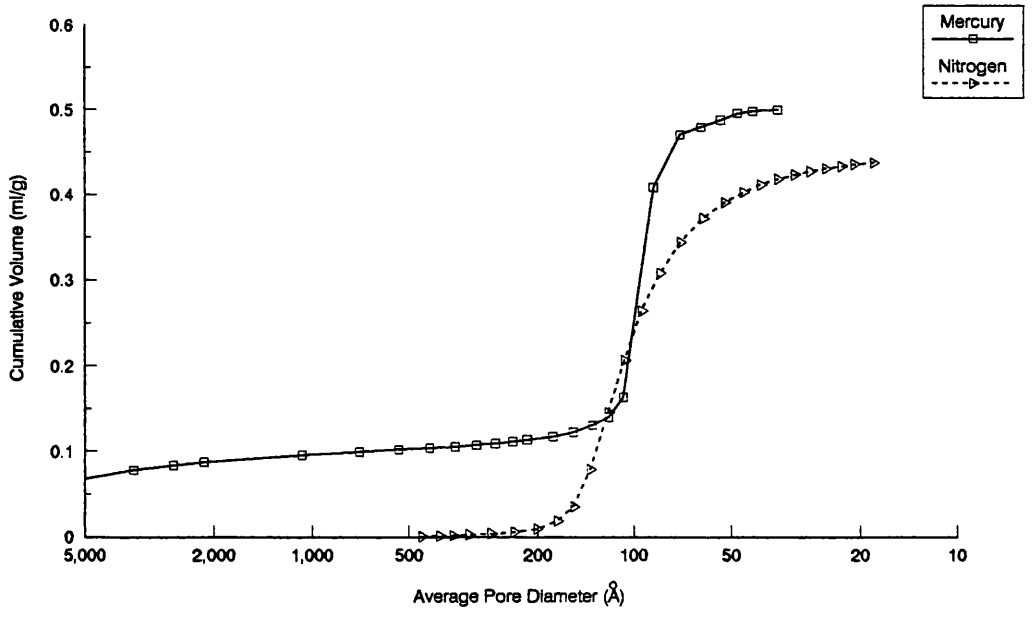

Figure 6.30.6. Comparison of mercury porosimetry and nitrogen adsorption techniques for 3.0%Pt-3.0%Re/Alumina

average pore diameter for both nitrogen adsorption and mercury porosimetry. The two techniques are in close agreement indicating that the catalysts have a uniform pore network.

Overall, comparing the results from both techniques several general conclusions can be reached:

1) When a support material like γ-alumina is impregnated with an aqueous metal solution there is a marked difference in the pore volume and surface area of the resultant catalyst if the loading is high enough. A small metal loading, say 0.3wt%, does not make a considerable difference to the surface area and pore volume whereas a 3.0wt% loading does. The presence of large platinum particles in the pore network is responsible for these differences.

2) The metal particles present in the pore network partially block the pores as shown by the entrapment of mercury during porosimetry experiments.

6.31. ELECTRON MICROSCOPY RESULTS

6.31.1. Pt-Re/Al_2O_3 Catalysts

The results of numerous HRTEM and EDX investigations are summarised in Table 6.31.1. Metal particles, if present, were detected using HRTEM and the composition of these particles ascertained using EDX spectroscopy. EDX spectra have additional signals present due to an alumina support (Al and O signals) and a carbon coated copper TEM grid (Cu and C) being used.

No metal particles were observed in EUROPT-3 after the calcination and reduction steps of the pretreatment. It was not until the catalyst had been used in the microreactor and then examined that platinum particles up to 20 nm in size were detected. EDX and micro-diffraction studies ascertained that these particles were platinum. In comparison small metal particles, 2 - 3 nm, were found to be present after the reduction stage on a EUROPT-4 catalyst. Once again after use in the microreactor particle aggregation occurred and platinum particles of between 10 and 20 nm were found to be present on the catalyst surface. The particle size distribution for both EUROPT catalysts was bimodal with a significant number of metal particles < 5 nm being detected. The platinum particles are very mobile upon the alumina surface under reforming conditions as shown by the particle aggregation. However, no Pt-Re alloy phase could be found on any EUROPT-4 catalyst examined in these studies.

The bimetallic 3.0wt%Pt-3.0wt%Re/Al_2O_3 catalyst was found to have particles

Table 6.31.1. Summary of TEM and EDX Results of Pt-Re/γ-Al_2O_3 Catalysts

	EUROPT-3	EUROPT-4	0.3wt%Re	3.0wt%Re	3.0%Pt3.0%Re Pt imp first
Dried	x	x	x	x	x
Calcined	x	x	x	x	1 - 10 nm Pt few ReO_x
Reduced	x	2 - 3 nm Pt	x	x	1 - 10 nm Pt more small Pt few ReO_2
Calcined	x	2 - 3 nm Pt	x	x	1 - 10 nm Pt
Reduced	x	2 - 4 nm Pt	x	x	1 - 10 nm Pt more small Pt
Reduced to 750°C			x	2 - 10 nm ReO_x	
Spent	1 -20 nm Pt	1 -20 nm Pt			< 100 nm Pt

'x' denotes that no particle was found in the sample

in the range from 1 - 10 nm present after being reduced in hydrogen at 400°C. A few very large particles, > 50 nm, were also observed on this catalyst surface. These particles were examined by EDX and micro-diffraction and were found to consist solely of platinum. A few rhenium oxide particles were detected on the catalyst.

Monometallic 0.3wt% and 3.0wt%Re/Al_2O_3 catalysts were found to resist particle aggregation under calcination and reduction at 400°C. However after reduction at 750°C rhenium or rhenium oxide particles were detected. A quantitative EDX analysis resulted in these particles being labelled as ReO_2 particles on this and the 3.0wt%Pt-3.0wt%Re/Al_2O_3 catalyst. A more detailed analysis of the Pt-Re catalysts used throughout this study and the calculation of the rhenium to oxygen ratio is presented in a recent publication by Huang *et al.* (212).

A selection of micrographs and EDX spectra of EUROPT-3 and -4 catalysts are presented in Figures 6.31.1 to 6.31.3.

6.31.2. Pt-Sn/Al_2O_3 Catalysts

Table 6.31.2 summarises the results from TEM and EDX studies on Pt-Sn/γ-Al_2O_3 catalysts. The approximate particle sizes are also outlined in this Table. One general aspect of all these catalysts was that the majority of small particles (< 5 nm) were composed solely of platinum and most of the large particles (> 10 nm) were bimetallic Pt-Sn particles.

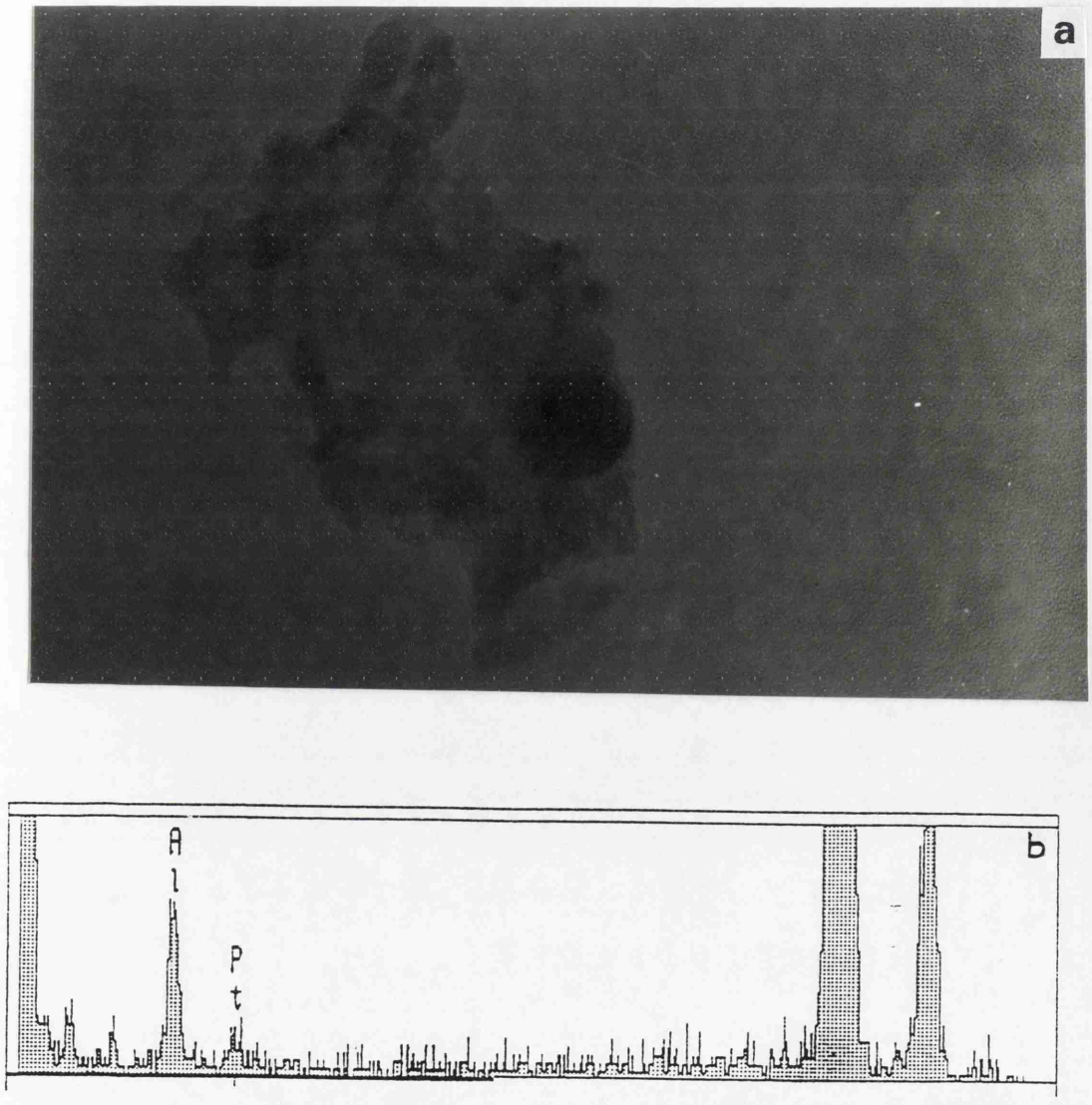

Figure 6.31.1. Reduced EUROPT-4 catalyst. (a) TEM micrograph; (b) EDX spectrum from one of the particles shown in the micrograph.

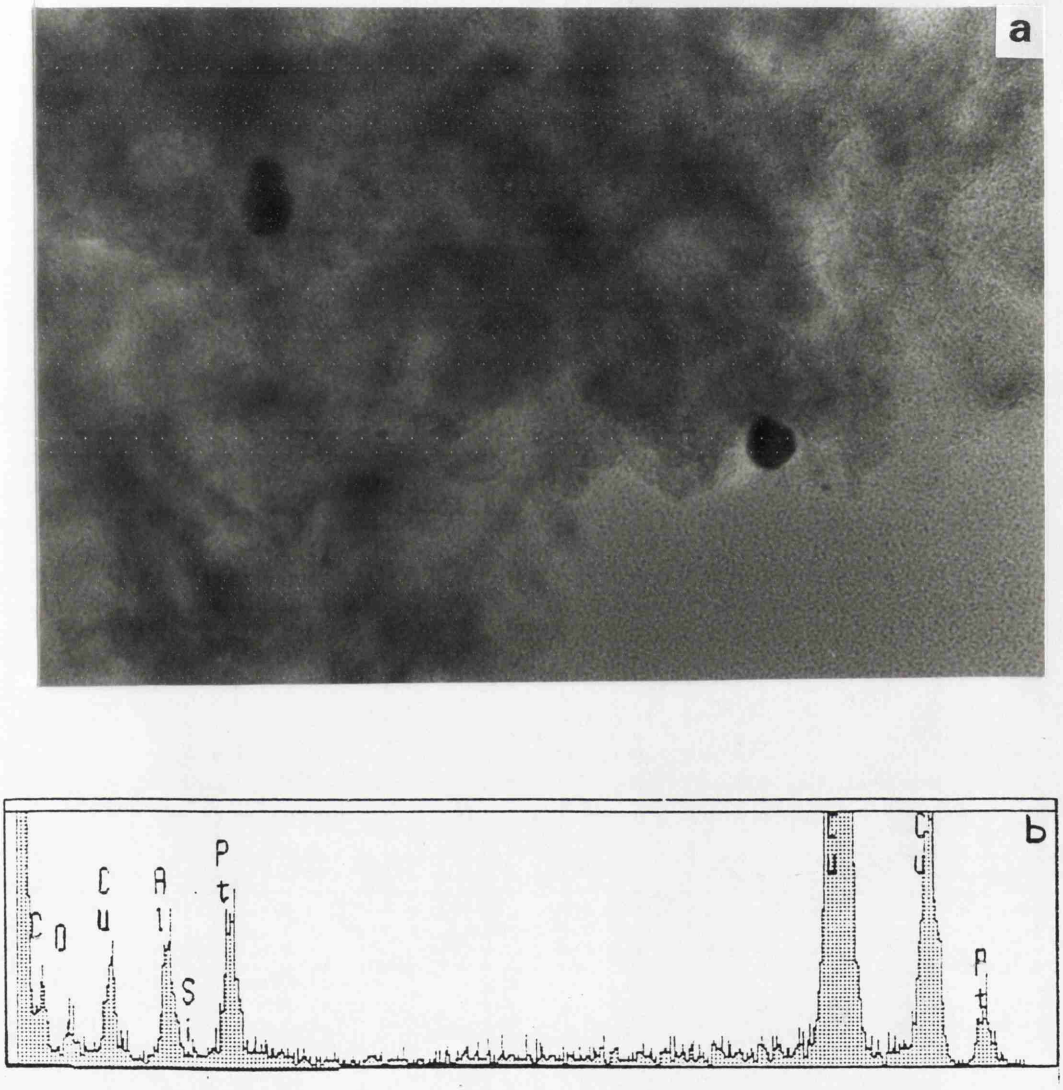

Figure 6.31.2. EUROPT-3 catalyst after use in n-octane reforming reactions. (a) TEM micrograph; (b) EDX spectrum for particle shown in the micrograph.

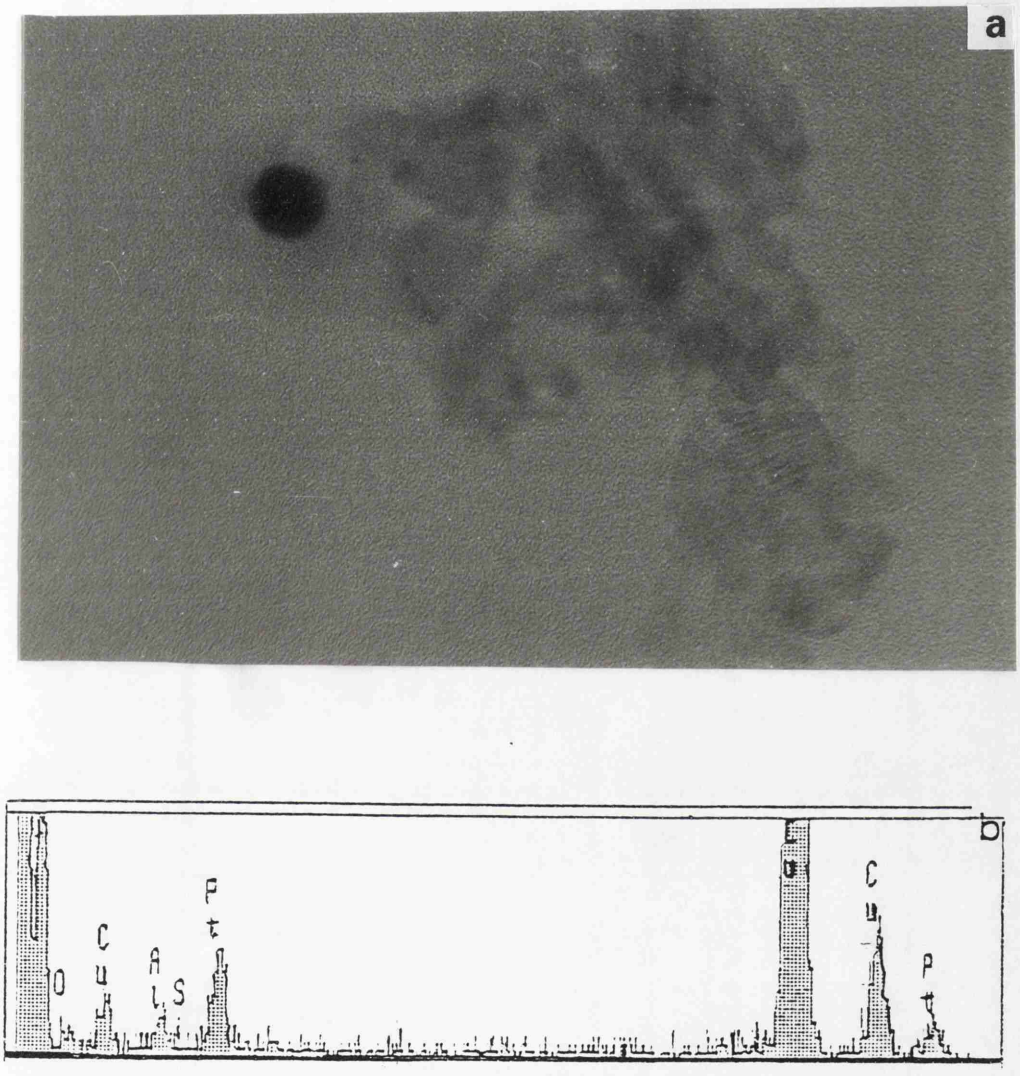

Figure 6.31.3. EUROPT-4 catalyst after use in n-octane reforming reactions. (a) TEM micrograph; (b) EDX spectrum for particle shown in the micrograph.

Table 6.31.2. Summary of TEM and EDX Results of Pt-Sn/γ-Al_2O_3 Catalysts

	0.3%Pt-0.3%Sn Sn imp first Patent	0.3%Pt-0.3%Sn Sn imp first	0.3%Pt-0.3%Sn Pt imp first	0.3%Pt-0.3%Sn Coimpregnated	0.3%Pt-0.3%Sn Sn imp first Methanol	1.0%Pt1.0%Sn Sn imp first	3.0%Pt3.0%Sn Pt imp first
Dried	x	x				x	x
Calcined	x	x	x	x	x	x	5 - 10 nm Pt
Reduced	x	few Pt	few Pt few Pt-Sn	x	~ 2 - 5 nm most Pt few Pt-Sn	few Pt-Sn few Pt	< 20 nm Pt. Pt-Sn
Calcined	x	few Pt	~ 2 - 4 nm few Pt	few Pt	~ 2 - 5 nm Pt-Sn Pt	a few Pt few Pt-Sn	< 20 nm, most Pt few Pt-Sn
Reduced	x	~ 2 - 3 nm few Pt	~ 2 - 4 nm few Pt	few Pt	~ 2 - 4 nm Pt	~ 2 - 5 nm few Pt & Pt-Sn	< 20 nm, most Pt-Sn minor Pt
Calcined						< 5 nm minor Pt-Sn most Pt	< 10 nm, most Pt few Pt-Sn
Reduced							~ 5 10 nm most Pt-Sn minor Pt
Spent	< 3 nm few Pt	< 15 nm, a few Pt-Sn minor Pt	< 20 nm, a few Pt-Sn minor Pt	< 20 nm, a few Pt-Sn minor Pt	< 20 nm, a few Pt-Sn minor Pt	< 80 nm, a few Pt-Sn minor Pt	< 100 nm a lot Pt-Sn minor Pt

'x' denotes that no particle was found in the sample

Quantitatively, the results of all the 0.3wt%Pt-0.3wt%Sn/Al_2O_3 catalysts, with the exception of the methanol catalyst, were similar to each other. Only a few metallic particles were observed after the reduction steps in the catalyst pretreatment. A general survey of all the TEM studies over a number of areas showed that the density of metallic particles was very low for the tin impregnated first, platinum impregnated first, coimpregnated and patent catalysts. This indicated that the dispersion of these catalysts is very high, in agreement with the CO chemisorption results. In contrast the density of particles was higher on the methanol catalyst and the particle sizes larger than expected.

No metal particles could be found on the catalyst prepared by the patented method until it had been used in the microreactor. Once this catalyst had been used, particles of < 3 nm could be detected. Particle aggregation occurred again in all 0.3wt%Pt-0.3wt%Sn/Al_2O_3 catalysts when subjected to reforming conditions. In general the particle size was < 20 nm in size after use with the majority of these particles being composed of Pt-Sn alloy phases. Figure 6.31.4 illustrates the 0.3wt%Pt-0.3wt%Sn/Al_2O_3 (coimpregnated) catalyst after use in n-octane reforming reactions.

On the 1.0wt%Pt-1.0wt%Sn/Al_2O_3 catalyst as metallic particles were detected until after the reduction step. Once again particle aggregation and further alloy formation occurred after use in the microreactor. Particles < 80 nm in size were found and most were bimetallic particles. However, the composition of the particles was found to vary considerably from particle to particle. Micro-beam diffraction was

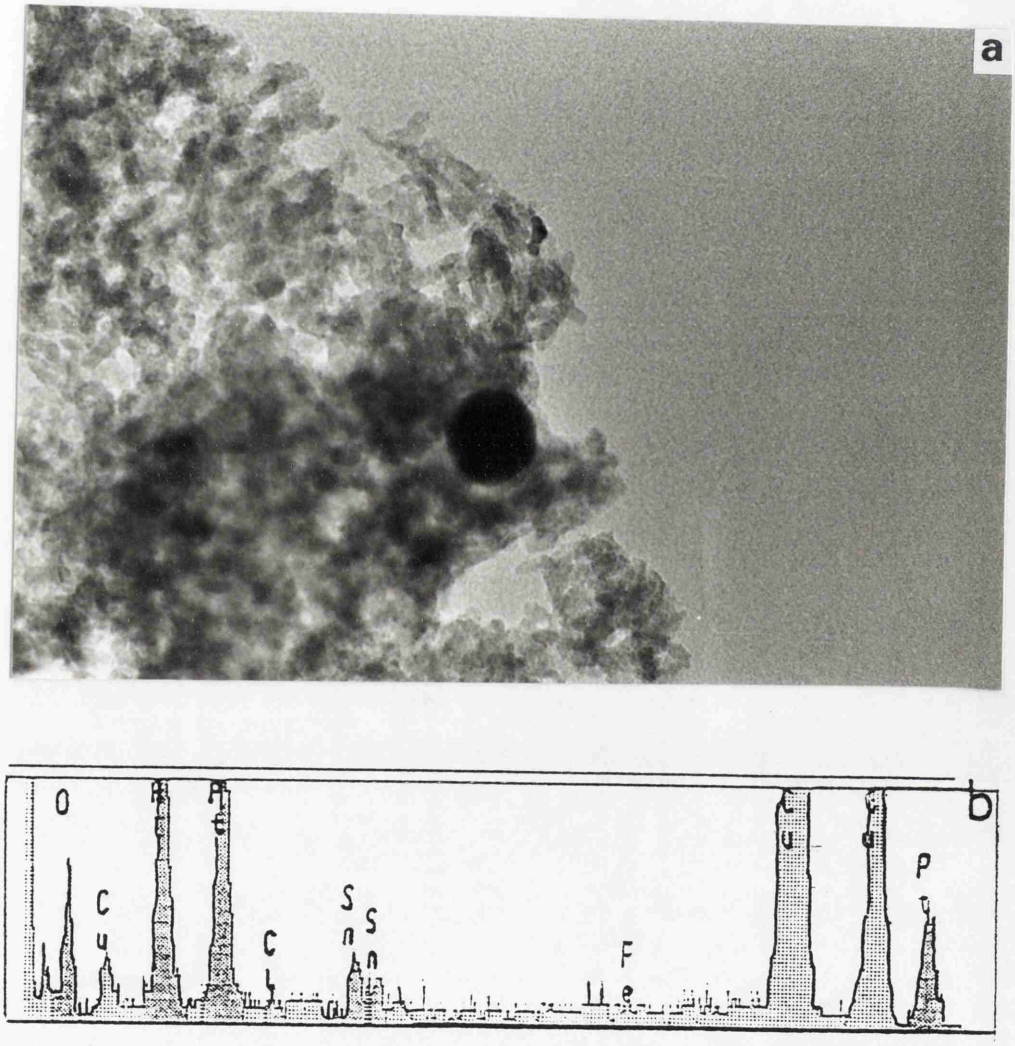

Figure 6.31.4 0.3wt%Pt-0.3wt%Sn/Al_2O_3 (Coimpregnated) catalyst after use in n-octane reforming reactions. (a) TEM micrograph; (b) EDX spectrum for particle shown in the micrograph.

carried out on several particles in addition to EDX analysis to identify the structural phase of the particles.

Figure 6.31.5 shows a particle on alumina and the corresponding EDX spectrum. The elemental ratio of Pt:Sn was found to be Pt/Sn = 0.8 and the micro-beam diffraction pattern was indexed to be the [121] pattern of the Pt-Sn alloy hcp structure. This clearly shows the existence of a Pt-Sn alloy phase after use in the microreactor.

The 3.0wt%Pt-3.0wt%Sn/Al_2O_3 catalyst had a larger particle size and density of particles than any other Pt-Sn catalyst studied. In the calcined catalyst most particles were composed of platinum while after reduction most were Pt-Sn alloy particles. After use in the microreactor, very large particles, up to 100 nm in diameter, were observed. Most of these particles were bimetallic in nature, however single platinum particles were also found. EDX analysis indicated that the two elements, platinum and tin, were not uniformly distributed over the catalyst surface. A more complete presentation and discussion of these catalysts is dealt with in a recent publication (198).

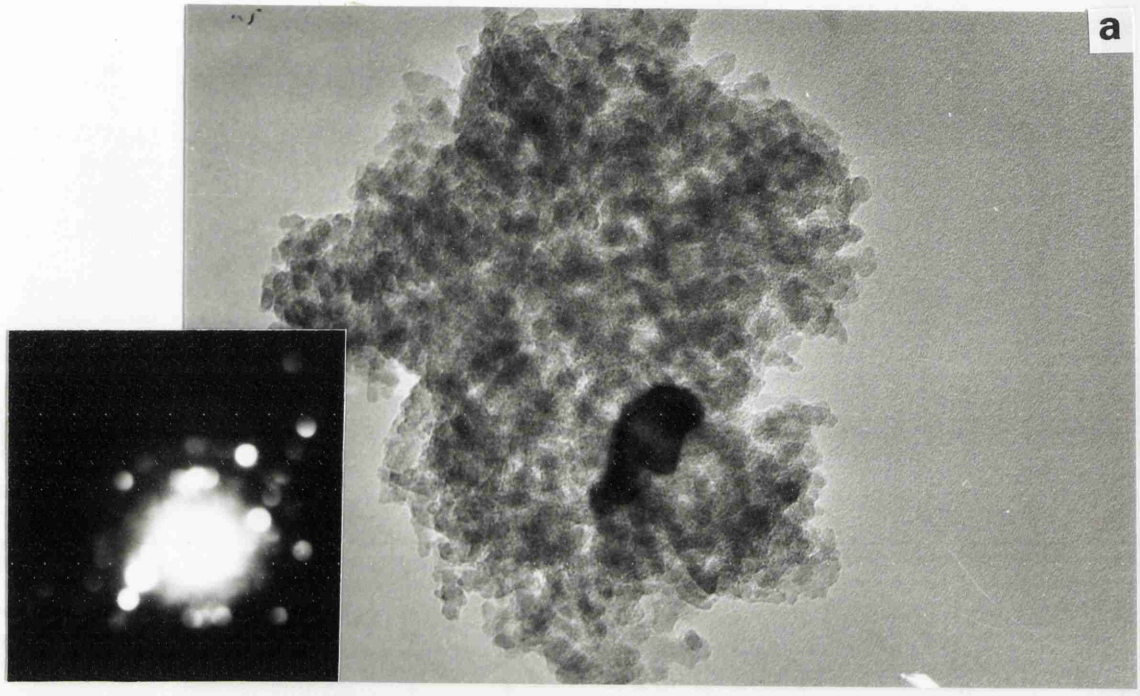

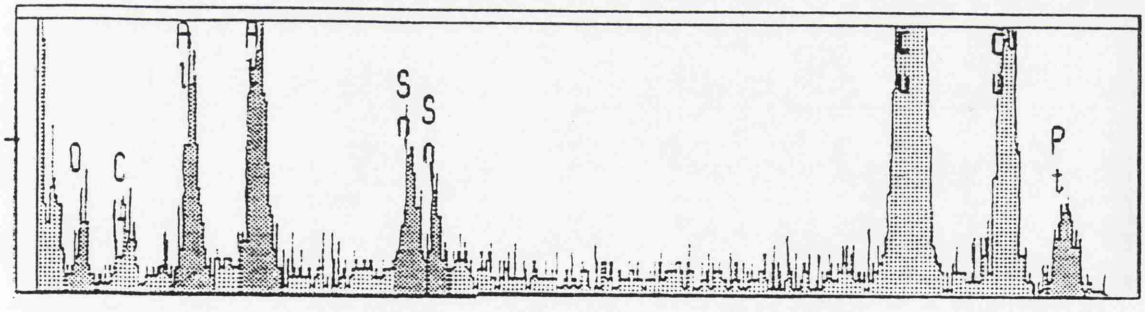

Figure 6.31.5. 1.0wt%Pt-1.0wt%Sn/Al_2O_3 catalyst after use in n-octane reforming reactions. (a) TEM micrograph, the inserted MBDP was the [121] pattern of the Pt-Sn alloy hcp structure; (b) EDX spectrum for particle shown in the micrograph.

6.31.3. Pt-Ge/Al_2O_3 Catalysts

The results obtained from HRTEM and EDX studies on a series of Pt-Ge/Al_2O_3 catalysts are summarised in Table 6.31.3. One general observation was that once the majority of the large particles (> 40 nm) were Pt-Ge alloy particles while the small particles (< 40 nm) were mainly platinum particles.

No metallic particles of any kind were found on the Ge impregnated first 0.3wt%Pt-0.3wt%Ge/Al_2O_3 catalyst after the standard pretreatment. It was not until the catalyst had been used in the microreactor that Pt and Pt-Ge particles were detected. The results of the Pt impregnated first 0.3wt%Pt-0.3wt%Ge/Al_2O_3 catalyst were similar except that a few particles were detected on the catalyst surface after the reduction step. TEM and EDX analysis of a particle on a spent sample of this catalyst found an elemental ratio of Pt/Ge = 1.45 suggesting a Pt_3Ge_2 structure for this particular particle.

However, the 0.3wt%Pt-0.3wt%Ge/Al_2O_3 coimpregnated catalyst was found to display unique properties when compared to the other 0.3wt% catalysts. After reduction a platinum rich Pt-Ge alloy and Pt particles were present upon the catalyst surface. This phenomenon was only seen after the previous 0.3wt%Pt-0.3wt%Ge/Al_2O_3 catalysts were used in the microreactor. However after use in reforming reactions several interesting features were noted. The micrograph in Figure 6.31.6a illustrates a particle which consists of 4 distinct regions; a, b, c and d, indicated on the micrograph. EDX analysis, Figure 6.31.6b, of the whole particle

Table 6.31.3. Summary of TEM and EDX Results of Pt-Ge/γ-Al_2O_3 Catalysts

	0.3%Pt-0.3%Ge Ge imp first	0.3%Pt-0.3%Ge Pt imp first	0.3%Pt-0.3%Ge Coimpregnated	1.0%Pt1.0%Ge Ge imp first	0.3%Ge
Calcined	x	x	x	x	x
Reduced	x	a few Pt particles	Pt and Pt rich Pt-Ge particles	Pt-Ge and Pt particles	x
Calcined	a few Pt particles	a few Pt particles	Pt particles	Pt-Ge and Pt particles	x
Reduced	a few Pt particles	a few Pt particles	Pt and Pt rich Pt-Ge particles	many Pt and Pt-Ge particles	x
Calcined			Pt particles	many Pt and Pt-Ge particles	x
Reduced			Pt and Pt rich Pt-Ge particles	many small Pt and Pt-Ge particles	x
Spent	a few Pt and Pt-Ge particles	a few Pt and Pt-Ge particles	Pt-Ge and Pt particles	Pt-Ge and Pt particles	x

'x' denotes that no particle was found in the sample

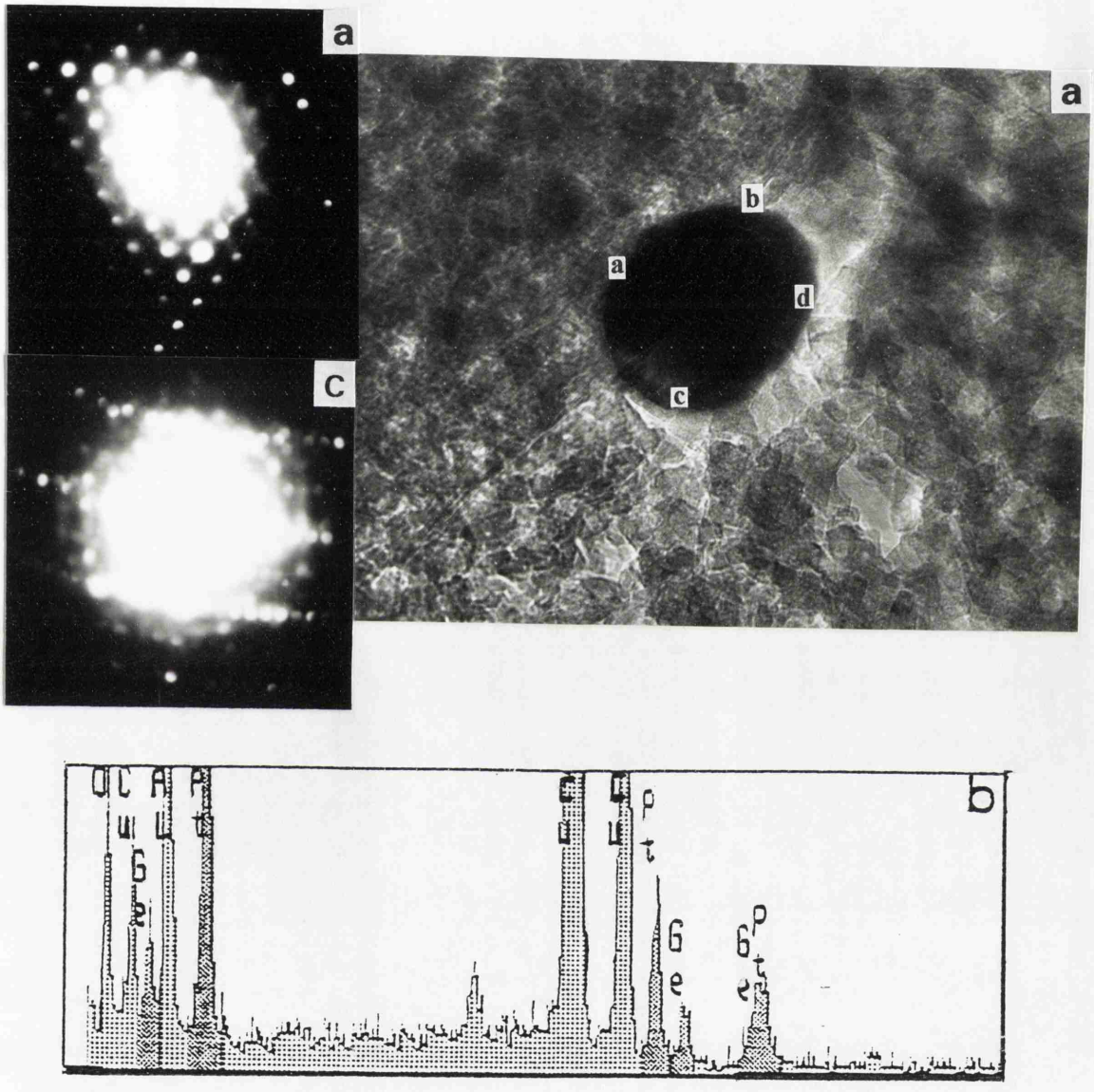

Figure 6.31.6. 0.3wt%Pt-0.3wt%Ge/Al_2O_3 (Coimpregnated) catalyst after use in n-octane reforming reactions. (a) TEM micrograph, the inserted MBDP of regions a and c. Region a was indexed to the [110] pattern of platinum. (b) EDX spectrum for particle shown in the micrograph.

determined the Pt/Ge ratio to be 2.02. Analysis of the distinct regions showed that region b had a Pt/Ge ratio equal to 2.57 and region c a ratio equal to 1.65. Furthermore the MBD pattern of region a was indexed to the [110] pattern of platinum. Figure 6.31.7a illustrates the diversity of the particles found upon the catalyst surface. The MBD pattern of this particle was indexed to the [031] pattern of the orthorhombic Pt_3Ge_2 structure. This demonstrates that different alloy phases and metallic germanium and platinum can coexist on the catalyst surface.

The 1.0wt%Pt-1.0wt%Ge/Al_2O_3 catalyst was similar to the coimpregnated catalyst in that both Pt-Ge alloy and Pt particles were present after the reduction step. One particle found on this catalyst after being used in the microreactor. Most of this particle was found to contain platinum with several areas being very rich in germanium. The MBD pattern of this particle did not match any pattern of known structures, but on closer examination the bright diffraction spots were found to match the [110] pattern of a face centred cubic (fcc) structure. However additional diffraction spots situated between any two bright spots led the particle to be indexed as a [110] pattern of a fcc structure with a lattice dimension double that of a platinum lattice dimension a_{Pt}. Therefore the particle had a superlattice structure with lattice dimensions $a = 2a_{Pt}$.

As noted in Table 6.31.3 no particles of any description could be distinguished on the monometallic 0.3wt%Ge/Al_2O_3 catalyst after calcination and reduction steps.

Overall, several phases, e.g. platinum, germanium and Pt-Ge alloys can coexist

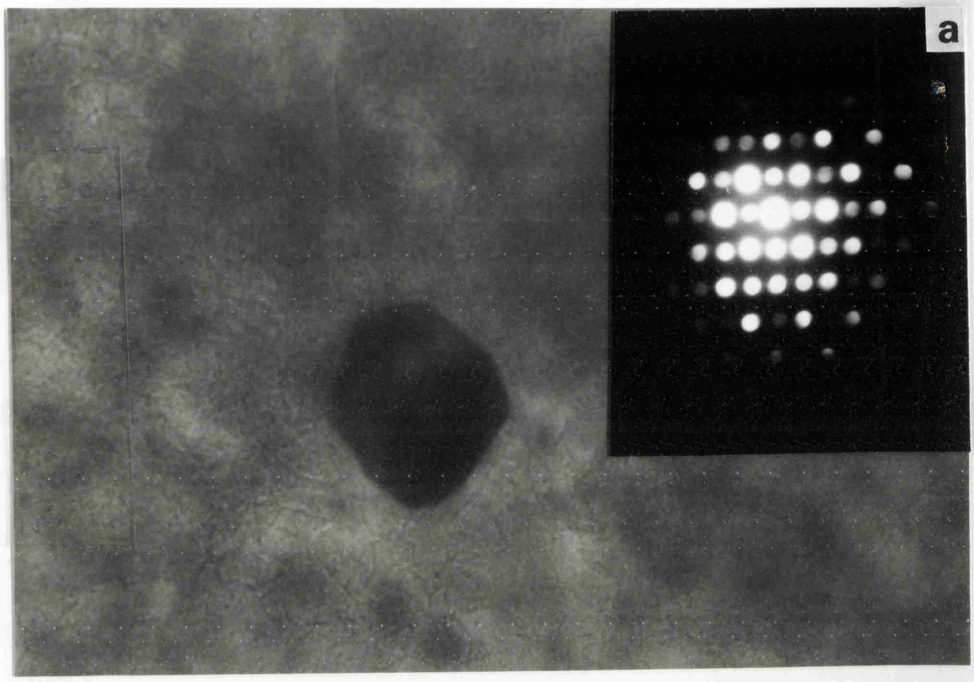

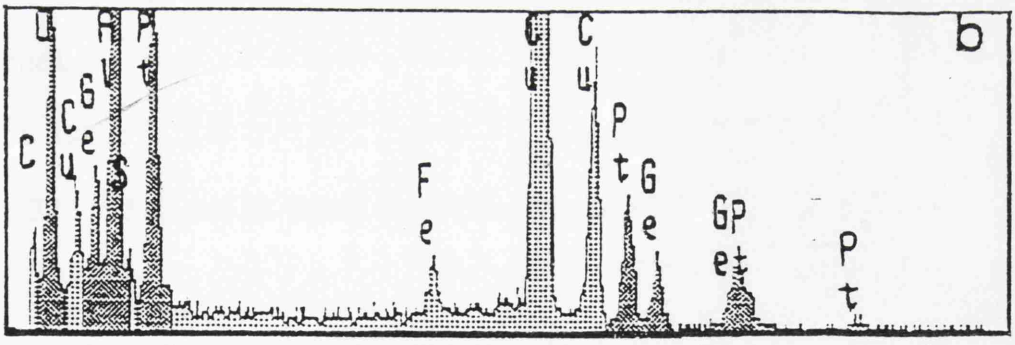

Figure 6.31.7. 0.3wt%Pt-0.3wt%Ge/Al_2O_3 (Coimpregnated) catalyst after use in n-octane reforming reactions. (a) TEM micrograph, the inserted MBDP of this particle was indexed to the [031] pattern of the orthorhombic Pt_3Ge_2 structure. (b) EDX spectrum for particle shown in the micrograph.

on the catalyst surfaces before but especially after use in n-octane reforming reactions. A complete discussion of these catalysts is given in a recent publication by Huang *et al.*(213).

6.32. CHARACTERISATION OF THE COKE DEPOSITS

The coke deposited upon the catalyst surface was investigated using FTIR spectroscopy. A typical spectra of the deposited coke is presented in Figure 6.32.1. The FTIR samples were prepared as KBr discs and were typically scanned 250 times to obtain a spectrum. The results obtained, shown in Table 6.32.1, were similar to the results reported previously in the literature (109, 167, 169, 171).

The identification and assignment of these bands shows that the coke is highly aromatic and is not altered considerably using alternative catalysts. This technique is obviously very limited but allows a good overall view of the coke to be ascertained.

Table 6.32.1. Selected IR Bands from Coke Deposits on Spent Catalysts

Frequency (cm^{-1})	
1420, 1437, 1458	CH stretching in CH_2 and CH_3
1491, 1588	Aromatic stretching
2856, 2926	Aromatic methylene stretches
2963	CH stretching in CH_2 and CH_3

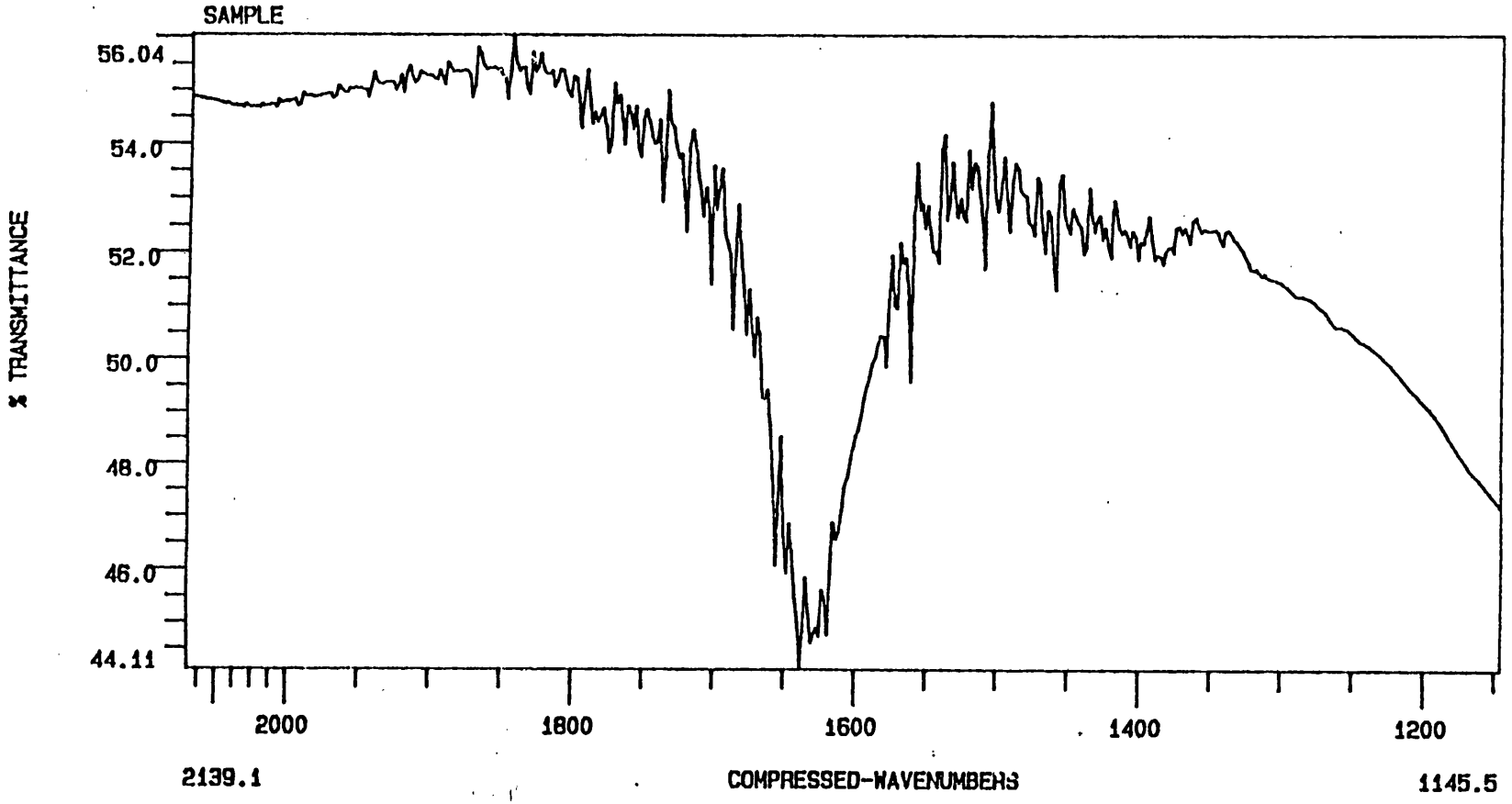

Figure 6.32.1. Typical Spectra of the Coke deposited on a Catalyst Surface after reaction at 510°C and 110 psig.

Chapter 7

Discussion

7.1. BRIEF SUMMARY OF THE RESULTS

From the results described in detail in the previous chapter, the studies of the reforming reaction of n-octane under typical industrial conditions over a series of mono- and bimetallic catalysts led to some very distinct trends in the yield and selectivity being identified. These are briefly summarised below.

The addition of a second metal, like rhenium, tin or germanium, to a monometallic Pt/Al_2O_3 catalyst resulted in many changes in the yield and selectivity from those of a monometallic catalyst. Obviously the different intrinsic nature of the second metal leads to different effects in the mixed metal catalysts. The most notable change, with respect to the monometallic catalyst, is in the behaviour of the bimetallic catalysts towards the dehydrocyclisation reaction. In general the addition of tin or, especially, rhenium as the second metal resulted in an enhanced selectivity at a steady value. The addition of germanium on the other hand had mixed effects, the activity and selectivity of individual catalysts depending heavily upon the method of preparation.

The selectivity towards hydrogenolysis follows a different trend compared to that of aromatisation. The addition of rhenium and in particular germanium resulted in a lower hydrogenolysis activity at a steady value. The addition of tin had little effect on the selectivity and similar values were reported for all $Pt\text{-}Sn/Al_2O_3$ catalysts.

The addition of a second metal to a monometallic catalyst in general lowered the deactivation rate and added a degree of stability to the reforming catalyst. The total conversion of n-octane under typical reforming conditions was enhanced by the addition of either rhenium or tin but the addition of germanium did not induce any great difference at the steady state. However, the greatly improved stability of this catalyst, i.e. no initial rapid fall in conversion, was found to be characteristic of all Pt-Ge/Al_2O_3 catalysts.

The addition of a small amount of sulphur to both the mono- and bimetallic catalysts led to dramatic improvements in the catalyst selectivity and stability. The selectivity to aromatisation increased while the selectivity to hydrogenolysis decreased with increasing sulphur content. Of all the catalysts tested, EUROPT-3 and -4 when sulphided to an appropriate level, were the most selective and least deactivated.

TEM and EDX studies of non-sulphided and sulphided Pt-Re/Al_2O_3 catalysts showed that, contrary to many previous studies (43, 45, 57), but in accord with others (42, 55, 60, 214), rhenium was not alloyed to platinum before or after use in catalytic reforming reactions. However the addition of either tin or germanium led to alloy particles being found on the catalyst surface in agreement with many workers (82, 85, 91, 215). The use of these electron microscopy techniques allowed the reduced and spent catalysts to be compared and any differences in the particle size and composition to be established.

In general the majority of all mono- and bimetallic catalysts, at 510°C and 110 psig, preferentially formed aromatics when reforming n-octane.

7.2. MONOMETALLIC EUROPT-3 CATALYSTS

The deposition of coke on the catalyst surface during a reforming reaction was found to alter the selectivity and activity of a catalyst. Coke deposition decreased with time on stream as illustrated in Table 6.1.3 and in Figure 6.1.8. The carbon mass balance (CMB) showed that after an initial rapid coking of the catalyst coke deposition decreased as less sites are available. The propane to methane ratio (Figure 6.1.7), a measure of the acidic and metallic sites, showed that the initial coke deposition took place on the metallic sites while subsequent coke was deposited mainly on the alumina support.

On examining the results from reforming n-octane on EUROPT-3.1 clearly the most significant reaction is aromatisation. The selectivity of the dehydrocyclisation reaction (Figure 6.1.6) increases initially to reach a value of 42%. This rise in the aromatisation activity is accompanied by a fall in the hydrogenolysis activity. The product yields of the C_8 aromatic species are much higher than those of either toluene or benzene (Figure 6.1.5). The formation of benzene and toluene is mainly via the dealkylation of C_8 aromatic species on the metallic sites of the catalyst (216, 217). The likelihood of two successive demethylation reactions occurring to produce benzene is extremely small explaining why toluene is produced in greater quantities than benzene. The initial decrease in both the yields of benzene and toluene is

almost certainly due to carbon deposition on the metallic sites poisoning this demethylation reaction.

Studies by Fogelberg *et al.* (218) have discovered that once C_8 aromatics form a six membered ring on the metallic component they are unable to readily undergo isomerisation reactions on a bifunctional reforming catalyst. Therefore the observed C_8 products, especially m- and p-xylene, cannot be formed by direct isomerisation of aromatic species. To achieve these products isomerisation must take prior to ring closure (218, 219).

Extensive studies by Pines and co-workers (217, 220-224) on non-acidic chromia/alumina catalysts have shown that the aromatisation of C_8 molecules can proceed via a variety of intermediates to form both m- and p-xylene. The aromatisation of 2,3,4-trimethyl pentane, for example, was found to proceed via a three or four membered ring to produce the desired reaction products (221). Since isomerisation is a primary reaction, it is likely that n-octane can isomerise to these i-octane species before undergoing aromatisation. The formation of i-octane increases at a time when secondary reactions like hydrogenolysis, hydrocracking and dehydrocyclisation decrease or are at a constant level.

Besides this monofunctional mechanism a bifunctional mechanism may also be responsible for the observed C_8 aromatic products. Davis (219, 225) showed that both m- and p-xylene could be produced via a five membered ring intermediate on a bifunctional catalyst. Sivasanker and Padalkar (226) when comparing a non-acidic

and an acidic catalyst found that the acidic sites as well as the metallic sites play an important role in the dehydrocyclisation of n-octane. These authors found that the acidic sites led to the increased production of i-octane which in turn produced more m- and p-xylene.

The decrease in all aromatic yields (Figure 6.1.5) during the reaction has been attributed by many authors (9, 142, 216) to the deposition of coke on the bifunctional catalyst. As the dehydrocyclisation activity is catalysed by both the monofunctional and bifunctional mechanisms, the initial decrease in the yield of aromatic products can be interpreted in terms of the severe coking and subsequent deactivation of the metallic sites. This agrees with work by Figoli *et al.* (227) and with work in this study where it has been shown that long term coking takes place on the support after an initial deposition on the metallic component.

Hydrogenolysis activity is significant at ~15% and is second to that of aromatisation (Figure 6.1.6). An initial rapid fall in the methane and ethane yields (Figure 6.1.1) was noted in this run. These products are formed by the breakage of a C-C bond upon the metallic sites of the support. This initial decrease in the hydrogenolysis reaction has been reported previously by many authors (9, 130, 135) and is postulated to be caused by the deposition of coke on the hydrogenolysis sites. This therefore decreases the number of platinum ensembles large enough to support this hydrogenolysis reaction.

Hydrocracking activity on EUROPT-3.1 could not be calculated due to the

inability to separate i- and n-butane products in all samples. However, there is an overall decrease in the hydrocracking activity with reaction time. Isomerisation activity increases in comparison to this decreasing hydrocracking activity as illustrated in Figure 6.1.6. Beltramini *et al.* (124) studying the reforming reactions on a Pt/Al_2O_3-Cl catalyst found similar results. These authors postulated that coke deposition upon the alumina surface was responsible for this phenomenon.

Hydrocracking and isomerisation reactions are both controlled by the acidic sites on a reforming catalyst. Isomerisation reactions can take place at less acidic sites than hydrocracking reactions (142, 228). It would therefore appear that most of the acidic sites on alumina are deactivated by coke deposition, decreasing the hydrocracking ability of the catalyst. However, EUROPT-3 had been doped with an optimum level of chlorine to enhance the acidic properties of the alumina support. It has been reported (131, 214) that the chlorine content on a reforming catalyst decreases with time on stream. Figoli *et al.* (131) reported that the hydrocracking activity increased while the isomerisation activity decreased with increasing chlorine content. Therefore an increase in the isomerisation and a corresponding decrease in the hydrocracking activity might suggest that chlorine has been removed from the most acidic sites of the catalyst during a reforming run. In consequence the variation in the activity of hydrocracking and isomerisation reactions in reality may be due to a combination of both coke deposition and chlorine removal from the catalyst surface during the reaction.

On EUROPT-3, at either 490 or 510°C, it is noticeable that there is a

predominance of i-paraffins over both cyclo- and n-paraffins (Tables 6.1.1 and 6.2.1). This is in keeping with many observations reported in the literature (3, 9) and has been explained by assuming cracking reactions proceed via a carbonium ion intermediate. This intermediate is able to form more stable alkyl cations by intramolecular rearrangements (9). On EUROPT-3.1 and -3.2 i-butane is the most abundant hydrocracking product (Figures 6.1.1 and 6.2.1). This is expected as primary cracking results in the following pairs of molecules, $C_4 + C_4$ and $C_3 + C_5$, per mole of n-octane. The subsequent cracking of butane by β-scission would result in the formation of unstable primary cations being generated and therefore is inhibited (9, 229).

The overall conversion of n-octane on EUROPT-3.1 decreased rapidly from 48 to 27% during this study as shown in Figure 6.1.9. A constant conversion had not been reached when the reaction was stopped after 50 hours. The conversion on EUROPT-3.2, Figure 6.2.7, is approximately 5% lower mainly due to the drop in the yield of aromatic products. The yields of all products, except for methane which increased, were lower than the corresponding yields on EUROPT-3.1.

The dominant reaction on EUROPT-3.2 is hydrogenolysis in contrast to that on EUROPT-3.1 where aromatisation predominates (Figures 6.1.6 and 6.2.6). The hydrogenolysis selectivity has increased 7% by decreasing the temperature by 20° as detailed in Table 7.2.1. This increase in hydrogenolysis selectivity is due inpart to the lower selectivity to aromatic products and inpart to the lower coke deposition on the catalyst surface.

Table 7.2.1. Summary of the % Selectivity to the major reactions and % Conversion on EUROPT Catalysts

Catalyst and Conditions Used	% Conversion	% Selectivity initially and after 40 hours on stream			
		Hydrogenolysis	Aromatisation	Isomerisation	Hydrocracking
EUROPT-3 (510°C, 110 psig)	Falls from 48 to 28%	Decreases from 18 to 16%	Increases from 35 to 42%	Increases from 0.1 to 0.3%	-
EUROPT-3 (490°C, 110 psig)	Falls from 47 to 24%	Decreases from 25 to 23%	Decreases from 19 to 8%	-	-
EUROPT-4 (510°C, 110 psig)	Falls from 57 to 41%	Decreases from 18 to 9.5%	Increases from 36 to a constant 58%	Increases from 0.3 to 1.0%	Decreases from 7.2 to 3.9%
EUROPT-4 (490°C, 110 psig)	Falls from 40 to 23%	Increases from 23 to 31%	Increases from 21 to 23%	Increases from 0.5 to 0.6%	-
EUROPT-4 (510°C, 130 psig)	Falls from 34 to 24%	Increases slightly from 20.3 to 21.3%	Increases from 28 to 34%	Increases from 0.19 to 0.21%	-

Aromatisation activity decreases with reaction time to a constant level of 9% on EUROPT-3.2, 32% lower than that on EUROPT-3.1 (Figures 6.1.6 and 6.2.6). Thermodynamically and kinetically this is expected as the formation of aromatics is favoured by high temperatures. Consequently, by decreasing the reaction temperature the aromatisation activity and selectivity trends have been altered considerably. The yield of toluene was dominant followed by C_8 aromatic species and finally benzene as detailed in Figure 6.2.5. The demethylation reaction seems to be favoured by a lower temperature as the yield of toluene predominates. This increased demethylation of C_8 aromatics to form toluene also explains the increased yield of methane. The second successive demethylation reaction to form benzene is still highly unfavoured. Toluene is also produced via the dehydrocyclisation of n-heptane. In either case the importance of the hydrogenolysis reaction at the lower reaction temperature is noted.

The rate of deactivation is slower and the % coke deposited upon the catalyst surface is lower on EUROPT-3.2 than on EUROPT-3.1 (Table 6.1 and Figures 6.1.9 and 6.2.7). The deactivation rate is lower due to less coke being deposited upon the catalyst surface as detailed by the carbon mass balance for both reactions (Tables 6.1.3 and 6.2.3). This lower rate of coke deposition results in fewer hydrogenolysis and hydrocracking sites being poisoned increasing the activity of both these reactions on EUROPT-3.2 when compared to EUROPT-3.1. Thermodynamically the decrease in both coke and aromatic formation is predicted. Consequently reforming reactions are usually carried out at higher temperatures as the aromatisation activity is many times greater although the coking rate, and therefore the deactivation rate, is

significantly higher.

The conversion of hydrocarbons on reforming reactions has been reported to increase with the reaction temperature (9, 12). As noted, under the reaction conditions used in this study, the conversion of n-octane on EUROPT-3 did not increase significantly at the higher reaction temperature. Despite the significant changes in the product yield of EUROPT-3.2 there was only 5% difference in the conversion throughout the entire run. The decreased aromatisation activity is heavily compensated by a corresponding increase in both the hydrocracking and hydrogenolysis reactions.

7.3. BIMETALLIC CATALYSTS

Electron microscopy investigations on both reduced and spent bimetallic catalysts indicated that there were some general similarities as well as differences between the various catalyst series.

It was very noticeable that particle aggregation occurred on all bimetallic catalysts with time on stream. This was most noticeable in the catalysts with the higher metal loadings, where particles of up to 100 nm in size were found after use in reforming reactions. The most important result from TEM and EDX studies was that two distinct types of platinum particles, 2 - 10 nm particles and very small particles < 1 nm, were identified on the catalyst surface for all bimetallic catalysts. It is the interaction of these small platinum particles with those of the second metal

on the alumina surface which is believed to be responsible for the improved selectivity and stability of these bimetallic catalysts over the corresponding monometallic catalysts. On all bimetallic catalysts the metal oxide, e.g. ReO_2, SnO, was stabilised by an interaction with the support. The addition of tin as the second metal is thought to form a tin aluminate complex with the alumina support similar to that reported by several authors (76, 230).

The formation of alloy particles was not observed on any Pt-Re/Al_2O_3 catalyst but was found on both Pt-Sn/Al_2O_3 and Pt-Ge/Al_2O_3 catalysts (Tables 6.31.1-6.31.3). Alloy formation was seen to increase with time and with metal loading on both Pt-Sn/Al_2O_3 and Pt-Ge/Al_2O_3 catalysts. The majority of both tin and germanium were present as oxides distributed on the alumina surface but a small fraction of each was reduced to the metallic state after reduction to form alloy particles with platinum. On both these series of catalysts it became apparent that several phases coexist upon the catalyst surface before and after use in reforming reactions, e.g. Pt, Ge and Pt-Ge alloy phases. Alloy formation was also highly dependent upon the method of catalyst preparation, e.g. the formation of a $[Pt(SnCl_3)_2Cl_2]^{2-}$ complex facilitates alloy formation under the conditions used in this study.

The presence of small platinum particles (< 1 nm) modified by the second metal is postulated to alter the aromatic selectivity of the bimetallic catalyst. The greater the number of small platinum particles modified in this manner the higher the aromatic selectivity.

7.3.1. The Effects of Coke Deposition

In the first 5-10 hours of a reforming reaction there is an initial rapid coke deposition on the metallic sites of a non-sulphided bimetallic catalyst. This is substantiated by both the carbon mass balance (CMB) and the propane to methane ratio of all these catalysts. The CMB shows the carbon deposition on a catalyst surface to decrease with time on stream after an initial large laydown. The propane to methane ratio, in comparison, increases rapidly to a maximum in this initial period indicating the rapid deactivation of the metallic hydrogenolysis sites by coke deposition.

The amount of coke deposited on both EUROPT-3.1 and -4.1 is 13.88 and 15.39% respectively. These values are very similar and are within experimental error of each other. These findings are in contrast to the results of many authors (7, 109, 216) who have reported that the level of coking is lower on the bimetallic catalyst when compared with a corresponding monometallic catalyst. The results would suggest that the addition of rhenium does not affect the rate of coking but rather the nature of the coke deposits themselves. The presence of rhenium intercepts the harmful graphitic coke precursors and hydrogenates them to less harmful species. The coke on a monometallic catalyst is more graphitic, that is it contains less hydrogen than on a bimetallic catalyst enforcing this theory.

The coke deposited on a Pt-Sn/Al_2O_3 catalyst is very dependent upon the method of preparation as detailed in Table 6.1. Previous studies by Völter *et al.* (63) found

that the coking rate of a Pt-Sn/Al_2O_3 catalyst was the same or higher than on a monometallic catalyst. In later work Völter and Kürschner (64) found that the addition of tin did not diminish the coking rate bur rather modified the nature of the coke deposition. In disagreement with these findings Burch and Garla (61) interpreted their decreased level of coking on a Pt-Sn/Al_2O_3 catalyst as being due to an interaction of tin and platinum on the alumina surface. Dautzenberg *et al.* (62) postulated that the level of coking decreased due to an ensemble effect, whereby the addition of tin breaks up the large platinum ensembles thereby diminishing the sites for coke deposition.

The increased coking rate on several Pt-Sn/Al_2O_3 catalysts is related to the increased cracking activity of these catalysts. This is partially compensated by an ensemble effect on the catalyst surface and by the presence of Sn^{II} species modifying the alumina support. The lower coking rate on the other Pt-Sn/Al_2O_3 catalysts has been attributed to a combination of the ensemble effect and the modification of the alumina by Sn^{II} species (61, 99).

Previous studies in the literature have shown that, in general, more coke is deposited on a Pt-Ge/Al_2O_3 catalyst than on a Pt-Re/Al_2O_3 catalyst under identical conditions. Franck and Martino (240) found that with n-heptane the coke content of their Pt-Ge/Al_2O_3 catalyst was three times that of their Pt-Re/Al_2O_3 catalyst. In a separate study Parera *et al.* (108) noted that a Pt-Ge/Al_2O_3 catalyst produced thirteen times as much coke as a Pt-Re/Al_2O_3 catalyst. These reactions were run under different conditions from those used in this study but more importantly the Pt-

Ge/Al_2O_3 catalysts used by Parera *et al.*(108) and Franck and Martino (240) all had a higher platinum content than germanium. In comparison all $Pt\text{-}Ge/Al_2O_3$ catalysts used in this study had an elemental ratio of Pt/Ge equal to one. With a larger platinum content it is feasible to presume that more hydrogenolysis sites and therefore coking sites will be present on the catalyst surface explaining the observed difference in coke deposition.

Significant changes in both the product yield and selectivity in the reforming of n-octane are observed when the reaction conditions are varied . The hydrogenolysis activity of EUROPT-4.2 increases from 23 to 31% in contrast to results obtained on EUROPT-4.1 where it decreases with time on stream (Table 7.2.1). This result is in contrast to those of Parera *et al.* (108) who reported that the hydrogenolysis activity increased with time on $Pt\text{-}Re/Al_2O_3$ catalysts. Kugelmann (241) and Le Page (8) postulated that a hydrogenolysis reaction had a high activation energy and was therefore favoured by higher reaction temperatures. Coke formation increases with reaction temperature (142) according to the results reported in Table 6.1 leading to more hydrogenolysis sites being blocked which in turn decreases the methane yield. A similar result was reported by Bond and Gelsthorpe (242) when studying the hydrogenolysis of alkanes on EUROPT-4.

The yield of methane on EUROPT-4.3 is greater than on EUROPT-4.1 after 20 hours on stream as shown in Table 7.2.1. The lower level of coking on this catalyst means that less hydrogenolysis sites are deactivated and therefore a smaller decline in the methane yield with time, when compared with EUROPT-4.1, is observed.

Isomerisation activity with both EUROPT-4.2 and -4.3 (Figures 6.4.5 and 6.5.6) increases with time, as with EUROPT-4.1 (Figure 6.3.6), as hydrocracking sites become deactivated and chlorine levels drop. The hydrocracking sites on both EUROPT-4.2 and -4.3 are not as strongly or as quickly deactivated as on EUROPT-4.1. Therefore selectivity to isomerisation reactions does not increase readily with time in agreement with less coke being deposited upon the catalyst.

7.3.2. Acid Catalysed Reactions

The isomerisation activity increases while hydrocracking activity decreases with reaction time on all bimetallic catalysts as was obtained with EUROPT-3.1. In all experiments the dominant hydrocracking species is i-butane. The behaviour of these two reactions may, as detailed in Section 7.2, be attributed to increasing coke deposition and decreasing chlorine content, with catalyst usage.

The addition of a second metal, e.g. rhenium, to a Pt/Al_2O_3 catalyst will induce changes in the bifunctional nature of the support. The interaction of ReO_2 with the alumina support modifies the acidity and explains the increase in isomerisation and hydrocracking reactions. However, the addition of either tin or germanium to a Pt/Al_2O_3 catalyst was found to alter the selectivity and acidity of the catalyst in a different manner. The addition of tin has been reported (89, 232-234) to alter the acidity of the catalyst by poisoning the most acidic sites on the support. The catalyst prepared by the patented method is disregarded as it was not prepared using the same γ-alumina support and will therefore have slightly different acidic properties. The

isomerisation activity increased by a factor of three on the 0.3wt%Pt-0.3wt%Sn/Al_2O_3 tin impregnated first and the coimpregnated catalysts (Figures 6.8.6 and 6.9.6) and decreased on the corresponding 0.3wt%Pt-0.3wt%Sn/Al_2O_3 methanol and platinum impregnated first (Figures 6.11.6 and 6.13.6) in comparison with EUROPT-3.1 (Figure 6.1.6). The poisoning of the most acidic sites on the support by tin means that more weakly acidic sites are available for isomerisation reactions. As both the tin impregnated first and coimpregnated catalysts have a large tin alumina interaction, as observed by TEM and EDX studies, this poisoning effect can be seen very clearly on these two catalysts in particular. When the tin-alumina interaction is not as strong, the poisoning effect will not be as large.

At a steady state the hydrocracking activity is similar for both the platinum and tin impregnated first and coimpregnated catalysts (Figures 6.8.6 and 6.9.6). The hydrocracking activity of the 0.3wt%Pt-0.3wt%Sn/Al_2O_3 catalyst prepared with a methanol solution (Figure 6.13.6) in comparison decreases to half the value on EUROPT-3.1 (Figure 6.1.6) suggesting that the acidic sites are deactivated by coke deposition throughout the run. Bacaud *et al.* (89) attributed the decreasing cracking activity on their Pt-Sn/Al_2O_3 catalysts to an increase in alloy formation on the catalyst. The alloy formation does increase with time on all these Pt-Sn/Al_2O_3 catalysts but coke deposition and decreasing chlorine levels are thought to result in a decrease in the cracking activity with time.

In this study it is not possible to comprehensively say that tin does poison the acidic sites of the alumina support as the precise chlorine content of these Pt-

Sn/Al_2O_3 catalysts is not known. However, as both platinum and tin are impregnated as chlorinated species in dilute HCl, the level of chlorine and therefore the acidity is believed to be high. Without the exact chlorine content we can only imply that tin does poison the most acidic sites of these catalysts. The isomerisation and hydrocracking activities will therefore be altered, but the poisoning effect of tin will reduce this effect.

In general the yield of both benzene and toluene increased on all 0.3wt%Pt-0.3wt%Sn/Al_2O_3 catalysts while that of C_8 aromatics decreased when compared with the yields observed on EUROPT-4.1. This is due to an increased isomerisation and cracking of n-octane to C_6 and C_7 species before undergoing dehydrocyclisation. This is highlighted by both the patent and the platinum impregnated first catalysts (Tables 6.11.2 and 6.13.2) which display an increased benzene and toluene selectivity when compared to both EUROPT catalysts (Tables 6.1.2 and 6.3.2).

The addition of germanium alters the acidity of the support in a different manner from that obtained with either rhenium or tin, as shown by the results detailed in Tables 7.3.1 and 7.3.2. The cracking activity has clearly been enhanced by the addition of germanium and increases by a factor of three for many of the Pt-Ge/Al_2O_3 catalysts in comparison with the EUROPT and Pt-Sn/Al_2O_3 catalysts. This result is in close agreement with those of Beltramini and Trimm (235) who reported that germanium enhanced the cracking ability of a Pt/Al_2O_3 catalyst for n-heptane reforming. Aboul-Gheit *et al.* (107) also noted that the addition of germanium altered the acidic properties of the catalyst. These authors reported a lower

Table 7.3.1. Summary of the % Selectivity to the major reactions and % Conversion on Pt-Sn/Al_2O_3 Catalysts

Catalyst and Conditions Used	% Conversion	% Selectivity initially and after 40 hours on stream			
		Hydrogenolysis	Aromatisation	Isomerisation	Hydrocracking
0.3%Pt-0.3%Sn (Pt impreg first)	Falls from 45 to 32%	Decreases from 25 to 20%	Increases from 36 to 40%	Increases from 0.1 to 0.15%	Decreases from 6.5 to 5.7%
0.3%Pt-0.3%Sn (Sn impreg first)	Falls from 52 to 39%	Decreases from 26 to 19%	Increases from 28 to 54%	-	-
0.3%Pt-0.3%Sn (Coimpreg)	Falls from 61 to 36%	Decreases from 20 to 15%	Increases from 40 to 54%	-	Decreases from 7 to 5%
0.3%Pt-0.3%Sn (Methanol)	Falls from 39 to 31%	Decreases from 22 to 17%	Increases from 26 to 45%	Increases slightly from 0.13 to 0.15%	Decreases from 8.5 to 2.6 %
0.3%Pt-0.3%Sn (Patent)	Falls from 33 to 15%	Decreases from 19 to 16%	Decreases slightly from 41.3 to 41.8%	Increases from 0.06 to 0.2%	-
1.0%Pt-1.0%Sn (Sn impreg first)	Increases from 39 to 45%	Decreases from 33 to 16%	Increases from 24 to 45%	-	-

Table 7.3.2. Summary of the % Selectivity to the major reactions and % Conversion on Pt-Ge/Al_2O_3 Catalysts

Catalyst and Conditions Used	% Conversion	% Selectivity initially and after 70 hours on stream			
		Hydrogenolysis	Aromatisation	Isomerisation	Hydrocracking
0.3%Pt-0.3%Ge (Pt impreg first)	Decreases from 32 to 31%	Decreases from 6 to 4%	Increases from 18 to 39%	Increases from 0.07 to 0.1%	Decreases from 26.5 to 17.8%
0.3%Pt-0.3%Ge (Ge impreg first)	Increases from 26 to 29%	Decreases from 12 to 4.6%	Increases from 22 to 29%	Increases from 0.07 to 0.21%	Increases slightly from 19.6 to 20.5%
0.3%Pt-0.3%Ge (Coimpreg)	Decreases slightly from 33.2 to 32.7%	Decreases from 9 to 5.4%	Increases from 18 to 49%	Increases from 0.15 to 0.24%	Decreases from 26 to 12.5%
1.0%Pt-1.0%Ge (Ge impreg first)	Decreases from 25.5 to15%	Decreases from 6.6 to 4.7%	Decreases from 29 to 21%	Decreases from 0.27 to 0.20%	Increases from 20 to 23%
0.3%Ge	Falls from 7.7 to 5.3%	Increases from 21 to 31.5%	Decreases from 7.8 to 5.1%	Decreases from 0.47 to 0.43%	Decreases from 28 to 22%

isomerisation and a higher hydrocracking activity for the bimetallic Pt-Ge/Al_2O_3 catalyst when compared to the monometallic Pt/Al_2O_3 catalyst.

The acidity of a Pt/Al_2O_3 catalyst would therefore seem to be enhanced by the addition of germanium to the catalyst. The bifunctional nature of the support is modified by an interaction with germanium oxide causing the observed changes in the acid catalysed reactions. This interaction is clearly noted when germanium is impregnated on to the alumina support first causing the hydrocracking activity to increase with time.

The increased acidity of a Pt-Ge/Al_2O_3 catalyst has altered the aromatic distribution from C_8 aromatics to benzene and toluene when compared to either EUROPT catalyst. This effect is greater than that found with the corresponding Pt-Sn/Al_2O_3 catalysts. This change in selectivity is caused by n-octane isomerising and cracking before undergoing dehydrocyclisation. From these results the selectivity to aromatics is seen to be very dependant upon the method of preparation as detailed in Table 7.3.2. When germanium is impregnated first, a lower selectivity to aromatic species is noted. The selectivity to aromatics increases when platinum is impregnated first and again if platinum and germanium are coimpregnated on to the alumina support. From the results detailed in Table 7.3.2 it is noticeable that as the hydrocracking activity of a catalyst increases the aromatisation activity decreases. This would suggest that a higher hydrocracking activity cracks n-octane to lower products, reducing the dehydrocyclisation. This can also be correlated with the degree of germanium interaction with the alumina support. The degree of

germanium interaction influences both the product distribution and the overall yield and selectivity of a catalyst. However, when germanium is impregnated first there is a large germanium interaction with the support resulting in a low selectivity to aromatic products due to the very high hydrocracking ability of the catalyst. This also explains the very high benzene yield on this catalyst (Table 6.24.1). The germanium interaction with the support in this catalyst and therefore the acidity of the support is too large to produce any beneficial effects. When platinum is impregnated first there is a much smaller germanium interaction with the support resulting in a lower hydrocracking selectivity of this catalyst (Table 7.3.2). This lower cracking selectivity of this catalyst meant that the highest C_8 aromatic yield on any Pt-Ge/Al_2O_3 catalyst was seen on this catalyst. Overall the lower cracking activity was beneficial in that a higher yield of aromatics was produced. When platinum and germanium are coimpregnated there is a balance between the metallic and acidic sites on the catalyst surface. The germanium interaction is lower than when germanium is impregnated first but higher than when platinum is impregnated first due to the competition for sites. The observed hydrocracking selectivity on the coimpregnated 0.3wt%Pt-0.3wt%Ge/Al_2O_3 catalyst is low in comparison with other Pt-Ge/Al_2O_3 catalysts. However the yield of both benzene and toluene has increased on this coimpregnated catalyst suggesting that n-octane is cracked preferentially to C_6 and C_7 species. The observed hydrocracking selectivity is lower than expected as a direct consequence. The 1.0wt%Pt-1.0wt%Ge/Al_2O_3 catalyst has the poorest selectivity and lowest conversion of all Pt-Ge/Al_2O_3 catalysts indicating that the optimum loading for these two components is 0.3wt%. The very low activity appears to be a result of the increased alloy formation found with this catalyst. It

is interesting to note that a bimetallic Pt-Ge/Al_2O_3 catalyst with a germanium loading of 0.3wt% has the highest activity for the hydrogenation of benzene (104).

7.3.3. Aromatisation Activity

The overall yield of aromatics on EUROPT-4.1 is almost twice that on EUROPT-3.1 after 50 hours on stream (Figures 6.1.6 and 6.3.6). The yield of aromatics on EUROPT-4.1 increases with time in contrast to EUROPT-3.1 where the yield decreases with time. The increasing aromatic yield on the bimetallic catalyst is surprising as many authors (109, 122, 231) reported that coke deposition on Pt-Re/Al_2O_3 catalysts decreased the dehydrocyclisation. However Bertolacini and Trimm (216) in their study of n-heptane reforming reactions on bimetallic catalysts also found that the overall aromatic yield increased with time before reaching a steady state. The highly dispersed platinum particles (< 1 nm) are modified by the presence of rhenium and this interaction results in an increased selectivity to aromatic products.

Similarly, a direct correlation between the aromatic selectivity and the interaction between small platinum particles and Sn^{II} stabilised on alumina has been discovered in the Pt-Sn/Al_2O_3 series of catalysts. The coimpregnated and tin impregnated first 0.3wt%Pt-0.3wt%Sn/Al_2O_3 catalysts both display a higher selectivity to aromatics (Figures 6.8.6 and 6.9.6) than all the other Pt-Sn/Al_2O_3 catalysts (Figures 6.11.6, 6.12.5 and 6.13.6) and EUROPT-3.1 (Figure 6.1.6). This improved selectivity is a direct result of a large interaction between Sn^{II} stabilised on the alumina surface and

the small platinum particles. The platinum particle size limited this interaction with the Sn^{II} species on the alumina support. The 0.3wt%Pt-0.3wt%Sn/Al_2O_3 catalyst prepared with a methanol solution had a lower platinum dispersion than the corresponding tin impregnated first catalyst prepared with an aqueous solution. This increase in the particle size resulted in a lower selectivity to aromatic products as detailed in Table 7.3.1. The beneficial Sn^{II} interaction would therefore appear to be limited to particles that are less than 1 nm in size. This view is reenforced by the claim that the 0.3wt%Pt-0.3wt%Sn/Al_2O_3 catalyst described in the patent literature had no alloy particles and very small platinum particles dispersed on the catalyst surface (Table 6.31.2). Despite a very low conversion the selectivity to aromatics at a steady state is almost identical to that of EUROPT-3.1 due to the Sn^{II} interaction with small platinum particles (Figures 6.1.6 and 6.12.5). When platinum is impregnated first on to alumina more alloy particles are formed and therefore the possibility of less interaction between Sn^{II} and small platinum particles results in a lower aromatic selectivity (Figure 6.11.6).

As with the related Pt-Re/Al_2O_3 and Pt-Sn/Al_2O_3 catalysts, the extent of the modification of the small platinum particles by germanium determines the selectivity and stability of a Pt-Ge/Al_2O_3 catalyst. With all Pt-Ge/Al_2O_3 catalysts initial aromatic yields decrease with decreasing alloy formation and with a decreasing number of platinum particles present on the catalyst surface. This again suggests that there is some degree of correlation between the platinum and germanium interaction and aromatic selectivity.

The coimpregnated 0.3wt%Pt-0.3wt%Ge/Al_2O_3 catalyst had the highest selectivity to aromatics and activity of all the Pt-Ge/Al_2O_3 catalysts. Besides the presence of alloy particles after reduction, this catalyst had more platinum particles present on the catalyst surface when compared with the platinum and especially with the germanium impregnated first catalysts. The subsequent modification of these particles by germanium led to an improvement in the aromatic selectivity as detailed in Table 7.3.2. Only the 1.0wt%Pt-1.0wt%Ge/Al_2O_3 catalyst contained a higher number of platinum particles and therefore a higher initial aromatic selectivity. However after 70 hours on stream due to particle aggregation and alloying the selectivity of the catalysts had changed accordingly. The 1.0wt%Pt-1.0wt%Ge/Al_2O_3 catalyst after use was found to contain larger particles and more alloy formation than the 0.3wt%Pt-0.3wt%Ge/Al_2O_3 catalysts. This increase in particle size and alloying decreased the number of small platinum particles modified by germanium, decreasing the overall yield of aromatics.

In conclusion, the aromatic selectivity of a 0.3wt%Pt-0.3wt%Ge/Al_2O_3 bimetallic catalyst is highly dependant upon the interaction of platinum and germanium particles. The greater the number of small platinum particles which are modified by the second metal, the higher the aromatic selectivity of that catalyst.

7.3.4. Hydrogenolysis Reactions

The hydrogenolysis activity of each bimetallic series of catalysts is characteristic of the second metal used. The hydrogenolysis selectivity, Table 7.2.1, for both

EUROPT-3.1 and -4.1 is initially similar but after 40 hours on stream the selectivity of the bimetallic catalyst falls below that of EUROPT-3.1 (Figures 6.1.1 and 6.3.1). The initial sharp decrease in the methane yield is particularly severe on EUROPT-4.1, 10.4 to 5.7%, in the first eight hours on stream, much more so than with EUROPT-3.1. This initial rapid decrease is due to rapid coke deposition on the metallic sites decreasing the number of large platinum ensembles available for this reaction. The propane to methane ratio of EUROPT-4.1, Table 6.3.3) indicates that the metallic sites are more deactivated by coke deposition than is the case with the corresponding monometallic EUROPT-3.1 catalyst. This increased carbon deposition on the metallic sites and the dilution of the platinum ensembles by rhenium means that less sites are able to support the hydrogenolysis reaction. Hydrogenolysis is supported by large platinum ensembles and so dilution of these ensembles, by rhenium addition or coke deposition, results in less sites being able to support this reaction. The increased coke deposition on the metallic sites means that less coke is deposited upon the support therefore explaining the increased selectivity to both hydrocracking and isomerisation reactions. This idea is in total contrast to that proposed by Ludlum *et al.* (236) and Bertolacini and Pellet (60) who postulated that rhenium influences coke deposition on the catalyst support.

In comparison the hydrogenolysis selectivity for all Pt-Sn/Al_2O_3 catalysts on the whole is similar to that on EUROPT-3.1 at a steady state (Tables 7.2.1 and 7.3.1). Initially the selectivity is influenced by the particle size on the reduced catalyst. If large particles are present more methane is produced initially before coke deposition deactivates these sites and alloy formation breaks up the large ensembles. As the

time on stream increases the formation of more Pt-Sn alloy particles this dilutes the platinum ensembles further.

In direct contrast to the other two bimetallic catalyst series, Pt-Ge/Al_2O_3 catalysts all display a diminished hydrogenolysis selectivity. The activity is approximately one third of that with EUROPT-3 and with Pt-Sn/Al_2O_3 catalysts (Tables 7.2.1 and 7.3.1) and approximately one half of that with EUROPT-4 (Table 7.2.1) at a steady value. The addition of germanium not only dilutes these large platinum ensembles but it readily forms a Pt-Ge alloy. A combination of these two effects results in the hydrogenolysis reactions having less chance of occurring, therefore the much lower yield. Germanium is more effective in forming an alloy with platinum than either platinum or rhenium diluting the platinum ensembles readily and decreasing the methane yield.

It was found with the Pt-Ge/Al_2O_3 series of catalysts that the method of preparation can greatly affect the selectivity and activity of a catalyst. A similar effect is observed with the Pt-Sn/Al_2O_3 catalysts. The most notable difference between all Pt-Sn/Al_2O_3 catalysts occurs when platinum is impregnated first on to the alumina support, followed by the tin. This order of sequential impregnation results in a colour change to red representing the formation of a trans $[Pt(SnCl_3)_2Cl_2]^{2-}$ complex (184, 185, 237, 238). The formation of this complex, only when platinum is impregnated first, has a detrimental effect on the catalyst selectivity as outlined in Table 7.3.1. This is highlighted in the results reported in Section 6.10, where the tin to platinum molar ratio was three. The formation of the

$[Pt(SnCl_3)_2Cl_2]^{2-}$ complex facilitates the formation of an alloy as all the available platinum was alloyed with the excess tin in the 0.3wt%Pt-0.9wt%Sn/Al_2O_3 catalyst. Sparks *et al.* (235) found that n-octane dehydrocyclisation decreases with increasing Sn/Pt ratios. These authors also found that all the platinum is converted into an alloy as the Sn/Pt ratio lies between three to five, depending on the support. This is in agreement with the results from this work. After 30 hours on stream the conversion of n-octane falls dramatically from 30 to 0% (Figure 6.10.1). At this stage all the platinum has alloyed with the tin leaving an excess of tin on the catalyst surface. This tin poisons the acidic sites of the catalyst support and as there are no platinum metal sites the activity of the catalyst decreases rapidly as there are few sites left to support any reaction.

A similar relationship has been noted previously by Baronetti *et al.* (70) who found that if the $[Pt(SnCl_3)_2Cl_2]^{2-}$ complex was formed, tin reducibility and Pt-Sn alloy formation increased. In contrast to the results reported in this work the complex was formed on both a platinum impregnated first and a coimpregnated catalyst. A molar ratio of Sn/Pt equal to six was used, compared to a ratio of one in this work, and this difference accounts for the observed difference as it is well documented that the higher the Sn/Pt ratio, the greater the probability of the red $[Pt(SnCl_3)_2Cl_2]^{2-}$ complex being formed (185, 237, 238).

7.3.5. Characteristic Trends Displayed by a Bimetallic Catalyst

One very notable general feature of all the 0.3wt% bimetallic catalysts is the increased yield and selectivity to n-paraffin products when compared to the monometallic EUROPT-3 catalyst. The yield of n-pentane, for example, increases by a factor of 50 on the EUROPT-4 catalyst (Tables 6.1.1 and 6.3.1) under identical conditions. This phenomenon together with an increase in the methane yield, has been reported previously by several authors (57, 132, 239) for a Pt-Re/Al_2O_3 catalyst. Shum *et al.* (239) explained these increases in terms of an increase in the multiple fission of the reactant molecule. However, in contrast to the results reported in this thesis, Shum *et al.* postulated that the increase in n-paraffins was characteristic of Pt-Re alloy formation. TEM and EDX studies (Table 6.31.1) revealed that both platinum and rhenium act independently on the catalyst surface. However, Pt-Sn alloy particles are formed with all the Pt-Sn/Al_2O_3 catalysts and an increase in methane selectivity was observed on these catalysts supporting the proposal by Shum and co-workers. Pt-Ge/Al_2O_3 catalysts while displaying an increased yield of n-paraffins and alloy particles had a significantly smaller yield of methane. As a consequence of alloy formation the large platinum ensembles are diluted resulting in a smaller yield of methane.

The formation of n-paraffins would appear to be a characteristic of bimetallic catalysts under the conditions used in this study. However, the formation of alloy particles and the change in methane yield are highly dependent on the second metal used and the reaction conditions.

In general, the stability of a Pt/Al_2O_3 catalyst has been vastly improved by the addition of a second metal to the catalyst. The deactivation rate is much lower especially with the germanium series of catalysts. Thus the initial sharp decline in the conversion often associated with monometallic catalysts is reduced to varying degrees with the bimetallic catalysts. This is especially true for $Pt\text{-}Ge/Al_2O_3$ catalysts where the sharp decline due to coke deposition on the metallic sites is not seen. It is suggested that this improved stability is due to the greater dilution of the platinum ensembles by germanium and alloy particles. In this study the conversion of n-octane reached a steady state with EUROPT-4.1 (Figure 6.3.7) but still decreased with EUROPT-3.1 (Figure 6.1.9) after 50 hours on stream indicating the increased stability of the bimetallic catalyst. The overall conversion of n-octane on EUROPT-4 is higher than on EUROPT-3 due to the increase in the aromatic yield seen with the bimetallic catalysts. The conversion of n-octane using both $Pt\text{-}Sn/Al_2O_3$ and $Pt\text{-}Ge/Al_2O_3$ catalysts is highly dependent on the method of preparation as discussed earlier.

Ako and Susu (243) regarded i-octane as an intermediate product that could undergo further conversion to a range of products. The conversion of i-octane to aromatics and light paraffins is increased by increasing the reaction temperature. The very low i-heptane yield on both EUROPT-4.2 and -4.3 (Tables 6.4.1 and 6.5.1) is due to the increased dehydrocyclisation to toluene the yield of which increased dramatically when compared to that observed with EUROPT-4.1 (Table 6.3.1).

7.3.6. Effects of Altering the Reaction Conditions

The most notable difference when altering the reaction conditions is observed in the aromatisation activity. The selectivity to aromatic products on EUROPT-4.2 and -4.3 (Figures 6.4.5 and 6.5.6) is approximately half that of EUROPT-4.1 (Figure 6.3.6). This result is predicted by thermodynamics as aromatic formation is favoured at high temperatures and low pressures (8, 241). Similar results were reported by Barbier *et al.* (132) and Figoli *et al.* (6). As with the corresponding EUROPT-3 catalysts a drop in the reaction temperature caused a similar change in the product distribution of the aromatic products. In contrast to EUROPT-3.2 the aromatisation selectivity (Figure 6.2.6) is almost three times higher when EUROPT-4.2 is used (Figure 6.4.5), resulting in an increase in both the methane and aromatic yields. The yield of all aromatic species on EUROPT-4.3 is lower than on EUROPT-4.1 as detailed in Table 7.2.1. Alternatively, in contrast the yield of o-xylene increases with time. This is a reflection of the suppression of the isomerisation reactions by the very active hydrocracking reactions resulting with the formation of less i-octane and, therefore, less m/p-xylene at this higher pressure.

In agreement with many studies (6, 109, 132, 181) the overall conversion increases with reaction temperature but decreases with an increase in pressure. The decrease in aromatisation is responsible for this difference although the increase in the hydrogenolysis selectivity partially compensates this. The overall conversion of EUROPT-4.2 is similar to that of EUROPT-3.2 (23 and 24% respectively) (Figure 6.4.5 and 6.2.6) although the yield of aromatics is significantly higher on the

bimetallic catalyst. The % coke deposited on the catalyst surface was found to be approximately 6% lower than that deposited on EUROPT-4.1, analogous to the EUROPT-3 catalysts. Increasing the pressure of the reaction has the advantage of decreasing coke deposits and the deactivation rate but is accompanied by an undesirable decrease in aromatisation and increase in hydrogenolysis reactions.

7.4. SULPHIDED CATALYSTS

The addition of sulphur to a reforming catalyst can either be beneficial or extremely detrimental to the activity and selectivity of the catalyst. This is illustrated by comparing the results obtained using fully and partially sulphided EUROPT-3 and -4 catalysts (Sections 6.18 to 6.23). Sulphur is a very selective poison when used in very small quantities as reported by many authors (36, 109, 244) but a highly destructive poison when used in sufficient quantities.

When presulphided EUROPT catalysts are compared with non-sulphided EUROPT catalysts several very distinct and important trends can be seen with increasing sulphur coverage. The most noticeable trend is the decreasing hydrogenolysis selectivity with increasing sulphur adsorption as shown in Table 7.4.1. Of all the possible reactions hydrogenolysis is suppressed the most by the addition of sulphur to either EUROPT-3 or -4 catalysts. This suppression is more pronounced with the bimetallic EUROPT-4 catalyst than with the monometallic EUROPT-3 catalyst. The suppression of hydrogenolysis by sulphur is best explained in terms of an ensemble effect. It is widely accepted that hydrogenolysis is a

Table 7.4.1. Summary of the % Selectivity to the major reactions and % Conversion on Sulphided EUROPT Catalysts

Catalyst and Conditions Used	% Conversion	% Selectivity initially and after 70 hours on stream			
		Hydrogenolysis	Aromatisation	Isomerisation	Hydrocracking
EUROPT-3 (4 pulses H_2S)	Decreases from 36 to 31%	Decreases from 6.2 to 2.9%	Decreases from 77.5 to 66.2%	-	-
EUROPT-3 (3 pulses H_2S)	Decreases from 34 to 31%	Decreases from 8.8 to 7.2%	Decreases from 53.7 to 52.4%	Decreases from 0.21 to 0.13%	Increases from 8.1 to 10.9%
EUROPT-3 (2 pulses H_2S)	Decreases from 21.5 to 15.9%	Decreases from 12.7 to 8.7%	Increases from 48.6 to 52.9%	Decreases from 0.25 to 0.2%	Decreases from 9.6 to 9.5%
EUROPT-4 (4 pulses H_2S)	Increases from 17.3 to38.1%	Increases from 0.55 to 1.21%	Increases from 73 to 77.7%	-	-
EUROPT-4 (2 pulses H_2S)	Increases from 16.6 to 52.3%	Increases from 3.8 to 6.1%	Decreases from 47 to 20%	Decreases from 0.14 to 0.08%	Increases from 10.1 to 20.8%

reaction that needs relatively large metal atom ensembles. The addition of sulphur effectively dilutes these metal ensembles on the catalyst surface. However in the bimetallic EUROPT-4 catalyst, sulphur bonds preferentially to rhenium forming a very strong Re-S bond in the process (55, 119). This Re-S species dilutes the platinum ensembles thus drastically diminishing the bimetallic Pt-Re/Al_2O_3 catalysts intrinsically high hydrogenolysis activity. The sulphur adsorbed on the monometallic catalyst is not as strongly bound and therefore more mobile and easier to displace by coke deposition. This explains why the bimetallic catalyst is much more sensitive to sulphur poisoning than the monometallic catalyst.

Sulphur adsorption on either EUROPT catalyst will take place preferentially on the metallic sites of the catalyst. This is especially true for the bimetallic Pt-Re/Al_2O_3 catalysts where a very strong Re-S bond is formed. Therefore, at low coverages the sulphur is adsorbed mainly on the metallic sites leading to an increased selectivity towards acid catalysed reactions. When the sulphur content is increased the acidic sites on the catalyst will be affected to a greater degree than at low coverages as more sulphur is adsorbed on to the alumina support.

These trends are very noticeable from the results obtained with presulphided EUROPT catalysts. At low sulphur coverage the hydrocracking activity is higher and the hydrogenolysis activity lower than that obtained with a non-sulphided catalyst under identical conditions (Figures 6.3.6 and 6.23.5). Isomerisation activity is initially similar on both catalysts as summarised in Tables 7.2.1 and 7.4.1. When the sulphur content is increased acid-catalysed and hydrogenolysis reactions decrease

indicating sulphur is poisoning both acid and metallic sites to a greater extent (Figures 6.19.5, 6.20.5 and 6.21.5). These results are similar to those reported by Apestiguia *et al.* (114). These authors found that when sulphiding a Pt/Al_2O_3-Cl catalyst, with H_2S, at low coverages the adsorption takes place mainly on the metal and strong Lewis acid sites of the support. On increasing the sulphur content adsorption on the support was found to predominate.

In contrast to hydrogenolysis and isomerisation activity the selectivity to dehydrocyclisation reactions increases with increasing sulphur content on both EUROPT-3 and -4 catalysts (Table 7.4.1). This feature is due in part to sulphur poisoning certain reactions therefore enhancing the selectivity to aromatic products. This increase in aromatisation activity is due mainly to the increase in yield of both benzene and toluene with increasing sulphur coverage. In direct contrast the yield of C_8 aromatics decreases with increasing sulphur content on both EUROPT catalysts (Tables 6.19.1 and 6.22.1) to a level below that observed on non-sulphided EUROPT catalysts (Tables 6.1.1 and 6.3.1). The adsorption of sulphur on to the surface of a EUROPT catalyst would therefore appear to enhance the formation of benzene and toluene while decreasing the C_8 aromatic formation. The observed increase in the yield of both benzene and toluene on a sulphided catalyst is a direct consequence of the increase in the hydrocracking and isomerisation activities when compared to a non-sulphided catalyst. This effect becomes more pronounced as the sulphur content increases with both the monometallic and bimetallic EUROPT catalysts. The addition of sulphur to both EUROPT catalysts has altered the selectivity from C_8 aromatic species to benzene and toluene.

The coke deposited upon the EUROPT-3 and -4 series of sulphided catalysts decreased with increasing sulphur adsorption as shown in Table 6.1. This result is expected as both sulphur and coke are deposited preferentially on the metallic hydrogenolysis sites. Consequently, as the sulphur coverage increases fewer sites are available to support coke deposition. In addition the adsorption of sulphur on to the catalyst will decrease the size of the platinum ensembles resulting in less coke being deposited upon the catalyst surface. This is in contrast to the work carried out by Dees (10) and Barbier and Marecot (248) who found an increase in the level of coking when the catalyst had been sulphided. These authors postulated that as hydrogenolysis had diminished, there would be an increase in the extent of alkene formation leading to a higher level of coking. However, with both EUROPT-3 and -4 catalysts, as the level of sulphur increases there is a distinct decrease in the level of coke deposited on the catalyst surface as shown in Table 6.1.

The conversion of n-octane on a sulphided and non-sulphided EUROPT-3 catalyst is similar once a steady level has been reached as shown in Figures 6.1.9 and 6.19.6. Initially the values are significantly lower on the sulphided catalyst as detailed in Tables 7.1.1 and 7.4.1. In stark contrast, while the conversion decreases with time on a non-sulphided EUROPT-4 catalyst (Figure 6.3.7) it increases on a sulphided EUROPT-4 catalyst (Figure 6.22.6). The initially low conversion is due to sulphur poisoning the hydrogenolysis sites which can also be rapidly deactivated by coke deposition on a non-sulphided catalyst. Therefore a certain degree of stability has been introduced to these catalysts by the addition of sulphur. The stability is a result of less coke being deposited and therefore fewer catalytic sites

on the sulphided catalyst being deactivated by coke. Biswas *et al.* (245), from their work on sulphur and coke poisoning, concluded that it was the combined action of both rhenium and sulphur that led to changes in the selectivity and in the catalytic behaviour. It has also been suggested that the Re-S bond sterically hinders graphitisation (246) of the carbonaceous overlayer on the catalyst metal sites. The dilution of the platinum ensembles by this Re-S bond results in a reduction in coke formation on the metal sites due to the inability to form multiple metal to carbon bonds (247).

In comparing the deactivation rate of a sulphided and non-sulphided EUROPT-3 catalyst (Figures 6.1.9 and 6.19.6) under identical conditions a very distinctive trend was noted. On sulphiding EUROPT-3 the deactivation rate is approximately five to six times lower than with a non-sulphided EUROPT-3 catalyst. With EUROPT-4 the conversion increased with time for the sulphided catalysts as detailed in Tables 7.2.1 and 7.4.1. The bimetallic Pt-Re/Al_2O_3 catalyst is considerably more deactivated than the corresponding monometallic catalyst at the same level of sulphur adsorption. This feature has been reported by numerous authors (115, 248-250) who noted that a Pt-Re/Al_2O_3 catalyst was extremely sensitive to the presence of sulphur on the catalyst.

This level of sulphur adsorption on the catalyst surface decreases with increasing time on stream during a reforming reaction. This is clearly illustrated in Section 6.18 when a poisoned EUROPT-3 catalyst is examined. Initially this catalyst produces only methane in any detectable quantity as shown in Table 6.18.1.

However after 74 hours on stream aromatic species and propane were detected indicating a change in the catalyst composition. When studying the carbon mass balance for this reaction, Table 6.18.2, it is noticeable that the difference between the carbon entering and exiting the microreactor increases with time on stream. Therefore carbon deposition upon the catalyst surface helps displace adsorbed sulphur allowing the observed reactions to occur after 74 hours on stream. This situation was found to hold for both fully sulphided EUROPT catalysts. When highly sulphided the production of aromatics was slower on the EUROPT-4 than on EUROPT-3 catalysts indicating that sulphur displacement by coke deposition was much slower on the bimetallic catalyst. This is to be expected, as much of the sulphur is strongly bound to rhenium. If this occurs on a highly sulphided catalyst it may be assumed that some sulphur will be lost from the catalyst surface in catalysts having lower initial levels of sulphur. Further work in this area using $H_2{}^{35}S$ to label the sulphur adsorbed on the catalyst would allow this postulate to be examined in greater detail.

From the results of these studies the optimum level of initial sulphiding would appear to correspond to the adsorption of 200 µl (4 pulses) of H_2S with a 0.4 g EUROPT catalyst sample. Reduction of this freshly sulphided catalyst at 400°C results in much of the reversible sulphur being desorbed from the catalyst surface (110, 111, 113, 114). It is the presence of this strong or irreversible sulphur which significantly enhances the selectivity and activity of the catalyst during a reforming reaction. This optimum level of sulphiding gave the lowest yield of hydrogenolysis products while enhancing the aromatic formation. The % coke deposited upon the

catalyst decreased as the initial level of sulphur adsorption increased.

In conclusion it is the effect of the irreversibly adsorbed sulphur which ultimately changes the selectivity and activity of a sulphided EUROPT catalyst. This sulphur is mainly deposited on the metallic sites (54, 113, 115) and breaks up the large platinum ensembles causing the observed decreases in the hydrogenolysis selectivity. On a bimetallic Pt-Re/Al_2O_3 catalyst the formation of a Re-S bond again breaks up the large platinum ensembles and impedes the formation of highly graphitic coke. It would therefore seem that it is the combined action of both rhenium and sulphur which is responsible for any differences observed between a sulphided EUROPT-3 and -4 catalyst.

7.5. GENERAL CONCLUSIONS

The reforming of n-octane under the conditions used in this study was significantly altered when a second metal, e.g. Re, Sn or Ge, was added to a monometallic Pt/Al_2O_3 catalyst. The increased selectivity and stability of a bimetallic catalyst have been clearly illustrated in this work.

Overall the improved selectivity and activity of the bimetallic catalyst depends upon the method of preparation. The improved aromatic selectivity on many bimetallic catalysts is governed by the highly dispersed small platinum particles interacting with the second metal on the catalyst support. The greater this interaction the higher the aromatic selectivity of a catalyst. The presence of these small

platinum particles has been verified by TEM and EDX studies on both freshly reduced and spent catalyst samples. Alloy formation is seen in both Pt-Sn/Al_2O_3 and Pt-Ge/Al_2O_3 catalysts but not in Pt-Re/Al_2O_3 catalysts under the reaction conditions used. However, the presence of a Pt-Re alloy has been reported for many Pt-Re/Al_2O_3 catalysts (43, 45, 57) using different catalysts and conditions. Alloying of the two metal components would therefore appear to be very dependent upon the catalyst pretreatment and the reaction conditions used.

A further advantage of using a bimetallic catalyst is the lower deactivation rate and consequently greater stability of these catalysts when compared with a monometallic catalyst. This allows the prolonged use on stream of these bimetallic catalysts before regeneration processes are required to return the catalyst to a higher level of activity. The Pt-Ge/Al_2O_3 series of catalysts was found to display the lowest deactivation rate and therefore greatest stability of all the non-sulphided catalysts examined in this study.

An improvement in the catalytic performance of both bimetallic Pt-Re/Al_2O_3 and monometallic Pt/Al_2O_3 catalysts was found to occur when the catalysts were doped with a small amount of sulphur. This addition of adsorbed sulphur resulted in a much lower hydrogenolysis rate and a higher selectivity to aromatics when compared with the non-sulphided catalysts. At a high sulphur coverage sulphur is adsorbed on both the hydrogenolysis sites on the metal and acidic sites on the support while a low sulphur coverage selectively favours the formation of aromatic products. The use of TEM and EDX in conjunction with these studies allowed the various metals

present in the catalyst to be studied in terms of particle size, changes in oxidation state and alloying. This proved to be invaluable and allowed a more accurate interpretation of the results obtained in the reforming reactions.

References

REFERENCES

1) Brock, W. H., 'The Fontana History of Chemistry', Fontana Press, London, 1992.

2) Satterfield, C.N., 'Heterogeneous Catalysis In Industrial Practice', 2nd Edition, M°Graw-Hill, New York, 1991.

3) Edmonds, T., 'Catalysis and Chemical Processes', (Pearce, R., and Patterson, W.R., Eds.), Leonard-Hill, London, 1981.

4) Gates, B.C., Katzer, J.R., and Schuit, G.C., 'Chemistry of Catalytic Processes', M°Graw-Hill, New York, 1979.

5) Sinfelt, J.H., 'Bimetallic Catalysts, Discoveries, Concepts and Applications', Wiley and Sons, New York, 1983.

6) Figoli, N.S., Beltramini, J.N., Martinelli, E.E., Sad, M.R., and Parera, J.M., Appl. Catal., **5**, 19, 1983.

7) Barbier, J., 'Catalyst Deactivation', (Delmon, B., and Froment, G.E., Eds.), Elseiver, Amsterdam, 1, 1987.

8) Le Page, J.F., 'Applied Heterogeneous Catalysis Design, Manufacture and Use of Solid Catalysts', Editions Technip, Paris, 1987.

9) Pines, H., 'The Chemistry of Catalytic Hydrocarbon Conversion', Academic Press, New York, 1981.

10) Dees, M.J., Ph.D. Thesis, Leiden University, 1991.

11) Sinfelt, J.H., 'Catalysis Science and Technology', Vol. 1, (Anderson, J.R., and Boudart, M., Eds.), Springer-Verlag, New York, 1981.

12) Richardson, J.T., 'Principles of Catalyst Developement', Plenium Press, New York, 1989.

13) Rossini, F.D., Pitzer, K.S., Arnett, R.L., Braum, R.M., and Pimental, G.C., Selected values of physical and thermodynamic properties of hydrocarbons and related compounds. API Res. Project 44, Pittsburgh, Carnegie Press, 1953.

14) Sinfelt, J.H., Advan. Chem. Eng., **5**, 37, 1964.

15) Foger, K., 'Catalysis Science and Technology', Vol. 6, (Anderson, J.R., and Boudart, M., Eds.), Springer-Verlag, New York, 223, 1984

16) Cotton, F.A., and Wilkinson, G., 'Advanced Inorganic Chemistry', 5th Edition, Wiley Interscience, New York, 1988.

17) de Boer, J.H., and Lippens, B.C., J. Catal., **3**, 38, 1964.

18) Lippens, B.C., and de Boer, J.H., J. Catal., **3**, 44, 1964.

19) Lippens, B.C., and Steggeron, J.J., 'Physical and Chemical Aspects of Adsorbents and Catalysts', Academic Press, New York, 171, 1970.

20) Kotanigawa, T., Yamamoto, M., Utiyama, M., Hattori, H., and Tanabe, K., Appl. Catal., **1**, 185, 1981.

21) Fripiat, J.J., Leonard, A.J., and Semaille, P.N., Proc. Brit. Ceram. Soc., 103, 1969.

22) Peri, J.B., J. Phys. Chem., **69**, 220, 1965.

23) Peri, J.B., Actes. Congr. Int. Catal., 2nd, Paris, **1**, 1333, 1960.

24) Tanabe, K., 'Solid Acids and Bases', Academic Press, New York, 1970.

25) Cai, T., Qü, J., Wong, S., Song, Z., and He, M., Appl. Catal., **97**, 113, 1993.

26) Krzywicki, A., Marczewski, M., Modzelewski, R., Pelszik., K., and Marinowski, St., React. Kinet. Catal. Lett., **13**, 1, 1980.

27) Krzywicki, A., and Marczewski, M., J. Chem. Soc. Faraday Trans. 1, **76**, 1311, 1980.

28) Basset, J., Naccache, C., Mathieu, M., and Pettre, M., J. Chim. Phys., **66**, 1522, 1969.

29) Hall, W.K., Lutinski, F.E., and Gerberich, H.R., J. Catal., **3**, 514, 1964.

30) Hightower, J.W., Gerberich, H.R., and Hall, W.K., J. Catal., 7, 57, 1967.

31) Haag, W.D., and Pines, H., J.Am. Chem. Soc., **82**, 2471, 1960.

32) Hightower, J.W., and Hall, W.K., Trans. Faraday Soc., **66**, 477, 1970.

33) Ciapetta, F.G., Dobres, R.M., and Baker, R.W., 'Catalysis', Vol. 6, (Emmett, P.H., Ed.), Rheinhold, New York, 497, 1957.

34) Cochran, C.N., and Russel, A.S., Ind. Eng. Chem., **42**, 1336, 1950.

35) Haensel, V., US Patent, 2 479 110, 1949.

36) Sterba, M.J., and Haensel, V., Ind. Eng. Chem., Prod. Res. Dev., **15**, 1, 1976.

37) Kluksdahl, H.E., US Patent, 3 415 737, 1968.

38) Johnson, M.F.L., and LeRoy, V.M., J. Catal., **35**, 434, 1974.

39) Johnson, M.F.L., J. Catal., **39**, 487, 1975.

40) Webb, A.N., J. Catal., **39**, 487, 1975.

41) Bolivar, C., Charcosset, H., Frety, R., Primet, M., Tournayan, L., Betizeau, C., Leclerq, G., and Maurel, R., J. Catal., **45**, 163, 1976.

42) M°Nicol, B.D., J. Catal., **46**, 438, 1977.

43) Bolivar, C., Charcosset, H., Frety, R., Primet, M., Tournayan, L., Betizeau, C., Leclerq, G., and Maurel, R., J. Catal., **39**, 249, 1975.

44) Yao, H.C., and Shelef, M., J. Catal., **44**, 392, 1976.

45) Menon, P.G., Sieders, J., Streefkerk, F.J., and Van Keulen, G.J.M., J. Catal., **29**, 188, 1973.

46) Isaacs, B.H., and Petersen, E.E., J. Catal., 77, 43, 1982.

47) Wagstaff, N., and Prins, R., J. Catal., **59**, 434, 1979.

48) Sermon, P.A., and Bond, G.C., Catal. Rev., **8**, 211, 1973.

49) Musso, J.C., and Parera, J.M., Appl. Catal., **30**, 81, 1987.

50) Kramer, R., and Andre, M., J. Catal., **58**, 287, 1979.

51) Mieville, R.L., J. Catal., **87**, 437, 1984.

52) Short, D.R., Khalid, S.M., Katzer, J.R., and Kelley, M.J., J. Catal., **72**, 288, 1981.

53) Cimino, A., de Angelis, B.A., Gazzoli, D., and Valigi, M., Z. Anorg. Allg. Chem., **460**, 86, 1980.

54) Biloen, P., Helle, J.N., Verbeek, H., Dautzenberg, F.M., and Sachtler, W.M.H., J. Catal., **63**, 112, 1980.

55) Kelley, M.J., Freed, R.L., and Swartzfager, D.G., J. Catal., **78**, 445, 1982.

56) Charcosset, H., Frety, R., Leclerq, G., Mendes, E., Primet, M., and Tournayan, L., J. Catal., **56**, 468, 1979.

57) Augustine, S.M., and Sachtler, W.M.H., J. Catal., **106**, 417, 1987.

58) Jossens, L.W., and Petersen, E.E., J. Catal., **76**, 265, 1982.

59) Peri, J.B., J. Catal., **52**, 144, 1978.

60) Bertolacini, R.J., and Pellet, R.J., 'Catalyst Deactivation', (Delmon, B., and Froment, G.E., Eds.), Elseiver, Amsterdam, 73, 1980.

61) Burch, R., and Garla, L.C., J. Catal., **71**, 360, 1981.

62) Dautzenberg, F.M., Helle, J.N., Biloen, P., and Sachtler, W.M.H., J. Catal., **63**, 119, 1980.

63) Völter, J., Lietz, G., Uhlemann, M., and Hermann, M., J. Catal., **68**, 42, 1981.

64) Völter, J., and Kürschner, U., Appl. Catal., **8**, 167, 1983.

65) Palazov, A., Bonev. C., Shopov, D., Lietz, J., Sárkanay, A., and Völter, J., J. Catal., **103**, 249, 1987.

66) Burch, R., J. Catal., **71**, 360, 1981.

67) Muller, A.C., Engelhard, P.A., and Weisang, J.E., J. Catal., **56**, 65, 1979.

68) Balakrishnan, K., and Schwank., J., J. Catal., **138**, 491, 1992.

69) Lieske, H., and Völter, J., J. Catal., **90**, 96, 1984.

70) Baronetti, G.T., de Miguel, S.R., Scelza, O.A., and Castro, A.A., Appl. Catal., **24**, 109, 1986.

71) Berndt, H., Mehner, H., Völter, J., and Meisel, W., Z. Anorg. Allg. Chem., **429**, 47, 1977.

72) Sexton, B.A., Hughes, A.E., and Foger, K., J. Catal., **88**, 466, 1984.

73) Kuznetsov, V.I., Duplyakin, V.K., Kovalchuk, V.I., Ryndin, Y.A., and Belyi, A.S., Kinet. Katal., **22**, 1481, 1981.

74) Kuznetsov, V.I., Duplyakin, V.K., Kovalchuk, V.I., Ryndin, Y.A., and Belyi, A.S., Kinet. Katal., **24**, 1183, 1982.

75) Kuznetsov, V.I., Belyi, A.S., Yurchenko, E.N., Smolikov, M.D., Protasova, M.T., Zatolokina, E.V., and Duplyakin, V.K., J. Catal., **99**, 159, 1986.

76) Davis, B.H., and Srinivasan, R., Plat. Metals Rev., **36(3)**, 150, 1992.

77) Li, Y.X., Stencel, J.M., and Davis, B.H., Appl. Catal., **64**, 71, 1990.

78) Gardner, S.D., Hoflund, G.B., and Schryer, D.R., J. Catal., **119**, 179, 1989.

79) Cox, D.F., and Hoflund, G.B., Surf. Sci., **151**, 202, 1985.

80) Gardner, S.D., Hoflund, G.B., Schryer, D.R., and Upchurch, B.T., J. Phys. Chem., **95**, 835, 1991.

81) Adkins, S.R., and Davis, B.H., J. Catal., **89**, 371, 1984.

82) Li, Y.X., Stencel, J.M., and Davis, B.H., React. Kinet. Catal. Lett., **37(2)**, 273, 1988.

83) Baronetti, G.T., de Miguel, S.R., Scelza, O.A., Fritzler, M.A., and Castro, A.A., Appl. Catal., **19**, 77, 1985.

84) Ushakov, V.A., and Moroz, E.M., React. Kinet. Catal. Lett., **27**, 351, 1985.

85) Srinivasan, R., de Angelis, R.J., and Davis, B.H., J. Catal., **106**, 449, 1987.

86) Davis, B.H., Proc. 10th Int. Congr. Catal., Budapest, 37, 1992.

87) Srinivasan, R., Rice, L.A., and Davis, B.H., J. Catal., **129**, 257, 1991.

88) Kuznetsov, V.I., Yurchenko, E.N., Belyi, A.S., Zatolokina, E.V., Smolikov, M.D., and Duplyakin, V.K., React. Kinet. Catal. Lett., **21**, 419, 1982.

89) Bacaud, R., Bussiere, P., and Figueras, F., J. Catal., **69**, 399, 1981.

90) Li, Y.X., Klabunde, K.J., and Davis, B.H., J. Catal., **128**, 1, 1991.

91) Hobson, M.C., Goresh, S.L., and Khare, G.P., J. Catal., **142**, 641, 1993.

92) Yurchenko, E.N., Kuznetsov, V.I., Melnikova, V.P., and Startsev, A.N., React. Kinet. Catal. Lett., **23**, 137, 1983.

93) Sinfelt, J.H., Via, G.H., and Lytle, F.W., J. Chem. Phys., **76**, 2779, 1982.

94) Meitzner, G., Via, G.H., Lytle, F.W., and Sinfelt, J.H., J. Chem. Phys., **87**, 6354, 1987.

95) Meitzner, G., Via, G.H., Lytle, F.W., and Sinfelt, J.H., J. Chem. Phys., **78**, 882, 1983.

96) Meitzner, G., Via, G.H., Lytle, F.W., and Sinfelt, J.H., J. Chem. Phys., **83**, 353, 1985.

97) Davis, B.H., J. Catal., **42**, 376, 1976.

98) Sachtler, W.M.H., and Van Santen, R.A., Advan. Catal., **26**, 69, 1977.

99) Coq, B., and Figueras, F., J. Catal., **85**, 197, 1984.

100) Balakrishnan, K., and Schwank, J., J. Catal., **132**, 451, 1991.

101) Sánchez, J., Segova, N., Moronta, A., Arteaga, A., Arteaga, G., and Choren, E., Appl. Catal., **101**, 199, 1993.

102) Jones, A., and M^{c}Nicol, B.D., 'Temperature Programmed Reduction for Solid Materials Characterisation', Marcel Dekker, New York, 1986.

103) Bouwman, R., and Biloen, P., J. Catal., **48**, 209, 1977.

104) Goldwasser, J., Arenas, B., Bolivar, C., Castro, G., Rodriguez, A., Fleitas, A., and Geron, J., J. Catal., **100**, 76, 1986.

105) Romero, T., Tejeda, T., Jaunay, D., Bolivar, C., and Charcosset, H., Proc. VIIth Iberoamerican Congr. Catal., La Plata, Argentina, 453, 1980.

106) Bolivar, C., Charcosset, H., Primet, M., Arenas, B., and Torellas, R., Proc. VIIIth Iberoamerican Congr. Catal., Huelva, Spain, 162, 1982.

107) Aboul-Gheit, A.K., Menoufy, M.F., and Ebeid, N.S., Appl. Catal., **4**, 181, 1982.

108) Parera, J.M., Querini, C.A., Beltramini, J.N., and Figoli, N.S., Appl. Catal., **32**, 117, 1987.

109) Biswas, J., Bickle, G.M., Gray, P.G., Do, D.D., and Barbier, J., Catal. Rev. Sci. Eng., **30(2)**, 161, 1988.

110) Apestiguia, C.R., Barbier, J., Plaza de los Reyes, J.F., Garetto, T.F., and Parera, J.M., Appl. Catal., **1**, 159, 1981.

111) Parera, J.M., Apestiguia, C.R., Plaza de los Reyes, J.F., and Garetto, T.F., React. Kinet. Catal. Lett., **15**, 167, 1980.

112) Barbier, J., Marecot, P., Tifouti, L., Guenin, M., and Frety, R., Appl. Catal., **19**, 375, 1985.

113) Menon, P.G., and Prasad, J., Proc. 6th Int. Congr. Catal., London, 1061, 1977.

114) Apestiguia, C.R., Trevizan, S.M., Garetto, T.F., Plaza de los Reyes, J.F., and Parera, J.M., React. Kinet. Catal. Lett., **20**, 1, 1982.

115) Apestiguia, C.R., and Barbier, J., J. Catal., **78**, 352, 1982.

116) Apestiguia, C.R., and Barbier, J., React. Kinet. Catal. Lett., **19**, 351, 1982.

117) Ponitzsch, L., Wilde, M., Tetenyi, P., Dobrovolszky, M., and Páal, Z., Appl. Catal., **85**, 115, 1992.

118) Gallezot, P., Datka, J., Massardier, J., Primet, M., and Imelik, B., Proc. 6th Int. Congr. Catal., London, **2**, 696, 1977.

119) Barbier, J., Lamy-Pitara, E., Marecot, P., Boitiaux, J.P., Cosyns, J., and Verna, F., Advan. Catal., **37**, 279, 1990.

120) Augustine, S.M., Alameddin, G.N., and Sachtler, W.M.H., J. Catal., **115**, 217, 1989.

121) Apesteguia, C.R., Brema, C.E., Garetto, T.F., Borgna, A., and Parera, J.M., J. Catal., **89**, 52, 1984.

122) Van Trimpont, P.A., Marin, G.B., and Froment, C.F., Appl. Catal., **17**, 161, 1985.

123) Voge, H.H., Good, J.M., and Greensfelder, B.J., Proc. 3rd World Pet. Congr., **4**, 124, 1951.

124) Beltramini, J.N., Martinelli, E.E., Churin, E.J., Figoli, N.S., and Parera, J.M., Appl. Catal., 7, 43, 1983.

125) Figoli, N.S., Beltramini, J.N., Querini, C.A., and Parera, J.M., Appl. Catal., **15**, 41, 1985.

126) Cooper, B.J., and Trimm, D.L., 'Catalyst Deactivation', (Delmon, B., and Froment, G.F., Eds.), Elseiver, Amsterdam, 63, 1980.

127) Zhorov, V.M., Panchekov, G.M., and Kartashev, Y.N., Kinet. Katal., **21(3)**, 776, 1980.

128) Davis, S.M., Zaera, F., and Somorjai, G.A., J. Catal., **77**, 439, 1982.

129) Gillespie, W.D., Hertz, R.K., Petersen, E.E., and Somorjai, G.A., J. Catal., **70**, 147, 1981.

130) Parera, J.M., Figoli, N.S., Traffano, E.M., Beltramini, J.N., and Martinelli, E.E., Appl. Catal., **5**, 33, 1983.

131) Figoli, N.S., Sad, M.R., Beltramini, J.N., Jablonski, E.L., and Parera, J.M., Ind. Eng. Chem. Prod. Res. Dev., **19**, 545, 1980.

132) Barbier, J., Churin, E., and Marecot, P., J. Catal., **126**, 228, 1990.

133) de Miguel, S.R., Martinez Correa, J.A., Baronetti, G.T., Castro, A.A., and Scelza, O.A., Appl. Catal., **60**, 47, 1990.

134) Barbier, J., Marecot, P., Martin, N., Elassal, L., and Maurel, R., 'Catalyst Deactivation', (Delmon, B., and Froment, G.F., Eds.), Elseiver, Amsterdam, 53, 1980.

135) Lankhorst, P.P., de Jongste, H.C., and Ponec, V., 'Catalyst Deactivation', (Delmon, B., and Froment, G.F., Eds.), Elseiver, Amsterdam, 43, 1980.

136) Carter, J.L., M^{c}Vicker, G.B., Weissman, W., Kmak, W.S., and Sinfelt, J.H., Appl. Catal., **3**, 327, 1982.

137) Barbier, J., Gorro, G., and Zhang, Y., Appl. Catal., **19**, 169, 1985.

138) Parera, J.M., Figoli, N.S., Beltramini, J.N., Churin, E.J., and Cabrol, R.A., 8th Int. Congr. Catal., Berlin, **2**, 593, 1984.

139) Querini, C.A., and Fung, S.C., J. Catal., **141**, 389, 1993.

140) Parera, J.M., Beltramini, J.N., Martinelli, E.E., Churin, E.J., Aloe, P.E., and Figoli, N.S., J. Catal., **99**, 39, 1986.

141) Parera, J.M., Verderone, R.J., and Querini, C.A., 'Catalyst Deactivation', (Delmon, B., and Froment, G.F., Eds.), Elseiver, Amsterdam, 135, 1987.

142) Franck, J.P., and Martino, G.P., 'Deactivation and Poisoning of Catalysts', (Oudar, J., and Wise, H., Eds), Marcel Dekker, New York, 205, 1985.

143) Sivasanker, S., and Ramaswany, A.V., J. Catal., **37**, 553, 1975.

144) Verderone, R.J., Pieck, C.L., Sad, M.R., and Parera, J.M., Appl. Catal., **21**, 239, 1986.

145) Parera, J.M., Figoli, N.S., Jablonski, E.L., Sad, M.R., and Beltramini, J.N., 'Catalyst Deactivation', (Delmon, B., and Froment, G.F., Eds.), Elseiver, Amsterdam, 571, 1980.

146) Parera, J.M., Traffano, E.M., Musso, J.C., and Pieck, C.L., 'Spillover of Adsorbed Species', (Pajonk, G.M., Teichner, S.J., and Germain, J.E., Eds.), Elseiver, Amsterdam, 1983.

147) Bishara, A., Murad, K.M., Stanislaus, A., Ismail, M., and Hussain, S.S., Appl. Catal., **7**, 337, 1988.

148) Appleby, W.G., Gibson, J.W., and Good, G.M., Ind. Eng. Chem. Proc. Des. Dev., **1**, 102, 1962.

149) Haldemann, R.G., and Bolty, M.C., J. Phys. Chem., **63**, 489, 1959.

150) Thomas, C.L., Div. Pet. Chem., ACS, **66**, 1586, 1944.

151) Parera, J.M., Figoli, N.S., and Traffano, E.M., J. Catal., **79**, 481, 1983.

152) Querini, C.A., Figoli, N.S., and Parera, J.M., Appl. Catal., **52**, 249, 1989.

153) Barbier, J., Gorro, G., Zhang, Y., Bournville, J.P., and Franck, J.P., Appl. Catal., **13**, 245, 1985.

154) Sato, Y., Kamo, M., and Setaka, N., Carbon, **16**, 279, 1978.

155) Lespade, P., Al-Jishi, R., and Dresselhaus, M.S., Carbon, **20**, 427, 1982.

156) Stencel, J.M., 'Raman Spectroscopy for Catalysis', Van Nostrand Rheinhold, New York, 1990.

157) Nikiel, L., and Jagodzinski, P.W., Carbon, **31(8)**, 1313, 1993.

158) Espinat, D., Dexpert, H., Freund, E., Martino, G., Couzi, M., Lespade, P., and Cruege, F., Appl. Catal., **16**, 343, 1985.

159) Tuinstra, F., and Koeng, J.l., J. Chem. Phys., **53**, 1126, 1970.

160) Nakamizo, M., Krammereck, R., and Walker, P.L., Carbon, **12**, 259, 1974.

161) Nakamizo, M., Honda, H., and Inagaki, M., Carbon, **16**, 281, 1978.

162) Nemanich, R.J., and Solin, S.A., Phys. Rev., **1320(2)**, 392, 1979.

163) Lespade, P., Marehand, A., Couzi, M., and Cruege, F., Carbon, **22**, 375, 1984.

164) Sinha, K., and Menendez, J., Phys. Rev., **B41**, 10845, 1990.

165) Posazheinikova, R.P., Buyanov, R.A., Koloniichuk, V.N., and Shadrin, L.P., J. Catal., **15**, 671, 1974.

166) Espinat, D., Freund, E., Dexpert, H., and Martino, G., J. Catal., **126**, 496, 1990.

167) Eberly, P.E., Kimbedin, C.N., Miller, W.H., Drushel, H.V., Ind. Eng. Chem. Proc. Des. Dev., **5**, 193, 1966.

168) Bellamy, L.J., 'The Infrared Spectra of Comple Molecules', Chapman and Hall, London, 13, 1975.

169) Wolf, E.E., and Petersen, E.E., Catal. Rev. Sci. Eng., **24(3)**, 329, 1982.

170) Parmaliana, A., Fruster, F., Nesterov, G.A., Paukshtis, E.A., and Giordano, N., 'Catalyst Deactivation', (Delmon, B., and Froment, G.F., Eds.), Elseiver, Amsterdam, 197, 1987.

171) Datka, J., Sarbak, Z., and Eischens, R.P., J. Catal., **145**, 544, 1994.

172) Blakely, D.W., and Somorjai, G.A., J. Catal., **42**, 181, 1976.

173) Butt, J.B., and Petersen, E.E., 'Activation, Deactivation and Poisoning of Catalysts', Academic Press, San Diego, 1988.

174) Myers, C.G., Lang, W.H., and Weisz, P.B., Ind. Eng. Chem., **53**, 299, 1961.

175) Bortekevich, M.I., Lenenter, M.E., Zabotin, L.I., and Berkovich, L.M., Kinet. Katal., **16**, 221, 1975.

176) Trimm, D.L., Appl. Catal., **5**, 263, 1983.

177) Sárkany, A., Lieske, H., Szilagyi, T., and Toth, L., 8th Int. Congr. Catal., Berlin, **2**, 613, 1984.

178) Maire, G., Luck, F., and Aeiyach, S., 8th Int. Congr. Catal., Berlin, **2**, 695, 1984.

179) Beltramini, J.N., Cabrol, R.A., Churin, E.J., Figoli, N.S., Martinelli, E.E., and Parera, J.M., Appl. Catal., **17**, 65, 1985.

180) Trimm, D.L., Catal. Rev. Sci. Eng., **16**, 155, 1977.

181) Christoffel, E.G., and Páal, Z., J. Catal., **73**, 30, 1982.

182) Beltramini, J., and Trimm, D.L., Appl. Catal., **31**, 113, 1987.

183) Tennison, S.R., Chem. Br., 536, Nov., 1981.

184) Bond, G.C., and Hellier, H., J. Catal., **7**, 217, 1967.

185) Davies, A.G., Wilkinson, G., and Young, J.F., J. Am. Chem. Soc., **85**, 1692, 1963.

186) Antos, G.J., US Patent, 3 929 683, Dec. 1975.

187) Jackson, S.D., Glanrille, B.M., Willis, J., McLellan, G., Webb, G., Moyes, R.B., Simpson, S., Wells, P.B., and Whyman, R.J., J. Catal., **139**, 207, 1993.

188) Dorling, T.A., and Moss, R.L., J. Catal., **7**, 378, 1967.

189) Herz, R.K., and McCready, D.F., J. Catal., **81**, 358, 1983.

190) Norton, P.R., Davies, J.A., Cresler, D.K., Sitter, C.W., and Jackson, T.E., Surf. Sci., **108**, 205, 1981.

191) Verbeek, H., and Sachtler, W.M.H., J. Catal., **42**, 257, 1976.

192) Gruber, H.L., J. Phys. Chem., **66**, 48, 1962.

193) Benson, J.E., and Boudart, M., J. Catal., **4**, 704, 1965.

194) Nacheff, M.S., Kraus, G.B., Weissman, W., Kmak, W.S., and Sinfelt, J.H., Appl. Catal., **3** 327, 1982.

195) Wilson, G.R., and Hall, W.K., J. Catal., **17**, 190, 1970.

196) Bouwman, R., and Biloen, P., Anal. Chem., **46**, 136, 1974.

197) Bouwman, R., Toneman, L.H., and Holscher, A.A., Surf. Sci., **35**, 8, 1973.

198) Huang, Z., Fryer, J.R., Park, C., Stirling, D., and Webb, G., (Submitted to J. Catal. for publication).

199) Bond, G.C., 'Catalysis by Metals', Academic Press, London, 1962.

200) Brunauer, S., Deming, L.S., Deming, W.E., and Teller, E., J. Am. Chem. Soc., **62**, 1723, 1940.

201) Brunauer, S., Emmett, P.H., and Teller, E., J. Am. Chem. Soc., **60**, 309, 1938.

202) Barrett, E.P., Joyner, L.G., and Halenda, P.P., J. Am. Chem. Soc., **73**, 373, 1951.

203) Gregg, S.J., and Sing, K.S.W., 'Adsorption, Surface Area and Porosity', 2nd Edition, Academic Press, London, 1982.

204) Spendal, L., and Bondart, M., J. Phys. Chem., **64**, 204, 1960.

205) Dorling, T.A., and Moss, R.L., J. Catal., **5**, 11, 1966.

206) Drake, L.C., Ind. Eng. Chem., **41**, 780, 1949.

207) M[ac]Dougal, G., and Ockrent, C., Proc. Roy. Soc., **180**, 151, 1942.

208) Ritter, H.L., and Drake, L.C., Ind. Eng. Chem. Analyt. Ed., **17**, 782, 1945.

209) Everett, D.H., and Haynes, J.M., 'Colloid Science', Specialist Periodical Reports, Chemical Society, London, Vol. 1, 123, 1973.

210) Rao, K.S., J. Phys. Chem., **45**, 506, 1941.

211) Katz, S.M., J. Phys. Chem., **53**, 1166, 1949.

212) Huang, Z., Fryer, J.R., Park, C., Stirling, D., and Webb, G., J. Catal., **148**, 478, 1994.

213) Huang, Z., Fryer, J.R., Park, C., Stirling, D., and Webb, G., (Submitted to J. Catal. for publication).

214) Roy, J.M., Ph.D. Thesis, University of Glasgow, 1992.

215) de Miguel, S.R., Scelza, O.A., and Castro, A.A., Appl. Catal., **44**, 23, 1988.

216) Beltramini, J.N., and Trimm, D.L., Appl. Catal., **32**, 71, 1987.

217) Csicsery, S.M., and Pines, H., J. Am. Chem. Soc., **84**, 3939, 1962.

218) Fodelberg, L.S., Gore, R., and Ranbg, B., Acta. Chem. Scand., **21**, 2041, 1967.

219) Davis, B.H., and Venuto, P.B., J. Catal., **15**, 363, 1969.

220) Csicsery, S.M., and Pines, H., J. Catal., **1**, 313, 1962.

221) Pines, H., and Goetschel, C.T., J. Org. Chem., **30**, 3530, 1965.

222) Pines, H., and Goetschel, C.T., J. Org. Chem., **30**, 3544, 1965.

223) Pines, H., and Goetschel, C.T., J. Org. Chem., **30**, 3548, 1965.

224) Pines, H., Goetschel, C.T., and Dembinski, J.W., J. Org. Chem., **30**, 3540, 1965.

225) Davis, B.H., Proc. 8th Int. Congr. Catal., Berlin, Vol. 2., 469, 1984.

226) Sivasanker, S., and Padalkar, S.R., Appl. Catal., **39**, 123, 1988.

227) Querini, C.A., Figoli, N.S., and Parera, J.M., Appl. Catal., **53**, 53, 1989.

228) Barbier, J., Appl. Catal., **23**, 225, 1986.

229) Voge, H.H., 'Catalysis', Vol VI, (Emmett, P.H., Ed.), Rheinhold, New York, 407, 1954.

230) Sachdev, A., and Schwank, J., Proc. XII Int. Congr. for E.M., **IV**, 278, San Francisco Press, San Francisco, 1992.

231) Parera, J.M., Querini, C.A., and Figoli, N.S., Appl. Catal., **52**, 249, 1989.

232) Davis, B.H., Westfall, G.A., Watkins, J., and Pezzanite, J., J. Catal., **42**, 247, 1976.

233) Sparks, D.E., Srinivasan, R., and Davis, B.H., J. Mol. Chem., **88**, 259, 1994.

234) Srinivasan, R., and Davis, B.H., J. Mol. Chem., **88**, 343, 1994.

235) Beltramini, J.N., and Trimm, D.L., 'Proc. XI Iberoamerican Congr. Catal., Guanajuato, Mexico, 1153, 1988.

236) Ludlum, L.H., Eischens, R.P., Prepr. Am. Chem. Soc. Div. Pet. Chem., 375, 1976.

237) Cramer, R.D., Jenner, E.L., Lindsay, R.V., and Stolberg, U.G., J. Am. Chem. Soc., **85**, 1692, 1963.

238) Young, J.F., Gillard, R.D., and Wilkinson, G., J. Chem. Soc., **5**, 5176, 1964.

239) Shum, V.K., Butt, J.B., and Sachtler, W.M.H., J. Catal., **99**, 126, 1986.

240) Franck, P., and Matrino, G., 'Progress in Catalyst Deactivation', (Figueiredo, J.L., Ed.), Martinus Nifhoff, The Hague, 355, 1982.

241) Kugelmann, A.M., Hydrocarbon Processing, 95, January, 1976.

242) Bond, G.C., and Gelsthorpe, M.R., J. Chem. Soc., Faraday Trans. I, **85(11)**, 3767, 1989.

243) Ako, C.T., and Susu, A.A., J. Chem. Biotechnol., **36**, 519, 1986.

244) Bartholomew, C.H., Agrawal, P.K., and Katzer, J.R., Advan. Catal., **31**, 135, 1982.

245) Biswas, J., Bickle, G.M., Gray, P.G., and Do, D.D., 'Catalyst Deactivation', (Delmon, B., and Froment, G.F., Eds.), Elseiver, Amsterdam, 553, 1987.

246) Sachtler, W.M.H., J. Mol. Chem., **25**, 1, 1984.

247) Van Broekhoven, E.H., Schoonhoven, J.W.F.M., and Ponec, V., Surf. Sci., **56**, 899, 1985.

248) Barbier, J., and Marecot, P., J. Catal., **102**, 21, 1986.

249) Coughlin, R.W., Hasan, A., and Kawakami, K., J. Catal., **88**, 163, 1984.

250) Shum, V.K., Butt, J.B., and Sachtler, W.M.H., J. Catal., **96**, 371, 1985.

Appendices

APPENDIX 1

MASS FLOW CONTROL

The Mass Flow Controller (MFC) used in this study operated by a thermal mass flow sensing technique.

The flow entered the MFC and passed through a restrictor (bypass element). This element produced a pressure drop which forced a percentage of the total flow through the sensor tube. The restrictor has very small passages to ensure a linear pressure drop with flow rate, thus maintaining a constant ratio of the flow through the restrictor to the sensor tube.

A constant input of power (P) was supplied to the heater, which was situated in the middle of the sensor tube (as shown below).

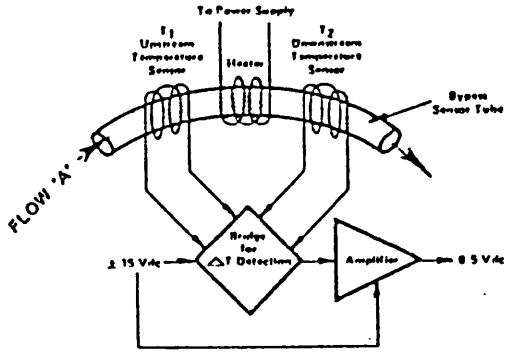

The flow through the sensor tube was measured thermodynamically. Therefore, at zero, or no flow conditions the heat reaching each temperature sensor was equal. So temperatures T_1 and T_2 were equal. When a gas flowed through the tube, the upstream sensor (T_1) is cooled and the downstream sensor (T_2) is heated. This

produced a temperature difference [T_2 - T_1] which was directly proportional to the mass flow rate. This is shown by the following equation:-

$$\Delta T = T_2 - T_1 = A\ P\ C_p\ m$$

where: ΔT = temperature difference.

C_p = Specific heat of the gas at constant pressure.

P = Power of the heater.

m = mass flow.

A = constant.

A bridge circuit interpreted the temperature difference and a linear 0-5 dc signal, directly proportional to the gas mass flow rate, was generated.

APPENDIX II

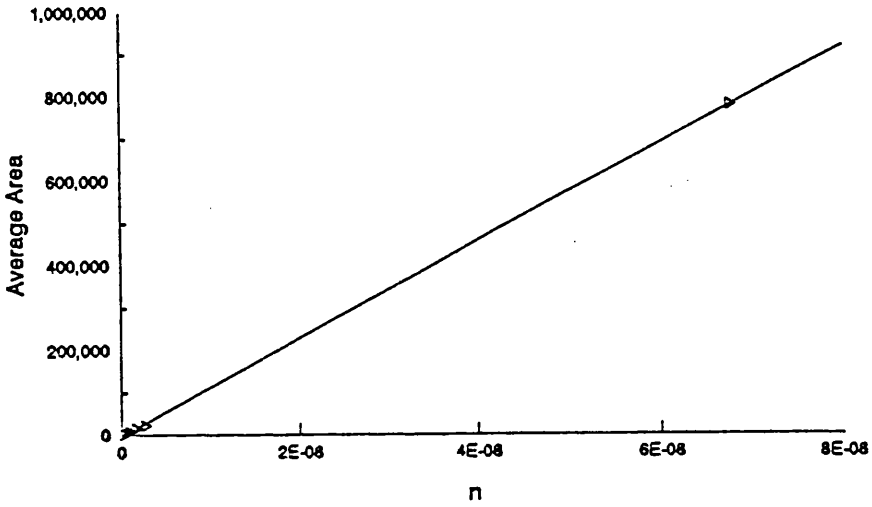

Calibration Of Benzene

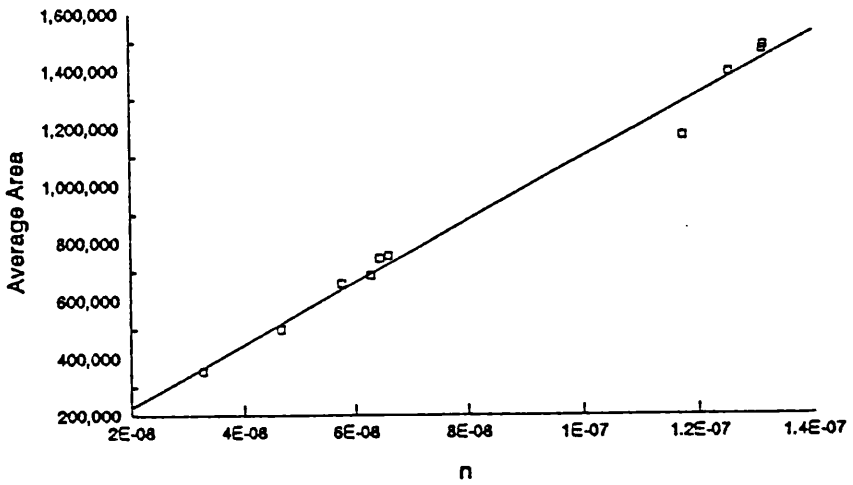

Calibration of Toluene

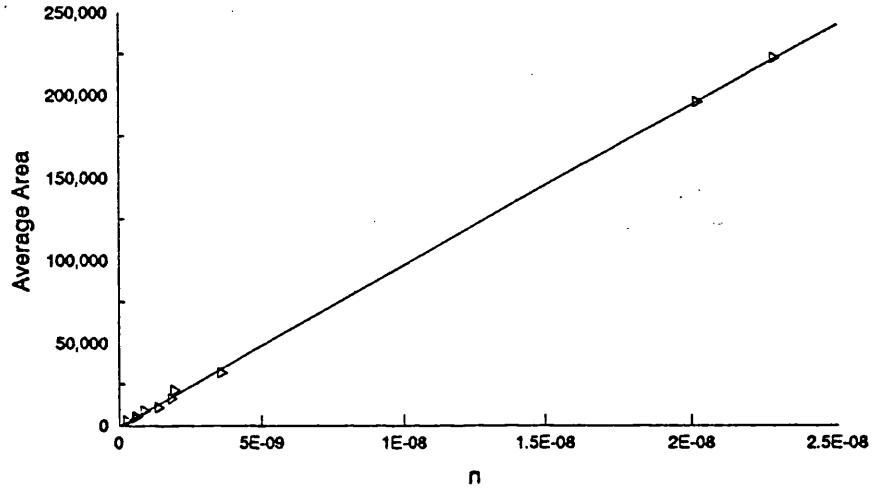

Calibration of Ethylbenzene

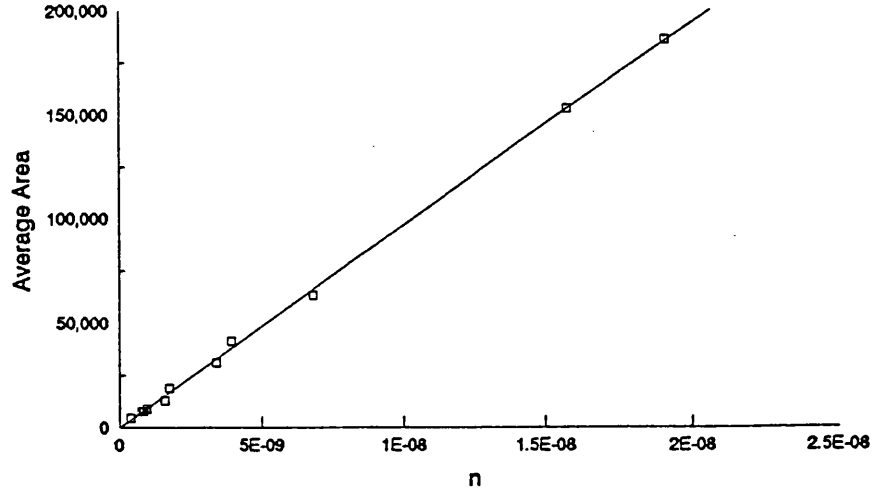

Calibration of m/p - Xylene

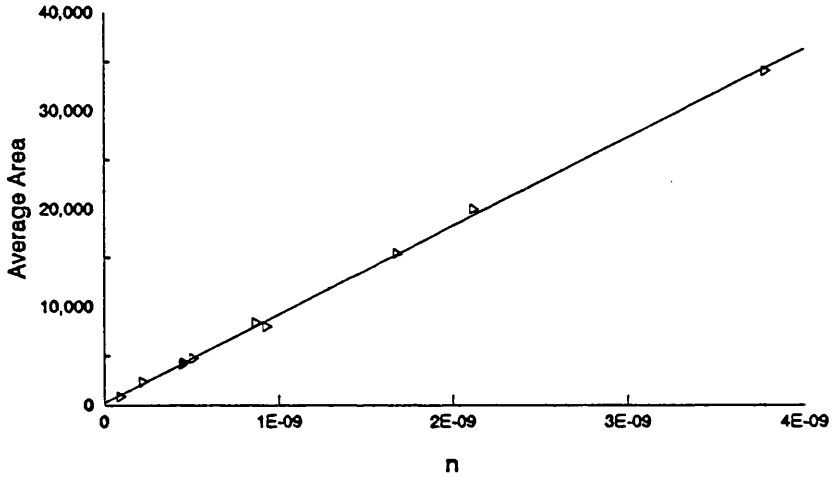

Calibration of o - Xylene

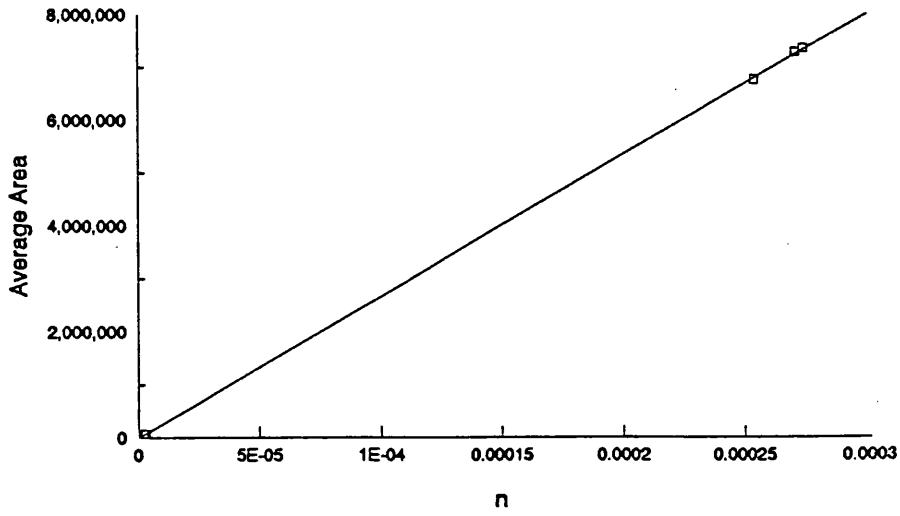

Calibration of Methane

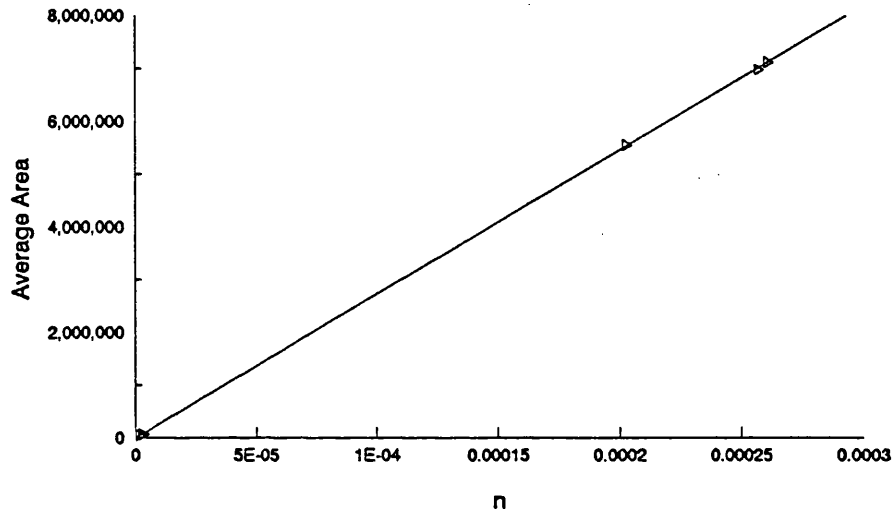

Calibration of Ethane

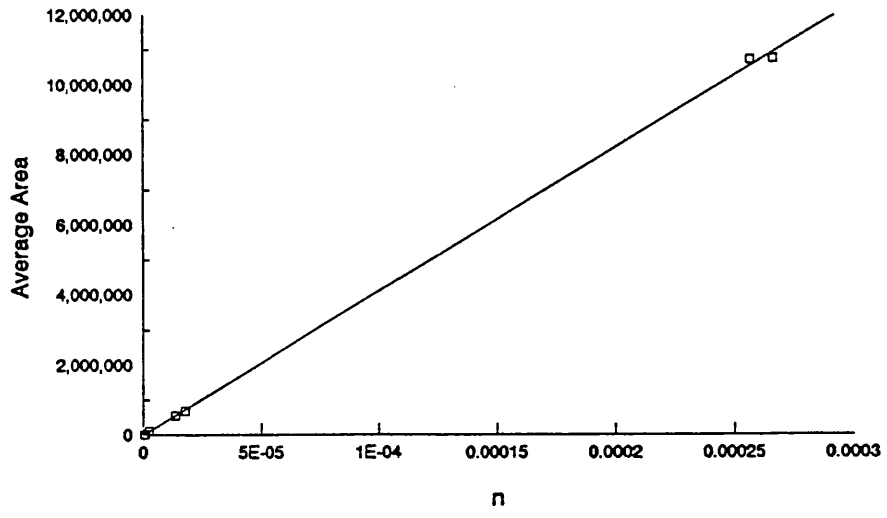

Calibration of Propane

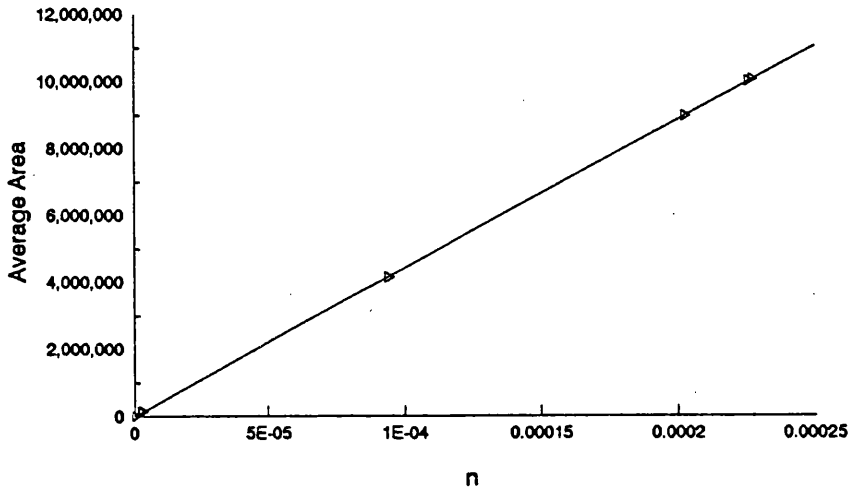

Calibration of i - Butane

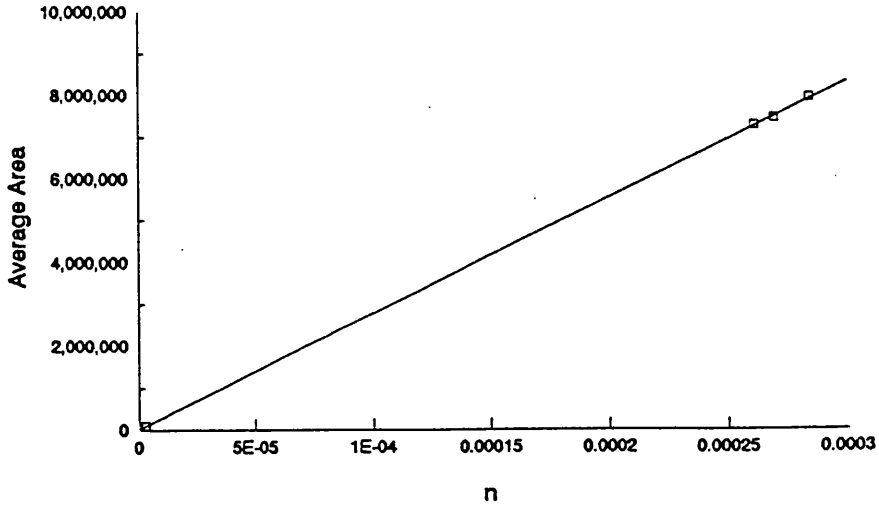

Calibration of n - Butane

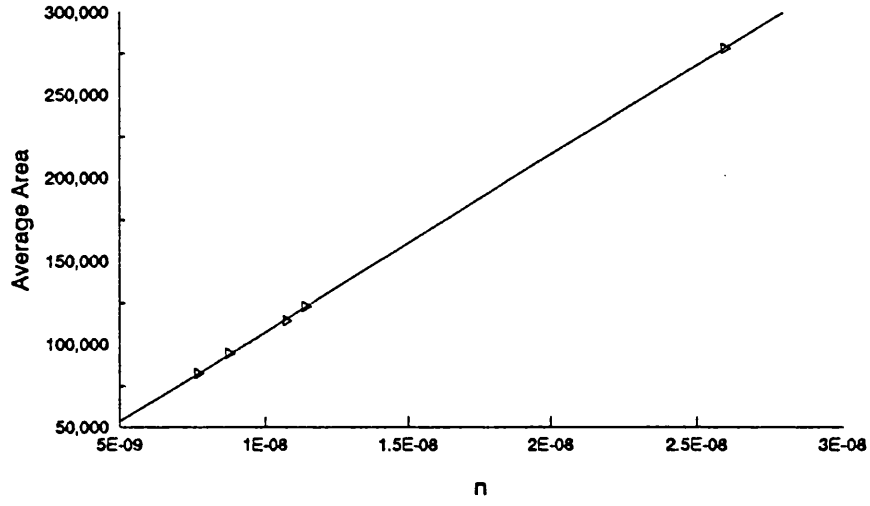

Calibration of Cyclopentane

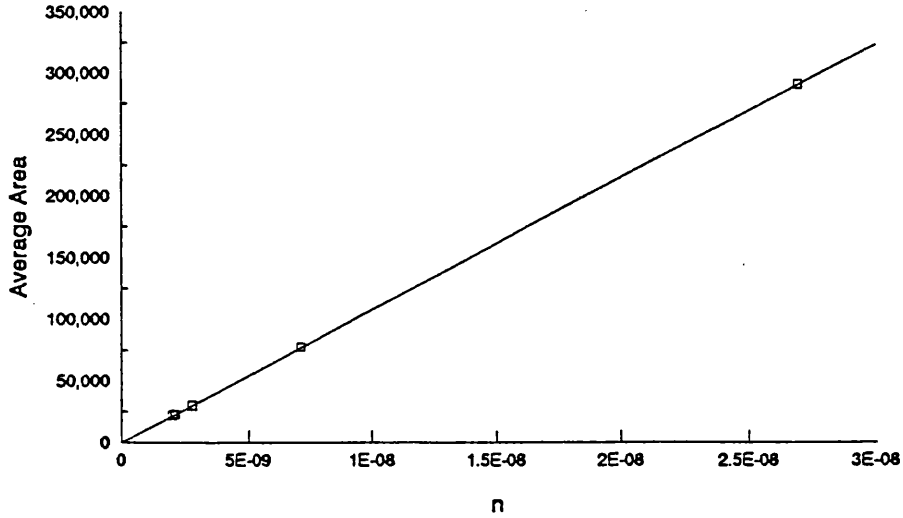

Calibration of i - Pentane

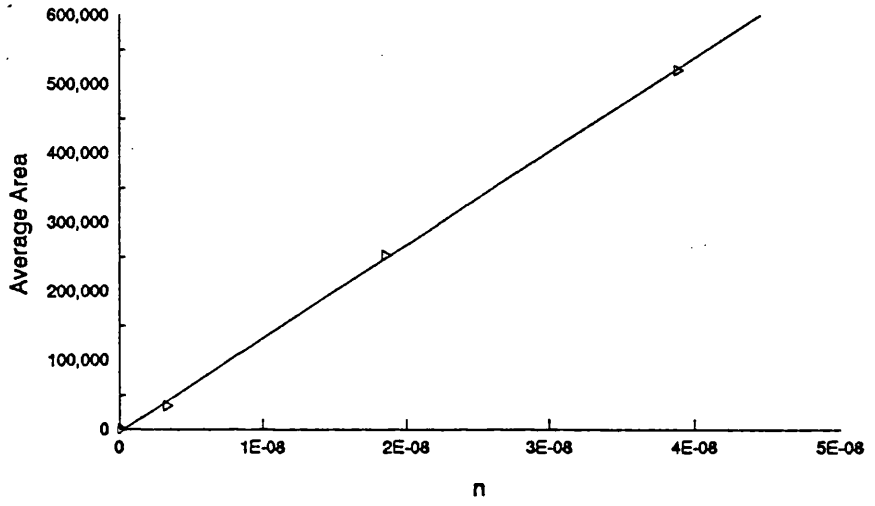

Calibration of n - Pentane

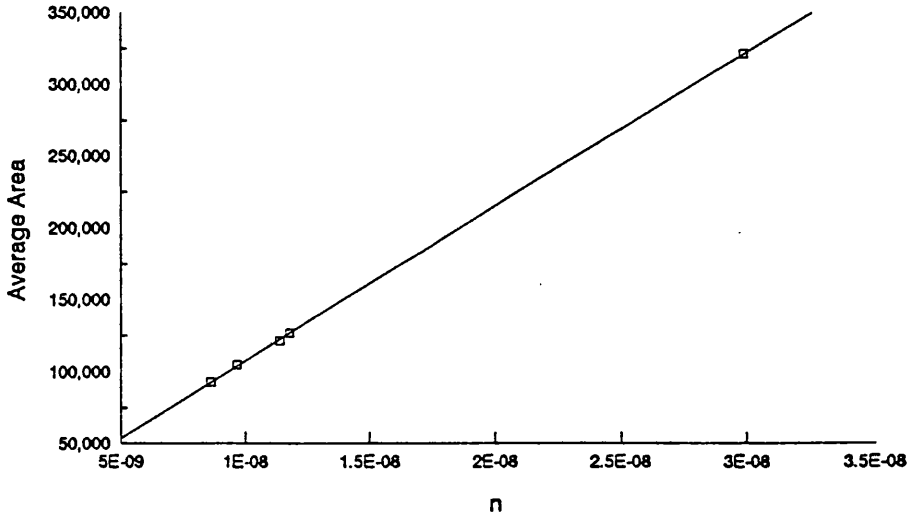

Calibration of Cyclohexane

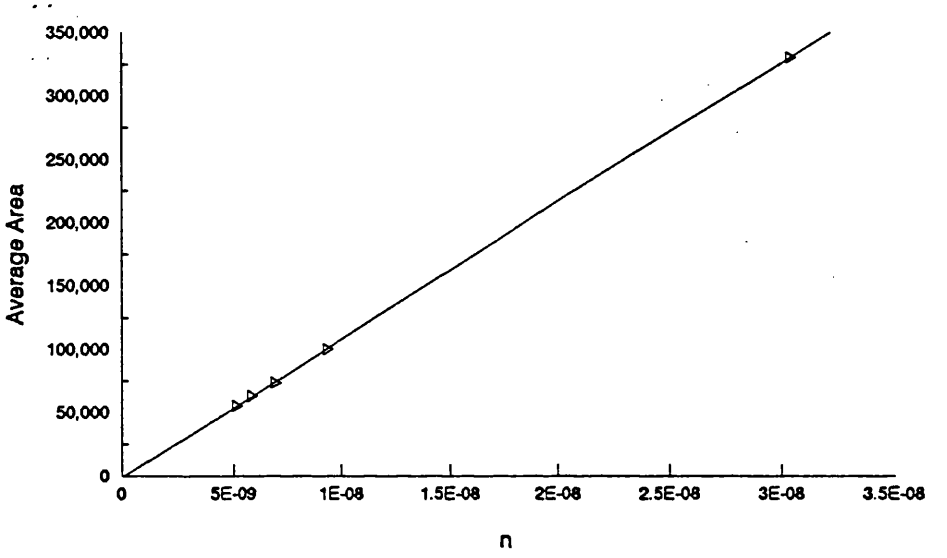

Calibration of i - Hexane

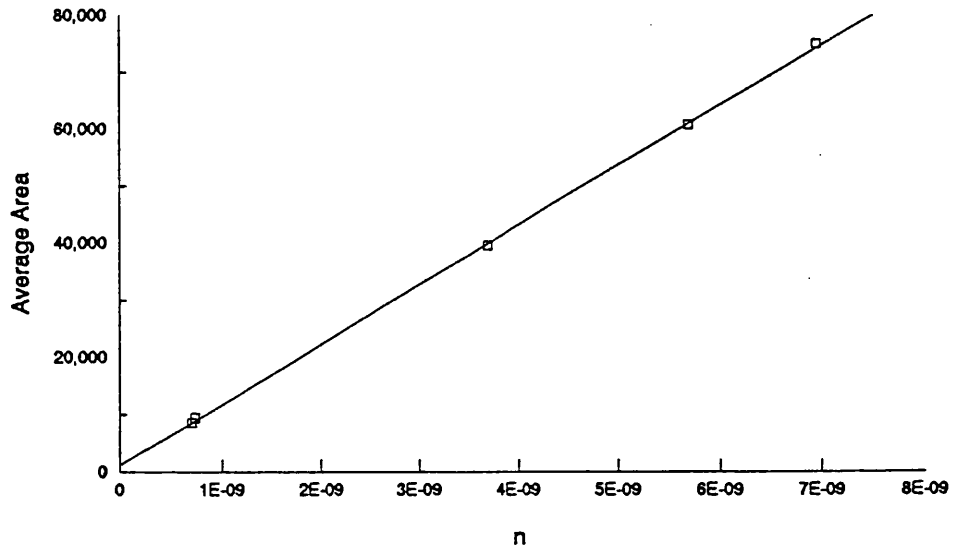

Calibration of n - Hexane

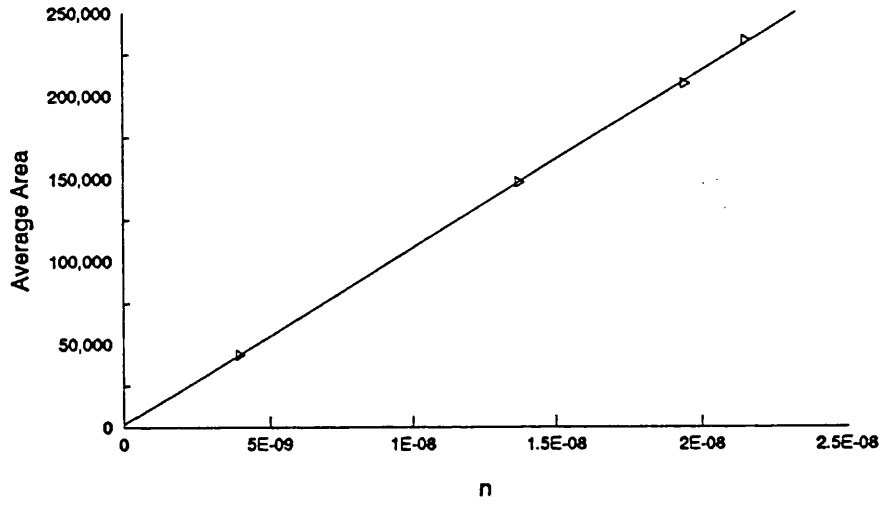

Calibration of Cycloheptane

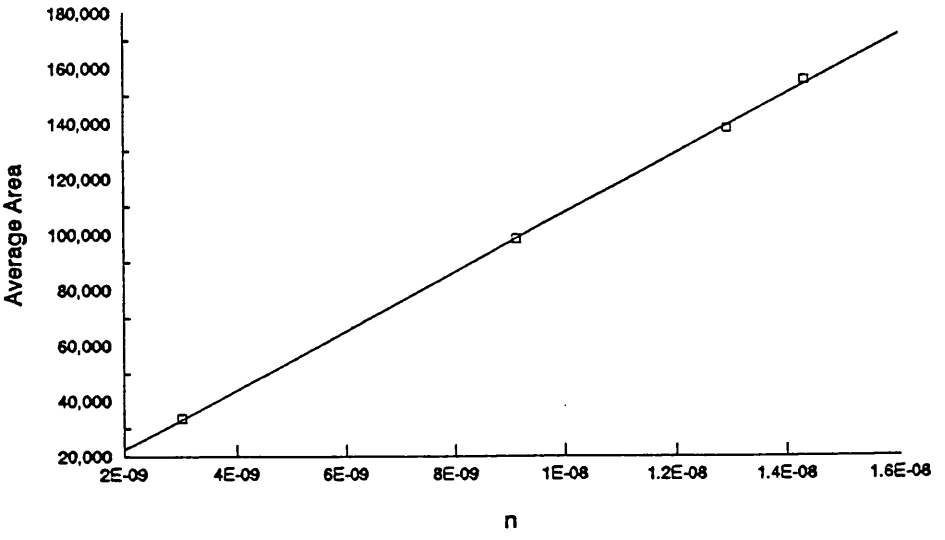

Calibration of i - Heptane

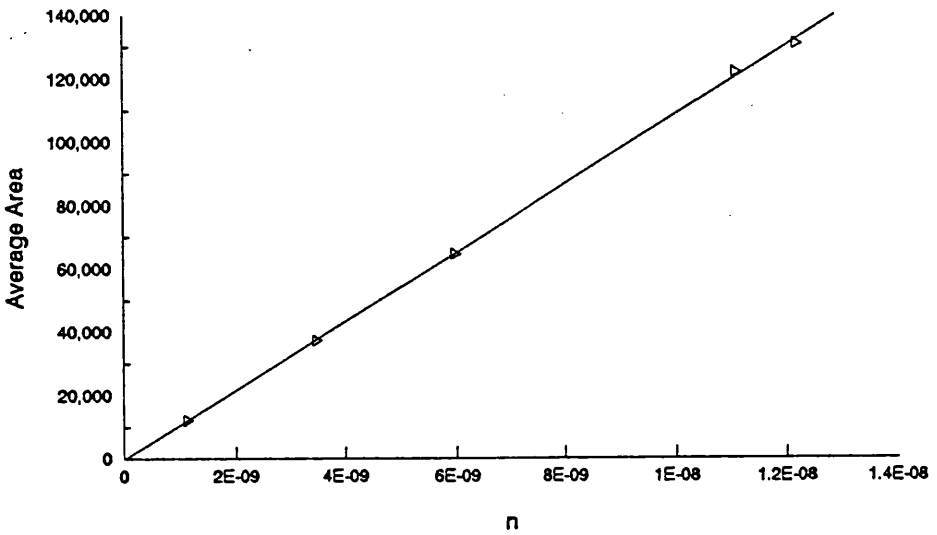

Calibration of n - Heptane

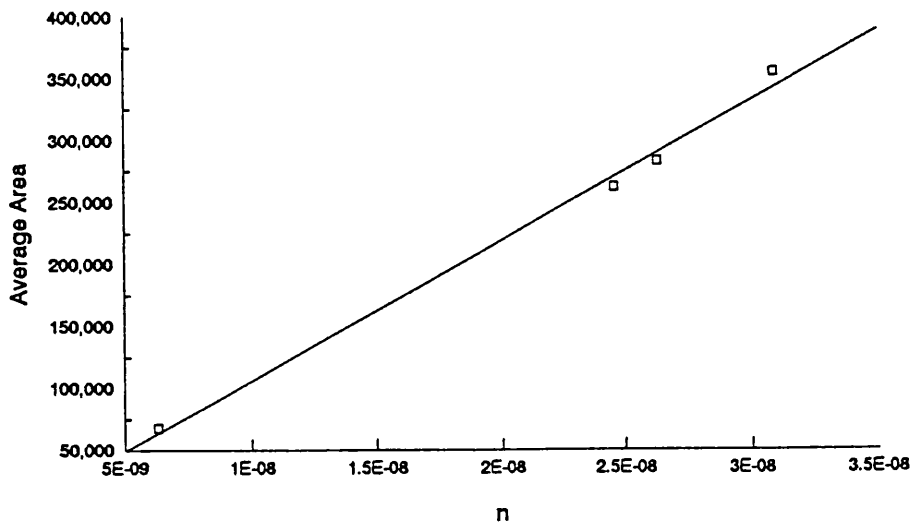

Calibration of Cyclooctane

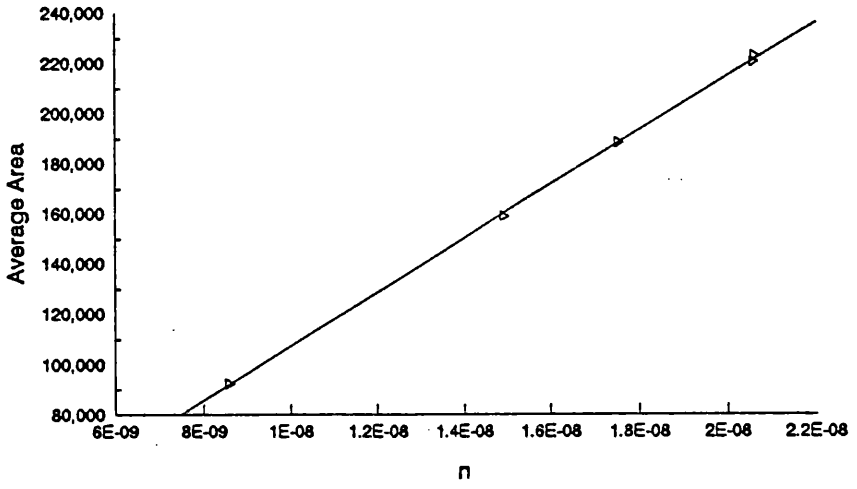

Calibration of i - Octane

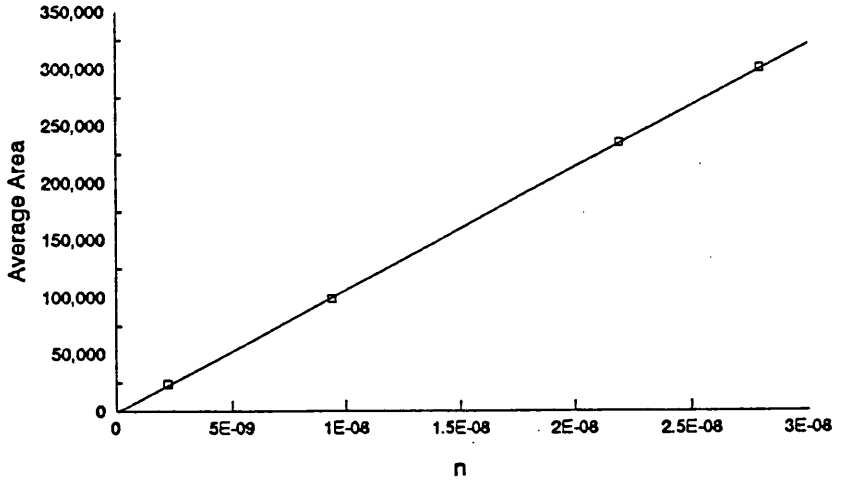

Calibration of n - Octane